IDŐJÁRÁS

QUARTERLY JOURNAL
OF THE HUNGARIAN METEOROLOGICAL SERVICE

Special Issue: Symposium on Climate Change and Variability – Agrometeorological Monitoring and Coping Strategies for Agriculture

Guest Editors: **Simone Orlandini, Mannava V. K. Sivakumar, Tor H. Sivertsen, and Arne O. Skjelvåg**

World Meteorological Organization
Weather • Climate • Water

CONTENTS

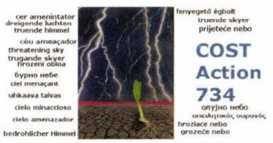

****

http://www.met.hu/Journal-Idojaras.php

VOL. 113 * NO. 1 – 2 * JANUARY – JUNE 2009

IDŐJÁRÁS

Quarterly Journal of the Hungarian Meteorological Service

Editorial Office: *Gilice tér 39, H-1182 Budapest, Hungary*
P.O. Box 39, H-1675 Budapest, Hungary
E-mail: bozo.l@met.hu or antal.e@met.hu
Fax: (36-1) 346-4809

Indexed and abstracted in Science Citation Index Expanded™ and Journal Citation Reports/Science Edition
Covered in the abstract and citation database SCOPUS®

Subscription by

mail: IDŐJÁRÁS, P.O. Box 39, H-1675 Budapest, Hungary
E-mail: kenderesy.k@met.hu or antal.e@met.hu

IDŐJÁRÁS

Quarterly Journal of the Hungarian Meteorological Service
Vol. 113, No. 1–2, January–June 2009

World
Meteorological
Organization
Weather • Climate • Water

Foreword

Agriculture is one of the most important industries in the world. It is estimated that nearly one out of every three people in the world is involved in farming, and agriculture provides all of the cereals, vegetables, meat, fish, and forestry products that we all depend on. Farmers and farming communities throughout the world have, in most instances, survived and developed by mastering the ability to adapt to widely varying weather and climatic conditions. However, the dramatic growth in human population is imposing enormous pressure on existing farming production systems. Human activities—primarily burning of fossil fuels and changes in land cover—are modifying the concentration of atmospheric constituents or properties of the Earth's surface that absorb or scatter radiant energy. Global atmospheric concentrations of carbon dioxide have increased 35% as a result of human activities since 1750 and now far exceed pre-industrial values determined from ice cores spanning many thousands of years. The primary source of the increased atmospheric concentration of carbon dioxide since the pre-industrial period is fossil fuel use, with land use change providing another significant but smaller contribution.

Farmers are expected to manage the more insidious effects of long-term climate change that may now be occurring at an unprecedented rate. Against the very unfavorable economic scenarios of the last decades, farmers have been struggling to maintain their income by continuously trying to increase yields in their production systems. Such increased productivity may be associated with increased economic and environmental risk as the farming systems become more vulnerable to climate variability and climate change. These existing pressures will demand the development and implementation of appropriate methods to address issues of vulnerability to weather and climate. These include agrometeorological monitoring and coping strategies for agriculture.

Awareness of the need to give greater attention to the issues of agrometeorological monitoring and coping strategies for agriculture led the Commission for Agricultural Meteorology (CAgM) of the World Meteorological Organization (WMO) at its fourteenth session held in New Delhi, India in 2006 to establish an Expert Team (ET) on "Climate Risks in Vulnerable Areas: Agrometeorological Monitoring and Coping Strategies" to determine the critical areas where the agricultural production is sensitive and vulnerable to climate change/variability in different regions; and to suggest continuous monitoring strategies for early detection in vulnerable areas. The team was asked to summarize the status of mitigation and adaptation strategies with respect to impacts of climate change/variability and also the status of coping with climate risks in agriculture, rangelands, forestry, and fisheries in vulnerable areas in the different regions. Another task of the team is to appraise and report on current capabilities in the analysis of climate risks and adaptation strategies in vulnerable areas and assess the status of progress in the project on "Climate Forecasts for User Communities" in agriculture, rangelands, forestry, and fisheries. Finally, the team was asked to develop methodologies for climate risk mapping for use by insurance industry.

WMO and the COST Action of the European Science Foundation have very fruitful ongoing collaboration in several areas and I am indeed very pleased that WMO and COST Action 734 on the "Impact of climate change and variability on European agriculture – CLIVAGRI" jointly organized the "Symposium on Climate Change and Variability-Agrometeorological Monitoring and Coping Strategies for Agriculture" in Oscarsborg, Norway on June 3–6, 2008. The symposium brought together experts from 27 countries from five continents including the members of WMO ET on Climate Risks in Vulnerable Areas: Agrometeorological Monitoring and Coping Strategies and those of COST Action 734 to discuss several important issues concerning agrometeorological monitoring and coping strategies for agriculture to deal with climate change and variability.

Fourteen papers presented at the Symposium are brought together in this special issue of IDŐJÁRÁS, and I hope this issue will serve as a major source of information to all agencies and organizations interested in the subject of climate change and variability, agrometeorological monitoring, and coping strategies for agriculture. I congratulate the editors of this special issue, *Drs Simone Orlandini, Mannava V. K. Sivakumar, Tor H. Sivertsen,* and *Arne O. Skjelvåg* for their hard work and dedication in putting this issue together and the Hungarian Meteorological Service for bringing out this issue of IDŐJÁRÁS.

(*M. Jarraud*)
Secretary-General
World Meteorological Organization
7bis, Avenue de la Paix
1211 Geneva 2
Switzerland

IDŐJÁRÁS

Quarterly Journal of the Hungarian Meteorological Service
Vol. 113, No. 1–2, January–June 2009

Editorial

This special issue of IDŐJÁRÁS contains the proceedings from the "Symposium on Climate Change and Variability – Agrometeorological Monitoring and Coping Strategies for Agriculture" held at Oscarsborg, Norway on June 3–6, 2008. The symposium was co-sponsored by COST ACTION 734 on the "Impact of climate change and variability on European agriculture – CLIVAGRI" and the World Meteorological Organization (WMO). The local organizers were the Plant Health and Plant Protection Division of the Norwegian Institute for Agricultural and Environmental Research and the Department of Plant and Environmental Sciences at the Norwegian University of Life Sciences.

The sessions of the symposium were structured and named according to the four working groups (WG) of COST 734, WG1: Agroclimatic indices and simulation models, WG2: Evaluation of the current trends of agroclimatic indices and simulation model outputs describing agricultural impacts and hazard levels, WG3: Developing and assessing future regional and local scenarios of agroclimatic indices, and WG4: Risks and foreseen impacts on agriculture.

Participants from WMO include the members of the Expert Team (ET) on Climate Risks in Critical Areas: Agrometeorological Monitoring and Coping Strategies in Vulnerable Areas of the WMO Commission for Agricultural Meteorology. The terms of reference of the ET were adopted and included as the bases of the symposium topics.

The symposium program was divided into four technical sessions, each of which covered specific topics covering agrometeorological monitoring and coping strategies for combating climate change and variability. The following is a brief description of the different technical sessions.

Session 1 covered "*Agroclimatic indices and simulation models*". The main theme was to review and assess current use of agroclimatic indices and simulation models like the crop growth models in Europe, and their application in analysis of impacts of climate change. Five papers from this session are presented in this special issue. In the first contribution, *J. Eitzinger et al.* presents an overview of the use of agroclimatic indices and process oriented models of crop growth in European agricultural research, specifically connected to the ongoing work of

WG1 of COST 734. The second contribution by *D. T. Mihailovic* and *B. Lalic* shows the connection between regional climatic models and parameterization schemes for describing the physics of dynamics (turbulent fluxes) and radiation balance of tall grass canopies. Several new results are shown. The paper by *Z. Dunkel* deals with a survey of drought definitions (concepts) and drought indices used in agrometeorology. The paper of *V. Vucetic* presents an analysis of the time trend of growing degree days in Croatia, using data from four different weather stations, and shows the results of global warming and growth of crops in Croatia. In the last paper, *Škvarenina et al.* presents a study on the occurrence of dry and wet periods at selected meteorological stations in Slovakia during the period 1951–2005. The parameters considered are the amount of precipitation, potential evapotranspiration, actual evapotranspiration, relative evapotranspiration, and a drought index. In certain lowland regions, the incidence of droughts seems to have increased significantly, and in certain highland regions the climate has become significantly more humid.

Session 2 covered "*Current trends of agroclimatic indices and simulation model outputs*". Three papers from this session are presented in this issue. In the first contribution, *Tsiros et al.* describe an agroclimatic zonation scheme for sustainable production in Greece using GIS and remote sensing data for the time period 1981–2001. In the second paper, *S. Orlandini et al.* have shown the results of calculating trends of agroclimatic indices applied to grapevine and olive trees in Central Italy. The third contribution by *K. C. Kersebaum et al.* deals with testing results of different CO_2 response algorithms against a FACE (German Free Air Carbon Dioxide Experiment) crop rotation experiment for a number of field crops.

Session 3 dealt with the topic of "*Developing and assessing future regional and local scenarios of agroclimatic indices*". Four papers from this session are included in this special issue. The first paper by *M. V. K. Sivakumar* and *R. Stefanski* presents a way of dealing with the threats of climate change connected to the conceptual framework of sustainability, impacts on agriculture, adaption, mitigation, and WMO initiatives for climate change adaption. The conclusion contains elements of strategies for combating climate change. The second contribution by *W. Smith et al.* contains certain perspectives on GHG emission from agricultural production systems in Canada, describing what is happening, and presenting ideas for long term strategies of mitigation and adaption to the emission of GHG. The paper by *R. Motha* discusses how adaptation strategies could be developed for sustainable agriculture by presenting examples from the USA. The conclusions contain ideas for an agricultural weather and climate policy, connecting policy makers and scientists. In the fourth paper, *O. H. Baadshaug* and *L. E. Haugen* describe the effect of climate change on grassland growth potential in the mountainous regions of southeastern Norway.

Session 4 dealt with "*Risks and foreseen impacts on agriculture*". Two papers from this session are included in this special issue. The paper of *B. Šiška* and *J. Takáč* presents drought analysis of agricultural landscapes as influenced by climatic conditions in the Slovak Republic. Agriculture in the different regions in Slovakia probably will be impacted by different climatic stresses in the future, but most of the country will experience drought conditions. *L. Dióssy* and *A. Anda* describe the consequences of climate change on maize microclimate in Hungary. The model analysis is based on climate change scenarios and different levels of CO_2 in the atmosphere.

Thanks to the strong collaboration between COST 734 and the Commission for Agricultural Meteorology of WMO, and to the excellent cooperation from the local organizers participants from 27 countries from five continents made presentations at the symposium in Oscarsborg. This provided an unique scientific occasion for discussing the important issue of climate change at the global level. Some of the participants are agronomists and biologists, while other participants have their background in physics and meteorology. The theme of the symposium is quiet relevant to the current concerns regarding climate change, and the short overview of the proceedings presented in this special issue shows that many aspects connected to geography as well as methods of research were discussed and a range of climate change consequences for agriculture was covered.

Simone Orlandini[1], *Mannava V.K. Sivakumar*[2], *Tor H. Sivertsen*[3], and *Arne O. Skjelvåg*[4]
Guest Editors

[1]University of Florence
[2]World Meteorological Organization
[3]Norwegian Institute for Agricultural and Environmental Research
[4]Norwegian University of Life Sciences

Acknowledgement—We would like to thank IDŐJÁRÁS for giving us the opportunity to present a cross-sectional view of the multidisciplinary themes of the work of COST 734 and the way in which the Oscarsborg symposium tried to address these themes in a systematic manner.

Conclusions and recommendations of the Oscarsborg symposium

Introduction

Participants in the WMO and COST Action 734 "Symposium on Climate Change and Variability – Agrometeorological Monitoring and Coping Strategies for Agriculture" held in Oscarsborg, Norway on June 3–6, 2008, met in four working groups to discuss the topic addressed by the symposium. The working groups developed conclusions and recommendations under the following major headings:

- Determination of critical areas for climate change and variability;
- Current status of strategies for mitigation, adaptation and sustainability;
- Current capabilities in the analysis of climate risks and adaptation;
- Coping with climate risks and foreseen impacts in agriculture.

Conclusions

Determination of critical areas for climate change and variability

- Global warming has been registered since the second half of the 20th century and is causing an increase in the frequency of various extreme weather events and natural hazards (such as droughts, heat waves, intensive precipitation, floods, storms, sea level rise, forest fires, water and wind soil erosion, etc) in many regions. This tendency is expected to continue in the future.

- Climate variability and change affect all sectors with a different level of their impacts. However, agriculture is considered among the most vulnerable sectors in many regions due to the negative impacts of unfavorable variations and changes in weather and climate.

- The most vulnerable agricultural regions are those:
  - adversely affected by current and projected climate variability and change,
  - damaged by occurrence of new pests, diseases, and weeds,
  - faced by insufficient financial resources and methodological experience.

Examples of such vulnerable regions in Europe include the Mediterranean region, the Balkan Peninsula, NW Russia, and likely Fennoscandia (thermal regime combined with change in snow cover).

Current status of strategies for mitigation, adaptation and sustainability

- Most agricultural systems are to some extent capable of mitigating greenhouse gas (GHG) emissions and adapting to changing climate, however, the extent to which this will occur is limited by lack of awareness, policy, economics, and a need for more food and energy.

- Gaps in research regarding climate change in agriculture limit our ability to take sufficient action to implement mitigation and adaptation measures.

- There has been little political and economic incentives to promote mitigation of GHGs from agricultural sources.

Current capabilities in the analysis of climate risks and adaptation

- Currently there is a wide range of indices for characterizing various types of droughts, but there is no standardized index that is universally acceptable.
- In the light of climate change, there is likelihood of floods and landslides in many vulnerable regions, and yet there does not seem to be a critical analysis of these two climate risks.
- Certain crops at certain phenological stages are highly susceptible to heat waves and there does not appear to be an operational warning system.
- Despite the availability of reasonably good frost warning systems, currently frost protection systems can not be universally employed as they are expensive.
- Cyclones/hurricanes do cause structural damages (farm implements, animals, and crops) and there does not seem an adequate assessment of their impacts on agriculture, forestry, and fisheries.
- Although the risk of forest fires in the light of climate change is increasing, there are no seasonal forecasts for controlling forest fires in the areas at risk.

Coping with climate risks and foreseen impacts in agriculture

- While acknowledging that farmers have always dealt with climate variability, the speed and magnitude of recent climate change has to be recognized as an increasing problem.
- Climate change is becoming an additional and more important driver in agricultural systems.
- Climate change impacts not only production services but also the protection and enviromental services (multifunctionality).

Recommendations

Determination of critical areas for climate change and variability

- Strengthen climate variability/change monitoring; develop/improve decision support systems and seasonal climate prediction by applying innovative techniques and approaches at local and regional level.
- Foster national/international/regional cooperation in the field of climate variability/change through exchange of know-how, information, etc.
- Develop common methodologies (e.g., determination of vulnerable regions – criteria; new agroclimatic zonation).
- Develop/improve/update and utilize adaptation and mitigation options for agriculture under climate variability/change (e.g., improving plant breeding and protection, assuring resistance to heat stress, dry spells, UV radiation negative effects).

- Promote work on climate variability/change related scientific uncertainties.
- Bring science to society by transmitting the climate variability/change and related impacts research results in appropriate way to the society including policy makers, stakeholders, end users, and broad community by:
  - Closer and direct contacts;
  - Increasing the knowledge of advisers, farmers (end users), etc.;
  - Incorporation of the media.

Current status of strategies for mitigation, adaptation and sustainability

- Develop a portfolio of agricultural strategies that includes adaptation, mitigation, technological development, and research (climate science, impacts, adaptation, and mitigation) to combat climate change.
- Integrate mitigation and adaptation frameworks into sustainable development planning on a priority basis.
- Assess long-term consequences of mitigation and adaptation strategies in agriculture and determine how these actions are affected by climate.
- Select the option of biofuel production as a viable adaptation and mitigation measure when it is not in conflict with essential food production, biodiversity issues, and land conservation.
- Integrate, where possible, agricultural systems with renewable energy systems such as wind, solar, and hydroelectric power.
- Ensure that developing countries play an increasing role in planning national and regional programmes on mitigation and adaptation to climate variability and climate change.
- Reduce the types of agriculture production which require large amounts of energy inputs per unit of food (e.g., meat and milk) to substantially reduce GHG emissions. This could be accomplished by applying a carbon tax on high-energy foods and transportation.

Current capabilities in the analysis of climate risks and adaptation

- Undertake, on an urgent basis, a comprehensive review of the existing drought indices, and recommend a limited set of indices that are universally acceptable and which could serve the needs of different regions and classes of droughts.
- Translate the current knowledge on floods and landslides into operational management systems that government and agencies could adopt.
- Adopt the current heatwave warning systems for humans to crops/cropping systems.
- Develop cost effective frost operational systems and raise awareness among the farmers about the frost damages.
- Undertake the assessment of the impacts of cyclones/hurricanes on agriculture, forestry, and fisheries systematically to develop operational systems in order to limit the losses to property, farms, and farm animals.

- Include in the agenda of the seasonal climate outlook fora, that are organized in different parts of the world, forecasts for the risks of forest fires and encourage the forest fire fighting community to be a part of the user community in these fora.
- Develop the most comprehensive information that could assist the locust-control community to address the increasing incidence of locusts.

Coping with climate risks and foreseen impacts in agriculture

- Ensure closer connection between studies of greenhouse gas emissions and climate change impacts.
- Encourage agrometeorologists to improve impact studies of climate variability and change.
- Make sure that coping strategies address both positive and negative impacts.
- Regionalize, on an urgent basis, climate change impact studies through regional organizations (e.g., Cost Actions) since climate variability is increasing and will be different in different regions.
- Promote the establishment of knowledge circles at different levels (scientists, decision-makers, and farmers at the local, regional, and national levels).
- Reinvigorate agrometeorological and related agricultural research in the light of climate change.

Mannava V. K. Sivakumar

World Meteorological Organization
7bis Avenue de la Paix, 1211 Geneva 2
Switzerland
Corresponding author: msivakumar@wmo.int

IDŐJÁRÁS

Quarterly Journal of the Hungarian Meteorological Service
Vol. 113, No. 1–2, January–June 2009, pp. 1–12

Applications of agroclimatic indices and process oriented crop simulation models in European agriculture

Josef Eitzinger[1], Sabina Thaler[1], Simone Orlandini[2], Pavol Nejedlik[3], Valentin Kazandjiev[4], Tor Håkon Sivertsen[5], and **Dragutin Mihailovic[6]**

[1]*Institute of Meteorlogy, University of Natural Resources and Applied Life Sciences, Peter-Jordan Str. 82, A-1190 Vienna, Austria; E-mail: josef.eitzinger@boku.ac.at*

[2]*Department of Agronomy and Land Management, University of Florence, Italy*

[3]*Slovak Hydrometeorological Institute, Bratislava, Slovak Republic*

[4]*National Institute of Meteorology and Hydrology, Sofia, Bulgaria*

[5]*Norwegian Institute for Agricultural and Environmental Reserach, Ås, Norway*

[6]*Faculty of Agriculture, University of Novi Sad, Novi Sad, Serbia*

(Manuscript received in final form February 24, 2009)

Abstract—During the past decades, many new software tools were developed to be used for agricultural research as well as for decision making. For example, crop and whole farm system modeling, pest and disease warning models/algorithms, models for irrigation scheduling or agroclimatic indices can help farmers significantly in decision making for crop management options and related farm technologies. The aim of Working Group 1 of COST 734 was a review and assessment of agroclimatic indices and simulation models relevant for various European agricultural activities. The key results, based on a survey by questionnaires among the COST 734 participating countries (see: www.cost734.eu) and a literature survey, are presented in this study. It includes an overview of most used agrometeorological or agroclimatic indices and process oriented crop models for operational as well as scientific applications, an analysis of the limitations for applications, and an overview of spatial applications in combination with GIS and remote sensing in Europe. The COST 734 survey showed, for example, that research activities regarding the development of agroclimatic indices in Europe are focused on indices on drought, phenology, frost, and heat stress. Process oriented crop models are mainly applied for wheat and maize, which is related to their importance in European crop production. In many cases there are still limitations of crop model applications in Europe, which are often related to the availability of input data. Spatial crop model applications including a combination with remote sensing data are still rare. There are a number of different models and indices in use, varying by regions and countries. From the survey it can be concluded that there is a need of standardization and harmonization of applications of agroclimatic indices as well as crop models in Europe in order to allow inter-comparison of the results and to improve the interpretation of results.

Key-words: agroclimatic indices, crop models, COST 734, European agriculture

1. *Introduction*

A review and assessment of agroclimatic indices (including meteorological, climatological, or agrometeorological indices, which are applied in agrometeorology) as well as crop simulation models relevant for various European agricultural activities was carried in the frame of the COST 734 action (see: www.cost734.eu). The survey was based on questionnaires and a literature survey. The detailed results are described in a COST 734 report (*Orlandini* and *Nejedlik*, 2008). It includes an overview of most used agroclimatic indices and process oriented crop models for operational and scientific applications, an analysis of the limitations for applications as well as an overview of spatial applications in combination with GIS and remote sensing in Europe. During the past decades many new software tools were developed to be used for agricultural research as well as for decision making. For example, crop and whole farm system modeling, pest and disease warning models/algorithms, models for irrigation scheduling or agroclimatic indices can help farmers significantly in decision making for crop management options and related farm technologies. In research, models can be used to simulate and analyze the complex interactions in the soil-plant-atmosphere system, for example in the important field of climate change impacts on crop water balance and crop yields. All these modeled systems and their interactions are simplifications and, therefore, include many different kind of uncertainties and limitations resulting from unknown trends in future technology and human activities, models simplified representation of reality, lack of knowledge on system responses, or lack of calibration data. Much research was done in Europe and worldwide in the field of model development, improvements, or comparisons of models.

2. *Agroclimatic indices and providers*

Indices are explicitly defined by equations, whereas indicators are relationships identified to quantified impacts. Both serve to simplify complex phenomena. Therefore, indices can be indicators once these relationships are quantified and measurable. Indicators can include also output values from mechanistic models, which uncover simplified relationships to impacts.

The following aspects are based on the findings of the COST 734 assessment. Many various indices are used in Europe for operational applications and in research. Indices are mostly used in agrometeorological monitoring and services operated by the national state bodies, such as in national meteorological and hydrometeorological institutes as well as their regional branches. Private agrometeorological services are scattered and usually concentrated on some specific points of service like extreme weather warning service or advisory services in case of plant protection against pests and diseases. In some cases, private companies selling chemicals or other materials and equipments to farmers, such as weather stations, include also some technical support and agrometeorological services and/or forecasting models (mostly pest and disease warning) as a part of their products. General agrometeorological information is mostly produced by national bodies such as meteorological services, which run the meteorological networks, and so they are also the owners of the data. In many cases, they cooperate with other national bodies providing them the data either free of charge or at commercial base.

The research activities regarding the development of the agrometeorological indices in Europe are focused on drought, crop responses such as phenology, and to a lesser extent, frost and heat stress (*Fig. 1*). The attention paid to research does reflect the practical use of indices in operational use. Relatively little attention is paid for example to the operational monitoring of drought and heat stress, while the majority of responding countries notices the research activities in this field.

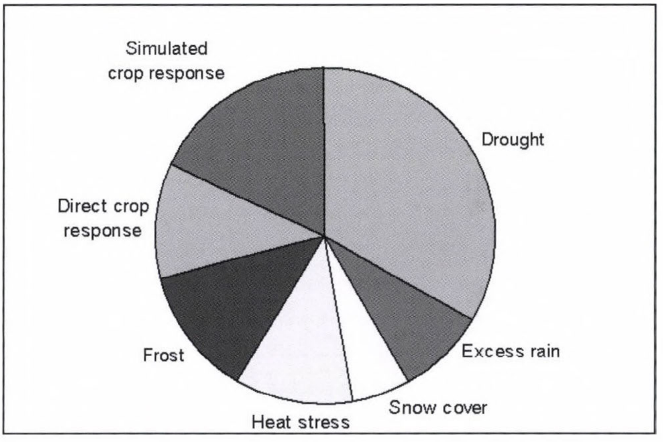

Fig. 1. Distribution of the numbers of agrometeorological indices used in research related to their purpose, according to the COST 734 survey.

In the following the main groups of indices applied in Europe relevant for agriculture are described. An extensive list of the various indices including literature can be found in *Orlandini et al.* (2008).

2.1. Drought

Drought indices are constructed to quantify the lack of water during certain periods, for example the negative deviation of precipitation from the normal in case of meteorological drought indices. Meteorological drought indices, however, do not always describe the real shortage of water for the crops. For agrometeorological drought indices, therefore, the focus is on crop water balance of crop stands during the plant growth and development cycle. The general problem of these indices is to include the physical and biological properties of the particular crop in order to reflect its sensitivity and limitations towards the lack of water supply during the vegetation period. A related problem is the definition of the time step used to calculate the particular indices.

The major part of the drought indices, as reported in the COST survey, is focused on pastcasting and some of them on nowcasting. These indices are often applied locally or regionally as they have to use multiyear measured values of the particular parameters recorded or calculated for a certain locality.

The major part of the indices in use are rather complex and deal with water balance components and precipitation measures. Indices defined in the calculation of water balance components are used in various modifications in almost all countries in the extent from national to a farm level. Both indices, based on water balance components and on precipitation only for a given period, are produced mainly by national weather services, as they run the meteorological networks at regional and national levels. Some institutes use the partial outputs of the models like WOFOST to define the days with the lack of water for the crops. In Slovenia, for example, the irrigation model IRRFIB is used for daily calculation of crop water balance for different regions. It represents an agricultural decision support tool, which is running inside the Slovene Agrometeorological Information System (SAgMIS) package.

From the standard indices, the standardized precipitation index (SPI), Palmer drought severity index (PDSI), percent of normal precipitation and rainfall percentiles are in operational use among other national services in Europe, at the Drought Management Center for South eastern Europe (DMCSEE). Relevant maps are published on the web page http://www.dmcsee.org/, and they are updated once per month (*Fig. 2*). Final data maps with two months delay are available after the 20th day of the current month. First-guess maps are available after the 5th day of the next month.

2.2. Excess rain

Excess rain as a water related phenomenon is observed in all European countries by simple measurements of daily sums of precipitation. Further to this parameter, the rainfall intensity is measured either by pluviographs or by weight rain gauges providing online signal. The major part of rainfall parameters are issued in the standard forecast of each meteorological service mainly at the regional scale. Some of the services provide special rainfall maps in their pastcasting, identifying the areas with high precipitation and/or anomalies.

In Greece, for example, apart from high precipitation pastcasting maps, an operational-research application of the non-hydrostatic model LM-COSMO of HNMS (Hellenic National Meteorological Service) has been used for forecasting excess rain events. The model has been used for the simulation of severe thunderstorms (*Avgoustoglou*, 2002). The data are collected from stations of the Hellenic National Meteorological Service and the Ministry of Agriculture. Generally, excess rain represents a damaging weather event and its characteristics are usually issued for general use stressing the regional differences.

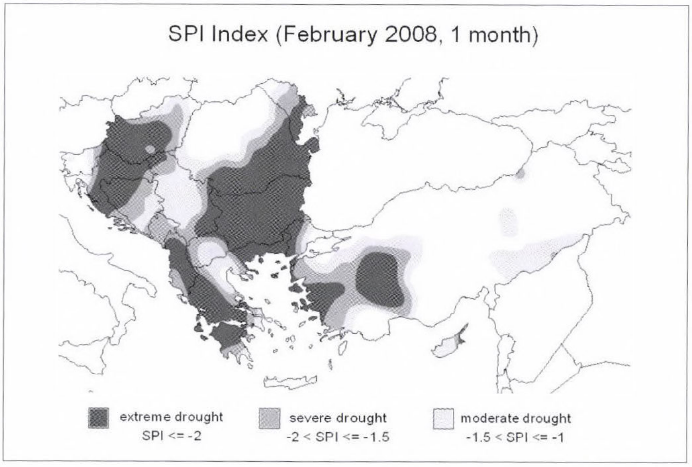

Fig. 2. Standardized precipitation index (SPI) for southeastern Europe issued for February 2008.

2.3. *Heat stress*

Heat stress is a complex phenomenon, depending on the definition and the sensitivity of the recipient. Factors such the height of temperature, duration, and rate of increase of the temperature as well as air humidity, radiation, and wind can modify the heat stress level of living organisms. The critical thresholds of temperatures for crops, for example, differ pretty much and they vary also according to the plant development stage. A threshold of heat stress usually refers to the daily mean temperature, over which a detectable reduction of growth or damages on plant begins. Heat stress prediction is naturally included in general weather forecasts, though there are very few services listed, which provide special heat stress related indices. A heat index forecast is provided, for example, by Hungarian Meteorological Service, which includes the forecast of daily average temperature above 25 °C. In Greece, forecasts of surface temperature and wind speed over Attica and neighboring areas are provided using the non-hydrostatic model MM5. This model has very high resolution (grid distance of 2 km), and the forecasts of the parameters are calculated every 18 hours (*Kotroni* and *Lagouvardos*, 2002).

2.4. *Frost*

Critical temperatures needed for frost damage to occur may vary depending on the temperature and the duration, while the temperature remains below freezing point, as well as on the sensitivity of the recipient. However, the common detection and prediction on frost conditions considers the duration of temperatures below 0 °C and daily minimum values. Frosts are frequently classified as either advective or radiative, and this also defines their impact on the different type of crops and possibilities for frost protection. During radiative frosts, local orographic conditions can modify near surface temperatures considerably, for example, the frost line does not reach more than 1–2 m above ground, so that only the crops close to the ground are affected by frost. These aspects make local frost prediction very difficult, and only generalized, large scale based assessments can be given by operational services.

Frost events are both forecasted and monitored by the national meteorological services in all countries. A standard weather forecast includes the forecast of the frost or the possibility of ground frost occurrence. However, only a few special indices in operational use focuse on nowcasting and pastcasting in Europe. Frost forecast is usually issued at the national level for general purposes, while specific indices for local assessments are mainly used by farmers (e.g., for frost irrigation scheduling), consultants, and insurance companies.

2.5. *Snow cover*

The presence of snow cover brings a valuable protection of plants against hard frosts during the winter. On the other hand, a long snow cover duration under unfavorable conditions can damage the crops, for example, by a forced occurence of fungs. Further, a frequent change of snow cover and bare soil, combined with freezing/thawing events can physically damage the roots of crops (e.g., winter cereals). The indices or algorithms dealing with snow cover are, beyond research applications, mostly focused on operational pastcasting, which, for example, is done daily at different spatial scales of 10 × 10 km grids in Finland to the regional and national scales in other European countries. In some cases the water content of the snow cover is announced which brings the possibility to estimate the amount of the water being stored in the snow as a water source in spring. Specific snow conditions are frequently observed in the Alpine region for detecting risk of avalanches.

2.6. *Specific events*

Further to the above described indices, several specific agrometeorological indices are in operational use, often focused on suitable conditions for crop management.

Relevant special weather forecasts for farmers and complex growing season information are provided by many European services, including institutional and privat services. Daily forecasts are, for example, provided at the scale of 10 × 10 km by the Finish Meteorological Service and a private company in Finland. This information includes probability of rain and frost, rain amount, temperature, relative humidity, wind speed and direction, index describing weather conditions for plant protection. The German Weather Service provides actualized 7-day forecasts up to 4 times a day, concerning the drying of hay and grain moisture of cereals and maize. Other parameters include potential and crop evpotranspiration soil temperatures as well as soil wetness and workability trends. Additionally, recommendations are given for the sowing day of winter cereals, oats, potato, sugar beets, and maize for the upcoming 6 days. Some services provide information about the workability of the soil with regard to the depth of the frozen soil considering also the impact of frost on lumps of clay during the winter.

Regarding the hail events, an operational project has been carried out in Greece, the Greek National Hail Suppression Project (NHSP) weather modification program. The objectives were to reduce hail damage and at the same time to examine and study the thermodynamic, dynamic, and microphysical characteristics of the potential hail producing clouds. Also, instability indices are calculated for Operational Hail Forecasting in Greece. In some countries specific radar services are installed for hail warning systems, such as in Serbia.

Forest/grass fire indices in various forms are in use in Mediterranean countries mainly. Considering increasing occurrence of forest fire events under the climate change, more frequent use of these indices is expected. The German Weather Service (DWD) provides a daily risk index for forest fire which combines several indices: a Swedish index (Angström), two German indices (Baumgartner, M-68), and the Canadian forest fire warning system (FWI: fire weather index, FFMC: fine fuel moisture code) (http://www.agrowetter.de/Agrarwetter/Waldbrand_en.html).

3. Crop response, pests and diseases monitoring

There are not many services monitoring the response of the crops to weather conditions regarding crop growth and phenological development. Operational phenological networks, which comprise a sufficient number of stations work, are mainly in the region of Central Europe (especially Germany). These networks are run by the meteorological services and systematically monitor phenological development stages of selected plants, and in several cases, crop development including some pheno-metric parameters, pests and diseases, as well as yields. The use of the data is mainly in pastcasting. In some cases some special parameters are monitored by remote sensing (e.g., greenness index). Remote sensing of phenological parameters is intensively used at the European scale by

JRC Ispra within the MARS project. A special set of parameters regarding the plant conditions close to the harvest is provided by the German Meteorological Service. Further to that, either standard (WOFOST) or specific (IPHEN) models are used to simulate the development of different plants.

On the other hand, crop parameters including yields and the level of pest and diseases occurrence are widely simulated by using either specific algorithms or partial outputs of crop growth models. Several agrometeorological services, often regionally based extension services, provide operational pest and disease warnings for specific crops in many European countries. A significant part of pest and disease warning is, however, carried out by farm based systems by using agrometeorological weather stations.

4. Process oriented crop simulation models

Mechanistic models have been studied for more than 50 years. The three most important "schools of development" from Australia, the Netherlands, and the United States include APSIM models (*Asseng et al.*, 2000), SUCROS based models (such as WOFOST) from the "School of De Wit" (*Van Ittersum et al.*, 2003), and the DSSAT family (such as CERES) of crop models (*Jones et al.*, 2003), although there are links between these models. As a result of the survey, in Europe, the most frequently used process oriented crop models for research or operational applications are CERES, WOFOST, and STICS, however, with distinct differences between countries. WOFOST is the only model, which is operationally integrated at the European level for the European crop yield prediction system, covering all countries.

It can be seen, that research applications dominate and that only few models are already applied operationally at the beginning of the 21st century. Often the number of national or European applications of the relevant models are related to established research institutions working on model developments. The main application of the crop models is in climate change impact research on agriculture, whereas the operational applications have the focus on crop yield forecasting. The applications often include an assessment of the dependence of growth, development, and yields of crops on limitations of soil-water regime. The assessment of crop development and yield response to related timing of crop management such as fertilizing, cultivation, irrigation, plant protection, etc., is another application. Rarely they are used for early warnings or mitigation of damages from extreme meteorological phenomena and processes.

Most crop simulation models in Europe are applied for annual crops, especially cereals and maize, reflecting the economically most important crops in Europe (*Fig. 3*). Regionally, however, also permanent grassland, potatoes, sugar beet, oilseeds, and others play an important role, which results in specific model applications.

Crop model applications are influenced by several uncertainties determining limitations of their use in research and practice (e.g., *Eitzinger et al.*, 2008). The main reported limitation for application of crop models in Europe is related to the input data. The reported most frequent problems are the availability or the low quality of the soil physical model input data (especially for spatial model applications), the lack of long term biophysical crop data for model validation and calibration and, in some cases, the availability or costs of meteorological data. This is related to the socio-economic conditions in countries and different local administration of data in the different regions of Europe. The reliability of data on climate scenarios or seasonal forecasts is another crucial point for the use of such models for operational purposes or for making long-term strategic decisions.

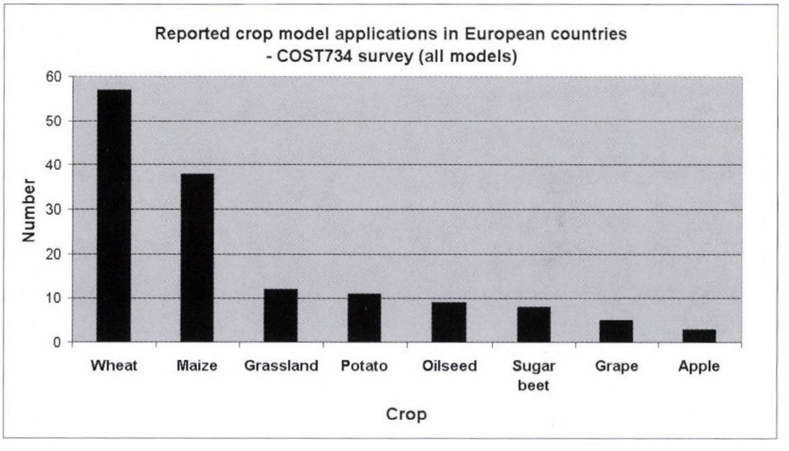

Fig. 3. Reported crop model applications (operational and research, one count per model and country) according to the COST 734 survey.

5. Spatial applications of models and indices

Spatial model applications, such as interfacing models with geographic information system (GIS), increase the possibilities of applying these models for regional planning and policy. Because of their relatively simple calculation methods, agroclimatic indices are often implemented in GIS in order to show spatial distribution and developments of the relevant calculated index. The most common examples of these are drought indices. Also several crop models are applied on spatial scales beyond the field level.

The most promising method to estimate crop yield over larger areas is combining crop growth models and remote sensing data. The main benefit of using remote sensed information is that it provides a quantification of the actual state of crop for large area, while crop models give a continuous estimate of growth over time. Only few applications of spatial crop growth monitoring systems are already operational in Europe. However, the general item of remote sensing data assimilation in crop models has been the subject of mainly methodological research in the last years. They have allowed to elaborate practical solutions, but the operational application is still limited by the large amount of data to be processed. The best known example of an operational application is the MARS Crop Yield Forecasting System (MCYFS) for food security for Europe and other parts of the world (http://agrifish.jrc.it/marsstat/), which is providing quantitative crop statistics at EU (for a 50×50 km^2 grid for NUTS units) and national levels, in near real time.

MCYFS was adapted also for national CGMS at a finer grid scale of 1×1 km^2 to 10×10 km^2 (for defined zones below NUTS level) for Belgium (B - CGMS; http://b-cgms.cra.wallonie.be/en/). B-CGMS is based on the existing European harvest forecasting system, but the data bases are supplemented and refined by Belgian physical (soil data) and technical (temperature sums, crop management) parameters. Satellite data are used as an aid to arrive at a quantitative estimate of production in B-CGMS, where at the European CGMS it is used for qualitative interpretation.

A national example of spatial agroclimatic monitoring is SIGA (Servicio de Información Geográfico Agrario-Service of Agrarian Geographics Information), an application running at the Ministry of Agriculture (Deputy Direction of annual crops) in Spain (*Sanchez et al.*, 2005). The application (SIGCH-GIS related to the management of annual crops) offers cartographic and alfanumerical information, thematic maps on agroclimatic variables, as well as information about the plan of productive regionalization of Spain for the application of the EC rules (EC-1251/1999) of the European Commission. There are also regional projects with similar characteristics like SITNA, such as a territorial information system developed by the regional government of Navarra region. SAgMIS is an internet based GIS information system managed by the Environmental Agency of the Republic of Slovenia, which includes in situ information on crop water balance and irrigation forecast. Maps of water balance for different areas in Slovenia can be obtained for different time scales upon request (*Sušnik* and *Kurnik*, 2004).

6. Concluding remarks

The COST 734 report contains probably the most complete overview on the big number of models and indices currently used in Europe for different operational and scientific applications in agriculture. Due to their simplicity, agroclimatological indices can be considered as valuable tools for research and operational applications. Particularly, the possibility of using wide temporal time steps (daily, weekly, monthly) makes these indices suitable for application with historical climatic series. There are few cases (e.g., drought indices, grapevine quality index), where indices also include thresholds describing the consequences of obtained values and recommended interventions needed to manage and to protect the agricultural systems from climate related impacts. The results of the questionnaires elaboration pointed out their large use at European level for many purposes, spatial (regional, national) and temporal (nowcasting, past-casting, etc.) scales. Especially for indices, it seems also to be clear, that there is a need of standardization and harmonization of applications in Europe in order to allow inter-comparison and to improve the interpretation of results. The more complex approaches, namely process oriented models, are still very limited in operational applications (especially crop yield models), except for the simple models, which focus on irrigation scheduling, or the widely applied models for pest and disease management. In research, however, process oriented crop models play a very important role in the assessment of global and climate change impacts on agriculture. A majority of these studies were carried out on a larger scale, neglecting the necessarily finer spatial resolution to be of relevance for local practical recommendations for farmers. One of the main difficulties for the spatial application of process oriented crop models in a high spatial resolution at the research level is often the lack of model input data (not available, high costs, expensive data management, etc.). On the other hand, new methods are being developed to overcome these problems by using GIS and integrating remote sensing data. Only very few examples exist for operational crop yield forecasting which integrate all these available tools, and they are only used at the expert level.

Beside the effects of climate change on crop productivity, which are the dominating studies till now, it is recommended that the modeling community should also have a closer look on other aspects such as soil fertility, and environmental issues like groundwater recharge and water quality, soil carbon stocks, erosion, trace gas emissions, etc., in the future. Therefore, integrated modeling approaches are required, which include the most relevant interactions in the soil-crop-atmosphere system. We, therefore, should also try to combine our modeling of climate change impacts with ideas and experiences of sustainable production.

Acknowledgment—This study was carried out within the COST 734 action, where many experts from various countries contributed in the survey. More details of the survey can be found in the COST 734 report.

References

Asseng, S., van Keulen, H., and *Stol, W.*, 2000: Performance and application of the APSIM Nwheat model in the Netherlands. *Eur. J. Agron. 12,* 37-54.

Avgoustoglou, E., 2002: Operational-research investigation of the model (LM-COSMO) at the

Hellenic National Meteorological Service. *Proceedings of 6th Hellenic Conference in Meteorology Climatology and Atmospheric Physics, Vol. 1.* Ioannina, 25-28 September 2002, 35-42.

Eitzinger, J., Formayer, H., Thaler, S., Trnka, M., Zalud, Z., and *Alexandrov, V.*, 2008: Results and uncertainties of climate change impact research in agricultural crop production in Central Europe. *Bodenkultur 59,* 1-4.

Jones, J.W., Hoogenboom, G., Porter, C.H., Boote, K.J., Batchelor, W.D., Hunt, L.A., Wilkens, P.W., Singh, U., Gijsman, A.J., and *Ritchie, J.T.*, 2003: The DSSAT cropping system model. *Eur. J. Agron. 18*, 235-265.

Kotroni, V. and *Lagouvardos, K.*, 2002: Fune grid weather forecasts over Attica, Greece: Results of one year operational use. *Proceedings of 6th Hellenic Conference in Meteorology Climatology and Atmospheric Physics, Vol. 1.* Ioannina, 25-28 September 2002, 132-137.

Orlandini, S. and *Nejedlik, P.* (eds.), 2008: Survey of agrometeorological practices and application in Europe regarding climate change impacts. *COST Report: COST ACTION 734 – Impact of Climate Change and Variability on European Agriculture* (available at : www.cost734.eu).

Sánchez, J.A., Cánovas, F., and *Lacasa, A.*, 2005: Un sistema de información geográfica (SIG) para el manejo de enemigos naturales, plagas y enfermedades en los cultivo de pimiento del Campo de Cartagena (Murcia) (in Spanish). *Agroinformación.com*

Sušnik, A., and *Kurnik, B.*, 2004: On-line irrigation support system in Slovenia. On-line agrometeorological application with decision support at the farm level. COST 718: Meteorological application to agriculture. *DINA Research Report,* no. 109, 113-128.

Van Ittersum, M.K., Leffelaar, P.A., van Keulen, H., Kropff, M.J., Bastiaans, L., Goudriaan, J., 2003: On approaches and applications of the Wageningen crop models. *Eur. J. Agron. 18,* 201-234.

IDŐJÁRÁS
Quarterly Journal of the Hungarian Meteorological Service
Vol. 113, No. 1–2, January–June 2009, pp. 13–22

Coupled land-air parameterization scheme (LAPS) and non-hydrostatic mesoscale model (NMM) for use in agricultural planning

Dragutin T. Mihailovic and **Branislava Lalic**

Faculty of Agriculture, University of Novi Sad,
Dositej Obradović Sq. 8, 21000 Novi Sad, Serbia; E-mail: guto@polj.ns.ac.yu

(Manuscript received in final form December 5, 2008)

Abstract—Characterization of climatic hazards for agriculture can be done using global circulation models (GCMs) and/or regional circulation models (RegGCMs). The GCMs provide credible information of climate, at least for subcontinental scales, while the RegCMs are used to determine specific characteristics of the weather in mesoscale. Regardless of whether these models provide meteorological data through either long-term or short-term runs, the land surface models are strong links between the underlying surface and the atmosphere. Recently they have been remarkably improved in the segment of the parameterization of turbulent fluxes inside and above the tall grass canopies, making them more relevant, in assessing how regional climate may affect agriculture. Except these schemes many other environmental/agricultural models (UV radiation, plant diseases, crop, irrigation models, etc.), linked with the new generation of non-hydrostatic mesoscale models, can provide highly sophisticated information for farmers and agricultural planners. In this paper we shortly describe environmental models, mostly designed in the Centre for Meteorology and Environmental Predictions, University of Novi Sad (Serbia). All of them are linked with the NMM non-hydrostatic mesoscale model for the purpose of an intensive use in agricultural planning. The description and comments are supported by the corresponding numerical simulations.

Key-words: GCMs model, RegCMs models, environmental/agricultural models, agricultural planning

1. Introduction

Agricultural planning – strategic (long-term) and tactical (short-term) – needs to appreciate climate-related and other risks to attain the producer's goals and spell out the sort of information that farmers need to aid their planning – e.g., climate, technical/management information, market. A key aspect needed in linking climate and weather risk to agricultural planners is to appreciate the overall management system in question from the viewpoint of decision makers. Managers need information for both tactical and strategic decision-making. Climate disasters can be divided into extreme events (e.g., tornadoes, hail, flash floods and severe thunderstorms, effect of prolonged drought and floods) and regional climate anomalies (mesoscale storms, small-scale severe weather phenomena). Global climate change may produce a large number of climatic disaster occurrences. This is based on the fact that a linear increase in the average of a climatic variable implicates a non-linear increase in the occurrence probability of extreme values of the variable. Assessing and forecasting the impacts of short-term climate variability and weather risk, as well as their relationship to extreme events could help mitigate the effects of climate variability and scheduling agricultural activities (*Everingham et al.*, 2002; *Meinke* and *Stone*, 2005).

Characterization of the climatic hazards for agriculture can be done using global circulation models (GCMs) and/or regional circulation models (RegCMs). The GCMs provide credible information of climate, at least for sub-continental scales, while the RCMs are used to determine specific characteristics of the weather in mesoscale. Regardless of whether these models provide meteorological data through either long-term or short-term runs, the land surface scheme is a remarkable link between the underlying surface and atmosphere. This link together with the mesoscale non-hydrostatic model is a base for use a number of environmental models (UV radiation, plant diseases, crop, irrigation, water, and chemical transfer in soil models, etc.) in agricultural science and practice for different purposes, particularly for planning.

The focus of this paper is directed to short description of environmental models, which are available in the Centre for Meteorology and Environmental Predictions (CMEP, in further text), Department of Physics, Faculty of Sciences, University of Novi Sad (Serbia). Most of them are designed in this institution and linked with the NMM non-hydrostatic mesoscale model for the purpose of an intensive use in agricultural tactic and strategic planning (*Mihailovic*, 2005; *Mihailovic* and *Lalic*, 2006). Descriptions are pursued by examples of corresponding numerical simulations.

2. *Short overview of the land-air parameterization scheme (LAPS)*

We will shortly summarize the main features of the LAPS by setting a focus on the parameterization of processes relevant in agricultural science and practice. The LAPS, developed at the Faculty of Agriculture and CMEP, University of Novi Sad (Serbia), describes mass, energy, and momentum transfer between the land surface and the atmosphere. This scheme is designed as a software package that can be run as part of an environmental model or as a stand-alone one. The LAPS includes modeling the interaction of the land surface and the atmosphere, under processes divided into three sections: subsurface thermal and hydraulic processes, bare soil transfer processes, and canopy transfer processes. They are: interaction of vegetation with radiation, evaporation from bare soil, evapotranspiration including transpiration and evaporation of intercepted water and dew, conduction of soil water through the vegetation layer, vertical water movement in the soil, surface and subsurface runoff, heat conduction in the soil, and momentum transport within and above the vegetation. A single layer "sandwich" approach for canopy is chosen for the physical and biophysical parameterization. The scheme has seven prognostic variables: three temperature variables (foliage, soil surface, and deep soil), one interception storage variable, and three soil moisture storage variables. For the upper boundary conditions the following forcing variables are used: air temperature, water vapor pressure, wind speed, short wave and long wave radiation, and precipitation at a reference level within the atmospheric boundary layer. The surface fluxes are calculated using resistance representation. The soil module is designed as a three-layer model, which is used to describe the vertical transfer of water in the soil. The LAPS uses the morphological and physiological characteristics of the vegetation community for deriving the coefficients and resistances that govern all the fluxes between the surface and atmosphere. The details about this scheme are available in many papers appeared in the last decade. However, the main features and recent redesign of the LAPS scheme can be found in *Mihailovic et al.* (2004) and *Mihailovic et al.* (2008).

3. The main features of the NMM non-hydrostatic regional model

In agricultural planning the non-hydrostatic mesoscale model (NMM), designed in the National Centre for Environmental Prediction (*Janjic*, 1994; *Janjic et al.*, 2001), with LAPS implemented in it (*Mihailovic*, 2003), is used in providing outputs for other models. The key features of the model are as follows: a fully compressible, non-hydrostatic or hydrostatic model; mass-based sigma-pressure hybrid terrain following system but with constant pressure surface above 400 hPa and Arakawa E-staggering; Adams-Bashforth and Crank-Nicholson time integration schemes; high-order advection scheme; scalar and energy conserving feature; Coriolis, curvature and mapping terms; one-way nesting; lateral boundary conditions suitable for real-data; and one-way nesting and full physics option to represent atmospheric radiation, surface and boundary layer, as well as cloud and precipitation processes. In the running procedure usually for the initial and boundary meteorological conditions, we use the NCEP objective global analysis gridded data with a 1° horizontal increment, for 23 pressure levels (up to 50 hPa). The lateral boundaries of the model domain are available every six hours from the NCEP data. In runs we work with a horizontal increment of 0.222° × 0.205° and a time step of 100 s. In the preparation phase, surface parameters, either observed or predefined (topography, sea surface temperature, soil and vegetation types, soil temperatures and wetness, slopes and azimuths of the sloping surfaces), were interpolated to the model grid. The topographic data set used is the one provided by the U.S. Navy with 10 × 10 arc min resolution. The vegetation data set is available from USGS with 30 arc s × 30 arc s resolution, following the classification by *Dickinson et al.* (1986). For soil textural classes, the UNEP/FAO data set was used, after converting from soil type to soil textural ZOBLER classes (*Zobler*, 1986). Albedo and surface roughness variations were computed in the preprocessing stage according to the vegetation type.

4. BAHUS model for providing the messages of occurrence of plant diseases: A short description

BAHUS is a biometeorological model fully developed in the CMEP. It is designed for providing the messages of occurrence of plant diseases and the proper time for pesticide application (*Mihailovic et al.*, 2001; *Mihailovic et al.*, 2002). Components of this model are: (1) input module – providing meteorological and biological data that are representative for a selected area; (2) modeling module – consisting of empirical relations and conditions related to the diseases occurrence and the intensity of infection, and (3) output module – giving following messages: risk of infection, duration of incubation period, time of the first symptoms, etc. Depending on the method selected in the modeling module, following meteorological data should be provided by input module: maximum air temperature, minimum air temperature, mean daily temperature, actual values of temperature, relative humidity, precipitation, and the duration of leaf wetness.

In the modeling module, BAHUS uses a method defined by *Mills* (1944), later modified by *Jones et al.* (1980), based on air temperature, relative humidity, and duration of leaf wetness in order to describe the intensity of apple scab infection. Requirements for fire blight blossom infection defined by *Steiner* (1990) are incorporated in degree-days (DD) by Mills (1955) and MARYBLIGHT methods (*Steiner* and *Lightner*, 1992). These methods are based on accumulation of DD and degree-hours (DH), which are defined as a number of degrees over the base temperature during one day and one hour, respectively (*Zoller* and *Sisevich*, 1979; *Mills*, 1955).

5. NEOPLANTA: A short description of the first Serbian UV index model

The numerical model NEOPLANTA is developed by *Malinovic et al.* (2006) in the CMEP. It computes the solar direct and diffuse UV irradiances under cloud-free conditions for the wavelength range 280–400 nm (with 1 nm resolution) as well as the UV index. Effects of O_3, SO_2, NO_2, aerosols, and nine different ground surface types on UV radiation are included. The model calculates instantaneous spectral irradiance for a given solar zenith angle, but there is also a possibility for calculation of the UV index for the whole day at half-hour intervals from sunrise to sunset. Also, there is a possibility of taking into account daylight saving time. Atmosphere in the model is divided into several parallel layers (maximum 40). It is assumed that the layers are homogeneous with constant values of meteorological parameters. The vertical resolution of the model is one kilometer for altitudes below 25 km, and 5 km above this height. The upper boundary of the highest layer in the model is 100 km. The model uses standard atmosphere meteorological profiles. However, there is also an option of including the real time meteorological data profiles from the high-level resolution mesoscale models. The required input parameters are the local geographic coordinates and time, or solar zenith angle, altitude, spectral albedo, and the total amount of gases. The model includes its own vertical gas profiles and extinction cross-sections, extraterrestrial solar irradiance shifted to terrestrial wavelength, aerosol optical properties for ten different aerosol types (*Hess et al.*, 1998), and spectral albedo for nine different ground surface types. Output data are spectral direct, diffuse, and global irradiance divided into the UV-A (320–400 nm) and UV-B (280–320 nm) part of the spectrum, biologically active UV irradiance calculated using the erythermal action spectrum by *McKinley* and *Diffey* (1987), UV index, spectral optical depth, and spectral transmittance for each atmospheric component. All outputs are computed at the lower boundary of each layer.

6. *Numerical simulations with coupled NMM – other environmental models*

To demonstrate how coupled NMM and different environmental models can provide sophisticated information for tactical and also strategic planning in this field, we designed three illustrative numerical simulations, which are widely recognizable in agricultural practice.

6.1. *Use of NMM model with the LAPS scheme for forecasting of extreme temperatures*

The air temperature at 2 m is a reliable indicator of the underlying surface's thermal state (i.e., the quality of the surface parameterization), because the surface temperature strongly affects the air temperature at 2 m. This temperature is determined diagnostically. From the diurnal course of 2-meter temperature are derived extreme temperatures, which are variables on the list of key parameters in the agricultural practice. In this case study, we performed a numerical simulation using the above mentioned NMM model coupled with the LAPS surface scheme (*Mihailovic*, 2003; *Mihailovic et al.*, 2008). The starting time of the simulation was 00:00 UTC, June 5, 2002, and the simulation period was 24 hours. The domain (*Mihailovic et al.*, 2008) was centred in 45.0°N, 19.0°E with (101, 99) cells distributed longitudinally and latitudinally. The domain had 651 grid cells. The cover types include water (22.7%), crops (i.e., short grass canopies) (39.9%), tall grass (4.3%), short grass patches (3.2%), evergreen needle leaf (2.6%), deciduous broadleaf (4.3%), and mixed woodland (23.0%), while the soil textural classes were water (22.7%), loamy sand (4.5%), sandy loam (11.5%), silt clay loam (36.6%), clay loam (19.7%), sandy clay (2.5%), and silt clay (2.5%). *Fig. 1* shows air temperature values obtained from the NMM plotted against observed values taken from the SYNOP data set of June 5, 2002. It compares the temperature extremes. For the temperature extremes, the simulated maxima are in better agreement with the observations than the simulated minima.

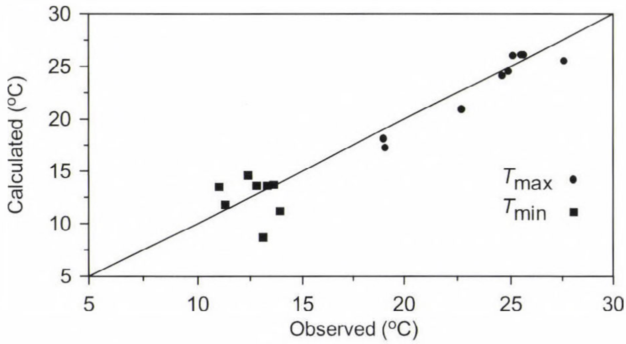

Fig. 1. Air temperatures at 2m obtained by the NMM (including LAPS) plotted against the observed values taken from the SYNOP data of June 5, 2002). Comparison for the temperatures extremes.

6.2. *An example of use the BAHUS model linked with the NMM model for plant diseases prediction*

In this numerical simulation we demonstrate an example of the assessment of meteorological conditions suitable for appearance of: (i) apple fire blight (infection intensity ranged as none, low, moderate, and high), (ii) grape downy mildew (duration of incubation period), and (iii) potato late blight (duration of incubation period) for Novi Sad area during spring period in year 2008. In the forecasting procedure we supposed, based on our experience, that biological conditions were satisfied: (i) for apple (flowering) after March 15 and (ii) grape and potato (certain stadium of growth) after April 20. Weather data file of the BAHUS input module included the following elements: (i) data from SYNOP data set describing previous weather conditions and (ii) the NMM model outputs including predicted state of weather (*Fig. 2*). Using these data the BAHUS model has been continuously run after March 15, in order to assess disease appearance risk on daily bases. Obtained results are presented in *Table 1*.

According to BAHUS model, until May 5, thermal and humidity conditions for fire blight, downy mildew and late blight appearance were not auspicious. Although on April 11 air temperature exceeds lower threshold for fire blight DH accumulation (*Fig. 2*), it was obvious that following temperature decrease will cause termination of the disease development process. On May 12, according to air temperature forecast (*Fig. 2*), at the end of the incubation period, downy mildew has been expected in next two days, while, in case of fire blight, epiphytic infection potential (EIP) should pass 100% on the same time. On May 26 and June 18, suitable conditions were also recorded for downy mildew appearance. However, for incubation period starting on June 12, a little bit longer duration has been expected due to forecasted temperature decrease (*Fig. 2*).

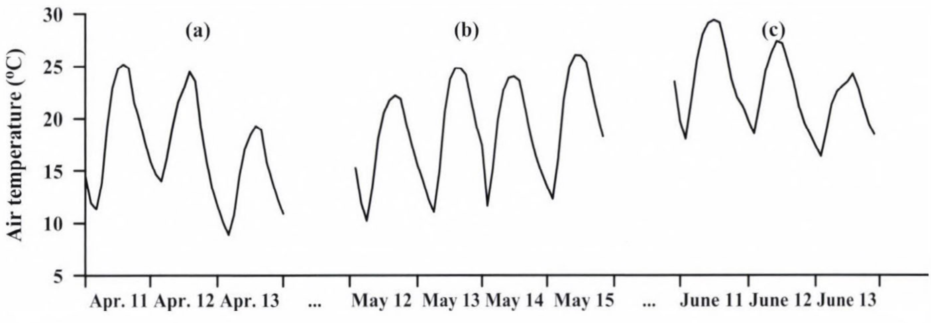

Fig. 2. NMM model forecast of 2m air temperature for periods: (a) April 11–13, (b) May 12–15, and (c) June 11–13 for year 2008.

Table 1. Simulated assessment of disease appearance (i.p. = incubation period) based on meteorological conditions

Date/Disease	Fire blight	Downy mildew	Late blight
Before April 11	no risk	no risk	no risk
April 11	hi risk – no infection	no risk	no risk
April 12	medium risk – no infection	no risk	no risk
April 13	medium risk – no infection	no risk	no risk
April 14	no risk	no risk	no risk
Before May 12	EIP = 15.7 – no infection	less than 2 days till the end of i.p.	no risk
May 13	EIP = 64.1 – no infection	end of i.p.	no risk
May 14	EIP = 123 – infection		no risk
Before May 26		last day of i.p.	no risk
Before June 11		i.p. in progress	end of i.p. in next 7 days
Before June 18		last day of i.p.	

6.3. The NEOPLANTA model for UV radiation prediction and its use in assessment of climate change impact on development of plant diseases

Based on an assessment of important diseases of wheat and other cereals, sugarcane, deciduous fruits, grapevine, vegetables, and forestry species, climate change may reduce, increase, or have no effect on some diseases (*Chakraborty et al.,* 1998). Changes will occur in the type, amount, and relative importance of pathogens and diseases. Host resistance may be overcome more rapidly due to accelerated pathogen evolution from increased fecundity at high CO_2 and/or enhanced UV-B radiation. However, uncertainties about climate change predictions and the paucity of knowledge limit our ability to predict potential impacts on plant diseases. Both experimental and modeling approaches are available for impact assessment research.

For the purpose of this paper we demonstrated the performance of this model by comparing UV index values, obtained by the coupled NMM and NEOPLANTA, with measurements recorded with a Yankee UVB-1 biometer (see *Yankee Environmental Systems Inc*., 2000). For the test, we have selected data for ten days, measured in the years 2003, 2004, and 2005, with cloudiness less than 0.2. The device used is located at the Novi Sad University campus (45.33°N, 19.85°E, 84 m a.s.l.). All other details about model run can be found in *Malinovic et al.* (2006). *Fig. 3* depicts comparisons between the calculated diurnal variations of UV index for cloudless days in 2003, 2004, and 2005. From this figure, it is seen that the NEOPLANTA model gives values that are very close to the observations.

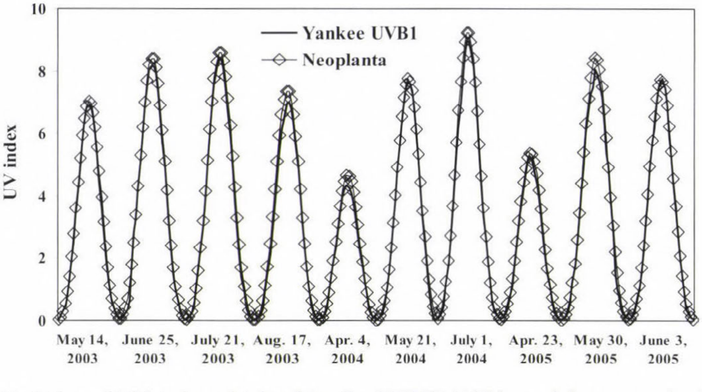

Fig. 3. Variation of UV index obtained by the NEOPLANTA model compared with the observations in Novi Sad for cloudless days.

As the development and implementation of mitigation strategies take long time, more research is urgently needed and we hope this paper will stimulate interest. For example, it is planned to carry out further research on the risk of the damages and yield losses in orchards and crop fields by plant diseases, increased UV radiation, and heat waves as a consequence of climate change. It will be done on the basis of analysis of outputs obtained by running (i) climate ECHAM model, (ii) regional NMM model with the LAPS scheme, (iii) NEOPLANTA UV radiation model, (iv) BAHUS model for forecasting the occurrence of plant diseases, and (v) a selected crop model. This assessment is particularly important for the central and southern parts of Europe which are potentially the most vulnerable regions in Europe regarding the climate change. It was one of the main reasons why the NEOPLANTA model has been developed, tested and prepared as a user friendly software that can be easily linked with the NMM model.

7. Conclusions

We considered a wide range of possibilities for use of coupled mesoscale non-hydrostatic model and land surface scheme for application in agriculture planning on both tactical and strategic levels. Specifically, in this paper we shortly described the NMM non-hydrostatic model and the LAPS scheme. Additionally, we briefly elaborated two environmental models (BAHUS – for prediction of plant diseases and NEOPLANTA – for prediction of UV radiation) which are fully developed in the Centre for Meteorology and Environmental Predictions, University of Novi Sad (Serbia). Finally, we performed numerical simulations with the coupled NMM-LAPS model and the aforementioned environmental models, giving three examples of forecasting the quantities which are on the list of key parameters that are important in agricultural practice and its planning activities.

Acknowledgement—The research work described in this paper has been funded by the Serbian Ministry of Science under the project "Modeling and Numerical Simulations of Complex Physical Systems", No. OI141035 for 2006-2010.

References

Chakraborty, S., Murray, G.M., Magarey, P.A., Yonow, T., Sivasithamparam, K., O'Brien, R.G., Croft, B.J., Barbetti, M.J., Old, K.M., Dudzinski, M.J., Sutherst, R.W., Penrose, L.J., Archer, C., and *Emmett, R.W.,* 1998: Potential impact of climate change on plant diseases of economic significance to Australia. *Australas. Plant Path. 27*, 15-35.

Dickinson, R.E., Henderson-Sellers, A., Kennedy, P.J., and *Wilson, M.F.,* 1986: *Biosphere–Atmosphere Transfer Scheme for the NCAR Community Climate Model. NCAR Tech. Rep. NCAR/TN-275 1STR*, pp. 69 [Available from NCAR, P.O. Box 3000, Boulder, CO 80307-3000].

Everingham, Y.L., Muchow, R.C., Stone, R.C., Inman-Bamber, G., Singels, A., and *Bezuidenhout, C.N.,* 2002: Enhanced risk management and decision-making capability across the sugarcane industry value chain based on seasonal climate forecasts. *Agr. Syst. 74*, 459-477.

Hess, M., Koepke, P., and *Schult, I.,* 1998: Optical properties of aerosols and clouds: The software package OPAC. *B. Am. Meteorol. Soc. 79*, 831-844.

Janjic, Z.I., 1994: The step-mountain eta coordinate model: Further developments of the convection, viscous sublayer, and turbulence closure schemes. *Mon. Weather Rev. 122*, 927-945.

Janjic, Z.I., Gerrity, J.P., Jr., and *Nickovic, S.*, 2001: An alternative approach to nonhydrostatic modeling. *Mon. Weather Rev. 129*, 1164-1178.

Jones, A.L., Lillevik, S.L., Fisher, P.D., and *Stebbins, T.C.*, 1980: A microcomputer-based instrument to predict primary apple scab infection periods. *Plant Dis. 64*, 69-72.

Malinovic, S., Mihailovic, D.T., Kapor, D., Mijatovic, Z., and *Arsenic, I.D.*, 2006: NEOPLANTA: A Short Description of the First Serbian UV Index Model. *J. Appl. Meteorol. Clim. 45*, 1171–1177.

McKinley, A.F. and *Diffey, B.L.* 1987: A reference action spectrum for ultraviolet induced erythema in human skin. *CIE Journal 6*, 17-22.

Meinke, H. and *Stone, R.C.*, 2005: Seasonal and inter-annual climate forecasting: the new tool for increasing preparedness to climate variability and change in agricultural planning and operations. *Climatic Change 70*, 221-253.

Mihailovic, D.T., 2003: Implementation of Land-Air Parameterization Scheme (LAPS) in a limited area model. *Final Report. The New York State Energy Conservation and Development Authority*, Albany, NY., 110 pp.

Mihailovic, D.T., 2005: LAPS – land surface scheme for use in crop modeling. *Workshop on Introducing Tools for Agricultural Decision-Making under Climate Change Conditions by Connecting Users and Tool-Providers (AGRIDEMA)*, 21 November–3 December 2005, Vienna, Austria. http://www.agridema.net (invited lecture).

Mihailovic, D.T., and *Lalic, B.*, 2006: Land- Air Parameterisation Scheme (LAPS) as a component in agrometeorological modeling. Abstracts, *Workshop on Environmental Fluid Mechanics as Elements in Agrometeorological Modeling*, 6-9 June, As, Norway (invited lecture).

Mihailovic, D.T., Koci, I., Lalic, B., Arsenic, I., Radlovic, D., and *Balaz, J.*, 2001: The main features of BAHUS – biometeorological system for messages on the occurrence of diseases in fruits and vines. *Environ. Modell. Softw. 16*, 691-696.

Mihailovic, D.T., Eitzinger, J., Koci, I., Lalic, B., Arsenic, J.I., and *Balaz, J.*, 2002: Biometeorological system BAHUS for predicting the occurrence of plant diseases and ensuring their efficient control. *Int. Workshop on Environmental Risk Assessment of Pesticides and Integrated Pesticide Management in Developing Countries*. Kathmandu, Nepal, 6-9 November, *Landschaftsokologie und Umweltforschung, 38*, 120-129.

Mihailovic, D.T., Alapaty, K., Lalic, B., Arsenic, I., Rajkovic, B., and *Malinovic, S.*, 2004: Turbulent transfer coefficients and calculation of air temperature inside the tall grass canopies in land-atmosphere schemes for environmental modeling. *J. Appl. Meteorol. 43*, 1498-1512.

Mihailovic, D.T., Lazic, J., Leśny, J., Olejnik J., Lalic, B., Kapor, D., and *Cirisan, A.*, 2008: A new design of the LAPS land surface scheme for use over and through heterogeneous and non-heterogeneous surfaces: Numerical simulations and tests. *Theor. Appl. Climatol.* (accepted).

Mills, W.D., 1944: Efficient use of sulfur dusts and sprays during rain to control apple scab. *N.Y. Agric. Exp. Stn. Ithaca Bull. 630*, pp. 4.

Mills, W.D., 1955: Fire blight development on apple in western New York. *Plant. Dis. Rep. 39*, 206-207.

Steiner, P.W., 1990: Predicting apple blossom infection by *Erwinia amylovora* using the Maryblyt model. *Acta Horticulturae 273*, 139-148.

Steiner, P.W. and *Lightner, G.W.*, 1992: *MARYBLYT: A Predictive Program for Forecasting Fire Blight Disease in Apples and Pears.* Version 4.0, University of Maryland.

Zobler, L., 1986: *A World Soil File for Global Climate Modeling.* NASA Technical Memorandum 87802. NASA Goddard Institute for Space Studies, New York, New York, U.S.A.

Zoller, B.G. and *Sisevich, J.*, 1979: Blossom populations of Erwinia amilovora in pear orchards vs. accumulated degree hours over 18.3 Celsius, 1972-1976. *Phytopatology 69*, pp. 1050.

Yankee Environmental Systems Inc., 2000: *UVB-1 UV Pyranometer. Installation and User Guide.* Version 2.0, Turner Falls.

IDŐJÁRÁS
Quarterly Journal of the Hungarian Meteorological Service
Vol. 113, No. 1–2, January–June 2009, pp. 23–37

Brief surveying and discussing of drought indices used in agricultural meteorology

Zoltán Dunkel

Hungarian Meteorological Service,
P.O. Box 39, H-1675 Budapest, Hungary; E-mail: dunkel.z@met.hu

(Manuscript received in final form January 8, 2009)

Abstract—The paper summarizes the indices used for identification of drought phenomenon in the agricultural meteorology practice. Many drought definitions and indices are known. Drought indices seem to be the simplest tools in drought analysis. The indices are classified into six groups, namely *atmospheric*, *precipitation*, *water balance*, *soil moisture*, *recursive*, and *remote sensing* indices. For each group typical expressions are given and analyzed for their performance and comparability. Taking into consideration that the drought is a compound concept, a few drought definitions are examined together with the drought indices. As any classification, the presented categories have got their limitation. The discussion on drought definition together with the survey of the indices tries to highlight the wide possible categorization of this very important phenomenon mainly from the meteorological point of view.

Key-words: drought, drought definition, drought index, meteorological drought, Palmer drought severity index, index surveying

1. Introduction

Drought is undoubtedly one of the human being's worst natural enemies (*WMO*, 1975, 1986). Among the extreme meteorological events, drought is possibly the most slowly developing and long existing event, and probably is the least predictable among the atmospheric hazards. Due to these characteristics, particularly their temporal character, drought cannot be compared with other natural hazards such as flood, hurricane, tornado, lightening, hailstorm, frost, or plague of locust, which also significantly can contribute to a nation's annual loss due to disadvantageous natural circumstances. We can record flood and drought in the same vegetation period in some part of the world. Because of its peculiar character, *drought* deserves the greatest scientific and operative/practical investigation. The goal was to collect the known and used drought indices and to compare their theoretical and practical advantages, limitations, interrelations, and numerical effectiveness. It seems to be necessary to re-evaluate the types of the indices and the definition itself. We can find interesting and important reviews (*Heim*, 2000; *Sivertsen*, 2005a, b) and almost impossible to refer all of them. Taking size limitations of present issue into consideration, only a summary of the definition and mathematical formulation will be given without any numerical evaluation. Some numerical evaluation was carried out in other particular reviews (*Jankó Szép et al.*, 2005; *http://drought.unl.edu*, 2008; *Mika et al.*, 2005).

More exact determination of drought could be made by means of plant-specific indicators of moisture deficiency, characterizing the water demand during the consecutive phenological phases of plants if the information was available and could be mathematically formulated. The drought is a compound concept. As a first guess, it seems that everybody determines it similarly. But, if we go into details, we can compare the phenomenon from different parts of the world; from different types of climate zones we cannot find an absolute acceptable definition and absolute categorization. It means, on one side, a prolonged absence or marked deficiency of precipitation, on the other side, a yield decrease caused by the precipitation deficit.

Many drought definitions are known. Several of them use meteorological parameters. Dealing with the drought problem we can take the following types of investigation, not only from the meteorological point of view:

—Drought frequency can be examined in long time series mainly using the long meteorological data series (for 30, 50, or 100 years). This is the *climatic description.*

—Based on territorial distribution of drought-affected areas for a given territory (region, country) generating homogeneous data series, the territorial distribution of drought tendency can be determined. This is the *regionalization.*

—Detection and prediction of drought during a given year (vegetation period) can be performed using weather information, to provide *forecast and warning of drought.*

—Direct detection of the plant water supply, the water stress detection is the key to *irrigation and plant protection advice.*

In all these approaches the same parameters and methods of drought identification can be used (*Budyko*, 1952; *Eitzinger et al.*, 2008; *Ivanov*, 1948; *Koshelenko* and *Volevakha*, 1971; *Ped*, 1975; *Sun* and *Ward*, 2007; *Theophilou*, 2006; *Tsiros et al.*, 2006; *Wilhite*, 2005), which can also be based on the same definition.

Without any ambition to give an absolute definition, that is acceptable for everybody, some kind of survey of the existing drought definitions will be introduced before the evaluation of drought indices. We start with the most authentic drought definition could be read in the International Meteorological Vocabulary (*WMO*, 1992). The survey will be not able to incorporate all existing drought indices, it only highlights the most important categories.

2. *Drought definitions and categories*

The problem involves a wide variety of definitions, indicators, indices, and methods of evaluation. As a consequence, almost all agrometeorologists, climatologists, and agronomists, engaged in this field, have their own time series, methods, and conclusions about the drought events. Drought may be studied from a number of different points of view. But, what is the drought, at all? If we would like to give any quantitative criteria for the drought, we must identify its quality before its parameterization. Drought has been defined very commonly and frequently as a period of precipitation deficiency (*Wilhite*, 1983). It seems to be a nice definition, but nobody speaks about drought in case of Sahara or other regions, where the weather is generally dry. In any case when we mention drought, we somehow involve the agricultural product into our consideration, or, more simply, the vegetation production or plant life cycle. It seems to be very easy to produce any combination of meteorological elements and define a threshold value, but if we neglect the behavior of natural or artificial vegetation, we cannot determine good or acceptable categories and threshold values to identify the drought situation. The International Meteorological Vocabulary (*WMO*, 1992), the most authentic source, gives two definitions of drought:

(1) *Prolonged absence or marked deficiency of precipitation;*

(2) *Period of abnormally dry weather sufficiently prolonged for the lack of precipitation to cause a serious hydrological imbalance.*

Both of them are very simple, but if we compare them with the definition given for the dry season: *Period of the year characterized by the (almost) complete absence of rainfall. The term is mainly used for low latitude regions*, we can state that is not very simple task to answer the question. Another category is given in the vocabulary, the *dry spell*. Its definition is more or less close to the drought: *Period of abnormally dry weather. Use of the term should be confined to conditions less severe than those of a drought.*

Drought may be identified from a number of different points of view. It means different things to various people, depending on their specific interest or historical, economical background. It is difficult to find a completely adequate definition of drought, which could be acceptable everywhere in the world. Sometimes the definition is confused with categories. To get a better understanding, some categories or types have been introduced, namely we can speak about the following terms:

— Atmospheric drought occurs if too high saturation deficit has been measured for a durable time. This category more or less refers to the dry spell category.
— Meteorological drought means a longer period of time with considerably less than average precipitation amounts. The definition is more or less the same given for drought in general.
— Agricultural drought has got two approaches. The first one is *the available soil moisture is inadequate*, the second one is: *yield is considerably less than the average because of water shortage*. As it was earlier mentioned, the real drought definition somehow should involve the less than normal vegetation production, so the agricultural drought seems to be close enough to the expected definition.
— Hydrological drought refers to a period of below-normal stream-flow. Another import approach is expressed in this category that the drought is not at all a very local phenomena, it occurs on a larger area, for example it is at least a problem of a water catchment.
— Physiological drought can occur when the plant is unable to take up water in spite of the present sufficient soil moisture. This situation refers to the circumstances when plant shows drought symptom but there is no drought at all in terms of the obvious drought related atmospheric conditions. This phenomenon could be caused by abnormally cold weather or in the case when the plant is infected.
— Socio-economical drought is some kind of integration of several drought categories. It implies any disadvantageous influence of the consecutively repeating dry spells. It is the lack of some economic goods due to meteorological, hydrological, and agricultural drought. In the specific case its definition can be close the definition of famine.

Following the structure of the picture is given in the homepage *http://drought.unl.edu* but making some modification we can summarize the categories and give a hierarchy in the definitions in the *Fig. 1*.

Anyway, we can determine *drought* as *a period during which prolonged and abnormal moisture deficiency produces reduced plant growth and productivity can cause significant loss in nation's economy*.

3. Drought indices definitions and categories

Drought index is *an index which is related to some of the cumulative effects of a prolonged and abnormal moisture deficit* (*WMO*, 1986). To describe the temporal and spatial distribution of drought or dry spell situation, we can mostly use meteorological parameters (*Budyko*, 1952). The practice is that any single meteorological element is unable to identify a drought situation, by itself, or, at least there are not uniform categories for drought in this case.

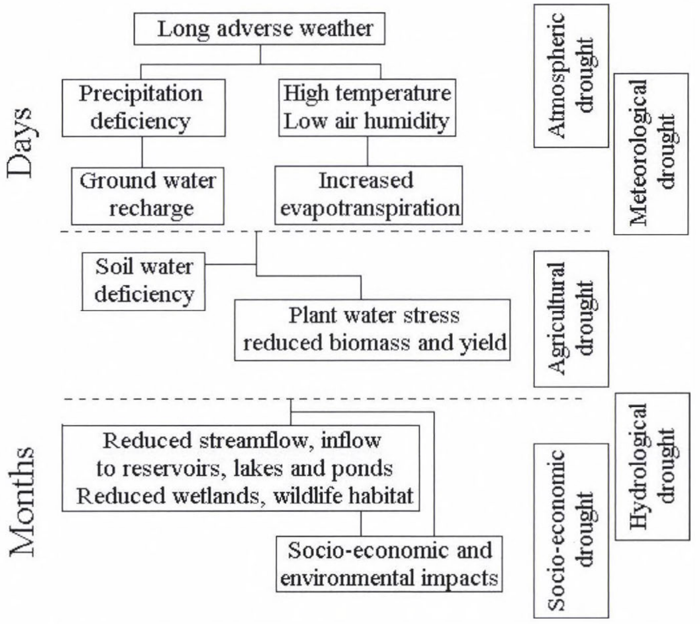

Fig 1. Logical scheme of the drought definition, in combination with the time frame and other water-, plant-, and environment-related phenomena (*http://drought.unl.edu,* 2008).

A more or less acceptable approach is to combine the meteorological variables in order to develop a so-called drought index. Some of these indices can be used only in special circumstances; the other ones can be used for wider area. Anyway, it is very difficult to give universal categories for drought situation that were suitable to determine the drought situation anywhere and anytime, and which could identify the drought for any types of vegetation.

The expectation of the everyday agronomic practice differs from the climatic approach, but the drought index and any kind of irrigation decision signal are not far from each other from meteorological point of view. Until now, many kinds of drought indices were developed, using classical meteorological variables. In this short paper we would like to give a short categorization of drought and dry spell indices, dealing with not only the traditional observations but with some possibilities of using remotely sensed information. The knowledge of temporal and spatial distribution of drought allows us to prevent its damage choosing proper (drought-resistant) species, or to build up a well-working irrigation system in the endangered area. The use of remote sensing technique gives new possibilities to detect the water deficit or drought situation. Vegetation indices derived from satellite's measurements give information about the plant cover of large area and can be the basis of the detection of general condition of vegetation. From this information we can derive a temporal change of water supply and water-stress status, too. Surface temperature measured from satellite or near the surface informs us about plant water supply, too. The practical use of the near-to-surface gradients and water vapor deficit, combined with other standard meteorological observations, opens new possibilities not only in the everyday coping with water deficit and drought but in the climatic detection, too.

In meteorology, it is a very common way to approach drought situation by generating an index using meteorological data. If an index is properly formulated, and its limitations are well recognized, then the index could be very useful. With very moderate criticism on their different types, we try to classify the reviewed indices. To compare drought or dry spell events either on spatial or temporal scale requires a quantitative expression. Drought indices appear to be more or less the simplest way to carry out this work. Nevertheless, finally we can use either a simple meteorological value with more or less 'natural' thresholds or a combination of meteorological elements, sometimes without any physical meanings. Following and partly modifying *Farago et al.* (1989), a compendium of indices are shown where the indices are grouped according to their similarity:

— atmospheric drought,
— indices of precipitation anomaly,
— aridity indices,
— soil moisture indices,
— combined or recursive indices, and
— indices based on remotely sensed information.

Independently of the categorization, the *drought index* is used very widely as a research and operative tool, not only within the agrometeorology, but in many related sciences, as well (*Alexandrov et al.*, 2008).

3.1. Indices of atmospheric drought

The standard signal of dry spell is the low humidity. The water vapor saturation deficit is commonly used for characterization of atmospheric drought, although the temporal scale for similar analysis is usually much shorter than a month, sometimes only a few days, but consequence of these days could be catastrophic in case of few species. These indices are not the commonly accepted indices (*Selyaninov,* 1958), but sometimes it is worth to introduce them mostly in the irrigation practice. The simplest form is a simple meteorological element, called saturation deficit (*WMO,* 1992),

$$E - e = E\,(1 - f),$$

where E is the pressure of the water vapor at saturation, e is the measured water vapor pressure, both of them given in SI unit, hPa, f is the relative humidity in percent. For a shorter period threshold values for the identification of atmospheric drought, the so-called *atmospheric dryness*, could be 20–29 hPa, for weak, 30–39 hPa for moderate, 40–49 hPa for intensive, and more than 50 hPa for very intensive dry spell. Dry conditions of longer periods can be described with threshold values of at least weak or moderate dryness.

3.2. Indices of precipitation anomalies

Any forms of drought are related to some antecedent and relative precipitation amounts for the previous period. This period could be last from 3–4 weeks to years. The drought occurs after the anomalous rainy season or period. For example, agricultural drought could be a consequence of dry autumn and winter period. Therefore, the simplest drought index is the deviation from a normal precipitation value. We can generate some combination of deviation, or can somehow normalize the deviation values for a better comparison of generalization. We have to stress that a good drought index is unimaginable without a long-term comparison with yield values before the establishment of threshold values.

Finally, the simplest expression of the difference from the normal could be defined as drought index, the so-called *precipitation index*:

$$P - m(P),$$

where P denotes the longer period's precipitation sum, $m(P)$ is its long term average, standard value, or *climate normal* for the same period. It could be expressed in standard precipitation unit, i.e., in mm. It is desirable to use as long as possible period for the generation of the mean value. The anomalies for non homogeneous regions or larger areas with different climatic conditions are not comparable. To avoid this problem, either relative amounts, or standardized values should be introduced.

Following the same categorization, other indices could be generated as relative values, like the r*elative precipitation amount or relative precipitation anomaly index:*

$$\frac{P}{m(P)} \quad \text{or} \quad \frac{P - m(P)}{m(P)}.$$

In practice both of them are multiplied by 100, and the index is used in percentage form. The difference could be normalized with the standard deviation of the precipitation data series. In this case we can introduce the s*tandardized precipitation anomaly index* (SAI):

$$\frac{P - m(P)}{d(P)},$$

where $d(P)$ is the standard deviation. Each relative index could be a drought indicator if its value is less than apreviously established threshold value, e.g., *75%* on an annual basis, or *50%* for a shorter period for example for a month. The use of other, slightly different levels was suggested by *WMO* (1975*)*. For a recent worldwide drought assessment, to outline desertification, smaller than 60% annual value was given for the relative precipitation anomaly index for more than two consecutive years.

3.3. Aridity indices

Aridity is the characteristic of climate relating to insufficiency of inadequacy of precipitation to maintain vegetation. For a single station, where the usual probability levels can be applied to choose particular threshold values in accordance with the hypothetical distribution of standard approximation of potential evapotranspiration, we can found many types of aridity indices. The simplest way to approximate the evaporation is using temperature alone or a kind of temperature sum and degree-days. The theoretical base form of the aridity index is the evapotranspiration/precipitation ration (*Bristov,* 1987; *Budyko*, 1952). The difference in the aridity indices is in the approximation of the evaporation (evapotranspiration). In principle, the aridity index looks like the following formulas:

$$\frac{P}{PE} \quad \text{or} \quad \frac{P}{\frac{R_n}{L}},$$

where PE is the evapotranspiration expressed in precipitation unit, i.e., mm, R_n is the radiation balance, and L is the latent heat of water vaporization. Taking into consideration the difficulty of evaporation calculation, many approaches were used to determine the evaporation substituting its value with other meteorological elements. The well known types from this category are as follows:

Lang's rainfall index

$$\frac{P}{T},$$

where P is the sum of precipitation for the examined period, expressed in precipitation unit, i.e., mm. T is the average temperature of the same period given in °C unit. It is a very simple approximation. A little more adjusted index using the similar variables is the

De Martonne aridity index

$$\frac{12P}{T+10},$$

written for monthly calculation. Similar construction is followed in the

Thornthwaite index

$$1{,}65\left[\frac{P}{T+12{,}2}\right]^{\frac{10}{9}}.$$

We have to mention that the form of the three last formulas is a typical *agrometeorological index* approach like different types of degree-days. Another type of this category is the degree-days approximation used in Selyaninov index. This index is known as hydro-thermal index. It uses daily values for the calculation of the period.

Selyaninov's hydro-thermal coefficient

$$\frac{P}{\sum\limits_{T\geq 10} T},$$

where T means the consecutive daily mean air temperature above 10 °C. The threshold values for categories of drought or aridity (*Selyaninov*, 1958) are 0.4–0.7 for very dry, 0.7–1.0 for dry, 1–1.3 for insufficiently wet category, and if the coefficient is higher than 1.3 the category is wet. A specific type of the supply-demand category is the comparison of standardized values of the temperature and precipitation in

Ped's drought index, 1st approximation

$$\frac{\Delta T}{d(T)} - \frac{\Delta P}{d(P)}.$$

Not only in the agricultural meteorology but in any near-to-surface energy transfer studies, a well known parameter is the Bowen ratio (*Skvortsov*, 1950) expressing the relation between latent and sensible heat transfer. Because of measurement difficulties, before the continuous data logging the Bowen ration was determined only among very restricted trial circumstances. Not only of its theoretical importance but of its growing direct measuring practice, we have to mention as an *aridity index* among the drought indices. Theoretically, the *Bowen ratio* could be expressed in the form

$$\frac{H}{LE},$$

where H denotes the sensible heat flux and LE is the latent heat flux. Both of them are given in standard flux unit, W $m^{-2}s^{-1}$.

3.4. Soil moisture indices

Using measured or calculated soil moisture data (*Budagovsky*, 1956), we can generate the same type of indices for expressing drought.

Relative soil moisture content

$$\frac{W}{AWC},$$

with W and AWC denoting the actual soil moisture and the available (or disponsible) water capacity for a fixed soil depth (e.g., the upper 1 m layer or the root zone for a given plant). Besides this well-known ratio, an extended form of Ped's (*Ped,* 1975) drought index incorporates the standardized value of the soil moisture amount.

Ped's drought index, 2nd approximation

$$\frac{\Delta T}{d(T)} - \frac{\Delta P}{d(P)} - \frac{\Delta W}{d(W)},$$

where $d(W)$ is the standard deviation of soil moisture content, as it was calculated for temperature and precipitation in the 1st approximation of *PDI*.

3.5. Recursive indices

Indices describing the moisture conditions for a relatively long time period through the integrated values of the related meteorological elements provide only a rough picture of the adverse conditions within this period. It is thought that, above all, the cumulative effect of prolonged moisture deficits (month by month) should be properly expressed. These indices proved to be of high utility in the delineation of meteorologically determined droughts or dry spell, which possess a kind of memory of which actual values depend on previous values of the related meteorological variables. Because of their calculation method, they could be called as *recursive* indices. A summarization of consecutive monthly precipitation is

Foley's anomaly index (*FAI*)

$$FAI_1 = \Delta P_1,$$

$$FAI_k = FAI_{k-1} + \Delta P_k.$$

The calculation starts with a simple difference for the 1st month. The kth month value is calculated using the *index* of the previous month adding the precipitation difference of the standard and actual precipitation value. Finally the series of the yearly indices could be produced to evaluate the drought tendency from climate change point of view (*Fensham* and *Holman*, 1999). Conceptually, the Bhalme-Mooley drought index (*BMDI*) can be considered as a simplified version of the well-known and widely used Palmer drought severity index (PDSI) (*Alley*, 1984). The base of the generation is the monthly precipitation amounts in the *Bhalme-Mooley drought index*

$$i_0 = 0,$$

$$i_k = c_1 i_{k-1} + \frac{SAI_k}{c_2},$$

$$BMDI = \frac{\sum_1^n i_k}{n}.$$

The coefficients c_1 and c_2 are region specific values. The *SAI* is the above mentioned *standardized precipitation anomaly index* (*Bhalme* and *Mooley*, 1980). The calculation is carried out for the vegetation period, starting in April, closing in September. Finally one number will be determined for the year as a sign of drought situation.

A very commonly used and accepted index is the *Palmer drought severity index* (PDSI). The PDSI index is based on the thorough analysis of the elements of surface water balance and on the comparison of their actual values to their climatically or physically potential values. The computing procedure of the PDSI consists of several steps. It considers monthly precipitation, evapotranspiration, and soil moisture conditions. In general, several methods can be used to calculate the potential evapotranspiration, a key variable of the water balance and also of the PDSI computation procedure. Palmer (*Alley*, 1984) applied the Thornthwaite-formula which is rather a climatic character; while later the Blaney-Criddle method provided better estimations (*Alley*, 1984), especially for vegetation specific alternatives. PDSI is standardized for different regions and time periods, which is useful in common assessment for a wide area with different climate. The steps of computation are:

— *Hydrological accounting.* Computation begins with a climatic water balance using series of monthly precipitation and temperature records. An empirical procedure is used to account for soil moisture storage by dividing the soil into two arbitrary layers. The upper layer is assumed to contain the available moisture at field capacity. The loss from the underlying layer depends on the initial moisture content, as well as on the computed *potential evapotranspiration* (PE) and *the available water capacity* (AWC). Runoff is assumed to occur if both layers reach their combined moisture capacity, AWC. In addition to PE, three more potential terms are used and defined as follows: *potential recharge* is the amount of moisture required to bring the soil to its water holding capacity. *Potential loss* is the amount of moisture that could be lost from the soil by evapotranspiration during a zero precipitation period. *Potential runoff* is defined as the difference between precipitation and potential recharge.

— *Calculation of climatic coefficients.* This is accomplished by simulating the water balance for the period of available weather records. Monthly coefficients are computed as proportions between climatic averages of actual vs. potential values of evaporation, recharge, runoff, and loss, respectively.

— *Calculation of CAFEC* (Climatically Appropriate for Existing Conditions) *values.* The derived coefficients are used to determine the amount of precipitation required for the CAFEC, i.e., *normal* weather during each individual month.

— *Moisture anomaly index.* Difference between the actual and CAFEC precipitation is an indicator of water deficiency or surplus in that month and station, expressed as $D = P–I$. These departures are converted into indices of moisture anomaly as $Z = K(j)D$, where $K(j)$ is a weighting factor, also accounting for spatial variability of the departures (D).

— *Calculation of drought severity.* In the final step the Z-index time series are analyzed to develop criteria for the start and end of drought periods and an empirical formula for determining PDSI

Palmer drought severity index

$$PDSI_k = PDSI_{k-1} + \frac{Z_k}{3} - 0{,}103\ PDSI_{k-1},$$

where Z is the moisture anomaly index. The equation indicates that PDSI of a given month strongly depends on its value in the previous months and on the moisture anomaly of the actual month. It causes strong autocorrelation of PDSI. In general, monthly PDSI time series range between –9 and +9, specifically, severe and extreme conditions are characterized by absolute values greater than 4 and 6, respectively. These thresholds may vary among the geographic regions of the world, whereas the original attribution (monthly PDSI time series range between –4 and +4) is considered to be the extremity threshold. Furthermore, drought events occur in the case of negative PDSI values, while positive values imply wet conditions. Compared to other traditional drought indices, PDSI can demonstrate several advantages. It is able to simulate moisture content of the soil month by month, and it is suitable to compare the severity of drought events at regions having rather different climate and seasons.

3.6. Indices based on remotely sensed parameters

The spectral reflectance of vegetation is markedly different from that of most soil materials (*Wagner et al.*, 1996). It is determined by the absorption of chlorophyll at blue and red wavelengths. In the near infrared the radiation is scattered by leaves. This results in generally high reflection which depends mainly on the geometry and size of the leaves. By contrast, vegetation reflectance is low in the visible region with small secondary maximum around 0.55 μm. When vegetation is stressed by shortage of water, and also at the end of the growing period, the chlorophyll absorption weakens and the ratio of near infrared to red or visible reflectance decreases. This ratio is the so-called *vegetation index*

$$\frac{NIR}{VIS},$$

where NIR denotes the reflected radiation in the near infrared interval and VIS denotes the red or visible intervals according to the satellite channel. It is, therefore, a measure for physiological activity of plants. In practice, the *normalized difference vegetation index* (NDVI)

$$\frac{NIR - VIS}{NIR + VIS}$$

is often used to characterize the state of vegetation. Because the state of vegetation highly depends on the water supply condition, we can use the normalized vegetation difference index as drought index. Stress induced by water shortage results in a reduction of the magnitude of the vegetation index. The NDVI is difficult to interpret in case of sparse vegetation, because also the reflectance of most soils increases slightly with wavelength.

The surface temperature can be measured remotely. The difference between the near surface and surface temperatures is the indicator of the latent and heat flux ration. Following the approximation of *Jackson et al.* (1981, 1984), a standardized index the so-called crop water stress index (CWSI) could be generated the
crop water stress index

$$\frac{PE - ET}{PE},$$

where *PE* denotes the potential, while *ET* the actual evapotranspiration. The CWSI in this theoretical form is neither drought nor remote sensing index. The remotely sensed surface temperature and the combination of other meteorological elements could be the base (*Bristow*, 1987) of the CWSI mainly used in irrigation advisory systems. Its consecutive daily values could be used as drought indices too. The difference of the surface and near surface temperatures (*Idso et al.*, 1981; *Seguin et al.*, 1994) could be alone a drought indicator. Using the well known degree day analogue we can generate the
stress degree day (*SDD*)

$$SDD = \sum_K (T_C - T_A),$$

where T_C is the remotely sensed surface (canopy), T_A is the standard air temperature of consecutive days of dry period.

4. Concluding remarks

Drought indices can be calculated at an individual weather station or for a larger area using data of many stations. A simple area-mean can be produced, or a weighted average can be computed. The goal in any cases is to generate a simple and well interpretable *number* or physical variable with its dimension, which can answer the question if there is a drought, or not. Sometimes, when soil moisture measurements or its reasonably good estimations are available, the respective soil moisture indices are more advantageous. Taking into consideration the data collection and computation capacity, we can use a very simple index (*Budyko, 1952*) and produce a quick, but rough result, or we can prepare a very sophisticated map using GIS technique (*Eitzinger et al.*, 2008). The use of remote sensing technique gives new possibilities for the research worker and decision makers mainly in the investigation of larger areas and longer time frames.

In the present survey, the systematic classification of *Farago et al.* (1989) was followed with some modifications, re-evaluations, and extensions. The investigations of indices showed limited agreement among the drought indices. Actually, the imperfect agreement is a direct consequence of the relative nature of drought and the related specific characteristics of all droughts and indices. It has been revealed that the best identification of drought can be achieved by recursive indices like the *Palmer-index*. It could be acceptable for the author to propose new, refined, or extended definitions of drought, by using the existing definitions of the phenomenon. The paper tried to summarize many drought indices with a restricted philosophical approach of how complicated and mixed the definitions and their explanations are. The only thing which should be highlighted is that many drought definitions and numerical categorizations exist, and it is almost impossible to determine any absolute categorization. On the other hand, we can exactly define the drought quantitatively as a numerical category, and qualitatively as a period with prolonged and abnormal moisture deficiency, which produces reduced plant growth and productivity, causing further significant loss in the economy of the affected nation or region.

References

Alexandrov, V., Matesescu, E., Mestre, A., Kepisnka-Kasparzak, M., Di Stefano, V., and *Dalezios, N.R.*, 2008: Summarising a questionnaire on trends of agroclimatic indices and simulation model outputs in Europe. In *Survey of Agrometeorological Practices and Applications in Europe Regarding Climate Change Impacts* (eds.: *P. Nejedlik* and *S. Orlandini*). COST-ESF, 115-153.

Alley, W.M., 1984: The Palmer Drought Severity Index: Limitations and assumptions. *J. Clim. Appl. Meteorol. 23*, 1100-1109.

Bhalme, H.N. and *Mooley, D.A.*, 1980: Large-scale drought/floods monsoon circulation. *Mon. Weather Rev. 108*, 1197-1211.

Bristow, K.L., 1987: On solving the surface energy balance equations for surface temperature. *Agr. Forest. Meteorol. 39*, 49-54.

Budagovsky, A.I., 1956: Meteorological factors and soil moisture influence on evaporation (in Russian). In *Irrigation Problems in Lower Amu-Darya River*. USSR RAS Publication, Moscow.

Budyko, M.I., 1952: *Climate Change and National Plan of Environment Modification of Arid USSR Areas* (in Russian). Gidrometeoizdat, Leningrad.

Eitzinger, J., Thaler, S., Orlandini, S., Nejedlik, P., Kazandjiev, V., Vucetic, V., Sivertsen, T.H., Mihailovic, D.T., Lalic, B., Tsiros, E., Dalezios, N.R., Susnik, A., Kersebaum, Ch.K., Holden, N.M., and *Matthews, R.*, 2008: Agrocliamtic indices and simulation models. In *Survey of Agrometeorological Practices and Applications in Europe Regarding Climate Change Impacts* (eds.: *P. Nejedlik* and *S. Orlandini*). COST-ESF, 15-92.

Farago, T., Kozma, E., and *Nemes, Cs.*, 1989: Drought indices in meteorology. *Időjárás 93*, 45-59.

Fensham, R.J. and *Holman, J.E.*, 1999: Temporal and spatial patterns in drought-related tree dieback in Australian savanna. *J. Appl. Ecol. 36*, 1035-1050.
Heim, Jr., R.R., 2000: Drought indices: A review. In *Drought* (ed.: *D.A. Wilhite*). Routledge Hazards and Disasters Series, 159-167.
http://drought.unl.edu, 2008
Idso, S.B., Jackson, R.D., Pinter, P.J., Jr., Reginato, R.J., and *Hatfield, J.L.*, 1981: Normalizing the stress-degree-day concept for environmental variability. *Agr. Forest. Meteorol. 32*, 249-256.
Ivanov, N.N, 1948: Landscape and climatic zones of continents (in Russian). *Bulletin of All-Union Geographical Society*. New Ser. Vol. 1.
Jackson, R.D., Idso, S.B., Reginato, R.J., and *Pinter, P.J., Jr.*, 1981: Canopy temperature as a crop water stress indicator. *Water Resour. Res. 17*, 1133-1138.
Jackson, R.D., Reginato, R.J., and *Idso, S.B.*, 1984: Wheat canopy temperatures: a practical tool for evaluating water requirements. *Water Resour. Res. 13*, 651-656.
Jankó Szép, I., Mika, J., and *Dunkel, Z.*, 2005: Palmer drought index as soil moisture indicator: physical interpretation, statistical behaviour and relation to global climate. *Phys. Chem. Earth 30*, 231-243.
Koshelenko, I.,V. and *Volevakha, V.A.*, 1971: Partial impacts of several meteorological factors on droughts formation. *Transactions of Ukrainian Research Hydrometeorological Institute*, N 101.
Mika, J., Horvath, Sz., Makra, L., and *Dunkel, Z.*, 2005: The Palmer Drought Severity Index (PDSI) as an indicator of soil moisture. *Phys. Chem. Earth 30*, 223-230.
Ped, L.A., 1975: On the new drought and over-moistening index (in Russian). *Transactions of the USSR Hydrometeorological Center*, Vol. 156. c., 19-39.
Seguin, B., Courault, D., and *Guérif, M.*, 1994: Surface temperature and evapotranspiration: application of local scale methods to regional scales using satellite data. *Remote Sens. Environ. 48*, 1-25.
Selyaninov, G.T, 1958: The nature and dynamics of the droughts. In *Droughts in the USSR, their Nature, Recurrences and Impact on Crops Yields* (in Russian). Gidrometeoizdat, Leningrad.
Sivertsen, T.H., 2005a: Discussing scientific methods and the quality of meteorological data. In *Use and Availability of Meteorological Information from Different Sources as Input in Agrometeorological Models* (eds.: *G. Maracchi, A. Mestre, L. Toulios*, and *B. Gozzini*). COST Action 718.
Sivertsen, T.H., 2005b: Reflections on the theme of classifying, documenting and exchanging meteorological data. *Atmospheric Science Letters, Vol. 6*, No. 3, John Wiley & Sons, London.
Skvortsov, A.A., 1950: On the question of heat and water exchange in the surface air (in Russian). *Transactions of Middle Asian State University, Vol. 22*, N 6.
Sun, L. and *Ward, M.N.*, 2007: Climate Downscaling: Assessment of the Added Values using Regional Climate Models. In *Climate Prediction and Agriculture* (eds.: *M.V.K. Sivakumar* and *J. Hansen*). Springer, 15-27.
Theophilou, M.K., 2006: Drought indices for the island of Cyprus. In *3rd HAICTA Int. Conference on Information System in Sustainable Agriculture* (eds.: *N.R. Dalezios* and *S. Tzortzios*). COST-University of Thessaly,Volos (Greece), 897-903.
Tsiros, E., Domenikitios, C., and *Dalezios, N.R.*, 2006: Aridity mapping with the use of NDVI and satellite derived degree days. In *3rd HAICTA Int. Conference on Information System in Sustainable Agriculture* (eds.: *N.R. Dalezios* and *S. Tzortzios*). COST-University of Thessaly, Volos (Greece), 853-865.
Wagner, W., Borgeaud, M., and *Noll, J.*, 1996: Soil moisture mapping with the ERS scatterometer. *Earth Observation Quarterly 54*, 4-7.
Wilhite, D.A., 1983: Government response to drought in the US; with particular reference to the Great Plain. *J. Clim. Appl. Meteorol. 22*, 40-50.
Wilhite, D.A., 2005: The role of disaster preparedness in national planning with specific reference to droughts. In *Natural Disasters and Extreme Events in Agriculture* (eds.: *M.V.K. Sivakumar, R.P. Motha*, and *H.P. Das*). Springer, 23-37.
WMO, 1975: Drought and agriculture. *WMO Technical Note 138*, Geneva.
WMO, 1986: Report on drought and countries affected by drought during 1974-1985. *WCP-118*, Geneva.
WMO, 1992: *International Meteorological Vocabulary*. WMO N°182, Geneva.

IDŐJÁRÁS

Quarterly Journal of the Hungarian Meteorological Service
Vol. 113, No. 1–2, January–June 2009, pp. 39–46

Secular trend analysis of growing degree-days in Croatia

Višnja Vučetić

Meteorological and Hydrological Service,
Grič 3, 10000 Zagreb, Croatia; E-mail:vucetic@cirus.dhz.hr

(Manuscript received in final form December 19, 2008)

Abstract—The growing degree-days (GDD) for different temperature thresholds above 5 °C at Croatian stations with long-term time series of meteorological data have been analyzed. The range of the mean annual GDD for the 5 °C threshold is from approximately 2000 °C in the highlands to 4200 °C in the mid-Adriatic. The results of the linear trend and the Mann-Kendall test indicate significant positive trends in annual GDD values at the 0.05 significance level for all thresholds in the northern and mid-Adriatic. A progressive test in the mid-Adriatic shows that the GDD for the 25 °C threshold has become significant since the early eighties and in the northern Adriatic since the early nineties. Such increase has a negative effect on plant growth and development on the Adriatic coast and islands.

Key-words: linear trend, climate change, growing degree-days, temperature thresholds, Croatia

1. Introduction

Degree-days, as a measure of accumulated air temperature deviation from the temperature thresholds, have many practical applications in various human-related activities such as home cooling and heating, power generation, and plant growth in agriculture (*Kadıoğlu et al.*, 1999).

Knowing how significantly air temperature affects plants, it is of the utmost importance to adequately define their reciprocal relationship. The simplest way of presenting the influence of air temperature on plants is by accumulating the required active air temperatures (degree-days). The beginning of vegetation depends on winter length and intensity, which is particularly important in the highlands, where the vegetation period is considerably shorter than in the rest of Croatia. Therefore, knowing the mean degree-days, it is possible to establish the temperature conditions in an area during a certain season, which helps the planning of plant cultivation.

The temperature thresholds typical for particular plant species in their different development stages are: absolute minimum, vegetation zero-point, optimal air temperature, and absolute maximum (*Penzar* and *Penzar*, 2000). With a drop in temperature below the vegetation zero-point, plant growth stops. However, if air temperature drops below the absolute minimum, the cold kills the plants. Plant activity is at its best at optimal air temperature. A growth in temperature above the absolute maximum results in the plants being killed by heat. Thus, one of the goals of this paper is to determine the degree-days above the different temperature thresholds, which is important for plant development. Since most recent climate research indicates an increase in growing-season temperatures, the second goal is to establish the existence of significant trends in degree-days for different temperature thresholds in Croatia using long-term time series of daily meteorological data.

2. *Material and methods*

Degree-days, also referred to as *heat units* or *temperature sums,* have been divided into cooling degree-days, when the temperature threshold is below 0 °C, and heating degree days, when the temperature threshold is equal to or above 0 °C. With most plant species, vegetation starts when enough temperature has been accumulated, i.e., above the 5 °C temperature threshold. Such specific degree-days are called growing degree-days. Therefore, the growing degree-days (GDD) have been analyzed for the 5 °C, 10 °C, 15 °C, 20 °C, and 25 °C temperature thresholds at five meteorological stations: Zagreb-Grič, Osijek, Gospić, Crikvenica, and Hvar, covering the different climatic regions of Croatia (*Fig. 1*).

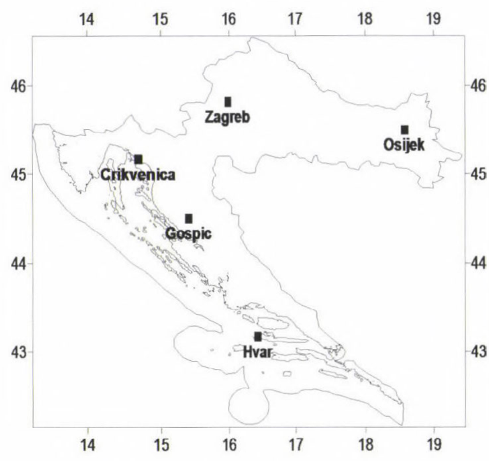

Fig. 1. Geographical position of Croatian stations with long-term time series of meteorological data.

In Croatia there are three types of climate: moderate continental climate in the north-western and eastern part of the country, mountain climate in the highest part of the land, and Mediterranean climate on the Adriatic coast and islands. The northern and eastern parts of the country are the lowest parts of Croatia. It is the Pannonian Plain, which is the main cereal-production region and the most important part of Croatia as regards agriculture. The highest region in Croatia is the Dinaric Alps. This region is characterized by leaf forests and common spruce forests, which are very important for the economy. The Adriatic coast and islands are mostly characterized by viticulture, Mediterranean fruit and olive growing, with little farming and a lot of rocky ground. Pine tree woods and Mediterranean macchia are predominant. In this region, tourism plays the most important role in Croatia.

The Zagreb-Grič and Osijek stations are situated in the region of moderate continental climate: Gospić with mountain, and Crikvenica and Hvar with Mediterranean climate. The data obtained from these stations are the secular series of daily maximum and minimum air temperatures for the period 1901–2000 (except Gospić, which covers 1902–2000). However, only Zagreb-Grič has an uninterrupted series of meteorological data, while Gospić misses 20 years, Hvar 19 years, Osijek six years, and Crikvenica four years.

As the GDD models span from the simple averaging method to complex methods (e.g., *Zalon et al.*, 1983; *McMaster and Wilhelm*, 1997; *Cesaraccio et al.*, 2001; *Schlenker et al.*, 2007), it is necessary to define the most suitable GDD method according to the different daily air temperature cycles of a specific climate region. Croatian research shows that the best methods are the simple averaging method, when daily minimum temperature is greater than the lower temperature threshold and the simple triangulation method, when the daily air temperature cycle is intercepted by the lower threshold (*Salopek*, 2007). In this study, the growing degree-days (GDD) have been defined by the simple averaging method as follows:

$$GDD = \sum_{i=1}^{n}(M_i - T), \qquad M = \frac{t_{\max} + t_{\min}}{2}, \qquad M_i > T, \tag{1}$$

where T is the temperature threshold, $t_{\max}$ is the maximum daily air temperature, $t_{\min}$ is the minimum daily air temperature, n is the number of days in the certain period, and M is the mean temperature.

The growing degree-days have been studied for the whole year as well as for the sub-periods: warm season from April to September and cold season from October to March, from multiannual data series and for the climatic period 1961–1990.

To determine the secular changes in GDD in Croatia, the linear trends of GDD for different temperature thresholds were analyzed. One of the methods for estimating the existence of a trend is the non-parametric Mann-Kendall rank test, based on the values of individual elements of the series and the position of these elements in the series (*Mitchell et al.*, 1966). Namely, if a linear trend exists, the values should increase or decrease chronologically. For significant linear trends at the 0.05 significant level a progressive analysis by *Sneyers* (1990) was used to determine the beginning of a linear trend and its significance.

3. Results and discussion

It would be normal to expect the GDD values to decrease as the temperature threshold increases (*Table 1*). For the lowest and highest temperature thresholds the GDD values have also been depicted graphically in *Fig. 2*. For the seleted Croatian stations there were three warmer periods: in the late twenties and fifties, and the last one starting in the early nineties of last century. A comparison of the secular series with the 30-year normal shows a positive deviation (higher mean annual values of GDD for the period 1901–2000), except at Hvar, which has a negative deviation up to the 10 °C temperature threshold and a positive deviation above it.

The highest mean values of the GDD for all thresholds are found in Hvar and the lowest in Gospić. A temperature mean above 25 °C is very rare in Gospić. As the Zagreb-Grič and Osijek stations are in the same climatic region, their mean annual and sub-period GDD values are similar. There is a bigger difference between the coastal stations in Crikvenica and Hvar than between the inland stations of Zagreb-Grič and Osijek. The annual and sub-period GDD values vary from year to year, as shown by the relatively high standard deviation values.

So far, research on degree-days in the Croatian highlands and lowlands over a 30-year period (1961–1990) has not indicated a significant trend for any temperature thresholds (*Vučetić* and *Vučetić*, 1994, 1996). However, the most recent results from the highlands (1951–2004) showed a significant increase in the number of degree-days for the 15 °C and 20 °C thresholds, which is a consequence of a significant increase in the maximum air temperature in spring and summer (*Vučetić* and *Vučetić*, 2006).

The linear trend results and the application of this test to the data above the defined temperature thresholds are shown in *Table 2*. Linear trends of the mean annual GDD values at the 0.05 significance level exist for the Zagreb-Grič, Crikvenica, and Hvar stations.While for Hvar they are valid for all thresholds in both seasons, for Crikvenica they apply only to the 5 °C threshold. The growth of GDD values at the Zagreb-Grič station, resulting mainly from a significant increase in minimum air temperature (*Vučetić*, 2003), can not be blamed only on global warming but also on the rapid growth of the city of Zagreb in the last hundred years. Linear trend analysis has not confirmed the existence of a significant trend in the annual and sub-period GDD values for Osijek and Gospić, except in Gospić by $T = 10$ °C for the cold season. In Gospić, a growth in the maximum and minimum temperatures has been noticed in winter and spring, but significance has been obtained only for the maximum air temperature in spring (*Vučetić* and *Vučetić*, 2006). This leads to the conclusion that an extreme temperature increase is still not sufficient for a significant increase in the annual GDD values.

Table 1. Mean (MEAN), standard deviation (STD), maximum (MAX), and minimum values (MIN) of growing degree-days (GDD) for different temperature thresholds (T) for selected Croatian stations during the year (Y), warm season (W, April–September), and cold season (C, October–March) in the periods 1961–1990 and 1901–2000

GDD (°C)	T = 5 °C			T = 10 °C			T= 15 °C			T = 20 °C			T = 25 °C	
	Y	W	C	Y	W	C	Y	W	C	Y	W	C	Y	W
ZAGREB-GRIČ														
1901–2000														
MEAN	2855.9	2404.9	451.0	1636.5	1512.9	123.6	736.0	720.5	15.5	186.5	186.3	0.1	11.2	11.2
STD	183.7	148.6	89.2	152.2	141.1	43.3	119.3	117.4	12.6	65.8	65.7	0.6	13.8	13.8
MAX	3523.7	2824.4	743.2	2098.1	1915.6	257.4	1044.6	1040.2	66.5	391.9	391.9	4.6	60.1	60.1
MIN	2468.4	2078.9	246.0	1280.8	1217.7	27.1	459.9	459.6	0.0	67.2	67.2	0.0	0.0	0.0
1961–1990														
MEAN	2817.2	2362.0	455.2	1597.5	1468.6	128.9	691.1	675.4	15.7	160.0	159.8	0.1	7.2	7.2
STD	160.7	115.7	89.7	126.5	110.0	44.4	89.9	88.2	13.1	43.0	43.0	0.4	6.6	6.6
MAX	3069.3	2598.0	645.0	1803.5	1688.7	226.5	851.8	837.4	66.5	248.2	248.2	1.5	27.4	27.4
MIN	2468.4	2086.1	332.0	1290.5	1217.7	70.9	459.9	459.6	0.3	67.2	67.2	0.0	0.0	0.0
OSIJEK														
1901–2000														
MEAN	2763.6	2361.7	403.5	1589.7	1476.3	114.7	712.1	695.9	17.2	173.7	173.2	0.3	9.9	9.9
STD	149.9	130.3	80.3	127.2	122.8	42.0	102.0	100.9	15.5	55.0	54.6	1.2	10.0	10.1
MAX	3223.1	2735.0	629.4	1922.7	1829.6	240.8	967.9	967.9	84.2	323.6	323.6	9.0	55.1	55.1
MIN	2415.1	2072.6	224.7	1320.2	1225.7	38.3	488.7	481.7	0.0	74.3	73.8	0.0	0.0	0.0
1961–1990														
MEAN	2739.8	2337.2	402.6	1565.8	1449.3	116.5	684.3	667.4	17.0	154.7	154.5	0.2	6.2	6.2
STD	148.5	117.6	82.9	118.7	111.2	39.6	89.7	88.8	15.7	41.9	42.0	0.6	6.7	6.7
MAX	2974.2	2540.7	562.5	1774.7	1649.9	240.8	845.2	827.8	84.2	239.5	239.5	2.9	26.9	26.9
MIN	2415.1	2072.6	271.4	1320.2	1225.7	61.0	488.7	481.7	1.0	77.4	77.4	0.0	0.0	0.0
GOSPIĆ														
1902–2000														
MEAN	2039.3	1766.2	272.2	985.3	932.6	54.8	298.7	296.8	4.0	25.1	25.1	0.0	0.3	0.3
STD	158.3	137.6	67.0	130.8	124.1	29.8	86.0	85.0	5.2	23.6	23.3	0.2	0.9	0.9
MAX	2511.5	2168.0	469.9	1328.8	1285.0	153.6	522.3	519.8	27.9	112.8	112.8	1.5	6.1	6.1
MIN	1689.9	1479.1	108.8	706.1	685.0	4.2	139.5	139.5	0.0	0.0	0.0	0.0	0.0	0.0
1961–1990														
MEAN	1968.8	1704.8	264.0	925.1	872.5	52.6	255.4	252.5	2.9	16.2	16.2	0.0	0.0	0.0
STD	125.9	107.1	60.7	97.5	92.2	26.0	56.7	56.1	3.4	11.9	11.9	0.0	0.1	0.1
MAX	2160.9	1878.1	409.4	1123.6	1071.0	122.0	373.4	368.9	11.5	45.6	45.6	0.0	0.4	0.4
MIN	1689.9	1479.1	154.3	706.1	685.0	4.2	139.5	139.5	0.0	0.7	0.7	0.0	0.0	0.0
CRIKVENICA														
1901–2000														
MEAN	3446.1	2632.2	814.6	1972.5	1724.5	248.0	940.1	898.0	42.1	282.8	281.6	1.3	25.3	25.3
STD	230.0	174.7	100.0	203.0	172.0	59.1	164.9	154.3	24.2	106.3	105.4	2.5	27.4	27.4
MAX	4057.4	3134.3	1061.5	2558.3	2219.3	397.6	1418.0	1344.4	118.7	617.8	617.8	13.9	130.3	130.3
MIN	3006.3	2275.3	554.9	1516.5	1377.0	107.3	615.0	607.3	0.0	71.6	71.3	0.0	0.0	0.0
1961–1990														
MEAN	3416.9	2599.9	819.5	1941.7	1691.5	250.5	910.8	867.3	43.8	265.4	264.7	1.0	20.4	20.4
STD	134.8	108.4	71.6	126.5	108.3	48.1	104.5	99.0	19.2	63.3	63.4	1.8	12.7	12.7
MAX	3650.2	2786.6	975.0	2199.0	1884.0	318.6	1128.0	1076.4	88.9	401.6	401.6	6.9	53.4	53.4
MIN	3117.9	2405.5	678.5	1684.2	1500.1	121.5	737.2	708.6	0.0	167.3	167.3	0.0	1.2	1.2
HVAR														
1901–2000														
MEAN	4209.1	2942.3	1268.4	2531.4	2030.2	499.7	1277.4	1161.2	117.6	460.2	452.9	9.1	56.3	56.3
STD	170.0	123.1	93.8	151.1	121.4	67.6	127.9	112.4	38.2	96.2	94.6	8.5	32.4	32.4
MAX	4644.2	3264.3	1470.9	2948.2	2349.2	649.6	1602.6	1453.8	199.9	709.6	697.2	47.6	166.1	166.1
MIN	3779.7	2692.6	1055.5	2158.3	1782.8	314.8	999.3	928.0	29.9	152.4	151.8	0.0	4.0	4.0
1961–1990														
MEAN	4225.8	2943.4	1282.4	2536.6	2029.4	507.2	1277.1	1155.1	121.9	459.1	449.8	9.3	53.6	53.6
STD	122.3	103.7	63.7	118.2	103.5	48.2	106.7	94.7	37.5	76.8	74.4	7.2	24.2	24.2
MAX	4406.8	3102.6	1433.8	2719.5	2187.6	602.0	1444.6	1309.2	189.6	600.6	593.0	22.6	106.5	106.5
MIN	3939.8	2709.3	1165.8	2248.8	1794.6	440.9	1016.1	937.7	37.1	300.8	300.4	0.0	11.4	11.4

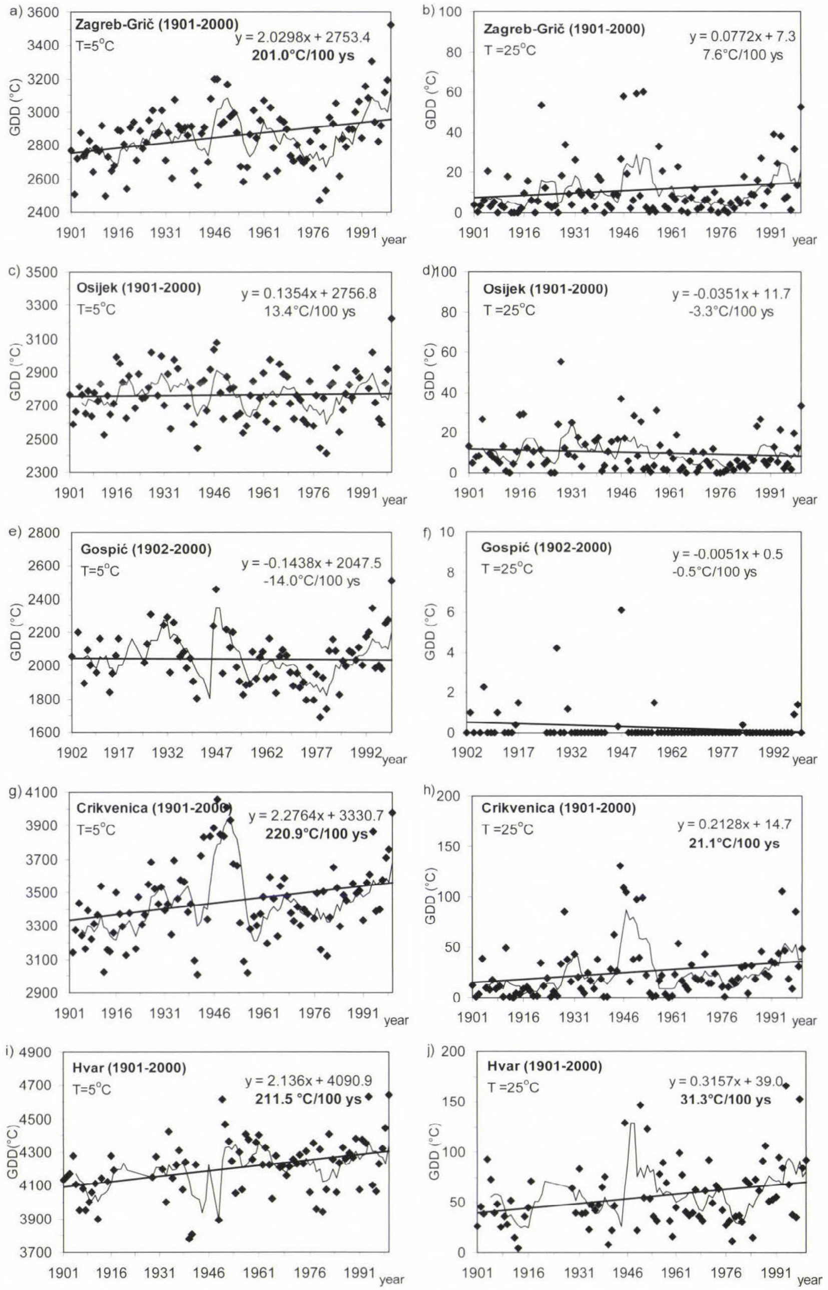

Fig. 2. Time series of the growing degree-days (GDD, diamonds) for the temperature thresholds of 5 °C and 25 °C, curves of the 5-year running average (thin line) and linear trends (thick line) for selected Croatian stations during the period 1901–2000. x is the number of years (1, 2, 3…) and the α significant level of 0.05 is bold according to the Mann-Kendal test.

Table 2. Linear trend of growing degree-days (°C/100 years) for different temperature threshold (T) for selected Croatian stations during the year (Y), warm season (W, April–September), and cold season (C, October–March) for the period 1901–2000. Linear trends at the 0.05 significant level are bolded according to the Mann-Kendal test

Trend	T = 5 °C			T = 10 °C			T= 15 °C			T = 20 °C			T = 25 °C	
	Y	W	C	Y	W	C	Y	W	C	Y	W	C	Y	W
Zagreb-Grič	**201.0**	**115.6**	**85.4**	**144.0**	105.4	**38.6**	76.7	71.3	**5.5**	35.0	35.0	–	7.6	7.6
Osijek	13.4	3.3	5.3	12.9	-2.4	12.0	-1.4	-9.6	-0.1	-12.7	-12.6	–	-3.3	-3.3
Gospić	-14.0	-25.1	33.4	-28.2	-35.5	**15.2**	-28.3	-33.5	0.7	-2.4	-2.4	–	-0.5	-0.5
Crikvenica	**220.9**	**143.9**	**73.6**	**177.7**	**140.1**	34.2	**142.2**	**127.9**	11.6	**94.0**	**93.8**	–	**21.1**	**21.1**
Hvar	**211.5**	**107.5**	**99.8**	**168.9**	**103.0**	**67.1**	**126.9**	**93.4**	**32.1**	**100.8**	**94.7**	–	**31.3**	**31.3**

A progressive test (*Sneyers*, 1990) of the annual GDD trend in Hvar shows that GDD growth started at the end of the 1940s (*Fig. 3*). It became significant in the early 1960s for the thresholds below 10 °C and in the early 1980s for the higher thresholds, while the significant period in Crikvenica started in the early 1990s. As most plants suffer from heat stress, the positive trend in GDD above 25 °C reveals an increasing negative effect of high temperatures on plants, especially on the Adriatic coast and islands.

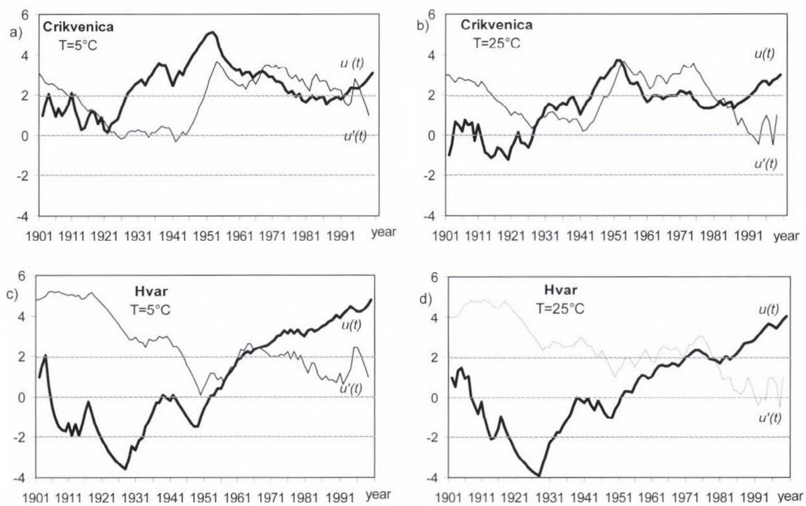

Fig. 3. The progressive trend test in growing degree-days for the temperature thresholds of 5 °C and 25 °C for the forward series $u(t)$ (thick line) and backward series $u'(t)$ (thin line) for Crikvenica and Hvar during the period 1901–2000. The positive $u(t)$ points show an increasing trend, while the negative $u(t)$ points are at a decreasing trend. In order to identify the beginning of the possible trend, $u(t)$ has been calculated from the first to the last date, forming a progressive onward test series. The backward test series $u'(t)$ has been formed in the same manner, calculated from the last to the first term. If there is no trend, the $u(t)$ and $u'(t)$ curves overlap several times, whereas in the case of a trend, the intersection point designates the beginning of the trend, becoming significant at the 0.05 level in the case when the absolute $u(t)$ exceeds the 1.96 value.

4. Conclusion

The significant positive trend in the growing degree-days for the 25 °C temperature threshold indicates that the mid-Adriatic coast and islands are subject to the highest vulnerability to climate change in Croatia. In this region, the growth in high temperatures and the risk of summer droughts account for high current vulnerability in agriculture and forestry. This vulnerable region has spread from the middle Adriatic to the northern Adriatic in the warm season, but there is no higher risk towards the inland mountains. If all available potential adaptation measures (particularly irrigation systems) were implemented in this region, the vulnerabilities could be brought to a lower level.

Acknowledgement—This research has been carried out as a part of the the projects: COST734 *Impacts of Climate Change and Variability on European Agriculture* (*CLIVAGRI*) and *Climate Variations and Changes and Response in Affected System* (004-1193086-3035) of the Ministry of Science, Education and Sport of Republic of Croatia.

References

Cesaraccio, C., Spano, D., Duce, P., and *Snyder, R.L.*, 2001: An improved model for determining degree-day values from daily temperature data. *Int. J. Biometeorol.* 45,161–169.

Kadıoğlu, M., Şen, Z., and *Gültekin, L.*, 1999: Spatial heating monthly degree-day features and climatological patterns in Turkey. *Theor. Appl. Climatol. 64*, 263–269.

McMaster, S.G. and *Wilhelm, W.W.*, 1997: Growing degree-days: one equation, two interpretations. *Agr. Forest Meteorol. 87,* 291–300.

Mitchell, J.M. Jr., Dzerdzeevskii, B., Flohn, H., Hofmeyr, W.L., Lamb, H.H., Rao K.H, and *Wallen, C.C.*, 1966: Climatic Change. *WMO Tech. Note 79*, Geneva, 58–75.

Penzar, I. and *Penzar, B.*, 2000: *Agrometeorology* (in Croatian). Školska knjiga, Zagreb.

Salopek, I., 2007: Different growing degree-day methods of calculation and their application in agriculture (in Croatian). *Theses*, Faculty of Agriculture, University of Zagreb, Zagreb.

Schlenker, W., Hanemann, W.M., and *Fisher, A.C.*, 2007: Water availability, degree days and the potential impact of climate change on irrigate agriculture in California. *Climate Change 81*, 19–38.

Sneyers, R., 1990: On the statistical analysis of series of observations. *WMO Tech. Note 143*, 1–15.

Vučetić, V., 2003: Climatic characteristics in the area of Sv. Ivana Zelina (in Croatian). *Proceedings of Conference of the Zelina area in past,* Sv. Ivan Zelina, Croatia, 15 December 2000, 361–378.

Vučetić, M. and *Vučetić, V.*, 1994: Degree days in the mountain area of Croatia. *Annalen der Meteorogie 30*, 356–360.

Vučetić, V. and *Vučetić, M.*, 1995: Degree days in the Croatian lowland. *Proceedings of International Conference of Climate Dynamics and the Global Change Perspective*, Krakow, Poland, 17–20 October 1995, 359–364.

Vučetić, V. and *Vučetić, M.*, 2003: Phenological characteristics in the area of Zavižan (in Croatian). *Šumarski list 7–8*, 359–372.

Vučetić, V. and *Vučetić, M.*, 2005: Temperature sums and climatic variations in the Parg region. *Hrv. meteor. časopis 40*, 217–220.

Vučetić, V. and *Vučetić, M.*, 2006: The phenological fluctuations as a possible signal of climatic changes in the Croatian mountain area. *Meteorol. Z., 15*, 237–242.

Zalom, F.G., Goodell, P.B., Wilson, W.W., and *Bentley, W.J.*, 1983: *Degree-days: The calculation and the use of heat units in pest management.* Leaflet n 21373. Division of Agriculture and Natural Resources, University of California, Davis.

IDŐJÁRÁS

Quarterly Journal of the Hungarian Meteorological Service
Vol. 113, No. 1–2, January–June 2009, pp. 47–54

Progress in dryness and wetness parameters in altitudinal vegetation stages of West Carpathians: Time-series analysis 1951–2007

Jaroslav Škvarenina[1], **Ján Tomlain**[2], **Ján Hrvoľ**[2], **Jana Škvareninová**[1], and **Pavol Nejedlík**[3]

[1]*Technical University Zvolen,*
T. G. Masaryka 24, 960 53 Zvolen, Slovak Republic
E-mails: jarosk@vsld.tuzvo.sk, janask@vsld.tuzvo.sk

[2]*Comenius University Bratislava,*
Mlynská dolina, 842 48 Bratislava, Slovak Republic
E-mails: tomlain@fmph.uniba.sk, hrvol@fmph.uniba.sk

[3]*Slovak Hydrometeorological Institute Bratislava,*
Jeséniova 17, 833 15 Bratislava, Koliba Slovak Republic
E-mail: pavol.nejedlik@shmu.sk

(Manuscript received in final form January 8, 2009)

Abstract—This article analyzes trends in the occurrence of dry and wet periods in altitudinal vegetation stages in the West Carpathian region of Slovakia for the period 1951–2007. The relative evapotranspiration, drought index, and radiation drought index were applied on meteorological data from eight meteorological stations representing the predominant vegetation stages in the investigated region. These indices were used to characterize humidity conditions. The radiation drought index ranges from 1.31 for the area heavily prone to drought (southern part), to 0.41 for the mountainous areas (northern part), where the sum of precipitation exceeds potential evapotranspiration. The relative evapotranspiration shows values as high as 97% in northern mountainous regions to the low value of 58% in the Danubian Lowland. A significant increase in the severity of drought was identified by means of the radiation drought index for the period 1951–2007 only in the Danubian Lowland (stage 1, oak vegetation). A significant trend in the case of humidity was determined in the mountains and in the northern part of East Slovakia.

Key-words: drought, drought index, radiation drought index, actual evapotranspiration, potential evapotranspiration, precipitation, relative evapotranspiration, vegetation stage

1. Introduction

In principle, drought is defined as the state of water deficit concerning soil, plants, and atmosphere (*Krečmer,* 1980). In agriculture and forestry, it is understood as an important meteorological factor, distressing all ecosystems. Drought features strongly vary from region to region. The primary cause of drought under the conditions prevalent in the investigated territory is a deficit at precipitation over a certain period of the growing season. Other climatic factors, such as high temperature, strong wind, and low relative humidity, can significantly aggravate its severity (*Hayes et al.*, 1999; *Heim*, 2002).

Altitude and topography are strong climate-differentiating factors. Consequently, under conditions of considerably broken topography in the West Carpathians, drought plays an extra-important role. The primary importance of climate from the point of view of the natural vegetation has already been pointed out by *Zlatník* (1976). The author defines the vegetation stages as basic units characterizing altitudinal climate conditions (vertical differentiation) through vegetation (biocenoses). The bio-geocenoses resulted from variability in altitude, exposure, and topography can be classified as belonging to 9 vegetation stages. The Slovak territory has been divided by *Zlatník* (1976) into altitudinal vegetation stages named after the significant tree or bush indicator species dominating the area. These stages are characterized by their dominant climax tree species as follows: stage 1, oak (*Quercus*) vegetation, stage 2, beech-oak (*Fagus-Quercus*) vegetation, stage 3, oak-beech (*Quercus-Fagus*) vegetation, stage 4, beech (*Fagus*) vegetation, stage 5, fir-beech (*Abies-Fagus*) vegetation, stage 6, spruce-fir-beech (*Picea-Abies-Fagus*) vegetation, stage 7, spruce (*Picea*) vegetation, stage 8, mountain pine (*Mughetum*) vegetation, stage 9, alpine vegetation (non-forest high mountain pastures).

The vegetation stages of lower elevations, i.e., oak vegetation (stage 1), oak vegetation with admixture of beech (stage 2), and beech vegetation with admixture of oak (stage 3) are rather arid during the vegetation period (from March to September). The precipitation deficit reaches 100–300 mm during the vegetation season. The beech vegetation (stage 4) is characterized by an equitable climatic water balance. The climate humidity increases in higher vegetation stages (beech vegetation with fir (stage 5) and fir with beech and spruce (stage 6)). Humidity belongs to the fundamental properties of mountain forests. The water balance reaches the highest values in the 8th vegetation stage of mountain dwarf pine and the 9th alpine stage, where the amount of precipitation considerably exceeds the evaporation requirements of the atmosphere. Within the annual balance, the surplus of precipitation water is approximately 1000 mm (*Škvarenina et al.,* 2004). Experiments confirmed that under optimum conditions of plant growth, the actual evapotranspiration (E) is proximate to the potential one (to the maximum possible evapotranspiration under the given climatic conditions from sufficient soil moisture – E_0). That is why the ratio E/E_o (relative evapotranspiration) and the drought index (E_o/P, where P is the total precipitation) enable the quantification of the deficit of water in the soil root zone for optimum plant growth (*Budyko* and *Zubenok*, 1961). The radiation drought index (B/LP), where B is net radiation and L is the latent heat of vaporization, expresses the energy of net radiation in amounts of heat needed to evaporate the annual precipitation total. The indices were proposed to characterize general environmental conditions and processes on the Earth's surface. It approximates the ability of precipitation to provide the water required by native vegetation for an undisturbed evapotranspiration process and is often used in ecological studies (*Tomlain*, 1996; *Tomlain*, 2004).

In this paper, for the first time, we present the relative evapotranspiration, radiation drought index, and drought index results for the altitudinal vegetation stages in Slovakia, covering the period 1951–2007.

2. Method

Relative evapotranspiration and drought indices express functional dependencies among all energy and water balance equation components of the locality (net radiation, air temperature and humidity, turbulent state of atmosphere, difference of saturation water vapor pressure at the temperature of evaporating surface and water vapor pressure in the air, precipitation, change of critical soil moisture during the year, and heat flux in the soil). The model resulted from common solution of the energy and water balance equations was performed at eight selected climatic stations in the investigated territory. The following data were taken as inputs into the model: air temperature and humidity, cloudiness, precipitation, and number of days with snow cover. The potential evapotranspiration was computed by the equation of water vapor diffusion in the atmosphere according to *Budyko* and *Zubenok* (*Budyko*, 1980), and the actual evapotranspiration was supposed to be proportional to the potential evapotranspiration:

$$E = E_o\, W / W_o, \qquad (1)$$

where the water storage W is specified as a moisture content stored in the upper soil layer of 1 m depth and W_o as a critical value above which E equals to E_o. W_o usually amounts to a layer of 100–200 mm of water with seasonal and regional variations. The average soil moisture, $W = (W_1 + W_2)/2$, is determined from the water balance equation by the method of step-by-step approximation (W_1 is the moisture stored in the soil layer at the beginning of the month, and W_2 is the same at its end). As the number of meteorological stations for which the potential evapotranspiration has been calculated was limited, we decided to use the method of representative climatic stations, where the station represents the climate-hydric conditions of a particular vegetation stage. The climatic stations were classified into the appropriate vegetation stages (stages 1–8). For stage 9 there were no data based on the map of vegetation stages (*Raušer* and *Zlatník*, 1966) and typological maps of the forest type groups (scale 1:200,000).

3. Results and discussion

Table 1 presents the average annual values of seven parameters affecting the humidity conditions at selected stations in 1951–2007 as well as their classification into vegetation stages. The distribution of stations in the territory is shown in *Fig. 1*. The territory of the West Carpathians is divided into the area of Pannonia (Pannonian Lowland) and the foothills to the north, influenced by Mediterranean climate, and the area of the inner Carpathians, influenced by sub-ocean mountainous climate and by the climate of both Northern and Baltic Seas. The line dividing these areas has been determined by *Zlatník* (1959) by the so-called main climatic line, where the Carpathian bow separates two European climatic areas. The area to the north of this line is quite wetter and colder than the southern one, which is drier and warmer. The northern part is favorable for the growth of spruce, unlike the southern part, where spruce grows only in the highest vegetation zone.

The E/E_0 is a suitable measure of the water sufficiency for vegetation. It approaches its lowest values of about 60% in the lowest areas. Towards the higher vegetation stages, the E/E_0 increases reaching more than 90% in stage 4 beech vegetation. However, in the mountain sites this measure partly loses its accuracy. By the 5th vegetation stage its resolution approaches only about 1–5%. Finally, the B/LP has appeared as the most suitable complex index for describing the humidity and drought phenomenon in the region. It keeps higher stability than E_0/P, while accounting both for energy and precipitation elements.

Table 1. Average annual values of net radiation (B) in kWh m^{-2}, precipitation (P) in mm, radiation drought index (B/LP), drought index (E_0/P), potential (E_0) and actual evapotranspiration (E) in mm, and relative evapotranspiration (E/E_0) in percentages at selected locations of Slovakia for the period 1951–2007 (L is the latent heat of vaporization)

Station	H(m)	B	P	B/LP	E_0/P	E_0	E	E/E_0	Vegetation stage
Hurbanovo	115	488	537	1.31	1.40	751	433	58	1, oak
Myjava	375	461	672	0.99	0.94	630	449	71	2, beech-oak
Kamenica and Cirochou	178	467	722	0.93	0.89	645	500	78	3, oak-beech
Plaveč	488	410	694	0.85	0.75	523	450	86	4, beech
Červený Kláštor	474	410	763	0.77	0.67	509	458	90	5, fir-beech
Oravská Lesná	780	392	1116	0.51	0.41	458	433	95	6, spruce-fir-beech
Ždiar-Javorina	1020	356	1258	0.41	0.34	426	414	97	7, spruce
Štrbské Pleso	1360	357	997	0.52	0.44	437	408	93	7, spruce, 8, mountain pine

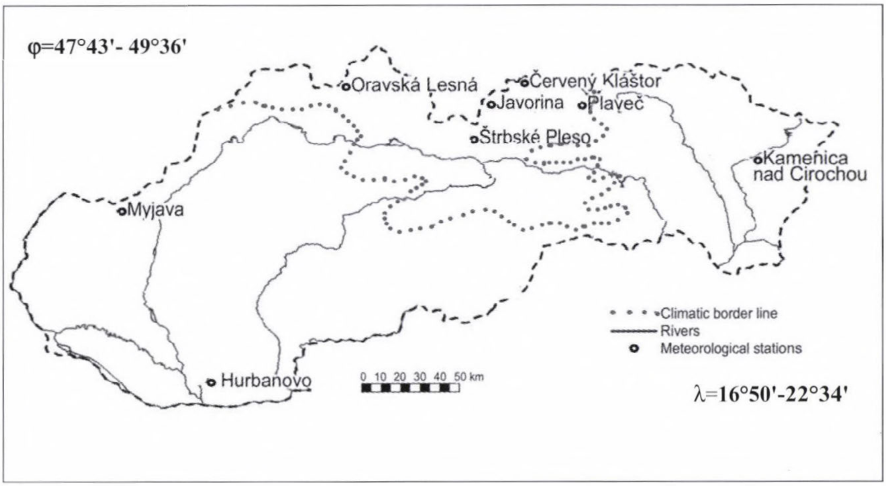

Fig. 1. The borders of Slovakia (dashed line) representing the West Carpathians with particular meteorological stations that represent conditions in the vegetations stages. The map displays the climatic border line (dotted line) and rivers (solid lines).

The E_o/P describes the relationship between the energy and precipitation inputs within particular vegetation stages. Beyond any expectations, the E_o/P index proved to be very sensitive to altitudinal changes and it was able to detect differences in bioclimatological conditions also in the comparatively small territory of the investigated region. As presented by Budyko (1980), the values of $E_o/P > 1$ indicate the territory of dry (arid) climate (steppe, forest-steppe). Values of $0.3 < E_o/P < 1$ specify forest bioms and values of $E_o/P < 0.3$ reveal the climate ecosystems of tundra or mountain forest of a temperate zone as well. The presented distribution of E_o/P values also corresponds to climate conditions in Slovakia. Warm forest-steppe formations dominated by oak, provides E_o/P values about 1. This represents the 1st vegetation stage (in the sense of Zlatnik classification) or a part of the 2nd vegetation stage dominated by beech-oak formations. Vegetation stages up to the E_o/P value of 0.3 represent the predominant area of Slovak forest; the values of index E_o/P decrease relatively proportionaly when related to both increasing altitude and precipitation amounts. The vegetation stages with $E_o/P < 0.3$ are of mountainous (boreal) climate, characterized by low temperatures and high precipitation amounts, with norway spruce and dwarf pine being the predominant tree species growing here.

The radiation drought index reaches the value about 1.3 in our driest region Hurbanovo. In mountainous areas which are rich in precipitation (Štrbské Pleso, Ždiar-Javorina) it moves about a mean value of 0.5. *Fig. 2* presents the regression dependence between the average annual values of the radiation drought index and the terrain altitude. Annual values of this index in the period 1951–2007 varied from 0.90 (1965, P = 827 mm) to 2.08 (2003, P = 333 mm) at

Hurbanovo, from 0.64 (1974, P = 1010 mm) to 1.68 (1961, P = 400 mm) at Kamenica nad Cirochou, from 0.76 (1987, P = 825 mm) to 1.55 (2003, P = 445 mm) at Myjava, from 0.53 (1980, P = 908 mm) to 1.15 (1971, P = 548 mm) at Červený Kláštor, from 0.62 (1985, P = 930 mm) to 1.31 (1961, P = 477 mm) at Plaveč, from 0.36 (1974, P = 1463 mm) to 0.72 (1959, P = 860 mm) at Oravská Lesná, from 0.25 (1980, P = 1630 mm) to 0.61 (1971, P = 908 mm) at Ždiar-Javorina, and from 0.35 (2004, P = 1299 mm) to 0.79 (1986, P = 690 mm) at Štrbské Pleso.

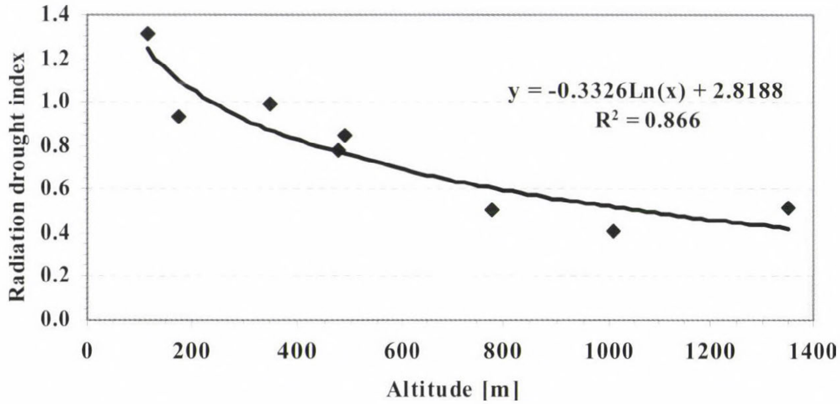

Fig 2. Logarithmic regression dependence of the radiation drought index annual values on the altitude (m a.s.l.) on the territory of Slovakia for the period 1951–2007.

The results presented in *Fig. 3* point out the overwhelming trend to aridity at the station in Hurbanovo, situated in the southern part of Slovakia. In Hurbanovo, as well as at other stations, linear and polynomial trends practically mingled one with another, so that only the linear trend is shown. This station represents the regions of most intensive agricultural production in Slovakia. Frequent occurrence of drought as well as its rising frequency negatively influences the production of the main crops in this region as well as in other regions of Central Europe (*Hlavinka et al.*, 2008; *Dubrovský et al.*, 2008). Further more, a statistically significant tendency to more intensive dry episodes in the region were stated by recent studies (*Brazdil et al.*, 2008). The next two stations with elevations below 500 m a.s.l. show practically no time trend in B/LP with relatively good water supplies as E_o/P drops below 1. B/LP starts to show the trend to lower values from the elevation around 500 m a.s.l. The stations situated to the north of the climatic line (Štrbské Pleso, Ždiar-Javorina, and Červený Kláštor) show an overwhelming trend to humidity during 1951–2007. Similar results are also presented by *Škvarenina et al.* (2008).

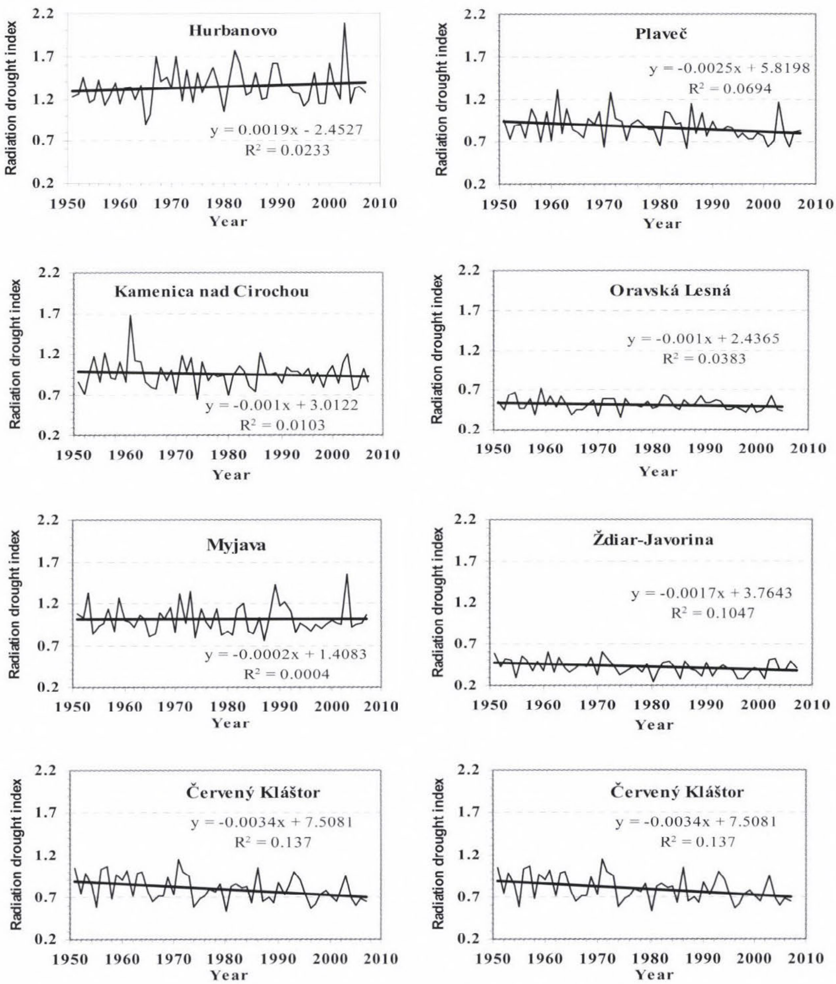

Fig. 3. Long-term course of the radiation drought index annual values at stations Hurbanovo, Kamenica nad Cirochou, Myjava, Červený Kláštor, Plaveč, Oravská Lesná, Ždiar-Javorina, and Štrbské Pleso for the period 1951–2007 with the linear trend.

4. *Conclusions*

- The calculations show that the radiation drought index is a suitable bioclimatic parameter. Its averages vary in a wide range from 1.31 in our driest region to 0.41 in mountain locations, but it is sensitive enough to indicate and reflect the diverse ecological conditions of the West

Carpathians from xerotherm oak plant communities to mountainous plant communities of spruce and dwarf pine.

- Maximum values of the radiation drought index for the processed period did not occur in the east and west parts of Slovakia in the same year.
- A significant increase in the severity of drought was identified from 1951 to 2007 only in the Danubian Lowland (stage 1, oak vegetation).
- In the mountains and in the northern part of East Slovakia, a significant trend of humidity increase was determined.

Acknowledgement—The study was supported by research grants VEGA No. 1/0515/08, 1/4393/07, 1/3528/06, from the Slovak Grant Agency for Science.

References

Brázdil, R., Trnka, M., Dobrovolný, P., Chromá, K., Hlavinka, P., and *Žalud, Z.*, 2008: Variability of droughts in the Czech Republic, 1881–2006. *Theor. Appl. Climatol.* (online first) 10.1007/s00704-008-0065-x.

Budyko, M.I., 1980: *Climate in the Past and in the Future* (in Russian). Gidrometeoizdat, Leningrad.

Budyko, M.I. and *Zubenok, L.I.*, 1961: The determination of evaporation from the land surface (in Russian). *Izv. Ak. Nauk SSR, Se. Geog. 6*, 3–17.

Dubrovský, M., Svoboda, M.D., Trnka, M., Hayes, M.J., Wilhite, D.A., Zalud, Z., Hlavinka, P., 2008: Application of relative drought indices in assessing climate change impacts on drought conditions in Czechia. *Theor. Appl. Climatol.* (online first) DOI 10.1007/s00704-008-0020-x.

Hayes, M.J., Sovoboda, M.D., Wilhite, D.A., and *Vanyarko, O.V.*, 1999: Monitoring the 1996 Drought by Standardized Precipitation Index. *American Meteorolog. Society 80,* 429-438.

Heim, R.R, 2002: A review of Twentieth-Century drought indices used in the United States. *B. Am. Meteorol. Soc. 83,* 1149-1165.

Hlavinka, P., Trnka, M., Semerádová, D., Dubrovský, M., Žalud, Z., Možný, M., 2008: Effect of drought on yield variability of key crops in Czech Republic. *Agr. Forest Meteorol.* (in press).

Krečmer, V., 1980: Bioklimatological explanatory dictionary of terms (in Czech). *Academia Praha.*

Raušer, J. and *Zlatník, A.*, 1966: Biogeography (map No. 21) (in Czech). *Atlas ČSSR*, Karto-grafický a reprodukční ústav, Praha.

Střelcová, K., Matejka, F., and *Kučera, J.*, 2004: Beech stand transpiration assessment – two methodical approaches. *Ekológia 23 (Suppl. 2/2004)*, 147-162.

Škvarenina, J., Križová, E., and *Tomlain, J.*, 2004: Impact of the climate change on the water balance of altitudinal vegetation stages in Slovakia. *Ekológia 23 (Suppl. 2/2004)*, 13-19.

Škvarenina, J., Tomlain, J., Hrvoľ, J., Škvareninová, J., and *Hlavatá, H.*, 2008: Occurrence of dry and wet periods in altitudinal vegetation stages of West Carpathians in Slovakia: time-series analysis 1951–2005 and prognosis of expected climatic changes. *National Climate Programme,* No. 12, Slovak Ministry of Environment, SHMI, Bratislava, 74-123.

Tomlain, J., 1996: Model computation of the climatic change impacts on potential and actual evapotranspiration changes on the territory of Slovakia (in Slovak). *National Climate Programme, No. 4,* Slovak Ministry of Environment, SHMI, Bratislava, 45-74.

Tomlain, J., 2004: Contribution to humid conditions of Slovakia. *Acta Meteorologica Universitatis Comenianae 33,* 21-30.

Zlatník, A., 1959: Waldtypengruppen der Slowakei.Vysoká škola zemědelská, Brno.

Zlatník, A., 1976: Forest phytocenology (in Slovak). Státní zemědelské nakladatelství, Praha.

IDŐJÁRÁS
Quarterly Journal of the Hungarian Meteorological Service
Vol. 113, No. 1–2, January–June 2009, pp. 55–68

Sustainable production zoning for agroclimatic classification using GIS and remote sensing

Emmanouel Tsiros, Christos Domenikiotis, and **Nicolas R. Dalezios**

School of Agricultural Sciences, Laboratory of Agrometeorology,
University of Thessaly, Fitokou Str, N. Ionia, 38446 Volos, Greece; E-mail: etsiros@uth.gr

(Manuscript received in final form December 31, 2008)

Abstract—Agriculture is a primary productivity sector which is highly dependent on environmental conditions. The agroclimatic potential of agricultural areas has to be assessed in order to achieve sustainable and efficient use of natural resources in combination with production maximization. Temperature and rainfall, in terms of quantity and spatiotemporal variability, are variables which determine the type of crops suitable to a given location. Rainfall variable can also be interpreted as availability of sufficient water required for production of given crops. These variables, in combination with soil type and geomorphology, also determine areas where high levels of production are appropriate, avoiding the threat of degrading the natural resources. In the current work, zones indicating water availability are combined with topographic features and soil types in order to identify areas for sustainable production. Firstly, aridity index (AI) and vegetation health index (VHI) are used in order to define zones adequate for sustainable farming according to water limitations. As crop growth is affected by water supply, these zones are named water limited growth environment (WLGE) zones. AI and VHI are computed on monthly time step for twenty hydrological years, from October 1981 to September 2001. VHI is derived from NOAA/AVHRR data, while in AI computations both satellite and conventional field data are used. Then, WLGE zones are combined with soil maps and a digital elevation model (DEM) of the area under investigation in order to define zones appropriate for sustainable production. The study area is the aquatic district of Thessaly, located in Central Greece. The current application has resulted in the definition of sustainable production zones by means of parallelepiped supervised classification using the two indices, soil maps and DEM. These zones can be further used for agroclimatic classification.

Key-words: sustainable production, WLGE, VHI, AI, remote sensing, GIS

1. Introduction

The climate is among the most important factors that determine the agricultural potentialities of a region and the suitability of a region for a specific crop, whereas the yield is determined by weather conditions (*Pereira*, 1982). Since agriculture is highly dependent on environmental conditions, a quantitative understanding of the climate of a region is essential for developing improved farming systems (*Reddy*, 1983).

Temperature and rainfall, in terms of quantity and spatiotemporal variability, are variables which determine the type of crops suitable to a given location (*Mavi* and *Tupper*, 2004). Even thought crop production depends on every environmental condition, almost all agroclimatic classifications take into account these variables. These climatic parameters in combination with soil type and geomorphology can determine areas where high levels of production are appropriate, avoiding the threat of degrading the natural resources (*Mavi* and *Tupper*, 2004).

Crop production requires the availability of sufficient water. In irrigated and rainfed agriculture, production is often constrained by water limitations during the growing season. Amount and distribution of rain during the growing season and supplemental irrigation along with soil characteristics and evapotranspiration losses determine the temporal pattern of water availability for plant use and the ensuing crop biomass and economic yield (*Arora* and *Gajri*, 1998).

The amount of rain needed for the production of a crop differs from region to region, mainly due to the decreasing "effectiveness" of rainfall in order to maintain plant growth due to the increasing evaporation (*Tow*, 1991). Effective rainfall is related to the moisture available in the plant's root zone, allowing the plant to germinate, emerge, and maintain its growth (*Mavi* and *Tupper*, 2004). There are many climatic and agroclimatic classifications seeking to describe the moisture conditions of crops (e.g., *Thornwaite*, 1948; *Reddy*, 1983). These classifications vary in complexity, ranging from the use of one parameter to methods incorporating a number of parameters. Most of these agroclimatic classifications used rainfall and potential evapotranspiration in order to delimit the growth environment of crops (*Badini et al.*, 1997).

Badini et al. (1997) investigated the water limited growth environment (WLGE) for millet cultivation in Burkina Faso, where rainfed production is a major source of food and income. They used aridity index (AI) and crop water stress index (CWSI) for defining such environments. AI incorporates rainfall and potential evapotranspiration. CWSI integrates all factors affecting water availability for crop growth but has the limitation of being crop specific.

One major application of remote sensing to agriculture is crop monitoring and assessment of vegetative stress. Satellite derived indices have been extensively used for identifying stress periods in crops or generally vegetation (*Steven* and *Jaggard*, 1995). In most cases the identification of vegetative stress is being held by the use of vegetation indices (*Domenikiotis et al.*, 2002; *Kogan*, 1995, 2001, 2002; *Tsiros et al.*, 2004).

Kogan (2001) proposed the vegetation health index (VHI) for monitoring the impact of weather to vegetation, and to use it for agricultural drought monitoring and mapping. Agricultural droughts reflect vegetation stress caused by the adverse climatic and hydrologic factors (*Bhuiyan et al.*, 2006; *Kogan*, 2002). VHI is a combination of vegetation condition index (VCI) and temperature condition index (TCI) derived by NOAA/AVHRR satellite data. In Greece, VCI and TCI have proven to be useful tools for the detection of agricultural drought (*Domenikiotis et al.*, 2002; *Tsiros et al.*, 2004).

In Greece, *Tsiros et al.* (2008) classified the WLGE using satellite derived VHI and AI. VHI represents overall vegetation health (moisture and thermal conditions) (*Kogan*, 2001) and is suitable for identification of vegetative stress, especially in cases where no specific crop is examined. AI represents climatic aridity and is used to determine the adequacy of rainfall in satisfying the water needs of crops.

The first objective of this study is to define a general methodology (not crop specific) for identifying WLGE using GIS and remote sensing. Therefore, the two indices are used to define zones adequate for agricultural use according to water limitations (WLGE zones). The second objective is to identify sustainable production zones in terms of water sufficiency, fertility (appropriate or not for agricultural use), desertification vulnerability, and altitude restrictions. Thus, WLGE zones are combined with soil maps and a digital elevation model (DEM). In order to apply new management techniques, transfer new technologies and plan alternative crops according to the bio-physical characteristics of each region, a quantitative understanding of the relationships among crop, climate, and soil are needed (*Badini et al.*, 1997). Defining areas of sustainable crop production is a major step for identifying agroclimatic zones, considering environmental limitations and the sustainable use of natural resources.

2. *Study area and preprocessing*

The study area is the geographical region of Thessaly (*Fig. 1*) and specifically the water district of Thessaly, located in Central Greece. Thessaly is a region of plains surrounded by mountains. The ridges of these mountains are the borders of the water district of Thessaly. Having higher percent of flatlands than any other district in Greece, 38.7% of the population is occupied in the primary productivity sector and thus, Thessaly is a major supplier of agricultural products.

The increase in agricultural activities and the intensive type of agricultural practices applied in Thessaly, resulted in an insufficient use of natural resources. Low and irregular amount of rain during the summer period lead to regional drought events which in combination with the oversized pumping and the bad management of irrigation water (old irrigation practices and network, increased water losses, more amount of irrigation water than needed) led to degradation of water resources and lowering of the ground water table. Thus, there is a necessity for identifying areas which are capable to fulfill crop water needs without aggravating the current conditions.

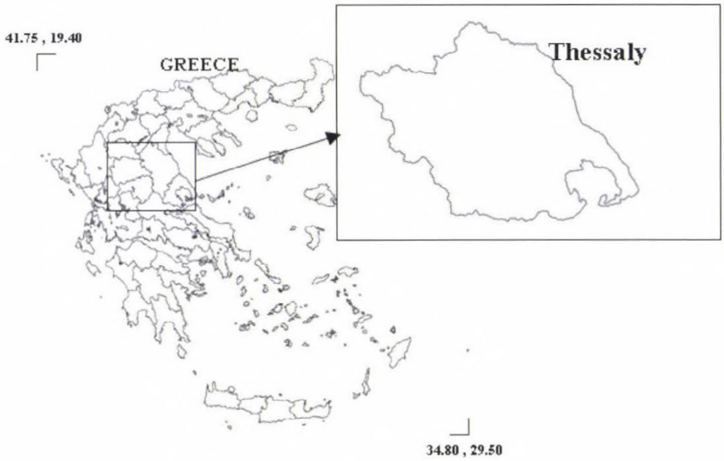

Fig. 1. Location of the study area.

The data base consists of NOAA/AVHRR satellite data and conventional data for 20 hydrological years, from October 1981 to September 2001. In specific:

- Normalized difference vegetation index (NDVI), channel 4 (CH4) and channel 5 (CH5) brightness temperature (BT) ten-day composite satellite images (8 × 8 km spatial resolution).
- Monthly rainfall maps with grid cell size 50 × 50 km (*ISPRA*, 2006).
- Mean monthly air temperature measurements from Larissa meteorological station (National Meteorological Service, NMS).
- Soil map of the study area (*Yassoglou*, 2004).
- Digital elevation model derived from 100m contours.

All satellite data are obtained on-line by NASA archives. NDVI maps are ten-day maximum value composite (MVC) images. CH4 and CH5 images are converted to BT using the equation provided by the info file of the data set. Using the ten-day images, NDVI and BT images are composed over a monthly period using the MVC and mean pixel value, respectively. Missing data due to cloud cover or sensor's technical problems are completed using monthly climatic values derived from the images of the time series which presented no blunders. Rainfall maps were produced using the data of ISPRA European database (*ISPRA*, 2006). The subset satellite images and rainfall maps cover the entire area of Greece. After all computations have been carried out, the area under investigation is isolated.

Before using NDVI and BT images, fluctuations induced by noise must be removed. The combination of the filtering and the MVC can significantly reduce the noise from residual clouds, fluctuating transparency of the atmosphere, target/sensor geometry, and satellite orbital drift (*Goward et al.*, 1991). Other noise can be related to processing, data errors, or simple random noise (*Kogan*, 1995).

In the current study, a "4253 compound twice" median filter (*Van Dijk et al.*, 1987) is applied to the NDVI images, whereas a "conditional" statistical mean spatial filter (window size ranging from 3×3 to 7×7, according to image needs) has been used for smoothing the BT series (*Tsiros et al.*, 2008). The BT series presented continuous spatial fluctuations, and thus, a spatial filter (statistical mean) has been preferred for smoothing channel 4 and channel 5 BTs. "Conditional" means that the filter is applied only to the pixels that presented errors.

3. Methodology

Remote sensing is a useful tool to analyze the vegetation dynamic. Several studies have shown that inter-annual differences in vegetation parameters are mainly driven by water availability (*Al-Bakri* and *Taylor*, 2003; *Weiss et al.*, 2004). Thus, AI and VHI are used in order to define zones adequate for sustainable farming according to water limitations (*Tsiros et al.*, 2008). As crop growth is affected by water supply, these zones are named water limited growth environment zones (*Badini et al.*, 1997). Furthermore, these zones are combined with soil maps and a DEM of the area under investigation in order to define zones appropriate for sustainable crop production due to water, soil, and altitude restrictions.

3.1. Water limited growth environment

The first index used to identify WLGE is VHI. VHI is a combination of VCI and TCI derived by a long term NDVI and channel 4 images from NOAA/AVHRR satellite. NDVI, is obtained by combining the channels 1 and 2, the visible and near infrared, respectively, of NOAA/AVHRR. NDVI is a quick and efficient way for the estimation of vivid vegetation. NDVI is indicative of the level of photosynthetic activity in the vegetation monitored, reflecting whether the vegetation is stressed or not. After stressed conditions, significant reduction in NDVI of the field is expected.

VCI and *TCI* characterize the moisture and thermal conditions of vegetation, respectively (*Bhuiyan et al.*, 2006; *Kogan*, 1995, 2001, 2002) and are given by the equations:

$$VCI = 100 \cdot \frac{NDVI - NDVI_{min}}{NDVI_{max} - NDVI_{min}}, \tag{1}$$

$$TCI = 100 \cdot \frac{BT_{max} - BT}{BT_{max} - BT_{min}}, \tag{2}$$

where *NDVI*, $NDVI_{max}$, and $NDVI_{min}$ are the smoothed ten-day normalized difference vegetation index, its multi-year maximum and minimum, respectively; *BT*, BT_{max}, and BT_{min} are the smoothed ten-day radiant temperature, its multi-year maximum and minimum, respectively, for each pixel, in a given area. Thermal conditions are especially important when moisture shortage is accompanied by high temperature, increasing agricultural's drought severity, having direct impact to vegetation's health. *VCI* and *TCI* vary from zero, for extremely unfavorable conditions, to 100, for optimal conditions. Thus, higher *VCI* and *TCI* values represent healthy and unstressed vegetation.

Both indices are based on the same concept. Maximum amount of vegetation is developed in years with optimal weather conditions, whereas minimum vegetation amount develops in years with extremely unfavorable weather (mostly dry and hot). Therefore, the absolute maximum and minimum values of NDVI and BT, calculated from several years, contain the extreme weather events (drought and no drought conditions). The resulted maximum and minimum values can be used as criteria for quantifying the environmental potential of a region (*Kogan*, 1995).

VHI represents overall vegetation health (*Kogan*, 2001). The five classes of VHI that represent agricultural drought are illustrated in *Table 1* (*Bhuiyan et al.*, 2006; *Kogan*, 2001). VHI is expressed by the following equation:

$$VHI = 0.5 \cdot (VCI) + 0.5 \cdot (TCI). \tag{3}$$

In *VHI* computation, an equal weight has been assumed for both *VCI* and *TCI*, since moisture and temperature contribution during the vegetation cycle is currently not known (*Kogan*, 2001).

Table 1. VHI drought classification schemes (*Kogan*, 2001)

VHI values	**Agricultural drought classes**
<10	Extreme drought
<20	Severe drought
<30	Moderate drought
<40	Mild drought
>40	No drought

The other index used to identify WLGE zones is AI. AI is a function of the ratio of precipitation to potential evapotranspiration. The categories as they are defined by the values of AI are illustrated in *Table 2* (*UNESCO*, 1979). In this study, AI represents climatic aridity and is used to determine the adequacy of rainfall in satisfying the water needs of crops. The index is calculated on multi-year basis, using monthly values. The potential evapotraspiration is calculated with the use of Blaney-Criddle method (*Tsiros et al.*, 2008). The method estimates potential evapotranspiration (ET_p) using monthly air temperature data, the ratio of daytime hours (month/year), and a weighted crop coefficient (C). Regarding the weighted crop coefficient, 12 maps with grid cell size of 100 × 100 m (one for each month) have been utilized. C values are defined according to land use provided by CORINE 2001 database.

Table 2. Characterization of an area according to aridity index, AI (*UNESCO*, 1979)

Category	**AI**
Extremely dry	<0.03
Dry	0.03 – 0.20
Semi-dry	0.20 – 0.50
Semi-wet	0.50 – 0.75
Wet	>0.75

In ET_p calculations, land surface temperature (LST) is used instead of air temperature. The generation of LST maps is based on the "split-window" algorithm from *Becker* and *Li* (1990), which uses the differential absorption effects in channels 4 and 5 for correcting atmospheric attenuation mainly caused by water vapour absorption. For estimating surface emissivity, the relationship given by *Van de Griend* and *Owe* (1993) is applied.

In order to avoid over-estimating ET_p, LST is converted to air temperature using a linear empirical relationship. The relationship has been derived by applying a regression analysis to the LST and air temperature data of the time series ($R^2 = 0.84$). Results are depicted in *Fig. 2*.

Since both indices have been computed, two maps are created. From the VHI images a final map is obtained using the frequency of occurrence of agricultural drought events. The derived map is combined with the climatic aridity map and led to the definition of WLGE zones. The generalized thematic classification scheme is illustrated in *Table 3*.

3.2. Soil map and DEM

Overlapping WLGE zones, a soil map, and a DEM of the study area has led to the definition of regions where crop production is sustainable and agriculture is the best suited agronomic use. Soil types are digitized according to fertility (appropriate or not for sustainable agricultural use) and desertification vulnerability. The sustainable agronomic use and the desertification risk according to soil category are adopted by *Yassoglou* (2004). Soil types are grouped into three classes during the digitization. Soils appropriate for agricultural use, controlled agricultural use, and no agricultural use. The classification pattern is illustrated in *Table 4*. Finally, the digitized vector map is converted to raster (grid) with cell size of 100 × 100 m.

As mentioned earlier, the DEM is constructed using 100 m interval contours. Three major crop growth zones are selected according to altitude limitations (*Danalatos*, 2007). The first, ranging from zero to 600 m, is appropriate for almost all crops. The second, ranging from 600 m to 900 m is appropriate for non-tropic crops and fruit trees (maize, winter wheat, apple trees, chestnuts, etc.). The last one, having altitude values higher than 900 m is not appropriate for crops. Again, the derived zones are converted to raster (grid) with cell size of 100 × 100 m.

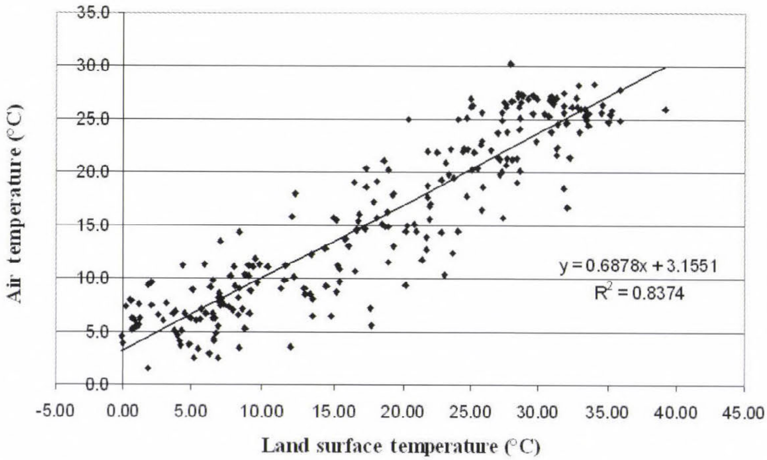

Fig. 2. Application of linear regression analysis to land surface temperature and air temperature.

Table 3. WLGE generalized classification scheme (*Tsiros et al.*, 2008)

Agricultural drought classes	Aridity classes	WLGE classes
Extreme drought	Extremely dry	Limited
Severe drought	Dry	Environment
Moderate drought	Semi-dry	Partially limited
Mild drought	Semi-wet	Environment
No drought	Wet	No limitations

Table 4. Classification scheme of soil types according to sustainable use and desertification vulnerability

Class name	**Sustainable agronomic uses**	**Desertification vulnerability**	**Soil types category**
No agricultural use	Wild nature,	Very high	Rock outcrops
	Forest		Leptosols, Regosols (low quality)
	Controlled pasture	High	Cambisols (medium-low quality)
Controlled agricultural use	Controlled agriculture and pasture	Medium	Regosols (medium quality)
			Cambisols (medium-high, high quality)
	Forest		Luvisols (medium quality)
Agricultural use	Agriculture	Low	Fluvisols, Vertisols, Luvisols (high quality)

3.3. Supervised classification

During the supervised classification, the parallelepiped technique is used in order to combine the WLGE zones, the soil map and the DEM and define the sustainable production zones. During the classification, the following rule pattern is used. Crop production is:

- "Unsustainable" in areas characterized by any of the "limiting" classes.
- "Sustainable under restrictions" when "partial limitations" regarding to WLGE or soil map or DEM (intermediate classes) exist.
- "Sustainable for non-tropic crops" in regions with "no limitations" and 600–900 m altitude range.
- "Sustainable" in areas with "no limitations" and altitude lower than 600 m.

4. Results and discussion

In this study, two satellite derived indices, VHI and AI are used to define areas where plant growth is limited by water availability. The calculation of the two indices resulted in the creation of two maps. One is characterizing areas according to the frequency of agricultural drought incidents (*Fig. 3a*) and the other is representing climatic aridity (*Fig. 3b*) for the period under consideration. *Figs. 3a* and *3b* show that there is no area in Thessaly water district where the climate regarding to AI is "dry" or "extremely dry", and "severe" and "extreme" drought events are frequent.

The definition of WLGE zones is the result of the combination of these two maps. The thematic classification scheme used is described as follows. A number has been assigned to every class of the two indices (five classes each). Number one corresponds to "wet" and "no drought" classes, grading the sequence up to five, which corresponds to "extremely dry" and "extreme drought" classes. By adding those numbers, three categories are utilized to delimit WLGE zones: (i) "limited" (values from 7 to 10) and (ii) "partially limited" (values from 3 to 6) growth environment, and (iii) the class where "no limitations" (values equal to two) exist according to water availability. The map of WLGE zones is presented in *Fig. 4*.

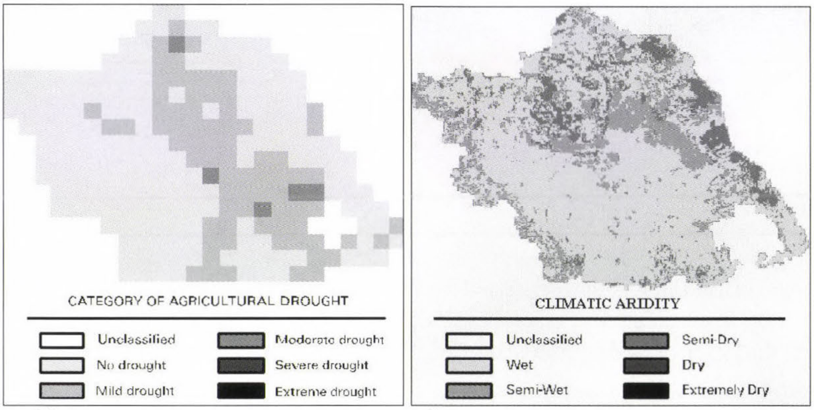

(a) (b)

Fig. 3. (a) Agricultural drought map of Thessaly water district derived using incidents frequency, (b) climatic aridity map of Thessaly water district.

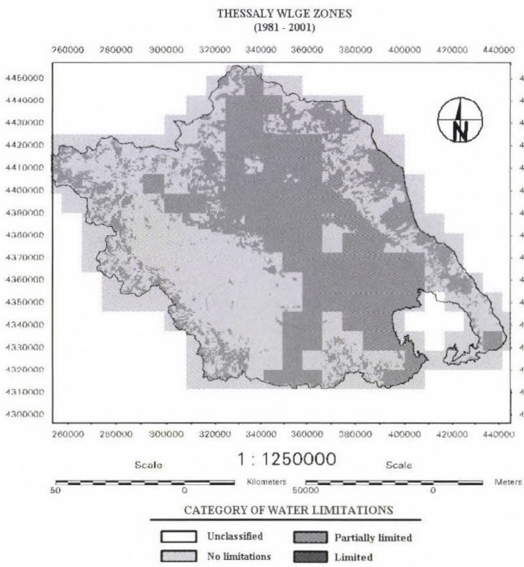

Fig. 4. Water limited growth environment zones of the water district of Thessaly.

Fig. 4 indicates that there is no area in Thessaly water district where plant growth is prohibited by water availability. The definition of "limited" growth environment indicates areas where moisture and rainfall cannot satisfy the water needs of crops or even a part of them. In order to satisfy crop requirements in those areas, large quantities of water supply from irrigation are required, leading to unsustainable use of water resources and increase of the cost of the final product. Areas of "partially limited" growth environment due to water availability need smaller amount of irrigation, whereas areas with "no limitations" even smaller. In such areas, a more effective use of water resources is being held, since a major part of crop water needs is supplied by rainfall and existing moisture conditions.

The combination of the WLGE zones, soil maps, and DEM resulted in the definition of sustainable production zones by means of parallelepiped supervised classification. The zones of sustainable use according to soil characteristics and the altitude based crop growth zones in Thessaly are depicted in *Figs. 5a* and *5b*, respectively, whereas the derived map of the sustainable production zones is presented in *Fig. 6*.

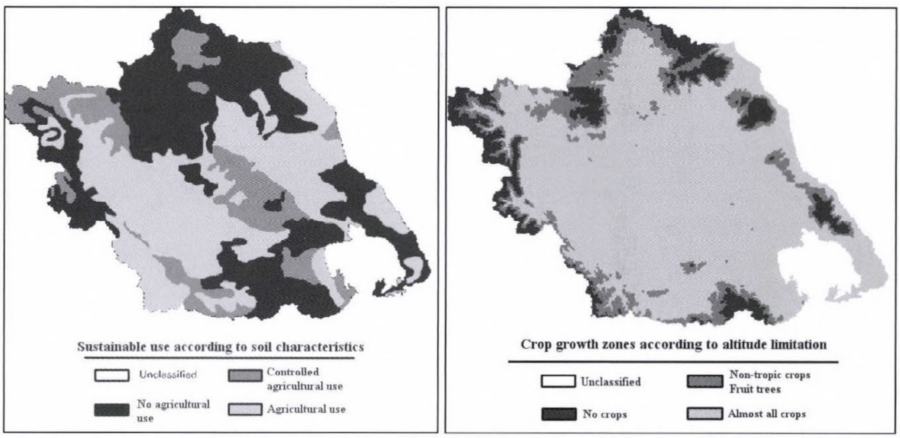

(a) (b)

Fig. 5. (a) Zones of sustainable use according to soil characteristics in Thessaly, (b) altitude based crop growth zones of Thessaly water district.

Fig. 6 shows that in the 35% of Thessaly water district agriculture is not a sustainable due to water, altitude, or soil limitations. The term "sustainable under restrictions" refers to the cultivation of crops that do not need large quantities as "input" regarding irrigation and fertilizers. Also, "sustainable under restrictions" indicates that the type of cultivation preferred to those areas is extensive and not intensive. Further work has to be done in order to define the type of crops and cultivation techniques applied to those areas. The sustainable production areas for non-tropic crops have small spatial coverage, because they are delimited by the relatively high altitudes. Lastly, sustainable production zones cover about 25% of Thessaly indicating that those areas of the water district are suitable for any agricultural use. But, in order to obtain sustainability, farming management practices such as crop rotation, use of crop cover, and combination with livestock grazing out of the growing season are essential. Most of the times, monocultures are not sustainable systems.

The main advantage of the methodology is that it uses satellite and raster data, providing continuous spatial and temporal information. In this way there are no fuzzy borders regarding the derived zones. Instead, methods that use conventional data are lacking the above advantages. But, despite the advantages, it is essential that the satellite data are calibrated and preprocessed properly before they are used as input data in any methodology. Lastly, another advantage of using these indices is that they are not crop specific.

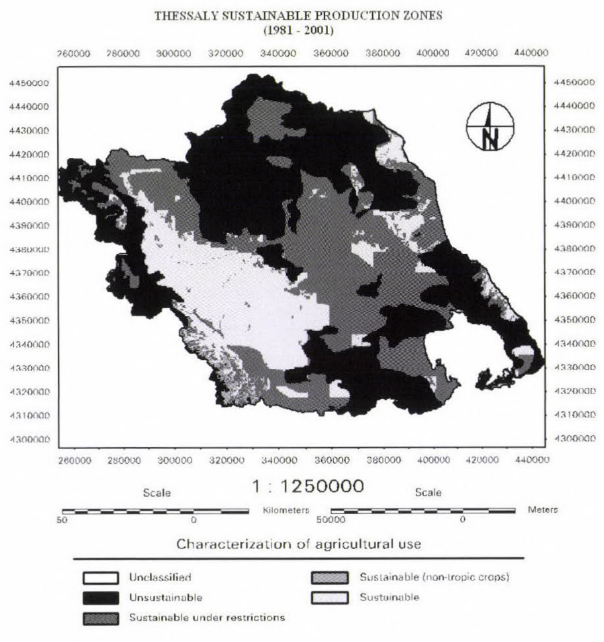

Fig. 6. Sustainable production zones of Thessaly water district.

5. *Conclusions*

The results of the current application justify the use of AI and VHI. Using VHI, areas frequently affected by agricultural drought are identified and excluded. The combination of the frequency of occurrence of such extreme events along with climatic aridity is useful for identifying areas unsuitable for crop production due to water availability. Such areas must be excluded from any sustainable management plan.

Thus, WLGE zones are important since they delineate areas where plant growth is limited by water availability. Moreover, the use of soil maps and DEMs excludes areas unsuitable for agricultural activities. Thus, the combination of WLGE zones along with soil maps and DEMs can be used to identify sustainable production zones. Such zones are essential in developing any sustainable development/farming plan, since they can be combined with crop specific agroclimatic indices in order to obtain agroclimatic zones.

The innovation of the proposed methodology consists of the joint use of the above described steps, as well as the classification of areas escalating the suitability of agricultural activities. Lastly, the methodology is not crop specific and has the advantage of providing total spatial coverage of the area under investigation.

Acknowledgments—This paper is part of the 03ED352 research project, implemented within the framework of the "Reinforcement Programme of Human Research Manpower" (PENED) and co-financed by National and Community Funds (25% from the Greek Ministry of Development-General Secretariat of Research and Technology and 75% from E.U.– European Social Fund). Data were provided by the National Meteorological Service of Greece, the Joint Research Centre of E.C. (ISPRA), and the Earth Observing System Data and Information System (EOSDIS).

References

Al-Bakri, J.T. and *Taylor, J.C.*, 2003: Application of NOAA–AVHRR for monitoring vegetation conditions and biomass in Jordan. *J. Arid Environ. 54*, 579–593.

Arora, V.K. and *Gajri, P.R.*, 1998: Evaluation of a crop growth-water balance model for analysing wheat responses to climate- and water-limited environments. *Field Crop Res. 59*, 213-224.

Badini, O., Stöcle, C.O., and *Franz, E.H.*, 1997: Application of crop simulation modeling and GIS to agroclimatic assessment in Burkina Faso. *Agric. Ecosyst. Environ. 64*, 233-244.

Becker, F. and *Li, Z.*, 1990: Towards a local split window method over land surfaces. *Int. J. Remote Sens. 11*, 369- 393.

Bhuiyan, C., Singh, R.P., and *Kogan, F.N.*, 2006: Monitoring drought dynamics in the Aravalli region (India) using different indices based on ground and remote sensing data. *International Journal of Applied Earth Observation and Geoinformation 8*, 289-302.

Danalatos, N., 2007: *An Introduction in Crop Production Simulation.* University of Thessaly Press, Volos, Greece.

Domenikiotis, C., Spiliotopoulos, M., Tsiros, E., and *Dalezios, N.R.*, 2002: Application of NOAA/AVHRR VCI for drought monitoring in Thessaly, Greece. *6th International Conference of Protection and Restoration of the Environment*, 1-5 July 2002, Skiathos, Greece, 1663-1670.

Goward, S.N., Markham, B., Dye, D.G., Dulaney, W., and *Yang, J.*, 1991: Normalized difference vegetation index measurements from the advanced very high resolution radiometer. *Remote Sens. Environ. 35*, 257-277.

ISPRA, 2006: *European Monthly Precipitation Database (1975-2006).* Joint Research Center of E.C., Varese, Italy.

Kogan, F.N., 1995: Application of vegetation index and brightness temperature for drought detection. *Adv. Space Res. 15*, 91-100.

Kogan, F.N., 2001: Operational space technology for global vegetation assessment. *B. Am. Meteorol. Soc. 82*, 1949-1964.
Kogan, F.N., 2002: World droughts in the new millennium from AVHRR-based Vegetation Health Indices. *EOS Transaction, American Geophysics Union 83*, 562-563.
Mavi, H.S. and *Tupper, G.J.*, 2004: *Agrometeorology: Principles and Applications of Climate Studies in Agriculture*. Food Product Press, Haworth Press Inc., New York.
Pereira, A.R., 1982: Crop planning for different environments. *Agr. Meteorol. 27*, 71-77.
Reddy, S.J., 1983: Agroclimatic classification of the semi-arid tropics I. A method for the computation of classificatory variables. *Agr. Meteorol. 30*, 185-200.
Steven, M.D. and *Jaggard, K.W.*, 1995: Advances in crop monitoring by remote sensing. In *Advances in Environmental Remote Sensing* (eds.: *F.M. Danson* and *S.E. Plummer*). Wiley.
Thornthwaite, C.W., 1948: An approach toward rational classification of climate. *Geogr. Rev. 38*, 55-94.
Tow, P.G., 1991: Factors in the development and classification of dryland farming systems. In *Dryland Farming-A Systems Approach* (eds.: V. Squires and P. Tow). Sydney University Press, Sydney.
Tsiros, E., Domenikiotis, C., Spiliotopoulos, M., and *Dalezios, N.R.*, 2004: Use of NOAA/AVHRR-based vegetation condition index (VCI) and temperature condition index (TCI) for drought monitoring in Thessaly, Greece. *EWRA Symposium on Water Resources Management*. Izmir, Turkey, 2-4 September 2004, 769-782.
Tsiros, E., Domenikiotis, C., Kanellou, E., Dalezios, N.R., and *Tzortzios, S.*, 2008: Identification of water limited growth environment zones using NOAA/AVHRR data. *4th International Conference HAICTA 2008*, 18-20 September 2008, Athens, 150-155.
UNESCO, 1979: *Map of the World Distribution of Arid Regions: Explanatory Note*. Man and the Biosphere. Technical Notes 7, Paris.
Van De Griend, A.A. and *Owe, M.*, 1993: On the relationship between thermal emissivity and the normalized difference vegetation index for natural surfaces. *Int. J. Remote Sens. 14*, 1119-1131.
Van Dijk, A., Callis, S.L., and *Sakamoto, C.M.*, 1987: Smoothing vegetation index profiles: An alternative method for reducing radiometric disturbance in NOAA/AVHRR data. *Journal of Photogrammetric Engineering & Remote Sensing 63*, 1059-1067.
Weiss, J.L., Gutzler, D.S., Coonrod, J.E., and *Dahm, C.N.*, 2004: Seasonal and inter-annual relationships between vegetation and climate in central New Mexico, USA. *J. Arid Environ. 57*, 507–534.
Yassoglou, N.J., 2004: *Soil Associations Map of Greece*. Greek National Committee for Combating Desertification, Agricultural University of Athens Press, Athens.

IDŐJÁRÁS

Quarterly Journal of the Hungarian Meteorological Service
Vol. 113, No. 1–2, January–June 2009, pp. 69–78

Current trends of agroclimatic indices applied to grapevine in Tuscany (Central Italy)

Simone Orlandini, Valentina Di Stefano, Paolo Lucchesini, Annalena Puglisi, and **Giorgio Bartolini**

Department of Agronomy and Land Management, University of Florence, Piazzale delle Cascine 18, 50144 Firenze, Italy; E-mail: simone.orlandini@unifi.it

(Manuscript received in final form January 15, 2009)

Abstract—Global warming is causing wide changes in atmospheric events with critical impacts on vegetations. Indeed, an increase of temperature variability has been observed, primarily due to increase in warm extremes. Temperature rising will lead to several consequences. For example, growing season lengthening is observed, but at the same time, plants grow faster, thus giving productions low in quality and quantity. Finally, concerning the Mediterranean region, it is evaluated that a greater water request is needed for irrigation. Besides, high maximum temperatures during summer months may cause drop in quality. On the opposite, concerning winter risks, earlier bud break will increase late frost risks. The aim of this study is to cover some aspects of warming temperature and phenological responses on grapevine in central Italy. The research is focused on climatic and agroclimatic indices calculated in 1955–2007 period. Regression trend, linear or non-parametric, depending on the distribution of data, was fitted to provide pictures of changes that have occurred.

Key-words: global warming, climate variability, rising temperature, phenology, quality, frost, *Vitis vinifera*

1. Introduction

A long history of grapevine (*Vitis vinifera*) is associated with the fitoclimatic Mediterranean area. Indeed, famous wine regions were established in this area during the Roman Empire, because it was recognized the fundamental link between the geographic location and the climatologic condition.

Nowadays this idea is the basis of the wine zoning. The wine style produced by regions is the result of the baseline climate, while climate variability determines vintage-to-vintage quality differences (*Jones*, 2003; *Jones* and *Hellman*, 2003). In particular, climate strongly affects the given wine style, because it has a deep influence on the optimum levels of sugar, acid, and flavor on grape. As for global warming, some studies highlight both positive and negative impacts in Europe. Among positive ones, the total surface suitable to cultivation foreseen by climatological models is going to increase and extend to European north latitudes and higher altitudes (*IPCC*, 2007; *Bindi et al.*, 2002). On the contrary, in southern areas of Europe, the benefits of the forecasted climate change will be limited, while the disadvantages will be predominant (*Maracchi et al.*, 2005). The Mediterranean area, in particular, shows high susceptibility to the most recent increase and variability of temperature: these strongly affect viticultural activities, modifying grapevine responses and determining the quality and quantity of vine production (*Jones* and *Hellman*, 2003). Among the other consequences, rising temperature is going to cause both geographical and varietal changes in grape cultivation (*Orlandini*, 2004).

As regard crops quality risks, high temperature and dry condition, especially in September, can be critical for grape quality, because they cause excessive fruit ripening, affecting fruit quality (*Schultz*, 2000).

Moreover, as for the impacts on the physiology, a few case studies point out that rising temperature in this area determines increase of water request and needs of monitoring. Indeed, even if grapevine is quite resistant to high summer temperature and drought, the increase of extreme conditions can be responsible of physiological stresses, such as the reduction of photosynthetic efficiency.

Concerning the phenology, higher minimum temperatures activate cellular split (*Nemani et al.*, 2001), thus causing advanced harvest. Moreover, a study conducted in the north-east part of Italy during the 1956–2002 period, shows an increase of thermal sum that determines earlier phenological phases (*Puglisi et al.*, 2005).

One of the most important indices used to investigate plant phenology is the growing season starting date, that is strongly related with air temperatures (*Fregoni*, 2002). For example, it is recently largely observed that a positive anomaly on the temperature trend during the growing season determines grape phases shift, with negative effect on vine quality. Indeed, it leads to the premature change of color, sugars accumulation, and partial or total failure of flavor ripening (*Mullins et al.*, 1992), in some cases enzyme inactivation (*Jones et al.*, 2005).

Moreover, the increase of interannual variability in temperature and precipitations makes adaptation to such continuous changes very expensive, thus winemakers have to be flexible in viticulture techniques planning and management beyond rescheduling crop operations (*Bindi et al.*, 2002). A study on Sangiovese and Cabernet Sauvignon in Italy revealed that warmer conditions will lead to shorter growth range and higher yield variability (*Bindi et al.*, 1996).

Finally, the more delicate grapevine growth phases, such as the very early ones, will be more and more vulnerable. In particular, bud-break will be affected by the late frost risk increase (*Nemani et al.*, 2001).

Assessment of the potential impacts of climate change on viticulture is demanded by scientists, policy makers, producers, and others to make decisions on policies and management practices that may minimize negative impacts and take advantage of positive impacts or opportunities.

On these bases, this study analyzes some climatic and agroclimatic indices trend to assess temperature changing and the consequent potential impacts on grapevine cultivation in Tuscany (central Italy).

2. *Material and method*

From a meteorological network, 22 stations were selected in Tuscany, Italy, for the 1955–2007 period (*Table 1*; *Fig. 1*). The following criteria were adopted to select stations: first, low percentage of missing data, because even if the techniques to reconstruct the series are known, it is preferable to start the analysis with original data; second, a long period covered by dataset, thirty years at least. Finally, stations must be distributed all over the territory to have a complete overview of the climate in Tuscany.

Table 1. Geographical information of the meteorological stations

Meteorological station	**UTM_X (m)**	**UTM_Y (m)**	**Altitude (m a.s.l.)**
Arezzo	730805	4815384	249
Boscolungo	633977	4888891	1340
Camaldoli	727025	4853030	1110
Castel del Piano	706920	4752060	596
Castelnuovo Garf.	613275	4885305	280
Elba Calamita	614306	4731893	380
Firenzuola	689640	4888022	454
Grosseto	669415	4735216	5
Livorno	606140	4822595	9
Lucca	620990	4855580	25
Massa	591800	4875450	38
Massa Marittima	653850	4768500	362
Montepulciano	726520	4774950	575
Orbetello	681025	4699970	1
Peretola	676985	4852101	38
Pisa	613017	4838671	3
Pistoia	653080	4867535	88
Pontremoli	570117	4913436	247
San Miniato	647740	4838630	132
Siena	687630	4799185	346
Vallombrosa	706000	4845450	972
Volterra	649965	4808235	465

Fig. 1. Meteorological station distribution in Tuscany.

In the first place, the dataset (period of 1955–2007) was verified as the GCOS (Global Climate Observing System) recommends: in order to avoid inhomogeneities or discontinuities in the climate record (caused by changes to the station, such as site location and instrumentation), time series were homogenized through the method described in *Brunetti et al.* (2006). After that, basic data exploration was carried out, considering absolute values and then differences between contiguous day values. Suspect values were coded as NA (not available). If neighboring stations with well correlated data were available, original suspect ones were reconstructed by statistical process. Afterwards, climatological mean and extreme temperature indices were selected in order to analyze climate and climatic variability. Climatic temperature indices were mean minimum (TN) and mean maximum temperature (TX). These indices were calculated both on seasonal and annual time scale. Extreme temperature indices were split in summer and winter and calculated only on the season when they showed effects. The summer period included June–August while winter period consisted in December–February. Selected summer extreme temperature indices were warm days and warm nights (*Manton et al.*, 2001; *Peterson et al.*, 2001; *Klein Tank* and *Können*, 2003; *Bartolini et al.*, 2008). For the winter period number of cold nights and number of days with minimum temperature lower than 0 °C (FD) were selected.

Concerning the potential impacts of climate change on grapevine, they were detected by applying agroclimatic indices such as growing degree days (GDD) related to the starting date of the most important phenological phases (bud-break, flowering, ripening) and expressed in doy (day of the year); length of growing season with 0 °C threshold (VGS0), thermal summation with 10 °C threshold in the period March–September (STA10), thermal summation with 10 °C threshold in the period April–October (STA10 Winkler), and Huglin index. These are good indicators of the interactions between climate trend and the physiological needs. In fact, to detect bud break trigger it must be considered that each species need a specific heat quantity to activate the phenological stages. Huglin index, as GDD index, is used in viticulture to explain temperature availability in a specific area. In particular, high values of this index reveal suitable areas for grapevine with late maturation, while low values fit for early maturation varieties. Huglin index is estimated by making use of maximum and mean daily temperatures. *Table 2* shows all the selected indices with the acronyms.

Table 2. Climatic and agroclimatic indices

Acronym	Unit	Description
TN (a)	°C	Mean of minimum temperature (annual)
TN (sp)	°C	Mean of daily minimum temperature (spring: March–May)
TN (s)	°C	Mean of daily minimum temperature (summer: June–August)
TN (au)	°C	Mean of daily minimum temperature (autumn: September–November)
TN (w)	°C	Mean of daily minimum temperature (winter: December–February)
TX (a)	°C	Mean of daily maximum temperature (annual)
TX (sp)	°C	Mean of daily maximum temperature (spring: March–May)
TX (s)	°C	Mean of maximum temperature (summer: June–August)
TX (au)	°C	Mean of maximum temperature (autumn: September–November)
TX (w)	°C	Mean of maximum temperature (winter: December–February)
TN90p*	°C	Number of days with daily minimum temperature higher than 90 percentile (1961–1990) calculated in summer period (July–August)
TX90p*	°C	Number of days with daily maximum temperature higher than 90 percentile (1961–1990) calculated in summer period (July–August)
FD (a)	Days	Annual number of days with minimum temperature lower than 0 °C
GDD Bud break	Day	Date of bud break: It is the doy (day of the year) when the summation of the differences between the mean daily temperature and the threshold temperature (10 °C) reaches a specific value
GDD Flowering	Day	Date of grape flowering: It is the doy (day of the year) when the summation of the differences between the mean daily temperature and the threshold temperature (10 °C) reaches a specific value
GDD Ripening	Day	Date of grape ripening: It is the doy (day of the year) when the summation of the differences between the mean daily temperature and the threshold temperature (10 °C) reaches a specific value
HI	Degrees	Huglin index: Daily summation of the mean between maximum and mean temperature calculated during the growing season (March-September) multiplied by a latitude coefficient
STA10	°C	Thermal summation (10 °C threshold): Daily mean temperature summation in the growing period (March–September)
STA10 Winkler	°C	Thermal summation (10 °C threshold): Daily mean temperature summation in the growing period (April–October)
VGS0	Days	Vegetative growing season (0 °C threshold): Number of days between the last and first frost events of the year

Data were analyzed to test the normality of the distribution with the Shapiro-Wilk normality test. If normal, the linear trend was fitted, otherwise the Theil-Sen (*Theil*, 1950; *Sen*, 1968) non-parametric test was applied.

Parametric and non-parametric regression was fitted to each index and meteorological station. Regression slope was evaluated in order to detect trends and changes occurred over the considered period.

3. Results

Table 3 shows all the results for each analyzed index. Climatic temperature indices (TN and TX) show a tendency to increase. In particular, the increase of annual maximum temperature (+0.9 °C/50 years) was similar to that of minimum temperature. Seasonal analysis shows a much greater increase of minimum and maximum temperatures in summer (+1.5 °C/50 years; +1.7 °C/50 years, respectively) and spring season (+0.9 °C/50 years and +1.1 °C/50 years, respectively).

Table 3. Trends of the climatological indices of the 22 meteorological stations (1955–2007)

S	Index	n°	n	N°	NN°	m	m1	m*	m1*
22	TN (a)	22 ; 0	0	20 ; 0	19 ; 0	+0.8		+0.9	
22	TN (sp)	21 ; 1	0	12 ; 0	10 ; 0	+0.9		+1.1	
22	TN (s)	22 ; 0	0	20 ; 0	20 ; 0	+1.5		+1.6	
22	TN (au)	18 ; 4	0	6 ; 0	5 ; 0	+0.6		+1.3	
22	TN (w)	20 ; 2	0	4 ; 0	2 ; 0	+0.5		+1.8	
22	TX (a)	22 ; 0	0	21 ; 0	21 ; 0	+0.9		+0.9	
22	TX (sp)	22 ; 0	0	16 ; 0	15 ; 0	+1.1		+1.3	
22	TX (s)	22 ; 0	0	22 ; 0	21 ; 0	+1.7		+1.7	
22	TX (au)	16 ; 6	0	1 ; 1	0 ; 1	+0.1		–1.3	
22	TX (w)	22 ; 0	0	6 ; 0	5 ; 0	+0.9		+1.2	
22	TN90p *	22 ; 0	0	20 ; 0	20 ; 0		+1		+18
22	TX90p *	22 ; 0	0	20 ; 0	19 ; 0		+1		+13
22	FD (a)	3 ; 19	0	0 ; 5	0 ; 3		–5		–15
22	GDD Bud break*	7 ; 12	3	0 ; 4	0 ; 2		–3		–16
22	GDD Flowering*	2 ; 18	2	1 ; 15	0 ; 13		–7		–9
17	GDD Ripening*	0 ; 17	0	0 ; 14	0 ; 14		–19		–23
22	HI	22 ; 0	0	18 ; 0	17 ; 0	+273		+318	
22	STA10	20 ; 2	0	19 ; 0	17 ; 0	+203		+236	
22	STA10 Winkler	20 ; 2	0	19 ; 0	18 ; 0	+219		+252	
22	VGS0*	11 ; 6	5	4 ; 1	4 ; 1		+5		+15

Legend:

S – number of stations for which it was possible to calculate the trend,

(a) annual, (sp) spring, (s) summer, (au) autumn, (w) winter,

The asterisk means that Theil-Sen method was applied to calculate the slope (non-normal distribution),

n° – number of stations with positive and negative trend, respectively,

n – number of stations with slope = 0,

N°– number of stations with statistically significant coefficient ($p < 0.1$) with positive and negative trend, respectively,

NN° – number of stations with statistically significant coefficient ($p < 0.05$) with positive and negative trend, respectively, m, m* – mean value of the regression coefficient for all the stations and mean value of the regression coefficient of the statistically significant stations ($p < 0.10$) (°C/50 year), respectively,

m1, m1* – mean value of the regression coefficient for all the stations and mean value of the regression coefficient of the statistically significant stations ($p < 0.10$) (days/50 year), respectively.

For the indices acronyms see Table 2.

Extreme summer temperature (TN90p and TX90p) indices show a positive trend too. In particular, the occurrences of warm nights show a greater increase than warm days (+17 days/50 years vs. +12 days/50 years). The number of days with minimum temperature lower than 0 °C (FD) highlights a slight decreasing trend.

Agroclimatological indices, in particular phenological phase indices, such as those referred to GDD, show an advanced tendency (*Fig. 2*). In particular, ripening phase shows a great advance tendency (–19 days/50 years).

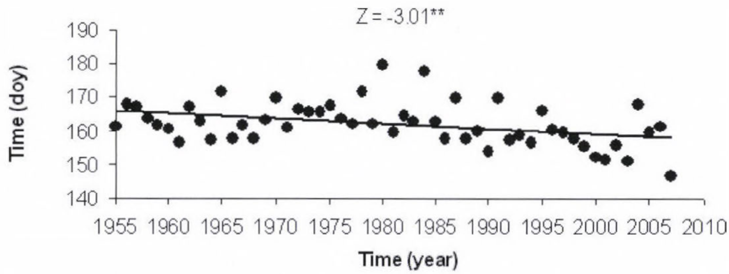

Fig. 2. Trend of the mean date of grapevine flowering for the 22 meteorological stations (1955–2007). ** = significance is greater than 99%; Z = standard normal distribution value; doy = day of the year.

The Huglin index (*Fig. 3*), according to the great rise of spring and summer temperatures, shows a generalized increasing trend in all over the region with a mean regional increase of 273 °C/50 years.

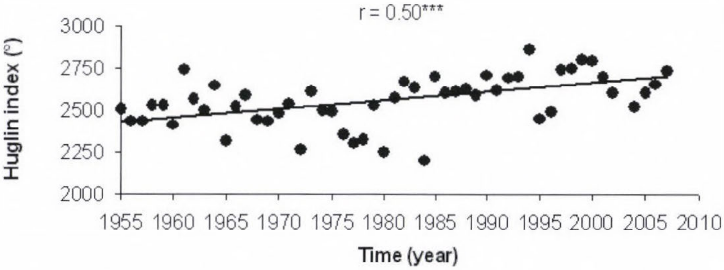

Fig. 3. Trend of the mean Huglin index for the 22 meteorological stations (1955–2007). *** = significance is greater than 99.9%; r = correlation coefficient.

Also STA10 (*Fig. 4*) and STA10 Winkler (*Fig. 5*) show positive trend (+203 °C/50 years and +219 °C/50 years, respectively). Vegetative growing season length with 0 °C threshold (VGS0) shows a slight positive trend (+5 days/50 year).

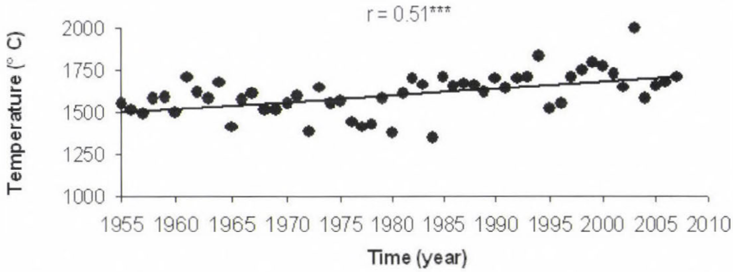

Fig. 4. Trend of the mean STA10 index for the 22 meteorological stations (1955–2007). *** = significance is greater than 99.9%; r = correlation coefficient.

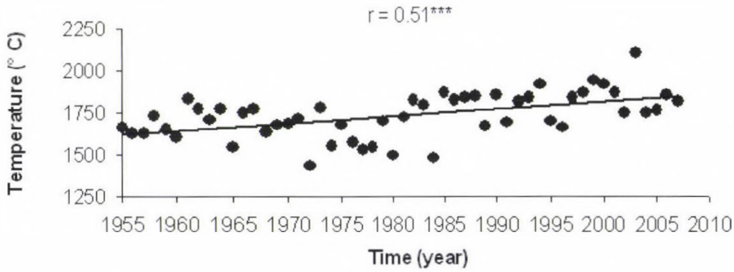

Fig. 5. Trend of the mean STA10 Winkler index for the 22 meteorological stations (1955–2007). *** = significance is greater than 99.9%; r = correlation coefficient.

4. Discussion and conclusions

The primary goal of this study was to assess Tuscany's annual and seasonal climatic and agroclimatic trend patterns, in order to more accurately represent local climate complexities and its potential impacts on grapevine. Moreover, the results of this study show a significant warming trend and a general advance in phenological phases confirming the global trend.

As grape quality is influenced by the temperatures in spring and summer, the observed temperature increase can produce physiological water stress and photosynthesis inefficiency (*Orlandini et al.*, 2005). Higher temperature summation lead to higher sugar accumulation in berry (*Gladstone*, 1992), less acidity and greater mean berry weight (*Fregoni*, 2002). Higher minimum temperatures speed up grape phenological phases and the advanced ripening affects the quality.

Huglin index shows general suitable conditions for grape varieties coming from southern region. Although frost day's trend is negative, late frosts damage risks are not decreased due to phenological general anticipations.

A more detailed research concerning the interannual variability by using standard deviation and moving average is need to understand the potential impacts on grapevine quality. Moreover, rainfall analysis and correlations with rising temperature may be useful to completely show the climate change effects on regional scale.

Acknowledgement—This study was performed with the support of Ente Cassa di Risparmio di Firenze.

References

Bartolini, G., Morabito, M., Crisci, A., Grifoni, D., Torrigiani, T., Petralli, M., Maracchi, G., Orlandini, S., 2008: Recent trends in Tuscany (Italy) summer temperature and indices of extremes. *Int. J. Climatol. 28*, 1751-1760, doi: 10.1002/joc.1673.

Bindi, M., Triossi, A., Moriondo, M., 2002: Mutamenti climatici e produzione vitivinicola europea. *L'Informatore Agrario 45*, 31-34.

Bindi, M., Fibbi, L., Gozzini, B., Orlandini, S., Miglietta, F., 1996: Modeling the impact of future climate scenarios on yield and variability of grapevine. *Climate Res. 7*, 213–224.

Brunetti, M., Maugeri, M., Monti, F., Nanni, T., 2006: Temperature and precipitation variability in Italy in the last two centuries from homogenised instrumental time series. *Int. J. Climatol. 26*, 345-381.

Fregoni, M., 2002: Adattamento della vite ai cambiamenti climatici futuri. *L'Informatore Agrario 45*, 29-30.

Gladstones, J., 1992: *Viticulture and Environment*. Winetitles, Adelaide.

IPCC, 2007: *Climate Change 2007: The Physical Science Basis. Contribution of Working Group I to the Fourth Assessment Report of the Intergovernmental Panel on Climate Change*. Edited by *S. Solomon, D. Qin, M. Manning, Z. Chen, M. Marquis, K.B. Averyt, M. Tignor,* and *H.L. Miller*. Cambridge, UK and New York, NY, Cambridge University Press. 996p. (Available online from http://www.ippc.ch)

Jones, G.V., 2003: *Climate and Terroir: Impacts of Climate Variability and Change on Wine*. Geoscience. Pper 4 from the "Terroir, geology andwinea tribute to simon j. haynes" Session held at The Geological Society of American Annual Meeting, Seattle, Washington, November 2, 2003.

Jones, G.V., Hellman, E., 2003: *Site Assessment: in "Oregon Viticulture"* (ed.: *E. Hellman*). 5th Edition, Oregon State University Press, Corvallis, Oregon, 44–50.

Jones, G.V., Whitem, White, M.A., Cooper, O.R., Storchmann, K., 2005: Climate change and global wine quality. *Climate Change 73*, 319-343.

Klein Tank, A.M.G., Können, G.P., 2003. Trend in indices of dayly temperature and precipitation extremes in Europe. *J. Climate 16*, 3665-3680.

Manton, M.J., Della-Marta, P.M., Haylock, M.R., Hennessy, K.J., Nicholls, N., Chambers, L.E., Collins, D.A., Daw, G., Finet, A., Gunawan, D., Inape, K., Isobe, H., Kestin, T.S., Lefale, P., Leyu, C.H., Lwin, T., Maitrepierre, L., Ouprasitwong, N., Page, C.M., Pahalad, J., Plummer, N., Salinger, M.J., Suppiah, R., Tran, V.L., Trewin, B., Tibig, I., Yee, D., 2001: Trends in extreme daily rainfall and temperature in southeast Asia and the south Pacific: 1961–1998. *Int. J. Climatol. 21*, 269–284, doi:10.1002/joc.610.

Maracchi, G., Sirotenko, O., Bindi, M., 2005: Impacts of present and future climate variability on agriculture and forestry in the temperate regions: Europe. *Climatic Change 70,* 117-135.

Mullins, M.G., Bouquet, A., Williams, L.E., 1992: *Biology of the Grapevine*. Cambridge University Press, Great Britain.

Nemani, R.R., White, M.A., Cayan, D.R., Jones, G.V., Running, S.W., Coughlan, J.C., Peterson, D., 2001: Asymmetric warming over coastal California and its impact on the premium wine industry. *Climate Res. 19*, 25-34.

Orlandini, S., Grifoni, D., Mancini, M., Barcaioli, G., Crisci, A., 2005: Analisi degli effetti della variabilità meteo-climatica sulla qualità del Brunello di Montalcino. *Rivista Italiana di Agrometeorologia 2*, 37-44.

Orlandini, S., 2004: La viticoltura di fronte ai cambiamenti climatici. Convegno IMaGONetafim "La vite e l'acqua", Sarteano, 26 Marzo 2004.

Peterson, T.C., Folland, C., Gruza, G., Hogg, W., Mokssit, A., Plummer, N., 2001: *Report of the Activities of the Working Group on Climate Change Detection and Related Rapporteurs. World Meteorological Organization Technical Document No 1071.* World Meteorological Organization, Geneva, Switzerland, 146.

Puglisi, A., Pastore, F., Orlandini, S., 2005: Analisi della variabilità climatica del territorio italiano. Implicazioni per la viticoltura. *Rivista Italiana di Agrometeorologia 9*, 70-71.

Schultz, H.R., 2000: Climate change and viticulture: An European perspective on climatology, carbon dioxide, and UV-B effects. *Australian Journal of Grape and Wine Research 6*, 2–12.

Sen, P.K., 1968: Estimates of the regression coefficient based on Kendall's tau. *Journal of the American Statistical Association 63*, 1379-1389.

Theil, H., 1950: A rank-invariant method of linear and polynomial regression analysis, I, II, III. *Nederlandse Akademie van Wetenschappen 53*, 396-392, 512-525, 1397-1412.

IDŐJÁRÁS

Quarterly Journal of the Hungarian Meteorological Service
Vol. 113, No. 1–2, January–June 2009, pp. 79–88

Testing different CO_2 response algorithms against a face crop rotation experiment and application for climate change impact assessment at different sites in Germany

K.C. Kersebaum[1,*], C. Nendel[1], W. Mirschel[1], R. Manderscheid[2], H.-J. Weigel[2], and K. -O. Wenkel[1]

[1]*Leibniz-Centre of Agricultural Landscape Research, Institute of Landscape Systems Analysis, Eberswalder Str. 84, D-15374 Müncheberg, Germany*

[2]*Johann Heinrich von Thünen-Institute (Federal Research Institute for Rural Areas, Forestry and Fisheries), Institute of Biodiversity, 38116 Bundesallee 50, D-Braunschweig, Germany*

(Manuscript received in final form December 5, 2008)

Abstract—In regional studies the effect of elevated CO_2 level on crop biomass and yield had not been considered in most cases, although several approaches were described in literature. Different algorithms describing CO_2 response on crop growth and crop water use efficiency have been integrated in the soil-crop model HERMES. The approaches are different in complexity and parameter requirement. Their suitability to explain crop growth responses and soil water dynamics observed in a six-year agricultural crop rotation (winter barley, sugar beet, winter wheat) under elevated atmospheric CO_2 level in a FACE experiment was tested. All algorithms were able to describe an observed increase in above-ground dry matter for all crops in the rotation. Increasing water use efficiency with rising CO_2 was also reflected. A combination of a semi-empirical Michaelis-Menten approach describing a direct impact of CO_2 on photosynthesis and a Penman–Monteith approach with a simple stomata conduction model for evapotranspiration yielded the best simulation result expressed by model performance indicators. Scenario simulations with and without CO_2 effect were performed for different sites in Germany for the present situation and the SRES-A1B scenario using statistically downscaled climate change scenarios from the WETTREG model. Results show that without consideration of the CO_2 effect mostly negative impacts on crop yields were simulated. Considering the CO_2 effect compensated the negative trend in most cases and turned yield effects to a positive impact.

Key-words: climate change, CO_2 effect, FACE experiment, crop yield, water use

* Corresponding author; E-mail: ckersebaum@zalf.de

1. Introduction

Climate change impact on food production is one of the key concerns of policy and research. Impact assessment usually requires spatial and temporal resolutions smaller than provided by the global climate models (GCM), since crop growth is temporary very sensitive, e.g., to radiation, temperature, soil moisture. Regional climate models *(Jacob et al.*, 2007*)* downscale the GCM results to a meso-climate level that can be used to assess climate effects on regional agriculture.

Climate change is expected to affect crop growth mainly by increasing temperatures, shifting distribution of precipitation, changing amount of precipitation, and rising atmospheric carbon dioxide concentration.

Describing the interactions of crop growth, soil processes, and weather variables in a simulation model is current state-of-art methodology to interpret downscaled GCM outputs for yield predictions. The effect of CO_2 on crop growth was recently implemented in agro-ecosystem models. Mainly two processes are affected: (i) in C3 plants, an increasing CO_2 would directly increase the photosynthesis rate (*Gaastra*, 1959) and (ii) a higher CO_2 would also lead to a decrease in stomatal conductance and thus to a higher water use efficiency *(Manderscheid* and *Weigel*, 2007*)*.

The impact of CO_2 on photosynthesis has been included in simulation models in different ways (*Tubiello* and *Ewert*, 2002). More simple approaches use an empirical relation between CO_2 and a crop specific radiation use efficiency (RUE) factor (e.g., *Bindi et al.*, 1996), others employ a CO_2 dependency of the photosynthesis-light response curve (e.g., *Porter*, 1993; *Goudriaan* and *van Laar*, 1994). Only few leaf-level biochemical algorithms are used, which require an extensive parameterization restricting their application to biochemical process research.

In this study, we integrated a number of selected algorithms into the soil-crop model HERMES to test their suitability to describe CO_2 impact on crop growth against data of a Free Air Carbon Enrichment (FACE) experiment (*Weigel* and *Dämmgen*, 2000). The best algorithm was then used in combination with downscaled climate change scenarios for simulations at different sites in Germany under the SRES-A1B scenario. Site selection considered locations with different climatic situations to demonstrate the combined climate change and CO_2 effect on crop yields of winter wheat.

2. Material and methods

2.1. The FACE experiment

At the experimental station of the von Thünen-Institute (vTI) at Braunschweig, Germany (52°18'N; 10°26'E), a three-year crop rotation (winter barley, sugar beet, winter wheat) was grown over two cycles at normal (~374 ppm) and elevated (~550 ppm) CO_2 levels. The crops were grown under optimum nutritional and moisture conditions. A FACE system, consisting of six rings with 20 m diameter was set up. Treatments included two rings equipped with blowers and enriched with CO_2, two rings operated with blowers and ambient air only and two rings without blowers. Subplots within the rings with 50% (N50) of the adequate nitrogen supply (N100) were established to study interactions between C and N. A detailed description is given by *Weigel* and *Dämmgen* (2000).

The soil is a loamy sand with 1.4% organic carbon (SOC) in the top soil. Soil texture allows a volumetric plant available water content (PAWC) of about 18% in the plough layer, which decreases slightly with increasing profile depth. Rooting depth is about 60 cm. During the experiment, soil moisture contents were determined gravimetrically. Fresh and dry weights of individual plant organs (culm, leaves, and ears, or tubers, respectively) were measured at intermediate harvests. At the final harvest, cereal grain yield was additionally quantified. Daily weather data were recorded at a nearby weather station.

2.2. The model framework

We tested the different CO_2 response algorithms within the HERMES model, which was designed to simulate crop growth, water and nitrogen uptake, and the nitrogen dynamics in the soil for applied purposes. This implies simple and robust model approaches, which are able to operate under restricted data availability. A more detailed description of the model is provided by *Kersebaum* (2007). Therefore, the characteristics of the model are described only briefly.

A capacity approach was used to describe soil water dynamics. The reference evapotranspiration was calculated using the Penman-Monteith method according to *Allen et al.* (1998). Crop specific potential evapotranspiration is calculated using crop specific factors (*kc*) during the growing season, which were linked to the developmental stages of the crops, and bare soil factors between harvest and crop emergence. Nitrogen mineralization and denitrification are simulated depending on temperature and soil moisture and nitrate content respectively.

Crop growth follows a generic approach, which is based on the SUCROS model. Daily net dry matter production by photosynthesis and respiration is driven by global radiation and temperature. Assimilates are partitioned depending on crop development stage, which is calculated from a thermal sum (degree-days) and modified, if applicable, by day length and vernalization. Root dry matter is distributed exponentially over depth with the rooting depth increasing with the thermal sum. Water and nitrogen uptake is calculated from potential evaporation and crop N status, depending on the simulated root distribution, and water and N availability in different soil layers. Crop growth is limited by water and N stress. Water and nitrogen stress accelerates crop ontogenesis for specific development stages. Crop yield was estimated at harvest from the weight of the storage organ.

The HERMES model was calibrated to the data of the control treatment of the FACE experiment, using the output variables soil moisture (sum of 0 – 60 cm soil depth), above-ground crop dry matter, and yield. Willmott's index of agreement (IoA) was used as a goodness-of-fit criterion (*Willmott*, 1981).

2.3. The CO_2 response algorithms

In order to equip the model with a suitable approach to describe CO_2 impact on crop growth, three algorithms were selected. The mechanistic and partly empirical character of the HERMES model determines the range of complexity the response algorithms have to match. The following approaches were selected:

(I) The Mitchell approach (*Mitchell et al.*, 1995) used a set of algorithms based on the ideas of *Farquhar* and *von Caemmerer* (1982) and *Long* (1991), calculating the maximum photosynthesis rate

$$A_{\max} = \frac{(C_i - \Gamma^*) \cdot V_{c\max}}{C_i + K_c \cdot \left(1 + \frac{O_i}{K_o}\right)}, \tag{1}$$

where C_i and O_i are the intercellular CO_2 and O_2 concentrations, respectively, Γ^* is the CO_2 compensation point of photosynthesis in absence of dark respiration, $V_{c\max}$ is the maximum Rubisco saturated rate of carboxylation, and K_c and K_o are Michaelis-Menten constants for CO_2 and O_2. The calculation of the latter four parameters is carried out according to *Long* (1991). Some modifications were applied to simplify the algorithms for suboptimal light conditions and light use efficiency.

(II) The Nonhebel approach is a much simpler approach extracted from the SUCROS87 model (*Nonhebel*, 1996). Here, *RUE* is directly affected by CO_2 as

$$RUE_{CO_2} = \left(\frac{C_a - \Gamma}{C_a + 2\Gamma}\right) \cdot E_0, \tag{2}$$

where C_a denotes CO_2 and E_0 the quantum use efficiency. Additionally, the maximum photosynthesis rate is influenced by CO_2 using

$$A_{\max(CO_2)} = \frac{C_a - \Gamma}{350 - \Gamma} \cdot A_{\max(350)}. \tag{3}$$

(III) The Hoffmann approach (*Hoffmann*, 1995) was similar to *Nonhebel* (1996) based on his own work with sugar beet and tree species, and on data previously obtained by *Gaastra* (1959). He adjusted A_{max} by the factor

$$K_{CO_2} = \frac{\dfrac{C_a - \Gamma^*}{k_1 + C_a - \Gamma^*}}{\dfrac{C_{a0} - \Gamma^*}{k_1 + C_{a0} - \Gamma^*}}, \tag{4}$$

where C_{a0} denotes the ambient CO_2 and C_a the elevated CO_2. Furthermore, $k_1 = 220 + 0.158 \cdot I_g$ and $\Gamma^* = 80 - 0.0036 \cdot I_g$, with I_g being the global radiation.

These three approaches were combined with a mixed Allen/Yu approach describing the CO_2 impact on crop transpiration. Evapotranspiration was calculated using the Penman and Monteith formula according to *Allen et al.* (1998) using the stomata resistance calculated as suggested by *Yu et al.* (2001) as

$$r_s = \frac{C_s\left(1 + \dfrac{D}{D_0}\right)}{a \cdot A_g}, \tag{5}$$

where a is a constant, A_g denotes the gross photosynthesis rate, D/D_0 describes the air water vapor deficit, and C_s is the ambient CO_2 concentration at leaf level, which was set equal to C_a in this case. D_0 and a were used for parameter calibration.

2.4. Model behavior under climate change scenarios

To demonstrate the combined effect of climate change and elevated CO_2 on wheat production, we selected 4 weather stations across Germany to cover the different climatic and soil conditions. The climate change scenarios were based on the SRES-A1B scenario and the output of the global climate model (GCM) ECHAM5/MPI-OMT63L31. The GCM output was downscaled using a statistical generation of classified weather situation sequences based on a data analysis of long term historical data of single meteorological stations by the WETTREG model (*Enke et al.* 2005). We selected 3 realizations (normal, wet, dry) for wetness for the period from 1961 to 2050. We used the time slice 1970–1989 as reference period and the time slice 2031–2050 for the projected future.

For each site, a typical soil profile was used. The characterization of the sites including the soil class, elevation, and the climatic conditions of the reference, as well as projected period are given in *Table 1*.

Table 1. Site characteristics and climatic changes estimated for the A1B scenario using the WETTREG model (*Enke et al.*, 2005) for selected locations across Germany. Numbers in parenthesis are changes in %

Station	Period	Hannover	Müncheberg	Hof	Weihenstephan
Latitude		52°28'N	52°52'N	50°19'N	48°24'N
Longitude		9°42'E	14°07'E	11°53'E	11°42'E
Altitude (a.s.l.)		55 m	62 m	567 m	470 m
Annual mean temperature (°C)	1970–1989	9.3	8.8	6.8	7.8
		(+8.8)	(+7.3)	(+10.8)	(+10.9)
	2031–2050	10.1	9.4	7.5	8.6
Annual precipitation (mm)	1970–1989	628	533	739	726
		(–5.1)	(–5.1)	(–3.5)	(–6.5)
	2031–2050	596	506	713	679
Precipitation winter (DJF) (mm)	1970–1989	156	131	182	118
		(+1.4)	(–7.6)	(+7.3)	(+12.9)
	2031–2050	158	121	195	133
Precipitation spring (MAM) (mm)	1970–1989	195	166	221	202
		(–3.4)	(–0.9)	(+3.6)	(+5.6)
	2031–2050	188	165	229	213
Precipitation summer (JJA) (mm)	1970–1989	181	165	230	272
		(–7.9)	(–3.0)	(–4.4)	(–5.8)
	2031–2050	167	160	220	229
Precipitation autumn (SON) (mm)	1970–1989	146	113	166	174
		(–9.1)	(–13.5)	(–8.8)	(–6.2)
	2031–2050	133	98	135	146
Soil		sandy loam	sand	sandy loam	silty loam

DJF = December, January, February; MAM = March, April, May; JJA = June, July, August; SON = September, October, November

3. *Results and discussion*

The Braunschweig FACE experiment showed two important results: increased CO_2 (i) enhanced crop growth for all investigated species and (ii) decreased evapotranspiration rate of the canopies resulting in higher soil moisture content (*Weigel et al.*, 2006). All algorithms tested within the HERMES model framework were able to describe the observed crop growth and soil moisture dynamics sufficiently under ambient and elevated CO_2 levels (*Table 2*). Since the Nonhebel and Mitchell approaches also affected the way of calculating photosynthesis under ambient CO_2 conditions, the simulation of the control treatment process yielded different results for all selected approaches. IoA yielded values of between 0.93 and 0.99 for the calibrated simulation of above ground dry matter (including tubers for sugar beet) and yield at sufficient N supply. *Fig. 1* shows the results using the combined Hoffmann/Yu/Allen approach. However, under limited N supply and under elevated CO_2 level the simulation performance was similar. For these variables, the Nonhebel approach performed slightly less satisfyingly than the others (*Table 2*). Such a performance is often found for single season crop growth simulations. However, for a six years rotation with three different crops this result is satisfying.

Table 2. Index of agreement IoA (*Willmott*, 1981) as a goodness-of-fit criterion for the simulation of the crop rotation experiment, using different approaches for the description of CO_2 impact on crop growth

CO_2 level ppm	Ambient		550		Ambient		550	
N level %	**100**	**50**	**100**	**50**	**100**	**50**	**100**	**50**
	Hoffmann				**Hoffmann + Allen/Yu**			
Above ground dry matter	0.99	0.98	0.99	0.99	0.99	0.99	0.99	0.99
Yield	0.98	0.96	0.97	0.94	0.98	0.98	0.97	0.97
Leaf area index	0.61	0.55	0.57	0.54	0.57	0.55	0.61	0.56
Soil moisture (0-60 cm)	0.77		0.76		0.79		0.82	
Mean IoA	**0.83**				**0.84**			
	Nonhebel				**Nonhebel + Allen/Yu**			
Above ground dry matter	0.95	0.94	0.98	0.96	0.95	0.99	0.98	0.98
Yield	0.93	0.94	0.95	0.93	0.93	0.94	0.95	0.92
Leaf area index	0.66	0.58	0.55	0.52	0.66	0.59	0.55	0.54
Soil moisture (0-60 cm)	0.77		0.77		0.85		0.85	
Mean IoA	**0.82**				**0.83**			
	Mitchell				**Mitchell + Allen/Yu**			
Above ground dry matter	0.99	0.95	0.99	0.99	0.99	0.95	0.99	0.99
Yield	0.98	0.98	0.97	0.96	0.97	0.97	0.97	0.96
Leaf area index	0.52	0.49	0.51	0.49	0.52	0.50	0.52	0.50
Soil moisture (0-60 cm)	0.78		0.78		0.80		0.83	
Mean IoA	**0.81**				**0.82**			

The simulation of soil moisture was compared to aggregated data (0 – 60 cm soil depth) and showed an IoA of 0.82 for calibrated conditions and 0.79 – 0.80 under elevated CO_2. When the CO_2 effect on transpiration was taken into account additionally, the overall performance improved slightly (*Table 2*) due to the better performance of the soil moisture simulation for all approaches (*Fig. 1c*). On the basis on above ground dry matter, yield, and soil moisture simulation, the Hoffmann approach in combination with the Allen/Yu approach performed best. However, the differences were marginal. *Fig. 1c* shows the measured and simulated soil water content under winter wheat in 2005 for ambient and elevated CO_2 level. The difference between the two CO_2 treatments expressed as the sum over six years corresponded well with the observed mean difference of approximately 20 mm water per year.

Application of the model with and without the combined Hoffmann/Yu/Allen approach for 4 selected sites in Germany shows different responses of crop yield to the projected climate change (*Fig. 2*). Without consideration of the CO_2 effect, only the site at Hof shows a beneficial trend for the wheat yield, because this elevated site is presently temperature limited. Therefore, crops would benefit from warming since precipitation is still sufficient. At the other sites, climate change without CO_2 would have a negative impact on crop yield mainly due to decreasing summer precipitation. Introducing the CO_2 effect in the model simulations in most cases leveled out the negative trend. Only at Müncheberg, the combination of poor sandy soil and very low precipitation could not be compensated completely by the CO_2 effect. Similar results for sites in Austria were published by *Alexandrov et al.* (2002). Separating the indirect from the direct CO_2 effect by switching off only the indirect effect shows, e.g., for the site at Hannover, that the indirect effect through the modified transpiration accounts for 2/3 of the total CO_2 effect simulated by the combined approach. The sites were selected exemplarily and neither represent wheat production areas in Germany nor give a representation of the whole specific regions, since they are only examples of one selected typical soil of the region.

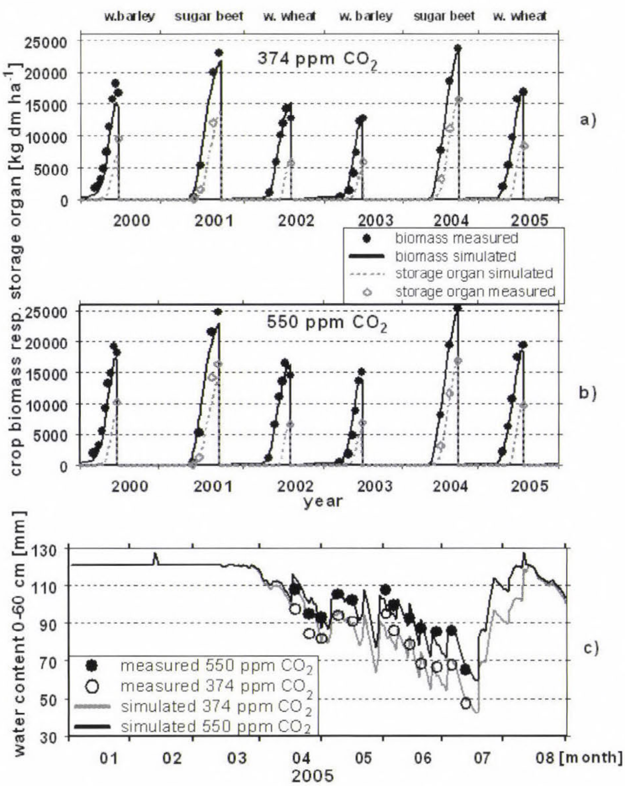

Fig. 1. Measured and simulated crop biomass (excluding root biomass) and storage organ mass of the Braunschweig FACE experiment for (a) 374 ppm CO_2 concentration, (b) 550 ppm CO_2 concentration, and (c) soil water contents (0 – 60cm) under winter wheat in 2005 in the 374 and 550 ppm plots (100% N treatment, simulation using the combined Hoffmann/Yu/Allen approach).

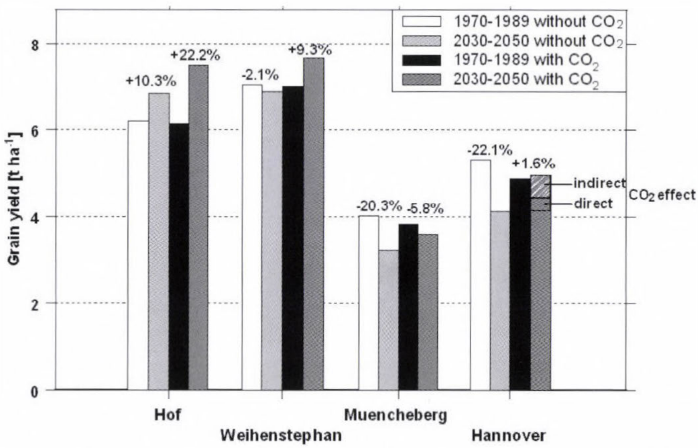

Fig. 2. Simulated impact of climate change scenario SRES-A1B on grain yield of winter wheat on selected sites across Germany with and without consideration of the CO_2 effect (combined Hoffmann/Yu/Allen approach).

4. Conclusions

For the simulation of expected climate change effects on regional agriculture an algorithm was found to successfully describe combined effects CO_2 levels, temperature, and moisture regime in a typical agricultural crop rotation in Germany. Application for 4 selected sites across Germany revealed that the simulated negative effect due to decreasing summer precipitation can be compensated in most cases if the combined CO_2 effect is considered. While sites at high elevation will benefit from global warming, the combination of poor sites and summer drought conditions resulted in yield reduction, which cannot be leveled out by the CO_2 effect.

Acknowledgement**—**The authors gratefully acknowledge funding from the German Federal Ministry of Education and Research (BMBF) within the "klimazwei" research program and from COST 734.

References

Alexandrov, V., Eitzinger, J., Cajic, V., Oberforster, M., 2002: Potential impact of climate change on selected agricultural crops in north-eastern Austria. *Glob. Change Biol. 8*, 372-389.

Allen, R.G., Pereira, L.S., Raes, D., Smith, M., 1998: *Crop Evapotranspiration. Guidelines for Computing Crop Water Requirements*. FAO Irrigation and Drainage Paper 56, Roma.

Bindi, M., Fibbi, L., Gozzini, B., Orlandini, S., Miglietta, F., 1996: Modelling the impact of future climate scenarios on yield and yield variability of grapevine. *Climate Res. 7*, 213-224.

Enke, W., Schneider, F., Deutschländer, Th., 2005: A novel scheme to derive optimized circulation pattern classifications for downscaling and forecast purposes. *Theor. Appl. Climatol. 82*, 51–63.

Farquhar, G.D., von Caemmerer, S., 1982: Modelling of photosynthetic response to environmental conditions. In *Encyclopedia of Plant Physiology* (eds.: *O.L. Lange*). *New series. Vol. 12B.* Physiological plant ecology. II. Water relations and carbon assimilation, 549-587.

Gaastra, P., 1959: Photosynthesis of crop plants as influenced by light, carbon dioxide, temperature, and stomatal diffusion resistance. *Mededel. Landbouwhogesch. Wageningen 59* (13), 1-68.
Goudriaan, J., van Laar, H.H., 1994: *Modelling Potential Crop Growth Processes.* Kluwer Academic Publishers, Dordrecht, The Netherlands.
Hoffmann, F., 1995: Fagus, a model for growth and development of beech. *Ecol. Model. 83*, 327-348.
Jacob, D., Barring, L., Christensen, O.B., Christensen, J.H., de Castro, M., Deque, M., Giorgi, F., Hagemann, S., Lenderink, G., Rockel, B., Sanchez, E., Schar, C., Seneviratne, S.I., Somot, S., van Ulden, A., van den Hurk, B., 2007: An inter-comparison of regional climate models for Europe: model performance in present-day climate. *Climate Change 81*, 31-52.
Kersebaum, K.C., 2007: Modelling nitrogen dynamics in soil-crop systems with HERMES. *Nutr. Cycl. Agroecosys. 77* (1), 39-52.
Long, S.P., 1991: Modification of the response of photosynthetic productivity to rising temperature by atmospheric CO2 concentrations – Has its importance been underestimated. *Plant Cell Environ. 14*, 729-739.
Manderscheid, R., Weigel, H.J., 2007: Drought stress effects on wheat are mitigated by atmospheric CO2 enrichment. *Agron. Sust. Dev. 27*(2), 79-87.
Mitchell, R.A.C., Lawlor, D.W., Mitchell, V.J., Gibbard, C.L., White, E.M., Porter, J.R., 1995: Effects of elevated CO_2 concentration and increased temperature on winter-wheat – Test of ARCWHEAT1 simulation model. *Plant Cell Environ. 18*, 736-748.
Nonhebel, S., 1996: Effects of temperature rise and increase in CO_2 concentration on simulated wheat yields in Europe. *Climate Change 34*, 73-90.
Porter, J., 1993: AFRCWHEAT2: a model of the growth and development of wheat incorporating responses to water and nitrogen. *Eur. J. Agron. 2* (2), 69-82.
Tubiello, F.N., Ewert, F., 2002: Simulating the effects of elevated CO_2 on crops: approaches and applications for climate change. *Eur. J. Agron. 18* (1-2), 57-74.
Weigel, H.J., Dämmgen, U., 2000: The Braunschweig Carbon Projekt: atmospheric flux monitoring and free air carbon dioxide enrichment (FACE). *J. Appl. Bot. 74*, 55-60.
Weigel, H.J., Manderscheid, R., Burkart, S., Pacholski, A., Waloszczyk, CK., Frühauf, O., Heinemeyer, O., 2006: Responses of an arable crop rotation system to elevated CO_2. In *Managed Ecosystems and CO_2 Case Studies, Processes, and Perspectives* (eds.: *J. Nösberger et al.*). *Ecol. Stud. 187*, 121-137.
Willmott, C.J., 1981: On the validation of models. *Phys. Geogr. 2*, 184-194.
Yu, Q., Goudriaan, J., Wang, T.D., 2001: Modelling diurnal courses of photosynthesis and transpiration of leaves on the basis of stomatal and non-stomatal responses, including photoinhibition. *Photosynthetica 39* (1), 43-51.

IDŐJÁRÁS
Quarterly Journal of the Hungarian Meteorological Service
Vol. 113, No. 1–2, January–June 2009, pp. 89–102

Climate change mitigation, adaptation, and sustainability in agriculture

Mannava V. K. Sivakumar* and **Robert Stefanski**

World Meteorological Organization,
7bis Avenue de la Paix, 1211 Geneva 2, Switzerland

(Manuscript received in final form January 19, 2009)

Abstract—Sustainability conveys the idea of a balance between human needs and environmental concerns. A common theme amongst definitions of sustainability is that sustainable agricultural systems remain productive over time. They should provide for the needs of current, as well as future generations, while conserving natural resources. The enhancement of environmental quality and careful use of resource base on which agriculture depends is viewed as a requisite for sustained agricultural productivity. The notion that sustainable agricultural systems maintain output in spite of major disturbances, e.g., such as those caused by projected climate change, is relevant to vulnerable areas, especially in the semi-arid and sub-humid regions of developing countries.

According to the Fourth Assessment Report of the WMO/UNEP Intergovernmental Panel on Climate Change (IPCC) released in 2007, semi-arid regions of Asia, Africa, and Latin America are likely to warm during this century, and freshwater availability is projected to decrease. Agricultural productivity in tropical Asia is sensitive not only to temperature increases, but also to changes in the nature and characteristics of monsoon. In the semi-arid tropics of Africa, which are already having difficulty coping with environmental stress, climate change resulting in increased frequencies of drought poses the greatest risk to agriculture. In Latin America, agriculture and water resources are most affected through the impact of extreme temperatures and changes in rainfall.

Climate change mitigation strategies which include interventions to reduce the sources or enhance the sinks of greenhouse gases have a marked management component aiming at conservation of natural resources such as improved fertilizer use, improved ruminant digestion, use of water harvesting, and conservation techniques. These strategies are equally consistent with the concept of sustainability. Adaptation strategies include initiatives and measures to reduce the vulnerability of agroecosystems to projected climate change, such as changing varieties, altering the timing or location of cropping activities, improving the effectiveness of pest, disease and weed management practices, making better use of seasonal climate forecasts, etc. It is essential to develop and integrate agriculture mitigation and adaptation frameworks for climate change into sustainable development planning at the national and regional levels to cope with the projected impacts of climate change.

Key-words: mitigation strategies, adaptation strategies, IPCC, mitigation and adaptation frameworks

* Corrsponding author; E-mail: msivakumar@wmo.int

1. Introduction

Climate change, a key global biophysical indicator, is widely accepted as the single most pressing issue facing society on a global basis, and the growing awareness of the impacts of climate change on agriculture is forcing decision makers to refocus on the sustainability of agricultural production. Broad concepts in sustainable agriculture encompass ecological, economic, and social parameters, whereas more narrowly defined concepts are mostly concerned with environmental issues such as optimal resource and environmental management (*McCracken* and *Pretty,* 1990). The notion that sustainable agricultural systems "maintain output in spite of major disturbance, such as caused by intensive stress or large perturbation" (*Conway*, 1985) is of particular relevance in the current concerns with the possible impacts of climate change on agroecosystems.

2. Observed climate change

The Intergovernmental Panel on Climate Change (IPCC) was established in 1988, by the World Meteorological Organization (WMO) and the United Nations Environment Program (UNEP), to assess scientific information on climate change, as well as its environmental and socioeconomic impacts, and to formulate response strategies. Climate change is defined by the IPCC as any change in climate over time, whether due to natural variability or as a result of human activity (*IPCC*, 2007b). Evidence from observations of the climate system has led to the conclusion that human activities are contributing to a warming of the Earth's atmosphere. This evidence includes an increase of 0.74 ± 0.18 °C in global average surface temperature over the last century, and an even greater warming trend over the last 50 years than over the last 100 years. Eleven years of the 12-year period between 1995 to 2006 are among the 12 warmest years since the instrumental record of global surface temperature was started in 1850 (*IPCC,* 2007b). Furthermore, higher temperatures along with decreased precipitation have been associated with observations of more intense and longer droughts over wider areas since the 1970s.

Changes in climate have also been manifested in altered precipitation patterns. Over the last century, the amount of precipitation has increased significantly across the eastern parts of North America and several other regions of the world (*IPCC*, 2007b). Many land areas have likely experienced an increase in the number and intensity of heavy precipitation (5 cm of rain or more) events (*IPCC*, 2007b). About half of the increase in total precipitation observed nationally in the United States has been attributed to the increase in intensity of storms (*Karl* and *Knight*, 1998).

During the 20th century, the changes in temperature and precipitation described above caused important changes in hydrology over large regions. One change was a decline in spring snow cover. This trend was observed throughout the Northern Hemisphere starting in the 1920s and accelerated in the late 1970s (*IPCC*, 2007b). Less snow generally translates to lower reservoir levels. The earlier onset of spring snowmelt exacerbates this problem. Snowmelt started 2–3 weeks earlier in 2000 than it did in 1948 (*Stewart et al.*, 2004).

Another manifestation of changes in the climate system is a warming in the world's oceans. The global ocean temperature rose by 0.10 °C from the surface to 700 m depth from 1961 to 2003 (*IPCC*, 2007b). Warming causes seawater to expand and thus contributes to sea level rise. This factor, referred to as thermal expansion, has contributed 1.6 ± 0.5 mm per year to global average sea level over the last decade (1993–2003). Other factors contributing to sea level rise over the last decade include a decline in mountain glaciers and ice caps (0.77 ± 0.22 mm per year), losses from the Greenland ice sheets (0.21 ± 0.07 mm per year), and losses from the Antarctic ice sheets (0.21 ± 0.35 mm per year) (*IPCC*, 2007c).

Other observations at smaller geographic scales lend evidence that the climate system is warming. For example, in the Arctic, average temperatures have increased and sea ice extent has shrunk (*IPCC*, 2007b).

3. *Future climate change*

Climate change projections indicate it to be very likely that hot extremes, heat waves, and heavy precipitation events will continue to become more frequent. Looking ahead, the *IPCC* (2007a) expects the warming in the 21st century to be greatest over land and at the highest northern latitudes. For the next two decades a warming of about 0.2 °C per decade is projected. Increases in the amount of precipitation are very likely in high latitudes, while decreases are likely in most subtropical land regions. For many parts of Africa the length of the growing period is projected to decrease over time (*Thornton et al.*, 2006) and projected losses in yield amount to 50% by 2020 for some countries (*IPCC*, 2007a).

Annual average river runoff and water availability are projected to increase by 10–40% at high latitudes and in some wet tropical areas, and decrease by 10–30% over some dry regions at mid-latitudes and in the dry tropics. The areas suitable for rainfed agriculture are expected to significantly decrease affecting adversely the land productivity potential of the continent (*Fischer et al.*, 2002).

4. *Climate change impacts*

An emerging but growing body of literature indicates that over the past three decades, the changes in the climate system described above—including the anthropogenic component of warming—have caused physical and biological changes in a variety of ecosystems (*Root et al.*, 2005; *Parmesan*, 2006; *IPCC*, 2007a) that are discernable at the global scale. These changes include shifts in genetics (*Bradshaw* and *Holzapfel*, 2006; *Franks et al.*, 2007), species' ranges, phenological patterns, and life cycles (reviewed in *Parmesan*, 2006). Most (85%) of these ecological responses have been in the expected direction (e.g., poleward shifts in species distributions), and it is very unlikely that the observed responses are due to natural variability alone (*IPCC*, 2007a).

Croplands, pastures, and forests that occupy 60 percent of the Earth's surface are progressively being exposed to threats from increased climatic variability and climate change. Abnormal changes in air temperature and rainfall and resulting increases in frequency and intensity of drought and flood events have long-term implications for the viability of these ecosystems (*FAO*, 2007).

IPCC (2007a) detailed many impacts on global and regional agriculture which impacts depend on the specific location and the magnitude of the warming.

- In general, the report states that increases in the frequency of droughts and floods are projected to affect local crop production negatively, especially in subsistence sectors at low latitudes.
- Globally, the potential for food production is projected to increase with increases in local average temperature over a range of 1–3 °C, but above this range, food production is projected to decrease.
- At lower latitudes, especially in the seasonally dry and tropical regions, crop productivity is projected to decrease for even small local temperature increases (1–2 °C), which would increase risk of hunger.
- Crop productivity is projected to increase slightly at mid- to high latitudes for local mean temperature increases of up to 1–3 °C depending on the crop, and then decrease beyond that in some regions.
- With the virtually certain likelihood of warmer and more frequent hot days and nights, there are projected to be increased insect outbreaks impacting agriculture, forestry, and ecosystems.
- Adaptations such as altered cultivars and planting times allow low- and mid- to high-latitude cereal yields to be maintained at or above baseline yields for modest warming.

They are too many region-specific climate change impacts on agricultural production to describe. For example, in many parts of Africa, it seems that warmer climates and changes in precipitation will destabilize the agricultural production. This is expected to undermine the systems that provide food security (*Gregory et al.*, 2005). *IPCC* (2007a) indicates that crop yields could decrease up to 30% in South Asia by the end of the century even if the direct positive physiological effects of CO_2 are taken into account. Several global studies indicate a probability of 10–40% loss in crop production in India with increases in temperature by 2080–2100 (*Rosenzweig et al.*, 1994; *Fischer et al.*, 2002; *Parry et al.*, 2004). From an analysis of climate risks for crops in 12 food-insecure regions conducted to identify adaptation priorities, based on statistical crop models and climate projections for 2030 from 20 general circulation models, *Lobell et al.* (2008) conclude that South Asia and Southern Africa are two regions that, without sufficient adaptation measures, will likely suffer negative impacts on several crops that are important to large food-insecure human populations.

In the Atlantic south, Continental south and Mediterranean zones of Europe, the greatest risks are reduced crop yields and conflicts over reduced water supply (*AEA Energy and Environment*, 2007). But in the Alpine, Boreal, Atlantic, and Continental north agro-climatic zones, a lengthened growing season and an extension of the frost-free period may increase the productivity of some crops and enhance the suitability of these zones for the growth of other crops. However, these changes will only be possible if there is sufficient water available (*AEA Energy and Environment*, 2007). Climate change is affecting many species attributes, ecological interactions, and ecosystem processes. Habitat change is already underway in some areas, leading to species range shifts, changes in plant diversity which includes indigenous foods and plant-based medicines (*McClean et al.*, 2005).

5. *Climate change and sustainability*

Sustainable agricultural systems remain productive over time (*Senanayake*, 1991) and should provide for the needs of current, as well as future generations, while conserving natural resources (*NRC*, 1991). The enhancement of the environmental quality and careful use of the resource base on which agriculture depends is viewed as a requisite to sustained agricultural productivity (*ASA*, 1989).

One important environmental force is climate, which can change over the long term and whose variation (with or without climatic change) has major implications for farming and sustainability. Agriculture's sensitivity to climate is influenced both by the nature of climatic variation and the nature of farming. Disasters are "caused" by the juxtaposition of a vulnerable activity and particular climatic conditions. For example, lack of economic activity and poverty renders African countries, especially the poorest communities in these countries, disproportionately vulnerable to climate change impacts.

The issues of climate change and sustainability have become well known worldwide, following the adoption of the United Nations' Agenda 21 and the United Nations Framework Convention on Climate Change (UNFCCC) at the 1992 Earth Summit in Rio de Janeiro, Brazil. Development, equity, and sustainability are integral elements of sustainable development. Hazards associated with climate change have the potential to undermine progress with sustainable development (*Berke*, 1995; *Wang'ati*, 1996). Therefore, it is important for sustainable development initiatives to explicitly consider hazards and risks associated with climate change (*Apuuli et al.*, 2000). The capacity to mitigate and adapt to climate change, and the associated mitigation and adaptation costs, depend critically upon the underlying development path, which in turn would be significantly influenced by sustainable development policies and actions.

Swart et al. (2003) point out that climate change and sustainable development have been addressed in largely separate circles in both research and policy. Nevertheless, there are strong linkages between the two in both realms. They argue that since the feasibility of stabilizing greenhouse gas concentrations is dependent on general socio-economic development paths, climate policy responses should be fully placed in the larger context of technological and socio-economic policy development rather than be viewed as an add-on to those broader policies.

Robinson et al. (2006) argue that manifold linkages exist between climate change and sustainable development, and that the focus has typically been on examining sustainable development through a climate change lens, rather than vice versa. They refer to the work of a panel of business, local government, and academic representatives in British Columbia, Canada, who were appointed to advise the provincial government on climate change policy. The panel found that sustainable development may offer a significantly more fruitful way to pursue climate policy goals than climate policy itself. Hence it is important to understand clearly the concept of sustainable agriculture and how it might help in coping with the projected climate change.

6. Climate change mitigation and adaptation

Climate change adaptation includes both short- and long-term responses to climate change, whereas mitigation refers to methods of reducing greenhouse gas emissions.

6.1. Climate change mitigation

When the topic of climate change is usually discussed, the focus is on the impact of the future climate changes on the agricultural sector. However, there is another aspect of climate change and agriculture, and that is the contribution of GHG emissions from agricultural sources (*Das*, 2004; *Desjardins*, 2004; *Smith et al.*, 2007; *Desjardins et al.*, 2007). According to the IPCC AR4, agriculture accounted for 10–12% (5.1 to 6.1 Gt CO_2-eq/yr) of total global anthropogenic emissions of greenhouse gases GHGs (*Smith et al.*, 2007). In separating the contribution from each GHG, agriculture accounted for about 60% of global anthropogenic emissions of N_2O and about 50% of CH_4.

Table 1 shows the percentage of world GHG emissions from agriculture by source in 2000 (*Vergé et al.*, 2007). This analysis for this table focused only on methane and nitrous oxide emissions. *Vergé et al.* (2007) state that carbon dioxide emissions from agriculture are mainly due to changes in land use such as clearing forests for agricultural development. Nitrous oxide emissions from agricultural soils represent the largest source of GHG emissions from agriculture. Nitrous oxide is produced in the soil during the process of converting ammonia to nitrate (nitrification) by soil microbes and by the conversion of nitrate into gaseous nitrogen (denitrification). Methane emissions by enteric fermentation (by-product of livestock digestion) is the second largest, and methane emissions from the fermentation of decomposing organic matter from rice paddies is the third. These three sources account for 86.2% of the GHG emissions from global agriculture. Globally, agricultural CH_4 and N_2O emissions have increased by nearly 17% from 1990 to 2005 (*Smith et al.*, 2007).

Table 1. Percentage of world GHG emissions from agriculture by source in 2000 excluding CO_2 (*Vergé et al.*, 2007)

Source	World GHG emissions from agriculture (%)
Agricultural soils (N_2O)	41.4
Enteric fermentation (CH_4)	30.1
Rice (CH_4)	14.7
N fertilizers (N_2O)	7.3
Manure management (CH_4)	3.4
Manure storage (N_2O)	3.1

6.1.1. Mitigation strategies

The IPCC AR4 (*Barker et al.*, 2007) defines mitigation as the technological change and substitution that reduces resource inputs and emissions per unit of output. Although several social, economic and technological policies would produce a reduction in emissions with respect to climate change, the term mitigation is defined as implementing policies to reduce GHG emissions and enhance sinks. The IPCC AR4 Working Group III Chapter on Agriculture (*Smith et al.*, 2007) noted that the most prominent mitigation options of GHG emissions in agriculture are improved crop and grazing land management such as improved agronomic practices, nutrient use, tillage, and residue management, restoration of organic soils that are drained for crop production, and restoration of degraded lands. Other options that offer significant mitigation potential include improved water and rice management; set-asides, land use change such as the conversion of cropland to grassland and agro-forestry; as well as improved livestock and manure management. The AR4 chapter on agricultural mitigation stresses that a practice effective in reducing emissions at one location may be less effective or even counterproductive elsewhere. Therefore, there is no universally applicable list of mitigation practices and that practices need to be evaluated for individual agricultural systems based on climate, soil, social issues, and historical patterns of land use and management.

Most of the mitigation strategies involve reducing nitrous oxide and methane emissions in agriculture. With regards to reducing CO_2 emissions in agriculture, increasing energy efficiencies in the transportation and building sector are important, but soil carbon sequestration is a mitigation strategy in which agriculture can directly plays a significant important role. The IPCC (*Smith et al.*, 2007) stated that soil carbon sequestration can provide an estimated 89% contribution to the total mitigation potential, while mitigation of CH_4 emissions and N_2O emissions from soils only account for 9% and 2%, respectively, of the total.

Desjardins (2004) provided an overview of agricultural practices to reduce GHG which include the following categories: livestock management; animal waste and nutrient management; crop management; soil management; and energy. *Edwards* (2007) notes that organic agricultural practices can reduce GHG emission in agriculture. These practices include the systematic application of manure and compost from animal and crop residues; crop-legume rotations; green manure with legumes; and agroforestry with multipurpose leguminous trees.

The AR4 report noted that the interactions between mitigation and adaptation in the agricultural sector need to be examined but differ in their spatial and geographic characteristics (*Smith et al.*, 2007). The report goes on to state that in many regions, non-climate policies related to economics, agriculture, and environment will have a larger impact on agricultural mitigation than climate policies. Also, current GHG emission rates may increase due to future population growth and changing diets. The report concluded that there is significant potential for GHG mitigation in agriculture and that current initiatives suggest that synergies between climate change policies, sustainable development, and improvement of environmental quality will be in the forefront in realizing mitigation potential in agriculture.

6.2. Climate change adaptation

As described earlier, climate change is expected to present new combinations of risks and potentially grave consequences. The secondary changes induced by climate change are expected to undermine the ability of people and ecosystems to cope with extreme climate events and other natural hazards. According to *Thomas* (2008), the world's drylands will face not only increasing temperatures with climate change but more importantly also disruptions to their hydrological cycles resulting in less and more erratic rainfall that will exacerbate the already critical state of water scarcity and conflicts over water allocation. In many regions of Africa, where small farmers depend on natural environment for their livelihoods, the high levels of poverty combined with rather poor infrastructure increases the vulnerability of local communities to climate change. Adaptation is a key factor that will shape the future severity of climate change impacts on food production (*Easterling et al.*, 2007) and is most relevant when it influences decisions that exist irrespectively of climate change, but which have longer-term consequences (*Stainforth et al.*, 2007).

According to *FAO* (2007), the two main types of adaptation are autonomous and planned adaptation. Autonomous adaptation is the reaction of, for example, a farmer to changing precipitation patterns through changing crops or planting dates. Planned adaptation measures, on the other hand, are conscious policy options or response strategies, often multisectoral in nature, aimed at altering the adaptive capacity of the agricultural system, or facilitating specific adaptations. Judicious use of water using supplementary irrigation systems, more efficient irrigation practices, and the adaptation and adoption of existing and new water harvesting technologies have been suggested as appropriate strategies to cope with these problems.

6.2.1. Adaptation strategies

Human adaptation to climate change impacts is increasingly viewed as a necessary complementary strategy to mitigation—reducing greenhouse gas emissions from energy use and land use changes in order to minimize the pace and extent of climate change (*Klein et al.*, 2007). Because adaptive strategies undertaken will have associated effects on carbon dynamics, it is important to consider carbon impacts of any proposed adaptive strategy.

In agriculture, forestry, livestock operations, water resources management, public health, and other fields impacted by climate change, there are typically a multiplicity of adaptation measures that may be taken (*Table 2*). In any given situation or context, though, the choice of adaptation measures may be difficult and constrained by their expense, the lack of knowledge on how to implement them, traditional beliefs, cultural practices, and others. Notwithstanding these impediments, farmers and others at risk from climate change (and including variability and extremes) can be provided with external help in a number of ways: insurance or other forms of financial assistance and risk spreading; drought relief in the form of cash or kind; information and advice; information and guidance; free or cheap seeds or replacement seed for seeds consumed, and so on (*Yohe et al.*, 2007). These are actions than can be taken to reduce exposure, vulnerability, or risk. For example, farmers in regions subject to drought can select the time of planting appropriate to their cropping systems.

For Europe, *AEA Energy and Environment* (2007) identified priority risks at the sector and farm level in the assessment of impacts and evaluated a number of possible adaptation responses (at both sector/policy level and farm level) with respect to the following issues: technical feasibility, potential costs of implementation, cost-effectiveness, ancillary benefits, and cross-sectoral implications (e.g., water, tourism, energy). Adaptation measures were further categorized as technical (e.g., introduction of new cultivars), management (e.g., changes in cropping patterns, soil, landscape, water), or infrastructural (e.g., changes in drainage, irrigation systems, access, buildings).

Table 2. Available adaptation measures

Sectors	Adaptation measures
Agricultural cropping	Choice of crop and cultivar: Use of more heat/drought-tolerant crop varieties in areas under water stress; Use of more disease and pest tolerant crop varieties; Use of salt-tolerant varieties; Introduce higher yielding, earlier maturing crop varieties in cold regions. Farm management: Altered application of nutrients/fertilizer; Altered application of insecticide/pesticide; Change planting date to effectively use the prolonged growing season and irrigation; Develop adaptive management strategy at farm level.
Livestock production	Breeding livestock for greater tolerance and productivity; Increase stocks of forages for unfavorable time periods; Improve pasture and grazing management including improved grasslands and pastures; Improve management of stocking rates and rotation of pastures; Increase the quantity of forages used to graze animals; Plant native grassland species; Increase plant coverage per hectare; Provide local specific support in supplementary feed and veterinary service.
Fishery	Breeding fish tolerant to high water temperature; Fisheries management capabilities to cope with impacts of climate change must be developed.
Development of agricultural biotechnologies	Development and distribution of more drought, disease, pest and salt-tolerant crop varieties; Develop improved processing and conservation technologies in livestock production; Improve crossbreeds of high productivity animals.
Improvement of agricultural infrastructure	Improve pasture water supply; Improve irrigation systems and their efficiency; Improve use/store of rain and snow water; Improve information exchange system on new technologies at national as well as regional and international level; Improve sea defense and flood management; Improve access of herders, fishers and farmers to timely weather forecasts.

Source: *Yohe et al.* (2007)

In a synthesis of research on adaptation options in Canadian agriculture, *Smith* and *Skinner* (2002) identified four main categories of adaptation options: (i) technological developments, (ii) government programs and insurance, (iii) farm production practices, and (iv) farm financial management. Most adaptation options were identified as modifications to on-going farm practices and public policy decision making processes with respect to a suite of changing climatic (including variability and extremes) and non-climatic conditions (political, economic, and social).

7. *Conclusions*

Western governments currently prioritize economic growth and the pursuit of profit above alternative goals of sustainability, health, and equality. Climate change and rising energy costs are challenging this consensus. The realization of the transformation required to meet these challenges has provoked denial and conflict, but could lead to a more positive response which leads to a health dividend; enhanced well-being, less overconsumption, and greater equality (*McCartney et al.*, 2008).

There is a need for better assessment of risks associated with variable and uncertain environmental conditions. This likely would involve documentation of climatic variation (temporal and spatial) so that probabilities of climatic conditions can be better estimated. This is different from mapping "normal" conditions, and it should focus on those climatic variables that are pertinent (for example, moisture during critical time periods) rather than readily available (such as mean annual temperature). This assessment of risks should include consideration of variation in other relevant external forces, including economic and policy conditions.

There is also a need for developing and promoting enterprises and management practices that are adaptive and sustainable in the variable and uncertain environment. Evaluations of existing and potential production systems according to their ability to sustain production and economic returns, as well as the consideration of policy vehicles (i.e., alternatives to the set of policies likely to be withdrawn) that might promote more sustainability, would help address this need.

References

AEA Energy and Environment, 2007: *Adaptation to Climate Change in the Agricultural Sector*. AGRI-2006-G4-05. Report to European Commission Directorate – General for Agriculture and Rural Development.

Apuuli, B., Wright, J., Elias, C., and *Burton, I.,* 2000: Reconciling national and global priorities in adaptation to climate change: with an illustration from Uganda. *Environ. Monit. Assess. 61*(1), 145–159.

ASA (American Society of Agronomy), 1989: Decision reached on sustainable agriculture. *Agronomy News, January*, p. 15.

*Barker, T., Bashmakov, I., Bernstein, L., Bogner, J.E., Bosch, P.R., Dave, R., Davidson, O.R., Fisher, B.S., Gupta, S., Halsnæs, K., Heij, G.J., Kahn Ribeiro, S., Kobayashi, S., Levine, M.D., Martino, D.L., Masera, O., Metz, B., Meyer, L.A., Nabuurs, G.-J., Najam, A., Nakicenovic, N., Rogner, H.-H., Roy, J., Sathaye, J., Schock, R., Shukla, P., Sims, R.E.H., Smith, P., Tirpak, D.A., Urge-

Vorsatz, D., Zhou, D., 2007: Technical Summary. In *Climate Change 2007: Mitigation.* Contribution of Working Group III to the Fourth Assessment Report of the Intergovernmental Panel on Climate Change (eds.: *B. Metz, O.R. Davidson, P.R. Bosch, R. Dave, L.A. Meyer*). Cambridge University Press, Cambridge, United Kingdom and New York, NY, USA.

Berke, P.R., 1995: Natural-hazard reduction and sustainable development: a global assessment. *Journal of Planning Literature 9*(4), 370–382.

Bradshaw, W.E. and *Holzapfel, C.M.*, 2006: Climate change: evolutionary response to rapid climate change. *Science 312*(5779), 1477-1478.

Conway, G.R.., 1985: Agroecosystem analysis. *Agr. Admin. 20*, 1-25.

Das, H.P., 2004: Adaptation strategies required to reduce vulnerability in agriculture and forestry to climate change, climate variability and climate extremes. In Management strategies in agriculture and forestry for mitigation of greenhouse gas emissions and adaptation to climate variability and climate change. *WMO Publication* No. 969. WMO, Geneva, Switzerland, 41-92.

Desjardins, R.L., 2004: The impact of management strategies in agriculture and agroforestry to mitigate greenhouse gas emissions. In Management strategies in agriculture and forestry for mitigation of greenhouse gas emissions and adaptation to climate variability and climate change. *WMO Publication* No. 969. WMO, Geneva, Switzerland, 30-41.

Desjardins, R.L., Sivakumar, M.V.K., and *de Kimpe, C.* (eds.) 2007: The Contribution of agriculture to the State of Climate. Special Issue *Agr. Forest Meteorol. 142.*

Easterling, W., Aggarwal, P. Batima, P., Brander, K., Erda, L., Howden, M., Kirilenko, A., Morton, J., Soussana, J.-F., Schmidhuber, S., and *Tubiello, F.*, 2007: Food, fibre and forest products. In *Climate Change 2007: Impacts, Adaptation and Vulnerability.* Contribution of Working Group II to the Fourth Assessment Report of the Intergovernmental Panel on Climate Change. (eds.: *M.L. Parry, O.F. Canziani, J.P. Palutikof, P.J. van der Linden,* and *C.E. Hanson*). Cambridge University Press, Cambridge, United Kingdom and New York, NY, USA, pp. 273-313.

Edwards, S., 2007: Role of organic agriculture in preventing and reversing land degradation. In *Climate and Land Degradation* (eds.: *M.V.K. Sivakumar* and *N. Ndiang'ui*). Springer, Berlin, Germany.

FAO, 2007: Adaptation to climate change in agriculture, forestry and fisheries: Perspective, framework and priorities. Food and Agriculture Organization of the United Nations, Rome, Italy.

Fischer, G., Shah, M., and *van Velthuizen, H.*, 2002: Climate change and agricultural vulnerability. *International Institute for Applied Systems Analysis, Vienna, Austria.* Available online at: www.iiasa.ac.at/Research/LUC/JB-Report.pdf.

Franks, S.J., Sim, S., and *Weis, A.E.*, 2007: Rapid evolution of flowering time by an annual plant in response to a climate fluctuation. *Proceedings of the National Academy of Sciences of the United States of America*, *104*, 1278-1282.

Gregory, P.J., Ingram, J.S.I., and *Brklacich, M.*, 2005: Climate change and food security. *Philos. T. Roy. Soc. B. 36,* 2139-2148.

IPCC, 2007a. *Climate Change 2007: Impacts, Adaptation and Vulnerability.* Contribution of Working Group II to the Fourth Assessment Report of the Intergovernmental Panel on Climate Change. Cambridge University Press, Cambridge.

IPCC, 2007b. *Climate Change 2007: The Physical Science Basis.* Contribution of Working Group I to the Fourth Assessment Report of the Intergovernmental Panel on Climate Change (eds.: *S. Solomon, D. Quin, M. Manning, Z. Chen, M. Marquis, K.B. Averyt, M. Tignor,* and *H.L. Miller*). Cambridge University Press, Cambridge, United Kingdom and New York, NY, USA, pp. 1-996.

IPCC, 2007c. Summary for policymakers. In *Climate Change 2007: The Physical Science Basis.* Contribution of Working Group I to the Fourth Assessment Report of the Intergovernmental Panel on Climate Change (eds.: *S. Solomon, D. Qin, M. Manning, Z. Chen, M. Marquis, K.B. Averyt, M. Tignor,* and *H.L. Miller*). Cambridge University Press, Cambridge, United Kingdom and New York, NY, USA.

Karl, T.R. and *Knight, R.W.*, 1998: Secular trends of precipitation amount, frequency, and intensity in the United States. *B. Am. Meteorol. Soc.79(2),* 231-241.

Klein, R.J.T., Hug, S., Denton, F., Downing, T. E., Richels, R., Robinson, G., and *Toth, F.L.*, 2007: Inter-relationships between adaptation and mitigation. In *Climate Change 2007: Impacts, Adaptation and Vulnerability.* Contribution of Working Group II to the Fourth Assessment

Report of the Intergovernmental Panel on Climate Change (eds.: *M.L. Parry, O.F. Caziani, J.P. Palutikof, P.J. van der Linden,* and *C.E. Hanson*). *Cambridge University Press, Cambridge, UK, pp. 745-777.*

Lobell, D.B., Burke, M.B., Tebaldi, C., Mastrandrea, M.D., Falcon, W.P., Naylor1, R.L., 2008: Prioritizing Climate Change Adaptation Needs for Food Security in 2030. *Science 319*, 607-610.

McCartney, G., Hanlon, P., and *Romanes, F.*, 2008: Climate change and rising energy costs will change everything: A new mindset and action plan for 21st Century public health. *Public Health 122*, 658-663.

McClean C.J., Lovett J.C., Küper W., Hannah, L., Sommer J.H., Barthlott, W., Termansen, M., Smith G.F., Tokumine S., and *Taplin J.R.D.*, 2005: *African plant diversity and climate change. Annals of the Missouri Botanical Garden 92,139-152.*

McCracken, J.A. and *Pretty, J.*, 1990*: Glossary of Selected Terms in Sustainable agriculture. Gatekeeper Series No. SA6, International Institute for Environment and Development, London.*

NRC (National Research Council), 1991: Toward Sustainability. A plan for collaborative research on agriculture and natural resource management. *Board on Science and Technology for International Development. National Academy Press, Washington DC.*

Parmesan, C., 2006: Ecological and evolutionary responses to recent climate change. *Annu. Rev. Ecol., Evol. Syst. 37,* 637-669.

Parry, M.L., Rosenzweig, C., Iglesias, A., Livermore M., and Fischer, G., 2004. Effects of climate change on global food production under SRES emissions and socio-economic scenarios. *Global Environmental Change* 14, 53–67.

Robinson, J., Bradley, M., Busby, P., Connor, D., Murray, A., Sampson, B., and *Soper, W.*, 2006: Climate change and sustainable development: realizing the opportunity. *Ambio 35*, 2-8.

Root, T.L., MacMynowski, D.P., Mastrandrea, M.D., and *Schneider, S.H.*, 2005: Human modified temperatures induce species changes: joint attribution. *Proceedings of the National Academy of Sciences of the United States of America, 102*(21), 7465- 7469.

Rosenzweig, C., Curry, B., Ritchie, J.T., Jones, J.W., Chou, T.Y., Goldberg, R., and *Iglesias, A.*, 1994: The effects of potential climate change on simulated grain crops in the United States. In Implications of Climate Change for International Agriculture: Crop Modelling Studies (eds.: *C. Rosenzweig, A. Iglesias*). U.S. Environmental Protection Agency, Washington DC, USA. pp. 1-24.

Senanayake, R.., 1991: Sustainable agriculture: definitions and parameters of measurement. *J. Sustain. Agr. 1*(4), 7-28.

Smit, B., Skinner, M.W., 2002: Adaptation options in agriculture to climate change: a typology. *Mitigation and Adaptation Strategies for Global Change 7*, 85–114.

Smith, P., Martino, D., Cai, Z., Gwary, D., Janzen, H., Kumar, P., McCarl, B., Ogle, S., O'Mara, F., Rice, C., Scholes, B., Sirotenko, O., 2007: *Agriculture.* In *Climate Change 2007: Mitigation.* Contribution of Working Group III to the Fourth Assessment Report of the Intergovernmental Panel on Climate Change (eds.: *B. Metz, O.R. Davidson, P.R. Bosch, R. Dave, L.A. Meyer*). Cambridge University Press, Cambridge, United Kingdom and New York, NY, USA.

Stainforth, D.A., Downing, T.E., Washington, R., Lopez, A., and *New, M.*, 2007: Issues in the interpretation of climate model ensembles to inform decisions. *Philos. T. Roy. Soc. 365,* 2163-2177.

Stewart, I.T., Cayan, D.R., and Dettinger, M.D., 2004: Changes in snowmelt runoff timing in Western North America under a 'business as usual' climate change scenario. *Climatic Change 62*, 217-232.

Swart, R., Robinson, J., and *Cohen, S.*, 2003: Climate change and sustainable development: expanding the options. *Climate Policy 3 Supplement 1*, S19-S40.

Thomas, R.J., 2008: Opportunities to reduce the vulnerability of dryland farmers in Central and West Asia and North Africa to climate change. *Agr. Ecosys. Environ. 126*, 36-45.

Thornton, P.K., Jones, P.G., Owiyo, T., Kruska, R.L., Herrero, M., Kristjanson, P., Notenbaert, A., Bekele, N., and *Omolo, A., with contributions from Orindi, V., Ochieng, A., Otiende, B., Bhadwal, S., Anantram, K., Nair, S., Kumar, V.*, and *Kelkar, U.*, 2006: Mapping climate vulnerability and poverty in Africa. *Report to the Department for International Development, ILRI, Nairobi, Kenya, May 2006, 200 pp. Online at http://www.dfid.gov.uk/research/mapping-climate.pdf*

Vergé, X.P.C., De Kimpe, C., and *Desjardins, R.L.*, 2007: Agricultural production, greenhouse gas emissions and mitigation potential. *Agr. Forest Meteorol. 142,* 255-269.

Wang'ati, *F.J.*, 1996: The impact of climate variation and sustainable development in the Sudano-Sahelian region. In *Climate Variability, Climate Change and Social Vulnerability in the Semi-Arid Tropics* (eds.: *J.C. Ribot, A.R. Magalhães,* and *S.S. Panagides*). Cambridge University Press, Cambridge, United Kingdom and New York, NY, USA, pp. 71–91.

Yohe, G., Burton, I., Huq, S., and *Rosegrant, M.W.*, 2007: Adaptation, mitigation and climate risk. A synthesis with emphasis on Asia. Prepared for Policy Forum *Agricultural and Rural Development for Reducing Poverty and Hunger in Asia: In Pursuit of Inclusive and Sustainable Growth.* 9-10 August 2007, Asian Development Bank, Manila, Philippines.

IDŐJÁRÁS

Quarterly Journal of the Hungarian Meteorological Service
Vol. 113, No. 1–2, January–June 2009, pp. 103–115

Some perspectives on agricultural GHG mitigation and adaptation strategies with respect to the impact of climate change/variability in vulnerable areas

Ward Smith[1], **Brian Grant**[1], and **Ray Desjardins**[1]

[1]*Agriculture and Agri-Food Canada, Research Branch, K.W., Neatby bldg., Ottawa, ON, Canada; E-mail: smithw@agr.gc.ca*

(Manuscript received in final form January 19, 2009)

Abstract—It is generally agreed that agricultural activities contribute to greenhouse gas (GHG) build up in the atmosphere which influences climate change and climate variability. Worldwide agriculture is responsible for about 13 percent of the total anthropogenic emissions. The scientific community has placed considerable efforts on developing ways to mitigate this effect through improvements in agricultural management practices. Improved management practices such as precision farming, implementation of less intensive tillage, changes in crop rotation, improved feed quality for better digestibility, improved manure handling, better water management of rice paddies, and biofuel/bioheat production are commonly employed as a means to mitigate GHG emissions. Even with all these mitigation measures, climate change is likely to have a wide range of effects on agricultural systems and we must adapt to these changes to ensure that agricultural production is not only maintained but is increased to support a growing world population. In some areas shifts in crop zones are expected, whereby cool season crops may be replaced by warm season crops and new cropping zones may open up for production. Most adaptation scenarios are likely to influence GHG emissions. Production of bioenergy crops, particularly lignocellulosic crops can, in some cases, provide a means to both mitigate net CO_2 emissions and adapt to a changing climate and world energy needs. There are numerous potential mitigation strategies to reduce GHG emissions from agriculture, but their effectiveness depends on climate, soil, and economic conditions which vary across regions. Process-based models can potentially act as a useful tool for examining the influence that climate change may have on mitigation and adaptation efforts. However, there are gaps in knowledge regarding processes that govern GHG emissions and much uncertainty regarding future trends in climate. In this paper the DeNitrification-DeComposition (DNDC) model was used to investigate the influence that a changing climate might have on GHG emissions in agricultural systems. Results indicate that N_2O emissions will be highly variable across different landscapes, and that net CO_2 emissions will generally increase, particularly in cooler regions. In regions with an average annual temperature of less than 10 °C, enhanced soil carbon decomposition due to increased temperatures is expected to cause a loss of approximately 70 kg CO_2 ha^{-1} y^{-1} by 2100.

Key-words: greenhouse gas, mitigation, adaptation, climate change, model

1. *Introduction*

Mitigating greenhouse gas (GHG) emissions and adapting to climate change will give rise to economic and environmental constraints. The agricultural sector is responsible for approximately 10–13% of total global anthropogenic emissions of GHGs (5.1 to 6.1 Gt CO_2-eq y^{-1} in 2005), and most of these emissions are in the form of CH_4 and N_2O (*Carter et al.*, 2007). Agricultural CH_4 and N_2O emissions have increased by nearly 17% from 1990 to 2005. Although net CO_2 exchange from agriculture soils is approximately at equilibrium, substantial mitigation potential exists in sequestering atmospheric CO_2.

The mitigation of GHG in agricultural systems is undoubtedly not the primary concern for farmers. Increased production costs and a need to maintain or re-establish sustainable agricultural systems are the driving forces for the agricultural sector. However, if concentration of GHGs continue to increase, the vulnerability of agriculture to changes in climate will be significant. Due to economic constraints, farmers in developing nations are considerably more vulnerable to climate change than those in developed countries. Implementation of long-term mitigation measures should help to minimize the impacts of climate change and reduce this vulnerability. There is an extensive range of potential agricultural mitigation measures for most regions, but the full potential to reduce GHG emissions will only be realized if economic and policy incentives are given. Due to the inevitability of climate change, adaptation of agricultural systems is also required to maintain or increase production.

There are some difficulties in assessing the potential impacts of future climate change on mitigation and adaptation strategies for agriculture. Empirical data cannot always be extrapolated to forecast future changes in GHG emissions from agriculture as the impacts of climate change are often dynamic. The use of process-based models, that have been verified against measurements, present a means of quantifying changes in GHG emissions from agricultural systems under future climate change scenarios. In this paper we will review the status of agricultural mitigation strategies that can potentially reduce GHG emissions under a changing climate. We will also review how adaptation measures can influence GHG emissions. Additionally, we will demonstrate how process based model can be used to predict changes in GHG emissions from agriculture under future climate.

2. *Mitigation of agricultural GHG emissions through improved management practices*

Numerous mitigation measures have been proposed to reduce GHG emissions from agricultural systems (*Smith et al.*, 2008a). Typically, the most promising practices are those that sequester carbon. *Smith et al.* (2007a) estimated that 90% of the total potential comes from sink enhancement. Mitigation measures that are particularly effective at reducing one GHG may, however, increase emissions of another thus it becomes important to quantify the emissions of CO_2, CH_4, and N_2O, simultaneously. In certain cases a change in albedo may also be an important factor in determining total radiative forcing of a management practice (*Janzen et al.*, 2008).

It is also important that mitigation measures be of long duration. Some practices may sequester soil carbon for a few years before reaching a new equilibrium with no further storage of carbon. Additionally, any sequestered soil carbon is vulnerable to being lost by either a change in practice or by a change in climate. Soil carbon may also be depleted in the future due to enhanced organic matter decomposition under a warming climate (*Smith et al.*, 2008b). Adaptation measures to minimize climate change impacts on crop production using improved water, soil, and disease management may also hamper mitigation efforts and fuel further changes in climate. Therefore, it is important to quantify the impact of adaptation measures. The impacts of land management, crop management, and livestock management on GHG emissions are discussed below.

2.1. Land management

Changes in land management can reduce GHG emissions by enhancing the removal of CO_2 and to a smaller extent CH_4 from the atmosphere. N_2O emissions can also be highly influenced by changes in water and nutrient management. Land management practices that impact GHG emissions include changes in tillage, nutrient, and water management, as well as the management of organic soils and degraded land (*Table 1*).

Reduction in the frequency of tillage is a widely accepted means to reduce carbon loss from soils. Advances in farm machinery and weed control methods have made this a viable strategy in many areas. Reduced tillage results in less water loss, less soil erosion, and a lower rate of organic matter decomposition. Soil disturbance through tillage aerates the soil and mixes residues into the profile providing substrates for enhanced decomposition of organic matter. The benefit of a reduction in tillage depends largely on climate and soil type. It is usually more beneficial in dryer soils which are not susceptible to water logging and disease. A reduction in the frequency of tillage can also affect N_2O emissions. Globally, the effects are not consistent, but in some areas a pattern can be discerned. For instance, in the semiarid regions of western Canada N_2O emissions are generally reduced (*Helgason et al.*, 2005), whereas in the humid east emissions often increase.

After years of intensive agriculture many soils have become less productive and thus fertilizer N use has been increased to compensate. Improved cultivars and management have also led to a higher fertilizer N requirement. Unfortunately, a large fraction of fertilizer N that is applied to crops remains unused or leaches out of the field and is subject to being transformed and emitted as N_2O. Improving N use efficiency by crops can yield both environmental and economic benefits. Frequent soil N testing is likely the most straightforward technique to improve nutrient management, although the cost of testing sometime limits its application. Applying the appropriate amount of nitrogen maximizes crop production and decreases N_2O formation. The use of slow release fertilizers, coated fertilizers, and nitrogen inhibitors has the potential to reduce N_2O production. Broadcast application of fertilizer often results in excess fertilizer application. Alternative fertilizer application techniques such as banding, precision, and deep placement can help alleviate over fertilization issues.

Table 1. Land management practices that reduce greenhouse gas emissions

Mitigation category	Practice	Impact on GHG emissions			Correlation of mitigation to adaptation
		CO_2	CH_4	N_2O	
Land management					
Tillage management	Reduction in tillage	↓↑		↓↑	Positive: Reduced tillage also helps maintain soil water and reduces soil erosion
	No tillage	↓↑		↓↑	
	Zone tillage	↓↑		↓↑	
Nutrient management	Slow release fertilizers or nitrogen inhibitors	↓		↓	Positive: Efficient N management means less energy use and cost per unit of food production
	Improved N scheduling to minimize loss	↓		↓	
	Reduce leaching and volatile losses	↓		↓	
	Placement of N (banding)	↓		↓	
	Timing of organic residue additions	↓↑	↓	↓	
Water management	More efficient irrigation (Trickle, subsurface)	↓		↓↑	Positive: Practices which conserve water often reduce GHG emissions and help maintain crop production as an adaptive measure
	Drainage in humid areas	↓		↓	
	Keeping soil cropped to rice dry in off season	↓↑	↓	↓	
	Deficit irrigation	↓↑		↓	
	Mulching with crop residue during fallowing	↓		↓↑	
	Draining wetland rice during the growing season (one to several times)	↓↑	↓	↓↑	
Managing organic soils and degraded land	Avoid drainage of wetlands	↓	↑	↓↑	Positive: Reclamation of degraded land can create a sustainable source of food production
	Maintain shallower water table in org. soils	↓		↓↑	
	Re-vegetation of organic soils	↓		↓↑	
	Improve fertility of degraded soils	↓		↓↑	
	Apply organic substrates to degraded soils	↓		↓↑	
	Retain crop residues and conserve water	↓		↓↑	

Although water management is not considered to be one of the more prominent mitigation options in agriculture, the potential benefits of acting as both a mitigation practice as well as an adaptation option are attractive. Mitigation of GHGs through water management is most applicable in regions where irrigation and drainage management is prevalent. Globally, irrigated rice production accounts for nearly 75% of all rice produced. Continuous flooding of rice paddies has been discussed as a potential mitigation measure that reduces the N_2O emissions in comparison to fields that use mid-season drainage management (*Zheng et al.*, 2000). Considering that nearly 80% of the land area currently dedicated to rice production in China uses midseason drainage (*Li et al.*, 2002), the potential for mitigation of N_2O emissions is significant. Note that low denitrification rates occur either when soils are saturated or at low in water content. If continuous flooding is not an option, then techniques that reduce the frequency and magnitude of irrigation events could also decrease the production of N_2O emissions, i.e., deficit irrigation, trickle, and subsurface (*Doerge et al.*, 1991). The use of crop residues as mulch can limit both evaporation losses as well as improve soil quality through the incorporation of organic matter along with reducing the impact of soil erosion (*Dahiya et al.*, 2007; *Bilbro* and *Fryrear*, 1994).

Increasing demand for food production from agriculture has caused farmers to reclaim organic soils and degraded land. Serious obstacles exist, however, before these areas are suitable for agriculture. Organic soils tend to be acidic and inherently have low fertility. The topsoil is typically very shallow and susceptible to erosion. The application of manure and the burning of crop residues are not always sufficient to keep degraded soils viable for continuous agriculture, so alternative nutrient additions are sometimes unavoidable. The application of phosphorus (P) can usually overcome the fertility constraints inherent in these types of soils but not without introducing a high cost to farmers. The opportunity to sequester soil carbon and increase the area of productive agricultural land should not be ignored. However, due to the inherently high cost of reclaiming these infertile soils, governments may need to provide incentives.

2.2. Crop management

Crop management includes practices that enhance removals of CO_2 from the atmosphere by improving crop selection, using rotations that include high input crops, changing to permanent cover or trees, reducing bare fallow, retaining crop residues, and avoiding biomass burning (*Table 2*). These practices stand to promote carbon sequestration by absorbing more CO_2 from the atmosphere and increasing carbon inputs in the soil.

Crop management can also contribute to reduce N_2O and CH_4 emissions through reduction of fertilizer inputs, using rice cultivars with low exudation rates, organic agriculture, and adjusting timing of planting, harvesting, and fertilizer additions.

Another way to mitigate GHG emissions is to replace fossil fuels with biofuels. Currently much effort is focused on bioenergy production using wheat and maize. It is debatable whether or not biofuel production using existing mainstream crop cultivars mitigates GHG emissions. There is also a major concern that biofuel production will displace agricultural land that would otherwise be used for food production. This is particularly a concern for third world countries where inexpensive food sources are necessary. However, much research is going into new forms of biofuel production using crop residues, lignocellulosic crops, or grasses and shrubs which can, in some cases, be grown on marginal or abandoned land. *Smith et al.* (2008a) predicted that biofuel production could reduce GHG emissions by over 600 Mt CO_2-eq y^{-1} at a market price of USD/20/t CO_2-eq.

Table 2. Crop management practices that reduce greenhouse gas emissions

Mitigation category	**Practice**	**Impact on GHG emissions**			**Correlation of mitigation to adaptation**
		CO_2	CH_4	N_2O	
Crop management					
Residue management	Retain crop residues	↓		↓↑	Positive: Crop residues are retained to reduce evaporation/water loss
	Avoid burning	↓		↓↑	
Change in land cover	Reduction in fallowing	↓		↓↑	Negative: Farmers may be required to increase fallow to store water in dryer conditions
	Cropland to Permanent grass/trees	↓		↓	
	More forage in rotations	↓		↓	
	Grassed waterways/field margins/ shelterbelts	↓↑		↓↑	Negative: Increased demand for food production may require more intensive agriculture
Improved crops/crop management	Improved varieties to enhance production	↓		↓↑	Positive: Increased crop production usually enhances soil carbon inputs
	Rice cultivars with low exudation rate	↓↑	↓	↓↑	
	Reduced fertilizer/pesticide inputs	↓↑		↓↑	
	Organic agriculture	↓↑		↓↑	
	Use catch or cover crops	↓		↓	
	Adjust fertilizer rate to crop needs	↓		↑	
Bioenergy	Biofuels from common crop cultivars	↓↑		↓↑	Positive: Biofuel production is an adaptation measure to meet global energy demands
	Biofuels from crop residues	↓		↓↑	
	Biofuels from Lignocellulosic crops	↓		↓↑	
	Bioheat from grasses and shrubs	↓		↓	Positive or negative: In some cases Biofuel crops may replace existing crops that become no longer suitable for production but in other cases they displace land that is needed for mainstream production

2.3. *Livestock and manure management*

Approximately 16% of the global atmospheric CH_4 emissions originate from livestock. The two main sources are enteric fermentation (83%) and manure management (17%) (*FAO*, 2007). It is well documented that the GHG emissions associated with livestock production are substantially higher than for crop production. Mean values of approximately 0.3 kg CO_2-eq per kg of soybean and 0.4 kg CO_2-eq per kg of corn have recently been calculated for these two crops in Canada. The GHG emission per kg of meat is substantially larger. The high emissions from livestock provide opportunities for reducing GHG emissions (*Table 3*). Emission intensities have been reduced in countries that have moved towards intensive production. For example, in Canada *Vergé et al.* (2008) reported a reduction of 5.9 kg CO_2-eq per kg of live weight for beef from 1981 to 2006. Gains in animal productivity as well as changes in animal management practices have contributed to this reduction in GHG emission intensity. Anaerobic digesters can also be used as an energy source thereby displacing emissions from fossil fuels. Other manure handling techniques such as more frequent applications to the field and mechanically separated solids, and handling manure in solid form can also reduce GHG emissions.

Table 3. Livestock and manure management practices that reduce greenhouse gas emissions

Mitigation category	**Practice**	**Impact on GHG emissions**			**Correlation of mitigation to adaptation**
		CO_2	**CH_4**	**N_2O**	
Livestock and manure management					
Grazing management	Grazing intensity and timing	↓↑	↓↑	↓↑	Positive: Improved grazing systems increase productivity
	Fertilizer or organic amendments	↓		↓↑	
	Irrigation (energy requirement)	↓↑		↑	
	Nutrient management	↓		↓	
	Reduce frequency of fires	↓	↓	↓↑	
	Species introduction	↓		↓↑	
Livestock management	Feeding more concentrates		↓	↓	Positive: More efficient feeding can enhance productivity Negative: In some areas breeds of livestock will need to be more resilient to heat and water stress. The dietary needs may be restricted by these requirements
	Adding more oilseeds to diet		↓	↓	
	Special agents and dietary additives		↓		
	Long-term management and improved breeding		↓	↓	
	Reduce confinement	↓	↓		
Manure and biosolid management	Anaerobic digestion to retrieve CH4 as an energy source		↓	↓↑	Positive: There are technologies which capture energy from manures
	Handling manure in solid form		↓	↓	
	More efficient use as nutrient source	↓		↓	
	Cooling of manure in lagoons or tanks, use of solid covers, mechanically separated solids, capturing emitted CH4		↓	↓↑	

3. Agricultural adaptation to limited water resources

Based on current climate model assumptions, it is predicted that there will be major shifts in global precipitation patterns and evaporation losses (*UNEP*, 1997; *Carter et al.*, 2007). Since many regions are already water stressed, any further declines in water resources would have an immediate impact on agroecosystems. Farmers would be forced to adopt water management techniques to ensure that agricultural productivity is minimally impacted. *Debaeke* and *Aboudare* (2004) identified six practices that farmers in dry land areas will need to employ to cope with future water limitations. These are: (1) increasing stored soil water at sowing to increase water availability, (2) increasing soil water extraction by crop by maximizing root extraction, (3) reducing the magnitude of soil evaporation and drainage, (4) optimizing the seasonal water use pattern during the growing season, (5) increasing crop tolerance to water stress, and (6) irrigating crops at the most-sensitive growth stages. These practices aim to improve water use efficiency by crops.

In soils that have low organic matter contents, the addition of farmyard manure or use of bio-fertilizers can help improve the soil structure and water holding capacity of these soils. Alternate deep tillage techniques can also increase soil water at sowing by encouraging water infiltration and by promoting deep root development. The deep tillage breaks up the sub soil which is often not ideal for root development. Stubble-mulch and minimum-tillage techniques can increase infiltration and lower evaporation. Evaporation of water was found to be reduced by 34–50% by leaving crop residues on the surface (*Sauer et al.*, 1996). The supply of water through irrigation at critical growth phases, deficit irrigation, would ensure that farmers can maintain productivity even when water resources are limited. Deficit irrigation can be accomplished by reducing the irrigation depth, refilling only part of the root zone, reducing the irrigation frequency, and various furrow wetting techniques (*Ali* and *Tualukder,* 2008).

Most of the water management practices mentioned are pertinent for dry land farming systems, but water management will also be important for rice production in many of the more humid regions. China and India produces much of their rice on irrigated lowlands which have relatively high water requirements. Irrigation water could be saved without yield loss by applying alternate wetting and drying or flush irrigation to rice systems, but in some cases this may increase N_2O emissions.

4. Modeling mitigation strategies to reduce GHG emissions

Future trends in climate will change the rate of GHG emissions from agroecosystems and will influence the effectiveness of mitigation strategies. We need to develop tools for estimating emissions under a changing climate. Due to limited data and the extreme number of variables in agricultural systems, it is difficult to extrapolate measured data to predict changes. In some cases, particularly for certain adaptation measures, no GHG emissions data are available.

The use of process-based models as prediction tools offers many advantages as they can simulate the highly diverse soils, farm management, and climatic conditions found in agroecosystems. They can simultaneously provide the interactions between all the GHG emissions and predict emissions over space and time. However, the biggest issue in using process-based models in various situations is that many of the processes observed are not fully understood. Therefore, process-based models require continuous development and verification to increase the confidence in the results.

Several researchers have used models to estimate GHG emission factors for different soils, crops, and climates (*Smith et al.*, 2001; *Desjardins et al.*, 2004;

Grant et al., 2004), but few have attempted to estimate the effect of climate change on these factors. Changes in climate are accompanied by many possible changes in agricultural management, whereby the length of the crop growing season may change, crop cultivars may change, it may no longer be viable to grow certain crops, different rates of fertilizer will need to be applied, irrigation or drainage may be required, and pest management strategies may need to change. The effect of climate on our agroecosystems in the future is highly uncertain, partly because our ability to predict climate change is uncertain. *Smith et al.*, (2008b) using the Century model found that climate change had little effect on no-till C sequestration factors, but had some influence on permanent cover factors. Both the SRES B2 and IS92a climate scenarios resulted in greater loss of soil C towards the end of the century. *Smith et al.*, (2007b) estimated ranges of emission factors for changes in agricultural management. The estimates were derived from empirical data and process-based models such as Daycent (*Del Grosso et al.*, 2001) and DNDC (*Li*, 2000). Based on these factors they estimated approximately 6000 Mg CO_2-eq y^{-1} as the global mitigation potential by 2030 and an economic potential of 1500–1600, 2500–2700, and 4000–4300 Mt CO_2-eq y^{-1} at carbon prices of 20, 50, and 100 USD/t CO_2-eq. No doubt there is much uncertainty involved in this process, but it is important to quantify the various mitigation options.

Adaptation methods and sometimes even mitigation measures may change with time as the climate becomes warmer, more arid, or more variable. For this review paper we also carried out a short study to serve as an example of how models may be applied to assess the effects of climate change on GHG emissions in some areas around the world. Ten locations were chosen across contrasting climatic zones, soils, and crops (*Table 4*). The purpose of this exercise was to gain a better understanding of how a changing climate might affect GHG emissions and not to fully characterize any given area.

Simulations were performed in a manner similar to that by Smith et al., 2008b. To generate future climate, 20 years of historical weather data (1970–1999) from a station at each of the 10 locations was used. A historical year was randomly selected from this 20-year period for each of the 100 years from 2000–2100. Thus each year from 2000 to 2100 had the same distribution and frequency of weather events as historical data. Seasonal changes in precipitation and temperature over time were applied based on estimates from the IPCC report on Climate Change: Impacts, Adaptation and Vulnerability (*Carter et. al.*, 2007). In this report AOCM predictions of seasonal changes in mean temperature and precipitation for the A2 emission scenario were estimated and averaged from 15 recent AOCM simulations to the end of the 21st century for 32 regions. We used the average of these ranges to indicate changes in temperature and precipitation for the ten chosen locations and applied the change in temperature and precipitation linearly over the time period from 2000 to 2100. Simulations were carried out both with and without CO_2 fertilization. A nonlinear rate of CO_2 fertilization was assumed based on the A2 scenario. Generalized agricultural management, including fertilizer application rates and scheduling, planting, and harvest dates, and tillage scheduling were used for each location. We created a few new crop profiles by adjusting optimum grain and total biomass and degree days to maturity such that the DNDC model could better match biomass production.

Table 4. Estimated change in yield from 2090–2100 in comparison to baseline yields from 1970–1999 using the DNDC model for the A2 climate change scenario

Location	Crop type	Average annual precipitation (cm)	Average annual temperature (°C)	Change in precipitation (%)	Change in temperature (°C)	Change in yield (CO_2 fertilization) (%)	Change in yield (no CO_2 fertilization) (%)
Australia	WF	29	17	–4.6	3.2	–6	–15
Canada	W	39	6	3.6	4.0	6	–4
Canada	W	47	2	18.1	5.2	–1	–7
India*	R/W	66	23	4.8	3.5	17	–3
China*	W/M	68	14	11.5	4.1	24	1
Germany	W	81	8	–19.1	3.9	–3	–19
Africa	M	92	28	1.3	3.4	–24	–25
Canada	M	99	6	5.5	4.3	21	–5
Brazil	M	121	27	–4.0	3.8	9	–3
China	R/R	146	17	11.5	4.1	–6	–13

W – wheat, F – fallow, R – rice, M – maize; / denotes two crops in same year ; * denotes irrigated systems

Crop yields were simulated under the A2 climate change scenario both with and without CO_2 fertilization. The resulting change in yield over the last 10 years from 2090–2100 in comparison to baseline yields from 1970–1999 is shown in *Table 4*. The average overall yield across the ten locations showed no change under the climate scenario when CO_2 fertilization was included, however, yield declined in simulations with no increase in CO_2 fertilization. Considering that recent research indicates some crops may reduce their rate of respiration and slow growth under higher temperatures (*Gill et al.*, 2002), we may not expect them to respond to increased CO_2 fertilization. Note that for the site in Mali, Africa a small increase in temperature resulted in a sizable decline in yield. This is because production at this location is already seriously hampered by poor soil quality, and the DNDC model indicates that any more stress could result in detrimental effects on crop yield.

Nitrous oxide emissions were extremely variable at several locations. Fertilizer rate was not adjusted to account for changes in growth which could result in over- or under-fertilization. At a subhumid location in Canada over-fertilization was not an issue. These results demonstrate the potential tradeoff that can occur between N_2O and CO_2 emissions (*Fig. 1*). At this location CO_2 flux from soils is increased due to enhanced decomposition of organic matter under higher temperatures. The denitrification process, on the other hand, is limited as soil-water availability declines and as a result less N_2O emissions occur. Some climate change studies have only looked at the effect of a changing temperature on GHG emissions but it is also of importance to examine the effects of a changing water regime. In semiarid and subhumid locations adaptation efforts will be required to maintain crop yields. Such measures might include selecting crops with improved water use efficiency, or a change in irrigation, or residue management. These changes should decrease soil carbon loss but will have variable effects on N_2O emissions.

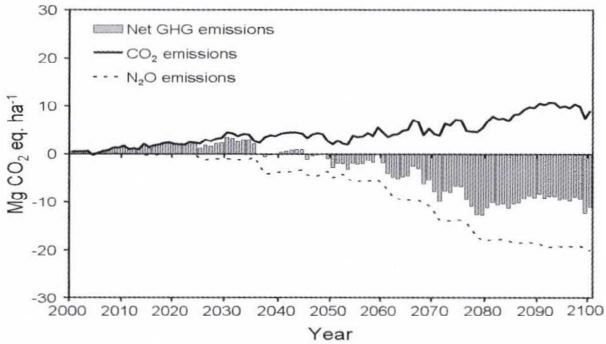

Fig. 1. Estimated influence of climate change on CO_2/N_2O emissions from a wheat crop in subhumid Canada, 2000–2100.

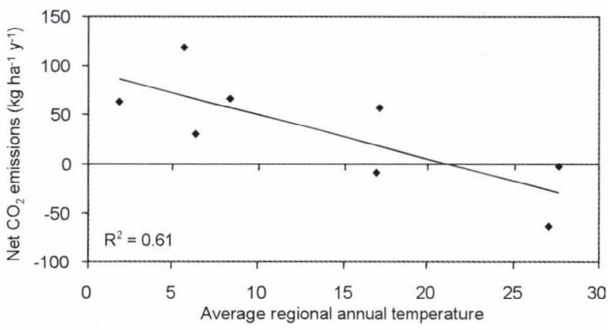

Fig. 2. Estimated effect of climate change by 2100 on CO_2 exchange from agricultural systems for a wide range of annual temperatures (see Table 4 for information on country selected).

An increase in temperature through climate change can result in enhanced soil organic matter decomposition and loss of soil carbon, which may offset some of the mitigative efforts. The results using the DNDC model indicate that soil carbon will be lost in cooler climatic zones but may be gained slightly in warmer regions (*Fig. 2*). In tropical regions soil carbon is often already in a degraded state, thus further increases in temperature have little effect. Furthermore, an increase in average annual temperature from 2 to 7 degrees will have more of an effect on decomposition than an increase from 28 to 33 degrees, largely because there are more frost free days, and the soil thaws much earlier in the spring.

5. Conclusions

Greenhouse gas emissions from most agricultural systems could be reduced, however, the extent to which reduction will occur is limited by policy, economics, and a need for more food production. Gaps in knowledge regarding the potential of various mitigation measures limit our ability to make recommendations. Policy and economic incentives will be needed to promote mitigation of GHG from agricultural sources. Reducing agricultural production that requires a large amount of energy input per unit of food (e.g., meat and milk) could substantially reduce GHG emissions. Biofuel production can be a viable adaptation and mitigation measure, but practices such as residue removal or growth of crops on marginal land should be promoted to avoid competition with mainstream agriculture. It is essential to assess long-term consequences of mitigation and adaptation strategies, determine how these actions are affected by climate, and develop strategies to combat climate change. Integration of mitigation and adaptation frameworks into sustainable development planning is required, especially in developing countries. It is imperative for countries to take a proactive and collaborative role in planning national and regional programs on mitigation and adaptation to climate variability and climate change.

References

Ali, M.H. and *Talukder, M.S.U.*, 2008: Increasing water productivity in crop production--A synthesis. *Agr. Water Manage.* (in press).

Bilbro, J.D. and *Fryrear, D.W.*, 1994: Wind erosion losses as related to plant silhouette and soil cover. *Agron. J. 86*, 550-553.

Carter, T.R., Jones, R.N., Lu, X., Bhadwal, S., Conde, C., Mearns, L.O., O'Neill, B.C., Rounsevell, M.D.A., and *Zurek, M.B.*, 2007: *New Assessment Methods and the Characterisation of Future Conditions. Climate Change 2007: Impacts, Adaptation and Vulnerability. Contribution of Working Group II to the Fourth Assessment Report of the Intergovernmental Panel on Climate Change.* M.L. Parry, O.F. Canziani, J.P. Palutikof, P.J. van der Linden and C.E. Hanson (eds.), Cambridge University Press, Cambridge, UK, 133-171.

Dahiya, R., Ingwersen, J., Streck, T., 2007: The effect of mulching and tillage on the water and temperature regimes of a loess soil: Experimental findings and modeling. *Soil Till. Res. 96*, 52-63.

Debaeke, P. and *Aboudrare, A.*, 2004: Adaptation of crop management to water-limited environments, *Eur. J. Agron. 21*, 433-446.

Del Grosso, S.J., Parton, W.J., Mosier, A.R., Hartman, M.D., Brenner, J., Ojima, D.S., and *Schimel, D.S.*, 2001: Simulated interaction of carbon dynamics and nitrogen trace gas fluxes using the DAYCENT model. In *Modeling Carbon and Nitrogen Dynamics for Soil Management* (eds.: *M. Schaffer, L. Ma* and *S. Hansen*). CRC Press, Boca Raton, Florida, 303–332.

Desjardins, R.L., Smith, W., Grant, B., Campbell, C., and *Riznek, R.,* 2004: Management strategies to sequester carbon in agricultural soils and mitigation greenhouse gas emissions. *Climatic Change 70*, 283-297.

Doerge, T.A., Roth, R.L., and *Gardner, B.R.,* 1991: *Nitrogen Fertilizer Management in Arizona. Report 191025*, Arizona Cooperative Extension, University of Arizona, Tucson, AZ.

FAO, 2007: Livestocks Long Shadow: environmental issues and options. *FAO Corporate Document Depository, Agriculture and Consumer Protection*, Rome 2007. Chapter 13, page 3.

Gill, R.A., Polley, H.W., Johnson, H.B., Anderson, L.J., Maherali, H., and *Jackson, R.B.*, 2002: Nonlinear grassland responses to past and future atmospheric CO_2. *Nature 417*, 279-282.

Grant, B, Smith, W.N., Desjardins, R.L., Lemke, R., and *Li, C.,* 2004: Estimated N_2O and CO_2 emissions as influenced by agricultural practices in Canada. *Climatic Change 65*, 315-332.

Helgason, B.L., Janzen, H.H., Chantigny, M.H., Drury, C.F., Ellert, B.H., Gregorich, E.G., Lemke, R.L., and *Pattey, E.,* 2005: Toward improved coefficients for predicting direct N_2O emissions from soil in Canadian Agroecosystems. *Nutr. Cyc. Agroecosys. 72*, 87-99.

Janzen, H.H., Desjardins, R.L., Rochette, P., Boehm, M., and *Worth, D.,* 2008: Better Farming, Better Air: A scientific analysis of farming practice and greenhouse gases in Canada. Agriculture and Agri-Food Canada, Ottawa, Ontario.

Li, C., 2000: Modeling trace gas emissions from agricultural ecosystems. *Nutr. Cyc. Agroecosys. 58*, 259–276.

Li, C., Qiu, J., Frolking, S., Xiao, X., Salas, W., Moore, B., Boles, S., Huang, Y., and *Sass, R.,* 2002: Reduced methane emissions from large-scale changes in water management in China's rice paddies during 1980–2000. *Geophys. Res. Lett. 29*(20), 33.1-33.4.

Sauer, T.J, Hatfield, J.L., and *Prueger, J.H.,* 1996: Corn residue age and placement effects on evaporation and thermal regime. *Soil Sci. Soc. Am. J. 60,* 1558–1564.

Smith, P.; Marco Bertaglia (Topic Editor), 2007a: Greenhouse gas mitigation in agriculture In *Encyclopedia of Earth* (ed.: *C.J. Cleveland*). Environmental Information Coalition, National Council for Science and the Environment, Washington, D.C.

Smith, P., Martino, D., Cai, Z., Gwary, D., Janzen, H., Kumar, P., McCarl, B., Ogle, S., O'Mara, F., Rice, C., Scholes, B., and *Sirotenko, O.,* 2007b: *Agriculture.* In *Climate Change 2007: Mitigation. Contribution of Working Group III to the Fourth Assessment Report of the Intergovernmental Panel on Climate Change. B. Metz, O.R. Davidson, P.R. Bosch, R. Dave, L.A. Meyer (*eds.). Cambridge University Press, Cambridge, United Kingdom and New York, NY, USA.

Smith, P., Martino, D., Cai, Z., Gwary, D., Janzen, H.H., Kumar, P., McCarl, B., Ogle, S., O'Mara, F., Rice, C., Scholes, B., Sirotenko, O., Howden, M., McAllister, T.A., Pan, G., Romanenkov, V., Schneider, U., Towprayoon, S., Wattenbach, M., and *Smith, J.,* 2008a: Greenhouse gas mitigation in agriculture. *Philos. T. Roy. Soc. B: Biological Sciences 363*(1492), 789-813.

Smith, W.N., Grant, B.B., Desjardins, R.L., Qian, B., Hutchinson, J., and *Gameda, S.,* 2008b: Potential impact of climate change on carbon in agricultural soils in Canada 2000–2099. *Climatic Change* (in press).

Smith W.N., Desjardins, R.L., and *Grant, B.,* 2001: Estimated changes in soil carbon associated with agricultural practices in Canada. *Can. J. Soil Sci. 81,* 221-227.

UNEP, 1997: *Climate change information kit. United Nations Environment Programme, Information Unit for Conventions.* Châtelaine, Switzerland, January 1997.

Vergé, X.P.C., Dyer, J.A., Desjardins, R.L., and *Worth, D.,* 2008: Greenhouse gas emissions from the Canadian beef industry. *Agr. Syst. 98*(2), 126-134.

Zheng, X., Wang, M., Wang, Y., Shen, R., Gou, J., Li, J., Jin, J., and *Li, L.,* 2000: Impacts of soil moisture on nitrous oxide emission from croplands: a case study on rice-based agro-ecosystem in Southeast China. *Chemosphere 2***,** 207–214.

IDŐJÁRÁS

Quarterly Journal of the Hungarian Meteorological Service
Vol. 113, No. 1–2, January–June 2009, pp. 117–127

Developing an adaptation strategy for sustainable agriculture

Raymond P. Motha

United States Department of Agriculture,
1400 Independence Avenue, Washington, D.C. 20250; E-mail: rmotha@oce.usda.gov

(Manuscript received in final form January 24, 2009)

Abstract—Agriculture is one of the most important economic sectors of global society. Agricultural production continues to expand into forest lands and marginal crop areas in an attempt to keep pace with the ever-increasing world population. Environmental damage is increasing, including erosion, salinity, desertification, deforestation, threats to biodiversity, and water scarcity. Moreover, climate change/variability is having a profound influence on agroecosystems, posing serious threats to food security, human health, and protection of the environment. Thus, comprehensive agrometeorological adaptation policy guidelines, focusing on preparedness, mitigation, and adaptation measures to support sustainable agricultural development, are needed to cope with the impacts of climate change/variability. Adaptation policy can not be an effective "stand alone" strategy, but should be incorporated into a broader policy objective. For example, adaptation to climate change should be a part of a broader socio-economic policy such as agricultural, forest, water resources, natural resources, or coastal-zone management policy. Poorer countries that will require resources to improve capacity in order to cope with impacts, undertake specific adaptation measures.

Key-words: climate change, sustainable agriculture, adaptation, preparedness, policy

1. Introduction

Farmers must cope with natural disasters and extreme weather events as part of their everyday farm management strategy to harvest their crops and raise their livestock. Droughts, floods, heat waves, and tropical cyclones, among other natural hazards, have enormous (and sometimes devastating) impacts on agriculture and the socio-economic well-being of the agricultural community. Thus, an important challenge for agrometeorologists is to develop or improve preparedness and adaptation strategies, especially in vulnerable regions where food and fiber production is most sensitive to vagaries of weather and climate. Equally important, however, are to find the ways and means to translate these strategies into meaningful products and services for local farming and extension systems; and, to help build the capacity to disseminate appropriate and timely information for the entire user community.

2. Preparedness, mitigation, adaptation, and emergency relief measures

It is within this framework that an effective agrometeorological adaptation policy is needed for the agricultural community to cope with natural disasters and climate change/variability. A disaster can be defined in terms of a natural hazard times the vulnerability. The natural hazard is an extreme weather or climate event such as drought, flood, heat wave, tropical cyclone, or other catastrophe such as wildfire, avalanche, earthquake, or tsunami. Vulnerability represents the social factors including land use practices, environmental degradation, water use trends, technology, urbanization, population growth, and population shifts.

Farmers have to cope with disasters and climate extremes throughout the growing season. Actions can be taken at the farm level to help farmers implement preparedness measures to cope with disasters, including better early warning communication and response systems. Feasible mitigation measures can help reduce vulnerability. Specific mitigation measures implemented by federal, state, or regional governments include drought monitor programs, water supply augmentation, public awareness/education programs, technical assistance on water conservation, water conservation programs, and emergency response programs. Specifically for agriculture, crop irrigation efficiency studies and scheduling, soil moisture monitoring, irrigation technology management, drought-tolerant crops, and innovative cultivation techniques to reduce crop water use are the primary mitigation measures. Adaptation strategies are measures or long-term plans to reduce the vulnerability of the agricultural or coastal communities to the natural hazards. These adaptation strategies need to be both proactive to address long-term coping strategies as well as reactive to provide resilience in the short-term.

A comprehensive framework to cope with natural disasters, which focuses on preparedness, mitigation, and adaptation, as well as emergency relief measures after a disaster strikes, is the ultimate goal of any policy initiative to support sustainable agricultural development efforts. There are other factors involved in this framework that have a significant impact on the ability to recover from climate extreme events. For example, with a shift from productive to marginal agricultural area, the impact of drought or flood on agriculture becomes a much more difficult challenge for climate sensitive farming and ranching, if remedial measures are not taken. The aim of this strategy is to move away from a mainly reactive approach to a disaster event (responding to a natural hazard that turns into a disaster) to a new paradigm based on a more comprehensive approach that include preventive measures, mainly aimed at reducing the likelihood that a natural hazard translates into a disaster.

Adaptation can help farmers to minimize or reduce the negative impacts of climate extremes on activities and ecosystems, and, perhaps to take advantage of potential beneficial changes (*Rosenzweig,* 2007). The response that can be taken may be directly by individual farmers based on a set of technology and management decisions available. These systems include shifting the crop calendar (planting, input schedules), cultivar changes, and crop rotation changes. Another response requires a concerted action facilitated by climate-specific regulations and incentives from local, regional, and national policies. These options include land use incentives, irrigation infrastructure, water management, regulations, and germplasm development programs. Both adaption responses are essential for sustainable agricultural systems.

3. Framework for an adaptation strategy

The development of adaptation policy must begin by identifying both the hazards and vulnerabilities, which then can be used to identify particular disaster scenarios. The disaster scenarios must account for all scales, ranging from actions to managing the local manifestations of global climate disaster, through to global measures to reduce hazards, and to reduce vulnerability. Ways and means of dealing with integrated climate disasters (or natural disasters) need to include the following elements: (1) adaptation to ensure that future developments reduce rather than increase potential disasters; (2) actions to mitigate the losses associated with disasters; and (3) measures to ensure that disasters do not reoccur after a disaster event. These measures should take into account both potential impacts on socio-economic and environmental systems in the local area.

Integrated planning and actions dealing with climate change (or natural disasters) allow the affected community to move beyond preparedness and contingency response and develop adaptation/response strategies to cope with climate change, variability, and extremes. Action must be taken at all governmental levels (international, national, and local) in order to deal with climate disasters and to move the policy from concept to practice. At the international level, an integrated international framework can promote partnerships for coping strategies, which incorporates elements of and builds on existing frameworks for addressing climate change, disaster reduction, desertification and others. At the national level, integrated climate disaster strategies, plans, and programs need to be built on the same institutional and administrative mechanisms as disaster risk management activities in order to address adaptation strategies for climate change (*Sperling* and *Szekely*, 2005).

Burton et al. (2002) describes a step-by-step formulation of an adaption policy. The process to develop an adaptation policy for natural disasters and future climate change begins by assessing current local vulnerabilities to present day climate, including its variability and extremes, and the ways that existing policy and development practice serve to reduce vulnerability.

The assessment of current vulnerability requires an understanding of key background information. What has been the recent pattern in climate variability and extremes? Are there any trends in their recent history of climate variability and extreme events, and if so, are there any discernible atmospheric oceanic features that can be attributed to the trends?

The next step in the policy development process involves the design of policy initiatives and alternatives, and their assessments and prioritization. In evaluating this phase of the exercise, some thought must be given to future conditions, including climate change and changes in the socio-economic environment, based on available evidence and/or sound reasoning. What are the prospects for economic and sustainable agricultural development? What are the prospects for adaptation and how much can vulnerability be reduced? What are the constraints and limitations to public policy for adaptation? What are the costs of adaptation measures and what benefits can be anticipated?

Adaptation policy can not be an effective "stand alone" strategy, but has to be incorporated into a broader policy objective. For example, adaptation to climate change in agriculture should be a part of a broader agricultural policy. The same applies to forests, water resources, coastal zone management, public health, natural ecosystems, infrastructure, and human settlements. Relevant policies are not limited to such socio-economic sectors, but can also include policies for dealing with natural hazards and coping with natural disasters (floods, droughts, tropical and extra-tropical storms, etc.). Governments may have national policies or special polices that are directed to regional developments, including rural and urban-centered regions or river-basins.

An assessment of current policy in agriculture, for example, will normally take into consideration the broad strategic objectives for agriculture in the national socio-economic and development context. Is the aim to expand commercial agriculture for export-led development? How much importance is given to local food security and the maintenance and improvement of agriculture-based livelihoods? Such policies also influence choice of crops and many other agricultural practices at the farm level. Of specific interest in the case of agriculture are other policies in related areas of natural resources and environmental management such as watershed protection and rehabilitation, soil erosion, soil salinity, the use of genetically modified crops, and so forth.

Costs of production are likely to rise in a changing climate, as producers adjust crop varieties and species, scheduling of operations, and land and water management techniques. Successful adaptation to climate change/variability may involve significant changes to current agricultural systems in order to maintain sustainability. Some of these changes may be costly. There may be a need for investment in new technologies and infrastructure; new irrigation systems may be required for aridity or precipitation instability, damages from flooding may increase in many regions, there may be greater application and/or development of new agricultural chemicals, particularly herbicides and pesticides. However, with respect to agricultural chemicals, environmental concerns and increasing problems with chemical pollution (discussed earlier) limit its successful application.

Adaptation is, in fundamental ways, inherently local, meaning that both natural disasters and climate change/extremes have their direct impacts mostly at the local level. Thus, response measures must be tailored to local circumstances. However, for these efforts to be robust, or, in many cases, even possible, they must be acted upon, guided, and supported by the national policies and strategies. For some countries, these, in turn, need to be facilitated through international measures.

The adaptation strategy for a country refers to a general plan of action for addressing the impacts of natural disasters and climate change and climate variability, including extremes. This requires a combination of coordinated policies and measures with the primary objective of reducing the country's vulnerability. The comprehensive strategy should be aimed at the national level, but addressing adaptation factors across all sectors, regions and vulnerable populations of the country. Policies refer to objectives, together with the means of implementation, with the goal to strengthen food security, for example.

Ways and means to achieve this objective may be to enhance farmer advice and information services, improved application of agricultural research and development, better seasonal climate forecasting services for agricultural applications, and sustainable agricultural development systems. Measures are focused actions aimed at specific issues. Measures can be individual interventions or they can consist of packages of related measures. Specific measures might include actions that promote the chosen policy directions such as implementing an irrigation project, setting up a farmer information, advice, and early-warning programme, developing a new scheme for crop insurance, establishing a system of grain storage to protect against drought or crop failure, or providing incentives to grow a specific crop. Each of these measures may contribute to the local, regional, and national goal of food security.

Easterling et al. (2004) discussed the strategy of "proactive adaptation" as opposed to reactive adaptation. In the reactive strategy, measures take effect after the climate event or disaster strike. In the reactive approach, coping with disasters or climate change/extremes can be very costly in terms of emergency response measures. For example, there is the possibility that irreversible impacts such as species extinction or unrecoverable ecosystem changes can occur. Unacceptable high agricultural losses and damages that expose lives and property to intense storm damages can also occur.

Proactive adaptation, unlike reactive adaptation, is forward-thinking and takes into account the inherent uncertainties associated with anticipated change.

Successful proactive adaptation strategies are, therefore, flexible; i.e., they are designed to be effective under a wide variety of potential climate conditions, to be economically justifiable (i.e., benefits exceed costs) and to increase adaptive capacity. Preparedness is the cornerstone for a proactive adaptation strategy.

4. Formulation of an adaptation strategy for sustainable agriculture

All countries should have national adaptation strategies with a broad view of future development paths and expected impacts of climate on agriculture, forests, fisheries, and other natural resources. The policy review needs to include the management of extreme weather events as well. It must be proactive, emphasize risk management, and preparedness as the cornerstone of its strategy, but must include emergency relief measures as fail-safe response steps.

Developed countries are well advanced in both resources and planning for adaptation strategies. However, even in the developed countries, there is a wide range of progress, with some very limited action pans to a few with well developed national adaptation strategies. Developing countries are more vulnerable and less able to adapt to changing climate. They also have a greater dependence on agriculture and national resources for subsistence-level economies. There is a tendency for many of these nations to have larger variations in weather; lower availability of critical resources such as water, productive land, production inputs, and capital. These vulnerabilities and limitations pose serious constraints on the ability of developing countries to cope with climate change and natural disaster issues.

The key issue is how governments and the international community can work together to assist developing countries with adaptation strategies and measures that are effective for local communities. The constraints are numerous, including expense, lack of knowledge on how to implement measures, and countervailing beliefs and cultural practices (*Yohe et al.*, 2007). Notwithstanding these impediments, farmers and others at risk in the local community from changing climate and natural disasters can be provided with external help. The provision of technical information, advice or guidance can be made more readily available through extension services in agricultural services; the provision of weather and seasonal climate forecasts and warnings can be improved; drought and flood emergency relief measures can be readily implemented; and insurance or other forms of risk management measures can be instituted. Adaptation measures need to be formulated into public policy. For example, with agricultural policies in place on crop and livelihood diversification, how drought and other climate variability or climate change influences agriculture can be factored into policy choices.

Knowledge is fundamental to any adaptation strategy. Knowledge is dynamic; it accumulates through observation, monitoring, and analysis; it can also degrade over time if the learning process is neglected; and research and development must be continually supported to ensure literacy and education levels improve and/or basic societal infrastructure does not decay. Education raises awareness, and over time, it changes societal values. Examples are consumer information, public awareness campaigns, and professional development. Monitoring, observation, and communication systems have to be created or strengthened for climate-related parameters, for indicators of climate change and impacts (e.g., sea-level rise, changes in species composition of ecosystems, extreme events monitoring, and for enhanced agroclimatic observations).

Technological change is a principal route of many recent human adaptations. Innovations in transportation, agriculture, and information systems have advanced adaptive capacity. However, while these advances have taken place in developed countries, developing countries have not benefited from these innovations. Thus, a major gap is still to be bridged. Science, research, and development (R&D) and technological innovations are needed to enable responses to natural disasters/climate change in general, and to enable specific responses to extreme events/climate variability, including economic valuation of adaptations, technological adaptations (development of drought or salt-resistant crop varieties), and investigations of new sources of groundwater and better resource management. It may be necessary to adapt existing technologies to fit with the adaptation demands; e.g., the development of more energy-efficient, low-cost desalination plants and new technologies to combat saltwater intrusion.

Adaptations can be divided into two categories: autonomous and planned adaptations (*Easterling et al*, 2007). Autonomous adaptation is the ongoing implementation of existing knowledge and technology in response to the changes in climate experienced, and planned adaptation is the increase in adaptive capacity by mobilizing institutions and policies to establish or strengthen conditions favorable for effective adaptation and investment in new technologies and infrastructure.

Examples of autonomous adaptation options include: altering inputs such as varieties and/or species to those with more appropriate thermal time and vernalization requirements; wider use of technologies to "harvest" water, conserve soil moisture and to use water more effectively; water management to prevent waterlogging, erosion, and nutrient leaching in areas with rainfall increases; altering the time or location of cropping activities, diversifying income by integrating other farming activities such as livestock raising; improving the effectiveness of pest, disease, and weed management practices through wider use of integrated pest and pathogen management; and, using seasonal climate forecasting to reduce production risk.

Options for effective planning and capacity building for adaptation include: policies to maintain climate monitoring and for effective communication of this information, including surveillance of pests, diseases, and other factors directly affected by climate; policies to support research, systems analysis, extension capacity, and industry and regional networks that provide information; need to invest in or develop technical options to respond to projected changes; where there are major land use changes, there may be a role for governments to support any transition; and, developing new infrastructure, policies and institutions to support management and land use arrangements by addressing climate change in development programs.

Risk and disaster management is another essential component of proactive adaptation. Proactive adaptation may necessitate periodic reassessment of the adequacy and preparedness of relief systems and programs, particularly in light of changing frequency and intensity of extreme events. Governments and insurance companies provide relief for such extreme climate events as hurricanes and tropical cyclones, floods, and droughts. Emergency plans, extreme events relief, and recovery measures also belong to this type of adaptation measure. Updating risk insurance rate tables may require anticipation of future climate/natural disaster risk changes. Proactive adaptation, therefore, may include fire mitigation programs such as prescribed burns and land use controls.

National drought policy has taken on even more importance with severe drought episodes in the late 1980's. Adaptation measures can also be grouped according to whether they are focused on one or more economic sectors (i.e., agriculture or multiple sectors). An example of a sectoral measure would be the introduction of improved agricultural varieties. In agriculture, for example, reduced rainfall and higher evaporation may call for drought tolerant crop varieties in a growing area. It may require a local, regional, and national drought policy to be implemented for long-term planning. Multi-sectoral measures include the use of improved watershed and coastal management methods, and more efficient irrigation management techniques. Multi-sectoral measures relate to the management of natural resources that span sectors; e.g. agricultural, water management, or river basin management. A third adaptation measure is called cross-sectoral measures, which includes such measures as the promotion of public awareness, agroclimatic research, and data collection. Sectoral measures may relate to specific adaptations that could be affected by natural disasters/climate change.

Science and technology have provided the knowledge and tools for the development of adaptation strategy formulation; a key component in the ultimate success in this framework is the engagement of stakeholders; i.e., individuals, local community groups, organizations (governmental agencies or non-governmental organizations and their networks). Relevant stakeholders need to be brought together to identify the most appropriate forms of adaptation. Furthermore, understanding the role of stakeholders in the decision-making process will assist in the implementation of adaptation policies.

Thus, an outline of an adaptation strategy for agriculture considers the following issues:

(1) Complete monitoring systems will allow policymakers to develop and adjust adaptation strategies based on sound observational data bases. Agrometeorologists can take a more active role in this aspect, as noted earlier in the discussion of the socialization of agrometeorology. It is becoming increasingly important to communicate and disseminate meaningful and appropriate information to the user community at the right time and in the right format for decision-making.

(2) Risk/disaster management measures include the development of early warning systems, in particular for extreme events like cyclones, droughts, floods, and ENSO occurrences. The success of this type of measure depends upon good communication systems and cooperation among users.

(3) In many cases, flexibility, durability, and resiliency to climatic variability and change can be enhanced via changes in infrastructure design characteristics. Agriculture extension services can be more proactive with farmers to inform them about changes in crop varieties and practices that may be better suited to changing climate conditions.

(4) Adopt preparedness measures and emergency response measures to help mitigate the impact of climate extremes and climate change.

(5) Avoid agricultural expansion into marginal lands, coastal lowlands, or other poor cropping areas that are prone to desertification, coastal erosion, or prone to flooding.

(6) Promote technological innovations that fit adaptation demands and will benefit both developed and developing countries, if possible.

(7) Public policy provides substantial guidance in adaptation formulation and strategy at the national level, and, planning and implementations at the local level. Coordination at all levels is absolutely essential for emergency preparedness and disaster planning.

(8) In summary, the ecosystem approach to adaptation measures involves the integrated management of land, water and other resources that promotes their conservation and sustainable use in an equitable way.

5. *Education and training*

It is essential to promote greater community education and training opportunities to meet the needs of the public, which correspond with the development of more robust warning systems, the increasing capacity to respond rapidly to disasters, and the recognition for comprehensive adaptation strategies in the community to cope with natural disasters and climate change. Some general focus areas include:

- Develop community awareness and self-management programs in relation to hazard management. The emphasis is on equipping community groups exposed to certain types of hazards with the knowledge to manage that hazard;
- Provide training programs in the effective use of agro-climate information, including climate predictions (which have the potential not only to help minimize heavy losses in poor years, but also to maximize yields in good years) and vulnerability scenarios;
- Promote communication strategies between stakeholders, including effective use of the media. Good services and methodologies are ineffective unless the user understands and applies the information provided. At the same time, it is important that users be able to feed back how the information can be improved (*Wright*, 2005).

Finally, the introduction of natural disaster/climate change and climate variability issues at different levels of the educational system must be in an ongoing process to help build capacity among stakeholders to support adaptation in the future and to develop appropriate research activities and a greater awareness among citizens. Furthermore, campaigns to raise public awareness and disseminate information in order to involve a broad array of stakeholders are necessary. These campaigns can also be an opportunity for adaptation decision-makers to better understand the perception and views of the public on the issues.

6. Conclusion

There are many illustrations of potential coping strategies each with challenges and uncertainties. There can be no generic strategy that can be formulated as a suitable solution for wide applications in diverse areas. However, the goal is to establish guidelines to meet the specific needs of the user community that be incorporated in the development of adaptation policy framework and adaptation measures.

References

Burton, I., Huq, S., Lim, B., Rlifosova, O., and *Schipper, E.,* 2002: From impacts assessment to adaptation priorities: The shaping of adaptation policy. *Climate Policy 2*, 145-149.

Easterling, W.E., Hurd, B.H., and *Smith, J.B.,* 2004: Coping with global climate change: The role of adaptation in the United States. Prepared for the Pew Center on Global Climate Change. Arlington, Virginia. 39pp

Easterling, W.E., Aggarwal, P.K., Batima, P., Brander, K.M., Erda, L., Howden, S.M., Kirilenko, A., Morton, J., Soussana, J.F., Schmidhuber, J., and *Tubiello, F.N.*, 2007: Food, fibre and forest products. *Climate Change 2007: Impacts, Adaptation and Vulnerability.* Contribution of Working Group II to the Fourth Assessment Report of the Intergovernmental Panel on Climate Change, M.L. Parry, O.F. Canziani, J.P. Palutikof, P.J. van der Linden and C.E. Hanson, Eds., Cambridge University Press, Cambridge, UK, 273-313p.

Rosenzweig, C., 2007: Climate Change and Agriculture: Learning Lessons and Proposing Solutions. The John Pesek Colloquium on Sustainable Agriculture, February 28 to March 1, 2007, Iowa State University, Ames, Iowa.

Sperling, F. and *Szekely, F.*, 2005: Disaster risk management in a changing climate. Discussion paper prepared for the World Conference on Disaster Reduction on behalf of the Vulnerability and Adaptation Resource Group (VARG). Washington, D.C.

Wright, W.J., 2005: Significance of training, education, and communication for awareness of potential hazards in managing natural disaster in Australia. In *Natural Disasters & Extreme Events in Agriculture: Impacts and Mitigation.* Springer-Verlag, 219-239p.

Yohe, G., Burton, I., Huq, S., and *Rosegrant, M.W.*, 2007: Climate Change: pro-poor adaptation , risk management, and mitigation strategies. 2020 Focus Brief on the World's Poor and Hungry People. Washington, D.C., IFPRI.

IDŐJÁRÁS
Quarterly Journal of the Hungarian Meteorological Service
Vol. 113, No. 1–2, January–June 2009, pp. 129–133

Effect of climate change on growth potential in the mountainous region of southeast Norway

Ole Hans Baadshaug and **Lars Egil Haugen**

Department of Plant and Environmental Sciences, Norwegian University of Life Sciences, P.O. Box 5003, N-1432 Ås, Norway; E-mail: ole.baadshaug@umb.no

(Manuscript received in final form December 10, 2008)

Abstract—The COUP–ENGNOR ley crop modeling system was calibrated on relevant yield data from field trials in southern Norway. This parameterized version was used to compare the potential ley production at Fokstua (62°N; 970 m a.s.l.) for the period 1961–1990 with that of a Hadley A2 climatic scenario for the period 2071–2100. The impact of a climatic change, which projects a temperature increase by 2–3 °C, and a lengthening of the growing season by approximately 1.5 months, is an appreciable increase in production potential, especially as to fodder quality and feed unit yield. This is due to a new harvesting regime, which favors an early first cut and thus allows two seasonal cuts. The impact of the increased production potential of the mountainous districts of southern Norway towards the end of this century are considered, including the value of ley plant breeding towards optimal combination of late seasonal growth with maximum winter hardiness.

Key-words: climatic scenario, crop model, cultivar, ley, mountainous area, regrowth, timothy, wintering

1. Introduction

A large part of the reclaimable land reserves in Norway lies in the mountainous areas of the southeastern parts at altitudes from 600 to 1000–1100 m a.s.l. In the marginal agroclimatic zones corresponding to this region, less than 30 percent of the arable soil is so far taken into cultivation for the whole country (*Grønlund*, 1990). In the most marginal zone, corresponding to approx. 900–1100 m a.s.l. in South Norway, at most some 15 percent of the potentially arable land is cultivated. These areas, in spite of their extremely short growing season, might still give a satisfactory dry matter (DM) yield when used for fodder production by a hardy perennial grass crop. One reason for the low utilization is that a satisfactory (DM) yield depends on one late cut, and thus to the cost of feed quality whether expressed as net energy (feed unit) or protein concentration in harvested DM. Both these quality traits decrease strongly with advancing grass development stage.

As the temperature climate ameliorates, cultivation will be possible and more profitable than today at higher altitudes, thus opening considerable areas in southeast Norway for increased food production. We have explored potentials and possible challenges by extending fodder production to higher altitudes in a future climate.

2. *Materials and methods*

The analytical tool of this work was the COUP – ENGNOR crop modeling system, in which the COUP model (*Jansson* and *Karlberg*, 2001) simulates soil moisture and crop water uptake based on daily values of global radiation, temperature, precipitation, relative air humidity, and wind speed. These data were the inputs to simulations of plant production by the ENGNOR model (*Baadshaug* and *Lantinga*, 2002), which calculates total and harvestable ley yield from the temperature, radiation, and soil moisture supply. The present model has been calibrated to weekly observations of growth rates of first and second growth of timothy at the University Experimental Farm. This has allowed a reliable description of the reduced regrowth capacity of the extremely hardy timothy cultivar Engmo (*Fig. 1*). In this study, the extrapolations into future climates were based on a regionally downscaled Hadley A2 scenario for the site Fokstua (62°N; 970 m a.s.l.) (*Engen-Skaugen*, 2007).

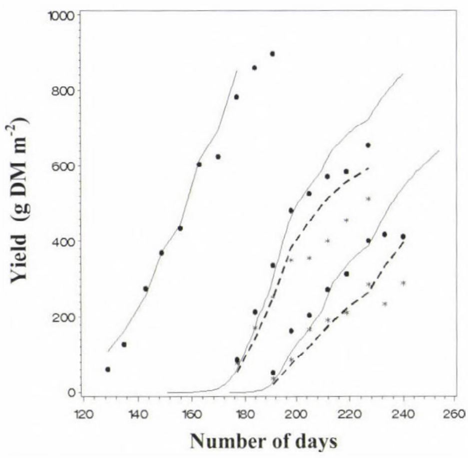

Fig. 1. Calibration of the ENGNOR ley crop model (curves) using first (left), and second growth rate observations (middle and right) at the University Experimental Farm (dots or stars) for two timothy cultivars, Engmo and Grindstad.

3. Results

The Hadley A2 scenario indicates only minor changes in the precipitation, whereas the air temperature (*Fig. 2*) will increase by 2–3 °C, implying a lengthening of the growing season by approximately 1.5 months. The effect of this change on the yield potential is seen from the comparison between the estimates for the 1961–1990 period and those of the 2071–2100 scenario (*Fig. 3*). The benefit of the climatic change may not be too striking when measured as a mere DM yield increase. The most important gain may be that of fodder quality, since the future climate will make possible two harvests in a season, a management regime which is not practical at this altitude in the present climate. The superior quality of young grass, especially as to net energy concentration, is more than ever appraised by milk and meat producers.

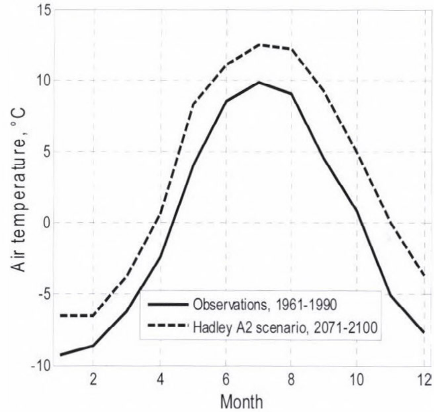

Fig. 2. Air temperature of the Hadley A2 scenario for the period 2071–2100 of Fokstua in southern Norway (62°N; 970 m a.s.l.), as compared with the observations during 1961 to 1990.

The results in *Fig. 3* are relevant for the timothy cultivar Grindstad, which is usually not considered as sufficiently winter hardy for the high altitudes. When choosing a more hardy cultivar, Engmo, to secure maximum winter survival, the yield gain from the warmer climate will be reduced (*Fig. 4*), due to the less vigorous second growth of this cultivar.

4. Discussion

The main limiting factors for agriculture in the marginal areas are the length of the growing season and the winter survival of perennial fodder crops, which usually are the only ones which can be grown. The expected increase of the seasonal temperature has a considerable positive effect on future plant production potential. However, the same is not necessarily in the case of wintering conditions. The main problems might be warm spells during the winter, which will be more frequent, and imply increased risks of ice crust formation on the grass fields. Therefore, in the case of timothy ley culture, the hardy cultivar Engmo will still be a highly actual choice, to the cost of reduced seasonal yield (*Fig. 4*), whenever more than one harvest is practiced.

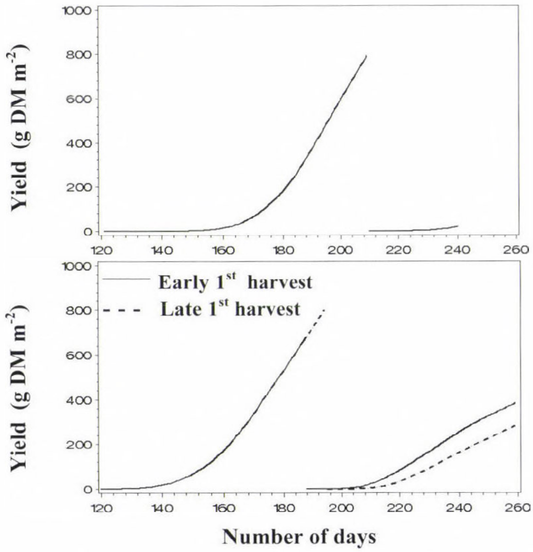

Fig. 3. Estimated yields of the Grindstad timothy ley at Fokstua (62°N; 970 m a.s.l.) for the period 1961–1990 (upper part) and for the scenario period 2071–2100 (lower part), using the ENGNOR crop growth model.

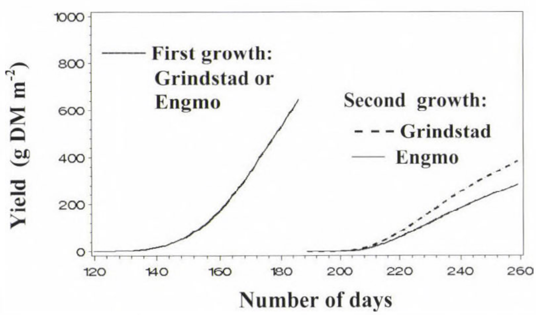

Fig. 4. Estimated yields of a timothy ley at Fokstua (62°N; 970 m a.s.l.) for the period 2071–2100 for the two contrasting timothy cultivars Grindstad and Engmo.

5. Conclusions

The projected climatic change will strongly increase the agricultural production potential of the mountainous areas of Norway. But, for a full benefit of the climatic change, the eternal challenge to the grass breeders still remains: to combine vigorous growth in the late growing season (see *Fig. 4*, Grindstad) with maximum winter hardiness (Engmo).

References

Baadshaug, O.H. and *Lantinga, E.A.*, 2002: *ENGNOR, a Grassland Crop Growth Model for High Latitudes*. Documentations. Report no 2/2002, Reports from UMB. Dept of Plant and Environmental Sciences, Norwegian University of Life Sciences. 18 pp.

Grønlund, A., 1990: Distribution of arable land in different agroclimatic zones (in Norwegian). In *Consequences of Increased Emissions of Climate Gases for Agricultural Production* (ed.: *A. Haglerød*). Report no. C-005-90, 21-25. The Norwegian Agricultural Economics Research Institute.

Engen-Skaugen, T., 2007: Refinement of dynamically downscaled precipitation and temperature scenarios. *Climatic Change 84*, 365-382.

Jansson, P-E. and *Karlberg, L.*, 2001: *Coupled Heat and Mass Transfer Model for Soil–Plant–Atmosphere Systems*. Royal Institute of Technology, Dept of Civil and Environmental Engineering, Stockholm, 325 pp.

IDŐJÁRÁS

Quarterly Journal of the Hungarian Meteorological Service
Vol. 113, No. 1–2, January–June 2009, pp. 135–143

Drought analyses of agricultural regions as influenced by climatic conditions in the Slovak Republic

Bernard Šiška[1*] and **Jozef Takáč**[2]

[1]*Department of Biometeorology and Hydrology, Slovak University of Agriculture in Nitra, Hospodárska 7, 949 01 Nitra, SK; E-mail:* bernard.siska@uniag.sk
[2]*Soil Science and Conservation Research Institute, Gagarinova 10, 827 13 Bratislava, SK; E-mail:* j.takac@vupop.sk

(Manuscript received in final form December 11, 2008)

Abstract—Drought analysis of the Slovak territorry was based on evaluation of climatic conditions during the growing season limited by daily mean air temperature $T > 10$ °C. Precipitation total (R in mm), and potential (E_0 in mm) and actual (E in mm) evapotranspiration were calculated for this period. Consequently, climatic index of drought ($E_0 - R$) and evapotranspiration deficits ($E_0 - E$) were evaluated on the background of agricultural productive regions. Climatic data from the database of the Slovak Hydrometeorological Institute in Bratislava in period of years 1960–1990 were used for evaluating the reference climate condition. Climatic stations used for GIS analyses were selected from the point of view of altitude, limiting plant production areas (up to 900 m a.s.l. – this altitude represents acreage 45,000 km^2) and spatial distribution. Climate change conditions were generated by general circulation model CCCM for emission scenario SRES B2.

According to the results, agricultural regions of the Slovak Republic will become more sensitive in conditions of climate change on drought occurrence as compared with climate conditions of the last normal period 1961–1990. While 5 categories of drought conditions were recognized on the territory of the Slovak Republic in the reference period 1961–1990, additional two very dry categories can be recognized in agricultural regions of Slovakia according to climatic indices of both drought and evapotranspiration deficit. This fact has serious effects on potential acreage of some crops. High totals of potential evapotranspiration can evoke occurrence of drought more frequently. This fact should be taken into account in the future on the levels of both crop selections and water saving rotations.

Key-words: climatic index of drought, evapotranspiration deficit, precipitation, drought, growing season, Slovakia

[*] Corresponding author

1. Introduction

Climatic conditions become the most important factor influencing variability of field crop yields in Slovakia today. Increase of annual mean air temperature by about 1 °C was occurred on most of climatic stations in Slovakia during last century. On the other hand, annual precipitations decreased by about 10% on lowlands of Slovakia (Danubian and east Slovakian lowlands) during this period. Precipitation totals varied also in mountainous regions, but no significant trend was found during last century (*Lapin et al.*, 2001). Increase of air temperature and shortage of precipitations create also conditions for drought occurrence, especially on lowlands of Slovakia. According to the outputs of the general circulation models (GCM), this trend is also supposed for future climate. Those facts call for analysis of drought occurrence in conditions of climate change on territory of the Slovak Republic.

According to the natural climate variability and the duration of drought, several levels of drought can be defined (*Hayes et al.*, 1999; *Heim*, 2002). For example, the difference between potential evapotranspiration and precipitation totals during growing season limited by mean air temperature $T \geq 10$ °C was defined as climatic index of drought for conditions of Central Europe. This index was frequently used in many works for evaluation of drought conditions (*Ditmarová et al.*, 2006; *Dubrovský et al.*, 2005; *Hlásný* and *Baláž*, 2008; *Tomlain*, 1997; *Trnka et al.*, 2007). This index was also used for agroclimatic regionalization of the Slovak Republic during the periods of 1931–1960 (*Kurpelová, et al.*, 1975) and 1961–1990 (*Šiška* and *Špánik*, 2008).

Evapotranspiration, as an important component of water balance, is also frequently used for evaluation of drought conditions in Slovakia. Spatial distribution of potential evapotranspiration was related to water needs of ecosystems (*Tomlain*, 1979; *Škvarenina et al.*, 2008), actual evapotranspiration was correlated to yield of some field crops (*Matejka* and *Huzulák*, 1995; *Vidovič* and *Novák*, 1987). Difference between potential and actual evapotranspiration defined as evapotranspiration deficit can be a good parameter for evaluating the drought condition of the landscape on agricultural level.

The aim of the paper is to evaluate drought occurrence in climate change conditions by means of GIS in Slovakia.

2. Material and methods

Climatic data from the database of the Slovak Hydrometeorological Institute (SHMI) in Bratislava were used for calculation of present climate ($1 \times CO_2$) in this paper. Climatic stations used for GIS analyses were selected with respect to agricultural productive types, altitude (up to 900 m a.s.l. – upper range of plant production), and spatial distribution. Evaluated acreage represents 45,000 km^2 –

90% of total area of Slovakia. Climatic data of the period 1961–1990 for 11 stations given in *Table 1* were used. These climatic stations represent 4 Slovak agroclimatic regions (productivity types).

Table 1. Agricultural regions and related climatic stations

Agricultural regions (productive type)	**Altitude (m a.s.l.)**	**Climatic stations**	**Altitude (m a.s.l.)**
Maize	< 200	Somotor	100
		Hurbanovo	115
		Nitra	143
		Piešťany	165
		Kamenica n/C.	178
Sugar beet	200 – 300	Rimavská Sobota	214
		Prievidza	260
		Košice	230
Potato	300 – 500	Bardejov	304
		Sliač	330
Mountainous	>500	Liptovský Hrádok	640

Temperature and drought characteristics were evaluated for growing seasons limited by daily mean air temperatures T >10.0 °C, henceforth signed by GS10. Daily mean air temperature sums (*TS* in °C), precipitation totals (R in mm), potential evapotranspiration (E_0 in mm), and climatic index of drought ($E_0 - R$ in mm) were calculated for GS10. Potential (E_0) and actual (E) evapotranspiration were calculated according to Budyko-Zubenok method (cit. in *Tomlain*, 1979).

In this study, two indices were selected for spatial evaluation of drought conditions for the territory of Slovakia: the climatic indices of drought and evapotranspiration deficit.

Since drought conditions are frequently observed during the whole growing season, calculation was applied for the whole growing season (GS10 period).

Climatic index of drought was calculated as:

$$K_{GS10} = E_0 - R, \tag{1}$$

where E_0 is the potential evapotranspiration during GS10 and R is the rainfall during GS10.

Evapotranspiration deficit was calculated as:

$$\Delta E_{GS10} = E_0 - E \tag{2}$$

where E_0 is the potential evapotranspiration during GS10, and E is the actual evapotranspiration during GS10.

Onset and end of GS10 were established according to numeric analyses (*Nosek*, 1972). GS10 is limited by biological temperature minimum of thermophil plants (by daily mean air temperature of $T \geq 10.0$ °C).

A raster model of geodata was applied for the spatial evaluation of the climatic parameters. Through the interpolation, the spatial change of the individual average meteodata was calculated. The method of regularized spline interpolation with tension and kriging was applied. Global radiation, air mean temperature, and precipitation for 2×CO_2 climate were generated by general circulation model CCCM 2000 (*Lapin et al.*, 2001). Consequently, potential and actual evapotranspirations were calculated.

Finally, by comparing the spatial distribution of the climatic indices of drought and evapotranspiration deficit for 1×CO_2 and 2×CO_2 scenarios, climate sensitivity of the agricultural regions of Slovakia to drought occurrence was evaluated.

3. Results

3.1. Duration of growing season

The main growing season (GS10) is limited by the onset and end of daily mean air temperature $T > 10$ °C, and it is the period when drought conditions are frequently observed.

The onset and end of GS10 in altitudinal profile of Slovakia are given in *Fig. 1*. As resulted from trend lines of the onset and end of GS10, the onset of GS10 would start significantly earlier by about 28 days in climate conditions of the 2×CO_2 climate in the whole altitudinal profile as compared to climate conditions of the 1×CO_2 climate. The end of the GS10 period will be delayed by about 14 days under the 2×CO_2 climatic conditions as compared to the 1×CO_2 climatic conditions.

The duration of the GS10 of the maize region related to the reference period 1×CO_2 is 175 days or which represents about 34% of total acreage of agricultural regions. Those conditions will occur on 80% of the total agricultural regions acreage in 2×CO_2 climatic conditions and the duration of GS10 can exceed 200 days in the Danubian lowland, east Slovakian lowland, and Zahorie lowland. Duration of GS10 influences positively photosythetically active period of maize and, therefore, also biomass creation. On the other hand, a longer duration of GS10 also increases the potential risk for drought occurrence.

3.2. Precipitation (R)

Generally it is supposed, that the precipitation total increases in 2×CO_2 climatic conditions. Except for the GCM (CCCM 2000), this fact is influenced also by a rising duration of GS10. An increase of *R* by about 60 mm in the lowlands of southern and eastern Slovakia and by 79–134 mm in northern Slovakia will probably not be sufficient. All regions should receive more than 390 mm precipitation during GS10 in 2×CO_2 climatic conditions, and a raising rainfall could favorably influence the yield of some crops (e.g., maize and other cereals). The distribution of precipitation generated by the GCM in the context of rising air temperatures and consequently increasing crop water demands during GS10 will, however, very probably result in increasing occurrence of drought conditions reducing yields of field crops.

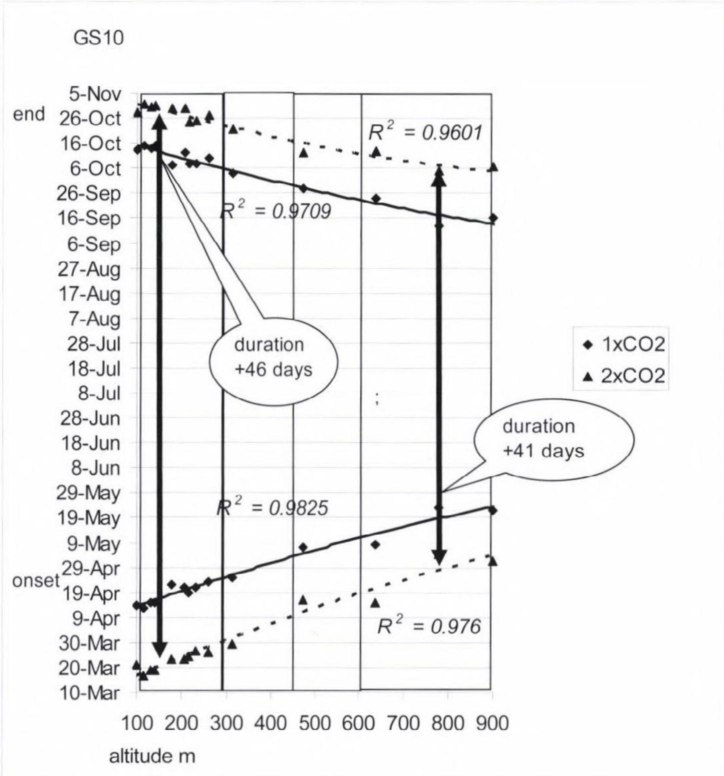

Fig. 1. Onset and end of growing seasons GS10 in dependence on altitude for 1×CO_2 and 2×CO_2 climates.

3.3. *Changes of evapotranspiration characteristics*

Evapotranspiration as a significant element of environmental water balance is a suitable indicator for moisture balance in any space and time scale. While potential evapotranspiration can be used as an indicator for estimating of water demand of the maximum productivity of ecosystems (*Šiška*, 1992), the exact estimation of actual evapotranspiration can lead to an actual assessment of biomass production (*Vidovič* and *Novák*, 1987).

Our study shows that potential evapotranspiration of E_0 > 450 mm during the GS10 period in the whole agricultural area, and even E_0 exceeding 700 mm, can be expected in the warmest areas of Slovakia (south of Danubian lowland, and the lowest areas of east Slovakian lowland). Such high E_0 totals call for the need of effective management with water resources and for building irrigation systems in most of the territory of Slovakia to eliminate negative effects on yield production.

3.4. Climatic index of drought

Climatic index of drought (*K*) was applied for the first time as index of agroclimatic regionalization of Slovakia by *Kurpelová et al.* (1975). The difference between potential evapotranspiration and precipitation during summer months was taken into account. Because drought conditions are frequently observed during the whole growing season, *K* was recalculated for the whole GS10 period (*Šiška* and *Špánik*, 2008).

The supposed air temperature increase and consequent increase of GS10 duration influence the E_0 increase in the 2xCO_2 climate on the whole area of Slovakia. During GS10, E_0 will increase in the lowlands of Slovakia by 160–170 mm, i.e., by 27–30%, on uplands by 106 mm, i.e., by 34%. E_0>500 mm can be expected in all agricultural regions of Slovakia, E_0 >750 mm can be expected in the warmest regions of Slovakia (south of Danubian lowland and east Slovakian lowland). Such high E_0 totals during the relatively short GS10 period (compared to GS5) will increase the potential of the occurrence of drought periods. Effective management of water resources can, therefore, eliminate the negative influences of evaporation demand on agricultural production in the majority of regions in Slovakia.

K_{GS10} is changing in the whole altitudinal profile of Slovakia significantly. The original classification scale of drought-wet conditions proposed by *Kurpelová et al.* (1975) was based on 50 mm differences of the index. According to this criterion, 5 categories of drought conditions can be defined for the reference (1×CO_2) climate. Most of the agricultural acreage belongs to the areas where wet conditions prevail in altitudes above 550 m. According to the calculations based on CCCM outputs, those conditions can be found in future in altitudes higher than 700 m. Other two categories of drought can be defined, where the deficit of water exceed 250 mm during GS10 (*Fig. 2*). These two new categories of drought will cover the most productive regions of the Slovak Republic – the Danubian and east Slovakian lowlands that represent the maize region productive type.

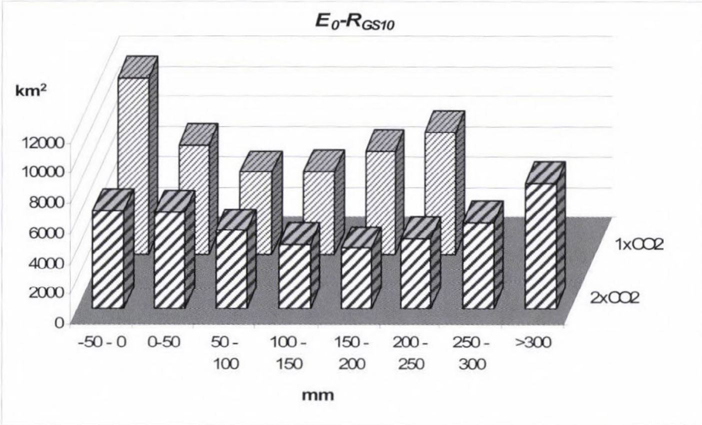

Fig. 2. Spatial distribution of climatic index of drought (K) during GS10 for $1\times CO_2$ and $2\times CO_2$ climates in Slovakia.

3.5. Evapotranspiration deficit

Evapotranspiration deficit ΔE as an important compound of water balance was also used for evaluation of drought conditions in Czechoslovakia (*Tomlain,* 1979). Except for meteorological factors, the calculation of actual evapotranspiration takes into account also soil water content and therefore, this parameter can better reflect drought conditions of agricultural regions.

According to the index ΔE, the territory of Slovakia looks even more vulnerable to drought than according to the previous index K. While $\Delta E \leq 100$ mm was calculated for sites with altitude over 300 m for the reference climate $1\times CO_2$, those conditions will be found in altitudes above 500 m for the $2\times CO_2$ climate (*Table 2*). These values represent potato and mountainous productive regions.

Table 2. Climatic index of drought (E_0-R) and evapotranspiration deficit (E_0-E) related to agricultural productive regions for $1\times CO_2$ and $2\times CO_2$ climates in Slovakia

Agro regions	E_0-R [mm]		E_0-E [mm]	
	$1\times CO_2$	$2\times CO_2$	$1\times CO_2$	$2\times CO_2$
Maize	150 – 250	250 – 360	130 – 220	240 – 350
Sugar beet	75 – 150	150 – 250	70 – 130	140 – 240
Potato	0 – 75	–20 – 150	30 – 70	90 – 140
Mountainous	<0	<–20	<30	<90

The classification scale of drought-wet conditions of this index is also based on 50 mm differences. According to this criterion, 5 categories of drought conditions can be defined for the reference ($1\times CO_2$) climate. As resulted from calculations based on CCCM outputs, two new very dry categories of drought can be introduced, where $\Delta E \geq 250$ mm (*Fig. 3*). Except for the Danubian and east Slovakian lowlands, these two categories of drought will cover also valleys of Slovakian rivers up to altitudes of 300 m. On the other hand, the acreage of agricultural regions, where $\Delta E < 50$ mm, will diminish under conditions of climate change.

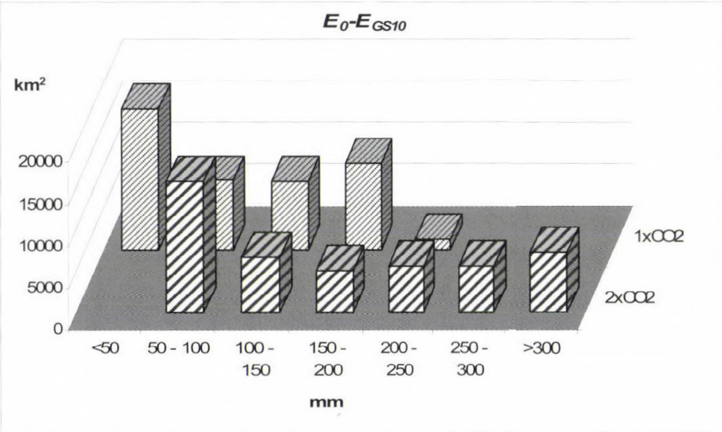

Fig. 3. Spatial distribution of evapotraspiration deficit ($E_0 - E$) during GS10 for $1\times CO_2$ and $2\times CO_2$ climates in Slovakia.

4. *Conclusions*

Drought conditions of agricultural regions were analyzed by climatic (climatic index of drought) and agroclimatic (evapotranspiration deficit) indices for the Slovak Republic.

It was found that the duration of the growing period (GS10) influences also the potential for drought occurrence.

According to both indices, two very dry and hot regions can be classified where the deficit of water exceed 250 mm. These two categories of drought will cover the most productive regions of the Slovak Republic – the Danubian and east Slovakian lowlands that represents the maize productive areas.

According to the evapotranspiration deficit, the agricultural regions of the Slovak Republic are more vulnerable under conditions of the applied climate change scenario as compared with K. $\Delta E \geq 250$ mm, except for Danubian and east Slovakian lowlands, will probably be recorded also in valleys of rivers up to altitudes of 300 m. Agricultural regions, where $\Delta E < 50$ mm, will probably disappear under conditions of this climate scenario in Slovakia.

According to K_{GS10}, most of the agricultural acreage belongs to areas where wet conditions prevail in altitudes above 550 m a.s.l. in the 1×CO_2 reference climate. As resulted from calculations based on CCCM outputs, those conditions will be found in altitudes higher than 700 m.

Except for agroclimatic planning issues, these facts should be taken into account in breeding strategies of new crop varieties suitable for the future climate of Slovakia.

Acknowledgments—This study was made with the help of grant project VEGA 1/4427/07: Design of new agroclimatic regionalization of plant production in condition of changing climate in Slovakia and aAV/1109/2004: Climate change and drought in the Slovak Republic and 6FP: CECILIA.

References

Ditmarová, Ľ., Kmeť, J., Střelcová, K., Gőmőry, D., 2006: Effects of drought on selected physiological parameters of young beech trees under stress conditions. *Ekológia (Bratislava) 25*, 1-11.

Dubrovský, M., Trnka, M., Svoboda, M., Gates, M., Šilháte, D., Žalud, Z., Semerádová, D., 2005: Drought conditions in the Czech Republic in present and changed climate. In *Proceedings of the European Geophysical Union*, Vienna. 25-29.

Hayes, M.J., Svoboda, M.D., Wilhite, D.A., Vanyarko, O.V., 1999: Monitoring the 1996 drought using the Standardized Precipitation Index. *American Meteorological Society 80*, 429-438.

Heim, R. R., 2002: A review of Twentieth-Century drought indices used in the United States. *B. Am. Meteorol. Soc. 83*, 1149-1165.

Hlásný, T., Baláž, P., 2008: The climatic water balance of Slovakia based on the FAO Penman-Monteith evapotranspiration. *Geografický časopis 60* (1), 15-30.

Kurpelová, M., Coufal, J., Čulík, J., 1975: *Agroclimatic Conditions of ČSSR* (in Slovak with English, German and Russian summary). Príroda, Bratislava

Lapin, M., Melo, M., Damborská, I., 2001: Scenarios of several physically plausible climatic elements (in Slovak). MoE SR Bratislava, *NCP SR 11*, 5-30.

Matejka, F., Huzulák, J., 1995: Analysis of relationships between winter wheat leaf water potential and atmospheric factors. *Biology 50*(1), 105-114.

Nosek, M., 1972: Methods in climatology (in Czech). Academia, Praha.

Šiška, B., 1992: *Potential Yield of Winter Wheat as Influenced by Actual and Potential Evapotranspiration in Western Slovakia* (in Slovak with English summary). PhD Thesis, VŠP Nitra, 1-100.

Šiška, B., Špánik, F., 2008: Agroclimatic regionalization of slovak territory in condition of changing climate. *Meteorologický časopis, 11*(1-2), 61-64.

Škvarenina, J., Tomlain, J., Hrvoľ, J., Škvareninová, J., 2008: Occurrence of dry and wet periods in altitudinal vegetation stages of West Carpathians in Slovakia: Time-Series Analysis 1951-2005. In *Bioclimatology and Natural Hazards* (eds.: *Strelcova et al.*). Springer-Verlag, New York, LLC (in print).

Tomlain, J., 1979: Estimation methods of potential and actual evapotranspiration (in Slovak with English summary). *Meteorologické zprávy 32*(2), 72-79.

Tomlain, J., 1997: Distribution of evapotranspiration in the territory of Slovakia in the period 1961-1990 (in Slovak with English resume). *Podzemná voda, Vol. III.*, No. 1, SAH Bratislava, 5-23.

Trnka, M., Dubrovský, M., Semerádová, D., Žalud, Z., 2007: Drought, precipitation index, Palmer drought indicies in Moravia and Silesia. In *Selected Natural Extremes and Their Impacts in Moravia and Silesia* (in Czech) (eds.: *R. Brázdil* and *K. Kirchner*). Masarykova universita, Český hydrometeorologický ústav, Ústav geoniky Akademie věd ČR Brno, Praha, Ostrava

Vidovič, J., Novák, V., 1987: Dependence of maize yields on crop evapotranspiration. *Rostlinná výroba 33*(6), 663-670.

IDŐJÁRÁS

Quarterly Journal of the Hungarian Meteorological Service
Vol. 113, No. 1–2, January–June 2009, pp. 145–156

Consequences of climate change on some maize characteristics in Hungary

László Dióssy[1] and **Angela Anda**[*2]

[1]*Ministry of Environment and Water,*
P.O. Box 351, H-1394 Budapest, Hungary; E-mail: diossy@mail.kvvm.hu

[2]*Department of Meteorology and Water, University of Pannonia,*
P.O. Box 71, H-8361 Keszthely, Hungary; E-mail: anda-a@georgikon.hu

(Manuscript received in final form December 10, 2008)

Abstract—The influences of global climate change on sensible and latent heat fluxes of maize were studied by using the simulation model of *Goudriaan* (1977). Eight scenarios were made, an increase of CO_2 content until doubling the recent content was included in the scenarios. Some of the scenarios were developed by downscaling the *IPCC* (2007) report (A2 and B2) to Hungary, and the others by taking into account more serious weather changes. Surprisingly, the distribution of intercepted radiation among sensible and latent heat fluxes in the individual scenarios was not significantly modified. A given increase in ambient air temperature caused a lesser rise in crop temperature at cob level, demonstrating the compensation role of the canopy. The moderate rise in crop temperature indicated that the plants did not suffer significantly from lack of water in any of the scenarios. However, there was a variation during the diurnal cycle. The doubled CO_2 concentration alone increased the net carbon assimilation rate of maize by 40%. Photosynthesis decreased only in cases with warmings higher than 6 °C. Decreased precipitation counteracted the positive influence of elevated CO_2 on carbon assimilation.

In other scenarios the latent heat flux increased in comparison to control run. This justifies the existence of reserve soil water at Keszthely, even in on extra hot day during July.

Key-words: micro-meteorological model, simulation, maize canopy, global warming

1. Introduction

The plant canopy architecture determines the energy and mass exchange creating the canopy microclimate, which affects the plant physiological processes. Thus, there is a long series of impacts from changes in environmental factors to plant responses. To investigate such complex relationships, simulation

[*] Corresponding author

models are the most suitable tools, because they draw attention to those fields where there is a lack of knowledge. The early works of *de Wit* (1965), *Monteith* (1973), *Shawcroft et al.* (1974), *Norman* (1979), *de Vries* (1975), and *Waggoner* (1975) can be considered as the beginning of crop growth simulation modeling. The first reflections on modeling were provided by *Passioura* at a relatively early date, in 1973. *Bouman et al.* (1996) has summarized the 30-year experience of the "Dutch school" dealing with the simulation modeling founded by *de Wit,* and outlined the way of further development.

The simulation models offer advantages in quantitative assumption of crop growth. Although the shortcomings of model application are well known, including limited accuracy of local climate change projections, the crop microclimate simulation model (CMSM) of *Goudriaan* (1977) provides complexity in crop-environment studies. The effect of increased atmospheric carbon dioxide concentration may be hypothesized by its direct effect as well as its effect on plant canopy temperature via evaporative cooling. The paramount importance of crop temperature is provided by the fact that it determines the intensity of physiological processes including photosynthesis through influencing intensity of biochemical processes. The aim of this examination was to present the expected changes based on various scenarios in crop temperature and intensity of photosynthesis to the area of Keszthely. The model results are illustrated by plants at fulfilled tasseling, a stage of phenological development that is certainly achieved in Keszthely in the month of July. Out of the three model layers regarding the energy distribution, we have chosen the middle one: the cob stratum in which physiological processes are the most intensive.

Topicality was grounded by the appearance of the latest climate scenarios published in *IPCC* 2007 Report, and its scenarios downscaled to Hungary (*Bartholy et al.,* 2007). At a certain part of the scenarios we used average changes (*Bartholy et al.,* 2007), while – due to the growing frequency of extreme weather phenomena – we have also drafted several notions regarding extreme hot days. However, due to the uncertain precipitation scenarios we have not widened this to the precipitation.

2. Material and methods

2.1. Source of model inputs

The model inputs are site- and plant-specific values (plant height, leaf density in different layers), soil characteristics (soil moisture content, physical soil properties), and hourly meteorological data (air temperature, global radiation, relative humidity, soil temperatures). The hourly meteorological elements were the driving variables of the model, which were transformed from the standard measurement level (Agrometeorological Research Station at Keszthely, 46°44'N; 17°14'E; 114.2 m above sea level) to the reference level required by the model. The automatic weather station equipped by Eppley pyranometer is a part of the observation network of the Hungarian Meteorological Service. Data from the preceding station back to 1961 are also included. The meteorological data measured under standard conditions were correlated to the reference level required by the model on the basis of former investigations by *Anda et al.* (2003). The leaf area and its density were measured in the field on 10 sample plants weekly, using a LI-3000A type leaf area meter. The soil moisture content in the upper 1 m was also measured in the field with thermo-gravimetric method at 10 cm intervals every 10 days.

Our test plant was a maize hybrid for which we have more than 30-year data with weekly observations of plant height, leaf area index, leaf breadth, density, etc. These values and relative water content of crop were parameters of the model. The observed soil water content also covers more than 30 years with weekly soil sampling and gravimetric determination of soil water down to a depth of 1 m for every 10 cm layer. Precipitation projections were converted into local soil water content expressed in terms of soil water potential, which in turn is the model input regarding crop water supply. The water, as a basis material of photosynthesis and a cooling substance for transpiration, determines crop energy balance together with the intensity of photosynthesis. Physical properties of the soil (heat capacity, heat conductivity, soil surface resistance, starting value of soil heat flux, diameter of soil particles) were the parameters of the model. The former and current atmospheric CO_2 concentrations as parameters were taken into account on the basis of the local measurements by *Dunkel* (1982) and the national measurements of *Haszpra* (2007). More details on plant and other data samplings are found in an earlier publication of *Anda* (2006).

A one-day detailed study by canopy simulation will only be presented for an "average day" in July. Weather, crop, and soil data for July between1961 and 1990 served as a reference in our simulation. We chose the month July for demonstration because the intensity of maize physiological processes is the highest during July. The one day resolution attributes to model construction. In some scenarios the influence of extreme hot days is also included in the study.

2.2. The applied scenarios

The **first scenario,** called the control scenario, is the same as presented in the *IPCC* (2007) Report. Mean values of July during 1961–1990 and a CO_2 concentration published by *Haszpra* (2007) at 340 ppmv were applied. Soil water potential was –7 bar.

The **second scenario,** called 1997–2006, represents the changes of recent years by data from 1997–2006. According to the last climate normal of Keszthely, the summer air temperature has been significantly higher by 0.6 °C as compared with the monthly mean of July of the period 1901–2000. Accumulated precipitation of the same month has decreased by about 10–15% in Keszthely, though it is not statistically significant. The soil water potential was equal to –7.7 bar. We estimated the atmosperic CO_2 concentration to be 380 ppmv on the basis of the background measurements.

The **third scenario**, called 2×CO_2, represents the impacts of the rising ambient air CO_2 concentration alone. We doubled the present CO_2 gas concentration (760 ppmv), and the meteorological inputs remained the same as in the control scenario. With this we estimated the expected change due to increased CO_2 concentration to the time period 2071–2100.

In scenarios four to eight – beside doubling the current CO_2 level (760 ppmv) – we gradually increased the air temperature and decreased the precipitation values compared to the basic run (1961–1990). The **fourth scenario**, called 3.8 °C/–15%, is based on the B2 scenario (*IPCC*, 2007). Mean summer temperature in Keszthely is estimated to rise by 3.8 °C and precipitation to decrease by about 15% (soil water potential: –9 bar).

The **fifth scenario**, called 4.8 °C/–25%, used the summer data of the A2 *IPCC* (2007) scenario for 2071–2100, downscaled to Hungary by the above mentioned method. It has estimated a stronger warming of +4.8 °C and a 25% decrease in precipitation. We have noted that standard deviation is rather high in both scenarios (±15%), which implies strong uncertainty. The soil water potential was settled to –10 bar.

In the **sixth scenario**, called 6.0 °C/–25%, we increased the average air temperature by 6.0 °C together with a 25% decrease in precipitation. This 6 °C rise is close to the value of the upper limit value (6.4 °C, annual average) in the *IPCC* Fourth Assessment Report (2007). The soil water potential was –9 bar.

Keeping that in mind we performed a further increase in the degree of warming up by involving the 1.4 times product of the upper temperature rise (6.4 °C) pertaining to Hungary (9 °C) in the last two scenarios. To evaluate the effects of the uncertainty of precipitation projects, we assumed a weak decrease in precipitation (–10%) in the **seventh scenario** (9 °C/–10%), and then a more significant drying (30% precipitation decrease) in the **eight scenario** (9 °C/–30%). Their soil water potentials were –7.7 and –11 bar. The comparison of these latter two scenarios provided opportunity to quantify the impacts on plant growth of the different amounts of precipitation.

2.3. Model description

2.3.1. Energy balance of canopy layers

The advantage of present study, the use of *Goudriaan*'s (1977) simulation model is that it could keep its high scientific level together with its relative simplicity. In 1989 the author himself published the critical evaluation and application problems of the model (*Goudriaan*, 1989). The modified versions of the model (*Chen*, 1984; *Goudriaan* and *van Laar*, 1994) are also user-friendly and suitable for the better knowledge of the relationship between plant and environment and for providing the consequences of scenarios like global warming (*Dióssy*, 2008). The time step in the model is one hour.

The CMSM of Goudriaan simulates the canopy microclimate as a function of plant, soil, and weather characteristics. Plant stand plays important role in the model feedback as partly influenced by earlier weather. One of the advantages of the model is that short-term and long-term influences are also incorporated in its structure.

The amount of intercepted radiation was determined after *Monsi* and *Saeki* (1953). Partioning of the intercepted radiation into sensible and latent heat fluxes was calculated on the basis of energy balance equations (*Goudriaan*, 1977):

$$0 = Rn - M - Q_H - \lambda E, \tag{1}$$

where Rn is the canopy net radiation [W m^{-2}], M is the metabolic storage [W m^{-2}], Q_H is the sensible heat flux [W m^{-2}], λE is the latent heat flux [W m^{-2}], and λ is the evaporation heat [kJ kg^{-1}].

The metabolic storage was neglected in the model. The sensible heat flux (Q_{Hi}) in the ith layer in the canopy is:

$$Q_{Hi} = \rho c_p \frac{T_{ci} - T_{ai}}{r_{aHi}}, \tag{2}$$

where T_{ai} is the air temperature in the ith layer [K], T_{ci} is the canopy temperature in the ith layer [K], r_{aHi} is the aerodynamic (boundary layer) resistance for sensible heat transfer in the ith layer [s m^{-1}], ρ is the air density [kg m^{-3}], and c_p is the specific heat of air [J kg^{-1} K^{-1}].

The latent heat flux (λE_i) in the ith layer can be calculated as follows:

$$\lambda E_i = \rho c_p \{e_s(T_{ci}) - e_s\} / [\gamma(r_{awi} + r_{ci})], \tag{3}$$

where $e_s\ (T_{ci}) - e_i$ is the difference between saturation vapor concentration at plant temperature and actual vapor concentration [m^3 m^{-3}], r_{awi} is the aerodynamic resistance for water vapor transfer in the ith layer [s m^{-1}], r_{ci} is the crop resistance in the ith layer [s m^{-1}], and γ is the psychrometric constant [0.5 g m^{-3} K^{-1}].

After calculating the sensible and latent heat, the air temperature (T_{ai}) in the ith layer was estimated as:

$$T_{ai} = T_{ai-1} + Q_{Hi} r_i / \rho c_p, \tag{4}$$

where r_i is the characteristic value of resistance against heat in the ith layer [s m^{-1}] when $i=1$ (when canopy is considered as one layer) and (T_{ai-1}) is the air temperature for the reference level. When canopy is divided into more than one layer, the $i-1$th layer means the bordering one. The crop temperature (T_{ci}) was calculated similarly to the air temperature:

$$T_{ci} = T_{ai} + (Q_{Hi} - Q_{Hi-1}) r_{H,i} / \rho c_p . \quad (5)$$

2.3.2. *Photosynthesis of the whole canopy*

Rate of net CO_2 assimilation (F) was considered empirically as follows:

$$F_n = (F_m - F_d)[1 - \exp(-R_v \varepsilon / F_m)] + F_d , \quad (6)$$

where F_m is the maximum rate of net assimilation, F_d is the dark respiration, R_v is the absorbed short wave radiation (per LAI), ε is the slope of the curve of F–R_v at low light intensities, or efficiency ($17.2 \cdot 10^{-9}$ kg J^{-1} light in maize). Contrary to crop temperature and sensible and latent heat fluxes, the photosynthesis is calculated independently of energy balance and for the whole canopy only (*Goudriaan*, 1977).

The validation of the CMSM pertaining to the location of model building was performed by several authors (*Stigter et al.*, 1977; *Singh* and *Jacobs* 1995). The publication of *Hiramatsu* and *Maitani* (1984) firstly drew attention to the problems for simulation during the night hours. The Hungarian verification of the model regarding both the microclimate and several plant characteristics was performed by *Anda* and *Lőke* (2003, 2005) and *Anda et al.* (2001, 2002).

2.3.3. *Assumption of crop water status*

The water status of the canopy influences both the transpiration and photosynthesis by setting a lower limit to stomatal resistance. The relation between this lower limit and relative water content is given by *Goudriaan* (1977). The relative water content is calculated as the ratio of actual and maximum water contents. The value of maximum water content is based on leaf thickness (2.5 10^{-3} kg m^{-2} times the leaf area index). The actual water content is an integral of water uptake minus transpiration rate (*Penman*, 1948). The first feedback is created by the relationship between transpiration and stomatal resistance. Another feedback functions through the water uptake, since lower water content of plants forces more water to flow from the soil. The soil water stress was supposedly set at -0.1 bar water potential, root resistance is a function of soil temperature, and plant stress is a function of the relative water content.

2.3.4. *Statistical evaluation*

We evaluated the significanct differences between model runs by using paired t-test that was performed by the free version of *STATA 5.0* (1996) program package. The process reduces the two-sample t-test to one-sample test since there is no possibility of repetition (thus, of calculation of standard deviation) of the model runs. The test compares the mean value of the sample to an expected mean value. According to the null hypothesis, if the mean value of differences is 0 then the two samples are statistically the same. If the mean value of differences is not 0 then the control and the given scenarios are significantly different. The significance level was fixed at 5% in the course of the process.

3. *Results and discussion*

3.1. *Energy use in the cob layer*

The energy distribution for sensible and latent heat fluxes of the individual scenarios were not significantly modified in comparison to the control scenario, the difference to the control did not exceed 10% in any treatments (*Table 1*) which is in the range of error of the models as evaluated by *Singh* and *Jacobs* (1996), who diagnosed overestimations of 9 and 10% regarding the amount of simulated latent and sensible heat, respectively. It is worth noting that soil moisture reserves in Keszthely, even during the extremely hot days of July, were it is big enough to allow the latent heat to increase as compared with the control run. However, in case of more serious precipitation decrease they will supposedly be reduced and cause drastic fallback in latent heat (evapotranspiration depression).

Table 1. Ratio of the sensible and latent heat fluxes in maize on an average day in July at Keszthely

Scenario/ fluxes	**1961–1990**	**1997–2006**	**2×CO_2**	**3.8 °C/ –15%**	**4.8 °C/ –25%**	**6.0 °C –25%**	**9.0 °C/ –10%**	**9.0 °C/ –30%**
Sensible heat (%)	32.3	32.2	35.4	32.1	32.4	31.4	26.0	29.3
Latent heat (%)	67.7	67.8	64.6	67.9	67.6	68.6	74.0	70.7

Though, the hardly changing energy ratios do not mean that the amounts of the sensible and latent heat were not modified by the different model runs as compared with the control runs. The changes produced by the individual scenarios are illustrated through the example of the latent heat. The narrowing of the stomata opening due to the doubled CO_2 concentration significantly decreased the latent heat by 14.2%. A further significant difference could be found on extremely hot days (at the temperature change of +9 °C), when the degree of modification depended also on water supply. In the scenario with a modest decrease in precipitation (only 10%) the energy spent on evaporation significantly increased, by 30.2%. If the average precipitation was reduced by 30%, the amount of latent heat increased only by 13.9% due to a reduced amount of available water. A comparison of the daily water loss of the individual scenarios with that of the control run also credibly reflected the differences determined in latent heat (*Fig. 1*). Change in soil moisture influences the movements of stomata. Interaction in soil water and transpiration is taken into account by calculation of stomatal resistance.

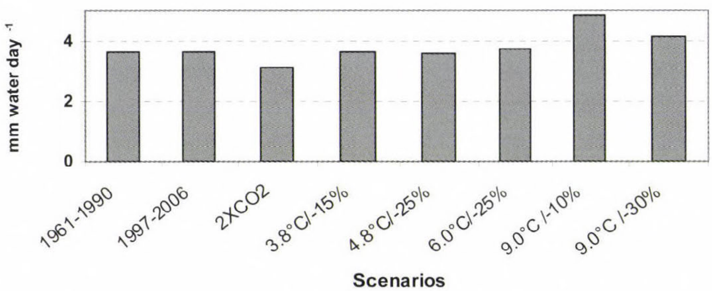

Fig. 1. Daily amounts of maize water losses (mm) in different scenarios at Keszthely during July.

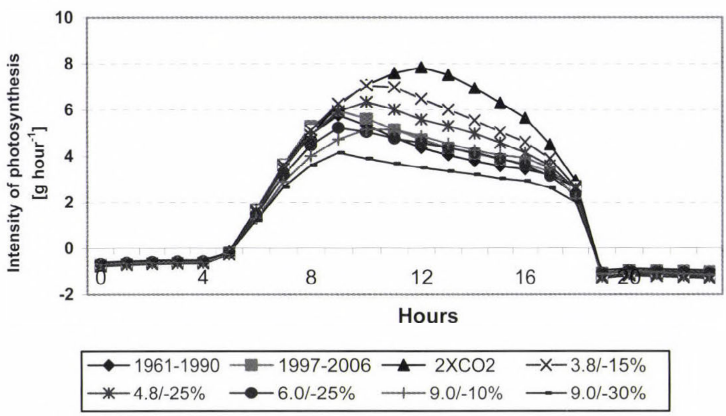

Fig. 2. Daily variation in the intensity of carbon assimilation in maize during July. Changes refer to 1961–1990.

Under the same weather conditions, the doubled CO_2 content significantly increased the net carbon assimilation rate of maize by 40% (*Fig. 2*). The balance of the photosynthetic rate of the past decade was positive (+7.1%), and increasing carbon assimilation are predicted by the fourth and fifth scenarios (14 and 24%). Photosynthesis decreased only in cases with warmings higher than 6 °C. A loss in photosynthesis will result from reduced amount of available soil water (precipitation); a good example of this relationship is the comparison of the two model runs with the same warming up of 9 °C but with different precipitation. At a decrease of 10% the daily carbon assimilation rate was reduced by 13%, while with a 30% less rainfall the rate was reduced by more than 30%. The model application suggests that in Hungary the future limiting factor of outdoor maize production without irrigation might be the precipitation.

3.2. Crop temperature inside the canopy

The simulated plant and air temperatures of the scenarios showed similar diurnal pattern but at different temperature in levels (*Fig. 3*) given by *Diószy* (2008). Air temperature was in all cases higher than leaf temperature as found also by *Singh* and *Jacobs* (1996), but the difference remained under 1 °C. This indicates that the plants did not suffer significantly from lack of water in any of the scenarios.

In the past decade the crop temperature at cob level, similarly to that of the air temperature, rose significantly by 0.6 °C. However, there was a variation during the diurnal cycle. From the second half of the night to the solar noon, the hourly rise in crop temperature was significantly higher for the past decade (1–1.5 °C per hour) (*Fig. 3*). The difference between the temperatures of the control and second scenarios decreased during early afternoon, and in the late afternoon it stabilized between – 0.2 and – 0.7 °C. Such a variation during the diurnal cycle was not found when comapring other scenarios with the values of the basic run of 1960 – 1990.

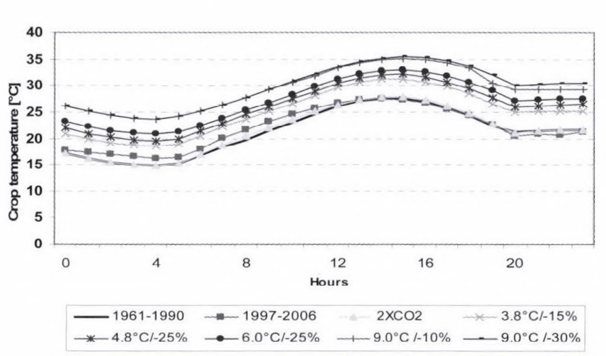

Fig. 3. Daily variations in maize crop temperature in the middle of the canopy (cob level).

The rise in plant temperature determined for the downscalings of the A2 and B2 scenarios to Hungary did not reach the rise of the ambient air temperature. This means that the cooling effect of the canopy transpiration on plant temperature was significant. In the scenarios with a smaller warming up, the degree of cooling was lower, only a couple of tenths of a degree. With simulating a greater warming up (above 6 °C), the canopy compensating effect on plant temperature still worked, but it was significantly reduced. The cooling effect of the canopy that mitigates the increase in plant temperature as compared with that of the ambient air emerged even in the last two scenarios (seventh and eighth). The cooling effect was 0.9 °C in the seventh scenario with low precipitation reduction, and only about the half of that, namely 0.5 °C in the eighth secenario with greater reduction in rainfall.

The optimum crop temperature range for maize in July is somewhere between 22–24 °C on average under Hungarian climatic conditions. At present, in most of the seasons there is enough precipitation for plant cooling to not override this optimum temperature. During global warming, the air temperature rise may increase the leaf temperature above this optimum level. Reduced precipitation may disturb the present balance, and farmers have to adapt to the changes for example by choosing more suitable crops for the given environment. One of the best tools in the hands of the Hungarian farmers to mitigate future impacts of climate change seems to be the use of irrigation to a greater extent.

4. Conclusions

The ratio of sensible to latent heat flux remained almost the same of all different scenarios. At a magnitude of less than 10% this was comparable to the overestimations by the crop microclimate simulation model in earlier simulations. It does not have the meaning that the absolute values of future projections were the same as the latent heat flux of control run. The doubled CO_2 level narrows the pore opening by about 14%. This may be a positive effect of global warming on the water loss of plants at Keszthely, where the water is the limiting factor of non irrigated maize growing. The latent heat flux of additional scenarios increased in comparison to control run. This justifies the existence of the reserve soil water at Keszthely even in an extra hot day during July.

Reduced transpiration and thus plant cooling at elevated CO_2 produced a moderate rise in plant temperature of 0.2 °C (in the third scenario). A given increase in ambient air temperature caused a lesser rise in crop temperature at cob level (place of yield formation in maize), demonstrating the cooling role of the canopy transpiration. This effect was detected even in extreme hot days.

Photosynthesis decreased only in cases with warmings higher than 6 °C. The photosynthesis was reduced by one third on an extremely hot day with 30% reduction in rainfall. This decline in photosynthesis may result in serious yield depression.

References

Anda, A., 2006: Modeling maize response to climate modification in Hungary. *Commun. Biometry Crop Sci. 1,* 90-98.

Anda, A. and *Lőke, Zs.*, 2003: Simulation of determiners maize transpiration, stomatal resistance and crop temperature and calculation of the intensity of photosynthesis (in Hungarian). *Növénytermelés 52,* 351-363.

Anda, A. and *Lőke, Zs., 2005: Microclimate simulation in maize with two watering levels. Időjárás 109,* 21-39.

Anda, A., Lőke, Zs., and *Burucs, Z.*, 2001: Microclimate of irrigated and non irrigated maize (in Hungarian). *Növénytermelés 50*, 249-260.

Anda, A., Lőke, Zs., and *Varga, B.*, 2003: Use of standard meteorological observation data as inputs of simulation models (in Hungarian). *Légkör XLVIII* (2), 28-33.

Anda, A., Lőke, Zs., and *Sz. Kirkovits M.*, 2002: Simulation of the components of water regime in maize (in Hungarian). *J. Central Eur. Agric. 3*, 95-103.

Bartholy, J., Pongrácz, R., and *Gelybó, Gy.*, 2007: Regional climate change in Hungary for 2071-2100. *Applied Ecol. and Environ. Res. 5,* 1-17.

Bouman, B.A.M., Keulen, H., Van Laar, H.H., and *Van Rabbinge, R.*, 1996: The „School of de Wit" crop growth simulation models: A pedigree and historical overview. *Agric. Syst. 52,* 171-198.

Chen, J., 1984: *Mathematical Analysis and Simulation of Crop Micrometeorology.* PhD. Thesis Wageningen University.

de Vries, D.A., 1975: Heat transfer in soil. In *Heat and Mass Transfer in the Biosphere. Part I: Transfer Processes in the Plant Environment* (eds.: *D.A. de Vries* and *N.H. Afgan*). John Wiley and Sons, New York.

de Wit, C.T., 1965: Photosynthesis of leaf canopies. *Agric. Res. Rep.* 663. Pudoc Wageningen, The Netherlands.

Dióssy, L., 2008: The influence of global climate change on air and soil temperatures in maize canopy. *Időjárás 112,* 125-139.

Dunkel, Z., 1982: Vertical profiles of CO_2 in maize canopy (in Hungarian). *Beszámolók az 1982-ben végzett tudományos kutatásokról.* Országos Meteorológiai Szolgálat, Budapest, 82-97.

Goudriaan, J., 1977: *Crop Micrometeorology: A Simulation Study.* Simulation Monographs. Pudoc, Wageningen.

Goudriaan, J., 1989: Simulation of micrometeorology of crops, some methods and their problems, and a few results. *Agr. Forest Meteorol. 47,* 239-258.

Goudriaan, J. and *van Laar, H.H.*, 1994: *Modelling Potential Crop Growth Processes.* Kluwer Academic Publishers, Dordrecht-Boston-London, p. 238.

Haszpra, L., 2007: 25 years history of CO_2 measurements in Hungary (in Hungarian). *Légkör 52*(1), 4-7.

Hiramatsu, Y.T. Seo & Maitani, T., 1984: Goudriaan's model of crop micrometeorology applied to the rice crop. *Berichte des Ohara Instituts für landwirtschaftliche Biologie.* Okayama Universität 18, 183-209.

IPCC, 2007: *Climate Change* (2007) *The Physical Science Basis. Contribution of Working Group I to the Fourth Assessment Report of the Intergovernmental Panel on Climate Change. Summary for Policymakers.* [*Solomon, S., Qin, D., Manning, M., Chen, Z., Marquis, M., Averyt, K.B., Tignor, H.L., Miller, G.* (eds)]. Cambridge University Press, Cambridge United Kingdom and New York, NY, USA, 996 pp. Available online: www.ipcc.ch

Monsi, M. and *Saeki, T.*, 1953: Über den Lichtfaktor in den Pflanzengesellschaften und seine Bedeutung für die Stoffproduktion. *Jap. J. Bot. 14*, 22-52.

Monteith, J.L., 1973: *Principles of Environmental Physics.* Edward Arnold, London, p. 271.

Norman, J.M., 1979: Modeling the complete crop canopy. In *Modification of the Aerial Environment of Crops* (eds.: *B.J. Barfield* and *J.F. Gerber*). Amer. Soc. of Agric. Eng., Michigan, 249-277.

Passioura, J., 1973: Sense and nonsense in crop simulation. *J. Aust. Inst. Agric. Sci. 39,* 181-183.

Penman, H.L., 1948: Natural evaporation from open water, bare soil and grass. *Proc. of the Royal Societiy A. 193*, 120-145.

Shawcroft, R.W., Lemon, E.R., Allen, L.H., Stewart, D.W. & Jensen, S.E., 1974: The soil-plant-atmosphere model and some of its applications. *Agric. Meteor. 14,* 287-307.

Singh, R.S. and *Jacobs, A.F.G.,* 1995: Validation of Goudriaan's model: A case study for maize. *Neth. J. Agr. Sci. 43,* 163-181.

SRES, 2000: Emission Scenarios. IPCC Summary for Policymakers. www.ipcc.ch/pdf/special-reports/spm/sres-en.pdf

STATA 5.0, 1996: Stata Corporation LP Texas, USA. Available online: www.stata.com

Stigter, C.J., Goudriaan, J., Bottemanne, F.A., Birnie, J., Lengkeek, J.G., and *Simba, L.,* 1977: Experimental evaluation of a crop microclimate simulation model for Indian corn (Zea mays). *Agr. Meteorol. 18*, 163-186.

Waggoner, P.E., 1975: Micrometeorological models. In *Vegetation and the Atmosphere* (ed.: *J.L. Monteith*). Academic Press Inc., London, Vol. 1, 205-228.

GUIDE FOR AUTHORS OF *IDŐJÁRÁS*

The purpose of the journal is to publish papers in any field of meteorology and atmosphere related scientific areas. These may be

- research papers on new results of scientific investigations,
- critical review articles summarizing the current state of art of a certain topic,
- short contributions dealing with a particular question.

Some issues contain "News" and "Book review", therefore, such contributions are also welcome. The papers must be in American English and should be checked by a native speaker if necessary.

Authors are requested to send their manuscripts to

Editor-in Chief of IDŐJÁRÁS
P.O. Box 39, H-1675 Budapest, Hungary
E-mail: antal.e@met.hu

including all illustrations. MS Word format is preferred in electronic submission. Papers will then be reviewed normally by two independent referees, who remain unidentified for the author(s). The Editor-in-Chief will inform the author(s) whether or not the paper is acceptable for publication, and what modifications, if any, are necessary.

Please, follow the order given below when typing manuscripts.

Title page: should consist of the title, the name(s) of the author(s), their affiliation(s) including full postal and e-mail address(es). In case of more than one author, the corresponding author must be identified.

Abstract: should contain the purpose, the applied data and methods as well as the basic conclusion(s) of the paper.

Key-words: must be included (from 5 to 10) to help to classify the topic.

Text: has to be typed in single spacing on an A4 size paper using 14 pt Times New Roman font if possible. Use of S.I. units are expected, and the use of negative exponent is preferred to fractional sign. Mathematical formulae are expected to be as simple as possible and numbered in parentheses at the right margin.

All publications cited in the text should be presented in the *list of references*, arranged in alphabetical order. For an article: name(s) of author(s) in Italics, year, title of article, name of journal, volume, number (the latter two in Italics) and pages. E.g., *Nathan, K.K.,* 1986: A note on the relationship between photosynthetically active radiation and cloud amount. *Időjárás 90,* 10-13. For a book: name(s) of author(s), year, title of the book (all in Italics except the year), publisher and place of publication. E.g., *Junge, C.E.,* 1963: *Air Chemistry and Radioactivity.* Academic Press, New York and London. Reference in the text should contain the name(s) of the author(s) in Italics and year of publication. E.g., in the case of one author: *Miller* (1989); in the case of two authors: *Gamov* and *Cleveland* (1973); and if there are more than two authors: *Smith et al.* (1990). If the name of the author cannot be fitted into the text: (*Miller,* 1989); etc. When referring papers published in the same year by the same author, letters a, b, c, etc. should follow the year of publication.

Tables should be marked by Arabic numbers and printed in separate sheets with their numbers and legends given below them. Avoid too lengthy or complicated tables, or tables duplicating results given in other form in the manuscript (e.g., graphs).

Figures should also be marked with Arabic numbers and printed in black and white or color (under special arrangement) in separate sheets with their numbers and captions given below them. JPG, TIF, GIF, BMP, PNG or EPS formats should be used for electronic artwork submission.

Reprints: authors receive 30 reprints free of charge. Additional reprints may be ordered at the authors' expense when sending back the proofs to the Editorial Office.

More information for authors is available: antal.e@met.hu

Published by the Hungarian Meteorological Service

Budapest, Hungary

INDEX 26 361

HU ISSN 0324-6329

IDŐJÁRÁS

QUARTERLY JOURNAL
OF THE HUNGARIAN METEOROLOGICAL SERVICE

CONTENTS

****

http://www.met.hu/Journal-Idojaras.php

VOL. 113 * NO. 3 * JULY – SEPTEMBER 2009

IDŐJÁRÁS

Quarterly Journal of the Hungarian Meteorological Service

Editorial Office: *Gilice tér 39, H-1182 Budapest, Hungary*
P.O. Box 39, H-1675 Budapest, Hungary
E-mail: bozo.l@met.hu or antal.e@met.hu
Fax: (36-1) 346-4809

Indexed and abstracted in Science Citation Index Expanded™ and Journal Citation Reports/Science Edition
Covered in the abstract and citation database SCOPUS®

Subscription by

mail: IDŐJÁRÁS, P.O. Box 39, H-1675 Budapest, Hungary
E-mail: kenderesy.k@met.hu or antal.e@met.hu

IDŐJÁRÁS
Quarterly Journal of the Hungarian Meteorological Service
Vol. 113, No. 3, July–September 2009, pp. 157–175

Study on the size dependence of complex refractive index of atmospheric aerosol particles over Central Europe

Diana Benkő[1], **Agnes Molnár**[2*], and **Kornelia Imre**[3]

[1]*Department of Earth and Environmental Sciences, University of Pannonia, P.O. Box 158, H-8201 Veszprém, Hungary; E-mail: benkodiana@freemail.hu*

[2]*Air Chemistry Group of Hungarian Academy of Sciences, P.O. Box 158, H-8201 Veszprém, Hungary; E-mail: amolnar@almos.uni-pannon.hu*

[3]*Department of Earth and Environmental Sciences, University of Pannonia, P.O. Box 158, H-8201 Veszprém, Hungary; kornelia@almos.uni-pannon.hu*

(Manuscript received in final form July 15, 2009)

Abstract—The aim of this paper is threefold: (1) to present our results on the complex refractive index regarding Central European background air; (2) to demonstrate the importance of the size dependence of the complex refractive index; (3) to study how the refractive index changes due to the aerosol hygroscopicity. The area of Central Europe is of great importance in modeling anthropogenic climate variations due to its relatively high aerosol burden and to the direct aerosol forcing effect. In this work the complex refractive index of the aerosol is calculated. The calculations are based on the size distribution measured for different aerosols species, as well as on the complex refractive indices of the different components. For this study, ambient aerosol samples were collected at K-puszta, in rural Hungary, by means of electric low pressure (ELPI) and Berner impactors, which make the estimation of the chemical mass closure possible. By using the data measured the complex refractive indices were determined in 8 size ranges (from 31 nm up to 1.7 μm (ELPI) and from 62.5 nm to 16 μm (Berner)), by assuming volume mixing rule. Our results show that the real refractive index of dry aerosol increases with particle size in the optically active range (0.1–1.0 μm) from 1.499 to 1.527. Contrary to the real part, the imaginary refractive index decreases with increasing particle size from 0.025 to 0.008. In a case study we show that the application of a size resolved refractive indices in Mie-calculations instead of a constant value may reduce the uncertainty of the estimation of scattering and absorption (extinction) coefficients and finally – through the single scattering albedo – of the direct aerosol radiation forcing. We found that the overall difference between extinction coefficients estimated by the two approaches varies in the range of –2% and 65%. Further, the absorption coefficient, calculated by applying a constant refractive index, overestimates the value calculated with a varying refractive index by 37%. In the case of the scattering coefficient the corresponding figure is equal to –4%. Finally, the study of hygroscopic mass growth of

* Corresponding author

the aerosol particles indicates that water uptake decreases the real part of the refractive index by 3% (at 86% relative humidity (RH)) compared to the dry aerosol.

Key-words: refractive index, volume mixing rule, size distribution, extinction coefficient, hygroscopic growth

1. Introduction

It is well known that aerosol particles in the atmosphere influence the transfer of solar radiation. For this reason, their effects on the radiative balance of the Earth - atmosphere system have to be considered in climate models. In these models, different physical, chemical, and optical properties of the aerosol should be taken into account. The optical properties of the aerosol are modeled by Mie-theory as a function of particle size distribution and composition determining the refractive index (e.g., *Hatzianastassiou et al.*, 2007). One of the problems arising during such modeling is that the composition and, consequently, the refractive index of the particles are inhomogeneous in space and time. Due to this variability, the direct aerosol radiation effect is also non-uniform as shown by different climate model outputs (e.g., *IPCC*, 2007; *Hatzianastassiou et al.*, 2007; *Kaufman et al.*, 2002; *Seinfeld*, 2008). Information on these parameters (chemical composition, spatial and temporal trends) for different locations and regions is, therefore, needed. More detailed regional input data make the predictions of global models more accurate (e.g., *Kaufman et al.*, 2002; *IPCC*, 2007; *Balkanski et al.*, 2007; *Randles et al.*, 2004; *Hatzianastassiou et al.*, 2007; *Stier et al.*, 2007; *Seinfeld*, 2008; *Ramanathan et al.*, 2007).

Aerosol studies carried out over Central Europe indicate that this area of the continent is characterized by high aerosol loading due to industrial and other anthropogenic sources. Model results show that in Central Europe the aerosol optical depth has significant local maximum with values between 0.1 and 0.2, similar to those found in the eastern US. It follows from the high aerosol burden that in this region both the shortwave atmospheric and the surface radiation forcing are important. As a consequence, the modeled shortwave radiation forcing referring to the total air column shows local minimum, between –1.0 and –2.0 W m^{-2} (*IPCC*, 2007; *Hatzianastassiou et al.*, 2007; *Kaufman et al.*, 2002; *Feczkó et al.*, 2004). These relatively high values indicate that data on the complex refractive index of aerosol particles from this region is of great importance. Unfortunately, only limited information on the complex refractive index is available for Central Europe (e.g., *Ebert et al.*, 2004; *Pesava et al.*, 2001; *Horvath*, 1995). Moreover, these data mainly correspond to urban environments not to regional background air. The main aim of this paper is to present complex refractive index for Central European background air.

As mentioned earlier, optical properties of the aerosol particles depend strongly on the particle size and refractive index. Furthermore, the refractive index itself is also a function of the size distribution. In spite of this, the dependence of the aerosol refractive index on particle size is generally not considered in climate modeling, due to different reasons, probably one of these is the lack of information on the size resolved complex refractive index. As noted before, only a few papers address the size resolved aerosol refractive index. For urban environments *Horvath* (1995) published data on the imaginary refractive index in the 15 nm–16 μm size range for Vienna, Naples, and Bologna; *Pesava et al.* (2001) reported the aerosol complex refractive index in the size range of 34 nm–15.6 μm for Vienna; *Iinuma et al.* (2000) studied the complex refractive index in Australian cities in the size interval of 0.1–1.0 μm. On the other hand, for rural environments, less information can be found: e.g., *Ebert et al.* (2004) discussed the complex refractive index of aerosol particles at Kleiner Feldberg, in the size range of 0.1–3.0 μm, while *Hand et al.* (2002) summarized the data obtained by different studies carried out in the Great Smoky Mountains National Park (size ranges of 0.12–0.28 μm, 0.2 μm, d<2.5 μm). In this paper we also aim to present additional data on the complex refractive index as a function of particle size for Central European rural air, for which no such information can be found in the literature. On the other hand, in a sensitivity study the effect of size resolved complex refractive index on the scattering and absorption coefficient is discussed.

The next problem arises from the hygroscopicity of aerosol particles. As is well known, increasing ambient relative humidity results in water uptake by the particles. The absorbed water changes the size distribution as well as the refractive index of the aerosol. However, in climate forcing estimations, although the hygroscopic growth of the particles is generally considered, the variation of the refractive index due to hygroscopicity is not usually involved. The effect of water uptake on the complex aerosol refractive index is taken into account only in few research studies (*Randles et al.*, 2004; *Iinuma et al.*, 2000). In the present paper the effect of the aerosol hygroscopicity on the aerosol complex refractive index is also discussed.

In summary, the goals of this paper are: (1) to present our results on the complex refractive index over Central European background air; (2) to demonstrate the importance of the size dependence of the complex refractive index; (3) to study changes in refractive index due to the aerosol hygroscopicity.

2. *Experimental*

2.1. Sampling and analysis

The aerosol sampling was carried out at K-puszta station (φ=46°58', λ= 19°35', h=125 m a.s.l.), in rural Hungary. This sampling site belongs to the GAW and EMEP networks, and is located in a forest clearing on the Great

Hungarian Plain. Because of the lack of nearby large emission sources, aerosol characteristics measured at K-puszta represent Central and Eastern European regional air.

In the calculations discussed in this study, the results of 92 aerosol samples overall are used, which were collected during different sampling periods between 1999 and 2002. The details of the sampling periods are given in *Table 1*. One can see from the table that all four seasons are represented. Since aerosol properties may vary significantly during the year, the results from the different sampling periods are distinguished from each other and are presented separately in the following (denoted as ELPI1-5). On the other hand, the results labeled as Berner correspond to the average of more than a whole year.

Table 1. Sampling periods

Sampling period	Date	Number of samples
ELPI1	July 11, 1999 – August 8, 1999	25
ELPI2	July 29, 2000 – August 14, 2000	26
ELPI3	January 31, 2001 – February 3, 2001	8
ELPI4	April 2, 2001 – April 6, 2001	9
ELPI5	October 23, 2001 – October 27, 2001	8
Berner	July 27, 2001 – October 28, 2002	16

76 and 16 aerosol samples were taken on Al-foils by an electric low pressure impactor (ELPI) and a 9-stage Berner impactor, respectively. The large number of ELPI samples is used for characterizing the complex refractive index of fine particles. While the ELPI instrument collects aerosol particles on 13 stages (in the range of 0.031–10.77 μm), in our work only the data of the first 8 stages (0.031–1.7 μm) are considered. This means that our results correspond to the fine particle size range, containing the optically active size interval. On the other hand, Berner impactor samples make it possible to study the size dependence of the refractive index in the 62.5 nm – 16 μm size range. Owing to higher aerosol masses collected, these latter samples were also used to investigate the effect of aerosol hygroscopicity on the refractive index.

The first step of the study is the determination of the mass concentration. In the case of ELPI samples, the mass concentrations in different size ranges are estimated from the conversion algorithm of the device (*ELPI User Manual*, 2003) based on the measured number size distribution; assuming spherical particles of unit density (see details in *Temesi et al.* (2001)). For the Berner samples, the mass is directly measured by weighting, applying a microbalance (the precision of the microbalance (Sartorius) is 10 μg). The dry mass of the samples is determined in an isolated box with low relative humidity (30%), which is adjusted by silica gel. Next, the mass growth of these samples due to their water uptake is measured as a function of increasing relative humidity.

For controlling the relative humidity, saturated solutions of different inorganic salts (NH_4NO_3 (64% RH); NH_4Cl (80% RH); KCl (86% RH)) were applied. Before weighing, the samples are kept at a given relative humidity for more than 48 hours in order to reach equilibrium with their surroundings (for more details see *Imre* and *Molnár*, 2008).

After sampling and weighing, all samples were chemically analyzed in the same way (see *Temesi et al.* (2001) for a detailed description of the analysis). It has to be mentioned, that in the case of Berner samples, the changes in the concentration of the measured inorganic components caused by the exposure to elevated humidities are not significant. This is confirmed by test measurements, which showed negligible differences (around 5%, within the analytical error) between the exposed and non-exposed samples.

The inorganic ion content (NH_4^+, SO_4^{2-}, NO_3^-) of the samples are measured by capillary electrophoresis (detection limit is 70 μg L^{-1}). On the basis of the results of the chemical analysis, the concentrations of the main inorganic compounds in the aerosol ($(NH_4)_2SO_4$, NH_4HSO_4, H_2SO_4, NH_4NO_3) are estimated by applying stoichiometry.

The concentration of the total organic carbon (TC) was measured by a TOC solid analyzer as carbon dioxide by catalytic combustion method with oxygen at 680 °C. The detection limit of carbon measurement is 2 μg (*Temesi et al.*, 2001).

Carbonaceous compounds (especially elemental carbon (EC)) in the particles are mainly responsible for the light absorption (the imaginary part of the refractive index) of the particles. For this reason, from the total carbon data, the concentrations of various carbonaceous species characterized by their different optical and chemical properties are estimated (elemental carbon, slightly absorbing HUmic-LIke Substances (HULIS), and non-absorbing carbon). In our former study (*Molnár et al.*, 1999), the total carbon concentration and absorption coefficient of fine aerosol (PM1) is compared. The results showed that 10% of the total carbon concentration in fine aerosol can be considered as elemental carbon. As mentioned before, direct sources (including traffic) cannot be found in the vicinity of the sampling site. This can be the reason why EC fraction in PM1 is quite low at K-puszta. Besides the lack of direct sources of EC, low EC/TC fraction can be also the result of relatively high organic carbon (OC) concentration due to the abundant biogenic precursors over the site. Significant formation of the secondary OC is followed by decreasing EC/OC ratio as already reported by, e.g., *Turpin* and *Hutzincker* (1995). On the other hand, low EC fraction is not unusual in background monitoring sites, e.g., in Hyytiälä. *Saarikoski et al.* (2005) reported 35 and 5% of OC and EC mass fractions for PM1, respectively. Calculating these fractions to EC/TC ratio, similar value can be obtained.

Not involving the particles smaller than 100 nm, the size distribution of EC and OC(TC) is rather similar (*Cabada et al.*, 2004; *Hitzenberger et al.*, 2006;

Miguel et al., 2004). *Jaffrezo et al.* (2005) stated that both in rural and suburban sites, EC and OC had "very same" distributions in the range of 0.1–1 μm both in winter and summer. Consequently, the OC/EC ratio has only slight size dependence in this size range.

According to the above mentioned reasons, in this work, elemental carbon concentration of all impactor stages is estimated as 10% of the TC concentration. On the other hand, HULIS concentration of the samples is also estimated from the TC data using the results of *Kiss et al.* (2002) and *Gysel et al.* (2004). These authors demonstrated that an average 35% of the TC concentration consists of HULIS in aerosol samples taken at K-puszta. Accordingly, in our calculations we accept this value for HULIS, while the rest of TC concentration is considered as non-absorbing organic carbon. Despite all assumptions, our results on the imaginary refractive index of aerosol particles can have importance, since data on the complex refractive index of aerosol particles are rather scarce. On the other hand, we note that due to the assumptions, these data should be considered as a first estimation of the imaginary part of the refractive index which needs to be confirmed by further studies.

2.2. Mass closure

On the basis of data obtained, the dry mass closure of the aerosol for each sample and impactor stage is estimated. The mass closure data are presented in *Table 2*. For Berner samples, obviously the mass concentrations measured at a relative humidity of 30% are used for this purpose. On the other hand, in the case of ELPI samples, we can assume that the mass concentrations determined relate to dry conditions. This assumption is based on the fact that in the overwhelming majority of cases during the sample collection by ELPI, the ambient relative humidity did not exceed 50%. It goes without saying that this assumption must be considered with caution. However, one can speculate that only a small quantity of water is absorbed by the particles under these conditions.

To establish the mass closure for each sample, the concentrations of $(NH_4)_2SO_4$, NH_4HSO_4, H_2SO_4, NH_4NO_3, EC, HULIS, and non-absorbing carbon are considered (see above). For the conversion of the last three "carbon" concentrations into mass concentrations we assume the following. In the case of EC, a factor of 1 is applied, while for HULIS a mass conversion factor of 1.9 is used. This value is based on the results of elemental composition (molar ratio of C:H:N:O) measurements carried out by UV, fluorescence, Fourier transform, and infrared studies (*Kiss et al.*, 2002; *Gysel et al.*, 2004). For the rest of TC (non-absorbing organic carbon), the conversion factor is adjusted in such a way to obtain a total carbon mass closure. By using this procedure the conversion factor for non-absorbing organic particles varied from sample to sample, but with a maximum value of 1.9.

Table 2. Mass closure of the aerosol samples. Concentrations are given in μg/m^3. *ROM stands for remaining organic material

Sampling period	Cut off (μm)	$(NH_4)_2SO_4$	NH_4HSO_4	H_2SO_4	NH_4NO_3	SiO_2	EC	HULIS	ROM*
ELPI1	0.061	0.007	0.049	0.046	0.011	0.000	0.000	0.000	0.082
	0.11	0.020	0.131	0.188	0.125	0.000	0.003	0.001	0.293
	0.178	0.041	0.274	0.402	0.388	0.043	0.000	0.007	1.010
	0.273	0.053	0.354	0.557	0.835	0.035	0.000	0.022	2.424
	0.419	0.082	0.548	0.849	1.695	0.029	0.000	0.024	6.004
	0.677	0.036	0.239	0.348	0.443	0.048	0.003	0.011	2.900
	1.05	0.015	0.102	0.146	0.039	0.016	0.010	0.009	1.254
ELPI2	0.061	0.021	0.143	0.156	0.014	0.018	0.025	0.004	0.040
	0.11	0.035	0.231	0.356	0.230	0.138	0.021	0.011	0.389
	0.178	0.050	0.335	0.526	0.620	0.357	0.037	0.032	0.985
	0.273	0.063	0.421	0.647	1.126	0.573	0.005	0.031	1.759
	0.419	0.080	0.531	0.835	2.033	1.356	0.000	0.102	4.372
	0.677	0.039	0.262	0.425	0.597	0.638	0.042	0.027	2.688
	1.05	0.029	0.195	0.307	0.061	0.089	0.067	0.014	1.940
ELPI3	0.061	0.015	0.098	0.126	0.004	0.007	0.021	0.018	0.018
	0.11	0.026	0.174	0.274	0.055	0.056	0.010	0.099	0.464
	0.178	0.044	0.291	0.457	0.211	0.042	0.017	0.205	1.383
	0.273	0.059	0.395	0.620	0.295	0.132	0.007	0.307	1.821
	0.419	0.101	0.674	1.059	0.693	0.258	0.000	0.837	5.423
	0.677	0.037	0.245	0.385	0.025	0.145	0.071	0.215	3.280
	1.05	0.017	0.113	0.178	0.005	0.001	0.020	0.023	1.458
ELPI4	0.061	0.016	0.106	0.146	0.035	0.021	0.028	0.024	0.063
	0.11	0.033	0.221	0.347	0.118	0.074	0.022	0.095	0.597
	0.178	0.060	0.402	0.632	0.300	0.159	0.006	0.186	1.578
	0.273	0.078	0.521	0.818	0.535	0.185	0.000	0.255	1.790
	0.419	0.135	0.901	1.415	1.208	0.372	0.000	0.904	8.122
	0.677	0.052	0.345	0.542	0.094	0.248	0.087	0.234	4.260
	1.05	0.020	0.132	0.208	0.013	0.022	0.042	0.037	3.613
ELPI5	0.061	0.018	0.118	0.133	0.014	0.000	0.022	0.013	0.000
	0.11	0.057	0.377	0.584	0.110	0.030	0.021	0.107	0.299
	0.178	0.219	1.458	2.170	0.206	0.133	0.042	0.404	1.763
	0.273	0.215	1.430	2.248	0.347	0.174	0.016	0.461	4.458
	0.419	0.239	1.588	2.495	0.727	0.287	0.096	0.890	8.266
	0.677	0.082	0.545	0.856	0.414	0.146	0.005	0.331	6.454
	1.05	0.051	0.336	0.529	0.147	0.019	0.052	0.166	5.260
Berner	0.0625	0.051	0.340	0.286	0.008	0.093	0.014	0.030	0.507
	0.125	0.067	0.444	0.513	0.179	0.127	0.010	0.065	0.303
	0.25	0.112	0.743	0.935	0.247	0.548	0.093	0.154	0.798
	0.5	0.075	0.502	0.508	0.109	0.639	0.109	0.187	0.942
	1	0.045	0.302	0.275	0.014	0.043	0.030	0.044	0.350
	2	0.060	0.402	0.435	0.003	0.000	0.002	0.053	0.317
	4	0.060	0.398	0.452	0.004	0.000	0.005	0.057	0.345
	8	0.052	0.347	0.335	0.005	0.000	0.000	0.053	0.335

In certain cases, especially for the first two stages of the ELPI and for the first stage of the Berner impactor, the total mass concentrations were lower than the sum of the concentrations of the species obtained from the chemical analysis. This is probably due to the uncertainty of the determination of low mass concentrations, as well as to the different measurement techniques. *Temesi et al.* (2001) and *Pesava et al.* (2001) already discussed this discrepancy and noted that its reason needs further consideration. Due to this problem, in the following these samples are excluded from calculations of the refractive index. Unfortunately, this step led to the exclusion of the entire first stage of ELPI impactor samples.

It is also to be noted that the sum of the mass concentration of the different species identified chemically is generally found to be lower than the total mass determined, mostly in the coarse size range. Thus, the undetermined aerosol mass fraction increases with the stage number (18–55%), and is likely caused by particles of crustal origin not indentified in this study. Since the soil type around the sampling site is sandy, in further calculations we suppose that this undetermined mass in the coarse mode consist of SiO_2. However, we also found some non-resolved mass in the fine size range. The results of *Mészáros et al.* (1997) show that in Hungary significant concentrations of Al, Fe, and Mn can be measured also in the fine mode. This makes it possible that crustal-like components are present in the fine mode aerosol. For this reason we speculate that even for fine particles the missing fraction is SiO_2 of crustal origin in agreement with the work of *Pesava et al.* (2001).

3. Calculation of the refractive index

After establishing the mass closure for each size selected sample, the complex refractive index is estimated by applying the volume mixing rule. In the calculations we assume that the particles are homogenously, internally mixed. This assumption is the most acceptable in the optically active size range (particles with diameters ranging between 0.1 and 1 μm), where the particles usually arise from the coagulation of smaller particles or from the condensation of low volatility vapors (*Guyon et al.*, 2005). In this way, the average complex refractive index (m) of the total aerosol is given by the following equation (e.g., *Ebert et al.*, 2002):

$$m = \frac{m_1 V_1 + ... + m_i V_i}{V_1 + ... + V_i} = \frac{n_1 V_1 + ... + n_i V_i}{V_1 + ... + V_i} - \frac{k_1 V_1 + ... + k_i V_i}{V_1 + ... + V_i} i, \qquad (1)$$

where m_i, n_i, k_i, and V_i are the complex refractive index, its real and imaginary parts, and the volume of particle group i, respectively.

In order to obtain the volume of the individual aerosol components from the mass measured chemically, their densities should be known. The densities of the inorganic compounds can be easily found in chemical handbooks, while some information on the density of EC, HULIS, and non-absorbing OC can be taken from recent research papers. *Guyon et al.* (2005) published a value of 1.2 g/cm^3 for EC; *Hoffer et al.* (2005) recommended a density of 1.569 g/cm^3 for HULIS; while according to *Turpin* and *Lim* (2001), for non-absorbing OC the value of 1.2 g/cm^3 can be applied. The summary of the densities considered in our calculations are listed in *Table 3*.

Table 3. Complex refractive indices ($m = n - ki$), $\lambda = 589$ nm. [a]*Weast* (1987), [b]*Stelson* (1990), [c]*Seinfeld* and *Pandis* (1998), [d]*Horvath* (1998), [e]*Hoffer et al.* (2005), [f]*Turpin* and *Lim* (2001), [g]*Guyon et al.* (2005)

Compound	**n**	**k**	**ρ (g/cm^3)**
$(NH_4)_2SO_4$	1.521	0 [a]	1.77
NH_4HSO_4	1.473	0 [a]	1.79
H_2SO_4 (97%)	1.426	0 [b]	1.84
NH_4NO_3	1.413	0 [a]	1.725
SiO_2 (550 nm)	1.550	0 [c]	2.2
EC	1.500	0.47000 [d]	1.2 [g]
HULIS	1.653	0.00187 [e]	1.569 [e]
Remaining organic material	1.400	0 [f]	1.2 [f]

As one can see from Eq. (1), for the calculation of refractive indices the knowledge of their real and imaginary parts is necessary. In *Table 3* both the real and imaginary parts of the refractive index are tabulated. The values for inorganic components can be found in appropriate handbooks and papers on the subject. However, for carbonaceous aerosol much less information can be found in the literature. In this work, the refractive indices of carbonaceous aerosol classified into three categories are estimated on the basis of the results published by the following authors: *Horvath* (1998), *Hoffer et al.* (2005), *Turpin* and *Lim* (2001). It has to be noted, that in *Table 3* the refractive indices refer to $\lambda = 550$ or 589 nm. Although the refractive index slightly varies in this wavelength range, in the calculation we neglect this unimportant variation.

One has to note that in the case of EC, the refractive index can vary within wide limits due to unknown density differences of black carbon. Besides, soot particles may contain un-burnt, mostly organic material components, which are not light absorbing (*Horvath*, 1995; *Ebert et al.*, 2002). In spite of these problems, we apply the commonly accepted value of $1.50 - 0.47i$, following the recommendation of *Horvath* (1998).

The complex refractive index of carbonaceous materials is also not well understood. For HULIS, *Table 3* contains the recent estimate of *Hoffer et al.* (2005). In their work, the optical properties of previously isolated HULIS were determined from the fine fraction of biomass burning aerosol during the LBA-SMOCC experiment. Hoffer and his co-workers measured the scattering and absorption coefficients of HULIS. On the basis of these results, and the size distribution of HULIS particles, the refractive index is derived from closure calculations. Finally, for the remaining, not light absorbing organic material, we consider a complex refractive index of 1.4 – 0*i*, as proposed by *Turpin* and *Lim* (2001).

4. Results and discussion

4.1. Size distribution of complex refractive index of dry aerosol

The complex refractive index is calculated individually for each aerosol sample. *Figs. 1a* and *1b* show the size distributions of the real and imaginary parts of the refractive index of dry aerosol. It has to be noted again, that the results on the imaginary part of the refractive index are first approximations based on TOC measurements and reasonable estimations (see details in Experimental).

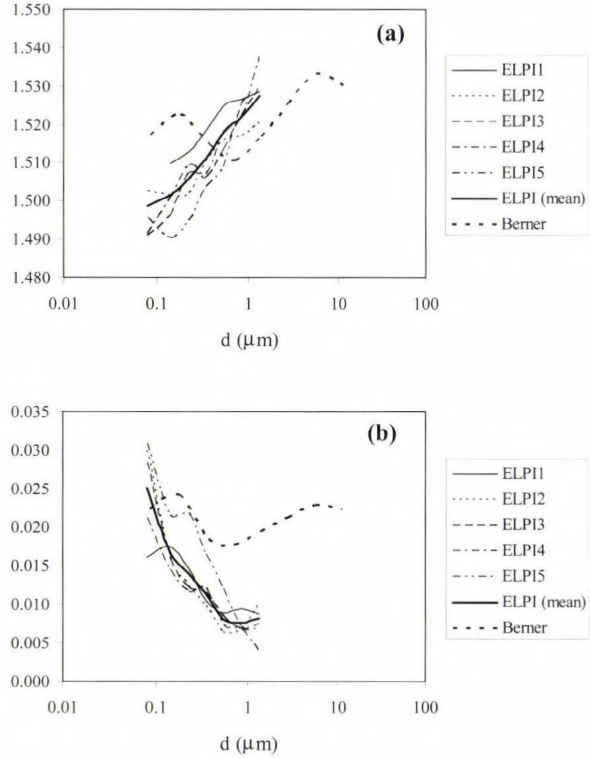

Fig. 1. Size distribution of the real (a) and imaginary (b) refractive index for dry particles.

The curves in these figures represent averages of the sampling periods (ELPI1-5 and Berner, see also in *Table 1*) and the mean distribution of all ELPI samples as ELPImean. The results clearly show that the real part of the refractive index increases, while the imaginary part (calculated from EC and HULIS) decreases with increasing particle size in the range of 0.1 – 1 μm. The data of both the real and imaginary parts in different ELPI campaigns are in good agreement with each other, indicating that seasonal variation is not important. The only exception is the ELPI5 data (referring to fall), when the carbon concentration – consequently, the imaginary part of the refractive index – is higher, probably due to biomass burning in this region. This assumption is confirmed by the aerosol composition (see data in *Table 2*). In ELPI5 samples the concentrations of carbonaceous compounds were the highest and the size distribution of TC was also different compared to the other sampling periods. According to ELPImean data set, the real part of the refractive index changes from 1.499 to 1.527, while in the case of the imaginary part, its value falls from 0.025 to 0.008, and has a local minimum around particle diameter of 1 μm.

On the other hand, the complex refractive index calculated from Berner samples has different size distribution. The real part of the refractive index does not vary as much as the ELPI data, and has a local maximum around 0.2 μm. The values above this size in the fine range are similar to all real refractive indices obtained form the ELPI samples. The imaginary refractive indices of the two different impactors are comparable; however, the values obtained from Berner samples are generally higher than the ELPI data. This discrepancy can be attributed to the different sampling periods of ELPI and Berner samples, different cut-off diameters and size resolution of the impactors (there are 4 and 7 data points in the fine size range in case of Berner impactor and ELPI, respectively), and to the large difference between the sample numbers (76 and 16 for ELPI and Berner impactors, respectively). Despite these facts, Berner samples are included into this work, because the refractive index in the coarse size range is only presented on the basis of these samples (as well as the effect of hygroscopicity, see later). The data in *Figs. 1a* and *1b* show that in the coarse mode, the real refractive index increases with the particles size; the imaginary part starts to increase after the local minimum around 1 μm.

Our results are compared to the refractive indices published by various authors in *Figs. 2a* and *2b*. Considering the value of the real refractive index (*Fig. 2a*), as well as its increasing tendency in the fine size range, our results are in good agreement with that of different authors, especially with the data presented by *Pesava et al.* (2001). Similar to our work, these authors applied the volume mixing rule for the estimation of the refractive indices of atmospheric aerosol from Vienna. The real part ranged between 1.455 and 1.495, with a peak in the 0.33 – 0.55 μm size interval. This difference can be attributed to the different sampling (urban – regional) environments and different analytical methods applied. Pesava and his co-workers made the chemical analysis by PIXE method. By means of this analysis nitrogen and carbon elements cannot be measured. For this reason, in their refractive index calculation the concentrations of carbonaceous compounds, ammonium, and nitrate ions are estimated. *Hand et al.* (2002) reported similar refractive index to our data, although they calculated and measured it by different methods. Data published by *Guyon et al.* (2005) represent the lowest refractive index, referring to Amazonian rural air. The authors compared the refractive indices derived from different approaches, and concluded that the real part of the refractive index obtained from an iteration procedure and from applying the volume mixing rule agreed well; the difference among them was ± 0.02. The highest refractive index were published by *Ebert et al.* (2004), who determined the size resolved complex refractive index for rural aerosol (Kleiner Feldberg, Germany) from individual particle analysis based on high-resolution scanning electron microscopy and energy-dispersive X-ray microanalysis. The values published by *Rault* and *Chazette* (2007), which were retrieved from a synergy between lidar, sunphotometer, and ground based in situ measurements in Paris, are also higher than our data. The difference in the applied methods may lead to the difference in values of the refractive indices. However, from the data presented in *Fig. 2* it is obvious that the smallest (*Guyon et al.*, 2005) and the largest (*Ebert et al.*, 2004; *Rault* and *Chazette*, 2007) refractive indices differ from our data within – 4 to + 5%, on average.

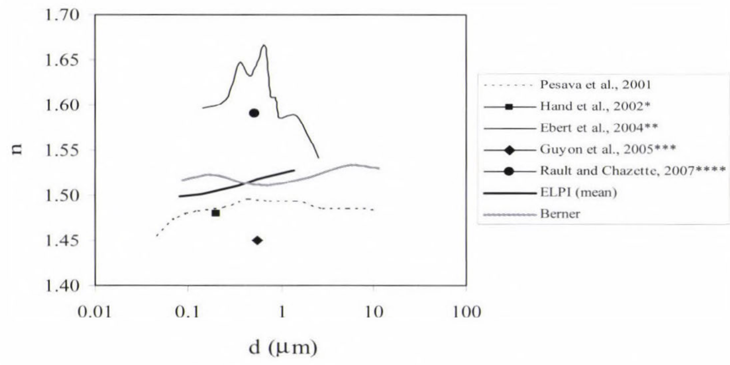

Fig. 2a. Variation of the real part of the refractive index published by different authors. Marking: *mean value; **mean value for rural air masses; ***mean value for background results obtained by applying volume mixing rule, ****$\lambda = 532$ nm.

Fig. 2b shows the variation in the imaginary refractive index published by different authors. In accordance with our results, *Horvath* (1995) found that the imaginary part shows a considerable decrease with increasing particle diameter. However, in the fine size range, *Horvath* (1995), *Pesava et al.* (2001), *Ebert et al.* (2004), *Raut* and *Chazette* (2007) reported higher imaginary refractive indices than the values presented in this work. This is probably due to the significantly different sampling sites. The results of authors referenced correspond to urban and urban influenced regional air affected by important anthropogenic sources (industrial and traffic), while our sampling site, K-puszta, represents regional background air. The imaginary refractive index published by *Guyon et al.* (2005) for Amazonian background air is also higher than values we found; however, these authors noted that their values might be overestimated.

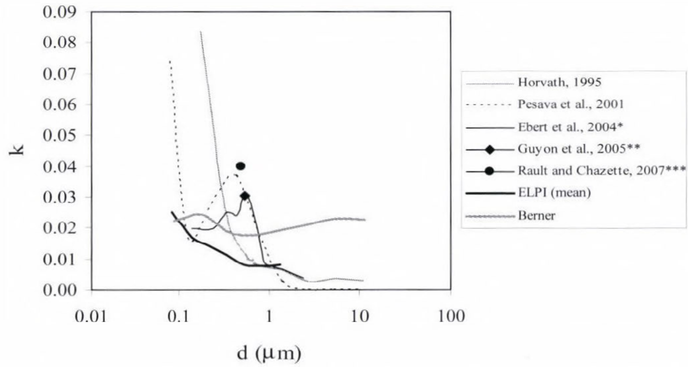

Fig. 2b. Variation of the imaginary part of the refractive index published by different authors. Marking: *mean value for rural air masses; **mean value for background results obtained by applying volume mixing rule, ***$\lambda = 532$ nm.

4.2. Importance of the size resolved refractive index

The importance of using a size resolved refractive index instead of a constant value can be evaluated if the scattering and absorption (extinction) coefficients are calculated by both approaches. In a case study we calculated the optical parameters (at 550 nm) in both ways, by applying the Mie-theory. In the calculations, the ELPI2 data set is used, and the results are tabulated in *Table 4*. In the first columns, the scattering, the absorption (the extinction) coefficients and the single scattering albedos are given which are calculated by means of the averaged (constant) complex refractive index and the mean number size distribution of ELPI2 data. Next, the same parameters are shown determined by considering the size distribution of the complex refractive index.

The results in both cases indicate that particles in the range of 0.273–1.05 μm (this interval is characterized by 0.34–0.84 μm geometric mean cut-off diameters) give the majority of the scattering and extinction coefficients. On the other hand, the contribution of smaller particles (in the 0.061–0.273 μm range) to the absorption coefficient is also important due to the relatively high TC concentration in this size interval. As a result, the difference between the absorption coefficients calculated by the two approaches is rather high. In the whole size range, the absorption coefficient resulting from constant refractive index overestimates the value calculated with a varying refractive index by 37%. In addition, the difference varies significantly with the particle size (see the last columns in *Table 4*). On the other hand, in this case study the difference between the scattering coefficients is not as high compared to the absorption coefficients; the overall difference is 4%, ranging from –3% to 17%. For the whole size range, the extinction coefficients determined by both approaches give similar values, which is the result of overestimation of the absorption and underestimation of the scattering coefficients. The overall difference is 1%, varying in the range of –2% and 65%. These numbers indicate that the deviation between extinction coefficients with a constant and a size resolved refractive index depends strongly on the particle size. Thus, we can conclude that the application of a constant refractive index instead of size resolved refractive index in Mie-calculations may enhance the uncertainty of the estimation of scattering and absorption (extinction) coefficients.

Table 4. Aerosol extinction coefficient (σ) and single scattering albedo (ω) calculated by applying size resolved and constant (1.510 – 0.01311i) refractive indices. Average of the size selected complex refractive index of ELPI2 data

Mean geometric diameter (μm)	**0.08**	**0.14**	**0.22**	**0.34**	**0.53**	**0.84**	**1.34**	**Σ**
Number concentration (cm^{-3})	**1460**	**983**	**524**	**228**	**118**	**15**	**2**	**3330**
				Constant refractive index				
σ_{ext} (Mm^{-1})	0.2	1.9	10.4	36.1	90.1	30.9	5.4	174.9
σ_{scat} (Mm^{-1})	0.1	1.5	9.4	33.7	85.4	28.3	4.2	162.6
σ_{abs} (Mm^{-1})	0.1	0.4	1.1	2.3	4.7	2.5	1.2	12.3
ω	0.46	0.78	0.9	0.94	0.95	0.92	0.78	0.93
				Size resolved refractive index				
σ_{ext} (Mm^{-1})	0.3	1.9	10.2	36.3	91.9	31.0	5.7	177.2
σ_{scat} (Mm^{-1})	0.1	1.4	9.2	34.5	89.5	29.7	4.9	169.4
σ_{abs} (Mm^{-1})	0.2	0.5	0.9	1.7	2.4	1.3	0.8	7.8
ω	0.27	0.74	0.91	0.95	0.97	0.96	0.86	0.96
				(Constant - Size resolved)/Constant				
$\Delta\sigma_{ext}$ (%)	65	2	-2	1	2	0	6	1
$\Delta\sigma_{scat}$ (%)	-3	-3	-1	2	5	5	17	4
$\Delta\sigma_{abs}$ (%)	123	18	-13	-26	-50	-49	-33	-37
Δω (%)	41	5	-1	-2	-3	-4	-10	-3

Finally, the effect on the single scattering albedo is evaluated. Single scattering albedo is one of the key parameters which determine the sign of the change in planetary albedo due to the aerosol layer, resulting in negative (cooling) or positive (heating) forcing of the Earth - atmosphere system. The boundary between the heating and cooling effect can be characterized by the critical single scattering albedo (at which the change in planetary albedo is zero). Besides, critical single scattering albedo depends strongly on the local albedo of the underlying surface. The more reflective the surface compared to the aerosol, the higher the critical value. If the single scattering albedo of the aerosol layer is higher than the critical value, the change of the planetary albedo is positive resulting in cooling effect, and *vice versa* (*Seinfeld* and *Pandis*, 1998; *IPCC*, 2007; *Seinfeld*, 2008; *Ramanathan et al.*, 2007; *Stier et al.*, 2007; *Randles et al.*, 2004).

The regions, where the single scattering albedo is close to the critical value, are sensitive to changes in the single scattering albedo. Small increase or decrease in this parameter (few %) can lead to change in the sign of the aerosol radiative forcing. Our results (last columns in *Table 4*) make it clear that the consideration of the size dependence of the complex refractive index instead of constant values may yield important variations in the single scattering albedo, which even can lead to change in the sign of radiative forcing of the Earth-atmosphere system. For this reason, mainly over the sensitive regions, the implication of the size distribution of the complex refractive index can decrease the uncertainty of the estimation of the aerosol direct radiative forcing.

4.3. Effect of hygroscopic mass growth on the refractive index

Increasing relative humidity results in water uptake by the aerosol particles. The water uptake of the particles changes their size as well as the chemical composition of the aerosol. Even, above the deliquescence relative humidity, water can be the most abundant compound in hygroscopic particles (e.g., *Randles et al.*, 2004). Taking into account the amount of the absorbed water measured (see paragraph 2.1), the complex refractive index of the wet aerosol was recalculated ($m_{water} = 1.33 - 0i$) by using the volume mixing rule. In *Fig. 3a*, the effect of hygroscopic mass growth on the real refractive index is plotted. One can see that the water uptake decreases the refractive index of the particles compared to the dry aerosol. Moreover, with increasing relative humidity, the size distribution of the refractive index changes, which is also shown in *Fig 3a*. Local minimum and maxima of the ‘dry’ curve become more significant with increasing relative humidity, due to the various hygroscopic mass growths in different size ranges caused by differences in the chemical composition. These results are in agreement with the data by *Iinuma et al.* (2000) who studied the effect of aerosol hygroscopicity in the air over Australian cities. At 80% RH, they reported –1% to –5% decreases in the real part in Canberra, while our results show a reduction between –3 and – 6%, probably due to the difference in the hygroscopic properties of the aerosol. We also have to note that water uptake decreases the imaginary part of the refractive index as shown in *Fig. 3b*, in accordance with the data of *Iinuma et al.* (2000). This decrease is obviously caused by the mass increase of the particles, as water is not light absorbing in the visible radiation range.

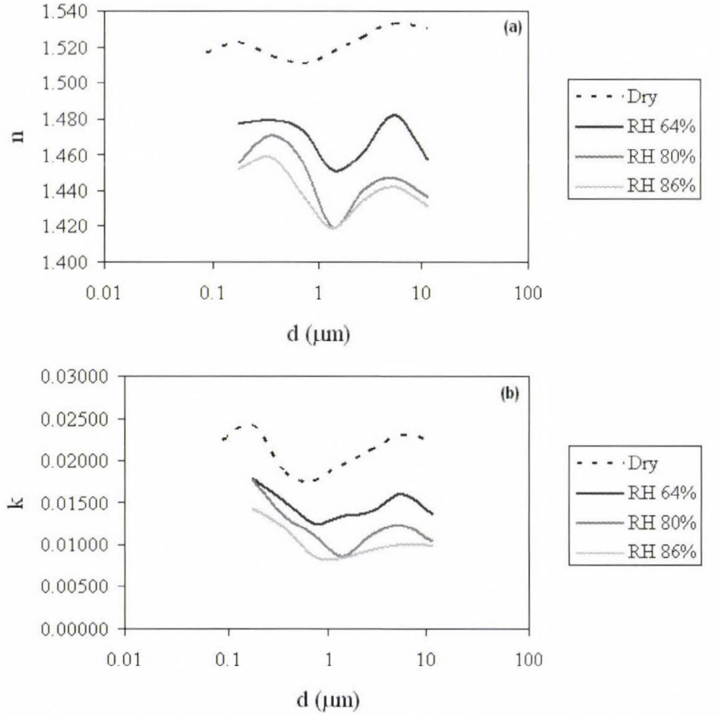

Fig. 3. The effect of hygroscopic mass growth on the real (a) and imaginary (b) refractive indices.

5. Summary and conclusions

The size dependent complex refractive index of dry ambient aerosol is estimated on the basis of the mass closure of the aerosol, as well as on the refractive indices and densities of different aerosol constituents. In the calculation, the approach of the volume mixing rule was applied. Calculations made by the Mie-theory indicate that the extinction coefficient and the single scattering albedo are different if the size resolved refractive index is used instead of a size-independent constant value. The study carried out also show that hygroscopic mass growth of the particles influence the refractive index. The main results obtained can be summarized as follows.

(i) In agreement with results published by different authors, in the optically active size range (0.1–1 μm) the real part of the refractive index of dry aerosol increases with particle size, while, at the same time, a significant decrease can be found in the imaginary refractive index. This latter parameter has a local minimum around particle diameter of 1 μm. Its size distribution is in close connection with the size dependent variation of EC concentrations.

(ii) No significant seasonal variation was found in the real or imaginary parts of the aerosol refractive index. However, during the fall, the imaginary part was found to be somewhat higher than in other seasons, probably due to some biomass burning in the region.

(iii) The absorption coefficient, calculated by applying a constant refractive index, overestimates the value calculated with changing refractive index by 37%. Further, an overall underestimation of 4% occurs in the case of the scattering coefficient, ranging from –3% to 17%. As the result of the overestimation of the absorption coefficient and underestimation of the scattering coefficient, the overall difference between the extinction coefficients is 1%, varying in the range of –2% and 65%. These numbers indicate that the deviation between extinction coefficients with a constant and a size resolved refractive index varies strongly with the particle size. We concluded that the application of a constant refractive index instead of size resolved values may enhance the uncertainty of the estimation of scattering and absorption coefficients.

(iv) It follows from our results that the consideration of the size dependence of the complex refractive index instead of constant values may yield changes (some %) in the single scattering albedo. Even this can lead to change in the sign of radiative forcing of the Earth-atmosphere system, mainly over sensitive regions, where the single scattering albedo is close to the critical value.

(v) Finally, our results show that water uptake by particles decreases the real part of their refractive index (by 5% at 86% relative humidity compared to the dry aerosol). Water uptake also decreases the imaginary part of the refractive index, which is obviously caused by the aerosol mass increase.

It goes without saying that our results on the size variation of dry complex refractive index should be confirmed by further similar studies. Moreover, more research is needed to clarify the effect of the hygroscopicity of aerosol particles on the refractive index.

Acknowledgements—The authors are indebted to the Hungarian Science Foundation (OTKA) for the financial support of this work (project numbers: T 047222 and TS 049845). The authors are grateful for the beneficial help from *Ernő Mészáros*.

References

Balkanski, Y., Schulz, M., Claquin, T., and *Guibert, S.*, 2007: Reevaluation of Mineral aerosol radiative forcings suggests a better agreement with satellite and AERONET data. *Atmos. Chem. Phys. 7,* 81–95.

Cabada, J.C., Rees, S., Takahama, S., Khlystov, A., Pandis, S.N., Davidson, C.I., Robinson, A.L., 2004: Mass size distributions and size resolved chemical composition offine particulate matter at the Pittsburgh supersite. *Atmos.Environ. 38,* 3127–3141.

Ebert, M., Weinbruch, S., Rausch, A., Gorzawski, G., Hoffmann, P., Wex, H., Helas, G., 2002: Complex refractive index of aerosols during LACE 98 as derived from the analysis of individual particles. *J. Geophys. Res. 107,* No. D21, 8121, doi:10.1029/2000JD000195.

Ebert, M., Weinbruch, S., Hoffmann, P., Ortner, H.M., 2004: The chemical composition and complex refractive index of rural and urban influenced aerosols determined by individual particle analysis. *Atmos. Environ. 38,* 6531-6545.

ELPI (Electric Low Pressure Impactor) *User Manual,* 2003, Dekati Ltd.

Feczkó, T., Mészáros, E., and *Molnár, A.,* 2004: Radiative forcing tendency due to anthropogenic aerosol particles and greenhouse gases in Hungary. *Időjárás 108,* 1-10.

Guyon, P., Boucher, O., Graham, B., Beck, J., Mayol-Bracero, O.L., Roberts, G.C., Maenhaut W., Artaxo, P., Andreae, M.O., 2005: Refractive index of aerosol particles over the Amazon tropical forest during LBA-EUSTACH 1999. *J. Aerosol Sci. 34,* 883-907.

Gysel, M., Weingartner, E., Nyeki, S., Paulsen, D., Baltensperger, U., Galambos, I., Kiss, G., 2004: Hygroscopic properties of water-soluble matter and humic-like organics in atmospheric fine aerosol. *Atmos. Chem. Phys. 4,* 35-50.

Hand, J.L., Kreidenweis, S.M., Kreisberg, N., Hering, S., Stolzenburg, M., Dick, W., McMurry, P.H., 2002: Comparison of aerosol properties measured by impactors and light scattering from individual particles: refractive index, number and volume concentrations, and size distributions. *Atmos. Environ. 36,* 1853-1861.

Hatzianastassiou, N., Matsoukas, C., Drakakis, E., Stackhouse Jr., P.W., Koepke, P., Fotiadi, A., Pavlakis, K.G., and *Vardavas, I.,* 2007: The direct effect of aerosols on solar radiation based on satellite observations, reanalysis datasets, and spectral aerosol optical properties from Global Aerosol Data Set (GADS). *Atmos. Chem. Phys. 7,* 2585–2599.

Hitzenberger, R., Ctyroky, P., Berner, A., Turšič, J., Podkrajšek, B., Grgić, I., 2006: Size distribution of black (BC) and total carbon (TC) in Vienna and Ljubljana. *Chemosphere 65,* 2106–2113.

Hoffer, A., Gelencsér, A., Guyon, P., Kiss, G., Schmid, O., Frank, G., Artaxo, P., Andreae, M.O., 2005: Optical properties of humic-like substances (HULIS) in biomass-burning aerosols. *Atmos. Chem. Phys. Discussions 5,* 7341-7360.

Horvath, H., 1995: *Size segregated light absorption coefficient of the atmospheric aerosol. Atmos. Environ. 29,* 875-883.

Horvath, H., 1998: Influence of atmospheric aerosols upon the global radiation balance. In *Atmospheric Particles IUPAC Series on Analytical and Physical Chemistry of Environmental Systems.* John Wiley, New York, Vol. 5, 543-596.

Iinuma, Y., Box, G.P., Gras, J.L., Keywood, M., & Ayers, G., 2000: Comparison of predicted and measured aerosol optical and physical properties in Australian cities. *Proc. 15th International Clean Air Conference.* Sydney, 2000. Clean Air Society of Australia & New Zealand, Mitcham, Vic., Australia, 227-231.

Imre, K. and *Molnár, A.,* 2008: Hygroscopic behaviour of Central European atmospheric background aerosol particles in summer. *Időjárás 112,* 63-82.

IPCC, 2007. *Forster, P., V. Ramaswamy, P. Artaxo, T. Berntsen, R. Betts, D.W. Fahey, J. Haywood, J. Lean, D.C. Lowe, G. Myhre, J. Nganga, R. Prinn, G. Raga, M. Schulz* and *R. Van Dorland,* 2007: *Changes in Atmospheric Constituents and in Radiative Forcing.* In *Climate Change 2007: The Physical Science Basis.* Contribution of Working Group I to the Fourth Assessment Report of the Intergovernmental Panel on Climate Change [*Solomon, S., D. Qin, M. Manning, Z. Chen,* *M. Marquis, K.B. Averyt, M. Tignor* and *H.L. Miller* (eds.)]. Cambridge University Press, Cambridge, United Kingdom and New York, NY, USA.

Jaffrezo, J.-L., Aymoz, G., and *Cozic, J.*, 2005: Size distribution of EC and OC in the aerosol of Alpine valleys during summer and winter. *Atmos. Chem. Phys. 5,* 2915–2925.

Kaufman, Y.J., Tanré, D., Boucher, O., 2002: A satellite view of aerosols in the climate system. *Nature 419,* 215-223.

Kiss, Gy., Varga, B., Galambos, I., Ganszky, I., 2002: Characterization of water soluble organic matter isolated from atmospheric fine aerosol. *J. Geophys. Res. 107,* No. D21, 8339, doi:10.1029/2001JD000603.

Mészáros, E., Barcza, T., Gelencsér, A., Hlavay, J., Kiss, Gy., Krivácsy, Z., Molnár, A., Polyák, K., 1997: Size distributions of inorganic and organic species in the atmospheric aerosol in Hungary. *J. Aerosol Sci. 28,* 1163-1175.

Miguel, A.H., Eiguren-Fernandez, A., Jaques, P.A., John R. Froines, J.R., Grant, B.L., Mayo, P.R., Sioutas, C., 2004: Seasonal variation of the particle size distribution of polycyclic aromatic hydrocarbons and of major aerosol species in Claremont, California. *Atmos. Environ. 38*, 3241–3251.

Molnár, A., Mészáros, E., Hansson, H.C., Karlsson, H., Gelencsér, A., Kiss, Gy., Krivácsy, Z., 1999: The importance of organic and elemental carbon int he fine atmospheric aerosol particles. *Atmos. Environ. 33,* 2745-2750.

Pesava, P., Horvath, H., Kasahara, M., 2001: A local optical closure experiment in Vienna. *J. Aerosol Sci. 32,* 1249-1267.

Ramanathan, V., Li, F., Ramana, M.V., Praveen, P.S., Kim, D., Corrigan, C.E., Nguyen, H., Stone, E. A., Schauer, J.J., Carmichael, G.R., Adhikary, B., Yoon, S.C., 2007: Atmospheric brown clouds: Hemispherical and regional variations in long-range transport, absorption, and radiative forcing. *J. Geophys. Res. 112,* D22S21, doi:10.1029/2006JD008124.

Randles, C.A., Russell, L.M., Ramaswamy, V., 2004: Hygroscopic and optical properties of organic sea salt aerosol and consequences for climate forcing. *Geophys. Res. Lett. 31,* L16108, doi:10.1029/2004GL020628.

Raut, J.C. and *Chazette, P.*, 2007: Retrieval of aerosol complex refractive index from a synergy between lidar, sunphotometer and in situ measurements during LISAIR experiment. *Atmos. Chem. Phys. 7,* 2797-2815.

Saarikoski, S., Mäkelä, T., Hillamo, R., Aalto, P.P., Kerminen, V.-M., Kulmala, M., 2005: Physico-chemical characterization and mass closure of size segregated atmospheric aerosols in Hyytiälä, Finland. *Boreal Environ. Res. 10,* 385–400.

Seinfeld, J.H. and *Pandis, S.N.*, 1998: *Atmospheric Chemistry and Physics.* John Wiley & Sons.

Seinfeld, J., 2008: Atmospheric science: Black carbon and brown clouds. *Nature Geoscience 1,* 15-16, doi:10.1038/ngeo.2007.62.

Stelson, A.W., 1990: Urban aerosol refractive index prediction by partial molar refraction approach. *Environ. Sci. Technol. 24,* 1676-1679.

Stier, P., Seinfeld, J.H., Kinne, S., and *Boucher, O.*, 2007: Aerosol absorption and radiative forcing. *Atmos. Chem. Phys. 7,* 5237–5261.

Temesi, D., Molnár, A., Mészáros, E., Feczkó, T., Gelencsér, A., Kiss, G., Krivácsy, Z., 2001: Size resolved chemical mass balance of aerosol particles over rural Hungary. *Atmos. Environ. 35,* 4347-4355.

Turpin, B.J., Hutzincker, J.J., 1995: Identification of secondary organic aerosol episodes and quantization of primary and secondary organic aerosol concentrations during SCAQS. *Atmos. Environ. 29,* 3527–3544.

Turpin, B.J., Lim, H.J., 2001: Species contributions to PM2.5 mass concentrations: Revisiting common assumptions for estimating organic mass. *Aerosol Sci. Technol. 35,* 602-610.

Weast, R.C., 1987: Physical constants of organic compounds. *CRC Handbook of Chemistry and Physics*, 68th Edition (ed.: *R.C. Weast*). CRC Press, Boca Raton, FL, B67-B146.

IDŐJÁRÁS
Quarterly Journal of the Hungarian Meteorological Service
Vol. 113, No. 3, July–September 2009, pp. 177–187

Determination of ambient air pollution: Tasks, methods, approaches

Krisztina Labancz[1*] and **István Matyasovszky**[2]

[1]*Hungarian Meteorological Service, P.O. Box 39, H-1675 Budapest, Hungary; E-mail: labancz.k@met.hu*

[2]*Department of Meteorology, Eötvös Loránd University, P.O. Box 32, H-1518 Budapest, Hungary; E-mail: matya@ludens.elte.hu*

(Manuscript received in final form June 20, 2009)

Abstract—Estimation of the level of ambient air pollution is a complicated task, which includes concentration measurements, modeling of dispersion and transport of air pollutants, and estimation of possible effects of a large number of different local sources. In this paper, a detailed description of the European ambient air quality legislation is presented indicating the tools for air quality control (monitoring, modeling, other methods) which should be applied by the member states. Hungarian regulation and the corresponding measurement and modeling activities are also described. Finally, a newly developed statistical method is presented, which can be a useful tool in planning an aimed measurement campaign to estimate the local ambient air quality around a new source. By the aid of this method the necessary time length and the best starting date of the measurement campaign can be estimated.

Key-words: ambient air quality, EU directives, legislation, assessment techniques, statistical model

1. Introduction

Ambient air quality is still a major problem in Europe, where long term exposure to air pollutants can cause damages to ecosystems, human health, and materials. Because of the health risks, the EU 2008 directive (*EU*, 2008) recommends member states to ensure that information about the level of ambient air pollution obtained by either measurements or other methods (e.g., modeling or objective estimation) are provided to the public. In order to follow these guidelines, a system of monitoring networks, air pollution transport and dispersion modeling activities, and studies of suitable objective estimation methods has to be set up.

* Corresponding author

In this paper, a description of the European ambient air quality legislation is presented indicating the tools for air quality control (monitoring, modeling, and other methods) which should be applied by the member states.

As the continental regional background air pollution is suitably calculated by long-range transport models run at the Europeans scientific centers, this paper focuses on the effect of the local sources on local scales. In urban areas, the total description of local ambient air quality by measurements requires many monitoring stations. Moreover, many suitable models exist for the calculation of air pollution dispersion and for chemical reactions, and the system of monitoring stations, modeling tools and available meteorological parameters provides relevant urban background air quality estimations (*Berkovicz et al.,* 1994). However, improved understanding of spatiotemporal variability in ambient air pollutant concentrations in urban areas is useful in many contexts and needs additional, mainly statistical estimation tools (*Morel et al.*, 1998; *Marshall et al.*, 2007; *Singh et al.*, 2009).

Statistical estimation methods play an important role in calculating air pollution around industrial site. Air quality around point sources and possible exceedances of short term limit values are not possible to determine without a large number of monitoring stations. The best way is to combine measurements and statistical estimation methods (*Rumburg et al.*, 2000; *McMillan et al.*, 2004). This paper presents a new statistical method for calculating the necessary time length of a measurement campaign to be carried out to estimate the local ambient air concentrations around a source.

2. Legislation

2.1. Regulation in the European Union

There are a number of EU laws that regulate air pollution. The Air Quality Framework Directive (*EU*, 1996) and its four daughter directives describe the basic principles as to how air quality should be assessed and managed, and list the pollutants for which air quality standards and objectives will be developed and specified in legislation. Other laws (the National Emission Ceilings Directive, sectoral emission laws) set national emission ceilings which must be achieved by 2010 through EU wide and national measures. Also, EU member states systematically exchange information on most effective abatement measures and coordinate their efforts in tackling transboundary air pollution.

The Air Quality Framework Directive sets concentration limit values or target values for a range of air pollutants. It defines minimum requirements for air quality assessments – through monitoring and modeling – that provide a good indication of air quality concentrations throughout the member states' territory. Where thresholds are exceeded, member states are expected to act.

Daughter directives complete the list of pollutants in details. For example, the First Daughter Directive (*EU*, 1999) sets the limit values for SO_2, NO_2 and NO_x, PM, and Pb in ambient air. The directive lists the limit values set in the member states' own legislation like the joint decree of the Minister of Environment and Water and the Minister of Health on the Hungarian limit values (*HU*, 2001a).

When the limit values are set, the ambient air quality shall be assessed in each member state. The directive sets the tools for air quality control which should be applied. Measurement is mandatory in zones with a population of more than 250,000 inhabitants, with high population concentration (agglomerations), and where the concentrations are near to or exceed the limit value. In zones with lower concentrations, member states can apply additional tools for quality control and the assessment of exceedances in addition to measurement data, e.g., air quality models and statistical methods. Based on the number of inhabitants and the limit value exceedances, the directive sets two limit values: a higher assessment level (tolerance limit), X, and a lower assessment level (acceptable limit), *Y*. The value of *X* and *Y* were determined by an expert group of the European Commission. *Table 1* shows the summary of recommended assessment techniques.

Table 1. Summary of requirements for measurements and other assessment methods

Type of zone	**Assessment technique**
Agglomeration, >250,000 inhabitants	Monitoring is mandatory even if levels are <X% of limit value
Zones with levels >*X* % of limit value	Monitoring is mandatory
Zones with levels <*X* % but >*Y*% of limit value	A combination of measurements and modeling may be used
Zones with levels <*Y* % of limit value	Modeling or objective estimation is sufficient

Determination of *X* and *Y* is based on the inter-annual variations and normalized standard deviation of data at monitoring stations. For NO_2 it is estimated, that there is a slight variation between stations, but the standard deviation is generally consistent for NO_2 throughout the European Union. The recommended values for *X* are 80% of the annual limit value and 60% of the hourly limit value, while for *Y* the values are 75% of the annual and 50% of the hourly limit values.

2.2. Measurements and modeling in Hungary

In Europe, there is a scientifically based and policy driven program, the EMEP (Co-operative Programme for Monitoring and Evaluation of the Long-range Transmission of Air Pollutants in Europe), which has a monitoring network for continuously measuring the regional background air pollution level. In Hungary, there is a background air pollution monitoring network of four stations, where air and precipitation samples and monitored values of about 20 elements are collected. The samples are analyzed in the laboratory of the Hungarian Meteorological Service. The urban ambient air pollution is monitored by an other network, the National Urban Air Quality Network carried out by the local environmental protection agencies. The network consists of 52 automatic stations measuring concentrations of 12 pollutants and 5 meteorological parameters. In addition to the monitoring of background values, there are aimed scientific measurements, as well as the Hungarian legislation ordains measurement campaigns in case of building a new source of air pollutants (an industrial unit, factory, or stack). In case of an aimed campaign, two important practical points are emerged: one is to determine the range area where the pollution emitted by the source has measurable effect on the surroundings and mark the places of sampling inside the range, and the other is to determine the optimal length of the measurement campaign.

Measurements are accurate and continuous in time, but point-wise in space, therefore, they operability is limited in space. The directives stimulate the use of models, which are less accurate but have better opportunities for spatial coverage. Depending on the size of the modeled area, there are different air pollution transport and dispersion models with global, regional, and local scales. The long-range transport of emitted air pollutants are modeled in the main European centers, like the EMEP, to regularly provide governments with qualified scientific information to support the development and further evaluation of the international protocols on emission reductions. On urban and local scales, every member states has its own air quality models. The Hungarian Meteorological Service runs models both on urban and local scales.

2.3. Regulation in Hungary

In Hungary, a governmental regulation (*HU*, 2001b) defines the ambient level of air pollution as "the average air pollution caused by other sources in given distance and time length around a given source". To calculate the effect of a new source, the concentration of air pollutants caused by the emission of the new source should be added to the above defined ambient level. The ambient air pollution consists of two components: one is the regional background concentration of pollutants calculated by global or regional long-range transport models; the other is the so-called supplementary pollution, the local effect of pollution sources in the vicinity of the examined source.

The total pollution in the surroundings of a given source is calculated by the sum of the ambient air pollution and the so-called excess pollution, which is also defined by the above mentioned regulation. By definition it is "the pollution near the given source caused by the emission of the source itself, the emission of the increased traffic, and the effect of the possibly modified air flow around the source".

3. *Tasks*

As a result of the above described regulations, estimating the level of ambient air pollution is a different kind of task than calculating the effect of a given source or modeling the transport of air pollutants. The task is to estimate the level of the permanently existing ambient concentrations which is made up of the emissions of local point-, line-, area-, or mobile sources, regional concentration levels, and long-range transport. Finally, the effect of a given source may be added to the estimated or calculated ambient level. Therefore, three types of the tasks can be formed:

- Evaluation of urban air quality on the base of the data measured by the urban monitoring network; analysis of characteristic weather situations.
- Urban air quality forecast calculated by an urban dispersion model using numerical weather prediction outputs and emission data.
- Calculating/estimating the effects of new local sources.

Let us take a close look at the third task! There is a village or smaller town, where no measurements were carried out in the past. A new industrial unit, factory or stack with significant pollution is planned to be built here. A study should be made on evaluation the effects of the new source and estimating the new air pollution level, which cause damage to the ecosystem and the human health in the town and its vicinity. The study should estimate if the sum of the original ambient air pollution and the effect of the new source would exceed the official limit values. The task has two parts: one is to estimate the original local ambient air pollution, the other is to calculate the effect of the new source. The later objective can be solved by the aid of a local scale dispersion model developed for regulatory purposes.

Based on the above described official definitions, the ambient level of air pollutants is composed of the regional background pollution and the effect of the local sources. Yearly average concentration values calculated for grid points over Hungary by the global or regional long-range transport models of European centers (like EMEP) are taken as regional background values. The real challenge of the task is to estimate the air pollution level caused by the local sources, as the emission of the sources, moreover, the local sources themselves are not known in most cases. The most one can do is relying on estimations. There are two ways of estimating the effect of local sources:

- The background concentrations of air pollutants calculated and reported yearly by the EMEP center is accepted as local ambient air pollution level. This choice is reasonable as the EMEP model uses the official emission data reported yearly by the member states, therefore, the local sources are taken into account indirectly. Moreover, long-range transport models give good spatial coverage of transboundary air pollution. The problem of this choice is that it does not give acceptable estimation for the possible limit value exceedances caused by the joint effect of the original and new local sources.

- The local air pollution level is estimated by an aimed measurement campaign. If the volume of the investment is big enough, the builder must carry on a measurement campaign at the place of the new source. Statistical methods can be useful tools in optimizing the time length and the starting date of the compulsory measurements, making it cost-effective and suitable.

4. *Statistical modeling*

To calculate the effect of a new pollutant source on its surroundings, the degree of the existing background pollution has to be estimated. There are two practical problems which make the estimation difficult: one is that often there are no measurements previously performed at the area nearby the new source, the other is that the time disposable for performing necessary measurements is highly restricted, no more than a few months. Therefore, the length of measuring period should be optimized. 14-year long time series of three pollutants were used for estimating the optimal length of measurements, assuming that the series of the two tasks have similar statistical features.

4.1. Data

A suitable dataset to conduct the statistical modeling was obtained from the National Urban Air Quality Monitoring Network carried out by the local environmental protection agencies. This ambient air monitoring program continuously observes the hourly and daily means of concentrations of 12 pollutants and 5 meteorological parameters. Data of 8 monitoring stations located in downtown and suburban areas of Budapest were available for the period of 1991–2005. In 2003, the structure of monitored data was changed to a certain extent: some stations were transferred, a new station started to work, and new elements (e.g., aromatic hydrocarbons) were taken into the monitoring program.

Time series of hourly NO_2, SO_2, and CO concentrations were chosen for the period of 1992–2005 measured at a downtown station (Baross Square, see *Fig. 1*). Time series observed at this station are the longest, most complete series. Unfortunately, the place of the station was changed in the beginning of 2006 because of street reconstruction works. Concentration of NO_2 describes the degree of air pollution caused by traffic, while SO_2 and CO indicate the urban background pollution and the pollution of industrial origin. This study is based on daily mean values of the three pollutants derived from the hourly data.

Figures show the results calculated for SO_2 as this pollutant best indicates the background pollution. Calculations for NO_2 and CO gave similar results.

Fig. 1. Urban air pollution monitoring stations in Budapest.

To estimate the optimal length of a measuring campaign, two important concentration measures – daily mean and limit value exceedance – were examined. This study presents the results for the reliable estimation of daily mean background concentration.

4.2. Estimation of necessary time length of measurements – mean concentration method 1

The first question addressed is how many daily measurements (n) are needed to ensure that the mean of these daily mean measured values lies within a specified interval (h) of the expected value with a large probability ($1-\varepsilon$)? Supposing that the time series of measured data comes from a first order autoregressive process, the solution is

$$n = \frac{1+a}{1-a}(\hat{s}\, y_\varepsilon / h)^2, \qquad (1)$$

where $y_\varepsilon = 1.64$, 1.96, 2.58 at $\varepsilon = 0.1$, 0.05, 0.01, respectively, furthermore, a is the one day lag autocorrelation and $\hat{s}$ is the adjusted empirical standard deviation. These latter two parameters can be estimated from data, while h is chosen as a specific portion of the standard deviation. Eq. (1) is based on the classical one-sample t-test (*Dévényi* and *Gulyás*, 1988) but taking into account autocorrelations of data. *Fig. 2* shows necessary measurement lengths (n) for $(1-\varepsilon)100\% = 90, 95$, and 99%.

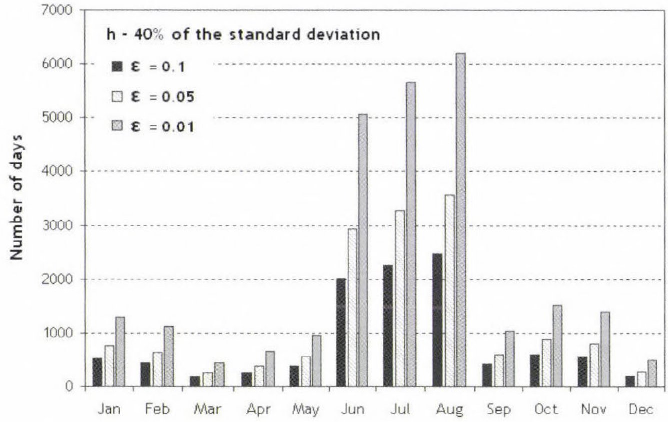

Fig. 2. Necessary measurement length in days for estimating daily average concentration of SO_2 using method 1.

Although quite high h values are chosen (20, 40, and 80% of the standard deviation), results obtained are not practically useful as the necessary measurement lengths are extremely large (from several hundred days to 6000 days when starting the measuring campaign in summer). Similar conclusions can be drawn for daily maximum concentrations, too.

The summer maximum is not surprising. Eq. (1) shows that the number of measurements n depends only on the autocorrelation a when h is chosen as a specific portion of the standard deviation. Since the main source of sulfur dioxide is the heating, the concentration of SO_2 in the air is steadily low in summer; therefore, the concentration series has high autocorrelation. On the other hand, in the heating season the volume of combustion is changing with the altering weather conditions, thus, the autocorrelation is low.

4.3. Estimation of necessary time length of measurements – mean concentration method 2

A much simpler and practically useful approach is to take the background concentration as the average concentration of a given particular year. The question is how long measuring period shorter than one year is necessary to form an average (within-year average) enough close to the annual average. The term "enough close" means that the null-hypothesis of having no systematic difference between the two averages is not rejected at a significance level $(1-\varepsilon)100\%$. The larger the value of ε the larger the certainty of having no systematic difference is. However, higher certainties require longer measuring periods. The answer depends on the starting date of measurements due to the annual course of pollutants concentrations. The test statistic z_i is used for the purpose as follows:

$$z_i = \frac{\overline{x}_i - \overline{x}_n}{\sqrt{\frac{1+a_i}{1-a_i} s_i^2 \frac{(n-i)^2}{in^2} + \frac{1+a_{n-i}}{1-a_{n-i}} s_{n-i}^2 \frac{n-1}{n^2}}}, \tag{2}$$

where $\overline{x}_i$ and $\overline{x}_n$ are the two means to be compared, n is the number of days of a year (n=365), a is the one day lag autocorrelation, and s is the standard deviation, while the subscripts refer to the number of days used to estimate the corresponding quantities. Eq. (2) is based on the Welsh test (*Dévényi* and *Gulyás*, 1988) considering autocorrelations of data. When i is not too small, the test statistic approximately follows the standard normal distribution under the null-hypothesis that the expectation of the difference between the annual and actual within-year average is zero (there is no systematic difference between averages). Significance levels chosen are 80, 90, and 95%. The analysis is performed again with data of Baross Square but using only the last two years.

Fig. 3 shows the minimum necessary measurement lengths for daily mean SO_2 concentrations. Months in the horizontal axis refer to the starting date of the measurements. Minimum necessary measurement lengths mean the shortest measuring period ensuring the acceptance of the null-hypothesis. The most appropriate start of the measurement campaign is in August (40 days) and July (85 days), or in February (120 days) in case of a winter starting. These measuring periods satisfy practical possibilities.

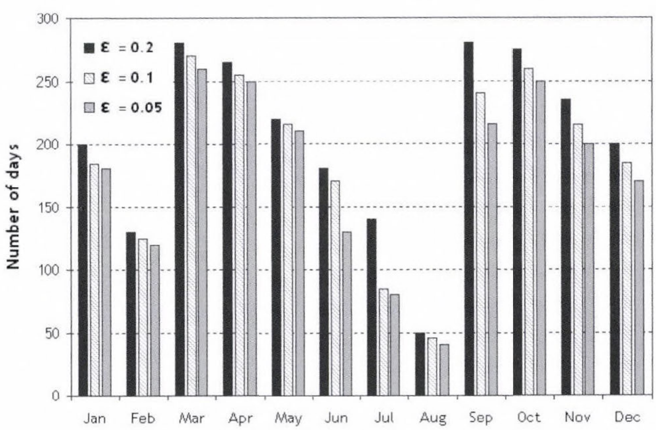

Fig. 3. Necessary measurement length in days for estimating daily average concentration of SO_2 using method 2.

Two local minimum appear in *Fig. 3,* at the end of winter and summer. Since the main source of sulfur dioxide is the heating, the measured concentrations of SO_2 are continuously above the mean value in winter; therefore, the mean concentration of the measuring period will approximate the yearly mean value after a relatively longer time period without heating. For estimating the yearly mean value, a good measuring period starts at the end of winter, when the volume of heating is quickly decreasing, thus the mean of measured values tends to the yearly mean value. Similarly, the measured concentrations are well below the mean value in summer, which again needs a longer averaging time period to tend to the yearly mean value. Hence, the beginning of autumn is the best period to reach the yearly mean by averaging values over a short period.

In addition to the average concentrations, the limit value exceedance should be examined in the prevailing measurement campaign. The builder of a new source should prove that the probability of limit value exceedance is very low. New statistical formulae developed for this purpose are being tested currently. The core of the method is to join typical meteorological conditions accompanied by possible limit value exceedances.

5. Conclusions and future plans

Description of the European ambient air quality legislation was presented in this study, indicating the tools for air quality control (monitoring, modeling, and other methods) which should be applied by the member states. Hungarian regulation and the corresponding measurement and modeling activities were also described. Measurements and modeling are the most important tools in the ambient air quality control, but other estimation methods are also recommended as assessment techniques in background areas and around industrial sources. A newly developed statistical method was presented in the paper which can be a useful tool in planning an aimed measurement campaign to estimate the local ambient air quality around a new source. By the aid of this method the necessary time length and the best starting date of the measurement campaign can be estimated on the base of daily mean concentration measurements carried out at another site. In the future, the method will be extended to limit value exceedances.

References

Berkowicz, R., Hertel, O., Sørensen, N.N., and *Michelsen, J.A.,*1994: Modelling air pollution from traffic in urban areas. In *Flow and Dispersion Through Obstacles* (eds.: *R.J. Perkins* and *S.E. Belcher*). Cambridge, UK, 28–30 March 1994, 121–142.

Dévényi, D. and *Gulyás, O.,* 1988: *Mathematical Statistics for Meteorologists* (in Hungarian). Tankönyvkiadó, Budapest, 443 pp.

Marshall, J.D., Nethery, E., and *Brauer, M.*, 2007: Within-urban variability in ambient air pollution: Comparison of estimation methods. *Atmos. Environ. 42,* 1359-1369.
McMillan, N., Bortnick, S.M., Irwin, M.E., and *Berliner, L.M.*, 2004: A hierarchical Bayesian model to estimate and forecast ozone through space and time. *Atmos. Environ. 39,* 1373-1383.
Morel, B., Yeh, S., and *Cifuentes, L.*, 1998: Statistical distributions for air pollution applied to the study of the particulate problem in Santiago. *Atmos. Environ. 33,* 2575-2585.
Rumburg, B., Alldredge, R., and *Claiborn, C.*, 2000: Statistical distributions of particulate matter and the error associated with sampling frequency. *Atmos. Environ. 35,* 2907-2920.
Singh, B., Carnevale, C., Pisoni, E., Volta, M., 2009: A comprehensive stochastic methodology to forecast ozone and PM10 in a metropolitan area. In *7th International Conference on Air Quality – Science and Application* (ed.: *R.R. Sokhi*). Istanbul, Turkey, 24 –27 March 2009 (in press).
EU, 1996: Council directive on ambient air quality assessment and management. Council Directive 1996/62/EC.
EU, 1999: Council directive relating to limit values for sulphur dioxide, nitrogen dioxide and oxides of nitrogen, particulate matter and lead in ambient air. Council Directive 1999/30/EC.
EU, 2008: Directive of the European Parliament and of the Council on ambient air quality and cleaner air for Europe. Council Directive 2008/50/EC, May 21.
HU, 2001a: Joint order of the Minister of Environment and Water and Minister of Health on air pollution limit values and limit values for emission of point sources (in Hungarian). 14/2001(V.9), KöM-EüM rend.
HU, 2001b: Decree of Government on some regulations on air quality protection (in Hungarian). 21/2001(II.14) Korm. rend.

IDŐJÁRÁS
Quarterly Journal of the Hungarian Meteorological Service
Vol. 113, No. 3, July–September 2009, pp. 189–202

Operator splitting in the Lagrangian air pollution transport model FLEXPART

Zsófia Kocsis[1*], **Zita Ferenczi**[1], **Ágnes Havasi**[2], and **István Faragó**[3]

[1]*Hungarian Meteorological Service, P.O. Box 38, H-1525 Budapest, Hungary; E-mails: kocsis.zs@met.hu; ferenczi.z@met.hu*

[2]*Department of Meteorology, Eötvös Loránd University, P.O. Box 32, H-1518 Budapest, Hungary; E-mail: hagi@nimbus.elte.hu*

[3]*Department of Applied Analysis and Computational Mathematics, Eötvös Loránd University, P.O. Box 32, H-1518 Budapest, Hungary; E-mail: faragois@cs.elte.hu*

(Manuscript received in final form February 18, 2009)

Abstract—Operator splitting is a widely applied computational procedure in the numerical integration of long-range air pollution transport models. It is based on a decomposition of the model problem into smaller sub-problems, which are connected through their initial conditions. In this paper we apply four different splitting techniques in the Lagrangian FLEXPART model. The results are compared with measurement data collected during the ETEX experiment.

Key-words: splitting methods, particle model, Langevin equation, ETEX experiment

1. Introduction

In the past few decades, special emphasis has been laid on the investigation of the mechanisms and effects of atmospheric pollution. Several by-products of industry, agriculture, and traffic are emitted directly into the air, where these pollutants go through further processes: they are transported by the wind and dispersed by turbulent eddies, undergo chemical transformations, and, finally, are removed from the air by some form of deposition. Thus, the air pollution process is a very complicated one, consisting of several simultaneous interrelated sub-processes. Our major tools for the description of changes in the pollutant concentrations are mathematical models.

The mathematical modeling of air pollution phenomena, especially long-range air pollution transport, is usually based on a highly complicated system of

* Correspondig author

differential equations. The high complexity of this system requires the application of numerical solution techniques. Since our natural expectation is real-time simulation, therefore, in addition to the accuracy of the results, the efficiency of the computations is a crucial requirement as well. If some "off-the-shelf" solver is applied directly to the system, then these two requirements can hardly be met at the same time. Therefore, procedures, that allow us to lead the solution of the system back to the solution of simpler systems for which sufficiently accurate as well as efficient methods exist, are of great significance. This is exactly what operator splitting attains.

The aim of the paper is to present different kinds of operator splitting methods and demonstrate their applicability in air pollution transport modeling. The experiments were performed with the FLEXPART model, developed by Andreas Stohl and adapted by the Hungarian Meteorological Service. Certain parts of the program package were modified for the inclusion of splitting. The effects of different splitting methods were investigated in computer experiments where the model results were compared with measurement data.

2. The FLEXPART model

The FLEXPART model has been developed for approximately ten years for the computation of long and medium range transport of air pollutants emitted by point sources, and has continuously been under development. Nowadays line, area, and volume sources can also be investigated by the model. The model computes the trajectories of the emitted pollutant particles, and their concentration changes along the trajectories as an effect of diffusion, dry and wet deposition, and radioactive decay. It can be used for operational runs as well as for research purposes. The source code of the model can be freely downloaded from the site http://transport.nilu.no/flexpart.

FLEXPART can be applied in two different modes, namely, in forward and backward mode. In the first case the path of the emitted pollutant is followed forward in time, while in the second case the trajectories are followed backward in time, and so the source of the pollutant can be found.

The input data for the model, i.e., the meteorological (analysis and forecast) fields are provided by the ECMWF numerical weather prediction model in gridded binary (GRIB) format (*ECMWF*, 1995). The interpretation of the data necessitates the use of a GRIB decoding software, which can also be accessed freely in the internet. FLEXPART uses five three-dimensional scalar fields, namely, the horizontal and vertical wind components, temperature, and specific humidity. The vertical layers of the input data should coincide with those of the ECMWF model, which are given in hybrid coordinate system. The model transforms the hybrid coordinates into pressure coordinates. Moreover, the model needs the following two-dimensional fields: surface pressure, total cloud cover, 10-meter horizontal wind components, 2-meter temperature and dewpoint, large-scale and convective precipitation, sensible heat flux, topography, surface cover, etc. The planetary boundary layer is parameterized by means of the Monin-Obukhov similarity theory.

The motion of the particles is composed of two components: the random wind velocities and an evolution part, which is supposed to be a Markov process. These two processes are described by the Langevin equation. The equation for the vertical wind component w can be given as

$$dw = -w\frac{dt}{\tau_{L_w}} + \frac{\partial \sigma_w^2}{\partial z}dt + \frac{\sigma_w^2}{\rho}\frac{\partial \rho}{\partial z} + \left(\frac{2}{\tau_{L_w}}\right)^{1/2} \sigma_w dW \,, \tag{1}$$

where w is the turbulent vertical wind component, σ_w is its standard distribution, τ_{L_w} is the Lagrangian time scale of the autocorrelation of the vertical wind, ρ is the air density, and dW is an increment. This kind of description of the turbulent motion has the advantage that it is simple, flexible, and able to combine the spatial and temporal changes of the turbulent properties (*Carvalho et al.*, 2007).

3. Operator splitting methods and their application in the FLEXPART model

Operator splitting is based on an appropriate decomposition of the right-hand side of an evolution equation. In the traditional formulation of these equations, the time derivative is on the left-hand side, and the right-hand side contains terms with no time derivative that describe the effects of different physical/-chemical sub-processes. The different sub-processes are treated separately, by coupling the corresponding mathematical problems through their initial conditions. This procedure has been widely used in various fields of applied mathematics, including air pollution meteorology (*Zlatev*, 1995) and circulation models (*Lanser* et al., 2001; *Havasi*, 2007).

Hereinafter we give a brief description of the operator splitting approach. For more details we refer to *Havasi et al.* (2001) and *Faragó* (2006). It is worthwhile to formulate the splitting procedure in general terms. Let **X** denote some normed space, and consider the abstract initial value problem

$$\left.\begin{aligned} &\frac{dy}{dt}(t) = Ay(t), \\ &y(0) = y_0, \end{aligned}\right\} \tag{2}$$

on $[0,T]$, where w: $[0,T] \rightarrow \mathbf{X}$ is the unknown function, and A is an operator $\mathbf{X} \rightarrow \mathbf{X}$. This abstract initial value problem can stand for a partial differential equation as well as for a system of ordinary differential equations, obtained, e.g., after spatial discretization of a partial differential equation. Assume that the operator A can be decomposed into a sum of two sub-operators, A_1 and A_2, such that a problem with only operator A_1 on the right-hand side and a problem with only operator A_2 on the right-hand side are easier to integrate than the original problem. We divide the time interval $[0,T]$ of the problem into n smaller sub-intervals of length $\tau = T/n$, called splitting time step.

The simplest and most natural splitting method is the sequential splitting, where – at each time step – we first solve a problem that contains only the operator A_1 on the right-hand side and then a problem with only A_2. The initial condition is always the solution of the previous sub-problem. (During the solution of the first sub-problem in the first time step, the initial condition specified for the original problem is used.)

To formulate the sequential splitting mathematically, denote by $S_1(t_n, \tau)$ the solution operator belonging to the sub-problem defined by A_1 on $[t_n, t_n+\tau]$, and by $S_2(t_n, \tau)$ that defined by A_2 on $[t_n, t_n+\tau]$. (We call solution operator the operator which assigns the solution at the end of the time step to that at the beginning of the time step. In our case $S_1(t_n, \tau)$ and $S_2(t_n, \tau)$ are the numerical solution operators of the sub-problems, however, they could be the exact solution operators as well, if the sub-problems were solved exactly.) If $y_{seq}(t_n)$ denotes the solution obtained by the sequential splitting at time level t_n, then the solution at time t_{n+1} reads

$$y_{seq}(t_{n+1}) = S_2(t_n,\tau)\, S_1(t_n,\tau) y_{seq}(t_n). \tag{3}$$

A more accurate splitting scheme is the Marchuk-Strang splitting (*Marchuk*, 1968, *Strang*, 1968), where at each time step we first solve a problem with A_1 over half a splitting time step, then a problem with A_2 over the whole time step, and, finally, a problem with A_1 again over half a time step:

$$y_{MS}(t_{n+1}) = S_1\left(t_n + \frac{\tau}{2}, \frac{\tau}{2}\right) S_2(t_n,\tau)\, S_1\left(t_n, \frac{\tau}{2}\right) y_{MS}(t_n). \tag{4}$$

A newly developed splitting scheme is the additive splitting (*Faragó et al.*, 2008), where both sub-problems use the same initial condition (the solution of the previous time step), which is subtracted from the sum of the two solutions:

$$y_a(t_{n+1}) = (S_1(t_n,\tau) + S_2(t_n,\tau)) y_a(t_n) - y_a(t_n). \tag{5}$$

The fourth method that we will study is called modified additive splitting (*Kocsis*, 2008), which has the algorithm

$$y_{ma}(t_{n+1}) = 0.5\left(S_1(t_n, 2\tau) + S_2(t_n, 2\tau)\right) y_{ma}(t_n). \quad (6)$$

Here the sub-problems are solved over time steps of length 2τ by using the same initial condition, and then the two solutions, obtained in this way, are symmetrically averaged. This modified method has better stability properties than the ordinary additive splitting, because the negative weights, which usually cause problems in proving the stability, are avoided in the time-stepping operator. Here and further on, by stability we mean the usual stability notion in numerical mathematics, namely, the continuous dependence of the numerical solution on the input data.

Originally, no operator splitting was used in the FLEXPART model, therefore, the source code had to be modified for the inclusion of operator splitting. The splitting procedure was applied to the Langevin equation describing both horizontal wind components

$$du = -u \frac{dt}{\tau_{L_u}} + \left(\frac{2}{\tau_{L_u}}\right)^{1/2} \sigma_u dU, \quad (7)$$

$$dv = -v \frac{dt}{\tau_{L_v}} + \left(\frac{2}{\tau_{L_v}}\right)^{1/2} \sigma_v dV, \quad (8)$$

where u and v are the turbulent horizontal wind components, σ_u and σ_v are their standard distributions, τ_{L_u} and τ_{L_v} are the Lagrangian time scales of the auto-correlations of the horizontal wind components, and dU and dV are increments.

During operator splitting, each of the above two equations were split into a pair of equations. For the component u these have the form

$$du = -u \frac{dt}{\tau_{L_u}}, \quad (9)$$

$$du = \left(\frac{2}{\tau_{L_u}}\right)^{1/2} \sigma_u du, \quad (10)$$

and we have similar equations for v. On the base of this decomposition, we prepared the computer code of all the four splitting schemes, presented in Section 3. In this manner, we obtained five different model versions, including the model with no splitting. The verification of these model versions with measurement data is presented in the next section. Further numerical investigations of the solutions obtained by different splitting methods can be found in *Kocsis* (2008).

4. Comparison of the model results with measurements

For the verification of the model versions measurement data collected during the European Tracer Experiment (ETEX) were used (*Nodop et al.*, 1998). In this section we present the ETEX project and the results of our comparisons.

4.1. The ETEX measurement program

The major aim of the ETEX project was a long-range experiment, in the framework of which a chosen air pollutant was emitted into the air under controled circumstances. In the autumn of 1994, two experiments were made (*Dop et al.*, 1998), during which perfluorocarbon (PMCH) particles were emitted into the air and monitored. This compound is appropriate for long-range atmospheric experiments, since it is non-toxic, not soluble in water, chemically inert, and does not harm the environment. Its background concentration is low and homogeneously distributed. The emission took place in France, near Monterfil and Treffandel (N 48° 3'33", W 2° 0'30"), 90 meters above sea level, from a 8-meter high chimney on October 23, 1994. Here the dominant wind direction is western/southwestern, and so the particles can be followed over a distance of as long as 2000 km. (A similar experiment was made on November 14, 1994, see *Nodop et al.*, 1998.)

On October 23, 1994, at 16:00 UTC, 340 kg of PMCH was emitted into the air during 12 hours, and then the concentration of this compound was measured throughout Europe, at 168 land measurement stations (including those in Hungary) and three aircrafts.

On the next day, the air mass over the area was still unstable, however, the winds weakened, since the cyclone moved forward to the north. On October 25, the wind direction changed to southerly at some places, and then again blew to southwest. On October 26, due to an anticyclone over the Black Sea, the southerly winds prevented the particles from spreading to the east (*Gryning et al.*, 1998).

Fig. 1 shows the spreading of the pollutant plume as time went by. 24 hours after the emission the plume reached Belgium, the Netherlands, and Germany. The plume decoupled, which is perhaps only a consequence of the visualization and the fact that the measurement network is sparse in the area (*Fig. 1a*). 12 hours later the plume had left France, and spread over the Benelux, Germany, and the Czech Republic (*Fig. 1b*). Some time later the position of the plume shows rotation in the northern-southern direction (*Fig. 1c*). 60 hours after the emission the plume began to separate into two parts: one with a center over Slovakia and one over the Northern Sea (*Fig. 1d*) (*ETEX*, 1998).

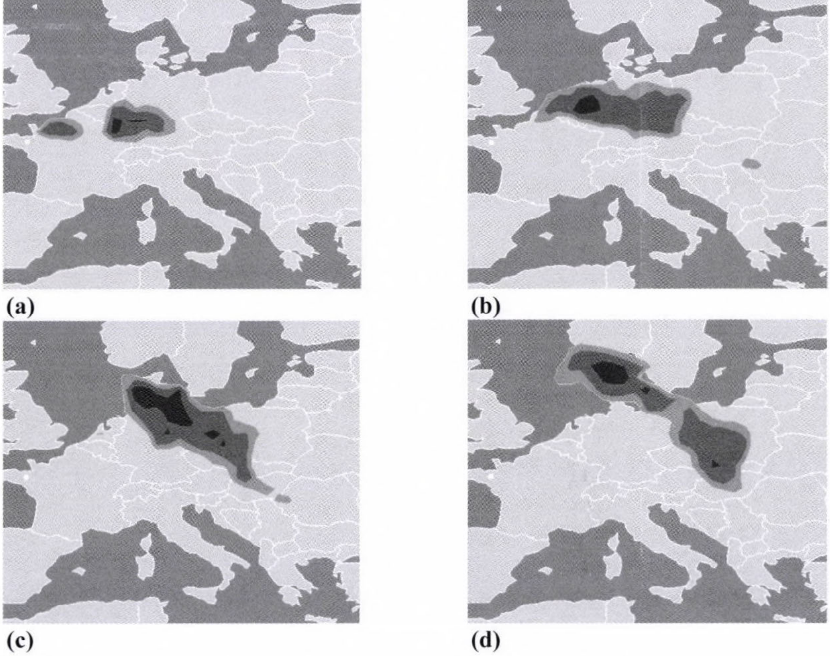

Fig. 1. The extension of the plume 24 (a), 36 (b), 48 (c), 60 (d) hours after the emission. Light grey: 0.01 ng/m^3, dark grey: 0.05 ng/m^3, black: 0.1 ng/m^3 (*ETEX*, 1998).

4.2. The results of the comparisons

Model versions obtained without splitting and with four different splitting schemes were run with the emission parameters specified by the ETEX experiment, and the 168 land stations were used as receptor points. Simulations were made by using the ECMWF analysis fields. The time integration steps were 900 seconds for the unsplit model, and 1800 seconds for the model versions with splitting. Our investigations were carried out for the beginning 54-hour period of the pollution transport. Comparisons were made by means of maps and several statistical indicators.

The maps shown in *Figs. 2* and *3* indicate the differences between the measurements and the five model versions. The left columns show the areas of overestimation, while the right columns indicate the areas of underestimation of the measurement data by the model versions. On the white areas the model results were exact.

24 hours after the emission, each model version overestimates the amount of pollutant over the central part of Germany (*Fig. 2*), on the area where the highest concentrations were measured (see *Fig. 1*). The only exception is the Marchuk-Strang splitting, which predicted higher concentrations for Luxemburg (*Fig. 2e*).

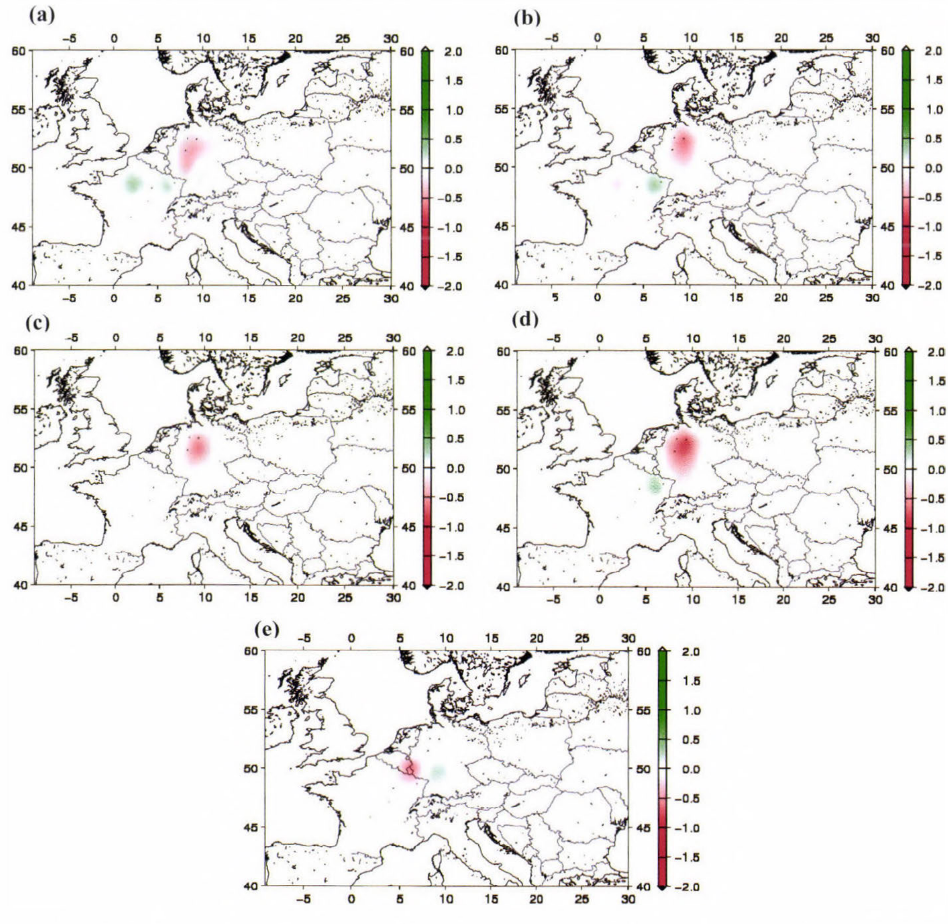

Fig. 2. Areas of underestimation (green) and overestimation (red) for the five different model versions 24 hours after the emission. (a) original, (b) sequential, (c) additive, (d) modified additive, (e) Marchuk-Strang. The tone of the colors shows the difference between the measured and modeled concentrations in ng/m^3.

54 hours after, the emission, all the model versions underestimate the concentration values in the same zone where the pollutant plume is located (*Fig. 3*). This underestimation is the smallest for the modified additive splitting (*Fig. 3d*). At some places we can find overestimation as well, namely, for the original unsplit model and for the modified additive splitting over the Baltic Sea (*Fig.*

3a, *3d*), while for the other splitting methods over the Benelux (*Fig. 3b*, *3c*, *3e*). The differences between the model results and the measurements are the largest for the Marchuk-Strang splitting, which overestimates the concentrations over huge areas of Western Europe.

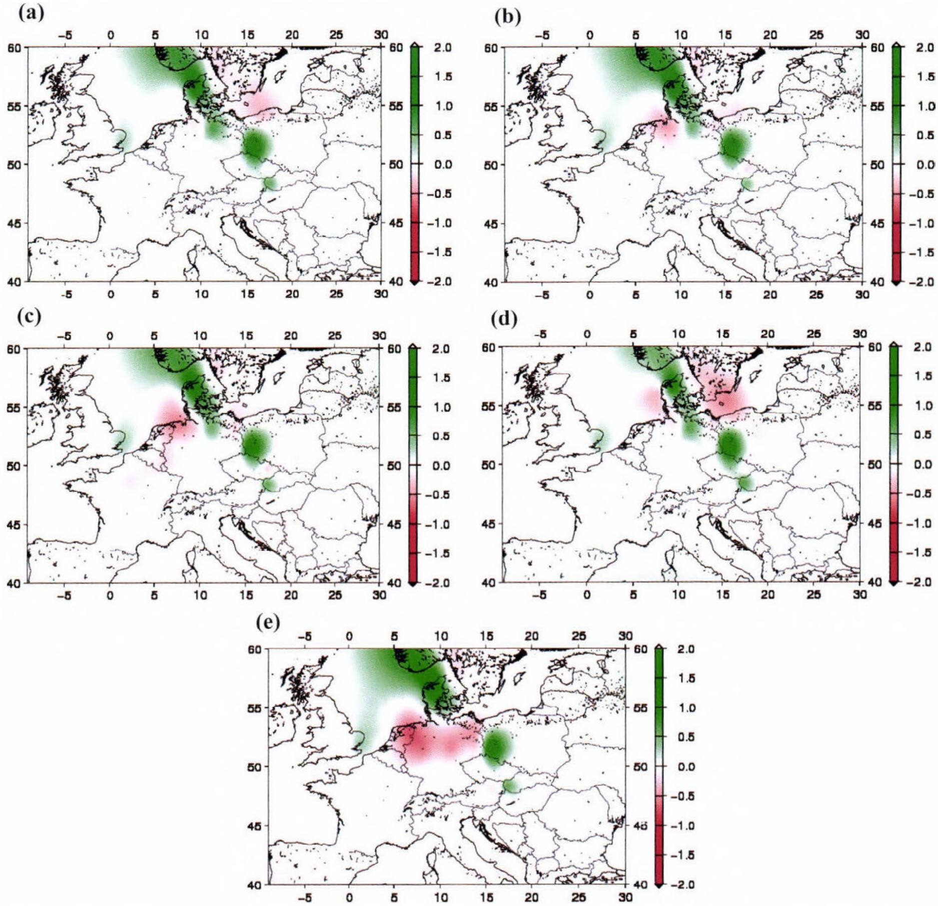

Fig. 3. The areas of underestimation (green) and overestimation (red) for the five different model versions 54 hours after the emission. (a) original, (b) sequential, (c) additive, (d) modified additive, (e) Marchuk-Strang. The tone of the colors shows the difference between the measured and modeled concentrations in ng/m^3.

In addition to the presented maps, we used several statistical indicators for the comparison of the different model versions. These indicators can be classified into two groups. The first group of indicators is used for characterizing the measure of the overestimation and underestimation, and includes, e.g., the bias

$$B_j = \frac{1}{N_j}\sum_{i=1}^{N_j}(P_{ji} - M_{ji}) \tag{11}$$

and the geometric mean error

$$MG_j = \exp\left(\frac{1}{N_j}\sum_{i=1}^{N_j}\ln P_{ji} - \frac{1}{N_j}\sum_{i=1}^{N_j}\ln M_{ji}\right). \tag{12}$$

In these formulas P_{ii}, M_{ji}, and N_j denote, respectively, the ith predicted value, the ith measurement value, and the number of measurements at time t_j. Indicators from the second group, such as the normalized mean square error

$$NMSE_j = \frac{1}{N_j}\sum_{i=1}^{N_j}\frac{(P_{ji} - M_{ji})^2}{\overline{P_j}\cdot\overline{M_j}} \text{ with } \overline{P}_j = \frac{1}{N_j}\sum_{i=1}^{N_j}P_{ji},\ \overline{M_j} = \frac{1}{N_j}\sum_{i=1}^{N_j}M_{ji}, \tag{13}$$

and the geometric mean variance

$$VG_j = \exp\left[\frac{1}{N_j}\sum_{1=i}^{N_j}(\ln P_{ji} - \ln M_{ji})\right], \tag{14}$$

measure the deviation of the model results from the measurements. If the above indicators are to be used for a time period with measurements at t_1,t_2,..., t_K, then we will use the global quantities

$$MG = \frac{1}{K}\sum_{j=1}^{K}MG_j, \qquad NMSE = \frac{1}{K}\sum_{j=1}^{K}NMSE_j, \qquad VG = \frac{1}{K}\sum_{j=1}^{K}VG_j. \tag{15}$$

The values of B and MG in *Table 1* show that all model versions overestimate the pollution, since $B > 0$ and $MG > 1$. The largest value of B was obtained for the Marchuk-Strang splitting, while the largest values of MG for the additive and sequential splittings. In terms of B the winner is the modified additive splitting, while in terms of MG it is the original unsplit version. From the values of B one can see that we have underestimation only for the original model.

The indicators do not inform us about the exact measure of over- and underestimation, since those can compensate each other due to the summation.

That is why the values of *NMSE* and *VG* should also be examined. According to the *NMSE* values, the modified additive and sequential splittings produced the best results, and the Marchuk-Strang splitting gave the biggest error. Note that overestimating models are characterized by a smaller *NMSE*, while underestimating ones by a larger *NMSE* (*Stohl et al.*, 1998). As opposed to the *NMSE*, the *VG* index is biggest for the sequential and additive splittings, and smallest for the unsplit model.

Table 1. Statistical indicators for the different model versions for the whole studied period

	Splitting method				
	No splitting	**Sequential**	**Marchuk-Strang**	**Additive**	**Modified additive**
B	-0.262	0.177	0.664	0.300	0.149
MG	4.93	10.40	6.02	10.02	7.71
NMSE	2.743	2.440	3.311	2.660	2.336
VG	0.816	1.135	1.086	1.122	0.990

Certainly, the above indices show temporal changes. To examine these changes, we fixed the time, averaged in space, and so obtained a value for each index at each time step. *Fig. 4* reveals that at the beginning of the studied period, each model version performs similarly, they all underestimate the concentrations, and then the splitting solutions start to overestimate the concentrations in a certain time period. The largest errors are obtained for the Marchuk-Strang splitting, which is probably due to the weaker stability properties of this method.

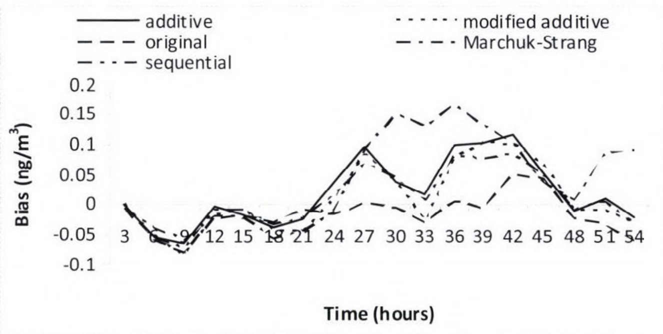

Fig. 4. Temporal changes of index *B* for the different model versions.

Fig. 5 shows the temporal changes of index *MG*. After a period of very small errors, the overestimation becomes dominant, however, the differences between the model versions are not so significant as for index *B*. At the end of the period, the values start to decrease, and the original model version and the modified additive splitting begin to underestimate the concentrations.

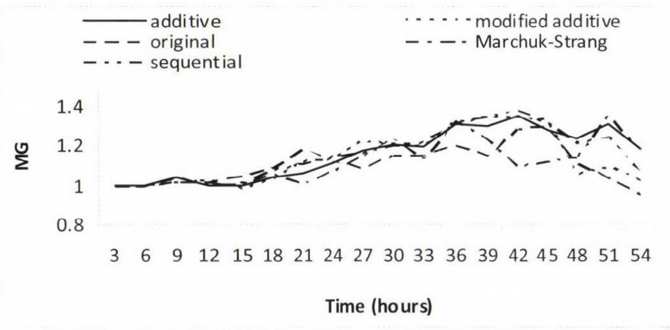

Fig. 5. Temporal changes of index *MG* for the different model versions.

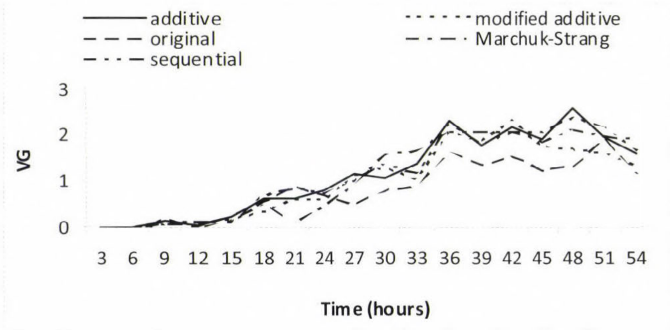

Fig. 6. Temporal changes of index *VG* for the different model versions.

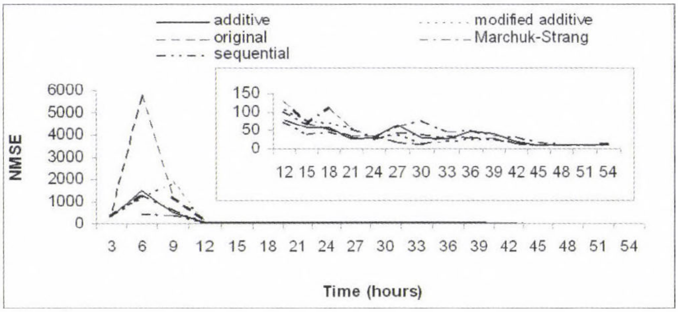

Fig. 7. Temporal changes of the index *NMSE* for the different model versions.

Fig. 6 shows the changes of index *VG* in time. The differences between the model versions are not significant. The best results are obtained for the original model version. In the case of the *NMSE*, see *Fig. 7*, the starting period is characterized by a big jump, which can be observed in each model version, and is especially significant in the unsplit case. The reason for this is that the concentration values differ from zero only in small areas, which results in division by a small value. There may also be errors in the vertical extension of the modeled plume (*Stohl* and *Wotawa*, 1997). The *NMSE* decreases at the end of the period for all model versions.

5. Conclusions

Four different operator splitting methods were introduced for the calculation of the trajectories in the Lagrangian FLEXPART model, namely, the additive, modified additive, sequential, and Marchuk-Strang splittings. The different model versions obtained in this way were verified with measurement data collected during the ETEX project. The main results of the examination can be summarized as follows:

- The different model versions tend to overestimate the measurements. According to the studied statistical indicators, the best results were obtained for the unsplit model and for the modified additive splitting, while the worst results for the Marchuk-Strang splitting. Therefore, the Marchuk-Strang splitting, which usually provides better accuracy than the other studied splitting methods, is not recommended to use in this model.
- The running time was reduced in all model versions where operator splitting was applied, except for the Marchuk-Strang splitting. The largest reduction was obtained for the modified additive splitting (by about 10%).

Acknowledgements—This work was supported by Hungarian National Research Founds (OTKA) No. F61016. *Ágnes Havasi* is a grantee of the Bolyai János Scholarship.

References

Carvalho, J.C., Vilhena, M.T., and *Thompson, M.,* 2007: An iterative Langevin solution for turbulent dispersion in the atmosphere. *J. Comput. Appl. Math. 206*, 534-548.

ECMWF, 1995: *User Guide to ECMWF Products 2.1*, Meteorological Bulletin M3.2, Reading, UK.

ETEX, 1998: *The European Tracer Experiment* (eds.: *F. Girardi, G. Graziani, D. van Velzen, S. Galmarini, S. Mosca, R. Bianconi, S. Bellasio, W. Klug,* and *G. Fraser*). European Communities, Italy, p. 107.

Faragó, I., 2006: Application of the operator splitting method for real-life problems. *Időjárás 110*, 379-395.

Faragó, I., Thomsen, P.G., and *Zlatev, Z.,* 2008: On the additive splitting procedures and their computer realization. *Appl. Math. Model. 32*, 1552-1569.

Gryning, S., Batchvarova, E., Schneiter, D., Bessemoulin, P., and *Berger, H.,* 1998: Meteorological conditions at the realize site during the two tracer experiments. *Atmos. Environ. 32*, 4123-4137.

Havasi, Á., 2007: Wave analysis of different splitting methods in the linearized shallow water equations. *IJCSE* 3, No. 4, 264-270.

Havasi, Á., Bartholy, J., and *Faragó, I.*, 2001: Splitting method and its application in air pollution modeling. *Időjárás 105*, 39-58.
Kocsis, Zs., 2008: *Numerical Investigation of the Transport of Air Pollutants* (diploma work; in Hungarian). Eötvös Loránd University, Budapest, Hungary.
Lanser, D., Blom, J., and *Verwer, J.*, 2001: Time integration of the shallow water equations in spherical geometry. *J. Comput. Phys. 171*, 1, 373-393.
Marchuk, G. I., 1968: Some application of splitting-up methods to the solution of mathematical physics problem. *Aplik. Mat. 13*, 103-132.
Nodop, K., Connolly, R., and *Girardi, F.*, 1998: The field campaigns of the European Tracer Experiment (ETEX): overview and results. *Atmos. Environ. 32*, 4095-4108.
Stohl, A., and *Wotawa, G.*, 1997: Validation of the Lagrangian particle dispersion model FLEXPART using ETEX data. In *ETEX Symposium on Long-range Atmospheric Transport, Model Verification and Emergency Response* (ed.: *K. Nodop*).Vienna, Austria, 13-16 May 1997, 167-170.
Stohl, A., Hittenberger, M., and *Wotawa, G.*, 1998: Validation of the Lagrangian particle dispersion model FLEXPART against large-scale tracer experiment data. *Atmos. Environ. 32*, 4245-4264.
Strang, G., 1968: On the construction and comparison of difference schemes. *SIAM J. Numer. Anal. 5*, 506–517.
van Dop, H., Addis, R., Fraser, G., Girardi, F., Graziani, G., Inoue, Y., Kelly, N., Klug, W., Kulmala, A., Nodop, K., and *Pretel, J.*, 1998: ETEX: European Tracer Experiment; observations, dispersion modeling and emergency response. *Atmos. Environ. 32*, 4089-4094.
Zlatev, Z., 1995: *Computer Treatment of Large Air Pollution Models*. Kluwer Academic Publishers, Dordrecht-Boston-London.

IDŐJÁRÁS

Quarterly Journal of the Hungarian Meteorological Service
Vol. 113, No. 3, July–September 2009, pp. 203–219

Estimation of the biospheric carbon dioxide balance of Hungary using the BIOME-BGC model

Zoltán Barcza[1*], László Haszpra[2], Zoltán Somogyi[3], Dóra Hidy[4], Katalin Lovas[5], Galina Churkina[6], and **László Horváth[2]**

[1]*Department of Meteorology, Eötvös Loránd University,*
P.O. Box 32, H-1518 Budapest, Hungary; E-mail: bzoli@elte.hu
[2]*Hungarian Meteorological Service,*
P.O. Box 39, H-1675 Budapest, Hungary; E-mails: haszpra.l@met.hu, horvath.l@met.hu
[3]*Forest Research Institute,*
Frankel L. u. 42-44, H-1027 Budapest, Hungary; E-mail: somogyiz@erti.hu
[4]*Institute of Botany and Ecophysiology, Szent István University,*
Páter K. u. 1, H-2103 Gödöllő, Hungary; E-mail: dori.hidy@gmail.com
[5]*Hungarian Meteorological Service,*
P.O. Box 38, H-1525 Budapest, Hungary; E-mail: lovas.k@met.hu
[6]*Max Planck Institute for Biogeochemistry,*
Hans-Knöll-Str. 10, D-07745 Jena, Germany; E-mail: churkina@bgc-jena.mpg.de

(Manuscript received in final form February 19, 2009)

Abstract—Here we estimate the biospheric carbon dioxide balance of Hungary using the adapted BIOME-BGC process oriented ecological system model. The model was calibrated using the Hungarian measurements of biosphere-atmosphere carbon dioxide exchange. After calibration, the model was run for the four major land cover types such as croplands, grasslands, deciduous and coniferous forests for the period of 2002–2007. Our calculations suggest that all Hungarian ecological systems together formed a net carbon dioxide source during the time period studied. Since agricultural fields cover more than 50% of the total area of Hungary, the net carbon dioxide flux is dominated by the carbon balance of croplands. The average net release of CO_2 is 8.7 Mt per year with significant interannual variation: the highest net emission was 21.6 Mt CO_2 in 2003, while the lowest was 1.2 Mt CO_2 in 2006. Due to the model limitations, simulated CO_2 release from croplands is most likely overestimated, thus, the present results provide an upper limit for the potential range of the carbon balance of Hungary. The model results highlight the strong dependence of the biospheric carbon dioxide balance on the weather conditions. The results are compared with the carbon budget estimations previously published for Hungary as well as with those reported to the United Nations Framework Convention on Climate Change.

Key-words: biospheric carbon balance, net ecosystem exchange, ecosystem model, upscaling, eddy covariance measurements, plant functional types, BIOME-BGC model, model calibration

[*] Corresponding author

1. *Introduction*

Atmospheric carbon compounds, especially carbon dioxide and methane, play a crucial role in the formation of Earth's climate through the greenhouse effect (*Jansen et al.*, 2007). Their atmospheric amount partly depends on the activity of the biosphere, which is partly climate controlled, but also considerably affected by human activities. Because of this strong coupling between the biogeochemical cycle of carbon and the climate, the understanding of the global carbon cycle, including its interactions and feedbacks is a prerequisite to any reliable climate prediction (*Cox et al.*, 2000; *Friedlingstein et al.*, 2006; *Denman et al.*, 2007).

During most of the Holocene, the biosphere was in approximate steady state with the atmosphere: on average, the biosphere absorbed approximately as much carbon dioxide from the atmosphere through photosynthesis as it released by respiration and by the decomposition of the dead organic material produced. However, in the 1980s, the measurements revealed that the biosphere was tending to be a net carbon dioxide sink. This net uptake partly balances the anthropogenic CO_2 emission (*Cao et al.*, 2002). Currently, less than half of the anthropogenic emission (fossil fuel burning, cement industry, deforestation, etc.) remains in the atmosphere increasing the greenhouse effect. Some 50–60% of the anthropogenic emission is taken up by the oceans and the terrestrial biosphere (*Denman et al.*, 2007). However, it is poorly known where and why the biospheric carbon dioxide uptake has increased. In a similar manner, we do not know how the biosphere will behave in the future.

The climate related behavior of the biosphere has been extensively studied all over the world. At present the European efforts are coordinated by the CarboEurope Integrated Project (IP) (http://www.carboeurope.org) financed by the 6th R+D Framework Programme of the European Commission. The primary aim of the project is to determine and constrain the European carbon dioxide budget with an accuracy of as high as possible on the basis of direct field measurements and application of ecosystem models. In addition to the present authors, other Hungarian scientists also participate in the project.

Most models used in CarboEurope-IP are of coarse spatial resolution, and more importantly they only use general parameterization for specific plant functional types uniform in the entire European region (*Janssens et al.*, 2003, 2005; *Vetter et al.*, 2007; *Gervois et al.*, 2008). To achieve a higher accuracy in the carbon dioxide budget estimation, the special features of smaller geographical regions should also be taken into account.

Information on the emissions and removals by certain elements of the biosphere is also collected annually for an increasing number of countries by the United Nations Framework Convention on Climate Change (UNFCCC) in the so-called national greenhouse gas inventory reports. In these reports, internationally approved methodology by the IPCC (*IPCC*, 1997, 2003, 2006) or peer-reviewed national methodologies must be applied. However, reports under the UNFCCC and, especially, its Kyoto Protocol may include only partial estimates for the terrestrial biospheric emissions and removals, while it is the *total* carbon dioxide budget that affects the CO_2 concentration of the air.

Hungary has also submitted her annual reports for almost two decades. However, although these reports take account of the vast majority of emissions and removals, not the whole budget is covered. The verification of these estimates is also necessary. In this verification, alternative methodologies and data sets should be used.

The present work is an attempt for the estimation of the *total* biospheric carbon dioxide balance of Hungary. For this purpose, the BIOME-BGC process oriented ecological system model (version 4.1.1) was adapted to the Hungarian conditions. The model results are compared with those CarboEurope results that can be related to Hungary, with the national land use dependent inventory data reported to UNFCCC, and with the Hungarian anthropogenic emission.

2. The BIOME-BGC model and its adaptation

BIOME-BGC was developed for the description of biosphere-atmosphere exchange of carbon dioxide, water, and nitrogen (*Running* and *Coughlan*, 1988; *Running* and *Gower*, 1991; *Running* and *Hunt*, 1993; *White et al.*, 2000; *Churkina et al.*, 2003; *Hidy et al.*, 2007). BIOME-BGC can simulate the biogeochemical cycles in evergreen and deciduous forests, shrubs, and grasses. The different ecological systems need different parameter values, thus, the model should be adapted to the systems studied (*White et al.*, 2000). The model also needs meteorological data, geographical and soil parameter values as input data, because these parameters convey the environmental constraints and conditions to the ecological systems. In order to use BIOME-BGC for the simulation of the carbon balance of large areas, the internal model parameters (ecophysiological parameters) are held constant, while the spatially varying soil and geographical parameters, and the temporally varying meteorological data are supplied to the model to reflect regional differences in the functionality of the different ecological systems. This assumption is only feasible if the spatial variability of the ecophysiological parameters is expected to be low. In case of Hungary, due to the relatively uniform climate, this assumption seems reasonable.

For the determination of the biospheric carbon dioxide balance, the area of Hungary was covered by a grid of $1/6 \times 1/6$ degree spatial resolution. The fraction of the different plant functional types and the characteristic soil type and weather condition were determined for each grid cell.

The determination of the land cover type is based on the CORINE CLC50 database (http://www.fomi.hu/corine/clc50_index.html). CLC50 was compiled based on satellite images taken between 1998 and 1999. It means that the spatial distribution of the different land use types is subject to uncertainty due to continuous land use change activities (reforestation, afforestation, land abandonment, etc.). Our modeling approach does not take into account the changes in land use during 2000–2007. CLC50 distinguishes among 78 land cover types. BIOME-BGC, similarly to the other models of the same kind, cannot distinguish among so many different land cover types because of the necessary simplifications and generalizations in the models (mostly caused by our insufficient knowledge and computing capacity). Therefore, the 78 different land cover types were aggregated into four basic, essentially different, categories: grasslands, agricultural fields, deciduous and coniferous forests (*Fig. 1*). The four general categories cover 81.83% of the country's area (agricultural fields: 52.95%, grasslands: 10.42%, deciduous forests: 16.72%, coniferous forests: 1.74%). The rest of the country's territory is covered by artificial land cover types (roads, built-up areas) and open water surfaces (lakes, rivers). Those areas are not handled by the model, therefore, in the present study they are considered as carbon neutral surfaces in biological sense. It does not mean that those areas are not important in the carbon cycle (e.g., anthropogenic emission can take place in the built-up areas, waters can take up or release carbon, etc.).

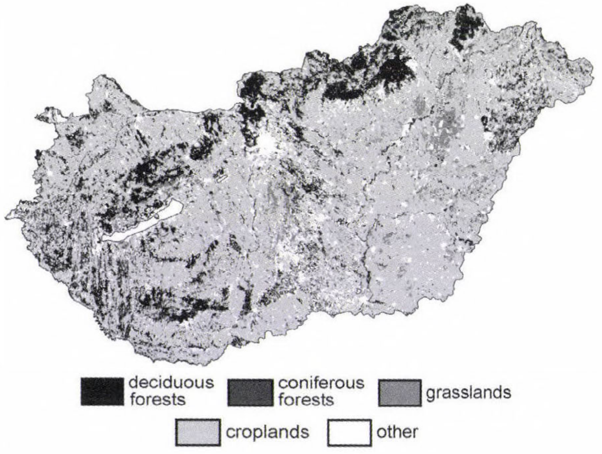

Fig. 1. Aggregated basic land cover types of Hungary used for the BIOME-BGC simulations. The map is based on the CORINE CLC50 land cover classification. Note that coniferous forests are hardly visible due to their small fraction and scattered geographical distribution.

BIOME-BGC and other process oriented biogeochemical models simulate the carbon dioxide exchange between the biosphere and atmosphere. The horizontal carbon transport (export or import of products, harvest, manure, or other carbon related materials from/to the territory studied) modifies the calculated geographical distribution of the balance. This type of geographical redistribution can be taken into account by means of additional calculations if needed (e.g., *Ciais et al.*, 2007). The results presented here are the carbon dioxide balance formed exclusively by the local biogeochemical processes (photosynthesis, respiration, chemical decomposition) and do not involve any horizontal transport. For the geographical distribution of the full carbon budget, the anthropogenic influence should be taken into account as part of the anthropogenic activity (burning of local/imported biomass, consumption of local/imported agricultural products, export/import of decomposable biospheric product/organic material, etc.). It should be noted that the model can only simulate the effects of the anthropogenic interventions (e.g., deforestation, afforestation, reforestation, irrigation, harvesting, herbage, other types of land management) on the carbon dioxide exchange in a rather limited way. Therefore, the model results are rather uncertain on recently disturbed, converted, or non-typically used lands.

Usually, the consistent biogeochemical data set required by a model is not available because of the lack of certain measurements, sampling and analytical errors, limited representativeness of the measurements, etc. Inconsistency in the input data causes transients in the beginning of the model runs not reflecting any real process, or phenomenon. The spin-up phase of the model run is used for the elimination of these transients. The only purpose of this phase is to transform the original, inconsistent input data into a consistent, steady state data set to be used for the actual simulation.

In the spin-up phase, the processes of a long (usually several decades long) period is simulated during which the soil-vegetation system reaches a steady state. This is one of the reasons why the model is unable to produce realistic carbon dioxide exchange data on recently and significantly disturbed lands.

For the spin-up the 1901–2000 period was used for which the basic meteorological data were available from the CRU TS 1.2 database (Climatic Research Unit [CRU], University of East Anglia) (*New et al.*, 2002). This database contains monthly average temperature, diurnal temperature range, and precipitation amount data on the same grid we use. For the preparation of the daily meteorological data (daily maximum and minimum temperature, daily precipitation) required by the model, a statistical weather generator (C2W) was used (*Bürger*, 1997). The missing daily meteorological parameters (average daytime temperature, average daytime vapor pressure deficit, average daytime global radiation) were generated by the MTCLIM model (*Thornton et al.,* 2000).

In the normal phase of the carbon dioxide exchange modeling (2002–2007), the grid-interpolated measurements of the Hungarian meteorological network were used. The interpolated data fields were produced by the Hungarian Meteorological Service applying the MISH method (http://www. cosis.net/ abstracts/ EGU05/07310/EGU05-J-07310.pdf).

Using the default, generalized parameter set of BIOME-BGC, the model approximates the carbon dioxide exchange of the different ecological systems with moderate accuracy. However, significantly better results can be achieved if the model is adapted to the real Hungarian conditions, that is the model is "calibrated". In the case of croplands and grasslands, the calibration was performed using Hungarian measurements (*Barcza et al.*, 2003; *Haszpra et al.*, 2005; *Nagy et al.*, 2007), while for deciduous and coniferous forests – in the lack of Hungarian measurements – the parameters were taken from the literature (*Pietsch et al.*, 2005).

In case of grasslands, measurements from three Hungarian monitoring sites (Bugac, Hegyhátsál, Szurdokpüspöki) were used. At all sites the biosphere-atmosphere exchange of carbon dioxide is directly measured using eddy covariance technique (*Barcza et al.*, 2003; *Haszpra et al.*, 2005; *Nagy et al.*, 2007). The calibration procedure of BIOME-BGC is published in the paper of *Hidy et al.* (2007).

The carbon exchange of crops is inherently affected by management practices (sowing, harvest, fertilization, etc.) that strongly influence the carbon, water, and nitrogen cycling through the ecosystem. Harvest causes a sudden drop in the standing biomass and alters the different carbon pools (aboveground biomass, litter), which in turn affects the carbon balance and the physiological response of the ecosystem to the environmental conditions. The current version of BIOME-BGC is unable to simulate disturbance and cropland management. However, considering larger regions where both winter and summer crops are present, the annual cycle of net ecosystem exchange (NEE) becomes more or less balanced in time (i.e., there is no sudden decrease in the NEE caused by harvest), as it is obvious from the large scale eddy covariance data measured over a mixed agricultural area in Hungary (*Haszpra et al.*, 2005; *Figs. 5* and *8*). The main cause of the balanced behavior is the conjoint presence of winter crops (e.g., winter wheat, harvested around June-July) and summer ones (e.g. corn, harvested around October–November). The measurement data suggest that the overall carbon balance can be approximated with the carbon dynamics of a perennial herbaceous ecosystem. In this sense, croplands can be handled as semi-natural grasslands without any sharp decrease in the standing biomass (thus, no modification in the model logic is needed for the simulation). This is the reason why BIOME-BGC can be used to simulate agricultural NEE with reasonable accuracy and handles crops as a kind of "super grass" (i.e., fertilized grass, see *Vetter et al.*, 2007) using the existing internal grass parameterization. This logic makes it imperative to use accurate measurement data for the calibration of the model to simulate super grass NEE in order to provide estimates that are comparable with the measured real cropland NEE. In Hungary the dominant land cover type is agriculture, thus, the success or failure of the present modeling activity strongly depends on the quality and proper use of the training data set.

The drawback of this grassland approach is the likely overestimation of NEE (higher CO_2 release) for the dormant season. The cause of this likely bias comes directly from cropland management: as part of the biomass is removed via harvest, it cannot decompose in the field and respire back to the atmosphere. In the model the biomass removal is not handled, thus, respiration is overestimated. As a consequence, the cropland NEE data presented here might be considered as an upper limit for cropland carbon balance.

The only monitoring project producing CO_2 net ecosystem exchange data for mixed agricultural fields in Hungary is carried out at Hegyhátsál (*Haszpra et al.*, 2001, 2005). The eddy covariance system installed at 82 m elevation above the ground has been providing regional scale NEE data since 1997. As the mosaic type mixed agricultural activity (including a mixture of winter and summer crops) can be considered typical in a large part of Hungary, the data measured here can be used for the calibration of BIOME-BGC (using the grass submodel) for the general Hungarian conditions. Calibration of the BIOME-BGC model was performed with the measured daily eddy covariance data using Monte Carlo Maximum Likelihood (MCML) approach (*Hollinger* and *Richardson*, 2005). The calibration was accomplished using nine years of measurement data (1997–1999, 2001–2006; *Haszpra et al.*, 2005). Modeled gross photosynthesis (gross primary production, GPP) explained about 80% of the measured GPP variance ($R^2 = 0.8$), while modeled total ecosystem respiration (Reco) explained about 72% of the total variance ($R^2 = 0.72$).

There are no Hungarian measurements available for deciduous and coniferous forests, therefore, the model calibration cannot be performed as it was implemented for grasslands and croplands. We used the data of *Pietsch et al.* (2005) recommended for BIOME-BGC. Their parameter sets were determined on the basis of measurements in oak (*Quercus robur/petraea*) and Scotch pine (*Pinus sylvestris*) forests. The measurements were carried out in low elevation regions of Austria and Czech Republic close to Hungary, where the climatic conditions are similar to those in Hungary.

Although oak is the dominant species among the Hungarian deciduous trees, significant areas are covered by Black locust (*Robinia pseudoacacia*) and other species. Thus, the generalized application of the oak parameter set may be considered as an oversimplification to characterize all Hungarian deciduous forests, but the parameterization cannot be refined without measurements on other species yet.

A better parameterization could be achieved using Hungarian forest inventory data (see, e.g., *Somogyi*, 2007), however, the calibration methodology for BIOME-BGC is not developed yet.

In summary, the main simplifications of our modeling approach are as follows: (a) BIOME-BGC is applied mainly to disturbed ecosystems, though the model logic is not prepared yet for the precise description of managed ecosystems; (b) the ecophysiological parameters for the different plant functional types are held constant during the simulation; (c) agricultural ecosystems are handled as "super grass", which means that harvest is not simulated but the annual course of NEE is well represented; (d) only a very limited number of tree species are simulated (oak and pine) in the lack of information about the spatial distribution of tree species and also in the lack of ecophysiological parameters for some of the other relevant tree species; (e) BIOME-BGC cannot simulate the effect of pests and diseases, and the long-term consequences of extreme weather events are not accounted for either; (f) the CLC50 database might be outdated due to land use change activities that are occurring in Hungary, which causes uncertainty in the simulation. Future research is essentially needed to address the above mentioned limitations of our modeling methodology.

3. Results

Using the input data and parameter sets presented above, the total Hungarian net biosphere-atmosphere CO_2 exchange has been calculated using daily time steps for 2002–2007 by means of BIOME-BGC. In the atmosphere-oriented studies like the present one, the net biospheric carbon uptake is denoted by negative sign, because the amount is a loss from the point of view of the atmosphere. Data are given in carbon amount throughout the paper (1 g C = 3.67 g CO_2, or 1 g CO_2 = 0.27 g C).

Fig. 2 shows the 6-year mean annual cycle of NEE for the different plant functional types averaged for all grid points. It can be seen in the figure, that the model captured the seasonal variation of the carbon exchange of the biosphere in all cases. On average, each plant functional type acts as a net carbon sink during the growing season (except for coniferous forests during July and August). Cropland NEE is balanced in time according to the modeling philosophy (super grass), that is in accordance with the measurement data (*Haszpra et al.*, 2005). Grassland carbon uptake decreases in time during the growing season because of its higher sensitivity to drought. These results are in accordance with the field evidence (*Barcza et al.*, 2003; *Nagy et al.*, 2007). During the dormant season, the ecosystems are net sources of CO_2, although for croplands it might be somewhat overestimated by the model (see above). Ecosystem respiration is the highest for deciduous forests probably due to decomposition of the high amount of organic matter. Respiration of coniferous forests is relatively low during the dormant season.

The daily data were aggregated for each year, for each grid cell, and for the entire area of Hungary taking into account the spatial extent of the different plant functional types in each individual grid cell. The annual sums of NEE for the different land cover types are presented in *Table 1* and also in *Fig. 3*. The data suggest that croplands are usually sources of carbon dioxide, grasslands are net sources or net sinks, while forest areas are usually net sinks. The balance shows that biosphere is a net source in Hungary. It seems that, on country level, the forests and croplands are the largest sinks and sources, respectively, but the contribution of grasslands must not be neglected, either.

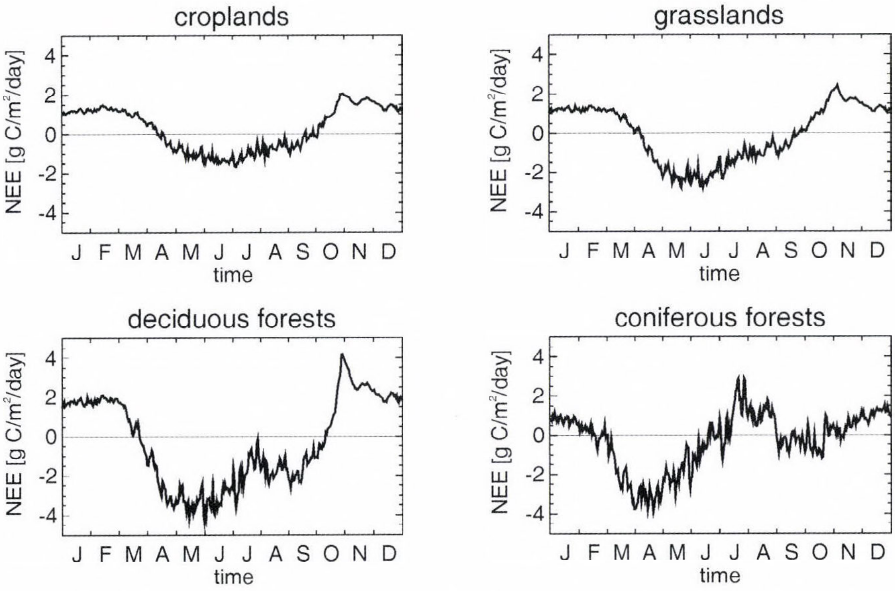

Fig. 2. Six-year mean annual cycle of modeled net ecosystem exchange of the different plant functional types averaged for all grid points. Negative NEE indicates carbon uptake by the vegetation.

Table 1. Biospheric carbon dioxide balance of Hungary estimated by the BIOME-BGC model for the time period of 2002–2007 (Mt C/year). Negative values indicate carbon uptake by the vegetation

	2002	**2003**	**2004**	**2005**	**2006**	**2007**
Croplands	5.12	4.06	4.92	5.55	4.85	3.86
Grasslands	-0.08	0.80	-0.60	-0.55	-0.94	0.32
Deciduous forests	-2.05	0.96	-3.09	-3.49	-3.40	-1.02
Evergreen coniferous forests	-0.18	0.08	-0.32	-0.25	-0.18	-0.12
Total	**2.81**	**5.90**	**0.91**	**1.26**	**0.33**	**3.04**

Our aim was not only to determine the average NEE but also to get information on the range of interannual variability (*Fig. 3*). The climate fluctuations significantly influence the activity of the biosphere and, thus, also its carbon balance. The climate variation in the study period (2002–2007) offered a unique possibility to study the effect of these fluctuations. 2003 was an extremely hot and dry year, which ended a long, increasingly warm and dry period followed by cooler and wetter years.

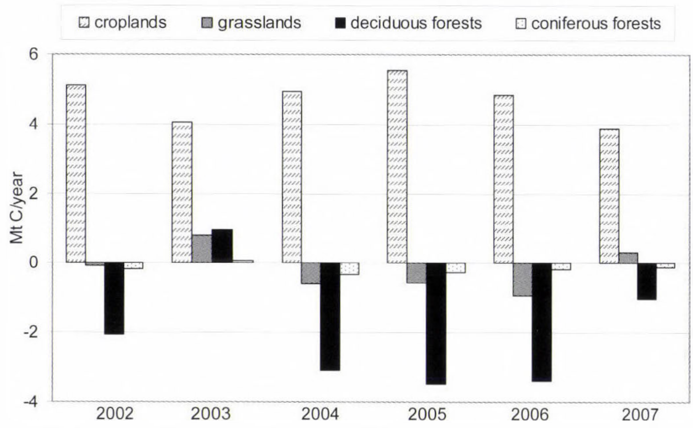

Fig. 3. Biospheric carbon dioxide exchange of the different land cover types for the entire country between 2002 and 2007 (Mt C/year) calculated using BIOME-BGC. Negative values indicate carbon uptake by the vegetation.

exchange data of the four basic land cover types for 2003 and 2004 (for two years with contrasting weather conditions, *Figs. 4* and *5*) show that agricultural fields were net carbon dioxide sources in both years, whereas grasslands were net sources in 2003, but net sinks in 2004 under the more favorable environmental conditions. These results are in accordance with the measurements presented in *Nagy et al.* (2007). In 2003, all ecological systems lost significant amount of organic material due to the extremely hot and dry weather.

The forests, storing a high amount of carbon, reacted more sensitively to the significant climate deviation than the agricultural fields and grasslands (*Figs. 4* and *5*). Except for the higher, cooler and wetter regions of the northern mountainous part of Hungary, both deciduous and coniferous forests were net carbon dioxide sources in 2003. In a significant area of the country the emissions exceeded 300 g C/m^2/year. However, in 2004, which was significantly cooler, and wetter than 2003, they became sinks at a similar rate.

Fig. 6 shows the annual mean biospheric carbon dioxide balance of Hungary for the entire study period (2002–2007). The figure was created from the BIOME-specific simulated NEE data taking into account the spatial extent of the specific land cover types for each grid cell. The figure shows that CO_2 uptake is generally associated with the forested areas (cf., *Fig. 1*). During 2003, almost the entire country became a net carbon dioxide source, only the mountainous regions in Northern Hungary and some other areas in Western Hungary acted as net sinks. It is interesting to see that in 2007, the western part of Hungary became an almost homogeneous net source, similarly to 2003.

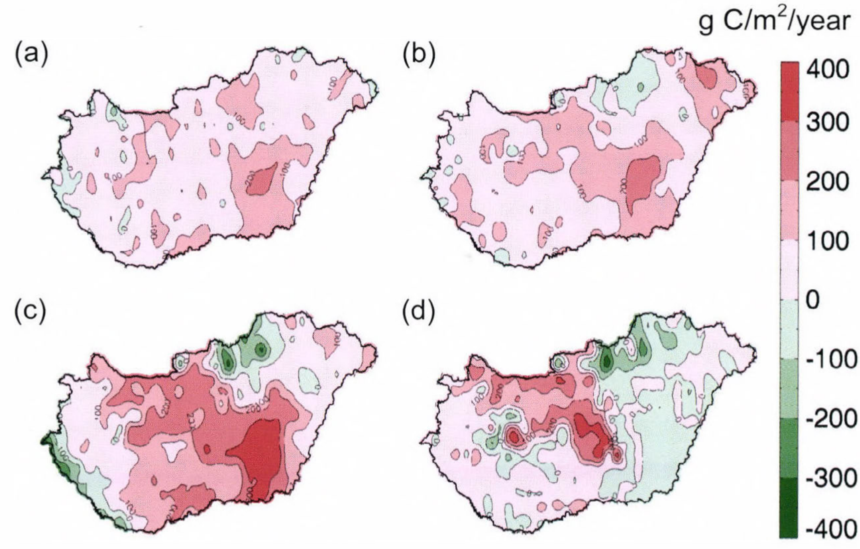

Fig. 4. Net carbon dioxide exchange of the different land cover types in 2003 (g C/m^2/year) estimated by the BIOME-BGC model. Negative values indicate carbon uptake by the vegetation. (a) croplands, (b) grasslands, (c) deciduous forests, (d) coniferous forests. Note that the numbers are only applicable where the specific plant functional types are present (see Fig. 1).

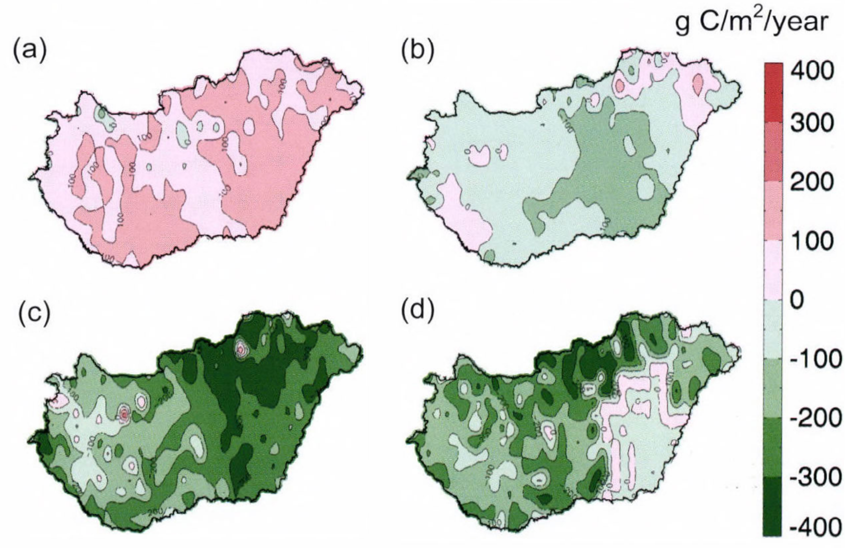

Fig. 5. Net carbon dioxide exchange of the different land cover types in 2004 (g C/m^2/year) estimated by the BIOME-BGC model. Negative values indicate carbon uptake by the vegetation. (a) croplands, (b) grasslands, (c) deciduous forests, (d) coniferous forests. Note that the numbers are only applicable where the specific plant functional types are present (see Fig. 1).

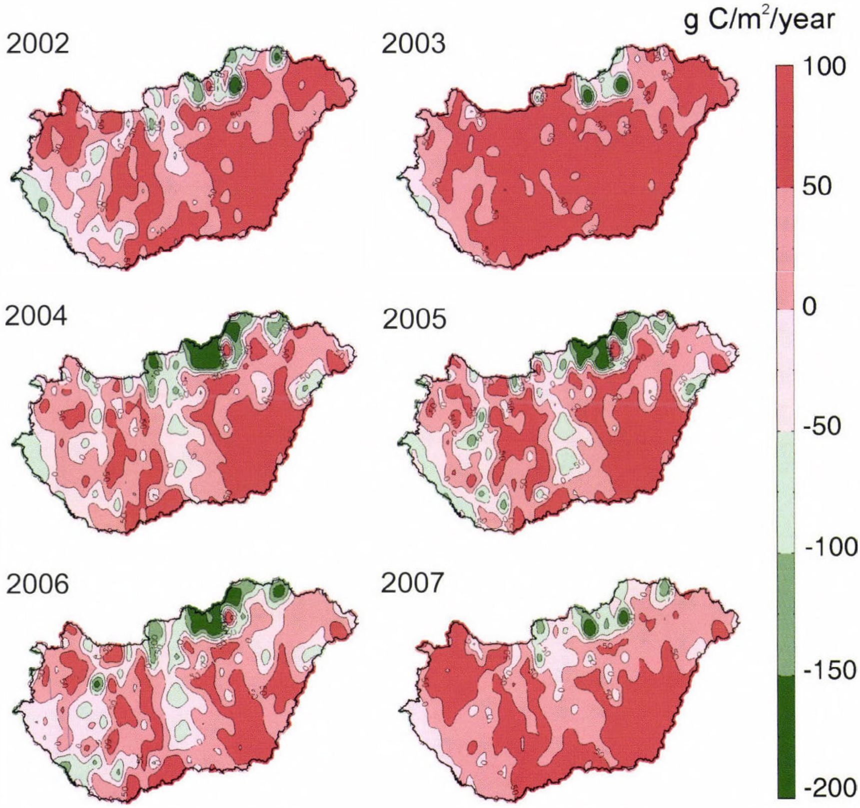

Fig. 6. Mean biospheric carbon dioxide balance of Hungary for the entire study period (2002–2007) estimated by the BIOME-BGC model (g C/m^2/year). The simulated, BIOME-specific NEE data were weighted for each grid cell. Negative values indicate carbon uptake by the vegetation.

4. Discussion

The model estimates in this study show that the net carbon dioxide balance of Hungary is positive, i.e., that the soil-vegetation system is a net carbon dioxide source on national level (*Table 1*). Its main cause is the significant net release from the agricultural fields. Any change in the ratio of the agricultural and forest areas would modify the biospheric carbon dioxide balance.

The model estimates were compared with the data reported by Hungary to the UNFCCC (*HMS*, 2008; see also *UNFCCC*, 2006). Under the UNFCCC, Hungary reported emissions of – 0.76, – 5.44, 0.24, – 0.85, and – 0.01 kt C/year for 2002, 2003, 2004, 2005, and 2006, respectively, for croplands and grasslands together, which are much lower emission estimates than those calculated by BIOME-BGC. On the other hand, Hungary reported net removals of 0.86, 1.31, 1.11, 1.58, and 1.27 Mt C/year for forests, which are considerably lower than those estimated by BIOME-BGC. At the same time, it is known that BIOME-BGC may tend to overestimate the annual net CO_2 release of croplands, but quantification of this likely overestimation needs further research. Some of the differences are due to known discrepancies in methodology. The IPCC deals with the estimation of greenhouse gas emissions and removals from human activities and takes into account yearly changes in land use instead of using one land use database. Accordingly, carbon stock changes on *managed land* in the relevant carbon pools are reported under the IPCC methodology that exludes reporting on unmanaged land, which is only required when unmanaged land is subject to land use conversion. As regards forests, Hungary reported under the UNFCCC the change only in biomass carbon pool, while soil and dead organic matter carbon pools have not been reported yet due to lack of appropriate databases. In cropland and grassland categories the changes in soil carbon pool are reported which are influenced by changes of the way land was used (abandonment of croplands and pastures, afforestation of croplands and grasslands, and tillage practices). In accordance with the IPCC methodology, the change in biomass in cropland category is estimated only for perennial woody crops. (The results of the sequestration of perennial woody biomass were not taken into account in the comparison.) For annual crops, the increase in biomass stocks in a single year is assumed to be equal to biomass losses from harvest and mortality in the same year. Thus, there is no net accumulation of biomass carbon stocks on cropland by the IPCC methodology under default assumptions. In grassland, where management practices are static, biomass carbon stocks are in an approximate steady-state, so the change in biomass carbon pool is neglected as well. Even though there are differences between the methodology of the IPCC and the model approach, this comparison clearly suggests that further studies are needed to identify the possible causes of the major differences. Due to the simplified methodology and limited data bases of both approaches, both the BIOME-BGC and the IPCC-based inventory approach should be analyzed and developed to harmonize estimates.

Fig. 7 shows the national biospheric carbon dioxide balance calculated by us and *Janssens et al.* (2005). Janssens and his coworkers (*Janssens et al.*, 2005) used a completely different approach: they estimated carbon budget based on changes in the carbon stocks, which means that they did not estimate biospheric NEE but the stock change. Of course NEE is related to the C stock change both in forests and croplands. In spite of the different methodology, their results are close to ours, though they only gave an overall value for the period studied. 2003 cannot be considered a typical year, therefore, its inclusion or exclusion significantly influences the 2002–2007 average.

It can be seen in *Fig. 7* that the significant net CO_2 release of the agricultural fields is remarkable in both cases. Because of the high share of the agricultural fields in the national net carbon dioxide balance and the related uncertainty in the model performance, the study of the agricultural carbon cycle could be an important target of the Hungarian research.

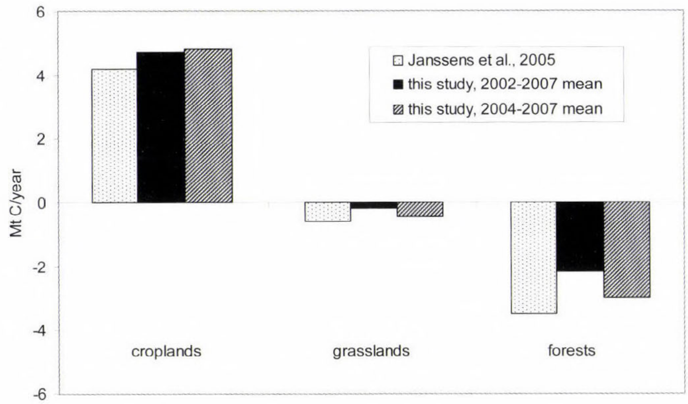

Fig. 7. Biospheric carbon dioxide balance of Hungary based on the country specific run of BIOME-BGC (present study), and on the data provided by *Janssens et al.* (2005). Negative values indicate carbon uptake by the vegetation. 2003 can not be considered a typical year (see text), thus, its inclusion or exclusion influences the average balance.

In order to illustrate the order of magnitude of our model results, it is interesting to mention that in the 2002–2005 period, the mean total anthropogenic carbon dioxide emission of Hungary, excluding emissions and removals from land use, land-use change, and forestry, was 60.75 million tons CO_2 (16.57 Mt C) (*HMS*, 2008). According to the model calculations presented, the biosphere in Hungary adds 8.7 million tons of CO_2 to this amount every year on average (2002–2007 mean) with significant interannual variation: the highest net emission was calculated for 2003 (21.6 Mt CO_2), while the lowest for 2006 (1.2 Mt CO_2).

Although forests sequester a significant amount of carbon dioxide, their CO_2 uptake may decrease or disappear with the warming climate, as it was experienced in 2003. According to the model results, the prevailing weather dramatically and rapidly influences the carbon dioxide exchange, i.e., the CO_2 uptake of the biosphere. This finding is supported by the measurements at Hegyhátsál where the net CO_2 exchange of the mixed agricultural lands changed significantly, from +69 g C/m^2/year (source) to –107 g C/m^2/year (sink) from 2003 to 2004 (*Haszpra et al.*, 2005).

Grasslands and forests are usually net carbon dioxide sinks. However, the uptake does not necessarily mean long term carbon storage. A large portion of the carbon dioxide taken up by croplands and grasslands may quickly return to the atmosphere through the consumption of the biomass by humans or animals. The total amount of carbon dioxide taken up by the forests is not stored in the forests forever either: the carbon content of the forest vegetation also returns into the atmosphere sooner (from firewood or due to disturbances) or later (from harvested wood products like furniture, buildings, other construction materials). The above mentioned processes must be taken into account in order to provide a full carbon budget of the biosphere. The extension of the present study with the quantitative estimate of horizontal carbon transport may provide a useful tool for constraining the total carbon budget of Hungary.

Acknowledgements—Biome-BGC version 4.1.1 was provided by the Numerical Terradynamic Simulation Group (NTSG) at the University of Montana. NTSG assumes no responsibility for the proper use of Biome-BGC by others. Use of the TV-tower and transmitter building at Hegyhátsál is kindly provided by Antenna Hungária Corporation. During the years, the measurements were/are supported by the U.S.-Hungarian Scientific and Technological Joint Fund (J. F. No. 162 and 504), the Agency of Industrial Science and Technology (Japan), the Bilateral Japanese-Hungarian Intergovernmental S&T Cooperation, the Hungarian National Scientific Research Fund (OTKA T7282, T23811, N31783, T42941), the Hungarian Ministry of Economy and Transport (GVOP-3.2.1.-2004-04-0107/3.0, GVOP-AKF-3.1.1.-2004-05-0358/3.0), the INTERREG IIIB CADSES program (5D038), furthermore, the EC's 5th and 6th R&D Framework Programme (EVK2-CT-1999-00013, EVK2-CT-2002-00163, GOCE-CT-2003-505572, GOCE-037005). The copyright owner of the CLC50 database is the Institute of Geodesy, Cartography and Remote Sensing, Budapest (FÖMI). The authors highly appreciate the help and advice of *T. Szentimrei*, *R. Hodossyné Rétfalvi*, *B. Birszki* (Hungarian Meteorological Service, Budapest, Hungary), *J. Szabó*, *L. Pásztor* (Research Institute for Soil Sciences and Agricultural Chemistry, Budapest, Hungary), *K. Trusilova*, *E. Tomelleri*, *M. Jung* (Max Planck Institute for Biogeochemistry, Jena, Germany), *Z. Nagy*, *K. Pintér*, *Z. Tuba* (Szent István University, Gödöllő, Hungary), *A. Kern* (Hungarian Academy of Sciences, Budapest, Hungary).

References

Barcza, Z., Haszpra, L., Kondo, H., Saigusa, N., Yamamoto, S., and *Bartholy, J.*, 2003: Carbon exchange of grass in Hungary. *Tellus 55B*, 187-196.

Bürger, G., 1997: On the disaggregation of climatological means and anomalies. *Climate Res. 8*, 183-194.

Cao, M., Prince, S. D., and *Shugart, H. H.*, 2002: Increasing terrestrial carbon uptake from the 1980s to the 1990s with changes in climate and atmospheric CO_2. *Global Biogeochem. Cy. 16*, 1069, doi:10.1029/2001GB001553.

Churkina, G., Tenhunen, J., Thornton, P., Falge, E.M., Elbers, J.A., Erhard, M., Grunwald, T., Kowalski, A.S., and *Sprinz, D.*, 2003: Analyzing the ecosystem carbon dynamics of four European coniferous forests using a biogeochemistry model. *Ecosystems 6*, 168–184.

Ciais, P., Bousquet, P., Freibauer, A., and *Naegler, T.*, 2007: Horizontal displacement of carbon associated with agriculture and its impacts on atmospheric CO_2. *Global Biogeochem. Cy. 21*, GB2014, doi:10.1029/2006GB002741.

Cox, P.M., Betts, R.A., Jones, C.D., Spall, S.A., and *Totterdell, I.J.*, 2000: Acceleration of global warming due to carbon-cycle feedbacks in a coupled climate model. *Nature 408*, 184-187.

Denman, K.L., Brasseur, G., Chidthaisong, A., Ciais, P., Cox, P.M., Dickinson, R.E., Hauglustaine, D., Heinze, C., Holland, E., Jacob, D., Lohmann, U., Ramachandran, S., da Silva Dias, P.L., Wofsy, S.C., and *Zhang, X.*, 2007: Couplings Between Changes in the Climate System and Biogeochemistry. In *Climate Change 2007: The Physical Science Basis.* Contribution of Working Group I to the Fourth Assessment Report of the Intergovernmental Panel on Climate Change [(*Solomon, S., D. Qin, M. Manning, Z. Chen, M. Marquis, K.B. Averyt, M. Tignor* and *H.L. Miller* (eds.)]. Cambridge University Press, Cambridge, United Kingdom and New York, NY, USA.

Friedlingstein, P., Cox, P., Betts, R., Bopp, L., von Bloh, W., Brovkin, V., Cadule, P., Doney, S., Eby, M., Fung, I., Bala, G., John, J., Jones, C., Joos, F., Kato, T., Kawamiya, M., Knorr, W., Lindsay, K., Matthews, H.D., Raddatz, T., Rayner, P., Reick, C., Roeckner, E., Schnitzler, K.-G., Schnur, R., Strassmann, K., Weaver, A.J., Yoshikawa, C., and *Zeng, N.*, 2006: Climate-carbon cycle feedback analysis: results from the C4MIP model intercomparison. *J. Climate 19*, 3337-3353.

Gervois, S., Ciais, P., de Noblet-Ducoudré, N., Brisson, N., Vuichard, N., and *Viovy, N.*, 2008: Carbon and water balance of European croplands throughout the 20th century. *Global Biogeochem. Cy. 22*, GB2022, doi:10.1029/2007GB003018

Haszpra, L., Barcza, Z., Bakwin, P.S., Berger, B.W., Davis, K.J., and *Weidinger, T.*, 2001: Measuring system for the long-term monitoring of biosphere/atmosphere exchange of carbon dioxide. *J. Geophys. Res. 106D*, 3057-3070.

Haszpra, L., Barcza, Z., Davis, K. J., and *Tarczay, K.*, 2005: Long-term tall tower carbon dioxide flux monitoring over an area of mixed vegetation. *Agr. Forest Meteorol. 132*, 58-77.

Hidy, D., Barcza, Z., Haszpra, L., Churkina, G., and *Trusilova, K.*, 2007: Parameter estimation for grassland carbon cycle using nonlinear inversion of Biome-BGC. *Cereal Res. Commun. 2*, 453-456.

HMS, 2008: *National Inventory Report for 1985-2006 Hungary*. Hungarian Meteorological Service, Budapest, Hungary. http://unfccc.int/national_reports/annex_i_ghg_inventories/national_inventories_submissions/items/4303.php

Hollinger, D.Y. and *Richardson, A.D.*, 2005: Uncertainty in eddy covariance measurements and its application to physiological models. *Tree Physiol. 25*, 873-885.

IPCC, 1997: Revised 1996 IPCC Guidelines for National Greenhouse Inventories [*Houghton, J.T., Meira Filho, L.G., Lim, B., Tréanton, K., Mamaty, I., Bonduki, Y., Griggs, D.J. and Callander, B.A.* (eds.)]. IPCC/OECD/IEA, Paris, France.

IPCC, 2003: Good Practice Guidance for Land Use, land-Use Change and Forestry [*Penman J., Gytarsky M., Hiraishi T., Krug, T., Kruger D., Pipatti, R., Buendia, L., Miwa, K., Ngara, T., Tanabe, K., Wagner, F.* (eds.)]. IPCC/IGES, Hayama, Japan.

IPCC, 2006: IPCC Guidelines for National Greenhouse Gas Inventories, Prepared by the National Greenhouse Gas Inventories Programme [*Eggleston H.S., Buendia L., Miwa K., Ngara T. and Tanabe K.* (eds.)]. Published: IGES, Japan.

Jansen, E., Overpeck, J., Briffa, K.R., Duplessy, J.-C., Joos, F., Masson-Delmotte, V., Olago, D., Otto-Bliesner, B., Peltier, W.R., Rahmstorf, S., Ramesh, R., Raynaud, D., Rind, D., Solomina, O., Villalba, R., and *Zhang, D.*, 2007: Palaeoclimate. In *Climate Change 2007: The Physical Science Basis.* Contribution of Working Group I to the Fourth Assessment Report of the Intergovernmental Panel on Climate Change [*Solomon, S., Qin, D., Manning, M., Chen, Z., Marquis, M., Averyt, K. B., Tignor, M.* and *Miller, H.L.* (eds.)]. Cambridge University Press, Cambridge, United Kingdom and New York, NY, USA. 433-497.

Janssens, I.A., Freibauer, A., Ciais, P., Smith, P., Nabuurs, G.-J., Folberth, G., Schlamadinger, B., Hutjes, R.W.A., Ceulemans, R., Schulze, E.-D., Valentini, R., and *Dolman, A.J.*, 2003: Europe's terrestrial biosphere absorbs 7 to 12% of European anthropogenic CO_2 emissions. *Science 300*, 1538–1542.

Janssens, I.A., Freibauer, A., Schlamadinger, B., Ceulemans, R., Ciais, P., Dolman, A.J., Heimann, H., Nabuurs, G.-J., Smith, P., Valentini, R., and *Schulze, E.-D.*, 2005: The carbon budget of terrestrial ecosystems at country-scale - a European case study. *Biogeosciences 2*, 15-26.

Nagy, Z., Pintér, K., Czóbel, Sz., Balogh, J., Horváth, L., Fóti, Sz., Barcza, Z., Weidinger, T., Csintalan, Zs., Dinh , N.Q., Grosz, B., and *Tuba, Z.*, 2007: The carbon budget of semi-arid grassland in a wet and a dry year in Hungary. *Agr. Ecosyst. Environ. 121/1-2*, 21-29. doi: 10.1016/j.agee.2006.12.003

New, M., Lister, D., Hulme, M., and *Makin, I.*, 2002: A high-resolution data set of surface climate over global land areas. *Climate Res. 21*, 1-25.

Pietsch, S.A., Hasenauer, H., and *Thornton, P.E.*, 2005: BGC-model parameters for tree species growing in central European forests. *Forest Ecol. Manag. 211*, 264-295.

Running, S.W. and *Coughlan, J.C.*, 1988: A general model of forest ecosystem processes for regional applications I. Hydrological balance, canopy gas exchange and primary production processes. *Ecol. Model. 42*, 125-154.

Running, S.W. and *Gower, S.T.*, 1991: Forest-BGC, A general model of forest ecosystem processes for regional applications II. Dynamic carbon allocation and nitrogen budgets. *Tree Physiol. 9*, 147-160.

Running, S.W. and *Hunt, E.R.J.*, 1993: Generalization of a forest ecosystem process model for other biomes, Biome-BGC, and an application for global-scale models. In *Scaling Physiological Processes: Leaf to Globe* (eds.: *J.R. Ehleringer, C.B.* Field). San Diego (CA): Academic Press, 141-158.

Somogyi, Z., 2007: A Kyotoi Jegyzőkönyv és az erdők (in Hungarian). *Erdészeti Lapok 142*, 152-154.

Thornton, P.E., Hasenauer, H., and *White, M.A.*, 2000: Simultaneous estimation of daily solar radiation and humidity from observed temperature and precipitation: an application over complex terrain in Austria. *Agr. Forest Meteorol. 104*, 255–271.

UNFCCC (United Nations Framework Convention on Climate Change), 2006: National greenhouse gas inventory data for the period 1990–2004 and status of reporting. *Report on national greenhouse gas inventory data from Parties included in Annex I to the Convention for the period 1990–2004.* FCCC/SBI/2006/26. http://unfccc.int/documentation/documents/advanced_search/items/3594.php?rec=j&priref=600004015#beg

Vetter, M. Churkina, G., Jung, M., Reichstein, M., Zaehle, S., Bondeau, A., Chen, Y., Ciais, P., Feser, F., Freibauer, A., Geyer, R., Jones, C., Papale, D., Tenhunen, J., Tomelleri, E., Trusilova, K., Viovy, N., and *Heimann, M.*, 2007: Analyzing the causes and spatial pattern of the European 2003 carbon flux anomaly in Europe using seven models. *Biogeosciences Discussions 4*, 1201-1240.

White, M.A., Thornton, P.E., Running, S.W., and *Nemani, R.R.*, 2000: Parameterization and sensitivity analysis of the Biome-BGC terrestrial ecosystem model: net primary production controls. *Earth Interactions 4*, 1-85.

IDŐJÁRÁS

Quarterly Journal of the Hungarian Meteorological Service
Vol. 113, No. 3, July–September 2009, pp. 221–231

Seasonal and spatial distribution of physiologically equivalent temperature (PET) index in Hungary

Ágnes Gulyás[1*] and **Andreas Matzarakis**[2]

[1]*Department of Climatology and Landscape Ecology, University of Szeged, P.O. Box 653, H-6701 Szeged, Hungary; E-mail: agulyas@geo.u-szeged.hu*

[2]*Meteorological Institute, Albert-Ludwigs-University of Freiburg, Werthmannstr 10, D-79085 Freiburg im Breisgau, Germany E-mail: andreas.matzarakis@meteo.uni-freiburg.de*

(Manuscript received in final form January 23, 2009)

Abstract—The aim of this study is to present a thermal human bioclimate analysis of Hungary by means of mapping, useing multiple linear regressions. The present study links geographical information with climatological data in order to generate a spatial distribution of PET values of a region. The distribution of average PET values of seasons are drawn at 1 km resolution. Meteorological data used to draw the maps was made with the help of data collation program at the Climatic Research Unit (University of East Anglia, Norwich, UK). The calculation of PET is performed with the aid of the RayMan model, which calculates the measures of the thermal human bioclimate. The calculated PET values show that the difference between the highest and lowest temperature areas is between 7–11 °C. This means two comfort level differences generally. The winter is an exception, when the whole country can be rated to the same physiological stress level.

Key-words: physiologically equivalent temperature, thermal comfort, mapping, Hungary

1. Introduction

Assessing the climatic capabilities of a certain area, bioclimatic aspects have higher and higher significance. In case of densely populated (urban) areas or extensively visited places (popular tourist destination, health resort), the effect of the climate on the inhabitants is an important question. A bioclimatic assessment is a complex task. The effect of the climate on the human body cannot be described by a single meteorological parameter. The air temperature, air humidity, wind, and radiation fluxes never act solely, but form a complex, so-called thermal factor. This complex factor induces certain physiological

* Corresponding author

responses on the human body. Several models and indices were created in the last decades to describe this mechanism and quantify thermo-physiological phenomenon occurring in the human body (*VDI*, 1998).

The recent models, based on the human energy balance, opened new dimensions. These models take into account the heat fluxes (sensible- and latent heat loss, thermal radiation) between the body and the environment as a basis, with several additional empirical factors. Thus the coupling of meteorological parameters and the characteristics of the body give more detailed picture. The output data of the models are different bioclimatological indices, which quantify the extent of the heat stress (*Fanger*, 1972; *Jendritzky et al.*, 1990; *Höppe*, 1993, 1999; *VDI*, 1998; *Matzarakis et al.*, 1999; *Spagnolo* and *de Dear*, 2003).

Assessments can be performed at different spatial and temporal levels, according to the purpose of the study (*Jendritzky et al.*, 1990; *Matzarakis et al.*, 1999; *Koch et al.*, 2005; *Zaninovic et al.*, 2006). Microscale (~1 cm−1 km) studies can be used to examine very small microclimatic phenomena, like, for example, bioclimatic properties of a building, street, or park (*Matzarakis*, 2001; *Mayer* and *Matzarakis*, 1998a,b; *Picot*, 2004; *Gulyás et al.*, 2006; *Knez* and *Thorsson*, 2006). The data produced by such researches, which provides, for instance, quantitative information about optimal street forms in order to regulate the climate comfort, can be applied by architects and urban designers (*Ali-Toudert* and *Mayer*, 2006; *Lin et al.*, 2006). Applied studies at local- and meso-climatic scales (~100 m–200 km) can provide data for urban planning or regional planning (e.g., tourism) (*Matzarakis et al.*, 2004; *Brandenburg* and *Matzarakis*, 2007). Mainly topographical methods are used in case of bioclimatic analysis of larger areas on the macroscale (>200 km). The fast development of geoinformatical methods opens new possibilities also in these studies. Nowadays, analysis of bioclimatic maps is an integral part of regional planning processes in countries with developed tourism infrastructure and industry (*Matzarakis et al.*, 2004; *Lin* and *Matzarakis*, 2008).

The aim of this study is to present a bioclimatic analysis of Hungary by means of bioclimatical mapping with the aid of geo-statistical methods. The present study links geographical information (*Hastings et al.*, 1999) with climatological data (*New et al.*, 1999, 2000, 2002) in order to generate a spatial distribution of the bioclimatological index PET in a region. The determination of PET is performed with the aid of the RayMan Model, which calculates the thermal indices mentioned above (*Matzarakis et al.*, 2000, 2007).

2. *Study area*

Although the original study was done for a larger area, this paper focuses on the description of bioclimatic properties in Hungary (*Fig. 1*).

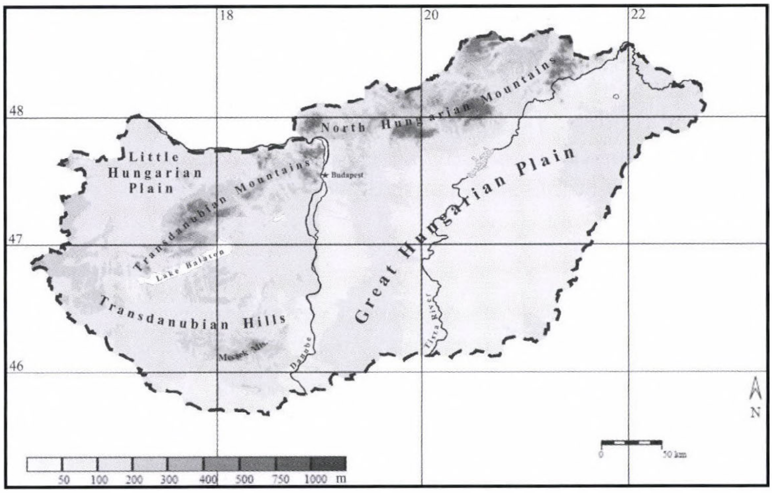

Fig. 1. Geographical location and topography of Hungary (the numbers are northern latitudes and eastern longitudes in degrees).

Hungary is situated in the Carpathian Basin almost in the central part of Europe, between the latitudes 45°48'N and 48°35'N and longitudes 16°05'E and 22°58'E, with an area of 93,030 km^2. As *Fig. 1* shows, it has three basic relief types: the low-lying regions (under 200 m above sea level) of the Great Hungarian Plain in the east, center, and southeast, and of the Little Hungarian Plain in the northwest, which together cover for two-thirds of Hungary's territory. There are the North Hungarian Mountains, the Transdanubian Mountains, and the hilly regions of Transdanubian Hills in the west and southwest.

The main characteristics of Hungary's climate and the frequent fluctuations in climatic factors are greatly due to the central position in Europe. Namely, Hungary is situated at the 'crossroads' of the East-European continental, the West-European oceanic, and subtropical Mediterranean climatic zones (*Pécsi* and *Sárfalvi*, 1964).

Using Köppen's classification, Hungary belongs to the climatic region *Cf*, which is characterized by a temperate warm climate with a rather uniform annual distribution of precipitation. Due to the relatively small spatial extension of the country and small vertical differences, the climate is quite uniform (*Justyák*, 2002).

Its annual mean temperature is 10.4 °C (in Budapest/Lőrinc). The spatial distribution of the temperature is mainly affected by the relief because of the small country size. The annual mean temperature decreases below 8 °C only in the North Hungarian Mountains, the highest peaks of the Transdanubian Mountains and close to the western border of the country. It has highest value on the southern side of the Great Hungarian Plain (just above 11 °C) (*Fig. 2*). The coldest month is January (–1.6 °C), the warmest is July (20.8 °C). Because of the small country area the radiation conditions are affected mainly by the clouds. The sunny hours are between 1700–2100 per year; this value is highest in the Great Hungarian Plain and lowest in the mountains. The yearly global radiation sum is the highest in southeast Hungary (above 5000 MJ m^{-2}), and lowest in the North Hungarian Mountains and near the western borders (below 4300 MJ m^{-2}) (*OMSZ*, 2003).

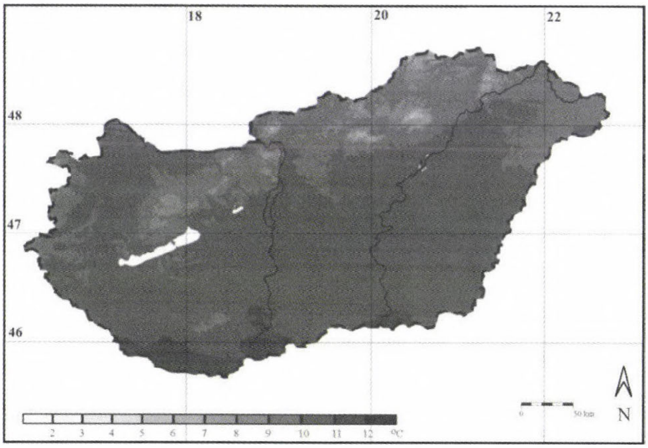

Fig. 2. The spatial pattern of the annual mean temperature in Hungary for the period 1961–1990.

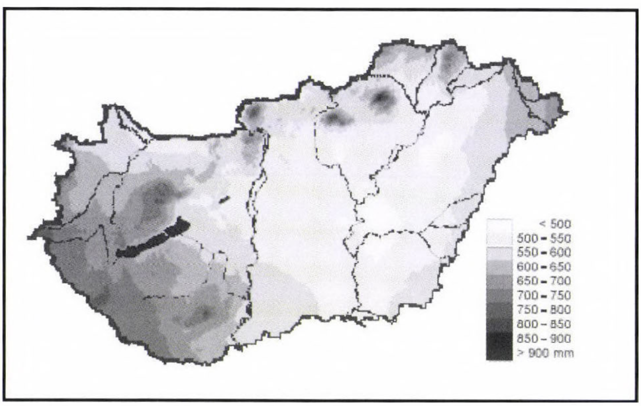

Fig. 3. Annual mean precipitation for the period 1965–1994 (*Szalai et al.*, 2005).

The annual mean precipitation is 612 mm, with high fluctuations between years. The temporal and spatial distribution of the precipitation is variable

(*Fig. 3*). Southwestern Transdanubia (with Mediterranean effect) and the higher mountain regions get considerably higher precipitation than the middle of the Great Hungarian Plain (800–1000 mm and 500–550 mm, respectively). Most of the precipitation falls in spring and summer (*WMO*, 1996). Homogenized datasets show that the climate of Hungary is getting warmer and drier in the last 100 years. This warming is similar to the global tendencies but with a higher extent (especially the summer temperatures and spring precipitation decline) (*Szalai et al.*, 2005).

3. Methods

Lots of thermal indices are used in bioclimatic studies to characterize the bioclimatic conditions of the surroundings on the human body. In this study one of the most widely used bioclimatic thermal indices, the PET is applied. PET evaluates the thermal conditions in a physiologically significant manner (*Höppe*, 1999; *Matzarakis et al.*, 1999). Meteorological parameters influencing the human energy balance, such as air temperature, air humidity, wind speed, and short- and long wave radiation (mostly the mean radiant temperature – T_{mrt} – is used to describe the radiation conditions, like the most important meteorological input parameter for the human energy balance during sunny weather in the hinterland), are represented in the PET values. PET also considers the heat transfer resistance of clothing and the internal heat production. The primary idea in the development of PET was the transfer of the actual thermal bioclimate to an equivalent fictitious indoor environment in which the same thermal sensation can be expected (*Mayer*, 1993). It is defined as the air temperature at which the human energy budget for the assumed indoor conditions is balanced by the same skin temperature and sweat rate as under the actual complex outdoor conditions to be assessed. The assumed indoor conditions are: $T_{mrt} = T_a$, $v = 0.1$ m^{-1}, $VP = 12.0$ hPa, where the T_{mrt} is the mean radiant temperature, T_a is the air temperature, v is the wind speed and VP is the vapor pressure.

PET has a widely known unit (°C) as an indicator of thermal stress and thermal comfort (*Table 1*). This makes the results easily understandable and comprehensible for potential users (according to its definition, PET values around 20 °C can be characterized as comfortable). This is especially the case for planners, decision-makers, and even the public who might be not familiar with modern human-biometeorological terminology (e.g., *Mayer* and *Höppe*, 1987; *Höppe*, 1999).

PET enables various users to compare the integral effects of complex thermal conditions outside with their own experience indoors. *Table 2* shows differences between PET values, calculated in typical summer and winter surroundings.

Table 1. PET for different levels of thermal sensation and physiological stress on human beings (during standard conditions where the heat transfer resistance of clothing is 0.9 clo and the internal heat production is 80 W) (*Matzarakis* and *Mayer*, 1996)

PET (°C)	Thermal sensation	Physiological stress level
	Very cold	Extreme cold stress
4		
	Cold	Strong cold stress
8		
	Cool	Moderate cold stress
13		
	Slightly cool	Slight cold stress
18		
	Comfortable	No thermal stress
23		
	Slightly warm	Slight heat stress
29		
	Warm	Moderate heat stress
35		
	Hot	Strong heat stress
41		
	Very hot	Extreme heat stress

Table 2. Examples of PET values under different environmental conditions

Character of the environment	T_a (°C)	T_{mrt} (°C)	v (m s^{-1})	VP (hPa)	PET (°C)
Typical indoor	21	21	0.1	12	21
Winter, sunny	-5	40	0.5	2	10
Winter, shaded	-5	-5	5.0	2	-13
Summer, sunny	30	60	1.0	21	43
Summer, shaded	30	30	1.0	21	29

One of the recently developed radiation and bioclimate models, the RayMan, is well-suited to calculate radiation fluxes (*Matzarakis*, 2002), and thus, all our calculations for T_{mrt} and PET were performed using this model. The RayMan model, developed according to the Guideline 3787 of the German Engineering Society (*VDI*, 1998), calculates the radiation flux in easy and complex environments on the basis of various parameters, such as air temperature, air humidity, degree of cloud cover, time of day and year, albedo of the surrounding surfaces, and their solid-angle proportions. The main advantage of RayMan is that it facilitates the reliable determination of the microclimatological modifications of different urban environments, since the model considers the radiation modification effects of the complex surface structure (buildings, trees) very precisely. Beside the meteorological parameters, the model requires input data on surface morphological conditions of the study area and on personal parameters.

The climate data used for this analysis were provided by the data collation program at the Climatic Research Unit (University of East Anglia, Norwich, UK) (*New et al.*, 1999, 2000, 2002). The required data for the thermal bioclimate analysis − air temperature, relative humidity, sunshine, and wind speed − are available at monthly resolution for the climate period 1961 to 1990 for the specific area. The calculated PET grid values have been used as dependent variables. They have been recalculated into a higher spatial resolution (1 km) by the use of geo-statistical methods – multiple linear regression – (independent variables were latitude, longitude, and elevation). The multiple regression of the three factors can be applied to construct maps (*Matzarakis* and *Mayer*, 1997). For this purpose the digital elevation data of the GLOBE data set was used (*Hastings et al.*, 1999).

4. Results

Fig. 4 show the spatial seasonal distribution of the PET in Hungary, with spatial resolution of 1 km. Like climatic parameters, the bioclimatic parameters also show homogeneous distribution, because the majority of the country is a plain with less than 200 m elevation above the sea level. The highest PET values can be observed throughout the whole year in the south (S, SE, SW) part of the country (except for the winter). The mountains show lover PET values, especially the North Hungarian Mountains, where the lowest seasonal values can be calculated. Generally, the differences are not too high, the difference between the highest and lowest values is around 7–10 °C, thus, there is no considerable difference between the thermal sensation categories. (Obviously, this is true for the average values, which hide the extremities.)

The difference between the highest and lowest PET values is ~7 °C in *spring* (March, April, May) (*Fig. 4a*). The highest PET value (11 °C) is calculated on the southern part of the Great Hungarian Plain (except for the Duna-Tisza Interfluve) and of Transdanubian Hills. The decrease of the PET value at higher elevations is more pronounced in the North Hungarian Mountains than in other mountains. This difference means two categories in the physiological stress level, according to the average spring PET values. Thus, the warmest areas can be classified to the moderate cold stress level, while the coldest to the extreme cold stress, while the majority of the area of the country belongs to the strong cold stress level zone.

In *summer* (June, July, August) the spatial distribution of the PET values is similar to the spring situation (*Fig. 4b*). The range of PET distribution is a little higher between the highest and lowest values: ~10.5 °C. There are a two categories difference (from the slight cold stress to the slight heat stress) on the area in summer, showing 14–24.5 °C end values. These averaged values cover the extremities which are typical in the Carpathian Basin. The higher PET values (~24.5 °C) around Lake Balaton have not only touristic importance.

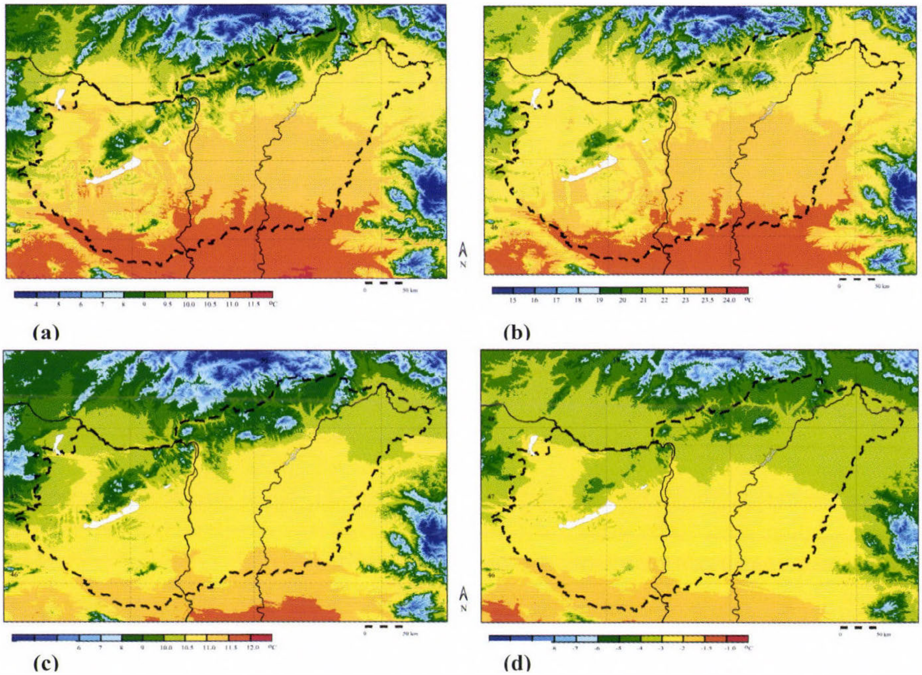

Fig. 4. Spatial distribution of PET in Hungary for (a) spring, (b) summer, (c) autumn, and (d) winter for the period 1961–1990.

The difference between the highest and lowest PET values is smaller again in *autumn* (September, October, November), it is around 7 °C (*Fig. 4c*). The values and their spatial distribution is similar to the situation in spring: 4–11 °C PET values, from the extreme cold stress to the moderate cold stress. The highest values restricted to the southern parts of the Great Hungarian Plain, the valley of Danube, and the south part of the Transdanubia. The tendency of the decrease in the southwest – northeast direction is clear on the region east of Tisza River. The pattern is more detailed in Transdanubia, due to the more diverse relief. The positive anomaly at the Lake Balaton can clearly be identified.

The bioclimatic situation of the *winter* (December, January, February) is the most homogeneous amongst the seasons (*Fig. 4d*), despite the higher difference between the lowest and highest PET values (9 °C). The lowest values can be observed at the highest peaks of the North Hungarian Mountains, covering small areas. The distribution on the Great Hungarian Plain also changed. The highest values can be observed only on the southern part of Transdanubia, possibly due to the Mediterranean effect (the Mediterranean cyclones have the strongest effect reducing continentality on this area during winter). The PET value on the Great Hungarian Plain decreases gradually from southwest towards northeast. The Transdanubian Mountains cannot be clearly separate from their surroundings in bioclimatic aspect. This is especially true in case of the Mecsek Mountains. (It has to be noted, however, that the deficiency of the interpolation and the not calculated exposition data together might cause this phenomenon.) There is no pronounced positive anomaly around the Lake Balaton in winter. These geographical distributions do not mean different categories at the physiological stress level. The whole area of the country can be categorized to the extreme cold stress, with different intensities.

5. Conclusions

- The main novelty of our study is the first publication of maps, based on the output of a modern bioclimatic index, which refers to the human energy balance. Moreover, these calculations were performed for the whole area of Hungary with a resolution of 1 km.
- Seasonal pattern with this resolution shows characteristic spatial structure, with high similarities between the spring-summer and autumn-winter season-pairs.
- Taken the whole area of the country into consideration, there are generally two comfort level differences between the highest and lowest averaged PET values. In summer it means that the thermal sensation on some areas shows cold stress, while on others it shows heat stress. Exception is the winter, when the whole area belongs to the same physiological stress level.
- The bioclimatic situation shows homogeneous distribution due to the relatively small latitudinal and longitudinal extent and low altitudes. The Transdanubian Mountains are not separated distinctly from their surroundings in a bioclimatological sense, especially in winter, when the Mediterranean cyclones reduce continentality on this area.
- The pattern of the Great Hungarian Plain shows a southwest-northeast gradient, that can be ascribed to the increasing continental effect.
- The surroundings of the Lake Balaton, which has touristic importance, show higher PET values than the neighbouring areas, throughout the whole year. This bioclimatological difference does not stand out characteristically, only in winter.

Finally, as we earlier mentioned, the analysis has been performed with no direct data from observations by climate networks. The application of the CRU database has certain limitations on the area of Hungary. The present method includes geographical latitude, longitude, and elevation, but not the aspect ratio, exposition, and land use, which could produce inappropriate results with the existing dataset. Climate modeling offers, in our opinion, diverse opportunities and possibilities of data in order to perform seasonal or monthly climate analysis. Due to the lack of available data sets, our results have not been compared to measured data, but we hope we will have opportunity to perform this analysis in the near future. Based on the existing data sets, several analyses for sensitive areas and sectors, i.e., agriculture, tourism, health, and regional planning can be performed, especially concerning expected climate change conditions.

Acknowledgements—The work of Ágnes Gulyás was supported by the Baden-Württembergisches Landesstipendium. Thanks to *János Unger* for proofreading and editing the manuscript.

References

Ali-Toudert, F. and *Mayer, H.*, 2006: Numerical study on the effects of aspect ratio and orientation of an urban street canyon on outdoor thermal comfort in hot and dry climate. *Build. Environ. 41*, 94-108.

Brandenburg, C. and *Matzarakis, A.*, 2007: Das thermische Empfinden von Touristen in der Region Neusiedlersee, *Ber. Meteor. Inst. Univ. Freiburg Nr. 16*, 67-72.

Fanger, P.O., 1972: *Thermal Comfort*. New York Mc Graw–Hill.

Gulyás, Á., Unger, J., Matzarakis, A., 2006: Assessment of the microclimatic and thermal comfort conditions in a complex urban environment: modelling and measurements. *Build. Environ. 41*, 1713-1722.

Hastings, D.A., Dunbar, P.K., Elphingstone, G.M., Bootz, M., Murakami, H., Maruyama, H., Masaharu, H., Holland, P., Payne, J., Bryant, N.A., Logan, T., Muller, J.-P., Schreier, G., MacDonald, J.S. (eds.) 1999: *The Global Land One-kilometer Base Elevation (GLOBE) Digital Elevation Model, Version 1.0*. National Oceanic and Atmospheric Administration, National Geophysical Data Center, 325 Broadway, Boulder, Colorado 80303, U.S.A. Digital data base on the World Wide Web (http://www.ngdc.noaa.gov/mgg/topo/globe.html)

Höppe, P., 1993: Heat balance modelling. *Experientia 49*, 741-745.

Höppe, P., 1999: The physiological equivalent temperature – a universal index for the biometeorological assessment of the thermal environment. *Int. J. Biometeorol. 43*, 71-75.

Jendritzky, G., Menz, H., Schirmer, H., Schmidt-Kessen, W., 1990: Methodik zur raumbezogene Bewertung der thermischen Komponente im Bioklima des Menschen (Fortgeschriebenes Klima-Michel-Modell). *Beitr. Akad. Raumforsch. Landesplan.* No. 114.

Justyák, J., 2002: *Climate of Hungary* (in Hungarian). Kossuth Egyetemi Kiadó, Debrecen, Hungary.

Knez, I. and *Thorsson, S.*, 2006: Influences of culture and environmental attitude on thermal, emotional and perceptual evaluations of a public square. *Int. J. Biometeorol. 50*, 258-268.

Koch, E., Marktl, W., Matzarakis, A., Nefzger, H., Rudel, E., Schunder-Tatzber, S., Zygmuntowski, M., 2005: Klimatherapie in Österreich. *Broschüre zu den Potentialen der Klimatherapie in Österreich. Bundesministerium für Wirtschaft und Arbeit.*

Lin, T.-P. and *Matzarakis, A.*, 2008: Tourism climate and thermal comfort in Sun Moon Lake, Taiwan. *Int. J. Biometeorol. 52*, 281-290.

Lin, T.-P., Matzarakis, A., Huang, J.-J., 2006: Thermal comfort and passive design strategy of bus shelters. *PLEA2006 - The 23 Conference on Passive and Low Energy Architecture*. Geneva, Switzerland.

Matzarakis, A., 2001: Die thermische Komponente des Stadtklimas. *Ber. Meteorol. Inst. Univ. Freiburg* Nr. 6.

Matzarakis, A., 2002: Validation of modeled mean radiant temperature within urban structures. *AMS Symposium on Urban Environment*, Norfolk, UK, 7.3.

Matzarakis, A. and *Mayer, H.*, 1996: Another kind of environmental stress: Thermal stress. *NEWSLETTERS* No. 18, WHO Collaborating Centre for Air Quality Management and Air Pollution Control, 7-10.

Matzarakis, A. and *Mayer, H.*, 1997: Heat stress in Greece. *Int. J. Biometeorol. 41,* 34-39.
Matzarakis, A., Mayer, H., Iziomon, M., 1999: Applications of a universal thermal index: physiological equivalent temperature. *Int. J. Biometeorol. 43*, 76-84.
Matzarakis, A., Rutz, F., Mayer, H., 2000: Estimation and calculation of the mean radiant temperature within urban structures. In *Biometeorology and Urban Climatology at the Turn of the Millenium* (eds.: *R.J. De Dear, J.D. Kalma, T.R. Oke, A. Auliciems*). Selected Papers from the Conference ICB-ICUC'99, WCASP-50, WMO/TD No. 1026. Sydney 2000, 273-278.
Matzarakis, A., de Freitas, C., Scott, D. (eds.), 2004: Advances in tourism climatology. *Ber. Meteorol. Inst. Univ. Freiburg Nr. 12,* 6-9.
Matzarakis, A., Rutz, F., Mayer, H., 2007: *Modeling radiation fluxes in simple and complex environments – Application of the RayMan model. Int. J. Biometeorol. 51,* 323–334.
Mayer, H. and *Höppe, P.*, 1987: Thermal comfort of man in different urban environments. *Theor. Appl. Climatol. 38,* 43-49.
Mayer, H., 1993: Urban bioclimatology. *Experientia 49,* 957-963.
Mayer, H. and *Matzarakis, A.*, 1998a: The urban heat island seen from the angle of human-biometeorology. *Proc. Int. Symposium on Monitoring and Management of Urban Heat Island.* Fujisawa, Japan, 84-95.
Mayer, H. and *Matzarakis, A.*, 1998b: Human-biometeorological assessment of urban microclimates' thermal component. *Proc. Int. Symposium on Monitoring and Management of Urban Heat Island.* Fujisawa, Japan, 155-168.
New, M., Hulme, M., Jones, P., 1999: Representing twentieth century space-time climate variability. Part I: Development of a 1961–90 mean monthly terrestrial climatology. *J. Climate 12,* 829-856.
New, M., Hulme, M., Jones, P., 2000: Representing twentiethcentury space-time climate variability. Part II: Development of 1901-1996 monthly grids of terrestrial surface climate. *J. Climate 13,* 2217-2238.
New, M., Lister, D., Hulme, M., Makin, I., 2002: A high-resolution data set of surface climate over global land areas. *Climate Res. 21*, 1-25.
OMSZ, 2003: *Climate Atlas of Hungary* (in Hungarian). Országos Meteorológiai Szolgálat, Budapest, Hungary.
Pécsi, M. and *Sárfalvi, B.*, 1964: *The Geography of Hungary. Corvina Press. 8°. XII.*, Budapest, 299 p.
Picot, X., 2004: Thermal comfort in urban spaces: impact of vegetation growth. Case study: Piazza della Scienza, Milan. *Italy Energy and Buildings 36*, 329–334.
Spagnolo, J. and *de Dear, R.*, 2003: A field study of thermal comfort in outdoor and semi-outdoor environments in subtropical Sydney Australia. *Build. Environ. 38*, 721-738.
Szalai, S., Bihari, Z., Lakatos, M., Szentimrey, T., 2005: Some Characteristics of the Climate of Hungary since 1901. Országos Meteorológiai Szolgálat, Budapest, Hungary. http://www.met.hu/pages/climate/Some_characteristics_of_the_climate_of_Hungary_since_1901.pdf
VDI, 1998: Methods for the human-biometeorological assessment of climate and air hygiene for urban and regional planning. Part I: Climate. *VDI Guidline 3787.* Beuth, Berlin.
WMO, 1996: *Climatological Normals (CLINO) for the Period 1961-1990.* WMO/OMM–No. 847, Geneva.
Zaninovic, K., Matzarakis, A., Cegnar, T., 2006: Thermal comfort trends and variability in the Croatian and Slovenian mountains. *Meteorol. Z. 15*, 243-251.

IDŐJÁRÁS

Quarterly Journal of the Hungarian Meteorological Service
Vol. 113, No. 3, July–September 2009, pp. 233–243

Reconciling the sequential probability ratio test with calibration

Alexander Jann

Central Institute for Meteorology and Geodynamics,
Hohe Warte 38, A-1190 Vienna, Austria; E-mail: Alexander.Jann@zamg.ac.at

(Manuscript received in final form June 10, 2009)

Abstract—A common strategy of meteorological calibration is to continuously screen the observational series for (occasional) abrupt changes and – once an alarm has been triggered – to assess how large that change is in order to correct for it. Starting with the analysis of a sequential probability ratio test strategy once proposed in radar meteorology, it is shown that an important enhancement is to combine this change-detection procedure with a dedicated change-point positioning procedure such that the individual capabilities of both methods are exploited. An additional crucial aspect is that – even with a good change-point location – initial estimates of the new state of the system may be quite imprecise, particularly in a real-time application because of small sample sizes. A subsequent rejection of the new calibration coefficient, hence, is not necessarily a sign of another change in the system – it might rather be due to a poor first guess which requires an update. By employing certain cautionary measures in this respect, finally a calibration approach based on comparatively simple statistical analysis principles is obtained, which should be attractive to meteorologists (as well as to practitioners in other disciplines) as it is sound, responsive, and easy to implement.

Key-words: real-time calibration, change-detection, change-point location, parameter estimation, sequential analysis

1. Introduction

Detection of changes in a system is a fundamental problem arising in many scientific disciplines as well as in engineering. There are applications where it suffices to know that a significant change has occurred and to stop the procedure then (e.g., to repair a damaged device). In other instances, however, it is impossible or at least impractical to do so, and it is demanded to estimate the parameters which statistically describe the new state in order to perform a sort of calibration by computational means. Meteorology repeatedly encounters the latter situation. Here are some selected relevant examples:

- In order to account for temporal changes in the sensor characteristics, meteorological satellite operators face a need of calibrating their instruments, for example by using targets on earth with known radiation characteristics (the so-called vicarious calibration). The updating rules apparently have been rather simple in the past, such as to replace the calibration coefficient by a mean of recent instantaneous values if the new value deviates by more than 1% from the former operational value (*van de Berg et al.*, 1995).

- In radar meteorology, much work has been devoted over decades to calibrate weather radars with raingages. The simplest models derived a single gage-to-radar adjustment factor, acknowledging that such a factor varies in time (in this case as the result of a complex mixture of technical and meteorological influences), and rules are needed how to update the calibration factor. One relevant analysis is by *Smith* and *Cain* (1983) who argued that one has to insist on the statistical significance of a suspected change in the series. Otherwise, new adjustment factors arbitrarily computed from time to time would reflect little more than fluctuations in random noise and very likely do more harm than good. Though a rule as the above-mentioned one for vicarious calibration tries, to some degree, to avoid overly often re-calibration, it still may be considered a bit too heuristic and not enough statistics-driven in the light of this analysis.

- The sequential probability ratio test (SPRT) strategy proposed by *Smith* and *Cain* (1983) was picked up later (*Jann*, 1996) in an effort to detect abrupt shifts in the height assigned to a satellite-derived quantity (in order not to mix information from different levels). The implementation was unsuccessful, however, and though some theoretical explanations for this failure were given, back then it could not be demonstrated how to eliminate the shortcomings of the concept.

- Many contributions on the change-detection and change-estimation subjects are also provided by climatologists who have to catch signals in their time series being caused by changes in instruments, etc., in order not to mistake them for a real response of the climate system. Though – unlike the first two applications – this one is not a real-time problem per se, this author recently found it rewarding to handle the statistical problem in a quasi-realtime fashion (*Jann*, 2006).

Benefitting from the experience gained in the last-quoted study, we are ultimately – more than a decade after first touching the subject – in the position to present hereafter a viable implementation of the SPRT for calibration purposes. The ambition behind the investigations documented here was to enhance a technique which we consider attractive for practical purposes because of its simple and transparent nature. It is not expected, however, that the found solution will nowadays have notable impact in the meteorological branch for which the Smith&Cain procedure was originally devised, as the simple segmentation model – with adjustment factors for a radar device held constant in-between breakpoints – appears to have fallen out of favor in this discipline and was superseded by more complex statistical approaches of blending precipitation data from different sources. Nevertheless, there are enough other types of meteorological data requiring straightforward quality control tools, so it appears worthwhile to describe in this note, how – through the addition of simple algorithmic components – we managed to augment the SPRT to better serve the needs of real-time calibration.

2. *Statistical techniques and their implementations*

2.1. The sequential probability ratio test

The principle of the sequential probability ratio test, employed by *Smith* and *Cain* (1983) for their detection of substantial changes in gage-to-radar rainfall amount ratios, is to sample values x_i of a normally distributed variable until the cumulative sum $\sum_i x_i$ confirms or opposes the null hypothesis of retaining an assumed value μ^* for the current population mean. Under the assumption of independently distributed observations x_i, the test decides between the null hypothesis H$_0$: $\mu-\mu^*=0$ and the two-sided alternative hypothesis H$_1$: $\mu-\mu^*=\pm\delta\sigma$, where μ is the (true) population mean, σ is the corresponding standard deviation, and δ is a tolerance parameter describing which deviation one is willing to admit. The SPRT test statistic writes

$$Y=\exp(-n\delta^2/2)\cosh\left((\delta/\sigma)\sum_i\left(x_i-\mu^*\right)\right). \qquad (1)$$

Given prescribed values of type I and type II errors (α and β, respectively), it is checked whether the test statistic satisfies $Y\geq(1-\beta)/\alpha$, in which case H$_0$ is rejected. Alternatively, if the test statistic falls below $\beta/(1-\alpha)$ for some *i*, H$_0$ is accepted. This is basically how far the original implementation of the SPRT (*Wald*, 1947) goes, detecting that at some (unknown) point in the past, the actual mean started to deviate substantially from its supposed value.

2.2. *A first attempt to exploit the sequential probability ratio test in meteorological calibration*

How to proceed in case of a rejection of H_0, as, e.g., in those mentioned practical meteorological applications, where there is need for a new estimate μ^* in order to continue? *Smith* and *Cain* (1983) proposed to simply average the values between the preceding decision of the sequential test and the current rejection decision (in case of an acceptance of H_0, the value μ^* was retained, and another SPRT check of this hypothesis commenced with the next observation). It would have been instructive to assess the performance of this approach using a simulated example like that of *Fig. 1a*!

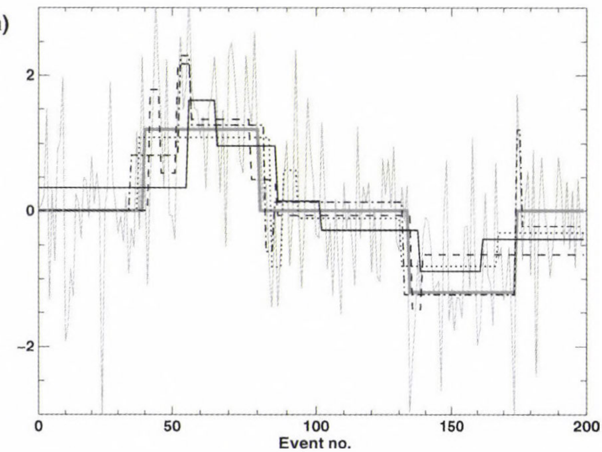

Fig. 1a. Light gray lines show a simulated 200-element time series sampled from a normally distributed population with standard deviation $\sigma=1$. Artificial shifts were applied according to an assumed course of the population mean, which is shown by the bold gray line. Black lines show population means as estimated by *Smith* and *Cain*'s (1983) sequential procedure with initial null hypothesis $\mu^*=0$ (for: $\delta=0.3$ (solid line), $\delta=0.5$ (dotted line), $\delta=0.7$ (dashed line), $\delta=0.9$ (dash-dotted line)).

As in the original report, let the initial null hypothesis be $\mu^*=0$, and $\alpha=\beta=0.1$. Take the curve for $\delta=0.3$: the first SPRT decision is to reject the null hypothesis $\mu^*=0$ at event No. 55; the average of the first 56 elements is 0.342, which is from a mixture of two populations and suits neither. Not surprisingly, this value is rejected ten events later, and from this small number of observations (though in principle 25 members of the second population have already been sampled), a new value of 1.633 is derived, being far off the specified actual value of 1.2. Many more examples of the following phenomena are observable in *Fig. 1a*:

1. quick rejections of unsuitable mean estimates (potentially leading to other highly noise-contaminated estimates which may then again cause rejections; thus, a chain of numerous poor estimates may be obtained even in cases where the mean remains perfectly stable for a long time after a jump),
2. "too late" decisions yielding mean estimates mixing many elements of two different populations with distinct mean.

Some more examples can be found in the original report by *Smith* and *Cain* (1983), where results likewise varied uncontrollably in dependence on δ. The fundamental reason for not being anywhere close to the truth (which is known by design in *Fig. 1*) is not difficult to find: parameter *estimation* tasks are delegated to the sequential probability ratio test, while it is merely a *decision* procedure (note how it does the latter job very well and repeatedly rejects the computed inadequate mean estimates). The two instructions to carry over when attempting to improve the scheme are: (1) once the SPRT indicates that a change has occurred, try to locate that change precisely; (2) yet even if this is done properly, be prepared that the first estimate μ^* could be highly noise-contaminated. Consequently, in the next section, we attempt to resolve the identified shortcomings by combining the detection procedure with a subsequent change-point positioning procedure plus a few cautionary measures on handling the derived mean estimates μ^*, i.e., a mechanism to possibly adapt such a poor hypothesis μ^* later, when more observations from the same population become available.

2.3. The proposed procedure combining change-point detection by the SPRT with separate change-point positioning and parameter estimation

It was argued above that there are two possible reasons why a hypothesis $\mu = \mu^*$ is rejected: one is an actual shift in the series, the other is a poor estimate of the mean, either by mixing populations or by having available too few observations. Therefore, for the case of two subsequent rejections of working hypotheses, the possible scenarios are

1. two actual shifts, or
2. one actual shift with a poor initial estimate of μ (which, using additional data, shall be tuned/updated; if it proves to be appropriate, the additional information shall also allow to shift the change point to a better position).

Consequently, one needs a change-point positioning procedure which evaluates both one-shift and two-shift configurations and is able to select the appropriate model. One candidate is the Schwarz criterion (*Schwarz*, 1978).

(Actually, a variant proposed by *Zurbenko et al.* (1996) is used, which resembles the Caussinus-Lyazrhi rule (*Caussinus* and *Lyazrhi*, 1997) in terms of penalizing the number of change points. See also the comparison results in *Caussinus* and *Mestre* (2004), supporting the choice made here).

$$(n/2)\ln s_a^2 + \nu \ln n \rightarrow \min! \tag{2}$$

where n is the sample size; s_a^2 is the variance of the adjusted series (i.e., for each supposed population the derived sample mean is subtracted from its members); ν designates the number of indicated change points. With this, all components are now assembled to formulate rules how decisions from the SPRT shall be handled in the calibration setting:

1. After an acceptance of the supposed mean, the last-detected shift has apparently been positioned adequately; it consequently may be fixed. As there are now more observations from the population available and one should in general benefit from this, if the hypothesized mean μ^* is recomputed from the larger sample, this is the action to be taken.

2. In case of a rejection after an acceptance, the partial series from the last change point onwards has to be investigated. We expect exactly one change point, so Eq. (2) is evaluated only for such configurations, i.e., $\nu=1$.

3. In case of another rejection after a rejection, the partial series from the last but one change point onwards has to be investigated. Because of the options listed above, the (modified) Schwarz criterion, Eq. (2), has to be investigated for all configurations with 1 or 2 change points.

4. At the very beginning, the procedure is initiated with an arbitrarily assumed hypothesis concerning μ, which easily may be inadequate. So, if the first decision of the SPRT is a rejection of that hypothesis, there is possibly no jump at all in the series investigated so far. Hence, the configurations with 0 or 1 change points have to be examined in this situation.

3. *Results*

For illustrating the mechanims, the same example as above is taken (*Fig. 1b*). It is a clear-cut one, i.e., the sample consists of simulated data satisfying the basic assumptions of the tests, without outliers, violent short-term fluctuations, or other peculiarities in the series, which could adversely affect the performance of the SPRT or the Schwarz test. As there is no point in probing and discussing the robustness of the basic tests in light of the existing literature about them, the focus here is on the proper combined implementation.

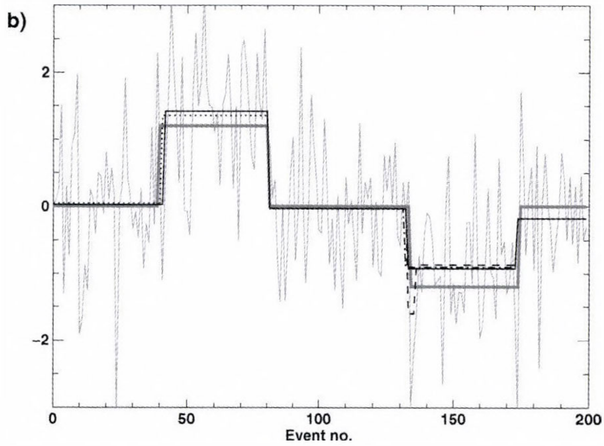

Fig. 1b. Courses of population means, as derived from the SPRT + Schwarz test combination with initial SPRT null hypothesis $\mu^* = 0$ (solid line: for $\delta = 0.3$, dotted line: $\delta = 0.5$, dashed line: $\delta = 0.7$, dash-dotted line: $\delta = 0.9$).

A hypothesis μ^* derived from elements M to N will be denoted as $\mu^*(M-N)$ hereafter. If change-points are fixed and a mean estimate is no longer subject to statistical inference, the asterisk is dropped: $\mu(M-N)$. The term "change-point" shall designate the position *after* which a change in the population mean is taking place. The prescribed values of the test series in *Fig. 1* (i.e., "the truth") are: $\sigma = 1$ (assumed to be known in advance, i.e., before starting the SPRT); $\mu(0-39) = \mu(81-133) = \mu(175-199) = 0$; $\mu(40-80) = 1.2$; $\mu(134-174) = -1.2$.

We start with the results for $\delta = 0.3$:

- Decision No. 1 of the SPRT: Rejection of the null hypothesis $\mu = 0$ at event No. 55; the Schwarz test applied to the series of the first 56 elements proposes to position a change-point at No. 41; $\mu^*(0-41) = 0.023$, and the new working hypothesis is taken from $\mu^*(42-55) = 1.297$.
- Decision No. 2 of the SPRT: Rejection of $\mu^* = 1.297$ at event No. 96; now the Schwarz test has to investigate all elements sampled so far and find out whether there are actually two change-points. It does in fact indicate a two-shift solution, confirming the change-point at No. 41 (which is definitively fixed $\rightarrow \mu(0-41) = 0.023$), and hypothesizing a new one at No. 80. The resulting new working hypothesis is $\mu^*(81-96) = -0.049$, the updated value for the mean of the preceding population $\mu^*(42-80) = 1.422$.

- Decision No. 3 of the SPRT: Rejection of $\mu^* = -0.049$ at event 152. The Schwarz test investigates elements 42 to 152 and proposes a two-step configuration with jumps at No. 132 and, again, at No. 80 (the population mean estimate for elements 42 to 80 is, therefore, definitively accepted as 1.422). The preliminary assumption is that $\mu^*(81-132) = -0.033$; the SPRT continues with $\mu^*(133-152) = -1.032$.
- Decision No. 4 of the SPRT: Rejection of $\mu^* = -1.032$ at event 185. The Schwarz test investigates elements 81 to 185 and once more votes for a two-step configuration with jumps at No. 132 and at No. 173: $\mu(81-132) = -0.033$; the preliminary assumption is that $\mu^*(133-173) = -0.924$; continuation of the SPRT with the new hypothesis $\mu^*(174-185) = -0.185$.
- No further SPRT decision is made until the end of the series. However, a final Schwarz test is performed for elements 133 to 199 to see if the final change-point shall possibly be readjusted on the basis of the latest information that has become available. The position of the break does not alter, however. Assuming that this indicates that elements 174 to 199 are from the very same population, the mean estimate changes slightly from –0.185 to –0.172.

The results for $\delta = 0.5$ should also be briefly considered here in order to illustrate how different the points of time of the SPRT decisions (and consequently the preliminary mean estimates) are and how stable the outcome after combination with the change-point positioning procedure nevertheless eventually is:

- Decision No. 1 of the SPRT: preference of null hypothesis over alternate hypothesis at event No. 18; $\mu^*(0-18) = -0.038$ used as new null hypothesis.
- Decision No. 2 of the SPRT: preference of null hypothesis over alternate hypothesis at event No. 36; $\mu^*(0-36) = -0.047$ used as new null hypothesis.
- Decision No. 3 of the SPRT: rejection of $\mu^* = -0.047$ at No. 44. The Schwarz test positions the change-point at no. 40; $\mu^*(0-40) = 0.051$; $\mu^*(41-44) = 1.003$.
- Decision No. 4 of the SPRT: preference of null hypothesis $\mu^* = 1.003$ over alternate hypothesis at event No. 87; $\mu(0-40) = 0.051$; $\mu^*(41-87) = 1.112$.
- Decision No. 5 of the SPRT: rejection of $\mu^* = 1.112$ at event no. 96, change point at position 80 suggested; $\mu^*(41-80) = 1.359$, new working hypothesis: $\mu^*(81-96) = -0.049$.

- Decision No. 6 of the SPRT: preference of null hypothesis $\mu^* = -0.049$ over alternate hypothesis at event No. 115; update: $\mu^*(81-115) = -0.039$.
- Decision No. 7 of the SPRT: rejection of $\mu^* = -0.039$ at no. 146, with a new change-point indicated at No. 132; $\mu^*(81-132) = -0.033$; $\mu^*(133-146) = -1.111$.
- Decision No. 8 of the SPRT: rejection of $\mu^* = -1.111$ at event No. 181, with the Schwarz test for elements 81 to 181 indicating two change-points at Nos. 132 and 173, $\mu^*(133-173) = -0.924$; $\mu^*(174-181) = -0.076$.
- No further SPRT decision observed. The final Schwarz test at the end of the series adjusts the last change-point by one position to No. 174.

Also the diagram for $\delta = 0.9$ in *Fig. 1b*) shows hardly any differences. For $\delta = 0.7$, 4 elements are pooled together in a separate population around event no. 132; though substantially deviating from the designed course of the population mean, there is little to discuss about this glitch here since it merely reflects the normal uncertainty inherent in statistical procedures (particularly when they are run with such high error probabilities as here). The important thing to note is that this questionable decision has only local impact as the analysis remains stable with mean estimates quickly returning to almost the same levels as for the other values of δ.

It is of course somewhat optimistic in the above experiment to assume that the process is known good enough to prescribe the right value of σ. *Smith* and *Cain* (1983) ran the SPRT using the standard deviation of the series under investigation. This choice, to some degree, has its point in retrospective experiments, since it is the optimum estimate for σ if there are no changes in the series, which in a heuristic sense gives this value the highest probability of being "correct". For the series in *Fig. 1b*, this standard deviation amounts to 1.19, and the SPRT/Schwarz combination was re-run with this value to assess the robustness against the inevitable uncertainties in a practical setting about the exact value of σ. Though SPRT decisions of course occurred at somewhat different times, the final results exhibited unspectacular deviations: only one shift of a change-point by one position was registered (namely, for the run with $\delta = 0.5$, the change-point at no. 40 moved to position 41, and the solution became identical to the one with $\delta = 0.3$ shown in *Fig. 1b*).

4. Discussion

For certain applications, there are very good reasons to select a sequential analysis procedure, since this area of mathematics strives for methods with the quickest possible reaction time to jumps in the series (already the inventor of the SPRT, *Wald* (1947), gave impressive numbers on this criterion). As one can see from a review like that of *Lai* (2001), also parameter estimation of the distribution after a change-point in a sequential framework has been the subject of mathematical research for long. However, the practical usage of many of the more sophisticated concepts has been fairly limited, and though apparently more and more procedures addressing the practitioners' requirements have surfaced in recent years, reality in meteorology (and elsewhere) indicates that so far they failed to supersede established simple procedures. Part of the cause appears to be a certain ambition to have change-point detection, change-point location, and parameter estimation altogether in a closed sequential framework, whereby one then arrives at relatively complex schemes. We found it supportive for our own approach towards the problem to identify precursors that separated change-point detection and change-point location for no other reason than being able to master the otherwise excessive computational demands. The first appearance of this approach apparently was due to *von Brandt* (1983), with the change-point positioning step based on a simplified version of the underlying sequential framework. The present paper takes the liberty to go a step further as the change-point location has no sequential background at all.

In fact, we presented a concept that allows to successfully employ a sequential analysis change-*detection* procedure like the SPRT in calibration problems, provided the change-point *location* is handled by another technique being tailored to this task and consulted in case of need. Though in principle the latter component alone would suffice to solve the problem, there are noteworthy practical advantages motivating the combination with the sequential change-detection. With an unknown number of change points in the series, expressions like the Schwarz criterion may quickly become impractical for longer series due to the combinatorial explosion of the number of configurations to check. A sequential analysis procedure in this case can be used to alert when the presence of a recent change is likely. Note that in the implementation presented above, the Schwarz criterion computations are constrained to $\nu \leq 2$, which keeps the number of possible combinations rather low and generally should be compatible with a real-time procedure. Of course, the number of detectable change-points in the whole series is still unlimited.

References

Caussinus, H. and *Lyazrhi, F.*, 1997: Choosing a linear model with a random number of change-points and outliers. *Ann. Inst. Stat. Math. 49*, 761-775.

Caussinus, H. and *Mestre, O.*, 2004: Detection and correction of artificial shifts in climate series. *Appl. Statist. 53*, 405-425.

Jann, A., 1996: Use of METEOSAT upper tropospheric humidity fields in synoptic practice. In *Proc. of the 1996 Meteorological Satellite Data Users' Conference*, September 16-20, 1996. Vienna, Austria, 265-272.

Jann, A., 2006: Genetic algorithms: Towards their use in the homogenization of climatological records. *Croatian Meteorological Journal 41*, 3-19.

Lai, T.L., 2001: Sequential analysis: some classical problems and new challenges (with discussion). *Stat. Sinica 11*, 303-408.

Schwarz, G., 1978: Estimating the dimension of a model. *The Annals of Statistics 6*, 461-464.

Smith, P.L. and *Cain, D.E.*, 1983: Use of sequential analysis methods in adjusting radar rainfall estimates on the basis of raingage data. *Report 83-2. Institute of Atmospheric Sciences, South Dakota School of Mines and Technology*, Rapid City, SD.

van de Berg, L., *Schmetz, J.* and *Whitlock, J.*, 1995: On the calibration of the Meteosat water vapour channel. *J. Geophys. Res. 100(D10)*, 21069-21076.

von Brandt, A., 1983: Detecting and estimating parameter jumps using ladder algorithms and likelihood ratio test. In *Proc. IEEE International Conference on ICASSP '83.* Boston, MA, 1017-1020.

Wald, A., 1947: *Sequential Analysis*. Wiley, New York.

Zurbenko, I., *Porter, P.S.*, *Rao, S.T.*, *Ku, J.Y.*, *Gui R.*, and *Eskridge, R.E.*, 1996: Detecting discontinuities in time series of upper-air data: Development and demonstration of an adaptive filter technique. *J. Climate 9*, 3548-3560.

GUIDE FOR AUTHORS OF *IDŐJÁRÁS*

The purpose of the journal is to publish papers in any field of meteorology and atmosphere related scientific areas. These may be

- research papers on new results of scientific investigations,
- critical review articles summarizing the current state of art of a certain topic,
- short contributions dealing with a particular question.

Some issues contain "News" and "Book review", therefore, such contributions are also welcome. The papers must be in American English and should be checked by a native speaker if necessary.

Authors are requested to send their manuscripts to

Editor-in Chief of IDŐJÁRÁS
P.O. Box 39, H-1675 Budapest, Hungary
E-mail: antal.e@met.hu

including all illustrations. MS Word format is preferred in electronic submission. Papers will then be reviewed normally by two independent referees, who remain unidentified for the author(s). The Editor-in-Chief will inform the author(s) whether or not the paper is acceptable for publication, and what modifications, if any, are necessary.

Please, follow the order given below when typing manuscripts.

Title page: should consist of the title, the name(s) of the author(s), their affiliation(s) including full postal and e-mail address(es). In case of more than one author, the corresponding author must be identified.

Abstract: should contain the purpose, the applied data and methods as well as the basic conclusion(s) of the paper.

Key-words: must be included (from 5 to 10) to help to classify the topic.

Text: has to be typed in single spacing on an A4 size paper using 14 pt Times New Roman font if possible. Use of S.I. units are expected, and the use of negative exponent is preferred to fractional sign. Mathematical formulae are expected to be as simple as possible and numbered in parentheses at the right margin.

All publications cited in the text should be presented in the *list of references*, arranged in alphabetical order. For an article: name(s) of author(s) in Italics, year, title of article, name of journal, volume, number (the latter two in Italics) and pages. E.g., *Nathan, K.K.,* 1986: A note on the relationship between photosynthetically active radiation and cloud amount. *Időjárás 90,* 10-13. For a book: name(s) of author(s), year, title of the book (all in Italics except the year), publisher and place of publication. E.g., *Junge, C.E.,* 1963: *Air Chemistry and Radioactivity.* Academic Press, New York and London. Reference in the text should contain the name(s) of the author(s) in Italics and year of publication. E.g., in the case of one author: *Miller* (1989); in the case of two authors: *Gamov* and *Cleveland* (1973); and if there are more than two authors: *Smith et al.* (1990). If the name of the author cannot be fitted into the text: *(Miller,* 1989); etc. When referring papers published in the same year by the same author, letters a, b, c, etc. should follow the year of publication.

Tables should be marked by Arabic numbers and printed in separate sheets with their numbers and legends given below them. Avoid too lengthy or complicated tables, or tables duplicating results given in other form in the manuscript (e.g., graphs).

Figures should also be marked with Arabic numbers and printed in black and white or color (under special arrangement) in separate sheets with their numbers and captions given below them. JPG, TIF, GIF, BMP, PNG or EPS formats should be used for electronic artwork submission.

Reprints: authors receive 30 reprints free of charge. Additional reprints may be ordered at the authors' expense when sending back the proofs to the Editorial Office.

More information for authors is available: antal.e@met.hu

Published by the Hungarian Meteorological Service

Budapest, Hungary

INDEX 26 361

HU ISSN 0324-6329

IDŐJÁRÁS

QUARTERLY JOURNAL
OF THE HUNGARIAN METEOROLOGICAL SERVICE

Special Issue: Climate variability of the past millennium in Hungary
Guest Editor: **Andrea Kiss**

CONTENTS

****

http://www.met.hu/Journal-Idojaras.php

VOL. 113 * NO. 4 * OCTOBER – DECEMBER 2009

IDŐJÁRÁS

Quarterly Journal of the Hungarian Meteorological Service

Editor-in-Chief

LÁSZLÓ BOZÓ

Executive Editor

MARGIT ANTAL

Editorial Office: Gilice tér 39, H-1182 Budapest, Hungary
P.O. Box 39, H-1675 Budapest, Hungary
E-mail: bozo.l@met.hu or antal.e@met.hu
Fax: (36-1) 346-4809

Indexed and abstracted in Science Citation Index Expanded™ and
Journal Citation Reports/Science Edition
Covered in the abstract and citation database SCOPUS®

Subscription by

mail: IDŐJÁRÁS, P.O. Box 39, H-1675 Budapest, Hungary
E-mail: kenderesy.k@met.hu or antal.e@met.hu

Editorial

Climate variability of the past millennium in Hungary

Due to recent environmental change issues, climate research of the past millennium has gained special interest in the past few decades. Among other things, this is caused by the fact that the process of making short- and medium-term climate projections requires much better understanding of climate cycles and past climate processes. The growing relevance of historical climate research can be seen as well in European climate studies. Within the framework of the currently ongoing European project (FP-6) entitled *Millennium – Climate and Its Past Dynamics*, significant efforts have been made, funded by the European Union, to provide complex and precise multi-proxy reconstructions of the variability of the European climate over the last thousand years. In a joint investigation by European scientists, studies and records from various fields and different parts of Europe, including Hungary and the Carpathian Basin are gathered.

Both in Hungary and the surrounding areas of the Carpathian Basin, either in the form of medium- or long-term climate reconstructions or impact case studies of weather anomalies and extremes, in the recent decades and especially in the last few years, a rapidly developing interest among scientists and historians can be perceived. In this issue we will present new results of long-term climate investigations in Hungary, provided by 16 scientists from various fields like paleoecology, geology, geochemistry, dendroclimatology, geography, and environmental history.

The paper of *Siklósy et al.* provides a reconstruction of climate variations that have occurred in the past millennium. In their paper temperature, precipitation, as well as vegetation changes in northeastern Hungary (Bükk Mountains), based on high-resolution stable isotope (oxygen, carbon) and trace-element analyses for a 1100-year long stalagmite record with decadal cycles, are discussed. While oxygen isotope content is mainly related to temperature and carbon is related to precipitation, a combined trace-element (Mg, Sr, and P) variation method was applied to detect changes in evapotranspiration. A significant result was that the predominantly wet and warm Medieval Warm Period, after a transition period of several dry spells, was followed by a colder, humid Little Ice Age.

In a study by *Sümegi et al.*, based on geoarchaeological methods (pollen, macrofossil, sediment analyses), a palaeoecological and palaeoclimatological reconstruction for northern Hungary was carried out for a period of two millennia. Also, based on the evidence derived from sediment depositions, after the high water level of Nádas Lake, which lasted until the mid-Holocene period, a 5000-year gap in deposits occurred due to the deepening of the lake basin in the Imperial period. At the same time as the depth of the lake was increasing, around 200 AD the water level decreased, which caused an eutrophication of the water. This process was followed by paludification, which occurred from ca. 1300 onwards. Their investigation suggests that warm conditions prevailed in the Imperial period, and then in the late Migration period. Once again, warm (and dry) conditions returned in the 8–12th centuries and ended around the mid-1200s.

Kern et al. carried out an investigation on August-July precipitation, focusing on the southern sections of the Bakony Mountains in west central Hungary, based on the ring widths of oak trees. Their reconstruction covers a period of 258 years, starting from 1746 AD. The reconstructed precipitation series suggests that very dry conditions occurred in the late 1740s, while the wettest part of the period occurred in the late 1700s. This was followed by a downward trend in precipitation, with short dry spells in the 1840s, 1860s, and 1940s. However, the driest period of the last 258 years in west central Hungary occurred in the period after the 1980s.

Following the three papers on data analysis, the review article of *Andrea Kiss* provides a synthesis of research in historical climatology and a study of hydrometeorological extremes in Hungary, based on documentary evidence, for the past millennium. In addition to compilations and analyses of long-term climate variability, case studies on hydrometeorological extremes (e.g., droughts and floods) and their impact over the past thousand years are also elaborated.

Andrea Kiss
Guest Editor
University of Szeged, Hungary

Acknowledgement—We would like to thank IDŐJÁRÁS for giving us the opportunity to present a cross-sectional view of the multidisciplinary themes of historical climate changes, mainly occurred in the last 1000 years, as well as for the support of the EU project called Millennium (No. 017008).

IDŐJÁRÁS

Quarterly Journal of the Hungarian Meteorological Service
Vol. 113, No. 4, October–December 2009, pp. 245–263

Reconstruction of climate variation for the last millennium in the Bükk Mountains, northeast Hungary, from a stalagmite record

Zoltán Siklósy[1*], **Attila Demény**[1], **István Szenthe**[2], **Szabolcs Leél-Őssy**[3], **Sebastian Pilet**[4], **Yin Lin**[5], and **Chuan-Chou Shen**[5]

[1]*Institute for Geochemical Research, Hungarian Academy of Sciences, Budaörsi út 45, H-1112 Budapest, Hungary; E-mail: siklosy@geochem.hu*

[2]*Múzeum krt. 5, H-1055 Budapest, Hungary*

[3]*Department of Physical and Applied Geology, Eötvös Loránd University, Pázmány P. stny. 1/C, H-1112 Budapest, Hungary; E-mail: losz@iris.geobio.elte.hu*

[4]*Institute of Mineralogy and Geochemistry, University of Lausanne, Bâtiment Anthropole, CH-1015 Lausanne, Switzerland; E-mail: Sebastien.Pilet@unil.ch*

[5]*Department of Geosciences, National Taiwan University, No. 1, Sec. 4, Roosevelt Rd., Taipei 106, Taiwan ROC; E-mail: river@ntu.edu.tw*

(Manuscript received in final form August 31, 2009)

Abstract—This paper presents the high-resolution stable isotope and trace element records from a stalagmite from Hungary (Kiskőhát Shaft, Bükk Mts.). Based on the variation of the isotopic and chemical composition of the carbonate deposit along the growth axis, changes in temperature and precipitation amount are assumed.

Our first results on the younger part (ca. last 1100 years) of the deposit suggest that not only major changes but several short period cycles can be recognized within the stalagmite, which are partly caused by temperature, precipitation amount, and vegetation changes. The oxygen isotope variation of the stalagmite can be explained mainly by the changes of the temperature, while carbon isotope ratios mainly reflect the changes in water recharge or precipitation amount. Combined trace element (Mg, Sr, and P) variations were used to reconstruct evapotranspiration changes.

The stalagmite recorded a generally wet and warm Medieval Warm Period, a colder but humid Little Ice Age, and several variably dry periods between.

Key-words: stalagmite, cave, paleoclimate, stable isotopes, trace elements, last millennium, Hungary

[*] Corresponding author

1. Introduction

During the past four decades, the majority of the paleoclimatological studies was concerned either with investigating marine records and/or polar ice cores. Efforts in reconstructing climate change from continental records have renewed interest in the use of speleothems as climatic proxies (e.g., *Gascoyne*, 1992; *Lauritzen*, 1995).

These deposits have specific advantages: stalagmites are widespread in continental area, they develop in relatively protected environments, practically free from re-deposition and alteration, and can be dated by absolute radiometric methods at relatively high precision. TIMS or ICP-MS uranium series dating of only a few 100 milligrams allow dating speleothem calcite with a precision better than 1% (*Shen et al.*, 2002).

Carbonate speleothems are formed when water saturated in CO_2 from the soil zone enters a cave where the CO_2 degasses. If degassing proceeds slowly in a stable-temperature environment, calcite can be precipitated in isotopic equilibrium with the parent drip water (*Hendy,* 1971). In this case, the reconstruction of environmental conditions existing during the formation of the calcite can be possible mostly based on the stable isotope analyses of speleothems.

Recently published preliminary studies in Hungary have reported significant isotopic and chemical variations within stalagmites related to interglacial/glacial climate transitions (Marine Isotope Stage 5e-5d; *Siklósy et al.,* 2008a) or volcanically induced climate changes (*Siklósy et al.*, 2007; *Siklósy et al.*, 2009). Speleothems that record decadal-scale environmental changes in the Carpathian Basin during the last millennium are of particular interest, as this time range is not fully covered by historical and/or instrumental climate records (e.g., *Réthly*, 1962; *Rácz*, 1989; *Kiss*, 2009). Although tree-ring growth series may preserve climatically induced climate proxy signals (*Kern* and *Popa*, 2007; *Kern et al.*, 2009) the lack of corresponding series further back in the past prevents the establishment of detailed studies. Ground-surface temperature (GST) may reflect past climate conditions, but the resolution and precision of the reconstruction for Hungary (*Bodri* and *Dövényi*, 2004) need to be improved for direct comparison with other records. Biostratigraphic evidences for Holocene climate changes (based on vertebrate paleontology) cover several localities in northeast Hungary (*Kordos*, 1977; *Kordos* and *Ringer*, 1991), however, the precise age control and the lack of continuous records prevent the establishment of high-resolution reconstruction for the last thousands of years.

There is a need, therefore, for well-dated climate records from this continental area to increase the input for general climate models. High-resolution geochemical data on speleothems may fill the gap also for this period.

In this study, we conducted complex trace element and stable C and O isotope analyses on a speleothem from Hungary (*Fig. 1*) acquired at high spatial and temporal resolution using various mass spectrometric techniques in order to test and validate independently recognized climate changes (e.g., Little Ice Age [LIA]) and to apply *geochemical results as a climate driven proxies* for future research.

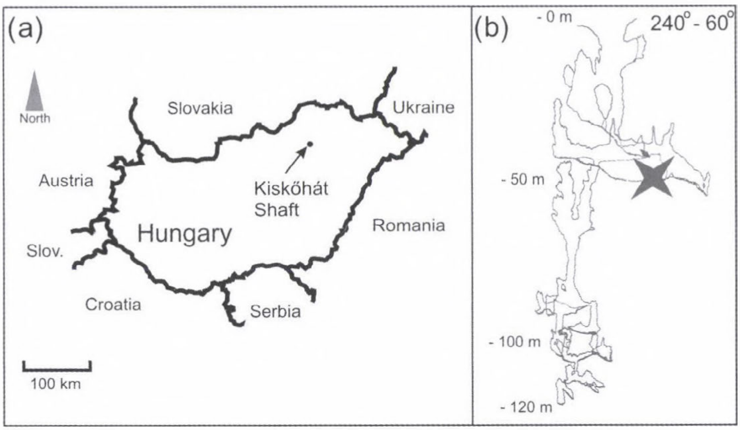

Fig. 1. Location of Kiskőhát Shaft in northeast Hungary (a) and vertical cross-section of the Kiskőhát Shaft with the sample location, indicated by a cross (mapped and created by the BEAC cave explorer group) (b).

2. *Site and sample*

The speleothem analyzed in this study originates from the Kiskőhát Shaft (*Fig. 1*), northeast Hungary (N 48° 4.086' and E 20° 29.422'). The cave is located at the southern rim of the Bükk Highland, at 915 m a.s.l. The 117 m deep inactive sinkhole opens up the cave with a total length of 479 m, situated in the Bükk National Park, under the Kiskőhát peak (938 m) at 915 m elevation, in Triassic limestone. The interior of the cave where the sample was located has a constant temperature of 5.5 °C, with only a minor variability over a year, except the shaft, close to the cave entrance, where freezing can occur during winter. In situ CO_2 measurements at the site revealed that the air masses within the cave can only change during wintertime because of the general, temperature dependent atmospheric circulation of sacklike chambers. When cold and dry winter air sinks into the cave, the environment may become totally dry and, therefore, the growth rate of the deposits becomes practically zero.

The stalagmite consists of dense, well-laminated dark crystalline and milky-colored calcite. Apparently, deposition has been continuous along the length of the sample (ca. 250 mm), except the top part of the stalagmite where hiatus in deposition are marked by small changes in crystal structure and layers of detrital inclusions (*Fig. 2*, shown by dotted lines). A polished section of the studied section of the stalagmite (ca. top 65 mm) was examined for calculating the number of growth bands along the growth direction.

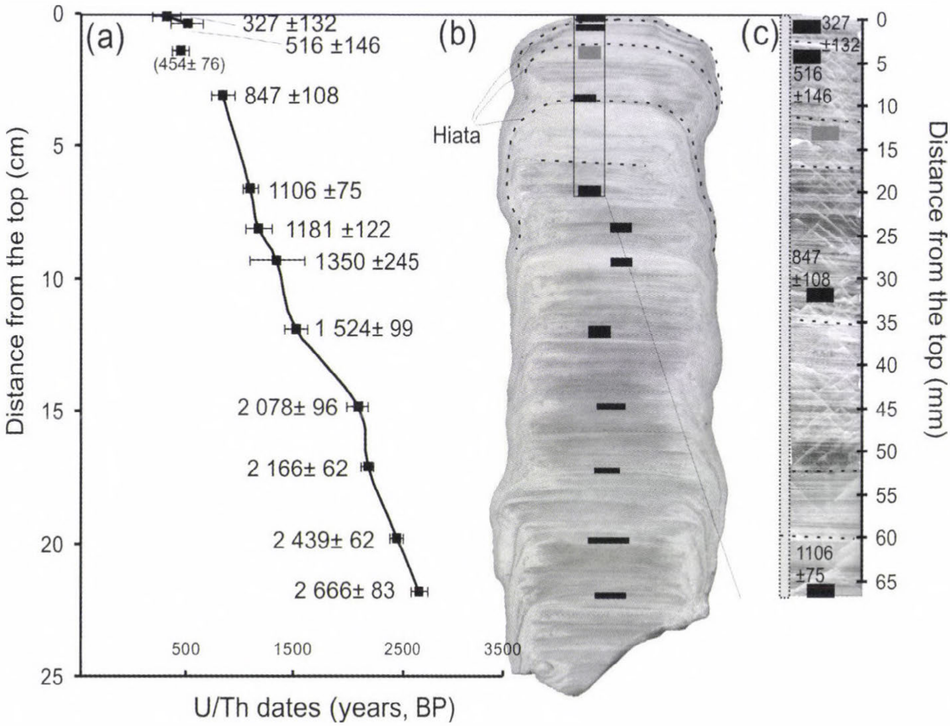

Fig. 2. The determined U-Th data series vs. the depth (a) of the studied Kiskőhát Shaft stalagmite (b), and the selected part for this study (c). Vertical gray bar shows the position of the stable isotope profile (c). Position of the Multi Collector-Inductively Coupled Plasma-Mass Spectrometry (MC-ICP-MS) age data are indicated by the black regions (b and c). Dotted line represents textural changes and/or hiata during the deposition of the stalagmite. Errors of the age data are also indicated.

3. *Methodology*

3.1. Age determination

To place the observed isotopic changes into a time frame for comparison with other records, *precise age determinations* of the cave deposits is required. The technique is based on the precipitation of small amounts of uranium at the moment of deposition of natural samples (e.g., calcite speleothems) in the absence of thorium. After carbonate deposition, a gradual increase of the ^{230}Th concentration occurs in the speleothem through radioactive decay of ^{234}U. The ratio ^{230}Th/^{234}U is a function of the speleothem age, which can be determined by chemical separation of ^{230}Th and ^{234}U from the sample and by measuring each nuclide (*Edwards et al.*, 1987; *Richards* and *Dorale*, 2003).

Subsamples (ca. 0.1–0.3 g) were drilled for U-Th chemistry (*Shen et al.*, 2003) and ^{230}Th-dated isotopic measurements on a multi-collector inductively coupled plasma mass spectrometer (MC-ICP-MS), Thermo Electron Neptune in the High-precision Mass Spectrometry and Environment Change Laboratory (HISPEC), Department of Geosciences, National Taiwan University. A triple-spike, ^{229}Th-^{233}U-^{236}U, isotope dilution method was employed to correct mass bias and determine uranium concentration (*Shen et al.*, 2002). A protocol, using one newly-developed MasCom secondary electron multiplier (SEM) with repelling potential quadrupole (RPQ), was employed. Only 1–4 ng of U is required to earn the 2-sigma reproducibility of 1–2‰. No significant difference between measurements of standards and carbonate samples on ICP-sector-field-MS (*Shen et al.*, 2002) and on MC-ICP-MS certify the developed MC-ICP-MS methodology.

Dating of the youngest part of the stalagmite was possible by applying the U-Th method due to its low detrital Th content. Age corrections are applied anyway, as even small amount of U-derived Th may have effect on the U/Th age for young samples. Thus, we used the corrected values for all dated subsamples (*Table 1*). The obtained ages are absolute ones and given as years BP (before present; here: before the chemistry date 2007 AD).

3.2. Stable isotopes

Carbon and oxygen isotope compositions of drilled calcite samples at a spatial resolution of ~0.5 mm were determined using the conventional H_3PO_4 digestion method (*McCrea*, 1950; *Spötl* and *Venneman*, 2003) at 72 °C and an automated GasBench II preparation unit attached to a Thermo Finnigan delta plus XP continuous flow mass spectrometer at the Institute for Geochemical Research in Budapest. Standardization was conducted using laboratory calcite standards calibrated against the NBS-19 standard. The results are expressed according to the following equation:

$$\delta^{18}O \text{ or } \delta^{13}C = \frac{R_{sample} - R_{standard}}{R_{standard}} \cdot 1000 \quad (‰). \qquad (1)$$

The variations of stable ^{18}O and ^{16}O or ^{13}C and ^{12}C are measures by a mass spectrometer relative to a standard, therefore expressed in a „delta" (‰) notation, here, relative to the carbonate standard named Vienna Pee Dee Belemnite (V-PDB). Reproducibilities for C and O isotope analyses are better than ±0.15‰.

In temperate regions, cave air is characterized by high-humidity (typically 95–99%), minimizing the evaporation that might otherwise cause kinetic isotope fractionation by preferred loss of easier water molecules ($H_2{}^{16}O$). In this case the variations in $\delta^{18}O$ value of a carbonate reflects primarily the changes in oxygen isotopic composition of precipitation in the area ($\delta^{18}O_{water}$) and the temperature of formation (*McDermott*, 2004 and references therein). Since the isotopic composition of dripping water is closely related to the meteoric precipitation at the studied region (*Harmon et al.*, 1979; *Yonge et al.*, 1985) and the cave temperature reflects the mean annual temperature at the surface (*Fairchild et al.*, 2006), the O isotope compositions of meteoric water that infiltrates into the cave, and from which the carbonate precipitates, reflect regional climate conditions. However, in order to interpret the $\delta^{18}O$ value of the stalagmite correctly, the factors that may influence the O isotope compositions of infiltrating water have to be listed here. As mentioned above, the $\delta^{18}O$ in cave seepage waters reflect the $\delta^{18}O$ of the local precipitation but may reflect evaporative processes that modify the $\delta^{18}O$ of the infiltrating water along the flow path from the surface across the vadose zone into the cave. The oxygen isotope composition of precipitation is temperature and site dependent.

Over the mid and high latitudes, *Rozanski et al.* (1993) calculated an average modern-day $\Delta\delta^{18}O_{precipitation}/\Delta T$ of approximately $+0.6‰/°C$. This value may have been different in the past, however, we may assume that the positive correlation remained. The equilibrium fractionation (*Friedman* and *O'Neil*, 1977) that accompanies calcite deposition from drip-waters inside the cave ($\Delta\delta^{18}O_{calcite}/\Delta T$) is approximately $-0.24‰/°C$ at 25 °C (*O'Neill et al.*, 1969). Since the temperature dependence of $\delta^{18}O$ in rainfall (ca. $+0.6‰/°C$) exceeds the calcite-water fractionation ($-0.24‰/°C$), in principle the *temperature dependency* of the O isotope compositions of meteoric water define the $\delta^{18}O$ value of the calcite (i.e., a positive correlation between $\delta^{18}O$ in the calcite and temperature).

The $\delta^{13}C$ values of the stalagmites can also provide important palaeoenvironmental information. The carbon isotopic composition of the drip water is the most important factor determining the $\delta^{13}C$ of speleothem carbonates. Carbon dissolved in drip water mainly derives from three sources: atmospheric CO_2, soil CO_2, and dissolution of the karstic host rock. Among these, the *amount of soil CO_2* has a major factor. Thus, changes of the vegetation activity or in the microbial activity within the oxidation process of soil organic matter plays a key role in the CO_2 production. Part of the precipitation will penetrate plant cover and pass through the soil and epikarst zone, where it takes up the CO_2, produced by plant respiration. The CO_2 uptake produces carbonic acid, which in turn dissolves limestone (Eq. (2)). The $\delta^{13}C$ value of soil CO_2 varies according to the photosynthetic pathway of plants (C3 and C4-types), however, the C4-type drought-adapted grasses can be ruled out for this region at the time range for this study (*Sümegi*, 2007). The $\delta^{13}C$ values of the stalagmite may become more positive also in case of above or within-cave phenomena, mostly related to rapid *outgassing* of CO_2, caused by stronger *ventillation* or *evaporation* which leads to kinetic fractionation, thus the enrichment of calcite precipitation (i.e., stalagmite) in isotopically heavier carbon isotope.

The carbon isotopic values, therefore, mainly reflect the influence of biogenic activity of soil above the cave and the degree of limestone dissolution. The driving force of karstification and speleothem deposition is the meteoric water circulation system in combination with soil carbon dioxide production, as expressed by the following equation:

$$CaCO_3(s) + CO_2(g) + H_2O(l)_{(precipitation)} <=>_{(dissolution)} Ca^{2+}(aq) + 2HCO_3^-(aq). \quad (2)$$

Table 1. U/Th isotopic compositions and ^{230}Th ages for Kiskőhát Shaft on MC-ICP-MS

	Distance (cm)	Weight	^{238}U	^{232}Th	δ^{234}U	[^{230}Th/^{238}U]	[^{230}Th/^{232}Th]	Age		Age		δ^{234}U initial	Growth rate
Sample ID	From the top	g	ppb	ppt	Measured[a]	Activity[b]	ppm[c]	Uncorrected	Error	Corrected[b,d]	Error	Corrected[e]	δm/yr
Kiskőhát 12.	0.1	0.298	35.7	356	317	0.0051	8.5	427	± 86	327	± 132	317	16
Kiskőhát 11.	0.4	0.249	33.9	334	335	0.0075	12.5	614	± 108	516	± 146	336	
Kiskőhát 10.*	1.4	0.352	41.8	100	374.6	0.0060	41	477	± 73	454	± 76	375	43
Kiskőhát 9.	3.1	0.222	38.7	58	349	0.0106	116.5	862	± 107	847	± 108	350	135
Kiskőhát 8.	6.6	0.332	39.4	115	358	0.0140	79.8	1135	± 70	1106	± 75	360	199
Kiskőhát 7.	8.1	0.221	34.0	60	349	0.0147	137.3	1199	± 121	1181	± 122	350	71
Kiskőhát 6.	9.3	0.159	27.1	171	366	0.0176	45.8	1412	± 240	1350	± 248	367	150
Kiskőhát 5.	11.9	0.416	35.4	47	374.6	0.0192	238	1537	± 98	1524	± 99	376	52
Kiskőhát 4.	14.8	0.116	37.4	177	391.9	0.0268	93.4	2123	± 85	2078	± 96	394.2	260
Kiskőhát 3.	17.1	0.197	35.0	98	396.0	0.0278	164.5	2193	± 56	2166	± 62	398.4	99
Kiskőhát 2.	19.8	0.171	128.1	215	420.3	0.0316	310.2	2455	± 60	2439	± 62	423.2	88
Kiskőhát 1.	21.8	0.143	340.0	2584	420.6	0.0352	76.5	2737	± 43	2666	± 83	423.7	

Analytical errors are 2s of the mean.

[a] $d^{234}U = ([^{234}U/^{238}U]_{activity} - 1) \times 1000$.

[b] $[^{230}Th/^{238}U]_{activity} = 1 - e^{-\lambda 230 T} + (\delta^{234}U_{measured}/1000)[\lambda_{230}/(\lambda_{230} - \lambda_{234})](1 - e^{-(\lambda 230 - \lambda 234)T})$, where T is the age.

Decay constants are 9.1577×10^{-6} yr^{-1} for ^{230}Th, 2.8263×10^{-6} yr^{-1} for ^{234}U, and 1.55125×10^{-10} yr^{-1} for ^{238}U (*Cheng et al.*, 2000).

[c] The degree of detrital ^{230}Th contamination is indicated by the [^{230}Th/^{232}Th] atomic ratio instead of the activity ratio.

[d] Age corrections were calculated using an ^{230}Th/^{232}Th atomic ratio of 2 (± 2) ppm.

[e] $\delta^{234}U_{initial}$ corrected was calculated based on ^{230}Th age (T), i.e., $\delta^{234}U_{initial} = \delta^{234}U_{measured}\ X\ e^{\lambda 234 * T}$, and T is corrected age.

*: U fraction lost during chemistry; estimate age using "Kiskőhát 11." U data.

3.3. Trace elements

As the speleothem grows, it incorporates trace elements into its structure, and their concentrations and ratios reflect environmental conditions at the time of deposition, e.g., temperature and water throughput (rainfall at the surface).

Trace element compositions were determined by laser-ablation (LA-)ICP-MS technique using a Perkin-Elmer ELAN 6100 DRC ICP-MS coupled with a LAMBDA PHYSICS excimer laser (193 nm) at the University of Lausanne. The measurements were performed using the following settings: laser: 7 Hz, 28 kV, energy ~170 mJ, fluency ~13 J/cm^2; spot size 60 μm, acquisition time: gas blank ~30s, data ~ 60s. Data were reduced using the CONVERT and LAMTRACE programs. NIST612 glass was used as external standard and Ca electron microprobe measurements served as an internal standard. BCR-2 glass was monitored during all analytical sessions for phosphoros and treated as unknowns during data reduction. The error is estimated to lie between 5–10% on a relative basis. With the applied method, elements incorporated into the structure of the calcite with low concentration and high spatial resolution could be followed along the growth axis.

In this paper we focus on prominent changes and cycles of the following trace elements: Mg, Sr, and P.

Mg can substitute Ca in the calcite lattice (*Mucci* and *Morse*, 1983). The main factors that can modify the Mg-signal in stalagmites are the following:

- Experimental results have demonstrated that Mg partitioning into calcite from water is temperature-dependent (*Mucci*, 1987; *Burton* and *Walter*, 1991). *Gascoyne* (1983, 1992) calculated that a 1 °C increase would increase the Mg content of the stalagmite with 7%, however, the long-term (millennial) temperature control on Mg abundance have proved to be over-simplified (*Fairchild et al.*, 2006).
- Under isothermal conditions or during short-term changes (yearly or decadal), variation in solution composition is much more important, hence Mg variation on decadal time scales reflects variations in solution Mg. This mostly reflect changes in hydrological parameters, with solution Mg / Ca tending to be lower under high flow-rate (i.e., wet) conditions, as a result of dilution.
- Furthermore, the enrichment of Mg in cave waters can be explained by prior low-Mg calcite precipitation from the cave waters along the flow path, which are consequently enriched in Mg. The partition coefficients (Kd) for Mg (and also for Sr) between cave waters and cave calcite are $<< 1$ (*Katz*, 1973; *Mucci* and *Morse*, 1983), therefore, Mg / Ca and Sr / Ca ratios increase in solutions that have precipitated calcite ("prior calcite precipitation"). This can explain co-variations of Mg and Sr in the seepage waters and consequently in the speleothem.

- Prolonged water residence time in the vadose zone linked to the reduced amount of precipitation may also enhance the Mg concentration in the solution and stalagmite due to the dissolution of the host rocks.

In the case of Sr variability, the increase in the speleothems can be interpreted by:

- Increased water residence time in the vadose zone and /or by an increase in prior calcite deposition caused by an increase in calcite saturation of the waters.
- In addition to varying solution Sr/Ca, the growth rate, or more specifically crystallographic changes can also influence Sr incorporation at higher growth rates (*Huang* and *Fairchild*, 2001). Higher Sr at a given Mg content represents faster growth rate of the stalagmite (*Huang et al.*, 2001).

Phosphate is one of the strongest adsorbents onto defect sites on the calcite surface (*Meyer*, 1984). It is directly linked

- to the vegetation productivity and its decay (*Fairchild et al.*, 2001), and
- the P incorporation into the calcite structure is sensitive to phosphate concentration in seepage water and rate of supply of dripwater (dilution).

Therefore, P concentrations can be used as an indipendent proxy together with carbon isotope values to estimate the change of biogenic activity. A control on P incorporation by rate of supply of inorganic P, rather than by defects produced during faster growth, is inferred from the lack of correlation of P and Sr in this case.

4. *Results*

4.1. ^{230}Th-^{234}U results of age determinations

Uranium-series dating results indicate that the stalagmite growth started some 2700 years BP. We obtained a total of 12 U-Th series dating along the growth direction (*Table 1*) and all subsamples were in stratigrapic order (*Fig. 2a*). The section selected for this study (ca. top 65 mm of the stalagmite) cover ca. 1100 ±75 years.

The age data demonstrate that the growth rate varied in time, from ca. 199 μm/year at the bottom of the studied section to ca. 16 μm/year at the top. This change may be due to the (i) real decreased rate in continuous growth or (ii) the presence of hiata. The visible laminae counts and width calculations using the CAROTA software (*Popa*, 1999) revealed that regular, high-frequency cycles can be recognized along the studied section (*Fig. 3a*) with a sum of 373 laminae within the determined age ranges for the studied section (from the bottom to the top of the stalagmite, between 1106 ± 75 and 327 ± 132 years BP, respectively). For the majority of the deposition, therefore, the stalagmite suffers from the lack of visible laminae. Fewer counted laminae than expected may probably represents brake during the stalagmite deposition. The average thickness of the bands is ca. 173 μm (*Fig. 3a*).

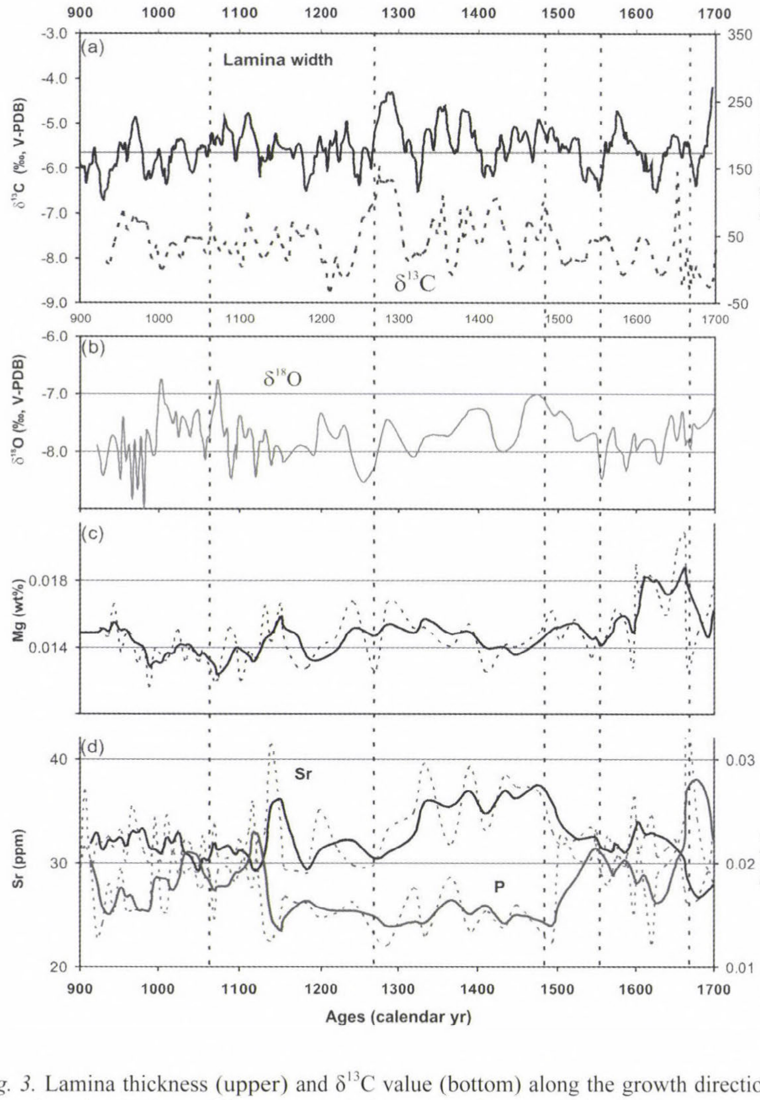

Fig. 3. Lamina thickness (upper) and $\delta^{13}C$ value (bottom) along the growth direction of the stalagmite. Horizontal line represents the average lamina width of 173 μm (a); Stable oxygen isotope composition of the studied section (b); Mg (c) and Sr-P (d) variations in the studied section of the Kiskőhát stalagmite. The thick line in each case shows smoothed data (3 running means). All data are plotted against the ages (calendar years or AD), based on the U-Th data. Vertical dotted lines mark the recognized textural changes and/or hiata (see *Fig. 2*).

The slowest growth rate based on the age-depth relationship (*Fig. 2a*) occurs at the top of the stalagmite, coinciding with the observed hiata. To put the observed changes in the isotopic composition and trace element concentration into the time-frame, U–Th ages along the growth direction were used to create time dependent proxy rather than distance.

In most speleothems from Hungary, growth rate changes and hiata during the deposition may indicate the occurrence of favorable (warm and humid) or unfavorable (cold and/or dry) conditions for calcite precipitation (*Siklósy et al.*, 2008a), thus, the observed features may represent climate changes.

4.2. Stable isotopes

The stable oxygen and carbon isotopic values were plotted against the ages (*Figs. 4a* and *4b*) according to the determined U-Th data of the selected section (ca. top 63 mm of the stalagmite). The profile consists of 125 samples obtained at ca. 0.5 mm increments. $\delta^{18}O$ values range between −9‰ and −6.7‰ (V-PDB) and $\delta^{13}C$ values range between −8.7‰ and −6‰ (V-PDB). The correlation between the two isotopes is very weak (0.13), and there is no systematic variation along a single growth layer, that suggest the sample deposited in isotopic equilibrium. However, distinct parts of the section studied (especially between ca. 1250 and 1500 AD) are characterized by fluctuations in both $\delta^{18}O$ and $\delta^{13}C$ values with higher correlation coefficient in response of possible kinetic fractionation. Processes including evaporation or rapid degassing of CO_2 from the cave dripwaters may explain this isotopic signal. In the case of $\delta^{18}O$ values (*Fig. 3b*), high-frequency cycles (with amplitudes of 1–1.5‰) are superimposed on low-frequency signals. Calcite at the bottom of the section exhibit $\delta^{18}O$ value of ca. −8‰ (V-PDB) with rapid fluctuations. Within a short period (at 1000 AD), a marked increase of >1‰ can be observed towards to less negative values of the section. These higher values remain and caracterize the section between 1000 and 1150 AD. Furter up-section, towards the younger part, lower averaged values were measured with some abrupt jumps towards higher $\delta^{18}O$ values, from which some coincide with similar $\delta^{13}C$ peaks. Between 1550 and 1680 AD there is a remarkable shift to lower $\delta^{18}O$, while the very top of the stalagmite (>1680 AD) shows slightly higher values again.

The carbon isotope composition of the stalagmite (*Fig. 3a*) is characterized by similar high-frequency cycles with even more abrupt changes. Smaller variability can be observed at the bottom part of the section (before 1200 AD), while more variable values of $\delta^{13}C$ are present between ca. 1200 and 1500 AD. An abrupt change at ca. 1250–1300 AD resulted the highest $\delta^{13}C$ value of the stalagmite. From this point to the top, a trend towards lower values appear with another sharp peak at 1650 AD, which coincides with darker calcite just below the observed hiata at the top of the section (dotted lines in *Figs. 2* and *4*).

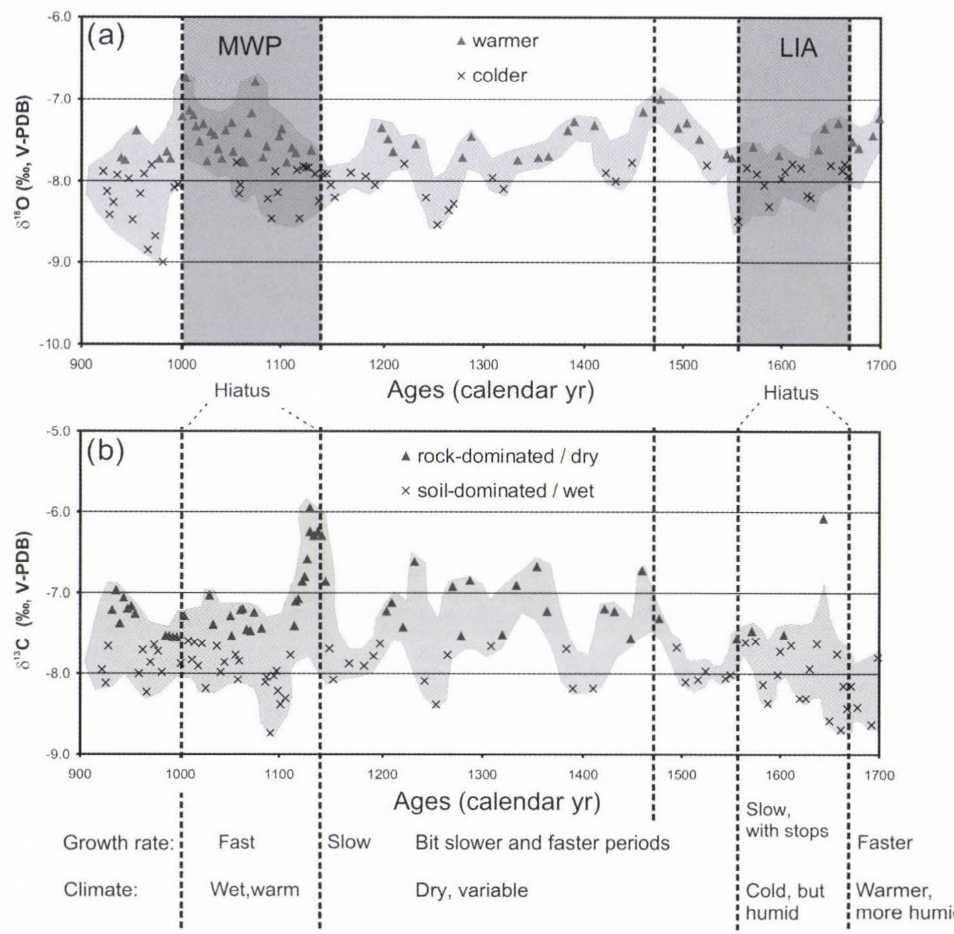

Fig. 4. Stable oxygen (a) and carbon (b) isotope record plotted against the age-relationship of the studied stalagmite. Vertical dotted line indicates hiata and/or marked textural changes during the selected growth period (see *Fig. 2*). See text for details.
(a) Triangles represent higher oxygen isotope values and crosses represent lower oxygen isotope values compared to the average of the total section.
(b) Triangles represent higher carbon isotope values and crosses represent lower carbon isotope values compared to the average of the total section.

4.3. Trace elements

Trace element data are plotted against the ages (AD) from the top of the sample (*Fig. 3c* and *d*). The stalagmite is practically free from detrital-derived impurities as the textural and prelimintary chemical scanning showed, therefore, they are not mentioned in this study or they are not responsible for the laminae observed in the stalagmite. The selected trace elements (Mg, Sr, and P) display similar oscillations along the studied section of the stalagmite, although there are some obvious differences (peaks and trends) at different parts of the concentration profiles.

Magnesium exhibits short-time cycles along the growth direction superimposed on a long-term increasing trend towards the top of the stalagmite (*Fig. 3c*). Low concentration appears between ca. 950 and 1100 AD, whereas the top part (between 1600 and 1680 AD) is characterized with higher Mg values. Mg shows no covariation with Sr or P.

Strontium displays high-frequency cycles superimposed on long-term changes as well. The highly variable Sr concentration clearly reveals a similar pattern as the $\delta^{13}C$ values in most of the section. The highest Sr values and peaks between 1300 and 1500 AD coincide with elevated $\delta^{13}C$ values, while there is a general decreasing trend between 1650 and 1700 AD for both profiles (*Fig. 3d*).

Phosphorus displays anticorrelation with Sr, but not with any other element (*Fig. 3d*). The overall anticorrelation is 0.61. The lowest values are observed between ca. 1150 and 1550 AD, with some troughs around 1600 AD. P peaks and elevated values (1000–1150 AD) generally encompass the lower values of Mg.

5. Discussion on the stable isotopes and trace element records

Before discussing the temperature and precipitation amount information obtained from the Kiskőhát Shaft, stable isotope data points were separated and colored according to their relative values to the averaged value of both (C and O isotope) datasets (*Fig. 4*), and plotted against the age.

As shown in *Fig. 2*, the older part of the studied section (35–40 mm to ca. 65 mm, which value represents ages between 847 and 1106 years BP) is characterized by faster growth rate (ca. 135 μm/year), opposit to the top of the stalagmite. In order to reconstruct the paleoenvironmental changes during this period, the $\delta^{18}O$ values of the stalagmite was first investigated. $\delta^{18}O$ of the seepage water is not controlled by the routing of the water but the composition of the local precipitation, thus the climate of the region (*Harmon et al.*, 1979; *Yonge et al.*, 1985). As abovementioned, higher $\delta^{18}O$ values of the precipitated carbonate primary reflect warmer climate. Evaporation may also have caused elevated $\delta^{18}O$ values, but this would be also indicated by the elevated Sr and Mg concentration. This period (between ca. 1000 and 1150 AD) is characterized by the highest values with positive shift of $\delta^{18}O$ (*Fig. 4)*, indicating warmer and/or arid climate conditions. This latter possibility can be ruled out, as the P and $\delta^{13}C$ show no systematic shifts towards low and high values, respectively, therefore towards drier conditions (*Fig. 3c* and *d*). Instead, the high P and the slight shift of $\delta^{13}C$ to more negative values imply increased soil biogenic activity, most probably due to the increased precipitation amount. Low Mg and decreasing Sr values can be also explained by dilution effect related to the elevated infiltration (i.e., wet conditions). According to the determined U–Th ages, this warmest period with the highest oxygen isotope values around 1000–1150 years may represent the Medieval Warm Period (MWP).

Just before this time period, the very bottom of the section (between ca. 900 and 1000 AD) represents colder and drier period, but the lack of interpretable data preceeding this time prevent the precise comparison.

In contrast to the MWP, the next few hundred years (ca. 1150–1500 AD) are characterized by highly variable geochemical parameters with sharp peaks of $\delta^{13}C$ values and Sr concentrations. In the case of Kiskőhát Shaft, the overall $\delta^{13}C$ values are determined by the contribution of biogenic CO_2 (plant respiration within the soil zone) and the degree of rock-water interaction. The resulted overall value is then modified or obscured by secondary processes as mentioned above (varying kinetic isotope effects, e.g., rapid degassing of CO_2 caused mostly by increased ventilation). In the case of the Kiskőhát Shaft, the $p(CO_2)$ of cave air falls strongly in winter because of the more ventilated system during cold seasons as a result of temperature dependent atmospheric circulation in sacklike chambers. This leads to a strong degassing of CO_2, therefore, a kinetic effect and an increase of $\delta^{13}C$ values in cave water. As the dissolved CO_2 degasses, the solution becomes supersaturated, and there is a tendency for $CaCO_3$ to precipitate. The maximum rates of $CaCO_3$ precipitation is, therefore, generated in the winter or cold periods, but only if the hydrologic system remains active for water infiltration.

As a result of slower flow rates within the karst system (i.e., dry climatic period), enhanced prior calcite precipitation along the flow-path may occur from waters due to Ca^{2+} supersaturations by CO_2-degassing. This prior calcite precipitation will lead to trace element enrichment (e.g., increased Sr and Mg concentration) of the dripping water and consequently in the stalagmite.

Sr incorporation into the calcite structure is dependent on precipitation rate. The overall good correlation between Sr, $\delta^{13}C$ (*Fig. 3a, d*) and – interestingly – also to lamina width, therefore, can be attributed to elevated precipitation rate most probably due to the temporal variations (i.e., sharp decrease) in $p(CO_2)$ in the cave air, which is mainly controlled by ventilation. We assume that both above mentioned processes, i.e., rapid degassing of CO_2 caused mostly by elevated, temperature dependent ventillation and prior calcite precipitation along the flow-path as a result of reduced precipitation amount occurred. Therefore, periods of low precipitation amount (dry conditions) and decrease in mean annual temperature (or longer winters) recorded during the deposition between ca. 1150 or 1200 and 1500 or 1550 AD. Low P concentration (*Fig. 3d*) supports our assumption, since the drier conditions prevent soil activity and, therefore, the biogenic production. Decreased soil biogenic CO_2 production via plant respiration and microbial activity leads to less negative $\delta^{13}C$ values, which, again record dry or drier conditions during the deposition of this part of the stalagmite. We assume that the increased $\delta^{18}O$ values may also represent drier conditions as a result of kinetic effect of evaporation events (e.g., at around 1280, 1400, and 1480 AD).

The rapid decrease of $\delta^{18}O$ values and change in trace element composition of the stalagmite imply remarkable change during the deposition at ca. 1500 AD. P shows rapid increase paralel to the decrease in Sr concentration, while Mg shifting towards more positive values. Textural studies indicate that there are small, but obvious variations in the petrographical features along the studied part of the stalagmite. The recognized hiata (vertical dotted lines in *Figs. 2* and *4),* represent ceased growth, especially near the top of the stalagmite (younger part). Non-uniform calcite growth rates were also shown by the age-depth relationship (*Fig. 2a*) and by the variable lamina width values (*Fig. 3a*). The lack of continuous growth reveals that the formation of the stalagmite suffer optimal conditions (i.e., warm and/or wet) in certain time period(s). The most remarkable hiatus can be seen close to the top of the stalagmite (ca. 1600–1700 AD). As the recent mean annual temperature in the cave interior is ca. 5.5 °C, we could exclude solely the temperature decrease for widespread freezing of the cave system. A gradual cooling would inevitability resulted in significant $\delta^{18}O$ shift for the deposited carbonate (*Siklósy et al.*, 2008b), however, in the case of Kiskőhát Shaft, only minor variability were observed before and after the growth cessation. Restricted growth can be explained by reduced drip rate of infiltrating water in dry periods, or because of heavy water flows in the wet season within the cave, when the water is no longer supersaturated for $CaCO_3$. This latter option can be ruled out as the trace element composition (especially Mg) exhibit higher values rather than the diluted, low values. The rapid increase in Mg after between 1600 and 1700 AD is possibly due to an important increase in water residence time followed by the cessation of speleothem growth as indicated by hiata at the top. Decreasing Sr concentration values after 1500 AD and especially after 1650 AD also suggest reduced growth rate. By the end of this process, stalagmite growth ceased. Therefore, our data suggest that the lack of infiltrated water would explain the marked growth break. It is important to distinguish internal and external dryness, as the second option would definitely imply regional climate variability, and the P concentration and $\delta^{13}C$ values would reflect aridity induced changes in the vegetation and soil system. On the contrary, P concentration increases and $\delta^{13}C$ values decrease, representing prosperous conditions in the soil zone. We, therefore, argued that internal ("within cave") dryness and, subsequently, the decrease in water availability during this period were responsible for the pausa of the growth. Water deficit in the interior can emerge by the advanced ventilation caused by enhanced winter (cold and dry) air masses entering the cave. In situ seasonal changes in $p(CO_2)$ were recorded and supported our assumptions. Therefore, we suggest that elevated ventilation during this time period was caused by longer winters. Based on the determined ages, this section of the studied stalagmite deposited during the LIA. As a consequence of external cooling, $\delta^{18}O$ of the stalagmite during this period exhibits lower values, while averaged growth rate decreased (to ca. 16 – 40 μm/year), according to the determied U–Th ages and distances (*Fig. 2a*). As a first approach, the observed ca. 2‰ isotopic shift between the MWP and LIA can be translated into temperature change using the above mentioned temperature dependency factor of the local precipitation (ca. + 0.6‰ / °C) and the equilibrium fractionation that accompanies calcite deposition from drip-waters (– 0.24 ‰ / °C) inside the cave. These two factors would result a range of ca. 5 °C cooling, which is higher than the realistic value. Thus, more complex scenario required for the interpretation of the isotopic record, therefore, we need to consider additional factors than solely the temperature dependency that may modify the $\delta^{18}O$ values of the calcite. We assume that a combination of the following processes shifted the $\delta^{18}O$ values of the stalagmite towards less negative values during the MWP:

- a slight evaporation of the local precipitation and the infiltrating water resulted in elevated $\delta^{18}O$ value for the dripping water, thus for the precipitated calcite as well, or
- the decrease of the ratio between winter/summer precipitation resulted in positive shift of the annual infiltrating water.

To summarize, the coldest years (most probably longer or colder winters) spans around from 1550 to ca. 1700 AD. The missing periods (hiata) and the relatively bigger age errors around the top of the stalagmite prevent the better resolution of the LIA, however, the minimum growth rate and the complex geochemical record support our assumptions.

6. Conclusions

We investigated the textural characteristics, stable carbon and oxygen isotope composition, and the trace element content of the subrecent part of a laminated stalagmite from northeast Hungary (Kiskőhát Shaft) in order to reveal a climate induced geochemical record for the last millennium. The high-resolution record from the cave deposit revealed a number of paleoenvironmental proxy. We interpreted the changes in this speleothem as a result of complex changes in the environmental parameters:

1. Cold and/or arid years (lower annual mean temperature or longer winter) reduce the average growth rate or even stop the growth of the stalagmite, while warm and humid periods results in optimal conditions for the accretion (faster growth rate).
2. More positive $\delta^{18}O$ values represent warmer periods (Medieval Warm Period), with a favorable conditions (wet and warm) for biogenic activity in the soil zone.

3. Cooling at the end of the Medieval Warm Period resulted in a reduced soil biogenic activity revealed by the increased stable carbon isotope values.
4. The climate experienced several warmings and coolings and important changes in the precipitation amount over the Medieval Warm Period – Little Ice Age transition, both with slower and faster growth rates, compared to the previous time period (MWP).
5. During the Little Ice Age, the cave was colder, the growth rate of the deposits was practically zero (presence of hiata). In the case of growing, stalagmite recorded colder but humid conditions.

Acknowledgements—This study was financially supported by the Hungarian Scientific Research Fund (OTKA T 049713). Measurements of U-Th isotopic compositions and ^{230}Th dates were supported by the National Science Council grants (94-2116-M002-012, 97-2752-M002-004-PAE & -005-PAE to C.C.S.). This paper is a contribution to the European Millennium Project (017008). Financial support of the Hungarian Meterological Society is greatly appreciated.

References

Bodri, L. and *Dövényi, P.*, 2004: Climate change of the last 2000 years inferred from borehole temperatures: data from Hungary. *Global Planet Change 41*, 121–133.

Burton, E.A. and *Walter, L.M.*, 1991: The effects of PCO_2 and temperature on magnesium incorporation in calcite in seawater and MgCl2–CaCl2solutions. *Geochim Cosmochim Ac 55*, 777–785.

Cheng, H., Edwards, R.L., Hoff, J., Gallup, C.D., Richards, D.A., and *Asmersom, Y.*, 2000: The half-lives of uranium-234 and thorium-230. *Chem Geol 169*, 17–33.

Edwards, R.L., Chen, J.H. Ku, T.-L., and *Wasserburg, G.J.*, 1987. Precise timing of the last interglacial period from mass spectrometric analysis of Th-230 in corals. *Science 236*, 175–192.

Fairchild, I.J., Baker, A., Borsato, A., Frisia, S., Hinton, W.R., McDermott, F., and *Tooth, F.A.*, 2001: Annual to sub-annual resolution of multiple trace-element trends in speleothems. *Journal of the Geological Society, London, 158*, 831-841.

Fairchild, I.J., Smith, C.L., Baker, A., Fuller, L., Spotl, C., Mattey, D., McDermott, F., and *E.I.M.F.*, 2006: Modification and preservation of environmental signals in speleothems. *Earth-Sci Rev 75*, 105–153.

Friedman, I. and *O'Neil, J.R.*, 1977: Compilation of stable isotope fractionation factors of geochemical interest. In *Data of Geochemistry* (ed.: *M. Fleischer*). *U.S. Geological Survey Professional Paper 440-KK, 6th Ed.*, Reston, VA.

Gascoyne, M., 1983: Trace element partition coefficients in the calcite-water system and their paleoclimatic significance in cave studies. *J. Hydrol. 61*, 213–222.

Gascoyne, M., 1992: Palaeoclimate determination from cave calcite deposits. *Quaternary Sci Rev 11*, 609–632.

Harmon, R.S., Schwarcz, H.P., O'Neil, J.R., 1979: D/H ratios in speleothem fluid inclusions: a guide to variations in the isotopic composition of meteoric precipitation? *Earth Planet Sc Lett 42*, 254–266.

Hendy, C.H., 1971: The isotopic geochemistry of speleothems 1. The calculation of the effects of the different modes of formation on the isotopic composition of speleothems and their applicability as palaeoclimatic indicators. *Geochim Cosmochim Ac 35*, 801–824.

Huang, Y., Fairchild, I.J., Borsato, A., Frisia, S., Cassidy, N.J., McDermott, F., and *Hawkesworth, C.J.*, 2001: Seasonal variations in Sr, Mg and P in modern speleothems (Grotta di Ernesto, Italy). *Chem Geol 175*, 429–448.

Huang, Y. and *Fairchild, I.J.*, 2001: Partitioning of Sr^{2+} and Mg^{2+} into calcite under karst-analogue experimental conditions. *Geochim Cosmochim Ac 65*, 47–62.

Katz, A., 1973: The interaction of magnesium with calcite during crystal growth at 25–90 °C and 1 atmosphere. *Geochim Cosmochim Ac 37*, 1563–1586.

Kern, Z. and *Popa, I.*, 2007: Climate–growth relationship of tree species from a mixed stand of Apuseni Mts., Romania. *Dendrochronologia 24*, 109–115.

Kern, Z., Grynaeus, A., and *Morgós, A.*, 2009: Reconstructed precipitation for southern Bakony Mountains (Transdanubia, Hungary) back to 1746 AD based on ring widths of oak trees. *Időjárás 113*, 299-314.

Kiss, A., 2009: Historical climatology in Hungary: Role of documentary evidence in the study of past climates and hydrometeorological extremes. *Időjárás 113*, 315-339.

Kordos, L., 1977: A sketch of the vertebrate biostratigraphy of the Hungarian Holocene. *Földrajzi Közlemények 25*, 144–160.

Kordos, L. and *Ringer, Á.*, 1991: Climatostratigraphic and archeostratigraphic correlation of Arviocolidae stratigraphy of the late Pleistocene in Hungary (in Hungarian). *MÁFI évi jelentése az 1989. évről*. Budapest, 523–533.

Lauritzen, S.E., 1995: High-resolution palaeotemperature proxy record for the last interglaciation based on Norwegian speleothems. *Quaternary Res 43*, 133–146.

McCrea, J.M., 1950: On the isotopic chemistry of carbonates and a paleotemperature scale. *J Chem Phys 18*, 849–857.

McDermott, F., 2004: Palaeo-climate reconstruction from stable isotope variations in speleothems: a review. *Quaternary Sci Rev 23*, 901–918.

Meyer, H.J., 1984: The influence of impurities on the growth rate of calcite. *J Cryst Growth 66*, 639–649.

Mucci, A., 1987: Influence of temperature on the composition of magnesian calcite overgrowths precipitation from seawater. *Geochim Cosmochim Ac 51*, 1977–1984.

Mucci, A. and *Morse, J.W.*, 1983: The incorporation of Mg^{2+} and Sr^{2+} into calcite overgrowths: influences of growth rate and solution composition. *Geochim Cosmochim Ac 47*, 217–233.

Popa, I., 1999: Aplicaţii informatice utile în cercetarea silvică. Programul CAROTA şi programul PROARB. *Revista pădurilor. 2*, 41–42.

Rácz, L., 1989: Climate history of the Middle and Modern Ages (in Hungarian). *Agrártörténeti Szemle 31*, 118–147.

Réthly, A., 1962: Natural disasters and calamities untill the year of 1700 (in Hungarian). Akadémiai Kiadó, Budapest.

Richards, D.A. and *Dorale, J.A.*, 2003: Uranium-series chronology and environmental applications of speleothems. *Rev Mineral Geochem 52*, 407– 460

Rozanski, K., Aragulas-Aragulas, L., and *Gonfiantini, R.* 1993: Isotopic patterns in modern precipitation. In *Climate Change in Continental Isotopic Records* (ed.: *P.K. Swart, K.C. Lohmann, J. McKenzie, S.* Savin). *Geophysical Monograph 78*. American Geophysical Union, Washington, DC, 1–36.

Shen, C.-C., Edwards, R.L., Cheng, H., Dorale, J.A., Thomas, R.B., Moran, S.B., Weinstein, S.E., and *Hirschmann, M.*, 2002: Uranium and thorium isotopic and concentration measurements by magnetic sector inductively coupled plasma mass spectrometry. *Chem. Geol. 185*, 165–178.

Shen, C.-C., Cheng, H., Edwards, R.L., Moran, S.B., Edmonds, H.N., Hoff, J.A., and *Thomas, R.B.*, 2003: Measurement of attogram quantities of ^{231}Pa in dissolved and particulate fractions of seawater by isotope dilution thermal ionization mass spectroscopy. *Anal Chem 75*, 1075–1079.

Siklosy, Z., Demeny, A., Vennemann, T.W., Kramers, J., Lauritzen, S.E. and *Leel-Ossy, Sz.*, 2007: Middle bronze age climate change recorded in a Hungarian stalagmite: triggering by volcanic activity? *Geophysical Research Abstracts, 9*: 1607-7962/gra/EGU2007-A-00777.

Siklósy, Z., Demeny, A., Leel-Ossy, Sz. and *Szenthe, I.*, 2008a: High-resolution stable isotope and U-Th study of Hungarian stalagmites, related to climate optima (in Hungarian). *Hungeo2008 abstract book*, 40–41.

Siklósy, Z., Demény, A., Pilet, S., Leel-Ossy, Sz., Lin, K. and *Shen, C.-C.*, 2008b: Stalagmite geochemistry and the timing of the last interglacial-glacial transition in Central Europe (NE Hungary). *EPICA2008* Conference Abstract.

Siklósy, Z., Demény, A., Vennemann, T.W., Pilet, S., Kramers, J., Leel-Ossy, Sz., Bondár, M., Shen C.-C. and *Hegner, E.*, 2009: Bronze Age volcanic event recorded in stalagmites by combined isotope and trace element studies. *Rapid Communications in Mass Spectrometry 23*, 801-808.
Spötl, C. and *Vennemann, T.* 2003: Continuous-flow isotope ratio mass spectrometric analysis of carbonate minerals. *Rapid Communications in Mass Spectrometry 17*, 1004–1006.
Sümegi, P., 2007: Late Quaternary environmental history of Hungary (in Hungarian). *D.Sc. Thesis for Hungarian Academy of Science*. University of Szeged, the Faculty of Science, Department of Geology and Palaeontology.
Yonge, C., Ford, D.C., Gray, J., and *Schwarcz, H.P.*, 1985: Stable isotope studies of cave seepage water. *Chem Geol 58*, 97–105.

IDŐJÁRÁS

Quarterly Journal of the Hungarian Meteorological Service
Vol. 113, No. 4, October–December 2009, pp. 265–298

Middle Age paleoecological and paleoclimatological reconstruction in the Carpathian Basin

Pál Sümegi[1,2*], Gusztáv Jakab[3], Péter Majkut[1], Tünde Törőcsik[1], and Csilla Zatykó[2]

[1]*Department of Geology and Paleoecology, University of Szeged, P.O. Box 658, H-6722 Szeged, Hungary*
E-mail: sumegi@geo.u-szeged.hu

[2]*Institute of Archaeology, Hungarian Academy of Sciences, Úri út 49, H-1014 Budapest, Hungary*

[3]*Institute of Environmental Sciences, Tessedik Sámuel College, Szabadság út 1-3, H-5540 Szarvas, Hungary*

(Manuscript received in final form November 19, 2009)

Abstract—Three programs of medieval environmental history research of fourteen sites was undertaken between 1998 and 2008 as part of the "*Evolution of the Hungarian mires, peats and marshes*", "*Environment history of Hungary*", and "*Geoarcheological investigations of Hungary*" projects. This present study was to demonstrate the facilities of paleoecological and paleoclimatological investigations (pollen, macrofossil, sediment works) completed on the core sequence of the Nádas Lake at Nagybárkány (Hungary). The Nádas Lake at Nagybárkány is a small peat-bog in the eastern Cserhát Mountains. The formation of the lake can be traced back to the late Glacial. The sediments deposited in the lakebed provide a record of climatic and hydrologic changes. A higher water level could be demonstrated from the late Glacial to the mid-Holocene, when the reed-beds covered a small area only. This was followed by a hiatus spanning about 5000 years, caused by the deepening of the lakebed during the Imperial Age, around 20–50 AD. The water level decreased and the water quality was more eutrophic. A reed-bed evolved around the lake. Paludification started with a bulrush floating mat phase at the close of the Middle Age, ca. 1300 AD. The initiation of the *Sphagnum*-bog underwent similar phases as in the other Hungarian peat-bogs. Although some anthropogenic disturbances can be reconstructed in the development of the peatland, some climatic effects and authogenic processes might be separated by paleoecological analyses.

Key-words: peatland development, macrofossils, pollen, geochemistry, paleoclimate, Holocene

* Corresponding author

1. Introduction

The application of macrofossil analysis to peat and lacustrine deposits enables to identify long-term vegetation changes in aquatic ecosystems. The composition of aquatic plant communities is largely influenced by the hydrological conditions prevailing in the basin harboring them. These, on the other hand, are highly prone to centennial-scale fluctuations in the climate. Former studies aimed at deciphering past climatic conditions via detailed analysis of peatland deposits primarily focused on the investigation of *Sphagnum*-peats of so-called ombrotrophic peatlands (*Barber et al.*, 2000; *Barber* and *Langdon*, 2001; *Barber* and *Charman*, 2005; *Mauquoy* and *Barber*, 1999). Due to various methodological problems, high-resolution quantitative macrofossil studies on the eutrophic peatlands of continental Europe were generally lacking so far. A slight modification of the method proposed by *Barber et al.* (1994) enabled us to retrieve proxy-climate data from the eutrophic peatlands of continental areas as well (*Jakab et al.*, 2004).

The total number of *Sphagnum* occurrences hardly exceeds 50, and in the central driest areas of the Great Hungarian Plain they are completely absent. Only sporadic *Sphagnum*-bogs are known in the country with a total number well below 20, most of them being extremely small with an area of a mere couple ha. Real raised bogs are completely missing. The majority of *Sphagnum*-bogs is restricted to the western parts of the country enjoying oceanic climatic influences, and to those of the areas of the Northern Mountains and the northern part of the Great Hungarian Plain, enjoying montane-type climatic influences of the Carpathians (*Boros*, 1968; *Szurdoki* and *Nagy*, 2002).

The present paper is discussing the findings regarding the development of small eutropic peat-bog from northern Hungary. Autogenic succession processes, climatic conditions, and anthropogenic influences largely contributed to creating the modern view of the referred peatland. Other aim was to put the reconstructed anthropogenic impacts and their changes to the context of the settlement strategies and landscape usages in the central parts of the Carpathian Basin.

Besides the radiocarbon-dated (Table 1) results (Tables 2–5) presenting some similarities and differences between local strategies in adopting and using marginal landscapes, this project will contribute to future research in Hungary on similar topics. In order to shed light onto the interrelations of vegetation changes and climate change, the model of *Davis et al.* (2001, 2003) was adopted in our work (Table 6). In our model the plants inferred from the palynological and plant macrofossil records were assigned to groups of plant functional types (*Prentice et al.*, 1998; *Peyron et al.*, 1998).

2. *Study site*

The Nádas Lake (360 m a.s.l.) at Nagybárkány lies on the northern side of Mt. Hármas-Határhegy, rising to a height of 516 m in the eastern Cserhát Mountains (*Fig. 1*). There are two other lakebeds in its vicinity, but these are smaller than the Nádas Lake. The lakebed has an elongated, north-west oriented form, with a strongly narrowing extension in the south. Its length is roughly 100 m, its greatest width is 40 m, and it covers an area of roughly 2000 m^2. The narrowing section is about 5–10 m wide. Accumulation in the catchment basin of the lake started in the late Glacial, when a mass movement (exactly rotation landslide) process was formed on the slope of the Miocene sandy and silty sediment covered land surface. A slump hollow formed in the source area between the landslide toe, and the scarp which was filled up by water forming a small round-form lake. This mass movement process is characteristic in the analyzed region. The annual rainfall is between 600–700 mm. The origin of the peat-bog's water is ombrotrophic and topogenic. There is not any visible watercourse in the drainage area.

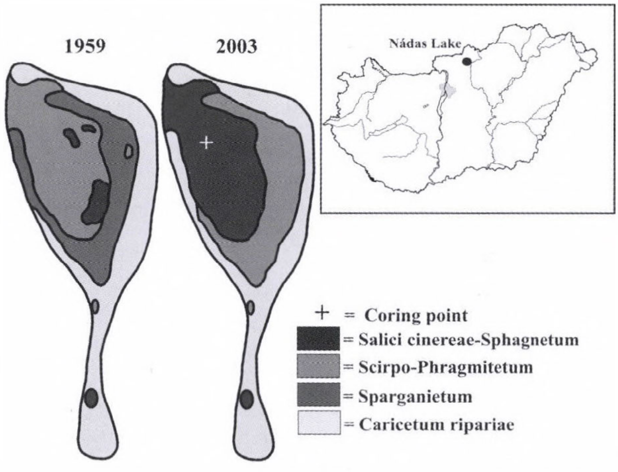

Fig. 1. Site location of the Nádas Lake and core location on the vegetation map in 1959 (after *Máthé* and *Kovács* (1959)) and in 2003 *Jakab-Sümegi* (2005).

The lakebed is fringed by a sessile oak forest. Three plant communities can be distinguished in the recent bog (*Fig. 1*). The central part of the bog is covered with Sphagnum willow swamp (*Salici cinereae-Sphagnetum recurvi*). This community is rather poor in species; it is characterized by a dominance of *Salix cinerea* and a carpet of *Sphagnum squarrosum*. This association is rather rare in Hungary, occurring in the well watered, undrained valleys of the Great Hungarian Plain and the Northern Mountains, as well as in smaller local hollows. The willow swamp is fringed by reed-beds (*Scirpo-Phragmitetum*), except on the western side. The reed-beds are similarly poor in species; the presence of *Lythrum salicaria, Lycopus europaeus*, and *Utricularia vulgaris* can be noted. Tall sedge communities (*Caricetum ripariae*) line the reed-beds. These communities are dominated by *Carex riparia*.

3. Methods

Overlapping cores were extracted using a Russian corer conforming to the general practice in quaternary paleoenvironmental studies. The samples submitted to lithological analyses were identical with the ones used for the paleobotanical, macrobotanical, and radiocarbon analyses. Results of pollen analyses of the peat-bog sequence were presented in *Juhász*, (2005) and *Juhász et al.* (2004).

The sampling of the 340-cm-deep, undisturbed sedimentary sequences from basin of the Nádas Lake was carried out using a 5-cm-diameter Russian type corer. The main lithostratigraphic features of the sedimentary sequence were determined and analyzed. For the description of the cores, the internationally accepted system and symbols of *Troels-Smith* method developed for unconsolidated sediments were adopted (*Troels-Smith*, 1955).

Radiocarbon dating of the sequence was obtained by both bulk and AMS (accelerator mass spectrometry) analyses. Four bulk samples of sediment were analyzed for radiocarbon ages at the Nuclear Research Centre of the Hungarian Academy of Sciences, Debrecen, Hungary, and one sample of plant macrofossils was analyzed for AMS date at the radiocarbon dating facility in Poznan, Poland. In order to allow comparison with other archaeological data, the dates were calibrated using the Oxcal v.3.9 calibration program (*Bronk Ramsey*, 2001), using atmospheric data of *Stuiver et al.* (1998). The original dates are indicated as uncal BP, while the calibrated dates are indicated as cal BC, cal BP, or cal AD (*Table 1*). Depth-age modeling and determination of the age of the samples were constructed by using radiocarbon data and sedimentation rate (*Bennett*, 1994; *Valanus*, 2008).

The core was divided into 4 cm samples. The organic content of the core samples was estimated by loss-on-ignition at 550 °C for 5 hours and the carbonate content by the further loss-on-ignition at 900 °C for 5 hours (*Dean*, 1974). The inorganic content was further analyzed using the sequential extraction method. *Mackereth* (1966) was the first to recognize the potential of geochemical investigations on the sediments of the catchment basin for the purpose of environmental reconstructions in his review of bulk chemical analyses on deposits from the Lake District. The application of bulk analysis, however, is quite problematic since it does not shed light unequivocally onto the origin of the chemical constituents (*Engström* and *Wright*, 1984). Mackereth' work was later enhanced by researchers working on the combination of chemical analyses with palynological investigations.

Table 1. Radiocarbon dates for the lake Nádas at Nagybárkány. Calibrated with Radiocarbon Calibration Program 4.4.2

Sample number	Depth (cm)	Sediment type	$\delta^{13}C$(PDB) ± 0.2 [‰]	^{14}C age (uncal BP)	cal AD/BC (2 σ)
deb-11110	NB-45	Peat	–28.02	100% ± 0.40 pM ^{14}C	1950–1960 cal AD
deb-11098	NB-100	Peat	–27.73	740 ± 60	1230–1300 cal AD
deb-11009	NB-180	Peat	–28.49	1600 ± 60	400–540 cal AD
deb-11100	NB-250	Charcoal	–27.52	6090 ± 60	4956–5146 cal BC
Beta-194559	NB-280	Charcoal	–24.90	8050 ± 40	6875–7061 cal BC

A new, so-called sequential extraction method (*Dániel*, 2004) with a long established history in the analysis of geochemical composition of lacustrine sediments was adopted in our work. From the full procedure, the step of water extraction for unseparated samples was sufficient to suit our analytical needs. As it was shown by previous works (*Dániel*, 2004), the most important paleo-hydrological and paleoecological data originate from water extraction samples. Distilled water was purified using a Millipore 5 Plus water purification system for water extraction samples. 100 ml distilled and purified water was added to 1.0 g sample and was shaken for 1 hour (*Dániel*, 2004), and then the water extract elements of Na, K, Ca, Mg, Fe were analyzed using a Perkin-Elmer AAS spectrometer. The results from the geochemical analyses are plotted against depth. Statistical procedures were used to zone the data. Principal components analyses computed on correlation matrices were preformed after logarithmic transformation of the geochemical data (*Rollinson*, 1993). The geochemical zones were identified by cluster analysis of principal components (*Dowdeswell*, 1982) using squared Euclidean distance and Ward aggregation method.

For the description of macrofossils, we used a modified version of the QLCMA technique (semi-quantitative quadrat and leaf-count macrofossil analysis technique) of *Barber et al.* (1994). Organic remains from peat and lacustrine sediments rich in organic matter can be divided into two major groups. Some remains can be identified with lower ranking taxa (specific peat components), while others cannot be identified using this approach (non-specific peat components). The most important specific peat components are seeds, fruits, sporogons, mosses, rhizomes, and epidermis (e.g., *Carex* species), leaf epidermis, other tissues and organs (hairs, tracheids, etc.), insect remains, and Ostracoda shells. The identification of herbaceous plant tissues was based on the procedure described by *Jakab* and *Sümegi* (2004). We defined the amount of peat components on the 1 cm^3 level, and the amount of seeds on the 3 cm^3 level. The samples were washed through a sieve with a 300 μm mesh size.

Concentration levels were determined by adding a known amount of indicator grains (0.5 g poppy seed, ca. 960 pieces) and by counting the poppy seeds and the remains using a stereo microscope in ten 10 mm by 10 mm quadrates in a Petri dish. Similarly to mosses, rhizomes can only be identified with a light microscope.

We removed a hundred monocotyledon remains and mounted them in water on microscopic slides for determining the percentages of individual taxa and of Monocot. undiff. The values for different moss species and UBF were determined using a similar procedure. We used the Psimpoll (*Bennett*, 1992) and Syn-Tax (*Podani*, 1993) programmes for plotting the analytical results.

4. *Results*

4.1. Chronology and sediment stratigraphy

Coring was carried out in the north-western part of the bog, now occupied by a willow swamp (*Fig. 1*). We found peat down to a depth of 110 cm, with an underlying water pocket (floating mat) down to 130 cm. Between 130–300 cm, we found peat and peat-mud with varying organic content. Between 300–340 cm, there was a silty lacustrine sediment layer (*Table 1*). The radiocarbon dates indicate a hiatus of roughly 4400 years (from 4970 BC to ca. 20–50 AD) between 248–240 cm, meaning that we have no data of any kind for this period. The results of the radiocarbon measurements analyses of the sequence described in this study are shown in *Table 2*.

Table 2. The lithological description of the sequence of Nádas Lake (*Jakab* and *Sümegi*, 2005)

Depth (cm)	*Troel-Smith* (1955) system	Description
0–40	Tb4 (Sphag.)	*Sphagnum* peat
40–110	Dg2Th1Tb1(Sphag.)	*Sphagnum* peat mixed with limus detritus, made up mostly of *Phragmites* (40–80 cm) and *Typha* rhizomes (80–100 cm)
110–130	–	Water
130–134	Dg2Tb1Th1	Burnt, charcoal rich peat layer with *Phragmites* rhizomes
134–255	Ld3Sh1 Tb+(Sphag.)Th+Tl+	Dark brown eutrophic lacustrine deposits (clayey silt) with varying organic content, large amount of wood fragments at 225 cm
255–277	As3Ld1 Th+Gs+(min.)	Pale yellow, brownish-grey slightly laminated silty clay with yellow spots
277–295	Ld3Sh1Tb+(Sphag.)Th+Gs+(min.)	Brownish-grey and pale yellow clayey silt with yellow spots
295–300	As3Ld1Gs+(min.)	Transitional layer
300–340	As3Ag1Gs+(min.)	Greenish-grey, clayey silt with frost marks (oligotrophic lacustrine deposists)

4.2. Geochemistry

A distinctive elemental and lithological stratigraphy was identified in the studied core sequence, which can serve as a potential record of paleohydrological and paleoecological history of the catchment basin of the Nádas Lake. According to the retrieved geochemical data (*Majkut*, 2009), 6 geochemical zones (*Table 3*) developed in the sediment profile of the core at Nagybárkány (*Fig. 2*).

Table 3. The geochemical zones and results from core sequence of the Nádas Lake (based on *Majkut* (2009))

Zone	cm	cal BP years	Geochemical changes
NBC-1	340–280	15,260 – 8800 late Glacial and early Holocene	The lake basin is characterized by the deposition of non-calcareous and low-organic content sediment. This sediment was predominantly inorganic (90–95%) and contained a high amount of water soluble Fe and K
NBC-2	280–240	8800 – 6000 early Holocene	The inorganic content (80–90%) decreased and there was a gradual increase in carbonate (5%) and organic (10–15%) content. The water soluble Fe, K content decreased, while the level of water soluble Ca, Mg input prior to this increase, indicating that the transformation of the vegetation continued and deciduous forest spread around the lake basin
NBC-3	240–190	2000 – 1500 Antiquity	There is a sudden upward decrease in the inorganic content of the deposits from the depth of 240 cm upwards, with an increase of the organic matter from the previous 10–15% to 70–80%. Elements to increase the level of included water soluble Ca and Mg suggest authigenic changes within the catchment (*Dániel*, 2004).
NBC-4	190–130	1500 – 700 Dark Age and early Middle Age	There is a gradual decrease in the organic content and water soluble Ca, Mg content accompanied by an increase in the inorganic content with water soluble Na content between 190–130 cm of the core profile. Previous studies (*Dániel*, 2004) have indicated that an increase of the abundance of these elements is indicative of both physical and chemical weatherings associated with soil erosion and human impact
NBC-5	110–40	700 – 0 late Middle Age and Industrial Age	A gradual increase in the organic content indicates decreasing soil erosion and human influences around the lake catchment basin. The water soluble Na, K, Ca, Mg content increased gradually in this zone. The observed composition of these elements may refer to the development of a floating mat, or a moss blanket on the water surface
NBC-6	40–0	Last 50 years	There is a rapid increase in the amount of water soluble Ca, Mg, K, and Na, as well as the organic content in this zone with peak values in the entire profile. According to the observed chemical composition of this zone, the emergence of a closed peat layer with mosses and the formation of a small peat-bog could have been inferred for the last 50 years

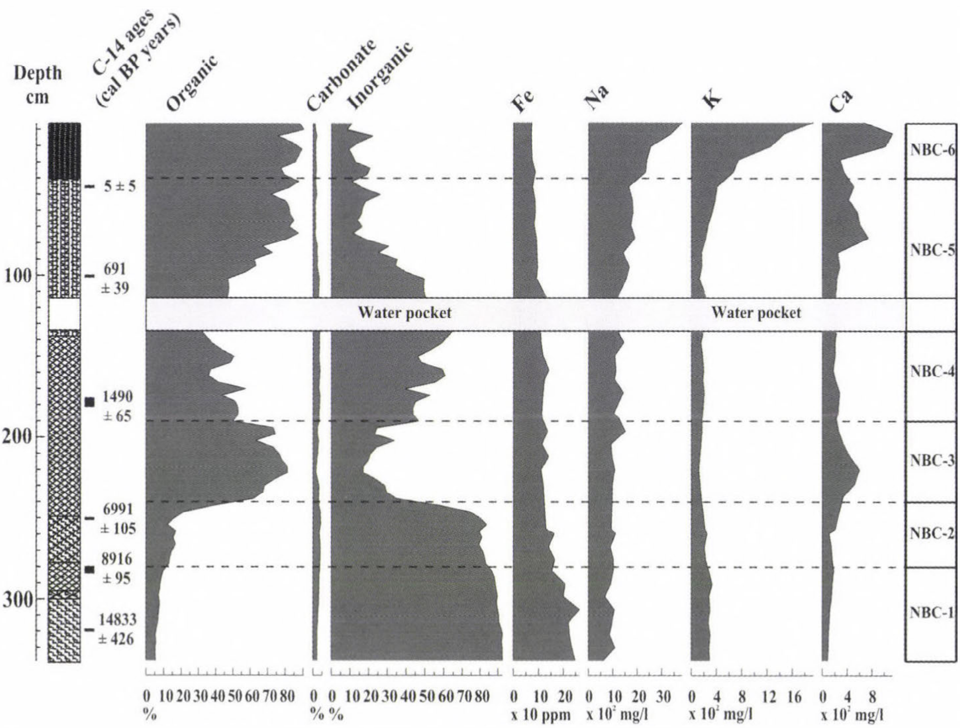

Fig. 2. Results of geochemical analyses (*Majkut*, 2009).

4.3. *Macrofossils*

The macrofossil zones are shown in *Table 4*. The profile was divided into nine zones on the basis of the analyses. The distribution of 15 most important peat components in the studied samples was evaluated using multivariate statistical methods in order to elucidate the major ecological, hydrological gradients of the individual macrofossil zones (*Jakab* and *Sümegi*, 2005). The ordination of variables (peat components) and objects (sediment samples) are depicted in *Figs. 3* and *4*.

Table 4. Macrobotanical zones and results from core sequence of Nádas Lake (based on *Jakab* and *Sümegi* (2005))

Zone	cm	cal BP years	Macrobotanical changes
NBM-1	340–288	15,260 – 10,000 late Glacial and early Holocene	The macrofossil concentration was rather low in the lower silty sediment which is poor in organic matter, suggesting high water level, oligo-mesotrophic water quality, and low vegetation cover. A narrow belt or patches of reed-beds probably lined the lakebed

Table 4 (continued)

Zone	cm	cal BP years	Macrobotanical changes
NBM-2	288–272	10,000 – 8000 early Holocene	The macrofossil concentration increased from 288 cm and reflected lower water level and mesotrophic water quality. The reed-bed at the edge of the lakebed probably formed a continuous belt by this period
NBM-3	272–247	8000 – 6000 mid-Holocene	The macrofossil concentration and the number of *Phragmites* decreased at 270 cm, marshland and bog species disappeared, suggesting a rise in the water level. In the second part of the zone, after 7000 cal BP, the macrofossil concentrations and the amount of *Phragmites* again increased, parallel to the renewed appearance of various *Sphagna* and moss species. These changes reflect another decrease in the water level and the spread of wetland vegetation
NBM-4	247–193	2000 – 1500 Antiquity	The radiocarbon measurements of the sediment samples between 187–176 cm indicated a hiatus of roughly 4400 years at the beginning of the zone. The extrapolation of the measurements suggest that this sediment hiatus developed around 2000 cal BP, during the Imperial Age, when the area was probably settled by Celtic man, who probably deepened the bog which had evolved by then
NBM-5	193 –103	1500 – 700 Dark Age and early Middle Age	The concentration of *Phragmites* rhizomes was quite high at the beginning of the zone, but declined continuously, parallel to the spread of *Typha*. The transition is marked by the lakebed's brief desiccation at 160 cm, with the significant increase of *Sphagnum squarrosum* peat-moss. The water quality was meso-eutrophic, changing to eutrophic from 160 cm. Between 130–110 cm there was a water pocket
NBM-6	103 –78	700 – 400 late Middle Age	The macrofossil concentration in this zone was extremely high. Many trees fell into the lakebed. The charcoal concentration also shows high values, reflecting the intensive exploitation of the environment. Thus, this zone represents the lake/bog transition
NBM-7	78 – 68	400 – 200 late Middle Age	A genuine floating mat phase
NBM-8	58 –33	200 – 0 Industrial Age	A *Sphagnum* bog (*Phragmiti communis-Sphagnetum*) developed in consequence of oligotrophication in the sampling area
NBM-9	33 – 0	Last 50 years	The *Sphagnum*-bog is replaced by a *Sphagnum* willow swamp in the last zone

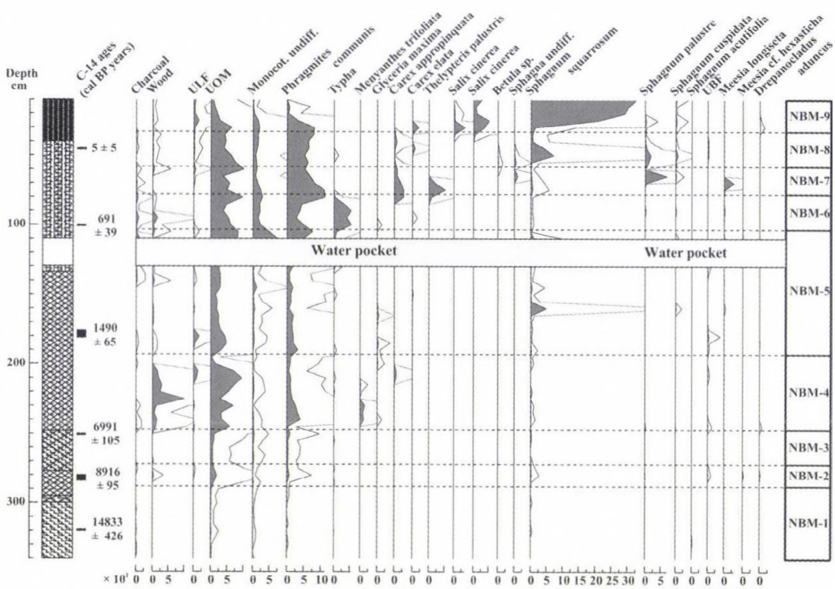

Fig. 3. Fossil plant tissues, mosses (pc cm^{-3}), and seeds (pc cm^{-3}) from Nádas Lake at Nagybárkány (*Jakab* and *Sümegi*, 2005).

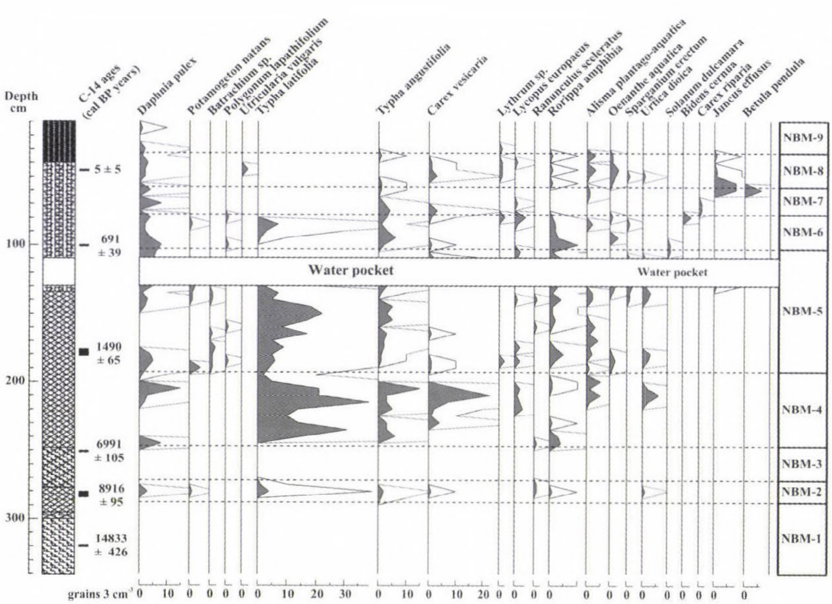

Fig. 4. Fossil plant tissues, mosses (pc cm^{-3}), and seeds (pc cm^{-3}) from the Nádas Lake at Nagybárkány (*Jakab* and *Sümegi*, 2005).

4.4. Pollen analysis

Samples taken between the depths of 340 and 0 cm yielded material suitable for evaluation. A summary of pollen analytical results is depicted in *Fig. 5*. *Table 5* shows the pollen zones of the lake Nádas.

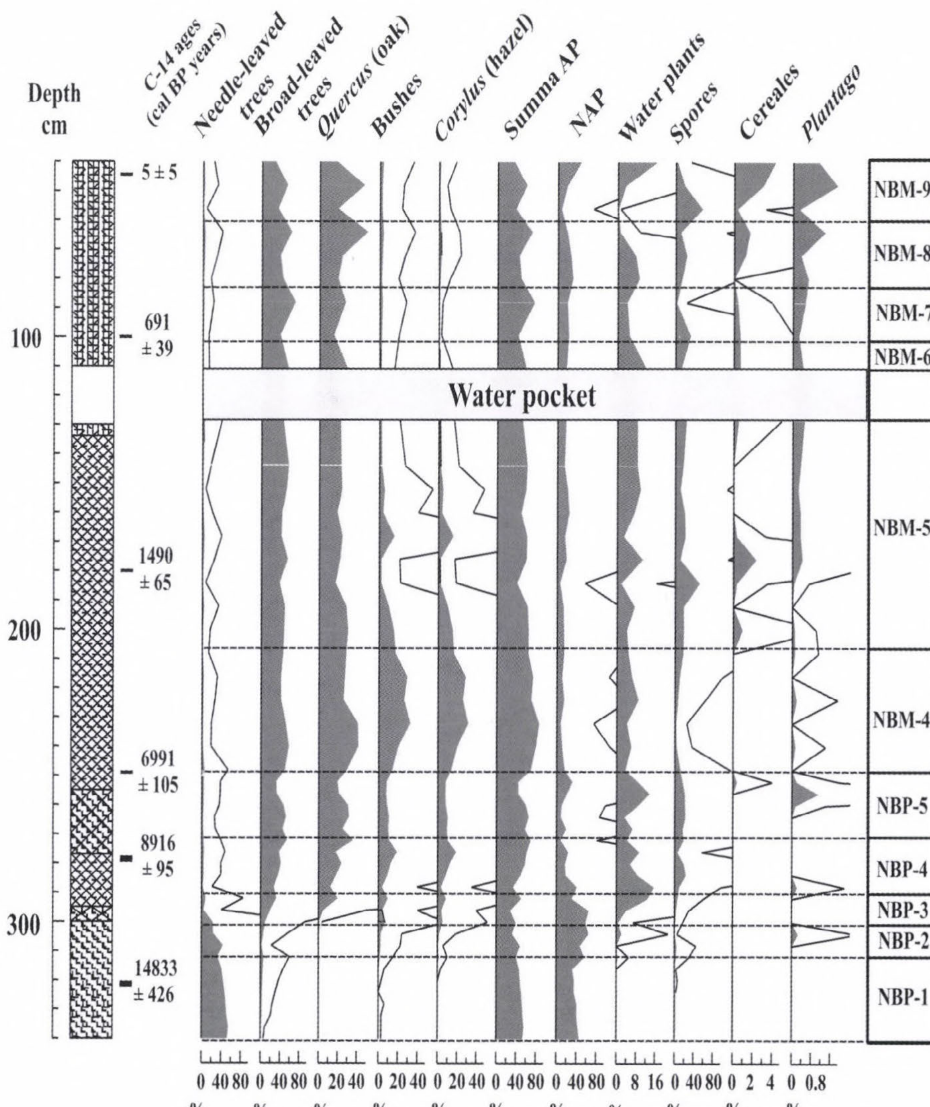

Fig. 5. Pollen zones and results from core sequence of Nádas Lake (based on *Juhász* (2005) and *Juhász et al.* (2004) (selected taxa)).

Table 5. Pollen zones and results from core sequence of Nádas Lake (based on *Juhász* (2005) and *Juhász et al.* (2004))

Zone	cm	cal BP years	Pollen composition changes
NBP-1	340–312	15,260 – 12,000 late Glacial	During the late Glacial, the surrounding hill slopes were covered by a mixed taiga vegetation with scattered patches of forest and steppe
NBP-2	312–304	12,000 – 10,000 transition	Open mixed taiga forest developed within *Pinus, Picea, Betula, Juniperus, Quercus* trees and *Corylus* scrub
NBP-3	304–292	10,000 – 9000 early Holocene	A species-rich mixed oak woodland appears early in this zone. There is a major decrease in the amount of pine at the beginning of the zone
NBP-4	292–272	9000 – 8000 early Holocene	A rapid spreading of *Fagus* and *Ulmus* can be traced within the newly developed mixed oak woodland accompanied by a gradual retreat of coniferous and steppe elements. The arboreal flora is dominated by oak and hazel with minor amounts of conifers and birch
NBP-5	272–248	8000 – 6000 mid-Holocene	The dominant elements of the flora in this zone are oak and hazel together with beech. Elm comprises the minor component of the flora. Evidence of the first human impacts was found in this zone. Selective logging of the woodlands is responsible for the change in the forest
NBP-6	248–192	2000 – 1600 Antiquity	In this zone, a mixed oak woodland was reestablished containing elements of hazelnut and scattered stands of *Fagus* and *Carpinus*. However, this woodland is characterized by a more closed canopy than the one present in the previous zone
NBP-7	192–136	1600 – 1000 Migration (Dark) Age	Besides the general dominance of oak, there is a sudden increase in the proportion of beech and hornbeam. The increased abundance of NAPs marks the gradual opening of the canopy from about 168 cm upwards. The presence of numerous weeds and cereals marks an intensive human activity in the analyzed area
NBP-8	104–72	900 – 300 Middle Age	The pollen profile points to the development of a closed canopy woodland with such dominant elements as *Salix* (40%) and *Quercus* (30–40%), together with *Fagus* and *Carpinus*. Other arboreal pollen (AP) types are rare. The presence of numerous weeds (*Plantago lanceolata* and *Centaurea cyanus*) and cereals marks an intensified human activity in the area
NBP-9	72–40	300 – 0 Industrial Age	The top of the pollen profile by *Juhász* (2005) is characterized by the development of an altered closed oak woodland with a presence of such AP species as beech and *Carpinus*
NBP-10	40–0	Last 50 years	Every 0.8 cm interval was analyzed for pollen. The pollen composition suggests forest regeneration process started around the peat-bog system

4.5. *Paleoecological zones*

According to the retrieved sedimentological, geochemical, pollen, and macrobotanical data, 6 paleoecological evolution phases developed in the sediment profile of the core at the lake Nádas (*Fig. 6*).

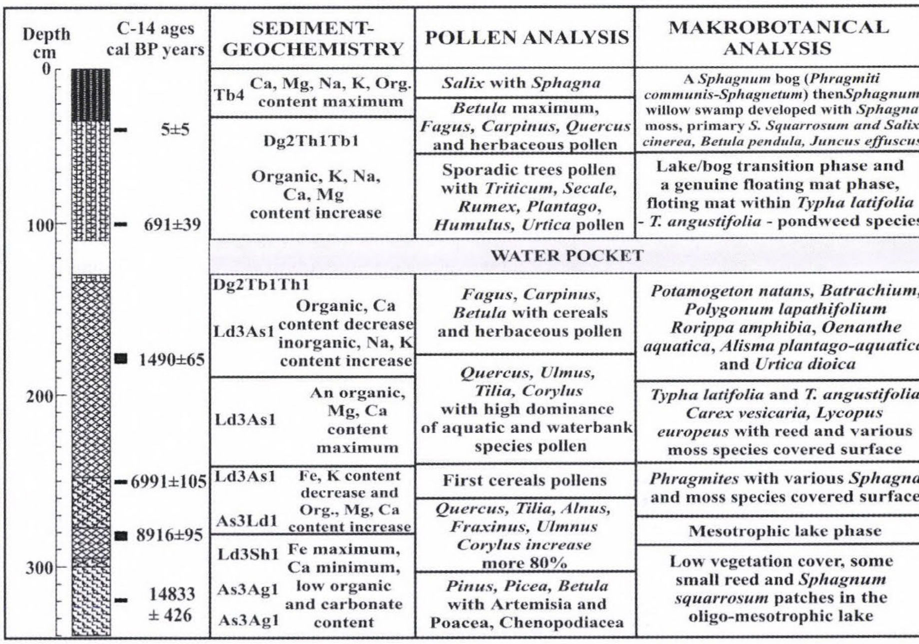

Fig. 6. Results of sedimentological, geochemical, pollen, and macrobotanical analyses.

4.5.1. *The first paleoecological phase, from late Glacial to early Holocene periods*

The lake base sediment is characterized by the deposition of non-calcareous and low-organic content sediment during the late Glacial and early Holocene periods. This sediment was predominantly inorganic (90 – 95%) and contained a high concentration of the water soluble Fe and K, and low concentration of water soluble Ca and Na.

The macrofossil concentration was rather low in the lower silty sediment which is poor in organic matter, suggesting high water level, oligo-mesotrophic water quality, and low vegetation cover. A narrow belt or patches of reed-beds probably lined the lakebed. The radiocarbon measurements indicated that this zone evolved at the time of the late Glacial up to the Pleistocene/Holocene transition. Rough peat-moss, *Sphagnum squarrosum*, a characteristic feature of the bog's recent vegetation, was already present at this time, even if in minimal amounts. The presence of peat-moss belonging to the *Acutifolia* section is noteworthy, coming from the damp soil of the surrounding coniferous forests.

During the late glacial and up until 10,000 cal BC, a coniferous forest steppe of Scots pine, spruce, and birch (*Pinus, Picea, Betula*) with several steppe elements surrounded the Nádas Lake at Nagybárkány. Pollen from the trees accounted for >50–60% of the total pollen with the remaining percentage composed of steppe elements such as the grasses (Gramineae), Chenopodiaceae, and *Artemisia.* The pollen compositions suggest that a cool climate phase developed around the catchment basin of Nádas Lake during the last phase of the Ice Age. Between 10,000–7000 cal BC, a dramatic change developed in the late-glacial boreal, type forest around the lake. There was a rapid decline in all dominant needle-leaved trees (*Pinus*, *Picea*) and an increase in the deciduous woodland elements. This deciduous woodland was composed of *Quercus, Tilia, Fraxinus, Alnus, Ulmus,* and *Corylus* and occurred for more 80% of the total pollen. This early postglacial diverse deciduous forest then persisted until anthropogenic activity effected the woodland at about 6000 cal BC. This pollen composition change indicates that a drastic climatic change developed during the early postglacial phase and the relative warm – rainy climatic Holocene climate was stabilized in the analyzed region.

4.5.2. The second paleoecological phase, mid-Holocene period

Up to the mid-Holocene, the inorganic content (80–90%) decreased and there was a gradual increase in carbonate (about 5%) and organic (10–15%) content. The water soluble Fe, K content decreased, while the level of water soluble Ca, Mg input prior to this increase indicates that the transformation of the vegetation continued and deciduous forest elements spread around the lake basin.

The macrofossil concentration increased from 288 cm. The number of *Phragmites communis* rhizomes and *Sphagnum squarrosum* leaves increased. *Typha angustifolia* and *Typha latifolia* made their appearance, together with the seeds of plants typical for reed-beds (*Ranunculus sceleratus, Rorippa amphibia, Alisma plantago-aquatica*) and *Daphnia* ephippiums. Bryophytes include the peatmoss *Sphagnum palustre* and other various mosses (*Drepanocladus aducus, Meesia* cf. *hexasticha*). The macrofossils reflect lower water level and mesotrophic water quality. The reed-bed at the edge of the lakebed probably formed a continuous belt by this period. The macrofossil concentration and the number of *Phragmites* decreased at 270 cm, and marshland and bog species disappeared, suggesting a rise in water level. In the second part of this zone, after 7000 cal BP, the macrofossil concentrations and the amount of *Phragmites* again increased, parallel to the renewed appearance of various *Sphagna* (*Sphagnum squarrosum, S. cuspidata, S. palustre*) and moss species

(*Drepanocladus aducus*). These changes reflect another decrease in the water level and the spread of wetland vegetation.

At approximately 5500 cal BC, the structure of the woodland altered once again with a large decline in the woodland pollen diversity, parallel with an increase of open gorund herbaceous types and an occurrence of cereal pollen. This change usually associated with anthropogenic activity. These results are consistent with archaeological data that has indicated development of Liner Pottery Culture within the Carpathian Basin at this time (*Kalicz* and *Makkay*, 1977). Some localities of this culture can be found around the analyzed region (*Bácsmegi* and *Fábián*, 2005).

4.5.3. The third paleoecological phase, Imperial Age

There is a sudden upward decrease in the inorganic content of the deposits from the depth of 240 cm upwards, with an increase of the organic matter from the previous 10–15% to 70 – 80%. Elements to increase the level of included water soluble Ca and Mg suggest authigenic changes within the catchment (*Dániel*, 2004). Probably Ca, Mg acceptor water plants, such as *Typha* and *Phragmites* colonized the analyzed catchment basin and the increase of the content water soluble Ca, Mg originated from the remains of these plants.

The macrofossil concentration suddenly increased at the beginning of the zone, with strikingly high UOM values, indicating an eutrophic marshland environment. The *Phragmites* cover expanded significantly over the lakebed. The zone contained high amounts of the leaf sheat epidermis of bogbean (*Menyanthes trifoliata*), which probably grew at the edge of the reed-bed facing the open water or in hollows. This section of the zone contained *Sphagnum squarrosum*. Reed declined in the second half of the zone, parallel to the expansion of bulrush (*Typha latifolia* and *Typha angustifolia*). This period is characterized by *Carex vesicaria* and various moss species (*Amblystegium serpens, Calliergonella cuspidata, Drepanocladus aduncus*). *Daphnia* ephippiums occurred in high numbers, and the spread of eutrophic marshland species, such as *Lycopus europaeus, Rorippa amphibia, Alisma plantago-aquatica*, and *Urtica dioica* could be noted. The macrofossils indicate lower water level and meso-eutrophic conditions at the beginning of the zone, and eutrophic conditions from ca. 1700 cal BP.

The radiocarbon measurements of the sediment samples between 187–176 cm indicated a hiatus of roughly 5000 years at the beginning of the zone. The extrapolation of the measurements suggest that this sediment hiatus developed around 1700 cal BP, during the Imperial Age, when the area was probably settled by Celtic or/and German groups, who probably deepened the peat-bog, which had evolved by then.

The closing of the forest canopy can be linked to the sudden increase of hazel (*Corylus*) from 15 to 30% and to the constantly high values of oak

(*Quercus*) in the first part of the zone. This is followed by the decline of hazel, while lime (*Tilia*) and elm (*Ulmus*) maintain a continuous presence, parallel to the re-appearance of *Fagus* and *Carpinus* at the end of the zone. The herbaceous vegetation has very low values, with a low amount of pollen grains. However, almost all taxa of the previous zone are present, even if only sporadically, but only grasses (Poaceae) and mugwort (*Artemisia*) have a continuous curve. Typical species of the wet zones, such as *Ranunculus*, *Lysimachia*, Apiaceae, can also be noted. The most important change in the local vegetation is the disappearance of *Sphagnum* moss with a very sharp decrease in the species of the earlier bogland vegetation, such as *Typha/Sparganium*, the Pteridophytes with Monolete spores (*Thelyptheris palustris*) and aquatic species (*Nuphar*, *Butomus*, *Potamogeton*).

4.5.4. The forth paleoecological phase, Migration Age

There is a gradual decrease in the organic content and water soluble Ca, Mg content accompanied by an increase in the inorganic content with water soluble Na content between 190–130 cm of the core profile. Previous studies (*Mackereth*, 1966; *Engström* and *Whright*, 1984; *Dániel*, 2004) have indicated that an increase of the abundance of these elements is indicative of both physical and chemical weatherings associated with soil erosion and human impact. The increase of the water soluble Na may indicate a drop in lake level as well during this phase.

The macrofossil concentration declined slightly in this zone. The concentration of *Phragmites* rhizomes was relatively low. Various pondweed species (*Potamogeton natans, Batrachium sp., Polygonum lapathifolium*) made their appearance, suggesting a relatively higher water level. *Sparganium erectum* became typical. The reed-bed was quite species rich, with species such as *Lycopus europaeus*, *Lythrum* sp., *Ranunculus sceleratus*, *Rorippa amphibia*, *Alisma plantago-aquatica*, *Oenanthe aquatica*, and *Urtica dioica*.

The concentration of *Phragmites* rhizomes was quite high at the beginning of the zone, but declined continuously, parallel to the spread of *Typha*. The transition is marked by the lakebed's brief desiccation at 160 cm, with the significant increase of *Sphagnum squarrosum* peat-moss. The water quality was meso-eutrophic, changing to eutrophic from 160 cm. Between 130–110 cm there was a water pocket. Between 110–100 cm, the number of *Phragmites* rhizomes increased significantly, suggesting that the extent of the open water diminished and that reed-beds also covered the sampling location. *Typha* (rhizome) appeared at the sampling location, although to a lesser degree only. The peak of *Rorippa amphibia* similarly indicates the decrease of the water level.

This zone is characterized by the opening up of the forest canopy and the increase of herbaceous elements. *Quercus* shows relatively constant values throughout the zone, while *Tilia* and *Ulmus* decline to very low values, parallel to the sudden rise of beech (*Fagus*) and hornbeam (*Carpinus*) at the beginning of the zone. *Betula* develops again in the forest with a constant level, except for a temporary minimum at 168 cm, while *Corylus* has a temporary maximum, followed by a decline to its previous level. *Alnus*, the typical taxa for the marginal zone of the peat-bog, is continuously present with low values, while *Fraxinus* shows a sporadic presence. Agricultural activity is reflected by the presence of cereals, *Plantago lanceolata*, *Centaurea cyanus*, and some nitrophilous taxa (*Urtica*) in this zone.

4.5.5. The fifth paleoecological phase, from Middle Age until 20th century AD

A gradual increase in the organic content indicates decreasing soil erosion and human influences around the lake catchment basin. The water soluble Na, K, Ca, Mg content increased gradually in this zone. The observed composition of these elements may refer to the development of a floating mat, or a moss blanket on the water surface.

The macrofossil concentration in this zone was extremely high. Many trees fell into the lakebed. The charcoal concentration also shows high values, reflecting the intensive exploitation of the environment. The expansion of bulrush at the sampling location can be noted (increase of *Typha* rhizomes), and the proportion of *Typha angustifolia* was higher than previously. *Typha angustifolia* gradually replaces *Typha latifolia*, indicating paludification and higher water level. This zone can be regarded as the first stage in the development of the present-day bog, when its central part was covered by floating bulrush mat at the expense of pondweed communities. It seems that the reed-bed broke loose from the sediment in consequence of rising water levels, leading to the formation of a floating mat. As a result of intensive oligotrophication, a floating reed swamp (*Phragmitetum communis thelypteridetosum*), then a *Sphagnum* bog (*Phragmiti communis-Sphagnetum*) developed in the sampling location with *Carex riparia* and *Carex appropinquata*. The zone is characterized by abrupt changes, reflecting further oligotrophication. There is a large-scale increase in marsh fern (*Thelypteris palustris*), which later decreases, parallel to the expansion of a rare moss, *Meesia longiseta*. Following the decline of the latter, the values of peat-mosses, especially of *Sphagnum palustris*, *Sphagnum squarrosum* increases. The high values of *Juncus effusus* are also characteristic for this zone.

According to the pollen composition (*Juhász*, 2005), this zone is characterized by a relatively closed vegetation cover. *Salix* is the dominant taxon, accounting for 40% of the total pollens. *Quercus* has high values too and shows a rise parallel to the decline of willow. Other tree taxa show a sporadic presence, except for beech (*Fagus*) and hornbeam (*Carpinus*), which are present with minor, but continuous curves, together with *Betula* and *Corylus*. Anthropogenic taxa are also present: the pollen grains of *Plantago lanceolata*, *Rumex*, and cereals (*Triticum* and also *Secale*) were identified. Cyperaceae, *Typha/Sparganium*, and aquatic species (*Lemna*, *Potamogeton*, *Butomus*) are present sporadically. The closing up of the forest canopy can be noted, with a dominance of *Quercus* and *Betula*.

4.5.6. The sixth paleoecological phase, 20th century

There is a rapid increase in the amount of water soluble Ca, Mg, K, and Na, as well as the organic content in this zone with peak values in the entire profile. According to the observed chemical composition of this zone, the emergence of a closed peat layer with mosses and the formation of a small peat-bog could have been inferred for the last 50 years.

The uppermost section of the pollen sequence is also dominated by oak, with some beech and hornbeam. Willow (*Salix*) is present and rises towards the end of the zone; the herbaceous vegetation (Poaceae and anthropogenic taxa) increases and dominates the landscape. The *Sphagnum*-bog is replaced by a *Sphagnum* willow swamp in the last zone. The recent expansion of *Salix cinerea* could be noted in the area (see *Fig. 1*). The number of reed species and reed-beds decreases, parallel to the increase of wood remains (wood, ULF). *Salix cinerea* remains (leaves, roots) are quite frequent. The values of *Sphagnum squarrosum* increase significantly.

Plantago lanceolata, Cerealia, *Urtica*, and *Rumex* have relatively high values. *Phragmites*, *Typha/Sparganium* are present in the local vegetation, together with *Thelypteris palustris*, although *Sphagnum* moss has lower values than in the previous zones. The very end of the pollen sequence was dated to 0 ± 60 uncalBP (1955 +/– 5 calAD), indicating a strong human impact on the vegetation cover, with high proportions of cereals, *Rumex*, and *Plantago lanceolata* among the herbaceous taxa. The size of the oak forest decreases and willow re-appears.

5. *Discussion*

5.1. Initial pond phase (late Glacial to mid-Holocene: 15,000 – 5000 cal BC yr)

The first phase of the analyzed region development, lasting until the mid-Holocene, was determined by relatively stable trophic conditions and smaller fluctuations in the water level. The water level somewhat decreased at ca. 6800 cal BC and the start of peat-bog initiation can be noted, probably in consequence of the onset of a warmer and drier climate. Species referring to paludification like *Sphagnum squarrosum* and *S. palustre* also turn up here. On the testimony of the pollen profiles (*Juhász et al.* 2004), this phase coincided with the appearance of thermophilous species rich oak forests. The water level again rose at 6000 cal BC and decreased after 5000 cal BC, enabling the expansion of reed-beds.

Between 15,000 – 5000 cal BC, inputs of K and Mg into the basin suggest that erosion of the slopes surrounding the lake basin was occurring and trophic conditions of the formed lake was oligotrophic (*Mackereth*, 1966; *Engström* and *Whright*, 1984; *Engström* and *Hansen*, 1985). The high content of water soluble Fe suggests that a combination of acidic silicate rich bedrock, coniferous trees and cool late Glacial climatic conditions resulted in podzol soil formation around the catchment basin. The deposited lacustrine sediments embedded minor pebbles as well till around 6000 cal BP in varying quantities. These must indicate abrasion of the shore in the lack of a closed reed belt.

According to the findings of geochemical analysis, the early Holocene lacustrine phase differed significantly from the previous pond stage in sedimentary, chemical composition and temperature conditions. While the earlier, late Glacial and lateglacial/postglacial transition lake environment can be characterized by sedimentation in a cold and oligotrophic water lacking Ca content and low vegetation cover, the early Holocene paleohydrological stage can be described as being relatively rich in Ca, with high carbonate and organic content and with a vegetation typical of easily warming water. The amount of Ca increased from about 100 to 200 ppm. Changes in the chemical composition refer to intensified erosion around the catchment basin and the transformation of the late Glacial oligotrophic lake into an open mesotropic lake phase. The increasing level of overland soil erosion into the catchment basin must have developed under increasing human impacts (e.g., woodland grazing). As shown by archeological data (*Bácsmegi*, 2005; *Bácsmegi* and *Fábián*, 2005), Neolithic Age communities settled around the analyzed region between 5500–5000 cal BC. These prehistoric human communities transformed their forested environment to open surface for arables and pasturelands. This type of human disturbance might trigger intensified soil erosion into the catchment basin.

5.2. Climate-driven mire phase (late Holocene: 0–1300 cal AD)

Abrupt geochemical changes indicate the emergence of a sedimentary hiatus in the catchment basin. It seems to us that this geological layer discordance formed by human impact. Results of the radiocarbon measurements are presented in *Table 1*, from which a sedimentary hiatus is apparent between 187–176 cm. This hiatus associated with a thin layer of burnt macrocharcoals. This, and a subsequent change in lacustrine stratigraphy from mesotrophic lake to reed peat show ca. 4000 years difference in age between adjacent samples. According to radiocarbon and sedimentological data of the core profile, this event coincides with a peat cutting in the Imperial Age when Barbarian groups (Celts, German tribes) occurred around the lake catchment basin (*Vaday,* 2005). Probably, one of these antique tribes cleaned the analyzed pond around 20-30 cal AD (*Figs. 5* and *6*). Then, after this cleaning procedure, a mass of water plants covered the artificially transformed pond surface (*Fig. 6*).

The *Phragmites* concentration in the sediment decreased during warmer periods in the Imperial Age and Middle Ages, parallel with an increase of *Typha* seeds and *Daphnia ephippia*. This reflects a competitive situation, characterized by alternating dominances of reed and bulrush in the lakebed. Reed and bulrush are both competitive species under favorable conditions.

In the pollen record, this phase is characterized by the opening up of the forest canopy and the increase of herbaceous elements (*Juhász*, 2005). It would appear that during periods of greater solar activity, the lake received more light, in part owing to the retreat of species forming higher and more closed forest canopy, like *Fagus* or *Carpinus*.

In order to shed light onto the interrelations of vegetation changes and climate change, the model of *Davis et al.* (2001, 2003) was adopted in our work. According to this model, some climatic changes, drier, wetter and warmer (*Table 6*), and cooler phases developed during last 2000 years (*Figs. 7* and *8*). One of the most important warmer climatic phases formed in the Imperial Age, then in the late Migration Age, and early Middle Age. The lake is fringed by high, steep slopes in the south and south-east, from where the high trees cast a shadow over the greater part of the lake. The expansion of phyto-planktons at the time of greater solar activity is indicated by an increase of *Daphnia* feeding on them. The expansion of phytoplankton leads to the development of looser sediments, encouraging the spread of *Typha*. The beginning and close of the Medieval Warm Period saw the maximum of solar activity (*Bradley et al.*, 2003). The end of this warm period at about 1250 AD was marked by the so-called medieval solar activity maximum, which caused serious droughts in Europe and North America. The sudden expansion of *Sphagnum squarrosum* can be noted at the time of the two maximums. *Phragmites* and *Typha* both declined at around 800 AD, suggesting the brief desiccation of the bed, when peat-moss temporarily covered the entire lakebed .

In the pollen record at ca. 600 cal AD, *Cyperaceae* and aquatic species (*Nuphar*, *Nymphea*, *Lemna*, *Butomus*) have a temporary minimum as well (*Juhász*, 2005). The water level decreased for a longer period of time around 1200–1300 cal AD, enabling the expansion of the reed-bed over the lake's entire surface and causing the reduction of open water. According to the geochemical data between 500–1300 cal AD, a drier and maybe a warmer phase formed (*Fig. 4*). The increase of the water soluble Na content shows that a decrease of the pond water level might have developed during this phase.

The referred period was coeval with one of the major crisis periods of medieval Hungary, the invasion of Mongolian tribes dated between 1241 and 1242. From the written record we do know that some chronicle writers blamed the Mongolian invasion of the country on the severe cold weather, while others related it to the unusual droughts hampering Europe during the summers of the 13th century. *Barber et al.* (2000) declared this period as the driest of the past 2000 years in the history of Europe. In Hungary, the extremely cold winter of

1241 was devastating regarding the political and economic fate of the country, when the river Danube was completely frozen enabling the Mongol tribes to safely cross the river and destroy the settlements of Transdanubia as well. As *Kiss* (2000, 2003) clearly stated, the controversies lying in the contrast of the extremely cold winters and summer droughts can easily be resolved. A complete freezing of the river Danube was not an unusual event in Hungary preceding the river regulations on the one hand. On the other hand, the summer droughts which might have struck Hungary as well at the time must have reinforced the devastating effects of famine attributable to the war itself as well. This warm and dry weather must have contributed to a complete desiccation of the Nádas Lake of Nagybárkány, when reed coverage must have extended to the entire lacustrine basin.

Table 6. Climatic parameters changes according to the pollen-based paleoclimatic reconstruction (used by pollen data based paleoclimatic reconstruciton methods of *Davis et al.* (2001))

Climatic parameters/Age AD	**100-200**	**200-300**	**300-400**	**400-500**	**500-600**	**600-700**	**700-800**	**800-900**	**900-1000**	**1000-1100**
MTCO (°C) The mean temperature of the coldest month	–2.0	–1.8	–2.1	–2.7	–3.0	–2.2	–1.9	–1.8	–1.9	–1.8
MTWA (°C) The mean temperature of the warmest month	+19.5	+19.7	+19.6	+19.5	+19.2	+19.7	+19.6	+19.8	+19.7	+19.7
TANN (°C) Annual temperature	+ 9.0	+ 9.2	+ 9.1	+ 8.9	+ 8.9	+ 9.2	+9.3	+9.4	+9.2	+ 9.5
PANN (mm) Annula precipitation	610	620	650	600	680	660	620	630	620	550
Continentality (°C) MTCO - MTWA	21.5	21.5	21.6	22.0	22.2	21.9	21.5	21.6	21.6	21.5
Water level of the pound based on macrobotanical data	low	low	rel. high	lowest	high	high	rel. low	rel. high	low	lowest
Climatic parameters/Age AD	**1100-1200**	**1200-1300**	**1300-1400**	**1400-1500**	**1500-1600**	**1600-1700**	**1700-1800**	**1800-1900**	**1900-2000**	**today**
MTCO (°C) The mean temperature of the coldest month	–2.5	–1.8	–2.2	–3.0	–2.2	–3.3	–3.5	–3.9	–3.6	–3.5
MTWA (°C) The mean temperature of the warmest month	+19.2	+19.9	+19.4	+18.5	+19.7	+18.2	+18.5	+19.0	+19.1	+ 19.0
TANN (°C) Annual temperature	+ 9.2	+ 9.6	+ 9.2	+ 8.8	+ 9.2	+8.3	+8.5	+8.2	+ 8.7	+ 8.8
PANN (mm) Annula precipitation	570	550	600	620	600	650	650	650	660	620
Continentality (°C) MTCO – MTWA	21.7	21.7	21.6	21.5	21.9	21.5	22.0	22.9	22.7	22.5
Water level of the pound based on macrobotanical data	low	lowest	low	rel. high	low	high	high	high	highest	**regu-lated**

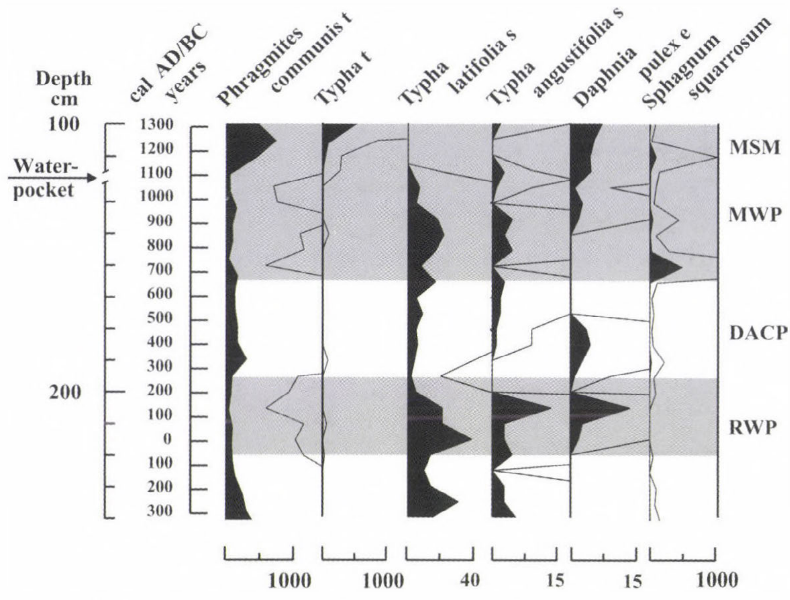

Fig. 7. Trophic fluctuations at the Nádas Lake between 330 BC and 1300 AD. The grey areas indicate periods with a warmer climate (MSM: medieval solar activity maximum; MWP: medieval warm period; DACP: Dark Ages cold period; RWP: Roman Age warm period; the interbedded water layer between 130–110 cm has been omitted).

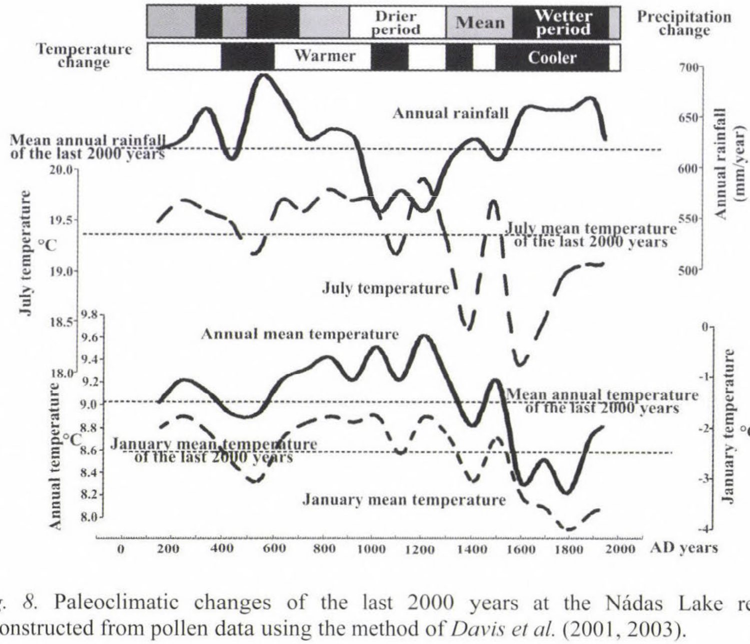

Fig. 8. Paleoclimatic changes of the last 2000 years at the Nádas Lake region reconstructed from pollen data using the method of *Davis et al.* (2001, 2003).

In the next part of the profile, there is major depositional hiatus spanning about 4400 – 4700 years. This must have emerged during the terminal part of the Iron Age, beginning of the Imperial Age around 20 –30 AD, preserving the signs of immense human impact. According to the available archeological record from the wider surroundings of the site, the area must have been controlled by Celtic herds at the time. The remains of Late Iron Age fortresses near Mátraszőlős and Kerekbikk are clear proof (*Vaday*, 2005). The area of Nádas Lake at Nagybárkány, which was a peatland at the time of the referred period, must have been systematically exploited by Celtic tribes. Peat must have been utilized in various forms ranging from fuel to litter, similarly to modern day utilizations observable in many parts of rural Ireland or Scotland (*Seymour*, 1984). An additional alternative might have been the use of the newly created ditches, which were the side-effects of peat mining, as water cisterns or reservoirs. Signs of similar activities could have been attested by Celtic tribes in the case of the Mohos Marshland at Kelemér and the Nyíres marshland of Csaroda for the periods of the late Iron Age – early Imperial Age (*Willis et al.*, 1998; *Sümegi*, 1999).

Some proxies from the referred period indicate a warming climate with perhaps a slight aridification, as seen by a concomitant increase in the amount of hazel, elm, and oak pollen grains accompanied by a retreat of lime (*Fig. 5*). In the light of this paleoenvironmental information one may assume, that the initiating peat exploitation and the artificial creation of cisterns must have been a feedback for this climatic change. Nevertheless, these activities might have been triggered by other factors as well, like a significant population growth or the foundation of a new settlement in the vicinity, not to mention a serious increase in livestock. The large proportions of macro- and micro-charcoal particles identified in the profile refer to intentional deforestation via burning, resulting in new open areas suitable for animal farming. These impacts can generally be connected to foundations of new settlements or the initiating construction of fortified settlements, around which woodland clearance was inevitable for defensive reasons (*Figs. 5* and *6*).

In the following part of the profile corresponding to the terminal part of Antiquity and the opening of the Age of Great Migrations, there is a gradual deceleration in the accumulation of organic matter in a continuously increasing trend, which was followed by alternating sudden increases and drops (*Fig. 2*). The growth period is characterized by an increase in Ca, followed by similar rises in Fe and Na. Nevertheless, when there is an increase in Fe and Na in the deposits, the ratio of Ca reaches a low. In the first part of the referred zone, there is an extremely rapid increase in the proportion of hazel pollen grains parallel with high values for oak pollen grains. Conversely, this is accompanied by a decrease in the amount of elm pollen grains and reed fragments preserved in the sediments. Afterwards, there is a very rapid decrease in the amount of oak pollen grains, reaching about two-third of their original value. Parallel with this phenomenon, large amounts of arboreal organic matter and unidentifiable organic matter appear in the deposits, accompanied by an increase in dissolved Ca as well. In the following part, oak seems to witness a slow recovery with a sudden increase in hazel pollen grains displaying a slow decrease afterwards till the end of the referred zone. All these biotic and chemical proxies seem to refer to rapid and very intensive human activities in the area. The large-scale rapid drop in oak pollen grains accompanied by an advent of lime and elm in the profile refers to selective deforestation, which must have been targeted the wood raw material itself as an ideal construction material and was not focusing on creating open areas for livestock primarily.

If the amount of available wood is proportional to changes seen in the pollen record, then one must assume a one-third decrease in the natural oak woodlands as a result of selective deforestation during the referred period, which is a very high number. Former environmental historical works speculated about the use of exploited wood in creating artificial objects within the lakebed or the exploited peatland area. This model assumes the construction of wood walls within the lakebed itself to give support to the newly formed cisterns, which seems plausible. Nevertheless, as it is seen from hard data depicted on the diagrams of *Figs. 5* and *6*, the majority of the oak stands logged down were 150-year-old at least, with a predicted volume of 800 m^3/hectar, assuming an annual growth of 8 m^3, which is a standard in forest management. This much log following the removal of branches and slicing by saw must have provided about 360 m^3 timber. The relatively small size and large proportion of retrieved timber remains call for the use of saw. If the logs were sawed into 10 cm thick, 30 cm wide and 1.5 m long timber pieces, ideal for construction of supporting walls, then for this purpose in case of a lakebed with a perimeter of 300 m, a volume of 45 m^3 timber must have been sufficient. As seen from the archeological record saw was known and utilized by late Iron Age Celtic tribes as well (*Caselli*, 1981).

The referred amount of timber could have been retrieved from an area of 1/8 hectars alone. Making predictions about the spatial extension of areas affected by logging is not an easy task. Nevertheless, the small size of the studied catchment basin (less than 100 m) and the origin of the preserved pollen grains in the deposits may help us to solve this conundrum. According to the findings of modern palynological studies in catchment basins, when the size of the basin is below 100 meters, 90% of the preserved pollen grains are of local origin with a small proportion of extralocal pollen grains (*Fig. 5*). As the largest radius of the studied catchment basin of Nádas Lake is well below this limit value, this might be rather promising in solving the above mentioned question. According to our model, the areas affected by deforestation during the referred period must have covered a radius of 300 m around the lake, reaching a maximum area of 20–30 hectars. This would suit both the spatial needs and the raw material demands of a smaller settlement with log houses and orchards, meadows, etc. As it is seen in the archeological record (*Bácsmegi* and *Guba*, 2007), people of the settlement must have been composed of Celtic groups surviving German, Dacian, and Roman attacks showing affinities to newly arriving German tribes as well. Moreover, based on the available absolute dates, the emerging settlement at the terminal part of the 4th and beginning of the 5th centuries AD might have been linked to the first appearance of Hun tribes in Central Europe, triggering the movement of lowland people to highland areas offering more safety.

After the formation of the settlement, the early period of the Age of Great Migrations (between the turn of the 4th–5th centuries AD and the terminal part of the 6th century AD) was characterized by a slow increase in the amount of oak pollen grains accompanied by the uniform accumulation of wood remains and a slow decrease in dissolved Ca in the deposits. All these imply the emergence of planned woodland management and the influences of a human group with a well-established economy for about two centuries. The use of oak woodlands in animal fodder and husbandry was a well-known established agricultural method offering efficient, cost-effective, and risk-free solutions in contrast to growing plants in arables used as fodder. Acorn has a relatively high nutrition value, with a high annual production rate of 15 tons/hectar, enabling efficient and cost-effective animal husbandry without the need of fodder plant production. As it can be seen in the pollen diagram (*Fig.5*), there is a minor peak of cereals at 200 cm corresponding to the opening of the 5th century AD, which further corroborates the permanent presence of human settlements and activities in the study area.

The next prominent change in the profile is observable at the depths of 190 and 130 cm corresponding to the period between the 6th and 9th centuries AD (*Fig. 6*). This zone is characterized by a decrease in organic and increase in inorganic components of the deposits (*Fig. 6*). The geochemical parameters also tend to be constant lacking any sudden transformations or outliers. These changes must have been triggered by a gradual retreat of reed fringing the lakebed. Nevertheless, the large amounts of wood remains as well as flue-ash in the initial part of the zone, as well as the inferred decrease in the amount of oak, hazel, lime, and elm pollen grains may indicate a smaller deforestation activity.

The presence of buttercups, known to carry toxics, can be clearly attested during the second half of the Age of Great Migrations. An increase of these plants may indicate the appearance of large livestock grazing meadows besides the survival of woodland grazing. The peak in the pollen ration of buttercups was noticed at a depth of 160 cm, followed by a gradual decrease, which must be attributed to an aridification of the climate on the one hand. On the other hand, a decrease in the importance of animal husbandry may be assumed as well. Based on the available plant macrofossils, this period is characterized by a decrease in the area of the peatland, which must be attributed to drier climatic endowments (*Figs. 7, 8*). This transformation, however, was by no means drastic, as peat-mosses managed to survive in the area, suffering only a minor decrease. Peat-mosses are capable to thrive in areas of the Carpathian Basin, where the rate of average annual rainfall is above 550 mm. So we may assume a similar value for the referred period in our study area, corroborated by results of pollen analysis as well (*Fig. 8*), assuming a rainfall value of 630–650 mm for the period between the 6th and 9th centuries. This value is well above the average of the past two millennia (620 mm).

Conversely, as it is clearly observable in the paleoclimate diagram based on pollen data (*Fig. 5*), the referred period is characterized by elevated mean annual, January, and July temperatures. Thus, as a result of higher temperatures, evaporation must have been higher as well during the second half of the Age of Great Migrations, between the 6th and 9th centuries. As a result of the elevated evaporation rate, drier conditions must have emerged with varying intensities related to micro-morphological and geographical setting. Conversely, the higher 100-year-long environmental historical data do not refer to such a drastic climatic change during the collapse of the Avar Empire, which might be blamed for its fall, e.g., famine following an extremely dry period. This question becomes even more exciting, when our data from the referred period of the Late Age of Great Migrations is compared with those for the periods of the Hungarian Conquest, the Arpadian Age, the late Middle Ages, or the New Age.

At a depth of 144 cm there is a rapid and considerable increase in the amount of willow pollen grains, overlain by layers embedding large proportions of wood remains, flue-ash, and burnt peatland mud. This overlying horizon is characterized by a drop in willow pollen grains implying a rapid burnt-down of the area of the peatland. The advent of acidic, toxic plants and those tolerating treading as seen in the pollen record during this horizon refers to an increasing importance of animal husbandry, implying human origin of the transformation. This horizon was dated to the 10th century, possibly marking a large demand for meat produce as a result of higher population densities following the foundation of the Hungarian state. In the zone between 130 and 110 cm there is an aquatic horizon implying the emergence of floating mats in the area (*Fig. 6*). The hollow stem of reed leaning over the lakebed must have served as a natural raft for successive plant generations, providing them habitat and sufficient nutrition, enabling the emergence of floating mats. The thickness of this layered plant complex may reach such proportions, which enables the advent of trees onto the mats as well as time passes, as was the case of Nádas Lake as well.

Based on chronometric data, the emergence of floating mats must be dated between the 11th and 16th centuries, seen in the continuous and steady increase in organic components and the advent of reed, willow, and bulrush to the area connected to the natural succession of the marshland. Nevertheless, two ash and wood remain peaks in this part of the profile can clearly be correlated with a significant drop in the amount of oak pollen grains. The ash peaks correspond to drops in reed fragments implying the development of natural or artificial fires in the reed zone fringing the lakebed. The second ash peak at 96 cm with a parallel increase in the ratio of weed and cereal pollen grains indicate a larger deforestation again attributable to mixed agriculture of crop cultivation and animal husbandry in the area. As shown by the archeological record (*Zatykó*, 2005), this period was characterized by multiple periods of plot shifts, deserting population, and revivals.

The first written record of the settlement of Nagybárkány can be dated to this period at around 1220, when it was the property of the Zách clade. The climate is characterized by natural cycles with a temperature maximum and a precipitation minimum during the 13th century. This climatic transformation resulted in real dry conditions yielding the extermination of peat-mosses from the area of the lake. Peat-mosses managed to conquer the lakebed only during the 16th century. When pollen-based paleoclimatic data for the 8th and 13th centuries are compared, it becomes clear that the 13th century transformations are much more pronounced. The aridity index must have been 4 times of that inferred for the 8th century as a result of the elevated temperatures and a drastic drop of annual rainfall. Yet as it was recorded in the written historical documents, the 13th century collapse of the Hungarian Kingdom were by no means the outcome of environmental changes, but rather political ones; the military defeat of the Hungarian troops by the Mongol tribes. The inland political fights and restructuring of the feudal social and political system is explained by historians by not the extreme dry conditions characterizing the period, but rather the loss of royal power, financial problems, and the collapse of the traditional latifundium system.

Conversely, several authors emphasize the role of extreme dry climate in the collapse of the Avar Empire and the resulting inland political tensions in a period, when the aridity index was much lower, relatively negligible compared to the 13th century conditions. Some papers postulated a „*devastating drought*" accompanied by famine waves which must have affected „*the warrior nation of the half-nomadic Avars*" (*Rácz*, 2008, pp. 54–55). Conversely, the statement according to which „*the more drought tolerant Slavic tribes could have been better suited to eliminate the hardships of draughts by withdrawing near oak woodlands and using acorn as fodder in the hard times*" (*Rácz*, 2008), was turned down by our paleoenvironmental data from the Nádas Lake, as this type of landscape use was present since the Age of Great Migrations in the area. Thus, this type of landscape economy must have emerged preceding the arrival of the Slavs to the area. Our paleoenvironmental data also calls for the re-evaluation of postulations made regarding the collapse of the Avar Empire. Since social processes and disturbances can only be linked to natural catastrophes if and only if there were such catastrophes in the referred area during the referred period. Based on our data, this problem must be treated with great caution, as highly different climatic conditions must have emerged in the area than stated by numerous recent paleoenvironmental studies (*Magny et al.*, 2008).

In contrast to the previous periods, the one starting from the 16th century till today is characterized by intensified rainfall and cooler conditions, resulting in a thriving of peatland conditions in the area of the Nádas Lake at Nagybárkány. The floating mats were turned into peatmossy reeds and willow peatland. This is the period when the highest organic content (around 80 – 85%) was recorded. Nevertheless, several inorganic peaks are observable as well reflecting soil erosion from the neighboring areas as a result of recurring deforestation activities. These transformations are observable at a regular centennial scale, which can be tracked to intentional forest management. Numerous ash peaks are observable in the lower part of the zone coinciding with a halt in the expansion of reed-beds. The continuous presence of weed, buttercup, and plantain pollen grains in the record refer to permanent human activities in the area and continuous disturbances. The most dynamic advent of peat-mosses is observable in the most recent periods attributable to a deserting population in the area.

5.3. Autogenous peat-bog phase (after 1300 cal BP)

The development of the present-day bog and the commencement of peat accumulation can be dated to the end of the early Middle Age. At around 1300 AD, the number of *Typha* rhizomes increases significantly, indicating a rise in the water level and the formation of a floating mat. The hydroseries of the bog was from this point on characterized by autogenic processes, with a tendency towards a gradual oligotrophication.

Based on detailed phytogeographical studies, floating mats of *Phragmites* and *Typha* are frequent components of lake shore vegetation in Hungary. The first signs of peat-bog formation from these floating mats can be seen in a massive expansion of *Thelypteris palustris*. As time goes by, peat-mosses also turn up on the mats (*Borhidi* and *Balogh*, 1970; *Balogh*, 2000a, b). Based on the paleobotanical investigations, the bog development passed through phases characterized by *Typha* → *Thelypteris palustris* → *Meesia longiseta* → *Sphagnum* spp.. This development shares numerous similarities with the formation of two other *Sphagnum*-bogs at the Csaroda–Báb Lake (*Jakab* and *Magyari*, 2000) and Kelemér-Nagy-Mohos (*Magyari et al.*, 2001), suggesting some sort of regularity in the formation of Hungarian *Sphagnum*-bogs. *Meesia longiseta* preceding the expansion of *Sphagna* is highly interesting. The taxon *Meesia longiseta* is a unique component of the flora of the Carpathian Basin with a single occurrence recorded in Hungary from 1885 (*Boros*, 1968). According to *Hall* (1979), the appearance of *Meesia longiseta* can be linked to a distinct phase of wetland succession, characterized by the transformation of the brown moss sedge floating mat into acidic *Sphagnum*-bog. This species was observed during the secondary succession of abandoned lakes used for retting hemp. *Odgaard* (1988) reported the same for *Meesia triquetra*.

Representatives of *Sphagna* seemed to have appeared in similar quantities during the middle part of the 17th century as today, followed by a complete drop till 0 BP. Surprisingly, the taxon *Sphagnum palustre*, indicating mesotrophic conditions, was present in the largest numbers. In the pollen record *Sphagnum* reaches a maximum peak at 70%, at the same time (*Juhász*, 2005). This expansion of *Sphagnum* coincides with the coldest period of the Little Ice Age (*Rácz*, 2001), which was also the coldest time of the past 2000 years (*Fig. 7*). The Little Ice Age dates from the middle part of the 16th till the middle part of the 19th centuries (*Bradley et al.*, 2003). The most significant cooling is put to the terminal part of the 16th century, when a major drop in the average temperatures is traceable across entire Europe (*Pfister*, 1999; *Pfister* and *Brázdil*, 1999).

As shown by archeological data (*Zatykó*, 2005), the traditional Medieval Age settlement system collapsed followed by the emergence of unpopulated areas in the analyzed region during the Ottoman occupation and scattered farmstead-like settlements from the 16th century onwards. The geochemical composition and the increasing amount of charcoal indicate that the human disturbance decreased around the analyzed catchment basin in the 18th century. According to the pollen analytical data, human impact on the vegetation became more intensive (*Juhász*, 2005). There was a rapid decrease in the amount of *Sphagnum palustre* preferring mesotrophic conditions (*Daniels* and *Eddy*, 1985). A rapid expansion of *Juncus effusus* indicates eutrophication, and the quick spread of weeds. Forest management, accompanied by increased soil erosion in the study area resulted in an enrichment of plant type nutrients on the marsh. The steady expansion of *Sphagnum squarrosum* refers to the emergence of an acidophil but eutrophic peatland in the area. *Sphagnum squarrosum* relatively tolerant to high Ca, bicarbonate levels, and pH (*Clymo*, 1973), and in mineral rich habitat with a high nutrient supply grow very fast (*Kooijman*, 1993). The expanding beds of *Sphagnum squarrosum* are capable of capturing and accumulating Ca via ion exchange (*Anschutz* and *Gessner*, 1954; *Clymo*, 1963; *Kooijman*, 1993). The recorded Ca content of the embedding sediments seems to display a strong correlation with the amount of peat-moss, which is a clear sign of the excellent Ca ion bonding capacity of peat-moss. Reed is also capable of accumulating Ca in its rhizomes similarly to peat-mosses (*Kovács et al.*, 1978; *Penksza et al.*, 1994; *Podani et al.*, 1979; *Tóth* and *Szabó*, 1958).

A smaller drop in the water-level can be dated to the turn of the 15th–16th centuries, reflected by the expansion of green algae and the retreat of alder, and the rise of aquatic species and reed. A secondary reforestation following forest clearance is reflected by the expansion of hornbeam around 1500. A slight rise in the water-level and a gradual reforestation can be noted during the Ottoman period. The warmer and drier climate observed at the paleoecological sites from 9th to 14th centuries coincides with the so-called Medieval Warm Period (MWP) in Europe, which is supposed to have been characterized by a warmer and wetter climate (*Lamb*, 1977). The opening of this period can be placed between the 9th and 11th centuries with differences regarding the applied analytical methods, sources of dating, and regions (*Bradley et al.*, 2003). On the contrary to the widely accepted idea of the warmer and wetter climate of MWP, in the cases of 14 Hungarian paleoecological sites, drier climate can be noted, in spite of high amount of precipitation. It appears that the increasing evapotranspiration, following the higher temperature led to a drier climate and a drop in the water-level of the lakes. These results concerning medieval (pre-15th-century) climatic processes are among the first data derived from the medieval layer of a sediment core extracted at the Hungarian sites and call the attention to the great importance of regional studies in order to refine further the local variations of climate conditions.

6. Conclusions

The development of the bog can be divided into three main phases in the light of macrofossil analysis. The first phase spanned the late Glacial to the mid-Holocene layers. The trophic conditions in this phase were oligo-mesotrophic and mesotrophic. The water level was high, although with minor fluctuations. A hiatus of roughly 4400 years can be noted in the sediment after this phase, owing to peat-cutting during the Imperial Age. The water level decreased slightly, the trophic conditions became eutrophic, and the lake was fringed by macrophyte vegetation. This period was characterized by the fluctuation of the lake's trophic conditions. This phase can be dated to the late Holocene, lasting until the end of the early Middle Age, at the beginning of the 14th century. The last phase, spanning the period up to the present, saw the paludification of the lake and the cessation of the open water surface.

The hydroseries was characterized by autogenic processes, with taxa *Thelypteris palusris* and *Meesia longiseta* playing a key role. Peat-mosses appeared in the same quantities during the coldest period of the Little Ice Age dated to the middle part of the 17th century as today. The subsequent periods saw a temporary decrease in their amounts. Forest management, accompanied by increased soil erosion in the study area resulted in an enrichment of plant type nutrients on the marsh during the past 200 years. The steady expansion of *Sphagnum squarrosum* refers to the emergence of an acidophil but eutrophic peatland in the area. Based on our findings, changes in the paleohydrology and aquatic vegetation of the bog were mainly driven by climatic changes and autogenic processes. Recurring human influences have also significantly modified the natural path of succession in the studied area.

7. Summary

The profile of the Nádas Lake at Nagybárkány speaks about continuous sedimentation from the Paleolithic till the opening of the Copper Age. Then during the opening of the Imperial Period, a major depositional hiatus emerged

in the deposits attributable to the creation of a water reservoir system by Celtic tribes in the lakebed. This initiated a secondary succession which enabled us to make inferences about the environmental historical evolution of the area for the past two millennia at a scale of centuries alone. With the help of paleoecological and geological data, a better reconstruction of climatic fluctuations was made from the Imperial Age up to modern times. As it was shown by our data, one must exercise caution in interpreting the correlations of environmental and social crises, e.g., in the case of the fall of the Avar Empire. An objective and correct approach is the careful and most elaborate utilization of available paleoenvironmental data from the area of the Carpathian Basin.

Acknowledgements—Authors would like to express their gratitude to the Headquaters of the Bükk National Park for granting access to the study area and to *Sándor Molnár* for his kind help in the fieldwork. This work was supported by grants OTKA T-034 392 and NKFP 5/0063/2002.

References

Anschutz, I. and *Gessner, F.*, 1954: Der Ionenaustausch bei Torfmoosen (*Sphagnum*). *Flora 141*, 178-236.

Bácsmegi, G., 2005: The Copper Age in the Nagybárkány area. In *Environmental archaeology in North-Eastern Hungary* (eds.: *E. Gál, I. Juhász* and *P. Sümegi*). Varia Archaeologica Hungarica, XIX. Budapest, 243-245.

Bácsmegi, G. and *Fábián, Sz.*, 2005: The Neolithic of Nagybárkány and its environs. In *Environmental archaeology in North-Eastern Hungary* (eds.: *E. Gál, I. Juhász* and *P. Sümegi*). Varia Archaeologica Hungarica, XIX. Budapest, 237-242.

Bácsmegi, G. and *Guba, Sz.*, 2007: *Mind of past ages* (in Hungarian). Szurdokpüspöki Önkormányzat Kiadványa, Szurdokpüspöki.

Balogh, M., 2000a: Classification of peatbogs (in Hungarian). In *Tőzegmohás élőhelyek Magyarországon: kutatás, kezelés, védelem* (Sphagnum-bogs in Hungary: research, conservation and management) (ed.: *E. Szurdoki*). CEEWEB Munkacsoport, Miskolc, 57-65.

Balogh, M., 2000b: On the succession of floating mat I. (in Hungarian). *Kitaibelia 5*, 9-16.

Barber, K.E. and *Charman, D.*, 2005: Holocene palaeoclimate records from peatlands. In *Global Change in the Holocene* (eds.: *A. Mackay, R. Battarbee, J. Birks* and *F. Oldfield*). Hodder Arnold, London, 210-226.

Barber, K.E. and *Langdon, P.G.*, 2001: Peat stratigraphy and climate change. In *Handbook of Archaeological Sciences* (eds.: *D.R. Brothwell,* and *A.M. Pollard*). Wiley, Chichester, 155-166.

Barber, K.E., Chambers, F.M., Maddy, D. and *Brew, J.*, 1994: A sensitive high resolution record of the Holocene climatic change from a raised bog in northern England. *The Holocene 4*, 198-205.

Barber, K.E., Maddy, D., Rose, N., Stevenson, A.C., Stoneman, R. and *Thompson, R.*, 2000: Replicated proxy-climate signals over the last 2000 yr from two distant UK peat bogs: new evidence for regional palaeoclimate teleconnections. *Quaternary Sci Rev 19,* 481-487.

Bennett, K.D., 1992: PSIMPOLL – A quickBasic program that generates PostScript page description of pollen diagrams. INQUA Commission for the study of the Holocene: working group on data handling methods. *Newsletter 8,* 11-12.

Bennett, K.D., 1994: Confidence intervals for age estimates and deposition times in late-Quaternary sediment sequences. *The Holocene 4*, 337-348.

Borhidi, A. and *Balogh, M.*, 1970: Die Enstehung von dystrophen Schaukelmooren in einem alkalischen See. *Acta Bot Hung 16*, 13-31.

Boros, Á., 1968: *Bryogeographie und Bryoflora Ungarns*. Akadémiai Kiadó, Budapest.

Bradley, R.S., Hughes, M. K. and *Diaz, H.F.*, 2003: Climate in medieval time. *Science 302*, 404-405.

Bronk Ramsey C., 2001: Development of the Radiocarbon Program OxCal. *Radiocarbon 43*, 355-363.

Caselli, G., 1981: *History of Everyday Things. The Roman Empire and the Dark Ages.* Macdonald and Company Publishers Ltd, London.

Clymo, R.S., 1963: Ion exchange in *Sphagnum* and its relation to bog ecology. *Ann Bot-London 27*, 309-324.

Clymo, R.S., 1973: The grows of *Sphagnum*: some effects of environment. *J Ecol 61*, 849-869.

Dániel, P., 2004: Geochemical analysis. In *The Geohistory of Bátorliget Marshland* (eds.: *P. Sümegi* and *S.* Gulyás). Archaeolingua Press, Budapest, 52-57.

Daniels, R.E. and *Eddy, A.*, 1985: *Handbook of European Sphagna.* Institute of Terrestrial Ecology, Hundtingdon.

Davis, B., Brewer, S., Stevenson, T. and *Juggins, S.*, 2001: *High resolution from low resolution; a new method for time-series pollen-climate reconstruction and its application in investigating abrupt Holocene climate change in Southern Europe/Mediterranean.* Abstracts of PAGES-PEPIII: Past Climate Variability Through Europe and Africa, Aix-en-Provence, France.

Davis, B.A.S., Brewer, S., Stevenson, A.C., Guiot, J., 2003: The temperature of Europe during the Holocene reconstructed from pollen data. *Quaternary Sci Rev 22*, 1701–1716.

Dean, W.E., 1974: Determination of carbonate and organic matter in calcareous sediments and sedimentary rocks by loss on ignition: comparison with other methods. *J Sediment Petrol 44*, 242-248.

Dowdeswell, J.A., 1982: Relative dating of Late Quaternary deposits using cluster and discriminant analysis, Audubon Cirque, Colorado Front Range. *Boreas 11*, 151-161.

Engström, D.R. and *Hansen, B.C.S.*, 1985: Postglacial vegetation change and soil development in southeastern Labrador as inferred from pollen and chemical stratigraphy. *Can J Bot 63*, 543-561.

Engström, D.R. and *Wright Jr., H.E.*, 1984: Chemical stratigraphy of lake sediments as a record of environmental change. In (eds.: *E.Y. Haworth* and *J.W.G. Lund*). *Lake Sediments and Environmental History.* University of Minnesota Press, Minneapolis, 11-68.

Hall, A.R., 1979: A note on the Quaternary history of *Meesia longiseta* Hedw. in Britain. *J Bryol 10*, 511-515.

Jakab, G. and *Magyari, E.*, 2000: New progress in the Hungarian mire succession studies: the use of palaeobryological and palynological techniques in the reconstruction of hydroseries (in Hungarian). *Kitaibelia 5*, 17–36.

Jakab, G. and *Sümegi, P.*, 2004: Identifying of herbaceous plant remains from peat on the basis of microscopic features (in Hungarian). *Kitaibelia 9*, 93–129.

Jakab, G. and *Sümegi, P.*, 2005: The evolution of Nádas-tó at Nagybárkány in the light of the macorfossil finds. In *Environmental Archaeology in North-Eastern Hungary* (eds.: *E. Gál, I. Juhász* and *P. Sümegi*). Varia Archaeologica Hungarica, XIX. Budapest, 67-77.

Jakab, G., Sümegi, P. and *Magyari, E.*, 2004: A new palaeobotanical method for the description of Late Quaternary organic sediments (Mire-development pathways and palaeoclimatic records from S Hungary). *Acta Geologica Hungarica 47*, 1–37.

Juhász, I., 2005: Preliminary palaeobotanical results from the Nádas-tó peat bog at Nagybárkány: the Late Holocene environmental history. In *Environmental Archaeology in North-Eastern Hungary* (eds.: *E. Gál, I. Juhász* and *P. Sümegi*). Varia Archaeologica Hungarica, XIX. Budapest, 79-85.

Juhász, I.E., Jakab, G. and *Sümegi, P.*, 2004: Vegetation dynamics of a small Sphagnum peat bog from North Hungary, from the Late Pleistocene until Late Holocene: palynological and macrobotanical data. *Abstracts of the 11th International Palynological Congress*, 2004, Granada.

Kalicz, N. and *Makkay, J.*, 1977: Die Linienbandkeramik in der Grossen Ungarischen Tiefebene. *Studia Archeologica, VII.* Budapest.

Kiss, A., 2000: Weather events during the first Tartar invasion in Hungary (1241-42). *Acta Geographica Szegediensis 37*, 149-156.

Kiss, A., 2003: „Ecce, in hyemis nivis et glaciei habundantia supervenit" – Weather, environmental crisis and the Mongol invasion (in Hungarian). In *Tatárjárás* (Mongol invasion) (ed.: *B. Nagy*). Osiris, Budapest, 439-452.

Kooijman, A.M., 1993: On the ecological amplitude of four mire bryophytes, a reciprocal transplant experiment. *Lindbergia 18*, 19-24.

Kovács, M., Précsényi, I. and *Podani, J.*, 1978: Anhäfung von Elementen im balatoner Schilfrohr (*Phragmites communis*). *Acta Botanica Sci. Hungarica 24*, 99-111.

Lamb, H.H., 1977: *Climate: Present, Past and Future 2*. Methuen Press, London.

Mackereth, F.J.H., 1966: Some chemical observations in post-glacial lake sediments. Proceedings *Royal Academy of Sciences 250*, 165-213.

Magny, M., Gauthier, E., Vanniere, B., Peyron, O., 2008: Palaeohydrological changes and human-impact history over the last millennium recorded at Lake Joux in the Jura Mountains, Switzerland. *Holocene 18*, 255-265.

Magyari, E., Sümegi, P., Braun, M., Jakab, G. and *Molnár, M.*, 2001: Retarded wetland succession: anthropogenic and climatic signals in a Holocene peat bog profile from north-east Hungary. *J Ecol 89*, 1019–1032.

Majkut, P., 2009: *Geoarcheological investigation on the basin of Nádas Lake at Nagybárkány* (in Hungarian). Diplomamunka, MSc, Szegedi Tudományegyetem, Földtani és Őslénytani Tanszék, Szeged.

Mauquoy, D. and *Barber, K.*, 1999: A replicated 3000 yr proxy-climate record from Coom Rigg Moss and Felicia Moss, The Border Mires, northern England. *J Quaternary Sci 14*, 263-275.

Máthé, I. and *Kovács, M.*, 1959: The Sphagnum bog of the Cserhát Mountains (in Hungarian). *Botanikai Közlemények 50*, 106–108.

Odgaard, B.V., 1988: Glacial relicts - and the moss Meesia triquetra in Central and West Europe. *Lindbergia 14*, 73-78.

Penksza, K., Turcsányi, G. and *Kovács, M.*, 1994: Element concentration cadastres of peat profiles in Nyírjes bog near Sirok in Hungary (in Hungarian). *Botanikai Közlemények 81*, 29-41.

Peyron, O., Guiot, J., Cheddadi, R., Tarasov, P., Reille, M., Beaulieu de, J.L., Bottema, S. and *Andrieu, V.*, 1998: Climatic reconstruction in Europe for 18,000 yr B.P. from pollen data. *Quaternary Res 49*, 183-196.

Pfister, C., 1999: *Wetternachhersage: 500 Jahre Klimavariationen und Naturkatastrophen (1496-1995)*. Haupt, Bern.

Pfister, C. and *Brázdil, R.*, 1999: Climatic variability in sixteenth-century Europe and its social dimension: A synthesis. *Climatic Change 43*, 5-53.

Podani, J., 1993: SYN-TAX 5.0: computer programs for multivariate data analysis in ecology and systematics. *Abstracta Botanica 17*, 289-302.

Podani, J., Kovács, M. and *Dinka, M.*, 1979: Chemical element analysis of reed from Balaton I. (in Hungarian). *Botanikai Közlemények 66*, 275-284.

Prentice, I.C., Harrison, S.P., Jolly, D. and *Guiot, J.*, 1998: The climate and biomes of Europe at 6000 yr BP: comparison of model simulations and pollen-based reconstructions. *Quaternary Sci Rev 17*, 659-668.

Rácz, L., 2001: *Magyarország éghajlattörténete az újkor idején* (Climate history of Hungary during Modern Age). JGYF Kiadó, Szeged.

Rácz, L., 2008: Environmental history of Hungary until Modern Age (in Hungarian). MTA Történeti Intézete, Budapest.

Rollinson, H., 1993: *Using Geochemical Data: Evaluation, Presentation and Interpretation*. Longman, London - Essex.

Seymour, J., 1984: *Forgotten Arts*. Dorling Kindersley Ltd., London

Stuiver, M., Reimer, P.J. and *Braziunas, T.F.*, 1998: High-precision radiocarbon age calibration for terrestrial and marine samples. *Radiocarbon 40*, 1127-1151.

Sümegi, P., 1999: Reconstruction of flora, soil and landscape evolution, and human impact on the Bereg Plain from late-glacial up to the present, based on palaeoecological analysis. In *The Upper Tisa Valley* (eds.: *J. Hamar, A. Sárkány-Kiss*). Tiscia Monograph Series, Szeged, 173-204.

Szurdoki, E. and *Nagy, J.*, 2002: Sphagnum dominated mires and Sphagnum occurrences of North-Hungary. *Folia Historico-Naturalia Musei Matraensis 26*, 67-84.

Tóth, L. and *Szabó, E.*, 1958: Über die chemische Zusammensetzung verschieder Schilfproben vom Balaton-See. *Annales Instituti Biologici (Tihany) Hungaricae Academiae Scientiarum 25*, 363-374.

Troels-Smith, J., 1955: Characterization of unconsolidated sediments (in Danish). Danmarks Geologiske Undersogelse *4*(3), 10.

Vaday, A., 2005: The Nagybárkány area in the Iron Age and the Roman period and Migration period. In *Environmental archaeology in North-Eastern Hungary* (eds.: *E. Gál, I. Juhász* and *P. Sümegi*). Varia Archaeologica Hungarica, XIX. Budapest, 45-347.

Valanus, A., 2008: Drawing the optimal dept-age curve on the basis of calibrated radiocarbon dates. *Geochronometria 31*, 1-5.

Willis, K.J., Sümegi, P., Braun, M., Bennett, K.D., Tóth, A. 1998: Prehistoric land degradation in Hungary: who, how and why? *Antiquity 72*, 101-113.

Zatykó, Cs., 2005: The medieval environment and settlement history of the Nagybárkány area. In *Environmental archaeology in North-Eastern Hungary* (eds.: *E. Gál, I. Juhász* and *P. Sümegi*). Varia Archaeologica Hungarica, XIX. Budapest, 405-409.

IDŐJÁRÁS

Quarterly Journal of the Hungarian Meteorological Service
Vol. 113, No. 4, October–December 2009, pp. 299–314

Reconstructed precipitation for southern Bakony Mountains (Transdanubia, Hungary) back to 1746 AD based on ring widths of oak trees

Zoltán Kern[1*], **András Grynaeus**[2], and **András Morgós**[3]

[1]*Institute for Geochemical Research, Hungarian Academy of Sciences, Budaörsi út 45, H-1112 Budapest, Hungary; E-mail: kern@geochem.hu*

[2]*Hungarian Dendrochronological Laboratory, Széher út 76/a, H-1021 Budapest, Hungary; E-mail: dendro@ludens.elte.hu*

[3]*Tokyo University of the Arts, 12-8 Ueno Park, Taito-ku, Tokyo, 110-8714, Japan; E-mail: andrasmorgos@gmail.com*

(Manuscript received in final form September 3, 2009)

Abstract—This paper presents a 258-year long precipitation reconstruction for the Balaton Highlands and the southern Bakony Mountains region. The reconstruction based on 22 living and 32 historical tree-ring width series from oak (*Quercus* sp.). Ring width series were standardized by regional curve standardization technique to preserve the low frequency information. Precipitation from August of the year preceding the formation of tree ring to the current July positively stimulates the growth of oaks, albeit May-June precipitation emerges as main growth regulator factor. Very dry period occurred in the late 1740s. Studied region has experienced the wettest period during the late 18th century since 1746. Since that time, a steady decreasing trend prevails over the fluctuations of regional precipitation. From this overall trend, the 1840s, 1860s, and 1940s stand out as drier periods. The post-1980s dry period was placed into a ~250 years context and found to be an unprecedented drought at the Balaton Highlands and the southern Bakony Mountains region.

Key-words: dendroclimatology, tree ring, Central Europe, drought, Balaton

1. Introduction

The only way to decide whether the 20th century climate is extreme or not is to investigate long records stretching well before the anthropogenically forced instrumental period (e.g., *Bradley,* 1999; *Bradley et al.,* 2003).

---

* Corresponding author

Bradley et al. (1987) analyzed 1487 instrumental precipitation series covering the northern Hemispheric land areas and pointed out significant regional differences in the fluctuation of past precipitation. They have already emphasized the dire necessity of investigations of past fluctuation of moisture regime on local-to-regional spatial scale. To fill this pronounced research need, paleoclimatic studies dealing with reconstruction of precipitation regime have taken enormous headway during the past decade. Amongst main sources of information on this field like documentary evidences (e.g., *Rodrigo et al.*, 1999; *Rácz*, 1999; *Garcia et al.*, 2003; *Diodato*, 2007) and speleothems (e.g., *Proctor et al.*, 2000; *Siklósy et al.,* 2009), tree rings play a leading part (e.g., *Brázdil et al.*, 2002; *Oberhuber* and *Kofler*, 2002; *Buckley et al.*, 2004; *Linderholm* and *Chen*, 2005; *Wilson et al.*, 2005; *Touchan et al.*, 2005, 2007; *Čufar et al.*, 2008).

The earliest sporadic instrumental rainfall data were recorded at Buda (1782), but the first continuous observations launched only in the mid-1800s (Buda 1841, Nagyszeben 1851) in the Carpathian Basin (*Hegyfoky*, 1910). These confirm that proxy based precipitation reconstructions have prominent importance also in the entire area girt with the arc of the Carpathians.

In addition, future continuation of warming on a global level is expected to procure reduction of annual precipitation in Hungary (*Bartholy et al.*, 2004, *Mika*, 2004, 2007) and, especially, the lake Balaton, prime tourist resource of Hungary, will be in risk, if precipitation declines in the future over the watershed (*Bartholy et al.*, 1995). So the knowledge about natural variability of moisture over its watershed is interesting not only from scientific but also from social and economical point of view.

This paper presents secular fluctuation of precipitation at the northern hilly part of the catchment area of the Lake Balaton. Variability of precipitation is reconstructed from tree-ring width variations of oak trees between 1746 and 2003. The low-frequency variability of present reconstruction is to be verified against longer instrumental record from the boarder vicinity of the study site. In addition, the tree-ring based reconstruction was compared to two other precipitation reconstructions, which are thought to have relevancy for the past fluctuation of the precipitation regime of the studied area.

2. *Materials and methods*

2.1. Tree-ring data

Fifteen mature oak trees (*Quercus petrea*, *Quercus pubescens*) were sampled by increment borer in November 2003. One or two cores were extracted from each tree. Due to exclusion of low quality samples, finally fourteen living oak trees (22 series) from Balaton Highland and southern Bakony Mts. (*Fig. 1*) developed a local oak chronology (*Kern*, 2007), and 32 historical timber samples derived from old buildings completed the 309 years long tree-ring width (TRW) chronology (1694 – 2003). Old timbers were collected from four villages close to the site of living trees, namely, Vöröstó, Nagyvázsony, Vigántpetend, and Örvényes (*Fig. 1*).

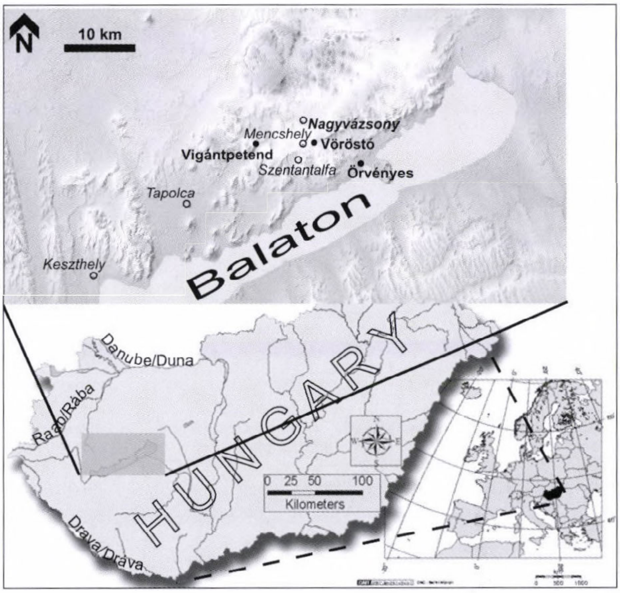

Fig. 1. Location of the study area (grey rectangle) and the precipitation gauge stations (marked by open circles and italics). Villages, from which historical wood samples originated, are marked by filled circles and bolds. From Nagyvázsony, both gauge records and historical timbers were used.

Living trees cover the 1766–2003 period, while historical samples distribute between 1694 and 1944.

Climate signal in raw ring width series are often biased by non-climatic effects (e.g., *Douglass*, 1919; *Cook*, 1985). To find the adequate method to eliminate non-climatic trends (e.g., age trend) from raw TRW series, the so-called standardization is always crucial in any dendroclimatological study.

Mean segment length (MSL) was 124 years in the data set. Applying any traditional standardization techniques (negative exponential function or digital filtering), frequencies lower than ~3/MSL could hardly be retained (*Cook et al.*, 1995). To avoid the loss of low frequency information, regional curve standardization (RCS) was applied (*Briffa et al.*, 1992; *Esper et al.*, 2003). Utilizing RCS technique, multi-centennial trends could be captured even though the mean sample length is below 50 years (*Wilson et al.*, 2004).

RCS uses the estimated biological growth curve of the studied species in the standardization. The estimated biological growth, regional curve (RC) of oak was determined as follows: first calculating the bi-weight robust mean (*Cook*,

1985) of the age-aligned series, after that fitting a cubic smoothing spline (*Cook* and *Peters*, 1981) with a 50% frequency-response cut-off at 10% of the series length (*Esper et al.*, 2003) (*Fig. 2*).

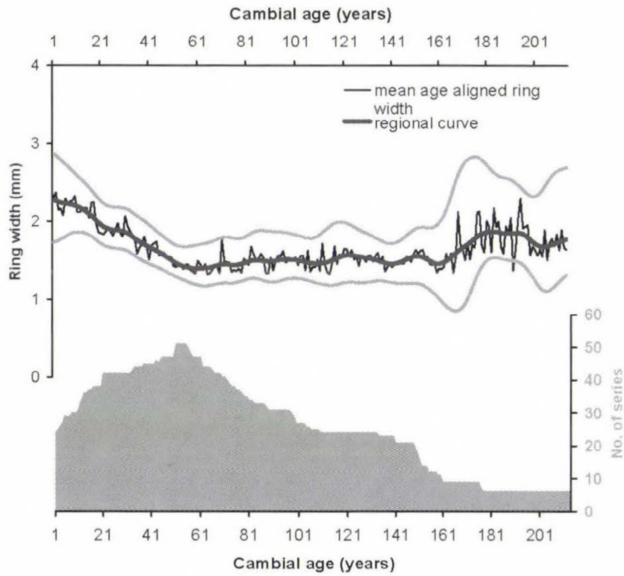

Fig. 2. Biological growth curve of oak. Upper graphics: thin black line: mean of age aligned series; thick black curve: regional curve (RC) obtained by fitting a cubic smoothing spline (50% frequency-response cut-off at 10% length); grey curves: 95% confidence intervals. Lower graph shows replication.

Twenty-five trees had the pith. In the other cases, missing rings to pith (pith offset) were estimated by the aid of graphics of concentric circles. Pith offset values for ten trees were less than 15, and the highest estimated pith offset was 50.

Indices were calculated as ratio of the measured ring width and the RC predicted value. Standardized series were rearranged by calendar date and average index was determined by bi-weight robust mean (*Cook*, 1985).

Uncertainty of the built chronology is represented by the 95% confidence interval calculated by bootstrap procedure (*Efron*, 1987). Stability of climate related signal preserved in the index series was controlled by the expressed population signal (EPS) statistic. Its widely accepted threshold is 0.85 (*Wigley et al.*, 1984). Mean interseries correlation (Rbar) and EPS were calculated for 50 years moving window with 25 years steps. Standardization and index calculation procedure was carried out using the ARSTAN software (*Cook* and *Krusic*, 2006). Variance adjustment was applied on the derived TRW chronology to minimize variance bias due to changing sample replication and the effect of fluctuating interseries correlation (*Osborn et al.*, 1997; *Frank et al.*, 2007).

2.2. *Precipitation data*

Monthly average precipitation totals were available from four nearby gauge-stations (Nagyvázsony 1901–2005, Tapolca 1901–2005, Mencshely 1960–1996 and 2001–2005, Szentantalfa 1900–1991 and 1998–2000) (*Fig. 1*). Since the use of averaged meteorological series yield better statistical connections in dendro-climatological analysis than individual stations (*Blasing et al.*, 1981; *Yeh et al.*, 2000), regional average precipitation series were estimated from these instrumental data. Monthly data were transformed to percentages of average monthly total of the 1961-1990 reference period (*WMO*, 1989). To accentuate the effect related to individual moisture regime of particular stations, monthly regional mean precipitation index series were calculated as non-weighted average percentage from the individual station-indices. Indices of May-June (MJ) and an annualized series were also determined. The annualized series were calculated as percentage of summarized monthly precipitation totals from the previous August to the current July.

These average percentage series were converted back to "absolute" precipitation values by multiplying each individual percentage data by the corresponding monthly, bimonthly, or annualized grand mean (mean of all stations' mean) calculated for the 1961–1990 reference period.

The longest continuous instrumental precipitation record in the region exists from the near-by Keszthely (*Fig. 1*). Early data (1861–1977) are available from Climate Explorer (*van Oldenborgh et al.*, 2005) and this series was updated to 2001.

2.3. *Relationship between tree growth and precipitation, precipitation reconstruction*

Relationship between annual increment of oak and precipitation was evaluated by computing Pearson's correlation coefficients from May of the previous year to October of the current year of formation of tree rings. In addition, MJ and annualized precipitation series were also involved into the correlation analysis.
To prevent the loss of natural amplitude due to the linear regression (*von Storch et al.*, 2005), rescaling technique was applied in reconstruction (*Esper et al.*, 2005). Period of instrumental precipitation data was divided into two subperiods: P1 (1901–1952) and P2 (1953–2003). Temporal stability of the reconstruction was tested in a split period calibration/verification procedure (*Fritts*, 1976). At first, mean and standard deviation of oak index for P1 were replaced by mean and standard deviation of instrumental data for P2, at second, role of subperiods was reversed.

Skill of reconstruction was tested by R^2 (explained variance), RE (reduction of error) and CE (coefficient of efficiency) statistics (*Cook et al.*, 1994). Values of R^2 are between 0 and 1. Higher value indicates more similarity, 1 means one series is the function of the others and vice versa. Potential values are $-\infty < RE, CE < 1$. If $RE > 0$ ($CE > 0$) it means that reconstruction better approximates data of the verification period than the mean of the calibration (verification) period. Obviously, CE is the more rigorous statistics.

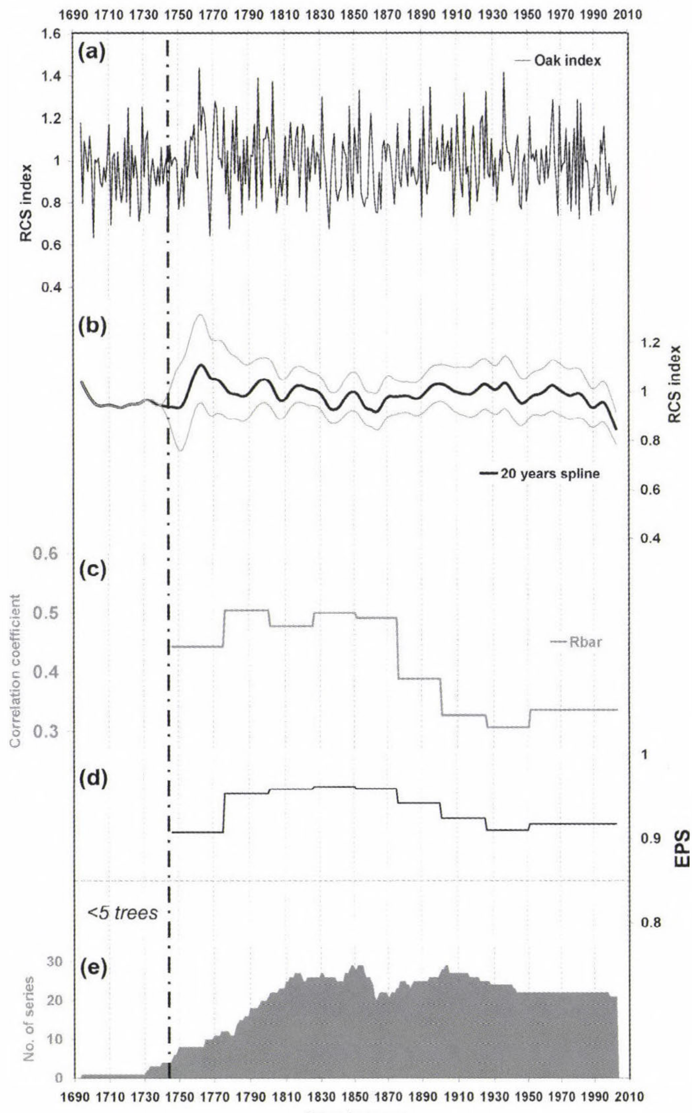

Fig. 3. Standardized oak index (a) and some signal strength statistics. (b) 20 years low pass filtered (cubic smoothing spline) indices. Light grey curves denote the bootstrapped 95% confidence interval. (c) Mean interseries correlation (Rbar). (d) Expressed population signal (EPS). Dashed horizontal grey line indicates the 0.85 level. (e) Sample depth. Dash dotted vertical line indicates 1745 AD. Before this date less than five trees build the chronology.

Two types of error were assigned as source of uncertainty (*Esper et al.*, 2007). On the one hand, chronology error was converted from the 95% confidence interval of the chronology (*Fig. 3b*). On the other hand, two standard error ranges derived from regression of 20 years smoothed reconstruction vs. instrumental data were regarded to quantify the 95% uncertainty designated as calibration error. Error terms were determined separately.

2.4. Independent precipitation reconstructions

Seven-graded monthly, seasonal, and annual precipitation indices were developed from documentary evidences for the Hungarian Kingdom (*Rácz*, 1999, hereafter R99) and available in printed form (*Rácz*, 2001). From the European gridded multi-proxy precipitation reconstruction (*Pauling et al.*, 2006, hereafter P06) seasonal totals could be extracted for the grid-cell (46.25°N; 17.25 × 46.75°N; 17.75°E) covering the studied area via internet (Climate Explorer (*van Oldenborgh et al.*, 2005)). R99 spans 1500–1850, while R06 spans 1500–2000.

3. Results

3.1. Characteristics of the TRW data

Chronology is still based on less than five trees before 1745. To avoid unreliable signal due to low replication, reconstruction is restricted to the well replicated period. Maximum replication is 29. Replication reaches its maximum level in three short periods, namely, 1903 – 04, 1852–55, and 1848 – 49 (*Fig. 3e*). Mean Rbar is 0.42 and mean EPS is 0.94 over the 1746 –2003 period. Minimum Rbar is 0.306 during the 1925 – 1960 period. A parting point (1875) appears in the Rbar statistics. Before this date, Rbar values are much higher than after. It indicates stronger common signal in the earlier part of the chronology when role of historical series is more dominant. This finding confirms the strict and excellent crossdate of the historical TRW series. EPS is steadily over the signal acceptance threshold (0.85) over the entire observation indicating robust chronology (*Fig. 3d*).

3.2. Relationship between oak index and precipitation

Correlation analysis revealed highly significant positive relationship between oak growth and May–June monthly precipitation of the year of tree-ring growth. The correlation coefficients are 0.36 and 0.41, respectively, exceeding the 99.9% significance level (*Fig. 4*). Calculating bimonthly (MJ) cumulated precipitation, the correlation coefficient reached 0.57 for the 1900–2003 period. All remaining months developed coefficients below 99% significance level. However, it is worthy to note that from August of previous year (pAug) to July, each coefficient is positive. Some of them (e.g., pDec, July) are above or (e.g., pAug, pSep) just slightly below the 90% significance level. This perception motivated the calculation of an annualized total precipitation summing monthly totals from previous August to current July. Involving this annualized precipitation into the analysis, correlation coefficient has even further improved (0.62). We can conclude that precipitation of May and June is the main growth regulator factor for oak growth in the southern Bakony Mts. and the Balaton Highlands, but moisture regime of complementary part of the previous August–current July period has also important effect. In the further steps, oak indices are to be calibrated against the annualized (i.e., previous August – current July) precipitation totals.

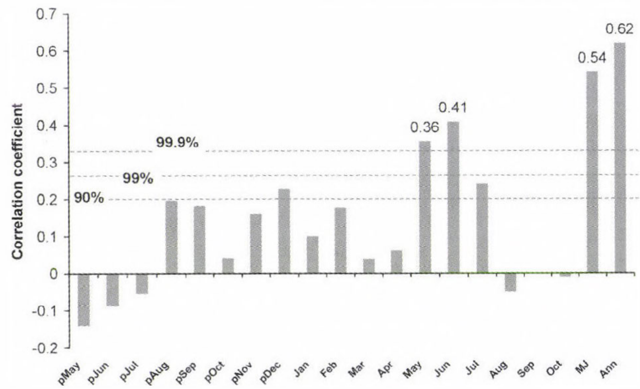

Fig. 4. Correlation coefficients computed between monthly precipitation and oak tree-ring index. Dashed horizontal lines denote 90%, 99%, and 99.9% significance levels for n=104 (1900–2003). Abbreviated months with 'p' mark months in the preceding year to formation of tree ring. 'MJ' means May–June bimonthly precipitation total. 'Ann' means annualized precipitation total summed from August of the previous year of growth to July of the current year. In the case of 'Ann' and months of previous year, comparison was restricted to 1901–2003.

3.3. Calibration and reconstruction

Split period calibration/verification procedure ensured the stability of reconstruction utilizing the rescaling technique (*Fig. 5*). RE and CE statistics yield above zero values in each case. In addition, verification statistics are fairly high, and squared correlation (R^2) exceeds the RE value settling any doubts about spurious significance (*McIntyre* and *McKitrick*, 2005).

As rescaling technique was well verified, final reconstruction (hereafter called OAK) has been prepared as mean and variance of oak index for the entire instrumental period (1901–2003) were set equal to mean and variance of regional precipitation (*Fig. 6a*).

The wettest and driest reconstructed years are 1795 (1033 mm) and 1768 (396 mm), respectively. The wettest decade in the OAK reconstruction is 1795 – 1804 (785 mm/yr). Driest decade on record is 1746–55 (613 mm/yr) and the second one is 1855 – 64 (620 mm/yr) (*Table 1*, *Fig. 6a*).

In general, a gradual long-term decreasing trend emerges as the dominant pattern of past changes. The trend seems to accelerate since the 1970s.

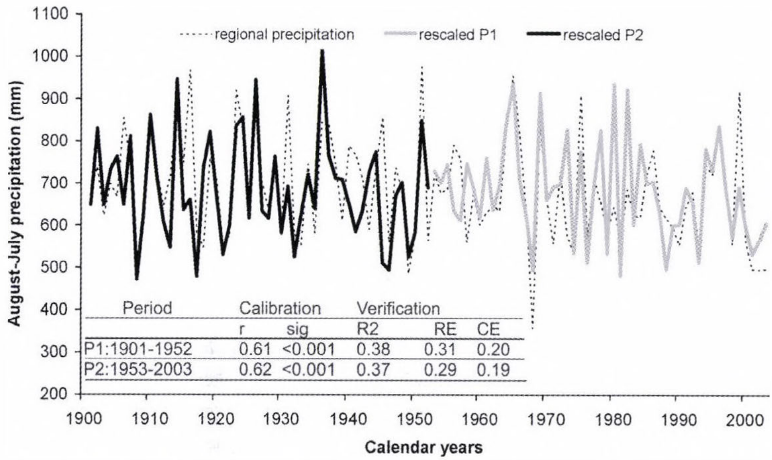

Fig. 5. Temporal stability of reconstruction by rescaling technique was tested. Dotted line: regional August–July precipitation. Grey line: estimated August–July precipitation rescaled by P1 period. Black line: estimated August–July precipitation rescaled by P2 period. Inset table: Split period calibration/verification statistics. r: Pearson's correlation coefficient, sig: significance of 'r', R2: explained variance, RE: reduction of error, CE: coefficient of efficiency.

4. *Discussion*

4.1. Extreme events and trends of past precipitation

On interannual scale, weak similarity can be found in extremes between instrumental and tree ring derived record (*Table 1*). Solely the driest instrumental year (1968) appeared and ranked third among the extremes of the modern part of OAK. Much more concurrences were found in the set of extreme decades. The driest rescaled decade is practically corresponding to the second driest instrumental one. Third driest decade is the same, but the driest decade from the instrumental period has also prominent place, ranked fourth, in the rescaled record. In addition, the wettest instrumental decade agrees, within a year shift, with the second one from the modern part of the rescaled record. Finally, the wettest rescaled decade significantly overlaps the third wettest instrumental one. Same as the instrumental data, each of the three rescaled driest decades appears in the second half of the century and practically the total post-mid-1980s period, covered by two non-overlapping decades, ranked into the drought top three. These correspondences further confirm the successful preservation of low-frequency precipitation signals in the OAK.

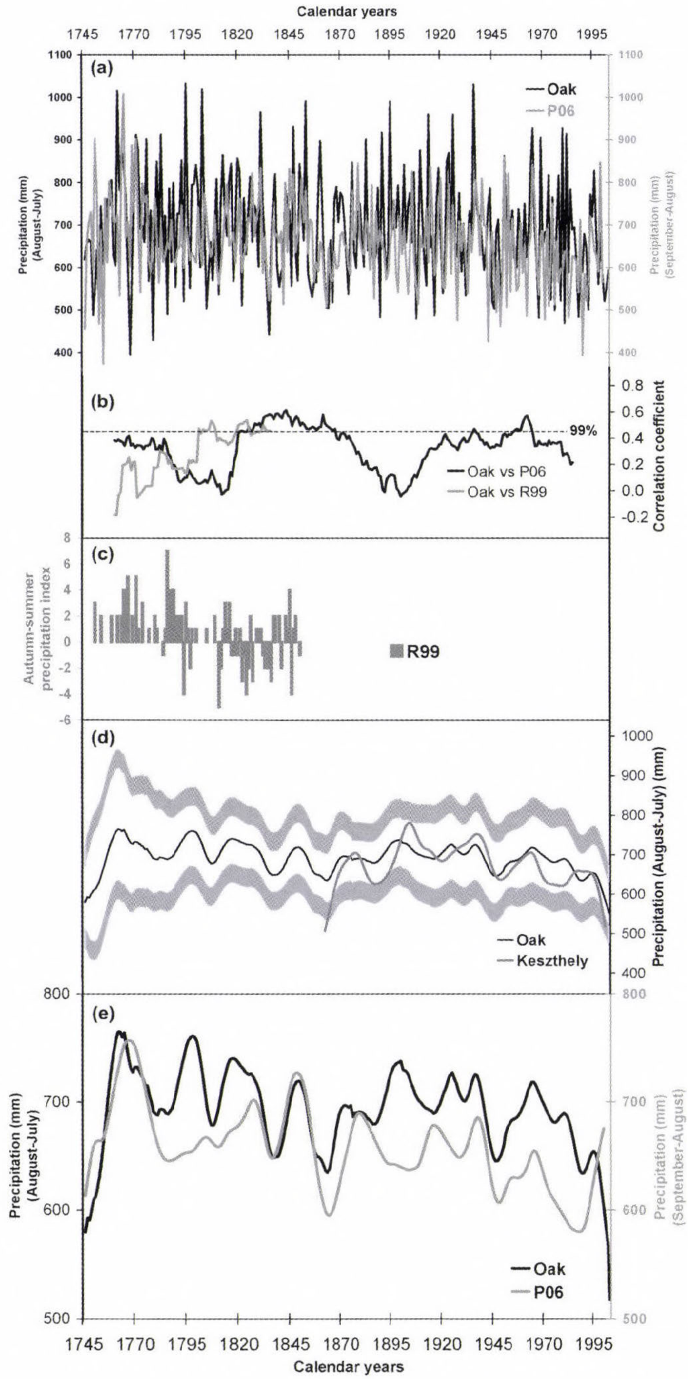

Fig. 6. (a) Reconstructed……→

Table 1. Three most extreme years and non-overlapping decades are listed from the instrumental and reconstructed era. Date in the 'year' column refers to the period from the previous August to the current July (i.e., 1968 means the period from August 1967 to July 1968). Date in the 'decade' column refers to the period from August ten years before to the current July (i.e., 1976 means the period from August 1965 to July 1976). 'Instrumental' means regional mean precipitation calculated from gauge records (see Section 2 for details)

		Instrumental (1901–2003)		**Rescaled (1901–2003)**		**Reconstruction (1746–1900)**	
		Year	**Decade**	**Year**	**Decade**	**Year**	**Decade**
Dry	1	1968	1976	1981	1994	1768	1755
	2	1949	1993	1908	1950	1779	1864
	3	2002	2003	1968	2003	1835	1842
Wet	1	1951	1945	1936	1927	1795	1804
	2	1916	1919	1914	1944	1803	1766
	3	1965	1932	1926	1973	1762	1821

Peering the extreme years in the reconstructed period, 1835 is nicely coinciding with the driest detected summer since 1800 in the eastern sector of Alps (*van der Schrier et al.*, 2006). The second driest (wettest) year was found as strong negative (positive) anomaly in reconstructed June aridity in southeast Slovenia (*Čufar et al.*, 2008).

The first studied decade was reconstructed as the driest one, but due to the larger uncertainty (mostly due to the widening chronology error (*Fig. 6d*)), absolute values are still less reliable. However, the second driest decade on record is a prominent dry period in the Alps (*Casty et al.*, 2005), especially in the eastern Alps (*Auer* and *Böhm*, 1994; *van der Schrier et al.*, 2006). Extreme Transdanubian drought from the late 1850s to the mid-1860s is nicely corroborated by documented desiccation of the lake Fertő (*Kiss*, 2001, 2004).

The wettest and the third wettest decades are in line with the statements of *van der Schrier et al.* (2006), as the first two decades of the 19th century was exceptionally wet periods also in the eastern part of the European Alps.

Fig. 6. (a) Reconstructed August–July precipitation of the Balaton Highlands and the southern Bakony Mts. over 1746–2003 based on oak ring widths (black line) and autumn-summer (previous September–current August) precipitation of the corresponding grid-cell of the P06 (*Pauling et al.*, 2006) reconstruction. (b) Coefficients of 31 years sliding window correlation computed between tree-rings based reconstruction and P06 (black) and R99 (grey). Dashed horizontal line denotes the 99% significance level. (c) Columns represent indices of the R99 reconstruction (*Rácz*, 1999). (d) Low-pass filtered (20 years cubic smoothing spline) reconstruction (black) and Keszthely gauge record (dark grey). The 95% uncertainty interval is presented as two separate bands related to chronology error (white) and to calibration error (grey). (e) Low-pass filtered (20 years cubic smoothing spline) tree-ring based reconstruction (black) and P06 (grey).

The longest continuous gauge record (Keszthely) was smoothed by a 20 years low-pass filter to verify the low-frequency signal of TRW based reconstruction (*Fig. 6d*). The independent record fits very well the fluctuation of OAK. Keszthely record excurses out from the range of uncertainty, solely, during its early decade. Though the 'low value' patterns are coherent between the records, it might be suspected that extreme low early gauge records are suffered from some negatively biasing homogeneity problem. Nevertheless, the similarity found with this independent record further confirms the fidelity of the oak ring width based precipitation reconstruction from the Balaton Highlands and the southern Bakony Mts.

4.2. Comparison with independent data

For the sake of better comparability of OAK, representing previous August–current July precipitation total as discussed above, with the seasonally resolved R99 and P06 ones were also annualized. Seasonal precipitation totals for P06 and indices for R99 were summed over the autumn-summer periods, respectively. By this way R99 and P06, in this study, differ from the original annual values of the reconstructions. Here they, indeed, represent the previous September–current August period. The one month shift in the theoretical time window of the reconstructions compared to OAK is unlikely to significantly affect their similarity or dissimilarity. Note that from 1800 to 1808 and before 1776, gaps are present in R99.

Sliding window correlation analysis revealed that OAK reconstruction and R99 shows significant similarity back to ~1800 (*Fig. 6b*). Similarity declines abruptly before. Observed worsening of relationship partially could be a consequence of gaps in R99. But we are to note that R99 gathered written evidences, practically, from the entire Carpathian Basin, so inherently and artificially reduced the ability to mirror reliably past changes on smaller spatial scales. For instance, 1786 designated as the wettest year in the observed period of R99 (*Fig. 6c*), based strongly on written evidences from the region of Miskolc and Sárospatak (northeast Hungary) (*Rácz*, 2001) and, in contrast, ranked seventh driest year by OAK during the reconstructed period in the southern Bakony Mts. (*Fig. 6a, b*).

Sliding window correlation analysis revealed that OAK reconstruction and P06 shows stable and significant similarity between ~1810 and ~1870 and quite well similarity (fluctuating around the 99% significance level) back to ~1920 (*Fig. 6b*). P06 lacks similarity in their interannual variability from the 1780s to 1810s and from the 1870s to the 1910s. Same periods present also the largest discrepancy in the low-frequency variability. In the latter case, the Keszthely gauge record verifies the fluctuation of OAK reconstruction. So we dare to conclude that P06 poorly reconstruct the fluctuation of precipitation during the above mentioned periods over the Balaton Highlands and the southern Bakony

Mts. region. After the 1910s, P06 presents similar fluctuations as OAK, but absolute values are consecutively below OAK (*Fig. 6e*). Another strange feature with P06 is that the trend for the recent decades is opponent with OAK. This sharply decreasing trend of OAK is verified by the local gauge records (*Fig. 4*, *Fig. 6d*). Since P06 also based on station data in recent century, an inadequate interpolation technique or non-representative station selection problem might be suspected.

However, the low precipitation at the earliest part of the record is coherent with P06 confirming the existence of the dry conditions during the late 1740s. In addition, the secular record of wet in the 1760s and the gradual decreasing trend since that time also agree in these independent precipitation reconstructions from the Balaton Highlands and the southern Bakony Mts. region.

5. *Conclusion*

We have presented a dendroclimatological reconstruction of August–July precipitation for the Balaton Highlands and the southern Bakony Mountains region since 1746. The reconstruction based on 22 living and 32 historical tree-ring width series from oak (*Quercus* sp.) samples. Ring width series were standardized by regional curve standardization technique (*Briffa et al.*, 1992; *Esper et al.*, 2003), regarding the biological character of oak's growth in the standardization procedure. By this way the low frequency climatic information was also effectively preserved in the tree-ring index.

A steady decrement has been appeared as an overall trend in the precipitation fluctuation since the mid-1700s. From this main pattern the 1840s, 1860s, and 1940s stand out as drier periods. The 1740s preceding the onset of this decreasing trend likely was also very dry. Derived precipitation reconstruction placed the late-20th century dry period into a secular context and suggests that the post-1980 drought period is unprecedented since 1746 at least. The low-frequency trend of the reconstruction from the mid-1800s century was verified by comparison with the longest nearby gauge record (Keszthely 1861–2001).

Present study pointed out weaknesses of two earlier precipitation reconstructions for the investigated region. A reconstruction developed on the base of written evidences (R99) aggregated documentary data over wide spatial distance, namely the entire Carpathian Basin, so owing to this methodological step, peculiarly in the case of precipitation, potential of R99 to detect past climate changes in local to regional scales has significantly reduced.

Data extracted from the corresponding grid from the European multi-proxy precipitation reconstruction (P06) showed poor similarity with this local reconstruction from the 1780s to the 1810s and from the 1870s to the 1910s. In addition, some problem (inadequate interpolation, non-appropriate station selection) during the instrumental era also might be suspected.

Reconstructed long-term gradual reduction of the precipitation associated with a changing seasonality (i.e., enhancing Mediterranean character (*Fogarasi*, 2004)) underlines that the climate of the Balaton Highlands and the southern Bakony Mts. significantly changed during the past centuries. Scenarios predict increasing aridity for Hungary (*Bartholy et al.*, 2004, *Gálos et al.*, 2007), especially over Transdanubia (*Szalai* and *Mika*, 2007) in future decades. Present results call the attention that agriculture and forestry have to face with this altered moisture regime by heavily depleted groundwater reservoirs.

Presented precipitation reconstruction also serves an objective basis to assess climatic conditions related to past historical events. Finally, we note that further improvements (e.g., extending the reconstructed time-span and reducing uncertainty) are possible and in progress.

Acknowledgements—The research was funded by OTKA T43666 and OTKA K67583. Budapest Tree-Ring Laboratory contribution No. 18.

References

Auer, I. and *Böhm, R.*, 1994: Combined temperature-precipitation variations in Austria during the instrumental period. *Theor Appl Climatol 49*, 161-174.

Bartholy, J.; Bogárdi, I. and *Matyasovszky, I.*, 1995: Effect of Climate Change on regional precipitation in Lake Balaton watershed. *Theor Appl Climatol 51*, 237–250.

Bartholy, J., Pongrátz, R., Matyasovszky, I. and *Schlanger, V.*, 2004: Expectable tendencies of global climate change in the Carpathian Basin (in Hungarian). In *Erdő és Klíma IV* (eds.: *Cs. Mátyás* and *P. Vig*). Nyugat-Magyarországi Egyetem, Sopron, Hungary, 57-68.

Blasing, T.J., Duvick, D.N., and *West, D.C.*, 1981: Dendroclimatic calibration and verification using regionally averaged and single station precipitation data. *Tree Ring Bull 41*, 37-43.

Bradley, R.S., 1999: Preface. *Climatic Change 43*, 1-2.

Bradley, R.S., Diaz, H.F., Eischeid, J.K., Jones, P.D., Kelly, P.M., and *Goodness, C.M.*, 1987: Precipitation fluctuations over Northern Hemisphere Land Areas since the mid–19th century. *Science 237*, 171–175.

Bradley, R.S., Hughes, M.K. and *Diaz, H.F.*, 2003: Climate in medieval time. *Science 30*, 404-405.

Brázdil, R., Štěpánková, P., Kyncl, T., and *Kyncl, J.*, 2002: Fir tree-ring reconstruction of March – July precipitation in southern Moravia (Czech Republic), 1376–1996. *Climate Res 20*, 223-239.

Briffa, K.R., Jones, P.D., Bartholin, T.S., Eckstein, D., Schweingruber, F.H., Karlén, W., Zetterberg, P., and *Eronen, M.*, 1992: Fennoscandinavian summers from AD 500: Temperature changes on short and long timescales. *Clim Dynam 7*, 111-119.

Buckley, B.M., Wilson, R.J.S., Kelly, P.E., Larson, D.W. and *Cook, E.R.*, 2004: Inferred summer precipitation for southern Ontario back to AD 610, as reconstructed from ring widths of *Thuja occidentalis*. *Canadian J Forest Res 34*, 2541-2553.

Casty, C., Wanner, H., Luterbacher, J., Esper, J. and *Böhm, R.*, 2005: Temperature and precipitation variability in the European Alps since 1500. *Int J Climatol 25*, 1855-1880. doi:10.1002/joc.1216

Cook, E.R. and *Peters, K.*, 1981: The smoothing spline: a new approach to standardizing forest interior tree-ring width series for dendroclimatic studies. *Tree Ring Bull 41*, 45-53.

Cook, E.R., 1985: A time series analysis approach to tree-ring standardization. *Ph.D. Dissertation*. The University of Arizona, Tucson.

Cook, E.R., Briffa, K.R. and *Jones, P.D.*, 1994: Spatial regression methods in dendroclimatology: a review and comparison of two techniques. *Int J Climatol 14*, 379–402.

Cook, E.R., Briffa, K.R., Meko, D.M., Graybill, D.A. and *Funkhouser, G.*, 1995: The 'segment length curse' in long tree-ring chronology development for paleoclimatic studies. *Holocene 5*, 229-237.

Cook, E.R. and *Krusic, P.J.*, 2006: ARSTAN4.1b_XP. http://www.ldeo.columbia.edu.

Čufar, K., De Luis, M., Eckstein, D. and *Kajfež-Bogataj, L.*, 2008: Reconstructing dry and wet summers in SE Slovenia from oak tree-ring series. *Int J Biometeorol 52*, 607-615. doi:10.1007/s00484-008-0153-8

Diodato, N., 2007: Climatic fluctuations in southern Italy since the 17th century: reconstruction with precipitation records at Benevento. *Climatic Change 80*, 411-431. doi:10.1007/s10584-006-9119-1

Douglass, A.E., 1919: *Climatic Cycles and Tree Growth. Vol. 1.* Carnegie Institution of Washington, Publication 289, Washington, DC, USA.

Efron, B., 1987: Better bootstrap confidence intervals. *J Amer Stat Assoc 82*, 171–185.

Esper, J., Cook, E.R., Krusic, P.J., Peters, K. and *Schweingruber, F.H.*, 2003: Tests of the RCS method for preserving low–frequency variability in long tree–ring chronologies. *Tree Ring Res 59/2*, 81–98.

Esper, J., Frank, D., Wilson, R.J.S. and *Briffa, K.R.*, 2005: Effect of scaling and regression on reconstructed temperature amplitude for the past millennium. *Geophys Res Lett 32*, L07711, doi: 10.1029/2004GL021236

Esper, J., Frank, D., Büntgen, U., Verstege, A., Luterbacher, J. and *Xoplaki, E.*, 2007: Long-term drought severity variations in Morocco. *Geophys Res Lett 34*, L17702, doi:10.1029/2007GL030844

Fogarasi, S., 2004: Change of Mediterranean Index on the karstic area of the Transdanubian Range and the connection with other elements of climate (in Hungarian). *Karsztfejlődés 9*, 251-268.

Frank, D., Esper, J. and *Cook, E.R.*, 2007: Adjustment for proxy number and coherence in a large-scale temperature reconstruction. *Geophys Res Lett 34*, L16709 doi:10.1029/2007GL030571

Fritts, H.C., 1976: *Tree Rings and Climate*. Academic Press, New York, p.567.

Gálos, B., Lorenz, P. and *Jacob, D.*, 2007: Climate change – drying tendency in Hungary? (in Hungarian). In *Erdő és Klíma* V (eds.: *Cs. Mátyás* and *P. Vig*). Nyugat-Magyarországi Egyetem, Sopron, Hungary, 57-67.

Garcia, R., Macias, A., Gallego, D., Hernández, L. and *Ribera, P.*, 2003: Reconstruction of the precipitation in the Canary Islands for the period 1595-1836. *Bull Am Met Soc 81*, 1037-1039.

Hegyfoky, K., 1910: Rainfall data from the 1851-1870 period (Supplementary for "The annual periodicity of precipitation in Hungary") (in Hungarian). *Meteorológiai és Földdelejességi Magyar Királyi Központi Intézet évkönyvei 37/* IV, 15-68.

Kern, Z., 2007: Tree-ring research in Balaton Highland and South Bakony Mts. (in Hungarian). In *Az erdő és a fa régészete és néprajza* (ed.: *Gömöri, J.*). MTA VEAB Soproni Tudós Társaság, Sopron, Hungary, 89-102.

Kiss, A., 2001: Die Veränderungen der natürlichen Verhältnisse des Komitates Sopron in XVIII-XIX. Jahrhundert. In *Bél Mátyás: Descriptio Comitatvs Semproniensis I.* (eds: *K. Szende* and *K. Kincses*). Quellen zur Geschichte der Stadt Ödenburg, Reihe C, Band 2. 76-89.

Kiss, A., 2004: Utilization of the Inundation Area at Lake Fertő before Regulation Works: Example of Sarród and its surroundings. *Acta Geographica Universitatis Szegediensis 38*, 39-49.

Linderholm, H.W. and *Chen, D.*, 2005: Central Scandinavian winter precipitation variability during the past five centuries reconstructed from *Pinus sylvestris* tree rings. *Boreas 34*, 43-52.

McIntyre, S. and *McKitrick, R.*, 2005: Hockey sticks, principal components, and spurious significance. *Geophys Res Lett 32*, L03710, doi:10.1029/2004GL021750

Mika, J., 2004: Regional climate scenarios: facts and doubts (in Hungarian). In *Erdő és Klíma IV* (eds.: *Cs. Mátyás* and *P. Vig*). Nyugat-Magyarországi Egyetem, Sopron, Hungary, 79-97.

Mika, J., 2007: New results and comparisons on regional features of the global warming in Hungary (in Hungarian). In *Erdő és Klíma* V (eds.: *Cs. Mátyás* and *P. Vig*), Nyugat-Magyarországi Egyetem, Sopron, Hungary, 13-30.

Oberhuber, W. and *Kofler, W.*, 2002: Dendroclimatological spring rainfall reconstruction for an inner Alpine dry valley. *Theor Appl Climatol 71*, 97-106. doi:10.1007/s704-002-8210-8

Osborn, T. J., Briffa, K.R. and *Jones, P.D.*, 1997: Adjusting variance for sample-size in tree-ring chronologies and other regional-mean time-series. *Dendrochronologia 15*, 89–99.

Pauling, A., Luterbacher, J., Casty, C. and *Wanner, H.*, 2005: Five hundred years of gridded high-resolution precipitation reconstructions over Europe and the connection to large scale circulation. *Clim Dynam 26*, 387-405. doi 10.1007/S00382-005-0090-8

Proctor, C.J., Baker, A., Barnes, W.L. and *Gilmour, M.A.*, 2000: A thousand year speleothem proxy record of North Atlantic climate from Scotland. *Clim Dynam 16*, 815-820. doi 10.1001/s003820000077

Rácz, L., 1999: *Climate History of Hungary Since 16th Century: Past, Present and Future.* Centre for regional studies of Hungarian Academy of Sciences discussion papers, No. 28, Pécs.

Rácz, L., 2001: *Magyarország éghajlattörténete az újkor idején* (Climate history of Hungary during Modern Age). JGYF Kiadó, Szeged, Hungary, 303 pp.

Rodrigo, F.S., Esteban-Parra, M.J., Pozo-Vazquez, D. and *Castro-Diez, Y.*, 1999: A 500-year precipitation record in Southern Spain. *Int J Climatol 19/11*, 1233-1253.

Siklósy, Z., Demény, A., Szenthe, I., Leél-Őssy, Sz., Pilet, S., Lin, Y. and *Shen, C.C.*, 2009: Reconstruction of climate variation for the last millennium in the Bükk Mts., northeast Hungary, from a stalagmite record. *Időjárás 113*, 245-263.

Szalai, S. and *Mika, J.*, 2007: Analysis and preciction of climate change and weather anomaly parameters important for forest cover (in Hungarian). In *Erdő és Klíma* V (eds.: *Cs. Mátyás* and *P. Vig*). Nyugat-Magyarországi Egyetem, Sopron, 133-143.

Touchan, R., Xoplaki, E., Funkhouser, G., Luterbacher, J., Hughes, M.K., Erkan, N., Akkemik, Ü. and *Stephan, J.*, 2005: Reconstruction of spring/summer precipitation for the Eastern Mediterranean from tree-ring widths and its connection to large-scale atmospheric circulation. *Clim Dynam 25*, 75-98.

Touchan, R., Akkemik, Ü., Hughes, M.K. and *Erkan, N.*, 2007: May-June precipitation reconstruction of southwestern Anatolia, Turkey during the last 900 years from tree-rings. *Quat Res 68*, 196-202. doi:10.1016/j.yqres.2007.07.001

van der Schrier, G., Efthymiadis, D., Briffa, K.R. and *Jones, P.D.*, 2006: European Alpine moisture variability for 1800-2003. *Int J Climatol 27*, 415-427. doi:10.1002/joc.1411

van Oldenborgh, G.J., Balmaseda M.A., Ferranti, L., Stockdale, T.N. and *Anderson, D.L.T.*, 2005: Evaluation of atmospheric fields from the ECMWF seasonal forecasts over a 15 year period. *J Climate 18*, 2970-2989.

Von Storch, H., Zorita, E., Jones, J.M., Dimitriev, Y., González-Rouco, F. and *Tett, S.F.B.*, 2004: Reconstructing past climate from noisy data. *Science 306*, 679-682. doi:10.1126/science.1096109

Wigley, T.M.L., Briffa, K.R. and *Jones, P.D.*, 1984: On the average value of correlated time series, with applications in dendroclimatology and hydrometeorology. *J Clim Appl Meteorol 23*, 201-213.

Wilson, R.J.S., Esper, J. and *Luckman, B.H.*, 2004: Utilising historical tree-ring data for dendro-climatology: a case study from the Bavarian Forest, Germany. *Dendrochronologia 21*, 53-68.

Wilson, R.J.S., Luckman, B.H. and *Esper, J.*, 2005: A 500 year dendroclimatic reconstruction of spring-summer precipitation from the Lower Bavarian Forest, Germany. *Int J Climatol 25*, 611-630. doi:10.1002/joc.1150

WMO, 1989: *Calculation of Monthly and Annual 30-year Standard Normals.* WCDP No. 10. WMO-TD/No. 341, Geneva

Yeh, H.-Y., Wensel, L.C. and *Turnblom, E.C.*, 2000: An objective approach for classifying precipitation patterns to study climatic effects on tree growth. *Forest Ecol Manag 139*, 41-50.

IDŐJÁRÁS

Quarterly Journal of the Hungarian Meteorological Service
Vol. 113, No. 4, October–December 2009, pp. 315–339

Historical climatology in Hungary: Role of documentary evidence in the study of past climates and hydrometeorological extremes

Andrea Kiss

Department of Physical Geography and Geoinformatics, University of Szeged, Egyetem u. 2, H-6722 Szeged, Hungary; E-mail: kissandi@earth.geo.u-szeged.hu

(Manuscript received in final form October 16, 2009)

Abstract—In the present paper, an overview of studies and investigations, related to the field of historical climatology and impact of hydrometeorological extremes based on documentary evidence, is presented. In addition to this, earlier investigations as well as the present stage of historical climatology in Hungary are discussed, based on research studies of climatologists, meteorologists, historians, and geographers. Besides compilations and analyses on long-term climate change, case studies on weather-related extreme events and anomalies of the last thousand years (such as droughts and floods) are also included. As regards climate variability and change, an overview is provided on the research based on lake water-level changes.

Key-words: historical climatology, climate reconstructions, extreme weather events, hydrometeorological extremes, climate anomalies, impact studies

1. Introduction

In the last decade, recent climate change issues and global warming have elicited deeper investigation of not only short, but also long-term changes and variability of climate, with special attention paid to extreme weather events and their consequences. In this respect, studying the climate variability of the last thousand years, historical climatology has begun to play a more important role, not only in other parts of Europe (*Brázdil*, 2000, 2003; *Pfister*, 2001; for the latest overview of European literature, see *Brázdil et al.*, 2005b and *Brázdil*, 2009), but also in Hungary. While there is an obvious general interest, especially among historians, related to environmental history and climatic changes in historical periods, and also a growing demand for a better understanding of the environment where human interactions took place, the climate and climate variability of the last thousand years are still relatively underinvestigated in the

Carpathian Basin and Hungary as well. In 1986, historical climatology was already listed as a separate field of higher education (*Draskóczy*, 1986); nowadays, it is treated among historians as a part of historical ecology and environmental history (*R. Várkonyi*, 2001). Nevertheless, while in the 1980s the actual research on historical climatology related topics played a somewhat marginal role in Hungary, attention was soon drawn towards this field as a result of conference presentations and publications of L. Rácz in Hungarian and international scientific journals and textbooks (*Rácz*, 1987, 1988, 1989, 1994, 1995, 1998, 1999a, 2001a, 2003a, 2003b, 2007 etc.).

Investigations that have some connection with historical climatology and topics are quite dependent on the databases and/or source collections available. The usual practice among scientists analyzing historical evidence is to take an existing database, regardless of the source quality, translation, or copying mistakes; as such, source criticism is still of marginal importance. In fact, due to these problems, most scientists do not dare to 'touch' historical databases at all. Since the building process of a database for detecting long-term changes may take decades and bring forth less attractive results in the period in between, historians usually concentrate on a specific event or series of events, with a special emphasis on the effects of extreme events or anomalies on human society. Another area of research, mainly carried out by motivated climatologists and meteorologists, is database enlargement. Among these databases the Réthly-collection, with its four volumes (*Réthly*, 1962, 1970, 1998, 1999), doubtlessly contains the most useful information.

2. *Antal Réthly and beyond: Compilations, data publishing, and reporting findings*

2.1. The role of scientific journals

The positivistic 19th century was the heyday of heroic collectors, whereas in the scientific literature of the 20th century, most of the historical data-collection efforts were carried out by climatologists and meteorologists. In the quarterly journal of the Hungarian Meteorological Service (IDŐJÁRÁS), from the beginning of the 20th century up to the 1970s, there was a separate section entitled "*Régi magyar megfigyelések*" (Early Hungarian observations), intended for publishing texts on historical weather events, early meteorological observations, and measurements. Though it was mainly *Antal Réthly* who published his concrete findings, there were other authors such as *Barna* (1960) with his Sárospatak observations, and early instrumental measurements from the mid-19th century and the Slovak climatologist, *Konček* (1972) on early instrumental measurements taken in late 18th century in Bratislava. Most of the evidence was extracted from the original sources; while in many cases Latin or German texts were published in Hungarian in translated excerpts; in some cases transcriptions in the original language (e.g., in Latin) were provided as well (e.g., *Csíkmadarasi Bogáts*, 1943).

From 1952 onwards, there was another journal, called *Légkör* (Atmosphere), which published reviews and descriptions on historical weather observations that were source related, and even if most of those reports were mainly of a short, descriptive nature, they succeeded in drawing attention to the topic and the field (*Csomor*, 1988, 1991, 1992; *Justyák*, 1991, 1992; *Ambrózy*, 1995; *Simon*, 1999). Much less in quantity and better in source-quality, local historians occasionally published sources for further climatological investigation. From these efforts, the importance of the Sopron archives and publication series in the local history journal of the *Soproni Szemle*, amongst others, should be mentioned, where contemporary sources were published, mainly (*Hegyi*, 1966; *Tirnitz*, 1974) or partly for the purpose of further climatological investigations (*Csatkai*, 1940; *Heimler*, 1942).

Besides the publishing works of journals and the Réthly-series, another compilation for the Kecskemét area was published as well. Although the Kecskemét-compilation of *Szilágyi* (1993, 1999) in part contains data taken from the Réthly-series, several additional, local history pieces of evidence were also included. Concerning criticism of historical sources, *Szilágyi* followed the Réthly-style; thus, including both contemporary and non-contemporary evidence in his compilation.

2.2. Role of the Réthly-collection in climate history analysis

Early weather reports, descriptions, observations, and measurements mostly mentioned in the IDŐJÁRÁS were later included in the four volumes of Antal Réthly's well-known compilation on weather events, extremes, and natural disasters of historical Hungary, for periods before 1900 (*Réthly*, 1962, 1970, 1998, 1999). This work, without any doubt, is of the utmost importance and provides a firm basis for further studies. Although Réthly as a meteorologist clearly did ask for the help of archivists and historians for collection, transcription, and translation works in several cases, data selection was clearly his own personal choice throughout the long and fruitful decades of his life. It is a notable fact that his selection criteria, source-quality judgements primarily formed, and provided the basis of evaluation for the existing Hungarian long-term climate reconstructions, descriptions, and most of the short-term surveys as well. As a motivated meteorologist and climatologist, Antal Réthly collected and included in his series all sorts of written information concerning the weather prior to 1900, regardless of the quality of these written materials as a historical source. Thus, contemporary, non-contemporary, and secondary-literature references were all included without much source criticism and validation. As he said in the Introduction of the first volume (*Réthly*, 1962, p. 13): "I included all the old weather data collected..."

Although in some particularly problematic cases and with clear contradictions, he did give his opinion, and thus, criticized some of the sources included in his series from the viewpoint of dating mistakes or general credibility of points, the vast majority of non-contemporary evidence as well as secondary literature references were included in exactly the same way as primary sources. Furthermore, we need to make distinction between the various volumes. While the first three books mainly contain texts or text-summaries taken from contemporary and non-contemporary sources as well as from secondary literature, originally written either in Latin, German, or Hungarian (or occasionally in other languages), in the fourth volume chiefly direct transcriptions of contemporary daily weather observations and early instrumental measurements of the 19th century, originally written in Hungarian, were gathered (*Réthly*, 1999). As such, there is a source-quality difference compared to the earlier, translated extracts, which in many cases were based on non-contemporary evidence. Unfortunately, in this last volume of 19th century daily observations, no clear reference on the availability of original sources are provided for each case, which makes proper investigations in some cases quite difficult.

In conclusion, when making use of the Réthly-series in any climatological analysis, we should enumerate the following sets of problems, which largely affect and concern the complete database included in the first three volumes of the Réthly-compilation:

(1) Up to the late 18th century, significant part of evidence included in the Réthly-collection is non-contemporary, which makes the Réthly-based analysis of the period rather problematic, due to the fact that non-contemporary evidence often contains the wrong dating of events, doubling or tripling events, etc. At the level of data analysis, another crucial problem is that while filtering out the non-contemporary evidence, in periods prior to the 17th century a significant part needs to be removed, and the same goes for some of the 18th century sources. This is especially true for the Middle Ages, whose part of the first volume contains information of acceptable source quality only in exceptional cases. For example, secondary literature without source references (*Bagi*, 1896; *Szentkláray*, 1880–1882; *Tőry*, 1952, etc.), as well as foreign source compilations like the one by *Hennig* (1904) or those by *Weikinn* (1958–1963), and texts of popular journals, newspapers (*Hasznos Mulatságok*) about curiosities which happened hundreds of years earlier, were included as well. In this respect, volumes of the Réthly-collection show clear similarities to other European compilations: none of them can be properly utilized without prior source validation (*Bell* and *Ogilvie*, 1978).

(2) Regarding the majority of the 16th–18th centuries and a part of the 19th century, sources (both contemporary and non-contemporary) were originally written not in Hungarian, but mainly in Latin or German, and rarely in other languages such as Turkish. Hungarian texts are mainly well extracted and

German texts were usually well translated and well extracted too. In some cases, however, there are clear problems (misinterpretations, gaps), for example, with texts taken from Latin, which without the help of other corresponding material can affect some of the index values (e.g., monthly reports taken from the volumes of *Sydenham*, 1769; or texts taken from the Jesuit diary of Levoča (in Hungarian: Lőcse), see Hungarian National Archives p. 478).

(3) In many cases, there are clear contradictions between the intervals provided by Réthly at the beginning of the actual source entry and the duration of a period mentioned in the actual text (e.g., an unknown length of time before a wine harvest is imprecisely recorded as the whole of October); similarly, some of the often equivalent events are misdated (problems of dating winter weather; or the huge amount of misdated materials, taken from secondary literature or from recent, unpublished private compilations or text collections, such the one by Florián Holovics or Gottlieb Bruckner – without mentioning original sources).

(4) Another dating problem especially of the late 16th century is that, although in the introduction Réthly draws attention to the question of proper dating due to the switch between Julian and Gregorian calendars occurring in different years in various parts of the Carpathian Basin, he clearly did not take it into consideration when providing the dates of events or periods in the actual text entries (see parts before and around late 16th – early 17th centuries in *Réthly*, 1962).

(5) Contemporary evidence is very much scattered in space, type, and time: observations or descriptions are rarely available from one place or even one region for a period of at least several decades, and even in these cases it is rare that one type of evidence (e.g., a family diary) contains a lot of detailed (monthly level) data for longer periods (for several decades at least). Hence the available data may be quite patchy; that is, it may have a low level of homogeneity.

(6) Parallel observations and descriptions would be of special importance to specify and check the credibility and quality of indices provided. Since in the majority of cases no parallel observation of appropriate quality on monthly or seasonal level is available in the Réthly-volumes, and contemporary indirect evidence, where it exists, often does not provide enough additional information, in many cases it is not possible to provide good-quality indices. Thus, the sources allow us to provide indices (i.e., the stage of deviations from normal values) only with some uncertainty in relatively clear cases without using further control evidence (independent, reliable sources).

As regards the temperature and precipitation indices of monthly or seasonal level, a great deal of evidence included in the Réthly collection is non-contemporary. Since non-contemporary evidence cannot form the main basis of analysis for further investigations, just the contemporary evidence entries should be used. These circumstances lead us to conclude that large portions of the materials should be excluded from a primary analysis. The remaining contemporary documentary evidence, on the other hand, does not provide a source that is large and detailed enough to draw long-term conclusions in appropriate quality and detail.

In summary, based on the above-mentioned main points, the Réthly-collection by itself cannot form the basis of an adequate long-term historical climatological reconstruction of the past 500 years, or longer. Therefore, significant and systematic database enlargement based on contemporary evidence, not only for the Middle Ages and early modern times but for the 19th century as well, is required.

3. Long-term reconstructions of historical climate

3.1. Index-based climate reconstructions of the last 500–1000 years

Apart from his studies in collecting weather and weather-related data, Antal Réthly carried out some basic analyses of selected evidence, such as the series of daily observations combined with early instrumental measurements, later published in the 18th century volume of his compilations (*Réthly*, 1970). Despite this, Réthly did not provide any further, long-term analysis based on his compiled database. Instead, somewhat earlier *Berkes* (1940) carried out some investigations on the long-term fluctuations of climate, first based on instrumental measurements, and then on the early-spring temperature-related evidence of the Kőszeg Book of Vinesprouts (*Berkes*, 1942). On a local scale, for the Kecskemét area in the central part of the Great Hungarian Plain, *Szilágyi* (1987, 1988a, 1988b, 1988c), besides his catalogue of weather events, mainly described extremes and anomalies reported from 1600 to 1873, highlighting winter temperature extremes as well as extremely dry periods.

The first and still most widely known and applied (7-scale) index-based temperature and precipitation reconstruction along with a description of weather conditions, for the past five hundred years, focusing on the regions of the former Hungarian kingdom, were published and analyzed by *Rácz* (1999b). In addition to the revised indices and historical investigations, in the extended textual analysis a clear attempt towards separating major regions can be seen (see also *Rácz*, 2001a, 2003c). Another concise statistical analysis of long-term temperature and precipitation conditions as well as of the frequency of strong winds were carried out for a thousand-year period, based on the documentary data included in the Réthly-compilation by *Bartholy et al.* (2004).

In the case of both existing long-term reconstructions and investigations of written weather records, the text data of the Réthly-series formed the basis of further research. Nevertheless, while Lajos Rácz did not include the analysis of medieval parts due to the strikingly low source quality of non-contemporary evidence, in the second reconstruction the complete Réthly-database of weather events, namely documentary evidence of the entire last millennium, was included. Although authors of the second reconstruction (*Bartholy et al.*, 2004) did distinguish between quality value classes of information (based on quantity-analysis), they only provided data for 50-year intervals: in this sense they concluded that the data for the entire 16th century and partly for the first half of the 17th century was of low quality; while from the quantity aspect, only the period of 1700–1850 was regarded as highly reliable (*Bartholy et al.*, 2003, 2004).

In essence, these reconstructions were carried out for historical Hungary, hence, practically, for the entire Carpathian Basin. In the last decade, however, there has been an increasing demand for high-resolution long-term temperature and precipitation information, divided on a (sub)regional basis, in fields such as landscape research or geomorphology (e.g., *Stankoviansky*, 2003; *Kovács* and *Rakonczai*, 2003; *Kovács*, 2004; *Kiss et al.*, 2006a), and this has a potential use in other well-established or emerging research fields, in the Carpathian Basin, like borehole climatology, dendroclimatology, speleology (*Bodri* and *Dövényi*, 2004; *Kern et al.*, 2004, 2009; *Siklósy et al.*, 2006, 2009; *Popa* and *Kern*, 2009), or fields of historical science that apply the results of historical climatology (e.g., *Laszlovszky*, 1994; *Kiss* and *Paszternák*, 2000; *R. Várkonyi*, 2001; *Szabados*, 2004). Furthermore, some interest from a climatology aspect can be seen as well, which can provide a climatological background to historical climate investigations (e.g., *Mika et al.*, 2000; *Mika* and *Lakatos*, 2008).

In Romania, *Cernovodeanu* and *Binder* (1993) provided a description of historical evidence taken from the Middle Ages onwards, based partly on source materials mentioned in the Réthly-series and partly on other, mainly contemporary written evidence related to the eastern parts of historical Hungary, namely Transylvania and the historical Partium (which today make up the western Romanian lowlands). In their investigations, the historical Romanian principalities (Walachia and Moldova) were also included. In the most westerly areas of the Carpathian Basin, a historical analysis of weather-related evidence was performed by *Strömmer* (2003) for the period of 1700–1830 for eastern Austria. In his recent investigations, *Rohr* (2007) provided a detailed account and a concise historical analysis of high and late medieval as well as early modern extremes that occurred in the eastern regions of the Alps.

Climate reconstructions of shorter periods are also available in Hungary, mostly in the form of case studies. From a climatological aspect, as early as in 1918, Antal Réthly carried out some statistical analyses, for example, on the early instrumental measurements and daily weather observations of Timişoara (in Hungarian: Temesvár) for the period of 1780–1803. Tables of results of this study were later included in his compilation (*Réthly*, 1970), together with a basic statistical analysis of other observations and early instrumental measurements of the same type (e.g., for Miskolc and Kežmarok (in Hungarian: Késmárk). This work, together with the digitalization process of the complete Timişoara-manuscript, was continued by *Csernus-Molnár* and *Kiss* (2008). A detailed historical and climatological analysis of well-documented periods, based on daily observations and early instrumental measurements was carried out in certain selected cases, in the present eastern parts of Slovakia, for some periods of the late 17th and early 18th centuries (*Brázdil* and *Kiss*, 2001; *Brázdil et al.*, 2008).

3.2. Phenological evidence and harvest results: The role of indirect information

As regards documentary sources containing regular observations of phenological data of a longer duration, up to now in Hungary the information content of the Kőszeg Book of vinesprouts has without doubt gained much interest. Looking for long-term evidence of climate fluctuation and change, *Berkes* (1942) was the first who investigated the connection between early spring temperature values and the length of vinesprouts illustrated each year on April 24. His evaluation was extended by *Péczely* (1982), who also raised an awareness of the connection between the quality of wine as another possible temperature indicator. Their works on Kőszeg vinesprouts were continued and a temperature reconstruction model, based on the length of vinesprouts, was developed by *Střeštík* and *Verő* (2000). Studying 20th-century data series, the connection between wine quality, quantity and climate is the topic of a recent investigation referring to the Tokaj wine region (*Makra et al.*, 2009).

By the early 1970s, *Bendefy* (1972a) in a conference report pointed out the possible reconstruction potential of wine harvest data series in town council protocols such as those in Kőszeg, Sopron, Szombathely, and Kecskemét. In a preliminary report he considered a 36-year periodicity in Hungarian vintage dates (*Bendefy*, 1972a); no information is, however, available for a continuation of this investigation. While some dates of Kecskemét vintages from the late 17th to the early 19th centuries were already published by that time (*Szabó*, 1934), the Kőszeg vintage dates, for the period of 1649–1820 (with gaps), were published a few decades later (*Szövényi*, 1965). Nevertheless, in both cases the actual series of dates formed a relatively less-important, additional part of two local history investigations. As a result, both sets of data have never been analyzed from a climatological point of view, or the later remarks on their significance. Moreover, in both cases it can be seen that they often provide not the date of beginning but a date 2–3 days after, or only one date during the wine harvest in general; thus, they did not concentrate on providing data for the beginning of an event. Following these early investigations, based on the original sources, a new interpretation of vine- and grain-related historical evidence (see *Fig. 1*) has been initiated within the framework of the EU project called Millennium (*Kiss,* 2008; *Kiss* and *Wilson*, 2009).

By looking for possible causes of economic wealth, crises, or periods of decline, economic historians can play an important role in identifying weather extremes or climate anomalies. Based on grain tithe accounts, for the bad harvest years of the late 16th century in the Žitný ostrov (in Hungarian: Csallóköz) area, the principal causes of a rainy period and Danube floods as well as wars were highlighted by *Zimányi* (1984). Using tithe series, *Landsteiner* (1999) studied vine harvest results of selected Central European towns, including Sopron, at the end of the 16th and the beginning of the 17th centuries and demonstrated, that similarly to other wine producing areas of Central Europe, the Sopron area had to face a decline in wine production in the late 16th century, mainly caused by adverse weather conditions.

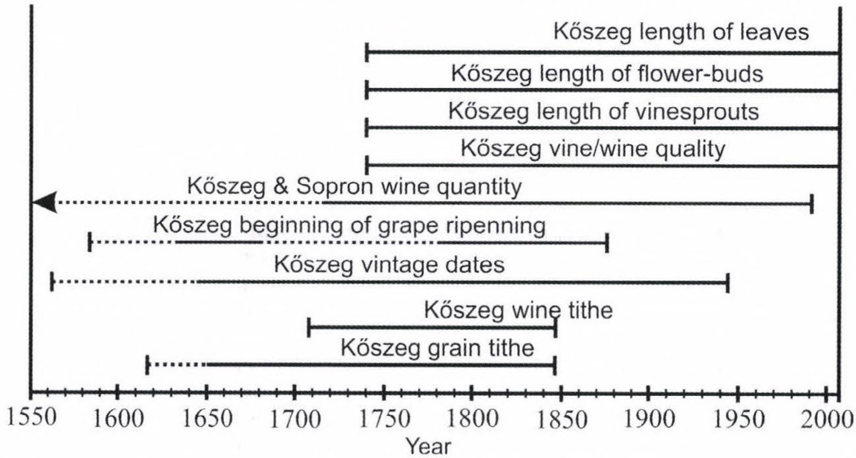

Fig. 1. Temporal coverage of recently available historical phenology evidence in Kőszeg (*Kiss*, 2008).

In the recent years, great interest has been shown in the possible agricultural consequences of climate change: based on evidence obtained from the Réthly-compilation, an analysis of phenological dates was done and phenophases information was examined (*Surányi*, 2006). However, owing to the quality and frequency of the data available in the Réthly-collection it is rather difficult to draw firm conclusions on this topic.

4. *Analysis of hydrometeorological extremes*

4.1. *Causes and consequences: Impact studies based on extreme events*

Series and combinations of extreme events and their consequences on the agriculture sector have, in some cases, gained more interest among agrarian and local historians. Some of the local history monographs, published in the period of the Austro-Hungarian Empire, contain particularly detailed accounts of natural disasters, induced by climate anomalies and weather extremes and their impact on local societies. Among others, a good example is the early monograph series by *Reizner* (1899–1900) about the local history of Szeged, where the great flood events of the Tisza in the Szeged area are described in an unusually detailed form, similar to the famine years, caused by a severe, prolonged drought of the late 1710s and 1720s. For instance in 1728, when the spring was particularly dry, and later this weather was combined with a great hailstorm over the plain, this caused the famous Szeged accusation case of witches. This witch-hunt, together with the historical background, was elaborated on in the first volume, together with primary sources (for a Central European context of witchcraft and weather, e.g., *Behringer*, 1999). This is of special importance, since the later monograph series of Szeged paid less attention to such issues (*Kristó*, 1985).

Droughts combined with extremely wet or cold periods caused the series of appealingly bad harvests in the Great Hungarian Plain, Transylvania, as well as in the Romanian principalities, which resulted in the great famine years of 1814–1817 in Bihar county (today, in Hungary and Romania), discussed by *Hodgyai* (1991). Also, the occurrence of the Maunder Minimum anomaly (1675–1715), as well as the cool summers of the 1830s and their adverse consequences on society in historical Hungary were discussed by *Rácz* (1994, 2001b). According to the author, as a consequence of cool summers there were bad harvests: these unfavorable conditions had an indirect influence on the decision-making policies of the contemporary Hungarian reform parliaments.

4.2. Droughts

In the central and eastern parts of the Carpathian Basin, especially in its lowland parts, mainly in the short-term but sometimes even in the long-term, severe droughts or a series of dry years probably had the most marked effects on the economy. Therefore, due to the well-known drought sensitivity of the semi-arid Great Hungarian Plain, droughts, said to be responsible for 22 known famines between 1790 and 1863 (*Érkövy*, 1863), have become a focal point of research. In historical research, the fields of local history and historical ethnography took a principal role in the study, description, and analysis of the effects of droughts on society, social relationships, economy, activities, and campaigns by the state and local authorities in finding solutions for crises which arose as a result of long dry spells. Since droughts had the greatest impact (greater than any flood event) in the aridification-endangered Great Hungarian Plain, studies usually concentrated on the most significant famines and mass extinction of cattle related to prolonged droughts of the late 18th and 19th centuries (*Györffy*, 1978; *Bellon*, 1996), but in some cases attention has also turned to the 1710s and 1720s (*Reizner*, 1899–1900).

Whereas floods caused problems in the previous decades but especially in the 1770s, the 1790s was without doubt the decade of droughts: investigating the great droughts of 1790 and 1794 (whose droughts also touched Moravia and Silesia – see *Brázdil et al.*, 2007), followed by famines, *Szabó* (1991) emphasized the significance of defence mechanisms developed by the society in 1791–1795 at both the local and regional levels in the north-central part of the Great Hungarian Plain, namely in Greater Cumania. Apart from the overwhelming importance of local history and historical ethnography research, looking for historical parallels of present drought events, to some extent environmental scientists also turned their attention towards this question (*Pálfai*, 1994). Nonetheless, without doubt great interest arose in the most influential drought of 1863, which is believed to have been primarily responsible for the fundamental and irreversible structural changes of Hungarian agriculture and as such, was widely discussed at both the regional and local level (*Reizner*, 1899; *Györffy*, 1978; *Bellon*, 1996; *Sipos*, 2001). In recent years, the possible connection between drought and the early 18th-century rise of witch accusations also became a topic of discussion among social historians (see, e.g., *Tóth*, 2008).

In two studies, mostly investigating the occurrence of famines in historical Hungary, the economic background, social consequences of droughts, and the response of the state are topics of discussion (*Gunst*, 1984a, 1984b). In his first article, the author suggests that due to the relatively low importance of crop production and consumption, and also due to the relatively low population density of the Carpathian Basin, droughts did not cause severe famines prior to the 18th century. Still, the number of famines caused by droughts increased from the early 18th century, when a great number of new settlers arrived in the country (*Gunst*, 1984a). Similar conclusions were reached in historical ethnography and local history studies, and he concluded that droughts of the Great Hungarian Plain and Transylvania in the 1850s and 1860s, and especially the well-known drought event of 1863 had probably the greatest impact on the long-term development and changes in agriculture, agricultural management, and economic development in Hungary. Moreover, this great drought event acted as a catalyst for the establishment of an independent Hungarian meteorological institute (*Gunst*, 1984b).

4.3. Floods

In Hungary another direction of historical research, which is also quite important in Central European investigations (e.g., *Brázdil et al.*, 2005a, 2007; *Glaser* and *Stangl*, 2004; concerning the Danube in Austria with emphasis on human response – see *Rohr*, 2005, 2007), focused on destructive historical floods: similar to well-known droughts, some of the especially destructive flood events were of especial interest and, as such, historians, hydrologists, as well as meteorologists studied them in great detail (in a European context, it is also reflected in the definition of historical hydrology – see *Brázdil et al.*, 2006). One of the early investigations was carried out by *Zawadovski* (1891). Apart from a detailed catalogue of data on water regulation, he listed the most destructive flood events that took place on larger rivers of the Carpathian Basin, especially from 1732 onwards, and sometimes he even gave a short overview on selected early modern floods as well. Although in most cases he did not provide clear evidence of his sources, in several cases he did refer to contemporary archival evidence. In addition, the author discussed some consequences (especially of material damage) of the greatest Danube floods in the late 18th and 19th century in the twin-town of Pest-Buda and Pest-Pilis-Solt County, like those of 1768, 1775, 1838, and 1876. Divided into small chapters, the author provided statistical information about damage in tabular form. Even if it is not completely free of errors, owing to the fact that no other comprehensive study of larger historical floods (Vol. 1) of the Carpathian Basin was carried out, this work became especially influential. Later investigations of hydrologists, usually including the obligatory short passages of a historical introduction, were largely based on the Zawadowski-catalogue.

Among the studies on individual flood events, most of the early studies were carried out on the 1838 ice flood at Pest-Buda (*Németh*, 1938; *Lászlóffy*, 1955), and the 1879 great Tisza flood at Szeged (for a concise overview of an early bibliography, see *Dégen et al.*, 1969; for a recent overview, see *Tóth*, 2009). These two events, together with their other consequences gained and still gain attention, and thus, separate chapters on several concise urban local history series, both old and new ones of Budapest and Szeged are usually devoted to the floods of great importance from the viewpoint of later urban development (*Gerevich*, 1975; *Kristó*, 1985). Furthermore, separate issues of the *Hidrológiai Közlöny* (*Hydrological Bulletin*) (1979: 59/6, 1988: 68/2) were published for the anniversaries of the great Pest-Buda and Szeged floods. In the past few decades, a new wave of analyses from both historians and environmental scientists were published for probably the most destructive flood event, namely the great 1838 Danube ice flood (*Faragó*, 1988; *Boldvay*, 1988; *Létay*, 1991 etc.), which practically destroyed the towns of Pest and Óbuda together with their suburbs. In this latter case, the meteorological conditions were also studied in detail (*Bodolainé Jakus*, 1988).

Based on data obtained from the Réthly-collection and the Zawadowski-catalogue, the connection between hard winters, ice cover, and ice floods of the Danube over a thousand year period are topics of discussion in the article by *Déri* (1989): due to the plentiful information available mostly for the period after 1820 and the impact of water regulations on ice cover, they were analyzed in more detail. Déri also emphasized the fact that, while significant efforts of water regulation works markedly reduced the chance of a looming destructive ice flood, still the danger was not over and, in the case of a hard winter, ice floods could cause significant damage even today. Mostly relying on the Zawadowski-catalogue, *P. Károlyi* (1970) studied the main periods and major consequences of significant flood events from the 18th century onwards of the Tisza valley from a hydrological viewpoint, with special emphasis on their impact on the later regulation works.

Other case studies on flood events are available in several individual articles, mainly done by local historians. Historical flood marks in Budapest were, for example, systematically described and investigated by *Rajna* (1979). Based on contemporary local history evidence, the most destructive flash floods and their impact on urban development were discussed in several local history articles (*Boronkai*, 1965; *Dobrossy* and *Veress*, 1978). In other studies, flood events of the River Maros (in Romanian: Mureş) in the 18th century (*Pálfai*, 1997; *Kiss et al.*, 2006b, 2008), those of the Drava river in the 16th–18th centuries (*Petrić*, 2007), and the main ice floods of the Danube between 1768 and 1799 together with related problems in the late 18th century development of Pest suburbs were discussed (*Kiss*, 2007). In a recent case study, the European aspects of great flood events in the winter and spring of 1784, including the Carpathian Basin, were also examined (*Brázdil et al.*, 2009).

5. Lake water-level changes: An interdisciplinary topic applying documentary evidence

As regards the lake-level variations related to climate variability, the investigations for Lake Balaton and Lake Fertő (in German: Neusiedlersee) should be emphasized.

By studying the water-level fluctuations of Lake Balaton, a great advantage can be detected in its shallowness as well as in the small, well-defined catchment situated at the west-central part of the Transdanubia in Hungary. In a book by *Bendefy* and *V. Nagy* (1969) on the water-level changes of Lake Balaton on a millennial scale, there is a clear attempt to apply contemporary medieval, early modern and modern documentary evidence. Although the book is still widely-accepted and used by scientists, the authors' interpretation of historical, cartographic, and archaeological evidence is often problematic and conclusions drawn are sometimes conceptual, and mostly related to the possible importance of human activity versus climate variability. As in some cases their results clearly contradict the other existing reconstruction, better accepted amongst historians and archaeologists (*Sági*, 1968; see also *Fig. 2*), a well-known, long-lasting debate (the so-called Balaton-debate), concerning medieval and early modern water levels, developed in the early 1970s (*Sági*, 1970; *Bendefy*, 1972b; *Sági* and *Füzes*, 1973). Another important difference was that, while in the case of the first water-level reconstruction human influence played an important role in the medieval and early-modern periods (*Bendefy* and *V. Nagy*, 1969; *Bendefy*, 1973), the other reconstruction viewed climate fluctuation as the factor primarily responsible for the historical water levels of Lake Balaton (*Sági*, 1968; *Sági* and *Füzes*, 1973).

On the other hand, in both papers there was a consensus on the fact that the average water-level of the Balaton underwent a slow rise in the high and later

Middle Ages, then this increase speeded up from the 16th century onwards. The changing human impact on the only natural outflow of the lake by itself, however, cannot be blamed for this significant increase, since the 14th century up to the mid-15th century contemporary sources show a survival of earlier utilization and management practices (mainly mills) of the waterflow (Fok/Sár river), even if in the 16th century, only the mills of the lower river sections (Sár river) were documented (*Kiss*, 2009). In the past few years, a multidisciplinary study, which included historical documentary evidence, was carried out by *Sümegi et al.* (2009a), and a comparison between the above-mentioned first water-level reconstruction and the available tree-ring evidence, connected to the 19th and 20th centuries, was published by *Kern* (2009).

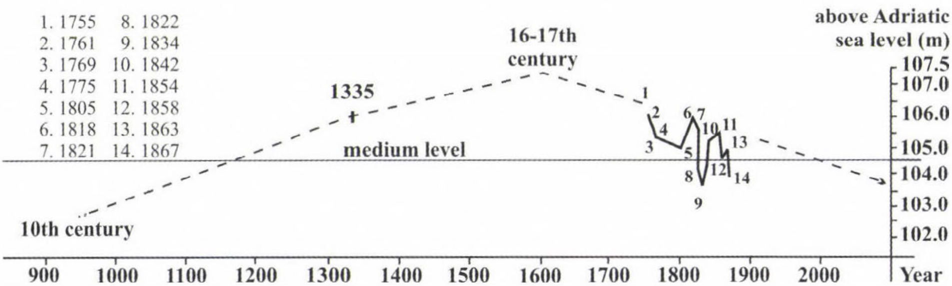

Fig. 2. The water-level changes of Lake Balaton in the past millennium, given by *Sági* and *Füzes* (1973).

Allegedly based on written evidence, the historical water-level changes of another lake, the Fertő (Neusiedlersee), which is even more sensitive to climate variability, was published by *Kopf* (1963). His extended reconstruction (*Fig. 3*), presumably based on documentary evidence, was widely accepted in the Hungarian scientific literature (*Zorkóczy*, 1975). Application possibilities are, however, strongly limited by the fact that Kopf made no mention at all of the sources used in the reconstruction (*Kiss*, 2004a).

In a similar way, although there was great interest and dozens of previous and later studies were carried out concerning the historical water-level changes of Lake Fertő (Neusiedlersee) and the Hanság (in German: Wasen) wetlands, most of the data was presented with no direct source-reference (*Nagy*, 1869; *Kövér*, 1930; *Haller*, 1941; *Károlyi*, 1955). They referred to earlier studies where, likewise, no reference concerning the source of information was provided (*Balsay et al.*, 1975; *Kováts*, 1982). As such, it is rarely possible to trace back all the original sources, based on literature entries. Other problems may occur when taking indirect written evidence into account: reconstruction attempts concerning medieval and early modern conditions often have interpretation problems of contemporary terminology (*Kiss*, 2004b). Quite similar problems have arisen in the scientific literature (*Bendefy* and *V. Nagy*, 1969) for the only natural outflow of Lake Balaton; namely the medieval Fok or Sár river (*Kiss*, 2009).

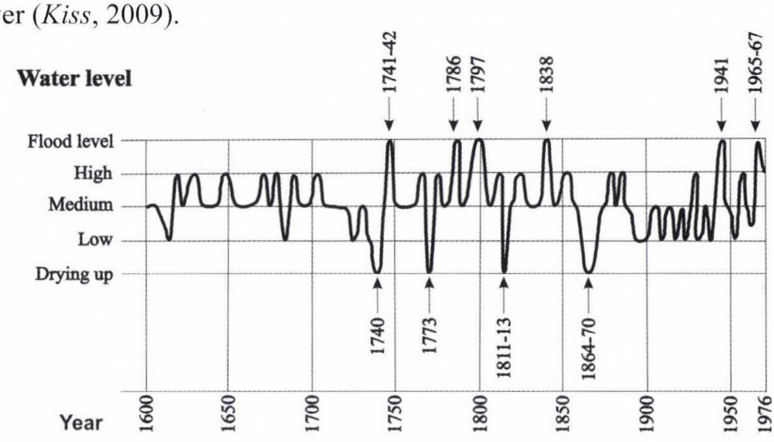

Fig. 3. Water-level changes of Lake Fertő (Neusiedlersee) in the last 400 years, elaborated by *Kopf* (1963), extended by *Zorkóczy* (1975).

6. *Medieval weather and climate: Sources and analysis*

From both medievalists and archaeologists, a growing interest could be seen to some extent from the 1960s (*Sági*, 1968), but especially from the 1990s onwards, with a particular emphasis on the Medieval Warm Epoch and the Little Ice Age transition (e.g., *Fügedi*, 1992; *Györffy* and *Zólyomi*, 1994, 1996; *Laszlovszky*, 1994; *Bálint*, 2003).

For the early Middle Ages, rather questionable attempts were made to relate the very scarce and problematic documentary evidence to a probable drought anomaly in the 8th century (*Györffy* and *Zólyomi*, 1994, 1996). Conversely, recent paleoenvironmental investigations suggest that droughts were more severe in the 13th century than in the 8th century (*Sümegi et al.*, 2009a; referring to 13th century conditions, see also *Sümegi et al.*, 2009b, 2009c). Concerning written sources, even much later, in the 11th–12th centuries only sporadic evidence is available (e.g., the battle of Ménfő: *Négyesi*, 1994), and these rarely provide the opportunity to draw some conclusions (*Kiss*, 2000a). Due to the growing amount of evidence, a few more detailed case studies have been occasionally carried out for particular, well-documented events of the 13th century like the hard winter conditions during the great or first Mongol invasion (*Kiss*, 2000b, 2003).

With the increasing amount of accurately dated 14th century legal evidence, in certain cases such as the 1340s, some great floods and presumed higher flood frequencies may be observed (*Kiss*, 1999). Concerning long-term changes, primarily based on archaeological and partly documentary evidence of the Visegrád royal palace and settlement, an interesting, early case study suggests that a significant increase of the average water level of the Danube began in the late medieval-early modern period (*Héjj*, 1988).

As regards the great subsistent crisis of 1315–1322 in Western Europe (*Kershaw*, 1973; *Jordan*, 1996), *Szántó* (2005, 2007) concluded that no contemporary evidence suggests that the crisis would have reached and had a significant impact in medieval Hungary. A recent investigation based on contemporary documents indicated that the European crisis of the mid-1310s reached and caused some problems in Hungary (*Vadas*, 2008).

Owing to the generally increasing amount of available medieval evidence, a review article was recently published on the medieval climate of Hungary (*Rácz*, 2007). Since very few studies have been published that directly analyze medieval weather and climate, it is a difficult task to provide any reliable conclusions on this subject. Therefore, database extension is of primary importance; up to now even key periods, like the 15th century with the most potential, have clearly been underinvestigated. Moreover, some contemporary legal documents (charters) suggest that not only direct but some indirect, landscape and hydrological evidence, for example the water-level conditions of larger lakes such as the Fertő (Neusiedlersee) in certain years, can also provide more useful information (*Kiss*, 2001; *Kiss* and *Piti*, 2005).

7. Conclusions and outlook

As we have seen, in Hungary climatologists and historians turned towards the study of climatic fluctuations and weather-related natural extremes at a relatively early period in history. This was partly due to the excellent potential arising from the immense amount of documentary evidence, largely available in present-day Hungary, but for historical reasons, for almost all of the Carpathian Basin as well. In this respect, it is clearly a positive point that the area of historical Hungary, meaning mainly Hungary, Slovakia, western Romania, northern Serbia, and the Transcarpathian region in Ukraine, is one of the areas in Central Europe with relatively early long-term historical climate reconstructions for the early-modern period (*Rácz*, 1999b, 2001a).

As a comparison, long-term (500-year or 1000-year) reconstructions on a monthly, seasonal basis (temperature, precipitation) are available in such areas of Central Europe as Switzerland (*Pfister*, 1988), the Czech Lands (*Brázdil* and *Kotyza*, 1995; *Dobrovolný et al.*, 2009a), and Germany (*Glaser*, 2001, 2008; *Glaser* and *Riemann*, 2009). A joint 500-year Central European seasonal temperature reconstruction, including the Czech Lands, Germany, and Switzerland, was recently carried out within the framework of the EU project called Millennium (*Dobrovolný et al.*, 2009b). Thus, an important future task will be to provide new index-based reconstructions, both for temperature and precipitation, based on an enlarged database of contemporary source evidence and a critical evaluation of sources.

Another promising direction for obtaining other long-term (mainly temperature-related) reconstructions is related to historical phenology evidence and other data series concerning agricultural activities (e.g., harvested amounts). Vine and grain phenology-based investigations, covering 500 years or more, have already been carried out in Central Europe (*Meier et al.*, 2007), which may eventually provide a good methodological background for the analysis of evidence either belonging to Hungary or other areas of the Carpathian Basin.

In spite of the good potential of contemporary documentary evidence, covering not just the early-modern period, but also the Middle Ages, in Hungary relatively little has been done on the systematic analysis of hydrometeorological extremes. This is especially true for flood evidence; even if dozens of more or less detailed case studies are available on one or another destructive drought or flood event, no systematic investigations have been carried out, unlike some other parts of Central Europe (see references in sub-chapter 4.3). Hence, another possible future direction of research is the systematic collection and analysis (e.g., frequency, classification, seasonality, causes, impact) of hydrometeorological extremes. Short- and long-term effects of extremes and anomalies on society had a further importance and have gained increasing interest in the past decade: impact studies and the role of human response have become a significant issue for environmental historians in Central Europe (e.g., *Behringer et al.*, 2005; *Pfister*, 1999, 2002; *Pfister* and *Brázdil*, 2006). As we saw earlier, in the form of individual events, in Hungary historical ethnographers and local historians played an important role in analyses, especially on droughts, and also on other hydrometeorological events like floods. As regards other types of impact, studies on the relationship between climatic fluctuations, frequency of extremes and landscape development might also be an interesting direction of further research (for Central European parallels, see, e.g., *Bork et al.*, 1998).

While no systematic collection and analysis of events have been carried out yet, after the source validation process the vast amount of contemporary evidence included in the Réthly-compilation could form a good starting point for systematic investigations covering a period of four hundred years or more. In this respect, the Middle Ages need to be treated differently: a completely new documentary source collection process has to be launched.

Acknowledgements—The present study was supported by the FP6 EU project Millennium No. 017008. The author would like to express her special thanks to *Rudolf Brázdil* (Masaryk University, Czech Republic) for his help and careful corrections. The author is also grateful to *Sheila Hicks* (University of Oulu, Finland), *József Laszlovszky* (Central European University, Hungary), *János Mika* (Hungarian Meteorological Service, Hungary), *Pál Sümegi* (University of Szeged, Hungary), and *Ágnes R. Várkonyi* (Eötvös Loránd University, Hungary) for their useful suggestions, and to *David P. Curley* (University of Szeged, Hungary) for proof-reading this article.

References

Ambrózy, P., 1995: Meteorological observations of David Fröhlich (in Hungarian). *Légkör 40*, No. 4, 23-24.

Bagi, L. (ed.), 1896: *Kecskemét múltja és jelene* (Past and present of Kecskemét). Tóth László Nyomdája, Kecskemét, 214 pp.

Balsay, L., Halupa, L. and *Komjáthy, F.*, 1975: Data on the history of forests in the Hanság area (in Hungarian). In *Az erdőgazdálkodás története Magyarországon* (History of Forestry in Hungary) (ed.: *Kolossváry, Sz.*). Akadémiai Kiadó, Budapest, 394-465.

Barna, U., 1960: Weather reports in Sárospatak between 1847-1853 (in Hungarian). *Időjárás 64*, 115-118.

Bartholy, J., Pongrácz, R. and *Molnár, Zs.*, 2003: Extremes and millennial trends in the Carpathian Basin using the Réthly documentary collection. American Meteorological Society, *17th Conference on Probability and Statistics in the Atmospheric Sciences*, Extended Abstracts, 1-12.

Bartholy, J., Pongrácz, R. and *Molnár, Zs.*, 2004: Classification and analysis of past climate information based on historical documentary sources for the Carpathian Basin. *Int J Climatol 24*, 1759-1776.

Bálint, M., 2003: Landscape development and soil formation in the Danube-Tisza Interfluve. In *People and Nature in Historical Perspective* (eds.: *J. Laszlovszky* and *P. Szabó*). Archaeolingua, Budapest, 157-174.

Behringer, W., 1999: Climatic change and witch-hunting: The impact of the Little Ice Age on mentalities. *Climatic Change 43*, 335-351.

Behringer, W., Lehmann, H. and *Pfister, Ch.* (eds.), 2005: *Kulturelle Konsequenzen der "Kleinen Eiszeit"*. Vandenhoeck&Ruprecht, Göttingen, 510 pp.

Bell, W.T. and *Ogilvie, A.E.J.*, 1978: Weather compilations as a source of data for the reconstruction of European climate during the medieval period. *Climatic Change 1*, 331-348.

Bellon, T., 1996: *Beklen. A nagykunsági mezővárosok állattartó gazdálkodása a XVIII-XIX. században* (Beklen. Animal husbandry of the towns in Greater Cumania in the 18-19th centuries). Karcag Város Önkormányzata, Karcag, 31-38.

Bendefy, L., 1972a: A 400-year phenological curve based on the ripening of Hungarian grapevines (in Hungarian). In *Anyag- és energiaáramlási ankét* (Meeting on material and energy flux) (eds.: *E. Szádeczky-Kardoss* and *É. Pécsiné Donáth*). Akadémiai Kiadó, Budapest, 31-33.

Bendefy, L., 1972b: The influence of natural and anthropogenic factors on the water-level changes of Lake Balaton (in Hungarian). *Földrajzi Értesítő 2-3*, 335-358.

Bendefy, L., 1973: Dykes at Jut and the high water-level conditions of Lake Balaton in the Turkish Period (in Hungarian). *Somogy megye múltjából 4*, 113-128.

Bendefy, L. and *V. Nagy, I.*, 1969: *A Balaton évszázados partvonalváltozásai* (Millennial shoreline changes of Lake Balaton). Műszaki Kiadó, Budapest, 215 pp.

Berkes, Z., 1940: Changes in climate or variability of climate? (in Hungarian) *Időjárás 44*, 155.

Berkes, Z., 1942: Éghajlatingadozások tükröződése a kőszegi szőlőhajtások hosszában / Spiegelung der Klimaschwankungen in dem Längenwachstum der Weinreben-Triebe in Kőszeg. *A M. Kir. Orsz. Meteorológiai és Földmágnességi Intézet Kisebb kiadványai, Új sorozat 15*, Budapest, 17 pp.

Bodolainé Jakus, E., 1988: Weather conditions of the 1838 ice flood of the Danube (in Hungarian). *Hidrológiai Közlöny 68*, 72-77.

Bodri, L. and *Dövényi, P.*, 2004: Climate change of the last 2000 years inferred from borehole temperatures: data from Hungary. *Global and Planetary Change 41*, 121-133.

Boldvai, F., 1988: About the ice flood of Pest 150 years ago (in Hungarian). *Légkör 33*, No. 2, 32-37.

Bork, H-R., Bork, H., Dalchow, C., Faust, B., Piorr, H-P. and *Schatz, T.*, 1998: *Landschaftsentwicklung in Mitteleuropa: Wirkungen des Menschen auf Landschaften*. Klett-Perthes, Stuttgart, 328 pp.

Boronkai, P., 1965: Floods in Sopron (in Hungarian). *Soproni Szemle 19*, 339-346.

Brázdil, R., 2000: Historical climatology: definition, data, methods, results. *Geografický časopis 52*, 99-121.

Brázdil, R., 2003: Historical climatology and its progress after 1990. In *People and Nature in Historical Perspective* (eds.: *J. Laszlovszky* and *P. Szabó*). Central European University, Department of Medieval Studies & Archaeolingua, Budapest, 197-227.

Brázdil, R., 2009: Historical climatology and its contribution to climate reconstruction in Europe. In *Nachhaltige Geschichte. Festschrift für Christian Pfister* (eds.: *A. Kirchhofer, D. Krämer, C.M. Merki, G. Poliwoda, M. Stuber* and *S. Summermatter*). Chronos Verlag, Zürich, 65-89.

Brázdil, R. and *Kotyza, O.*, 1995: *History of Weather and Climate in the Czech Lands I (Period 1000-1500)*. Zürcher Geographische Schriften 62, Zürich, 260 pp.

Brázdil, R. and *Kiss, A.*, 2001: Daily weather observations at Košice, Slovakia, in the period 1677-1681. *Meteorologický časopis 4*, 3-14.

Brázdil, R., Dobrovolný, P., Elleder, L., Kakos, V., Kotyza, O., Květoň, V., Macková, J., Müller, M., Štekl, J., Tolasz, R. and *Valášek, H.*, 2005a: *Historical and Recent Floods in the Czech Republic* (in Czech). Masaryk University, Czech Hydrometeorological Institute, Brno, Praha, 370 pp.

Brázdil, R., Pfister, Ch., Wanner, H., von Storch, H. and *Luterbacher, J.*, 2005b: Historical climatology in Europe – the state of the art. *Climatic Change 70*, 363-430.

Brázdil, R., Kundzewicz, Z. W. and *Benito, G.*, 2006: Historical hydrology for studying flood risk in Europe. *Hydrolog Sci J 51*, 739-764.

Brázdil, R., Kirchner, K. Březina, L, Dobrovolný, P., Dubrovský, M., Halásová, O., Hostýnek, J., Chromá, K., Janderková, J., Kaláb, Z., Keprtová, K., Kotyza, O., Krejčí, O., Kunc, J., Lacina, J., Lepka, Z., Létal, A., Macková, J., Máčka, Z., Mulíček, O., Roštínský, P., Řehánek, T., Seidenglanz, D., Semerádová, D., Sokol, Z., Soukalová, E., Štekl, J., Trnka, M., Valášek, H., Věžník, A., Voženílek, V. and *Žalud, Z.*, 2007: *Selected Natural Extremes and Their Impacts in Moravia and Silesia* (in Czech). Masaryk University–Czech Hydrometeorological Institute and Institute of Geonics–Academy of Sciences of the Czech Republic, Brno, Praha, Ostrava, 432 pp.

Brázdil, R., Kiss, A., Luterbacher, J. and *Valášek, H.*, 2008: Weather patterns in eastern Slovakia 1717-1730, based on records from the Breslau meteorological network. *Int J Climatol 28*, 1639-1651.

Brázdil, R., Demarée, G.R., Deutsch, M., Garnier, E., Kiss, A., Luterbacher, J., MacDonald, N., Rohr, Ch., Dobrovolný, P., Kolář, P. and *Chromá, K.*, 2009: European floods during the winter 1783/1784: scenarios of an extreme event during the 'Little Ice Age'. *Theor Appl Climatol*, doi 10.1007/s00704-009-0170-5.

Cernovodeanu, P. and *Binder, P.*, 1993: *Cavalerii Apocalipsului. Calamitățile naturale din trecutul României (până la 1800)* (Knights of the Apocalypse. Natural disasters of Romania up to 1800). SILEX–Casă de Editură S.R.L., București, 255 pp.

Csatkai, E., 1940: Sopron chronicles I.: Chronicle of Daniel Petz senior and junior (in Hungarian and German). *Soproni Szemle 4*, 133-203.

Csernus-Molnár, I. and *Kiss, A.*, 2008: Instrumental measurements and weather reports in Temesvár [Timişoara] (in Hungarian). In *IV. Magyar Földrajzi Konferencia tanulmánykötet* (Research papers of the Fourth Conference on Geography in Hungary) (eds.: *V. Szabó, Z. Orosz, R. Nagy*, and *I. Fazekas*). Debreceni Egyetem, Debrecen, 205-211.

Csíkmadarasi Bogáts, D., 1943: Reports of János Vásárhely, Calvinist priest of Sepsiszentgyörgy [Sfântu Gheorghe] about the weather conditions of the years 1722-1764 (in Hungarian and Latin). *Időjárás 47*, 143-145, 235-236.

Csomor, M., 1988: Extreme winters in Hungary in the 19th century (in Hungarian). *Légkör 33*, No. 4, 31.

Csomor, M., 1991: Early Hungarian observations: the winter of 1791 (in Hungarian). *Légkör 36*, No. 2, 29.

Csomor M., 1992: Early Hungarian weather observations (1791/1792) 200 years ago (in Hungarian). *Légkör 37*, No. 3, 31.

Dégen, I., Lászlóffy, W. and *Károlyi, Zs.*, 1969: *A szegedi árvíz 1879* (The Great Flood of 1879 in Szeged). Vízügyi történeti füzetek 1, VIZDOK, Budapest, 80 pp.

Déri, J., 1989: Ice floods of the Danube in the last Millennium (in Hungarian). *Hidrológiai Közlöny 69*, 151-158.

Dobrossy, I. and *Veres, L.*, 1978: *Miskolci árvíz 1878-1978* (Flood in Miskolc 1878-1978). Herman Ottó Múzeum, Miskolc, 66 pp.

Dobrovolný, P., Brázdil, R., Valášek, H., Kotyza, O., Macková, J. and *Haličková, M.*, 2009a: A standard paleoclimatological approach to temperature reconstruction in historical climatology: an example from the Czech Republic, A.D. 1718–2007. *Int J Climatol 29*, 1478–1492.

Dobrovolný, P., Moberg, A., Brázdil, R., Pfister, Ch., Glaser, R., Wilson, R., van Engelen, A., Limanówka, D., Kiss, A., Haličková, M., Macková, J., Riemann, D., Luterbacher, J. and *Böhm, R.*, 2009b: Monthly and seasonal temperature reconstructions for Central Europe derived from documentary evidence and instrumental records since AD 1500. *Climatic Change*, doi 10.1007/s10584-009-9724-x.

Draskóczy, I., 1986: Historical climatology (in Hungarian) In *A történelem segédtudományai* (Auxiliary sciences of history) (ed.: *I. Kállay*). Eötvös Loránd Tudományegyetem Bölcsészettudományi Kar, Budapest, 307-316.

Érkövy, A., 1863: *Az 1863. évi aszályosság a Magyar Alföldön* (Drought in 1863 on the Great Hungarian Plain). Országos magyar gazdasági egyesület, Pest, 103 pp.

Faragó, T. (ed.), 1988: *Pest-budai árvíz 1838* (Flood in Pest-Buda 1838). Főv. Szabó Ervin Könyvtár, Budapest, 515 pp.

Fügedi, E., 1992: Historical demography of medieval Hungary (in Hungarian). *Történeti demográfiai füzetek 10*, 10-60.

Gerevich, L. (ed.), 1975: *Budapest története* (History of Budapest). Akadémiai Kiadó, Budapest, 288-300.

Glaser, R., 2001: *Klimageschichte Mitteleuropas. 1000 Jahre Wetter, Klima, Katastrophen*. Primus-Verlag, Darmstadt, 227 pp.

Glaser, R., 2008: *Klimageschichte Mitteleuropas. 1200 Jahre Wetter Primus-Verlag, Klima, Katastrophen.* Wissenschaftliche Buchgesellschaft, Darmstadt, 227 pp.

Glaser, R. and *Stangl, H.*, 2004: Climate and floods in Central Europe since AD 1000: Data, methods, results and consequences. *Surv Geophys 25*, 485-510.

Glaser, R. and *Riemann, D.*, 2009: A thousand-year record of temperature variations for Germany and Central Europe based on documentary data. *J Quaternary Sci 24*, 437-449.

Gunst, P., 1984a: Hungersnöte und Agrarausfuhr im spätmittelalterlichen Ungarn (1700-1848). *Agrártörténeti Szemle 26*, 11-18.

Gunst, P., 1984b: Droughts and the Hungarian state. From the 18th century to 1945 (in Hungarian). *Agrártörténeti Szemle 26*, 438-457.

Györffy, L., 1978: Memory of the 'horrible year' and the great famine of 1863 (in Hungarian). *Szolnok megyei múzeumok közleményei 1*, 91-103.

Györffy, Gy. and *Zólyomi, B.*, 1994: Landscape of the Carpathian Basin and the 'Etelköz' thousand years ago (in Hungarian). In *Honfoglalás és régészet* (Conquest and archaeology) (ed.: *L. Kovács*). Balassi Kiadó, Budapest, 13-37.

Györffy, Gy. and *Zólyomi, B.*, 1996: The Carpathian Basin and the 'Etelköz' thousand years ago (in Hungarian). *Magyar Tudomány 96*, 899-918.

Haller, J., (1941) 1998: *Moson vármegye történelmi földrajza* (Historical geography of Moson county). Mosonmagyaróvári Helytörténeti Füzetek 9. Mosonmagyaróvári Hansági Múzeum, Mosonmagyaróvár, 318 pp.

Hegyi, F., 1966: Judgement day in the Sopron area in 1789 (in Hungarian). *Soproni Szemle 20*, 378.

Heimler, K., 1942: Sopron chronicles II: chronicle of Georg Payr and Michael Payr 1584-1700 (in Hungarian and German). *Soproni Szemle 6*, 1-94.

Hennig, R., 1904: *Katalog bemerkenswerter Witterungsereignisse von den ältesten Zeiten bis zum Jahre 1800.* Abhandlungen des Königlich Preussischen Meteorologischen Instituts. Vol. 2, No. 4. A. Asher, Berlin, 93 pp.

Héjj, M., 1988: Observations concerning settlement geography. Visegrád in the 14th-16th centuries (in Hungarian). In *Visegrád 1335. Tudományos tanácskozás a visegrádi királytalálkozó 650. évfordulóján* (Visegrád 1335. Scientific workshop on the 650th anniversary of the Visegrád royal meeting) (ed.: *J. Köblös*). Pest Megyei Levéltár, Budapest, 63-67.

Hodgyai, M., 1991: Hunger years in Bihar between 1814-1817 (in Hungarian). *Történelmi Szemle 33*, 59-69.

Jordan, W.Ch., 1996: *The Great Famine. Northern Europe in the Early Fourteenth Century.* University Press, Princeton, 316 pp.

Justyák, J., 1991: Weather reports in Széchenyi's diary (in Hungarian). *Légkör 36*, No. 2, 15-18.

Justyák, J., 1992: Weather of Debrecen based on early reports: 1820-1837 (in Hungarian). *Légkör 37*, No. 3, 19-21.

Károlyi Z., 1955: Development of water-regulation issues of the Hanság wetlands and Lake Fertő (in Hungarian). *Vízügyi Közlemények 37*, 291-332.

Kern, Z., 2009: Connection between oak tree ring width of the Balaton Uplands and the water-level changes of Lake Balaton (in Hungarian). In *Környezettörténet* (Environmental history) (ed.: *M. Kázmér*). Hantken kiadó, Budapest, 357-366.

Kern, Z., Fórizs, I., Nagy, B., Kázmér, M., Gál, A., Szántó, Z., Palcsu, L., and *Molnár, M.*, 2004: Late Holocene environmental changes recorded at Gheţarul de la Focul Viu, Bihor Mountains, Romania. *Theor Appl Karstology 17*, 51-60.

Kern, Z., Grynaeus, A. and *Morgós, A.*, 2009: Reconstructed precipitation for southern Bakony Mountains (Transdanubia, Hungary) back to 1746 AD based on ring widths of oak trees. *Időjárás 113*, 299-314.

Kershaw, I., 1973: The Great Famine. *Past and Present 59*, 3-50.

Kiss, A., 1999: Some weather events in the fourteenth century II (Angevin period: 1301-1387). *Acta Climatologica Universitatis Szegediensis 32-33*, 51-64.

Kiss, A., 2000a: Evidence on weather in 11-12th-century Hungary (in Hungarian). In *Magyaroknak eleiről* (About the ancestors of Hungarians) (eds.: *F. Piti* and *Gy. Szabados*). SzKM, Szeged, 249-263.

Kiss, A., 2000b: Weather events during the first Tatar invasion in Hungary (1241-42). *Acta Geographica Universitatis Szegediensis 37*, 149-156.

Kiss, A., 2001: Hydrology and Environment in the Southern Basin of Lake Fertő/Neusiedlersee in the Late Middle Ages. *Medium Aevum Quotidianum 44*, 61-77.

Kiss, A., 2003: „Ecce, in hyemis nivis et glaciei habundantia supervenit" – Weather, environmental crisis and the Mongol invasion (in Hungarian). In *Tatárjárás* (Mongol invasion) (ed.: *B. Nagy*). Osiris, Budapest, 439-452.

Kiss, A., 2004a: Utilization of the inundation area at Lake Fertő before the regulation works: Example of Sarród and its surroundings. *Acta Geographica Universitatis Szegediensis 38*, 39-49.

Kiss, A., 2004b: Waterflows in the basin of great lakes: Fertő and Balaton rivers? (in Hungarian). In *Víz a tájban* (Water in the landscape) (ed.: *Gy. Füleky*). Gödöllői Agrártudományi Egyetem, Gödöllő, 325-331.

Kiss, A., 2007: "Suburbia autem maxima in parte videntur esse deleta" – Danube icefloods and the pitfalls of urban planning: Pest and its suburbs in 1768–1799. In *From Villages to Cyberspace*. (ed.: *Cs. Kovács*). University Press, Szeged, 271-282.

Kiss, A., 2008: The 'Millennium' FP6 EU projekt – possible role of Hungarian documentary evidence in the European millennial climate reconstruction (in Hungarian). In *IV. Magyar Földrajzi Konferencia tanulmánykötet* (Research papers of the Fourth Conference on Geography in Hungary) (eds.: *V. Szabó, Z. Orosz, R. Nagy*, and *I. Fazekas*). Debreceni Egyetem, Debrecen, 163-169.

Kiss, A., 2009: „Rivulus namque, qui dicitur Fuk, fluens de prefatu lacu" – Fok, Sár, Foksár (in Hungarian). In *Antropogén ökológiai változások a Kárpát-medencében* (Ecological changes of anthropogenic origin in the Carpathian Basin) (eds.: *B. Andrásfalvy* and *G. Vargyas*). Studia Ethnologica Hungarica 9, L'Harmattan and PTE Néprajz–Kulturális Antropológia Tanszék. Budapest, 49-63.

Kiss, A. and *Paszternák, I.*, 2000: Where was Urkony located? Historical geographical and archaeological evidence for studying the topography of a medieval village (in Hungarian). *Soproni Szemle 52*, 402-419.

Kiss, A. and *Piti, F.*, 2005: The 'fok' of the Fertő (in Hungarian). *Soproni Szemle 59*, 164-184.

Kiss, A. and *Wilson, R.*, 2009: Analysis of late spring-summer temperatures for Western Hungary based on vine, grain tithes and harvest records. European Geosciences Union, *Geophysical Research Abstracts*, Vol. 11, 10945.

Kiss, A., Sümeghy, Z. and *Danku, Gy.*, 2006: The severe winter of 1783-1784 and the ice flood of the Maros river (in Hungarian). In *Táj, környezet és társadalom* / Landscape, Environment and Society (bilingual Hungarian and English volume, with English abstracts) (eds.: *A. Kiss, G. Mezősi* and *Z. Sümeghy*). Szegedi Tudományegyetem, Szeged, 353-362.

Kiss, A., Sümeghy, Z. and *Fehér, Z. Zs.*, 2008: 18th-century floods of the Maros river and the regional consequences of a typical winter flood event (in Hungarian). In *Tájváltozások a Kárpát-medencében: Az erdélyi táj változásai* (Landscape changes in the Carpathian Basin: Changes of the Transylvanian landscape) (ed.: *Gy. Füleky*). Környezetkímélő Agrokémiáért Alapítvány, Szent István Egyetem, Gödöllő, 94-100.

Kiss, T., Nyári, D. and *Sipos, Gy.*, 2006a: Blown sand movement in historical times in the region of Csengele (in Hungarian). In *Táj, környezet és társadalom* / Landscape, Environment and Society (bilingual Hungarian and English volume, with English abstracts) (eds.: *A. Kiss, G. Mezősi* and *Z. Sümeghy*). SzTE, Szeged, 373-382.

Konček, M., 1972: Über die ersten meteorologischen Aufzeichnungen in Bratislava (Pressburg) aus dem Ende des 18. Jahrhunderts. *Időjárás 76*, 51-53.

Kopf, F., 1963: Wasserwirtschaftliche Probleme des Neusiedler Sees und des Seewinkels. *Österreichische Wasserwirtschaft 15*, 190-203.

Kovács, F., 2004: Evaluation of environmental changes in the Danube Tisza Interfluve, with special emphasis on drought problems (in Hungarian). In *II. Magyar Földrajzi Konferencia tanulmánykötet* (Research papers of the Second Conference on Geography in Hungary) (eds.: *G. Barton* and *G. Dormány*). Szegedi Tudományegyetem TFGT, Szeged, 1046-1072.

Kovács, F. and *Rakonczai, J.*, 2003: Analysis of the 200-year environmental changes of a strictly protected area in the Kiskunság National Park, Hungary. In *Dealing with Diversity. Proc. of the 2nd International Conference of European Society for Environmental History*. Charles University, Prague, 263-268.

Kováts, Z., 1982: A Fertő tó mederviszonyai / Bettverhältnisse des Neusiedlersees. In *A Fertő-tó természeti adottságai* / Naturverhältnisse des Neusiedlersees (in Hungarian with German abstracts) (eds.: *Z. Kováts* and *E. Kozmáné Tóth*). Országos Meteorológiai Szolgálat, Budapest, 13-40.

Kövér, F.J., 1930: *A Hanság földrajza* (Geography of the Hanság area). Szeged városi nyomda és könyvkiadó Rt., Szeged, 99 pp.

Kristó, Gy. (ed.), 1985: *Szeged története* (History of Szeged). Vol. 2, Somogyi Könyvtár, Szeged, 846 pp.

Landsteiner, E., 1999: The crisis of wine production in late sixteenth-century Central Europe: Climatic causes and its economic consequences. *Climatic Change 43*, 323-334.

Laszlovszky, J., 1994: „Per tot discrimina rerum" Zur Interpretation von Umweltveränderungen im mittelalterlichen Ungarn. In *Umweltbewältigung. Die historische Perspektive* (eds.: G. *Jaritz* and *V. Winiwarter*). Verlag für Regionalgeschichte, Bielefeld, 37-55.

Lászlóffy, W., 1955: Flood of 1838 and the water regulation works of the Danube (in Hungarian). *Vízügyi Közlemények 20*, 39-44.

Létay, M., 1991: Flood in Óbuda in 1838: for the 150th anniversary of the catastrophy (in Hungarian). *Tanulmányok Budapest múltjából 24*, 17-26.

Meier, N., Rutishauser, Th., Pfister, Ch., Wanner, H. and *Luterbacher, J.*, 2007: Grape harvest dates as a proxy for Swiss April to August temperature reconstructions back to AD 1480. *Geophysical Research Letters 34*, L20705, doi 10.1029/2007GL031381.

Makra, L., Vitányi, B., Gál, A., Mika, J., Matyasovszky, I. and *Hirsch, T.* 2009: Wine quantity and quality varioations in relation to climatic factors in the Tokaj winegrowing region (Hungary). *Am J Enol Viticult 60*, 312-321.

Mika, J. and *Lakatos, M.*, 2008: Extreme weather tendencies in Hungary based on empirical and model approaches. *J Environ Geography 1*, 57-66.

Mika, J., Domonkos, P. and *Lakatos M.*, 2000: Meteorological revision of indirect temperature series (in Hungarian). In *Erdő és Klíma* (Forest and climate) (ed.: *K. Tar*). Debreceni Egyetem, Debrecen, 171-184.

Nagy, I., 1869: Early floods of the Fertő (in Hungarian). *Századok 3*, 690-709.

Négyesi, L., 1994: Battle of Ménfő (in Hungarian). *Hadtörténeti Közlemények 3*, 136-146.

Németh, K., 1938: *A pest-budai árvíz 1838-ban* (Flood of Pest-Buda in 1838). Budapest Székesfőváros Közönsége, Budapest, 387 pp.

Pálfai, I., 1994: Memory of the extraordinary drought of 1794 (in Hungarian). *Hidrológiai Tájékoztató 34*, 16-17.

Pálfai, I. 1997: Floods of the Maros in the 18th century (in Hungarian). *Hidrológiai Tájékoztató 37*, 34-35.

Petrić, H., 2007: Drava river flooding in Varaždin and Koprivnica parts of Podravina (Drava river region – between Croatia and Hungary) in the period of 17th-19th centuries. *Podravina 12*, 136-147.

Péczely, Gy., 1982: The Kőszeg 'Book of Vinesprouts' (in Hungarian) *Légkör 27*, No. 3, 24-27.

Pfister, C., 1988: *Klimageschichte der Schweiz: 1525-1860: das Klima der Schweiz von 1525-1860 und seine Bedeutung in der Geschichte von Bevölkerung und Landwirtschaft.* Haupt Verlag, Bern, Stuttgart, 394 pp.

Pfister, C., 1999: *Wetternachhersage. 500 Jahre Klimavariationen und Naturkatastrophen (1496-1995).* Paul Haupt, Bern, 304 pp.

Pfister, C., 2001: Klimawandel in der Geschichte Europas. Zur Entwicklung und zum Potenzial der Historischen Klimatologie. *Österreichische Zeitschrift für Geschichtswissenschaften 12*, 7-43.

Pfister, C. (ed.), 2002: *Am Tag danach. Zur Bewältigung von Naturkatastrophen in der Schweiz 1500-2000.* Paul Haupt, Bern, 263 pp.

Pfister, C. and *Brázdil, R.*, 2006: Social vulnerability to climate in the "Little Ice Age": an example from Central Europe in the early 1770s. *Climate of the Past* 2, 115-129.

P. Károlyi, Zs., 1970: Data to the flood-history of the Tisza-valley (in Hungarian). *Vízgazdálkodás 10*, 150-152, 191-192.

Popa, I. and *Kern, Z.*, 2009: Long-term summer temperature reconstruction inferred from tree-ring records from the Eastern Carpathians. *Climate Dynamics 32*, 1107-1117.

Rajna, Gy., 1979: Flood marks in Budapest (in Hungarian). *Tanulmányok Budapest múltjából 21*, 361-392.

Rácz, L., 1987: Climate variabilities in the Carpathian Basin between 1490-1700 (in Hungarian). *Légkör 32*, No. 4, 29-31.

Rácz, L., 1988: Changes in the climate of the Great Hungarian Plain between 1490-1779 based on historical sources (in Hungarian). *Alföldi Tanulmányok 12*, 34-47.

Rácz, L., 1989: About the climate history of the Little Ice Age (in Hungarian). *Agrártörténeti Szemle 31*, 185-190.

Rácz, L., 1994: The climate of Hungary during the Maunder Minimum Period. In *Climatic Trends and Anomalies in Europe 1675-1715* (eds.: *B. Frenzel, C. Pfister* and *B. Gläser*). *Palaeoclimate Research 13*, Fischer, Stuttgart, 95-108.

Rácz, L., 1995: Climate history of the Carpathian Basin in the early modern period (in Hungarian). *Történelmi Szemle 37*, 487-508.

Rácz, L., 1998: Climate history source collections of Antal Réthly and the reconstruction of climate changes (in Hungarian). *Légkör 43*, No. 4, 2-6.

Rácz, L., 1999a: Climate history of Hungary from the 16th century to the present day (in Hungarian). *Magyar Tudomány 44*, 1127-1139.

Rácz, L., 1999b: *Climate History of Hungary Since 16th Century: Past, Present and Future.* Centre for Regional Studies of Hungarian Academy of Sciences, Pécs, 158 pp.

Rácz, L., 2001a: *Magyarország éghajlattörténete az újkor idején* (Climate history of Hungary during Modern Age). JGYF Kiadó, Szeged, 303 pp.

Rácz, L., 2001b: "... rains made harvests impossible..." Weather anomalies in the 1830s (in Hungarian). In *Ezredforduló-századforduló-hetvenedik évforduló* (Millennium–hundred years anniversary–seventieth anniversary) (ed.: *Zs. Újváry*). PPKE BTK, Piliscsaba, 367-379.

Rácz, L., 2003a: Environmental crisis in Hungary during the Modern Epoch. In *Exploitation and Overexploitation in Societies Past and Present* (eds.: *B. Benzing* and *H. Bernd*). LIT Verlag, Münster, 107-114.

Rácz, L., 2003b: The Climate History of Central Europe in the Modern Age. In *People and Nature* (eds.: *J. Laszlovszky* and *P. Szabó*). CEU Press, Budapest, 229-246.

Rácz, L., 2003c: Long-term trends of climate changes in the Great Hungarian Plain (in Hungarian). In *A fenntartható fejlődés és az Alföld* (Sustainable development and the Great Hungarian Plain) (eds.: *T. Baukó* and *I. Nagy*). MTA Társadalomkutató Központ, Budapest, 9-28.

Rácz, L., 2007: Climate changes in the Carpathian Basin during the medieval period (in Hungarian). In *Dixit et salvavi animam meam* (eds.: *Cs. Jancsák, G.F. Kiss, P. Zakar* and *A. Döbör*). Belvedere Meridionale, Szeged, 57-78.

Reizner, J., 1899-1990: *Szeged története* (History of Szeged). Vols. 1-2, 4, Szeged Szab. Kir. Város Közönsége, Szeged, 388, 358, 577 pp.

Réthly, A., 1962: *Időjárási események és elemi csapások Magyarországon 1700-ig* (Weather events and natural disasters in Hungary until 1700). Akadémiai Kiadó, Budapest, 450 pp.

Réthly, A., 1970: *Időjárási események és elemi csapások Magyarországon 1701-1800* (Weather events and natural disasters in Hungary 1701-1800). Akadémiai Kiadó, Budapest, 622 pp.

Réthly, A., 1998: *Időjárási események és elemi csapások Magyarországon 1801-1900-ig* (Weather events and natural disasters in Hungary 1801-1900). Vol. 1, Országos Meteorológiai Szolgálat, Budapest, 616 pp.

Réthly, A., 1999: *Időjárási események és elemi csapások Magyarországon 1801-1900-ig* (Weather events and natural disasters in Hungary 1801-1900). Vol. 2, Országos Meteorológiai Szolgálat, Budapest, 1369 pp.

Rohr, Ch., 2005: The Danube floods and their human response and perception (14th to 17th C). *History of Meteorology 2*, 71-86.

Rohr, Ch., 2007: *Extreme Naturereignisse im Ostalpenraum. Naturerfahrung im Spätmittelalter und am Beginn der Neuzeit*. Böhlau Verlag, Köln, Weimar, Wien, 640 pp.

R. Várkonyi, Á., 2001: Historical ecology (in Hungarian). In *A történelem segédtudományai* (Auxiliary sciences of history) (ed.: *I. Bertényi*). Osiris, Budapest, 307-316.

Sági, K., 1968: Water-level tendencies of Lake Balaton in the light of historical and cartographical data (in Hungarian). *Veszprém megyei múzeumok közleményei 7*, 441-468.

Sági, K., 1970: Natural scientific sides of a historical debate (in Hungarian). *Földrajzi Értesítő 19*, 200-207.

Sági, K. and *Füzes, M.*, 1973: Recent data to the question of the water-level tendencies of the Balaton before 1863 (in Hungarian). *Somogyi múzeumok közleményei 1*, 247-261.

Siklósy, Z., Demény, A., Vennemann, T. W., Kramers, J., and *Leél-Őssy, Sz.*, 2006: Stable isotope compositions of speleothems from Hungary: climate conditions and local variations. European Geosciences Union, *Geophysical Research Abstracts*, Vol. 8, 06905.

Siklósy, Z., Demény, A., Szenthe, I., Leél-Őssy, Sz., Pilet, S., Lin, Y. and *Shen, C.-C.*, 2009: Reconstruction of climate variation for the last millennium in the Bükk Mountains, northeast Hungary, from a stalagmite record. *Időjárás 113*, 245-263.

Simon, A., 1999: Some climate extremes of the 19th-century, based on the source collection of Antal Réthly (in Hungarian). *Légkör 44*, No. 3, 29-33.

Sipos, I., 2001: *Makó és az 1863. évi országos aszály* (Makó and the regional drought of 1863). *Szirbik Miklós Társaság füzetei 14*, Makó Város Önkormányzata, Makó, 28 pp.

Stankoviansky, M., 2003: Gully evolution in the Myjava Hill Land in the second half of the last millennium. *Geographia Polonica 76*, 89-107.

Střeštík, J. and *Verő, J.*, 2000: Reconstruction of the spring temperatures in the 18th century based on the measured lengths of grapevine sprouts. *Időjárás 104*, 123-136.

Strömmer, E., 2003: *Klima-Geschichte. Methoden der Rekonstruktion und historische Perspektive. Ostösterreich 1700 bis 1830*. Franz Deuticke, Wien, 325 pp.

Surányi, D., 2006: Phenological extremes on fruit-types in the Carpathian Basin between the 6th and 19th centuries (in Hungarian). *Agro-21 füzetek 47*, 70-84.

Sümegi, P., Majkut, P., Páll, D.G., Persaits, G., Pomázi, P., Bodor, E., Jakab, G. and *Törőcsik, T.*, 2009a: Environmental reconstruction for Fenékpuszta in the Migration period (in Hungarian). In *A hadak útján 9. Konferenciakötet* (On the military route 9. Conference papers) (eds.: *A. Nagy* and *Sz. Bíró*). Xantus János Múzeum, Győr, 79-88.

Sümegi, P., Majkut, P., Jakab, G., Persaits, G. and *Törőcsik, T.*, 2009b: Environmental reconstruction for Nagybárkány (Cserhát-hills) (in Hungarian). In *A hadak útján 9. Konferenciakötet* (On the military route 9. Conference papers) (eds.: *A. Nagy* and *Sz. Bíró*). Xantus János Múzeum, Győr, 89-99.

Sümegi, P., Jakab, G., Majkut, P., Törőcsik, T. and *Zatykó, Cs.*, 2009c: Middle Age palaeoecological and palaeoclimatological reconstruction in the Carpathian Basin. *Időjárás 113*, 265-298.

Sydenham, T., 1769: *Opera Medica. Editio Novissima, aliis omnibus quae praecesserunt multo emaculatior, et novis Additamentis ditior*. Tomus Secundus. Apud Fratres de Tournes, Genevae [Genève], 288-339.

Szabados, Gy., 2004: Country defence during the German wars 1030–1052 (in Hungarian). In *Gyepűk, várak, erődítmények és egyéb honvédelmi létesítmények a Kárpát-medencében (895-1920)* (Barriers, castles, fortresses and other objects of national defence in the Carpathian Basin 895-1920) (eds.: *S. Frisnyák* and *Gy. Csihák*). Nyíregyházi Főiskola Földrajz Tanszéke, Nyíregyháza, Zürich, 35-45.

Szabó, K., 1934: *Kecskemét szőlő- és gyümölcstermelésének múltja* (Vine and fruit production of Kecskemét in the past). Katona József Társaság, Kecskemét, 84 pp.

Szabó, L., 1991: Drought in Greater Cumania at the end of the 18th century (in Hungarian). *Zounuk 6*, 99-112.

Szántó, R., 2005: Natural catastrophy and hunger in 1315-1317 (in Hungarian). *Világtörténet 27*, 50-64.

Szántó, R., 2007: Environmental changes in Europe in the first decades of the 14th century (in Hungarian). *Középkortörténeti tanulmányok 5*, 159-164.

Szentkláray, J., 1880-1882: *Száz év Dél-Magyarország ujabb történetéből: 1779-től napjainkig* (Hundred years from the recent history of South-Hungary: from 1779 to the present). Csanád Egyházmegyei Ny., Temesvár [Timişoara], 520 pp.

Szilágyi, T., 1987: Very cold, snowy winters in Kecskemét 1 (in Hungarian). *Légkör 32*, No. 4, 2-6.

Szilágyi, T., 1988a: Very cold, snowy winters in Kecskemét 2 (in Hungarian). *Légkör 33*, No. 1, 2-7.

Szilágyi, T., 1988b: Very dry, drought years in Kecskemét 1 (in Hungarian). *Légkör 33*, No. 3, 20-25.

Szilágyi, T., 1988c: Very dry, drought years in Kecskemét 2 (in Hungarian). *Légkör 33*, No. 4, 18-20.

Szilágyi, T., 1993: *Szélsőségek Kecskemét időjárásában* (Extremes in the weather of Kecskemét). *Bács-Kiskun megyei Levéltári Füzetek 10*, Bács-Kiskun Megyei Önkormányzat Levéltárának kiadványai, Kecskemét, 155 pp.

Szilágyi, T., 1999: *Időjárási események Kecskeméten a XVII-XIX. században. Forráskiadvány* (Weather events in Kecskemét in the 17-19th centuries. Source collection). Kaloprint, Kecskemét, 473 pp.

Szövényi, I., 1965: The importance of vine harvest in the economy of old Kőszeg (in Hungarian). *Savaria 3*, 259-281.

Tirnitz, J., 1974: 18th century reports on the climatic conditions of Sopron and the natural disasters affecting the town: 1725-1800 (in Hungarian). *Soproni Szemle 28*, 165-178.

Tóth, B., 2009: *A szegedi nagyárvíz képeskönyve* (Picture book of the great flood in Szeged). 3rd edition, Bába Kiadó, Szeged, 285 pp.

Tóth, G.P., 2008: Trial by water – swimming of witches: procedures of ordeal in witch trials. In *Witchcraft Mythologies and Persecutions. Demons, Witches, Spirits*. Vol. 3, (eds.: *G. Klaniczay* and *É. Pócs*). Central European University Press, Budapest, 129-163.

Tőry, K., 1952: *A Duna és szabályozása* (Water regulation of the Danube). Akadémiai Kiadó, Budapest, 454 pp.

Vadas, A., 2008: Documentary evidence on weather conditions and an environmental crisis in 1315-1317: Case study from the Carpathian Basin. *J Environ Geography 1*, 67-76.

Weikinn, C., 1958-1963: *Quellentexte zur Witterungsgeschichte Europas von der Zeitwende bis zum Jahre 1850. Hydrographie.* Vols. 1-4, Akademie-Verlag, Berlin, 531, 486, 586, 381 pp.

Zawadowski, A., 1891: *Magyarország vizeinek statisztikája* (Statistics concerning the waters in Hungary). Vol. 1, Orsz. Magy. Kir. Statisztikai Hivatal, Budapest, 450 pp.

Zimányi, V., 1984: Grain yields in the villages of the Csallóköz [Žitny ostrov] area, based on tithe accounts (in Hungarian). *Agrártörténeti Szemle 26*, 458-505.

Zorkóczy, Z., 1975: Data of the lake basin, catchment area and water economy (in Hungarian). In *A Fertő-táj Monográfiáját előkészítő adatgyűjtemény. 2. kötet: Természeti adottságok: A Fertő-táj hidroszférája és vízgazdálkodása* (Data collection for the preparation of the Monography of the Fertő. Vol. 2: Natural conditions: Hydrosphere and the water economy of the Fertő area) (eds.: *L. Aujeszky, F. Schilling* and *S. Somogyi*). Vízgazdálkodási Kutató Intézet, Budapest, 5-43.

IDŐJÁRÁS

VOLUME 113 * 2009

BUDAPEST, HUNGARY

AUTHOR INDEX

TABLE OF CONTENTS
Papers

SUBJECT INDEX

A

H

I

L

M

N

O

P

R

S

GUIDE FOR AUTHORS OF *IDŐJÁRÁS*

The purpose of the journal is to publish papers in any field of meteorology and atmosphere related scientific areas. These may be

- research papers on new results of scientific investigations,
- critical review articles summarizing the current state of art of a certain topic,
- short contributions dealing with a particular question.

Some issues contain "News" and "Book review", therefore, such contributions are also welcome. The papers must be in American English and should be checked by a native speaker if necessary.

Authors are requested to send their manuscripts to

Editor-in Chief of IDŐJÁRÁS
P.O. Box 39, H-1675 Budapest, Hungary
E-mail: antal.e@met.hu

including all illustrations. MS Word format is preferred in electronic submission. Papers will then be reviewed normally by two independent referees, who remain unidentified for the author(s). The Editor-in-Chief will inform the author(s) whether or not the paper is acceptable for publication, and what modifications, if any, are necessary.

Please, follow the order given below when typing manuscripts.

Title page: should consist of the title, the name(s) of the author(s), their affiliation(s) including full postal and e-mail address(es). In case of more than one author, the corresponding author must be identified.

Abstract: should contain the purpose, the applied data and methods as well as the basic conclusion(s) of the paper.

Key-words: must be included (from 5 to 10) to help to classify the topic.

Text: has to be typed in single spacing on an A4 size paper using 14 pt Times New Roman font if possible. Use of S.I. units are expected, and the use of negative exponent is preferred to fractional sign. Mathematical formulae are expected to be as simple as possible and numbered in parentheses at the right margin.

All publications cited in the text should be presented in the *list of references*, arranged in alphabetical order. For an article: name(s) of author(s) in Italics, year, title of article, name of journal, volume, number (the latter two in Italics) and pages. E.g., *Nathan, K.K.*, 1986: A note on the relationship between photosynthetically active radiation and cloud amount. *Időjárás 90,* 10-13. For a book: name(s) of author(s), year, title of the book (all in Italics except the year), publisher and place of publication. E.g., *Junge, C.E.*, 1963: *Air Chemistry and Radioactivity.* Academic Press, New York and London. Reference in the text should contain the name(s) of the author(s) in Italics and year of publication. E.g., in the case of one author: *Miller* (1989); in the case of two authors: *Gamov* and *Cleveland* (1973); and if there are more than two authors: *Smith et al.* (1990). If the name of the author cannot be fitted into the text: *(Miller,* 1989); etc. When referring papers published in the same year by the same author, letters a, b, c, etc. should follow the year of publication.

Tables should be marked by Arabic numbers and printed in separate sheets with their numbers and legends given below them. Avoid too lengthy or complicated tables, or tables duplicating results given in other form in the manuscript (e.g., graphs).

Figures should also be marked with Arabic numbers and printed in black and white or color (under special arrangement) in separate sheets with their numbers and captions given below them. JPG, TIF, GIF, BMP, PNG or EPS formats should be used for electronic artwork submission.

Reprints: authors receive 30 reprints free of charge. Additional reprints may be ordered at the authors' expense when sending back the proofs to the Editorial Office.

More information for authors is available: antal.e@met.hu

Published by the Hungarian Meteorological Service

Budapest, Hungary

INDEX 26 361

HU ISSN 0324-6329